

26th Benelux Meeting

on

Systems and Control

March 13 – 15, 2007

Lommel, Belgium

Book of Abstracts

The 26th Benelux meeting on Systems and Control is sponsored by

ICCoS (Identification and Control of Complex Systems),
a Scientific Research Network of the Research Foundation - Flanders (FWO-Vlaanderen),



and supported by the

Belgian Programme on Interuniversity Poles of Attraction DYSCO
(Dynamic Systems, Control and Optimization), initiated by the Belgian State,
Prime Minister's Office for Science.



Jan Swevers, Johan Schoukens, Rik Pintelon, Patrick Guillaume, Jan Van Impe, Ilse Smets, Bram Demeulenaere and Bart De Moor (eds.)

Book of Abstracts 26th Benelux Meeting on Systems and Control

Katholieke Universiteit Leuven - Departement Werktuigkunde
Celestijnenlaan 300B, B-3001 Heverlee (Belgium)

Alle rechten voorbehouden. Niets uit deze uitgave mag worden vermenigvuldigd en/of openbaar gemaakt worden door middel van druk, fotocopie, microfilm, elektronisch of op welke andere wijze ook zonder voorafgaandijke schriftelijke toestemming van de uitgever.

All rights reserved. No part of the publication may be reproduced in any form by print, photoprint, microfilm or any other means without written permission from the publisher.

D/2007/5769/1
ISBN 9789073802841

Part 1

Table of Contents

Tuesday, March 13, 2007

Les Arcades
Welcome and Opening

Chair: B. De Moor 10:40–10:55

Plenary Lecture Les Arcades
Sampling in Signal Processing
Graham C. Goodwin
Chair: Johan Schoukens 11:30–12:30TuP01 Les Arcades
Control applications 1
Chair: D. Lefeber 14:00–16:05TuP01-1 14:00–14:25
Velocity control of a 2D dynamic walking robot 19
G. van Oort University of Twente
S. Stramigoli University of TwenteTuP01-2 14:25–14:50
Application of constraint-based task specification and estimation for sensor-based robot systems to a laser tracking task 20
T. De Laet Katholieke Universiteit Leuven
W. Decré Katholieke Universiteit Leuven
J. Rutgeerts Katholieke Universiteit Leuven
H. Bruyninckx, J. De SchutterTuP01-3 14:50–15:15
Sensor-based control using the Open Robot RealTime Toolkit 21
R. Smits Katholieke Universiteit Leuven
P. Soetens Flanders' Mechatronics Technology Centre
H. Bruyninckx Katholieke Universiteit LeuvenTuP01-4 15:15–15:40
Image Based Robotic Apple Harvesting 22
K. Donné Katholieke Hogeschool Limburg
S. Boedrij Katholieke Hogeschool Limburg
W. Beckers Katholieke Hogeschool Limburg
J. Baeten, E. ClaesenTuP01-5 15:40–16:05
Mechatronics and Control for Atomic Force Microscopy at Video-Rate 23
G. Schitter Delft University of TechnologyTuP02 Bloemenzaal
Control
Chair: A. Stoorvogel 14:00–16:05TuP02-1 14:00–14:25
Dealing with Flexible Modes in 6 DOFs Robust Control 24
T.A.E. Oomen Technische Universiteit Eindhoven
O.H. Bosgra Technische Universiteit EindhovenTuP02-2 14:25–14:50
Multivariable Ellipsoidal Unfalsified Control 25J. van Helvoort Technische Universiteit Eindhoven
B. de Jager Technische Universiteit Eindhoven
M. Steinbuch Technische Universiteit EindhovenTuP02-3 14:50–15:15
Linear Control Design of Time-Domain Constrained Systems 26W. Aangenent Technische Universiteit Eindhoven
M.J.G. van de Molengraft Technische Universiteit Eindhoven
M. Steinbuch Technische Universiteit EindhovenTuP02-4 15:15–15:40
Solving control-to-facet problems using output feedback 27L.C.G.J.M. Habets Technische Universiteit Eindhoven
P.J. Collins Centrum voor Wiskunde en Informatica
J.H. van Schuppen Centrum voor Wiskunde en InformaticaTuP02-5 15:40–16:05
H infinity Control for Nonlinear Systems Based on SOSDecomposition 28
X. Wei Delft University of Technology
M. Verhaegen Delft University of TechnologyTuP03 Impressario zaal
Reservoir monitoring & control
Chair: P. van den Hof 14:00–16:05TuP03-1 14:00–14:25
Closed-Loop Oil and Gas Reservoir Management 29S.G. Douma Shell SIEP-EPT
D.R. Brouwer Shell SIEP-EPT
J.D. Jansen Shell SIEP-EPT/Delft University of TechnologyTuP03-2 14:25–14:50
Real-Time Estimation of Well Inflow Parameters Using Only Pressure and Temperature Measurements 30M. Leskens TNO Science and Industry
S. Belfroid TNO Science and IndustryTuP03-3 14:50–15:15
Parameterization of reservoir properties for closed-loop reservoir management 31J.F.M. van Doren Delft University of Technology
M.J. Zandvliet Delft University of Technology
P.M.J. Van den Hof Delft University of Technology
O.H. Bosgra, J.D. JansenTuP03-4 15:15–15:40
Adjoint-Based Well Placement Optimization Under Production Constraints 32M. Handels Delft University of Technology
M.J. Zandvliet Delft University of Technology
D.R. Brouwer Delft University of Technology
J.D. JansenTuP03-5 15:40–16:05
A hierarchical system approach toward improved oilreservoir management 33
G.M. van Essen Delft University of Technology
P.M.J. Van den Hof Delft University of Technology
J.D. Jansen Shell SIEP-EPT/Delft University of Technology
O.H. Bosgra

TuP04	System theory 1	Western zaal	14:00–16:05	TuP05-4	15:15–15:40
Chair: F. Callier				<i>Real-time Dynamic Optimization of Crystal Yield in a Fed-batch Crystallization of Ammonium Sulphate</i>	42
				A. Mesbah	Delft University of Technology
				L.C.P. Spierings	Delft University of Technology
TuP04-1		14:00–14:25		TuP05-5	15:40–16:05
<i>(In)equivalence of Discrete Time LPV State-Space and Input/Output Representations</i>			34	<i>Stabilization of the Optimally Scheduled Cyclic Operation of an Hybrid Chemical Plant</i>	43
R. Toth	Delft University of Technology			I. Simeonova	Université catholique de Louvain
P.S.C. Heuberger	Delft University of Technology			F. Warichet	Université catholique de Louvain
F. Felici	Delft University of Technology			G. Bastin	Université catholique de Louvain
P.M.J. Van den Hof				D. Dochain, Y. Pochet	
TuP04-2		14:25–14:50		TuP06	Seaside zaal
<i>Reachability analysis and verification of hybrid systems using Ariadne</i>			35	System identification & experiment design	
A. Casagrande	University of Udine		Chair: V. Wertz		
P. Collins	Centrum voor Wiskunde en Informatica				
T. Villa	University of Verona			14:00–16:05	
TuP04-3		14:50–15:15		TuP06-1	14:00–14:25
<i>On a balanced canonical form for continuous-time lossless systems</i>			36	<i>Frequency domain identification of linear slowly time-varying systems</i>	44
R.L.M. Peeters	Universiteit Maastricht			J. Lataire	Vrije Universiteit Brussel
B. Hanzon	University College Cork			R. Pintelon	Vrije Universiteit Brussel
M. Olivi	INRIA Sophia-Antipolis			TuP06-2	14:25–14:50
TuP04-4		15:15–15:40		<i>Estimating the power spectrum and sample variance of the fourier coefficients using overlapping sub-records</i>	45
<i>Matrix Factorization and Stochastic State Representations</i>			37	K. Barbé	Vrije Universiteit Brussel
B. Vanluyten	Katholieke Universiteit Leuven			J. Schoukens	Vrije Universiteit Brussel
J.C. Willems	Katholieke Universiteit Leuven			R. Pintelon	Vrije Universiteit Brussel
B. De Moor	Katholieke Universiteit Leuven			TuP06-3	14:50–15:15
TuP04-5		15:40–16:05		<i>Finite-Time Experiment Design with Multisines</i>	46
<i>Realization of Rational Systems</i>			38	X.J.A. Bombois	Delft University of Technology
J. Nemcova	Centrum voor Wiskunde en Informatica			S. Taamallah	National Aerospace Laboratory (NLR)
TuP05	Chemical reactors	Emanuel zaal	14:00–16:05	M. Barenthin	KTH
Chair: I. Smets				TuP06-4	15:15–15:40
TuP05-1		14:00–14:25		<i>Hybrid optimization of optimal temperature inputs for the accurate estimation of microbial cardinal temperatures</i>	47
<i>Design of an inferential sensor for a chemical batch reactor</i>			39	E. Van Derlinden	Katholieke Universiteit Leuven
G. Gins	Katholieke Universiteit Leuven			K. Bernaerts	Katholieke Universiteit Leuven
I.Y. Smets	Katholieke Universiteit Leuven			F. Logist	Katholieke Universiteit Leuven
J.F. Van Impe	Katholieke Universiteit Leuven			J.F. Van Impe	
B. Pluymers, W. Van Brempt				TuP06-5	15:40–16:05
TuP05-2		14:25–14:50		<i>Stable Approximations of Unstable Models</i>	48
<i>Parameter Identification to Enforce Practical Observability - Application to (Fed-)batch Bioprocesses</i>			40	T. D'haene	Vrije Universiteit Brussel
G. Goffaux	Faculté Polytechnique de Mons			R. Pintelon	Vrije Universiteit Brussel
L. Bodizs	Ecole Polytechnique Federale de Lausanne			TuE01	Les Arcades
A. Vande Wouwer	Faculté Polytechnique de Mons			Control applications 2	
P. Bogaerts, D. Bonvin			Chair: M. Steinbuch		
TuP05-3		14:50–15:15			16:35–18:40
<i>State observer for fed-batch reactor with uncertain kinetics</i>			41	TuE01-1	16:35–17:00
F. Sauvage	Université catholique de Louvain			<i>Sub nano positioning</i>	49
D. Dochain	Université catholique de Louvain			J. van Hulzen	Delft University of Technology

TuE01-3	17:25–17:50	TuE03-2	17:00–17:25
<i>Dealing with Instability in Hybrid Stepper Motors . . .</i>	51	<i>Effects of a recently discovered voltage-dependent current on the electrical activity of midbrain dopaminergic neurons: modeling and experiments</i>	60
J. Stolte	Technische Universiteit Eindhoven	M. Bonjean	University of Liege
A. Veltman	Technische Universiteit Eindhoven	O. Waroux	University of Liege
P.P.J. van den Bosch	Technische Universiteit Eindhoven	V. Seutin	University of Liege
TuE01-4	17:50–18:15	R. Sepulchre	
<i>Contactless Planar Actuator with Manipulator - Experimental Setup for Control</i>	52	TuE03-3	17:25–17:50
M. Gajdusek	Technische Universiteit Eindhoven	<i>Actigraphy as a way of distinguishing sleep from wake . . .</i>	61
A.A.H. Damen	Technische Universiteit Eindhoven	J. Tilmanne	Faculté Polytechnique de Mons
P.P.J. van den Bosch	Technische Universiteit Eindhoven	J. Urbain	Faculté Polytechnique de Mons
TuE01-5	18:15–18:40	M.V. Kothare	Lehigh University
<i>Switched Linear Controller Breaks Waterbed Effect . . .</i>	53	A. Vande Wouwer, S.V. Kothare	
R.A. van den Berg	Technische Universiteit Eindhoven	TuE03-4	17:50–18:15
A.Y. Pogromsky	Technische Universiteit Eindhoven	<i>A system identification approach to kinetic modeling of metabolic networks of eukaryotic cells from experimental data</i>	62
J.E. Rooda	Technische Universiteit Eindhoven	J. Shi	Delft University of Technology
TuE02	Bloemenzaal	A.J. den Dekker	Delft University of Technology
	Traffic, motion control	P.J.T. Verheijen	Delft University of Technology
Chair: B. De Schutter		W.A. van Winden, M. Verhaegen, J.J. Heijnen	
TuE02-1	16:35–17:00	TuE03-5	18:15–18:40
<i>Swarm Intelligence Methods for Traffic Control</i>	54	<i>Adaptive minimal model for glycemia control in critically ill patients</i>	63
J.M. van Ast	Delft University of Technology	T. Van Herpe	Katholieke Universiteit Leuven
R. Babuska	Delft University of Technology	G. Van den Berghe	Katholieke Universiteit Leuven
B. De Schutter	Delft University of Technology	B. De Moor	Katholieke Universiteit Leuven
TuE02-2	17:00–17:25	TuE04	Western zaal
<i>Consensus problems with distributed delays, with application to traffic flow models</i>	55	System theory 2	
W. Michiels	Katholieke Universiteit Leuven	Chair: J. Willems	16:35–18:40
C.I. Morarescu	University of Bucharest		
S.-I. Niculescu	Supélec	TuE04-1	16:35–17:00
TuE02-3	17:25–17:50	<i>Contact structures: a tool for modeling and analyzing thermodynamical systems</i>	64
<i>Hierarchical traffic control and management with intelligent vehicles</i>	56	A. Favache	Université catholique de Louvain
L.D. Baskar	Delft University of Technology	D. Dochain	Université catholique de Louvain
B. De Schutter	Delft University of Technology	B. Maschke	Université Claude Bernard, Lyon 1
J. Hellendoorn	Delft University of Technology	TuE04-2	17:00–17:25
TuE02-4	17:50–18:15	<i>Growth rate of a switched homogeneous system</i>	65
<i>Stabilization of Collective Motion in Three Dimensions . . .</i>	57	S. Emre Tuna	University of Liege
L. Scardovi	University of Liege	TuE04-3	17:25–17:50
R. Sepulchre	University of Liege	<i>On the circle criterion for feedback systems with both unbounded observation and control</i>	66
TuE02-5	18:15–18:40	P. Grabowski	AGH University of Science and Technology
<i>Time-varying delays in Networked Control Systems . . .</i>	58	F.M. Callier	University of Namur
M. Cloosterman	Technische Universiteit Eindhoven	TuE04-4	17:50–18:15
N. van de Wouw	Technische Universiteit Eindhoven	<i>Pseudo-Gradient and Lagrangian Boundary Control Formulation of Electromagnetic Media</i>	67
H. Nijmeijer	Technische Universiteit Eindhoven	D. Jeltsema	Delft University of Technology
TuE03	Impressario zaal	A.J. van der Schaft	University of Groningen
	Bio / Human		
Chair: C. Ionescu		TuE04-5	18:15–18:40
TuE03-1	16:35–17:00	<i>Observable graphs</i>	68
<i>Why must the brain take into account the eyes translations during active head movements</i>	59	R.Jungers	Université catholique de Louvain
P. Daye	Université catholique de Louvain	V.D. Blondel	Université catholique de Louvain
V. Wertz	Université catholique de Louvain		
Ph. Lefèvre	Université catholique de Louvain		

TuE05	Bio reactors	Emanuel zaal	17:50–18:15	
Chair: J. Van Impe		16:35–18:40	<i>Disturbance Accommodated Control</i> 77	
TuE05-1		16:35–17:00	M.L.G. Boerlage Technische Universiteit Eindhoven	
<i>Productivity optimization of cultures of <i>S. cerevisiae</i> through a robust control strategy</i> 69			B. de Jager Technische Universiteit Eindhoven	
L. Dewasme	Faculté Polytechnique de Mons		M. Steinbuch Technische Universiteit Eindhoven	
F. Renard	Faculté Polytechnique de Mons			
A. Vande Wouwer	Faculté Polytechnique de Mons			
TuE05-2		17:00–17:25	TuE06-4	18:15–18:40
<i>Application of Robust Control to the Activated Sludge Process</i> 70			<i>Variance calculation of covariance-driven stochastic subspace identification estimates</i> 78	
R. David	Faculté Polytechnique de Mons		E. Reynders Katholieke Universiteit Leuven	
A. Vande Wouwer	Faculté Polytechnique de Mons		R. Pintelon Vrije Universiteit Brussel	
J.-L. Vasel	University of Liege		G. De Roeck Katholieke Universiteit Leuven	
I. Queinnec				
TuE05-3		17:25–17:50		
<i>Asymptotic behavior and bistability of a biochemical reactor distributed parameter model</i> 71				
A.K. Dramé	University of Nevada			
D. Dochain	Université catholique de Louvain			
J.J. Winkin	University of Namur			
TuE05-4		17:50–18:15		
<i>The effect of feedback on the stability of biochemical reaction systems</i> 72				
M. Sbarciog	Ghent University			
M. Loccufier	Ghent University			
E. Noldus	Ghent University			
TuE05-5		18:15–18:40		
<i>Analysis of nonlinear biochemical networks: the hybrid approach</i> 73				
M.W.J.M. Musters	Technische Universiteit Eindhoven			
N.A.W. van Riel	Technische Universiteit Eindhoven			
TuE06	Seaside zaal			
Chair: J. Vandewalle	Blind identification	16:35–18:40		
TuE06-1		16:35–17:00		
<i>Operational Acoustic Modal Analysis: Sensitivity-based mode shape normalisation</i> 74				
G. De Sitter	Vrije Universiteit Brussel			
P. Guillaume	Vrije Universiteit Brussel			
TuE06-2		17:00–17:25		
<i>Operational Modal Analysis Using Transmissibility Measurements</i> 75				
C. Devriendt	Vrije Universiteit Brussel			
P. Guillaume	Vrije Universiteit Brussel			
TuE06-3		17:25–17:50		
<i>Reference-based combined deterministic-stochastic subspace identification for modal analysis applications</i> 76				
E. Reynders	Katholieke Universiteit Leuven			
G. De Roeck	Katholieke Universiteit Leuven	8		

Wednesday, March 14, 2007

Plenary Lecture	Les Arcades
Parametric Time Domain Methods for Non-Stationary Random Vibration Identification: An Overview of Methods and Applications	
Spilios D. Fassois	
Chair: R. Pintelon	08:30–09:30

Plenary Lecture	Les Arcades
Quantization in Signal Processing and Control	
Graham C. Goodwin	
Chair: P. Guillaume	10:00–11:00

WeM01	Les Arcades
Control applications 3	
Chair: J. Camino	11:15–12:30

WeM01-1	11:15–11:40
<i>Global chassis control under varying road conditions</i> 79	
M. Gerard	Delft University of Technology
M. Verhaegen	Delft University of Technology
WeM01-2	11:40–12:05
<i>Hydraulic CVT slip control: new challenges</i> 80	
S. van der Meulen	Technische Universiteit Eindhoven
B. de Jager	Technische Universiteit Eindhoven
M. Steinbuch	Technische Universiteit Eindhoven
B. Veenhuizen	

WeM01-3	12:05–12:30
<i>Controller design for the active control of gearbox noise: preliminary results</i> 81	
B. Stallaert	Katholieke Universiteit Leuven
S.G. Hill	Flanders' Mechatronics Technology Center
W. Symens	Flanders' Mechatronics Technology Center
J. Swevers, P. Sas	

WeM02	Bloemenzaal
Special session: "target round-robin"	
Chair: W. Van Moer	11:15–12:30

WeM02-1	11:15–11:40
<i>Special Session: A round-robin benchmark for the Large Signal Network Analyzer</i> 82	
Y. Rolain	Vrije Universiteit Brussel
W. Van Moer	Vrije Universiteit Brussel
C. Gaquière	Université des Sciences et Technologies de Lille
D. Duceau, M. Fernandez Barciela, D. Schreurs, M. Vanden Bossche, F. Verbeyst	

WeM03	Impressario zaal
Tubular reactors	
Chair: J. Winkin	11:15–12:30

WeM03-1	11:15–11:40
<i>Multiple-objective optimisation of jacketed tubular reactors</i> 83	
P.M. Van Erdeghem	Katholieke Universiteit Leuven
F. Logist	Katholieke Universiteit Leuven
I.Y. Smets	Katholieke Universiteit Leuven
J.F. Van Impe	
WeM03-2	11:40–12:05
<i>Classic vs. flow reversal operation of jacketed tubular reactors</i> 84	
F. Logist	Katholieke Universiteit Leuven
A. Vande Wouwer	Faculté Polytechnique de Mons
J.F. Van Impe	Katholieke Universiteit Leuven
I.Y. Smets	
WeM03-3	12:05–12:30
<i>Solving large-scale Lyapunov equations with multigrid</i> 85	
B. Vandereycken	Katholieke Universiteit Leuven
S. Vandewalle	Katholieke Universiteit Leuven
WeM04	Western zaal
Game theory	
Chair: P. Van Dooren	11:15–12:30
WeM04-1	11:15–11:40
<i>Playing Clobber on a Cycle</i> 86	
V.D. Blondel	Université catholique de Louvain
C. de Kerchove	Université catholique de Louvain
J. M. Hendrickx	Université catholique de Louvain
R. Jungers	
WeM04-2	11:40–12:05
<i>Adaptive Missile Guidance Laws using game Theoretic Equilibria</i> 87	
E.J. Trottemant	Delft University of Technology
WeM04-3	12:05–12:30
<i>Computability of solutions of dynamical games</i> 88	
P.J. Collins	Centrum voor Wiskunde en Informatica
L. Sella	Centrum voor Wiskunde en Informatica
WeM05	Emanuel zaal
Bio-modelling	
Chair: A. Vande Wouwer	11:15–12:30
WeM05-1	11:15–11:40
<i>Application of a Weibull-type model to Listeria innocua inactivation at dynamic conditions of lactic acid and pH</i> 89	
A. Verhulst	Katholieke Universiteit Leuven
M. Janssen	Katholieke Universiteit Leuven
A.H. Geeraerd	Katholieke Universiteit Leuven
F. Devlieghere, J.F. Van Impe	
WeM05-2	11:40–12:05
<i>NN-based Software Sensors in Yeast and Bacteria Fed-Batch Processes</i> 90	
L. Dewasme	Faculté Polytechnique de Mons
A. Vande Wouwer	Faculté Polytechnique de Mons
X. Hulhoven	Université Libre de Bruxelles
Ph. Bogaerts	

WeM05-3	12:05–12:30
<i>Modeling AI-2 type quorum sensing in <i>Salmonella Typhimurium</i></i>	91
A.M. Cappuyns	Katholieke Universiteit Leuven
K. Bernaerts	Katholieke Universiteit Leuven
S.C. De Keersmaecker	Katholieke Universiteit Leuven
J. Vanderleyden, J.F. Van Impe	

WeM06	Seaside zaal
	System identification applications
Chair: M. Kinnaert	11:15–12:30

WeM06-1	11:15–11:40
<i>Computer Based Real Time Aircraft Model Identification</i>	92
T.J.J. Lombaerts	Delft University of Technology
Q.P. Chu	Delft University of Technology
J.A. Mulder	Delft University of Technology

WeM06-2	11:40–12:05
<i>A Frequency Domain Identification Algorithm for Single Ended Line Measurements</i>	93
C. Neus	Vrije Universiteit Brussel
P. Boets	Vrije Universiteit Brussel
L. Van Biesen	Vrije Universiteit Brussel

WeM06-3	12:05–12:30
<i>Transmission line modelling exploiting 'common-mode' signals</i>	94
W. Foubert	Vrije Universiteit Brussel

WeP01	Les Arcades
	Control applications 4
Chair: H. Van Brussel	14:00–16:05

WeP01-1	14:00–14:25
<i>State feedback control of switching server flowline with setups</i>	95
J.A.W.M. van Eekelen	Technische Universiteit Eindhoven
E. Lefeber	Technische Universiteit Eindhoven
J.E. Rooda	Technische Universiteit Eindhoven

WeP01-2	14:25–14:50
<i>Model and actuator improvements for surge control</i>	96
J. van Helvoirt	Technische Universiteit Eindhoven
B. de Jager	Technische Universiteit Eindhoven
M. Steinbuch	Technische Universiteit Eindhoven

WeP01-3	14:50–15:15
<i>A four-channel adaptive structure for high friction tele-operation systems in contact with soft environments</i>	97
T. Delwiche	Université Libre de Bruxelles
M. Kinnaert	Université Libre de Bruxelles

WeP01-4	15:15–15:40
<i>Real-time Optimal Power Balance Control Using Nodal Prices</i>	98
A. Jokic	Technische Universiteit Eindhoven
P.P.J. van den Bosch	Technische Universiteit Eindhoven
M. Lazar	Technische Universiteit Eindhoven

WeP01-5	15:40–16:05
<i>Control Issues in Rotor-Bearing Interactions</i>	99
H.M.N.K. Balini	Delft University of Technology
C.W. Scherer	Delft University of Technology

WeP02	Bloemenzaal
	Distributed systems
Chair: H. Hellendoorn	14:00–16:05

WeP02-1	14:00–14:25
<i>Modelling and identification of a SMB process</i>	100
V. Grosfils	Université Libre de Bruxelles
C. Levrie	Faculté Polytechnique de Mons
M. Kinnaert	Université Libre de Bruxelles
A. Vande Wouwer	

WeP02-2	14:25–14:50
<i>Model Approximation for Distributed Parameter Systems</i>	101
S.K. Wattamwar	Technische Universiteit Eindhoven
S. Weiland	Technische Universiteit Eindhoven
L. Ozkan	IPCOs

WeP02-3	14:50–15:15
<i>Mathematical performance analysis of a temperature controlled bulk storage room</i>	102
S. van Mourik	University of Twente
H. Zwart	University of Twente
K. Keesman	Wageningen University

WeP02-4	15:15–15:40
<i>An algebraic approach to control theory for PDE</i>	103
H. Trentelman	University of Groningen
D. Napp	University of Groningen

WeP02-5	15:40–16:05
<i>Distributed waveform reconstruction for Adaptive Optics</i>	104
R.M.L. Ellenbroek	Delft University of Technology
M.H.G. Verhaegen	Delft University of Technology
N. Doelman	TNO Science and Industry

WeP03	Impressario zaal
	Optimization
Chair: S. Vandewalle	14:00–16:05

WeP03-1	14:00–14:25
<i>Efficient Numerical Solution of SDPs Derived from the Generalized KYP Lemma</i>	105
G. Pipeleers	Katholieke Universiteit Leuven
L. Vandenberghe	University of California, Los Angeles
B. Demeulenaere	Katholieke Universiteit Leuven
J. Swevers, J. De Schutter	

WeP03-2	14:25–14:50
<i>Efficient dynamic optimization for Nonlinear Moving Horizon Estimation</i>	106
N. Haverbeke	Katholieke Universiteit Leuven
M. Diehl	Katholieke Universiteit Leuven
B. De Moor	Katholieke Universiteit Leuven

WeP03-3	14:50–15:15
<i>Design of dynamically optimal B-spline motion inputs: experimental results</i>	107
J. De Caigny	Katholieke Universiteit Leuven
B. Demeulenaere	Katholieke Universiteit Leuven
J. Swevers	Katholieke Universiteit Leuven
J. De Schutter	

WeP03-4	15:15–15:40	WeP05-2	14:25–14:50
<i>Optimising the robust stability of time-delay systems via nonsmooth eigenvalue optimisation 108</i>			
J. Vanbervliet	Katholieke Universiteit Leuven	G. Pipeleers	Katholieke Universiteit Leuven
W. Michiels	Katholieke Universiteit Leuven	B. Demeulenaere	Katholieke Universiteit Leuven
		J. Swevers	Katholieke Universiteit Leuven
		J. De Schutter	Katholieke Universiteit Leuven
WeP03-5	15:40–16:05	WeP05-3	14:50–15:15
<i>Young's Modulus Reconstruction Using a Constrained Gauss-Newton Method 109</i>			
J. Camino	Katholieke Universiteit Leuven	H. Hadiyanto	Wageningen University
M. Sette	Katholieke Universiteit Leuven	A.J.B van Boxtel	Wageningen University
M. Diehl	Katholieke Universiteit Leuven	G. van Straten	Wageningen University
		D.C. Esveld, R.M. Boom	Wageningen University
WeP04	Western zaal	WeP05-4	15:15–15:40
Signal processing		<i>Towards economic optimal dynamic plantwide operation 118</i>	
Chair: Y. Rolain	14:00–16:05	A.E.M. Huesman	Delft University of Technology
		O.H. Bosgra	Delft University of Technology
WeP04-1	14:00–14:25	WeP05-5	15:40–16:05
<i>Time averaging in solid substrates 110</i>			
V. Beelaerts	Vrije Universiteit Brussel	<i>A note on cooperative linear quadratic control 119</i>	
F. De Ridder	Vrije Universiteit Brussel	J.C. Engwerda	Tilburg University
R. Pintelon	Vrije Universiteit Brussel		
J. Schoukens, F. Dehairs			
WeP04-2	14:25–14:50	WeP06	Seaside zaal
<i>An estimation approach to system inversion 111</i>			
S. Gillijns	Katholieke Universiteit Leuven	Identification in presence of nonlinear distortions	
B. De Moor	Katholieke Universiteit Leuven	Chair: W. Van Moer	14:00–16:05
WeP04-3	14:50–15:15	WeP06-1	14:00–14:25
<i>Bayesian filtering and smoothing techniques in gait analysis 112</i>			
F. De Groot	Katholieke Universiteit Leuven	<i>Some Practical Applications of a Nonlinear Block Structure Identification Procedure 120</i>	
T. De Laet	Katholieke Universiteit Leuven	L. Lauwers	Vrije Universiteit Brussel
I. Jonkers	Katholieke Universiteit Leuven	J. Schoukens	Vrije Universiteit Brussel
J. De Schutter		R. Pintelon	Vrije Universiteit Brussel
WeP04-4	15:15–15:40	WeP06-2	14:25–14:50
<i>Review of filtering methods for removal of resuscitation artifacts from human ECG signals 113</i>			
I. Markovsky	Katholieke Universiteit Leuven	<i>Detection of Nonlinearities when Measuring Respiratory Impedance 121</i>	
S. Van Huffel	Katholieke Universiteit Leuven	C. Ionescu	Ghent University
A. Amann	Innsbruck Medical University	A. Caicedo Dorado	Ghent University
		M. Gallego	Ghent University
		R. De Keyser	
WeP04-5	15:40–16:05	WeP06-3	14:50–15:15
<i>A positioning technique for GSM, using the signal strengths of one antenna site 114</i>			
N. Deblauwe	Vrije Universiteit Brussel	<i>Estimating the FRF Matrix and the Level of Nonlinearity for Multivariable Systems using a Single Periodic Broadband Excitation 122</i>	
L. Van Biesen	Vrije Universiteit Brussel	K. Smolders	Katholieke Universiteit Leuven
		J. Swevers	Katholieke Universiteit Leuven
WeP05	Emanuel zaal	WeP06-4	15:15–15:40
Optimal control 1		<i>Extending the Best Linear Approximation for Frequency Translating Systems 123</i>	
Chair: B. de Jager	14:00–16:05	K. Vandermot	Vrije Universiteit Brussel
		W. Van Moer	Vrije Universiteit Brussel
		Y. Rolain	Vrije Universiteit Brussel
		R. Pintelon	
WeP05-1	14:00–14:25	WeP06-5	15:40–16:05
<i>Optimal control in a data-based context 115</i>			
A.J. den Hamer	Technische Universiteit Eindhoven	<i>Experimental stability analysis of nonlinear feedback systems 124</i>	
M.J.G. van de Molengraft	Technische Universiteit Eindhoven	L. Vanbeylen	Vrije Universiteit Brussel
G.Z. Angelis	Philips	J. Schoukens	Vrije Universiteit Brussel
M. Steinbuch			

WeE01	Control applications 5	Les Arcades	17:00–17:25
Chair: R. Boel			
		16:35–18:15	
WeE01-1		16:35–17:00	
<i>Overview of the Control Architecture used for the Biped Lucy</i> 125			
B. Vanderborght	Vrije Universiteit Brussel		Université catholique de Louvain
R. Van Ham	Vrije Universiteit Brussel		Université catholique de Louvain
B. Verrelst	Vrije Universiteit Brussel		Université catholique de Louvain
M. Van Damme, D. Lefeber			
WeE01-2		17:00–17:25	
<i>Design and control of Pneumatic Artificial Muscle actuators for fatigue testing</i> 126			
K. Deckers	Vrije Universiteit Brussel		University of Liege
P. Guillaume	Vrije Universiteit Brussel		Université catholique de Louvain
D. Lefeber	Vrije Universiteit Brussel		University of Liege
WeE01-3		17:25–17:50	
<i>Proxy-Based Sliding Mode Control of a 2-DOF Pneumatic Manipulator</i> 127			
M. Van Damme	Vrije Universiteit Brussel		Katholieke Universiteit Leuven
B. Vanderborght	Vrije Universiteit Brussel		ENSEA-CNRS
R. Van Ham	Vrije Universiteit Brussel		Katholieke Universiteit Leuven
F. Daerden, D. Lefeber			
WeE01-4		17:50–18:15	
<i>Long-Stroke Six Degree of Freedom Planar Actuator Topology</i> 128			
C.M.M. van Lierop	Technische Universiteit Eindhoven		Technische Universiteit Eindhoven
J.W. Jansen	Technische Universiteit Eindhoven		Technische Universiteit Eindhoven
A.A.H. Damen	Technische Universiteit Eindhoven		Technische Universiteit Eindhoven
P.P.J. van den Bosch			
WeE02	Miscellaneous	Bloemenzaal	16:35–17:00
Chair: H. Hellendoorn			
		16:35–18:15	
WeE02-1		16:35–17:00	
<i>Vibration reduction using dynamic absorbers</i> 129			
F. Petit	Ghent University		University of Liege
M. Loccufier	Ghent University		University of Liege
WeE02-2		17:00–17:25	
<i>Observer design for real-time controlled restraint systems</i> 130			
E.P. van der Laan	Technische Universiteit Eindhoven		Université catholique de Louvain
WeE02-3		17:25–17:50	
<i>Robust low-complexity controller design applied to integrated clutch control</i> 131			
G.J.L. Naus	Technische Universiteit Eindhoven		Université catholique de Louvain
R. Huisman	DAF Trucks N.V.		Université catholique de Louvain
M.J.G. van de Molengraft	Technische Universiteit Eindhoven		Massachusetts Institute of Technology
WeE03	Numerical techniques	Impressario zaal	17:00–17:25
Chair: V. Blondel			
		16:35–18:15	
WeE03-1		16:35–17:00	
<i>Symmetric Non-negative Matrix Factorization</i> 132			
N.D. Ho	Université catholique de Louvain		Technische Universiteit Eindhoven
P. Van Dooren	Université catholique de Louvain		Technische Universiteit Eindhoven
WeE03-2		17:25–17:50	
<i>Maximizing Pagerank via outlinks</i> 133			
C. de Kerchove	Université catholique de Louvain		Université catholique de Louvain
L. Ninove	Université catholique de Louvain		Université catholique de Louvain
P. Van Dooren	Université catholique de Louvain		Université catholique de Louvain
WeE03-3		17:50–18:15	
<i>Optimization of the RADICAL contrast for ICA</i> 134			
M. Journée	University of Liege		University of Liege
P.-A. Absil	Université catholique de Louvain		Université catholique de Louvain
R. Sepulchre	University of Liege		University of Liege
WeE04		Western zaal	
		Nonlinear dynamics	
Chair: R. Sepulchre			16:35–18:15
WeE04-1			16:35–17:00
<i>Phase feedback in MEMS resonators</i> 136			
R.M.C. Mestrom	Technische Universiteit Eindhoven		Technische Universiteit Eindhoven
R.H.B. Fey	Technische Universiteit Eindhoven		Technische Universiteit Eindhoven
H. Nijmeijer	Technische Universiteit Eindhoven		Technische Universiteit Eindhoven
WeE04-2			17:00–17:25
<i>Modelling the dynamics of cluster formation</i> 137			
D. Aeyels	Ghent University		Ghent University
F. De Smet	Ghent University		Ghent University
WeE04-3			17:25–17:50
<i>Rigid body attitude synchronization: a consensus approach</i> 138			
A. Sarlette	University of Liege		University of Liege
R. Sepulchre	University of Liege		University of Liege
N. Leonard	Princeton University		Princeton University
WeE04-4			17:50–18:15
<i>Opinion dynamics model: on the 2R conjecture</i> 139			
V.D. Blondel	Université catholique de Louvain		Université catholique de Louvain
J.M. Hendrickx	Université catholique de Louvain		Université catholique de Louvain
J.N. Tsitsiklis	Massachusetts Institute of Technology		Massachusetts Institute of Technology
WeE05		Emanuel zaal	
		Learning 1	
Chair: O. Bosgra			16:35–18:15
WeE05-1			16:35–17:00
<i>Iterative learning control with an identified time-varying robot model</i> 140			
W.B.J. Hakvoort	Netherlands Institute for Metals Research		Netherlands Institute for Metals Research
R.G.K.M. Aarts	University of Twente		University of Twente
J. van Dijk	University of Twente		University of Twente
J.B. Jonker			
WeE05-2			17:00–17:25
<i>Robust Iterative Learning Control</i> 141			
J. van de Wijdeven	Technische Universiteit Eindhoven		Technische Universiteit Eindhoven
O. Bosgra	Technische Universiteit Eindhoven		Technische Universiteit Eindhoven

WeE05-3	17:25–17:50
<i>Reinforcement learning in aerospace control</i> 142	
E. van Kampen	Delft University of Technology
Q.P. Chu	Delft University of Technology
J.A. Mulder	Delft University of Technology
WeE05-4	17:50–18:15
<i>Fuzzy approximation in continuous-space reinforcement learning</i> 143	
L. Busoniu	Delft University of Technology
B. De Schutter	Delft University of Technology
R. Babuska	Delft University of Technology
WeE06	Seaside zaal
Identification of nonlinear systems	
Chair: X. Bombois	16:35–18:15
WeE06-1	16:35–17:00
<i>On the Equivalence between some Block Oriented Nonlinear Models and the Nonlinear Polynomial State Space Model</i> 144	
J. Paduart	Vrije Universiteit Brussel
J. Schoukens	Vrije Universiteit Brussel
L. Gommé	Vrije Universiteit Brussel
WeE06-2	17:00–17:25
<i>Identification of Linear and Nonlinear Systems using Signal Processing Techniques</i> 145	
G. Kerschen	University of Liege
F. Poncelet	University of Liege
J.C. Golinalval	University of Liege
A.F. Vakakis, L.A. Bergman	
WeE06-3	17:25–17:50
<i>Crystal detector as calibration standard for Large Signal Analysis</i> 146	
L. Gommé	Vrije Universiteit Brussel
J. Schoukens	Vrije Universiteit Brussel
Y. Rolain	Vrije Universiteit Brussel
W. Van Moer	
WeE06-4	17:50–18:15
<i>Online identification of a nonlinear battery model for hybrid electrical vehicles</i> 147	
P.J. van Bree	Technische Universiteit Eindhoven
A. Veltman	Technische Universiteit Eindhoven
P.P.J. van den Bosch	Technische Universiteit Eindhoven
W.H.A. Hendrix	

Thursday, March 15, 2007

Plenary Lecture	Les Arcades
Nonlinear Dynamic Optimization in Control Engineering – Algorithms and Applications	
Moritz Diehl	
Chair: J. Swevers	08:30–09:30
Plenary Lecture	Les Arcades
Sampling and Quantization in Modelling and System Identification	
Graham C. Goodwin	
Chair: I. Smets	10:00–11:00
ThM01	Les Arcades
Control applications 6	
Chair: K. Keesman	11:15–12:30
ThM01-1	11:15–11:40
<i>Mathematical performance analysis of a temperature controlled bulk storage room</i> 148	
S. van Mourik	University of Twente
H. Zwart	University of Twente
K. Keesman	Wageningen University
ThM01-2	11:40–12:05
<i>Optimal control design for a solar greenhouse</i> 149	
R.J.C. van Ooteghem	Wageningen University
ThM01-3	12:05–12:30
<i>Control-oriented model of a dwelling coupled to a water-to-water heat pump</i> 150	
R. Lepore	Faculté Polytechnique de Mons
S. Nourricier	Faculté Polytechnique de Mons
F. Renard	Faculté Polytechnique de Mons
H. Diricq, M.-E. Duprez, E. Dumont, C. Renotte, V. Feldheim, M. Frère	
ThM02	Bloemenzaal
Model reduction	
Chair: J. Scherpen	11:15–12:30
ThM02-1	11:15–11:40
<i>An efficient Gaussian proposal in SMC methods</i> 151	
S. Saha	University of Twente
ThM02-2	11:40–12:05
<i>Model Reduction Based On a Cross-Energy Function For Nonlinear Systems</i> 152	
T.C. Ionescu	University of Groningen
J.M.A. Scherpen	University of Groningen
ThM02-3	12:05–12:30
<i>Model Reduction through Proper Orthogonal Decompositions for Multidimensional Systems</i> 153	
F. van Belzen	Technische Universiteit Eindhoven
ThM03	Impressario zaal
MPC 1	
Chair: R. De Keyser	11:15–12:30

ThM03-1	11:15–11:40	ThM05-3	12:05–12:30																																																																																								
<i>Flood prevention combining model predictive control with expert knowledge</i>	<i>154</i>	<i>Automatic classification of primary frequency control behavior</i>	<i>162</i>																																																																																								
T. Barjas Blanco	Katholieke Universiteit Leuven	B. Cornélusse	University of Liege																																																																																								
B. De Moor	Katholieke Universiteit Leuven	C. Wéra	Elia System Operator																																																																																								
P. Willems	Katholieke Universiteit Leuven	L. Wehenkel	University of Liege																																																																																								
J. Berlamont																																																																																											
ThM03-2	11:40–12:05	ThM06	Seaside zaal																																																																																								
<i>Model Based Controllers for a Solar Power Plant</i>	<i>155</i>	State estimation																																																																																									
M. Gálvez-Carrillo	Université Libre de Bruxelles	Chair: O. Bosgra	11:15–12:30																																																																																								
R. De Keyser	Ghent University																																																																																										
C. Ionescu	Ghent University																																																																																										
ThM03-3	12:05–12:30	ThM06-1	11:15–11:40																																																																																								
<i>Multi-Agent Control for Large-Scale Transportation Systems</i>	<i>156</i>	<i>State estimation for distributed control of a semi-active suspension system for a passenger</i>	<i>163</i>																																																																																								
A.N. Tarau	Delft University of Technology	M. Witters	Katholieke Universiteit Leuven																																																																																								
B. De Schutter	Delft University of Technology	J. Swevers	Katholieke Universiteit Leuven																																																																																								
J. Hellendoorn	Delft University of Technology	P. Sas	Katholieke Universiteit Leuven																																																																																								
ThM04	Western zaal	ThM06-2	11:40–12:05																																																																																								
Nonlinear control systems		<i>Interval Estimation with Confidence Degree - Application to AUV Positioning</i>	<i>164</i>																																																																																								
Chair: J. Rogge	11:15–12:30	G. Goffaux	Faculté Polytechnique de Mons																																																																																								
		A. Vande Wouwer	Faculté Polytechnique de Mons																																																																																								
		M. Remy	Faculté Polytechnique de Mons																																																																																								
ThM04-1	11:15–11:40	ThM06-3	12:05–12:30																																																																																								
<i>Modular Reconfigurable Flight Control</i>	<i>157</i>	<i>Constrained estimation with truncated Gaussians</i>	<i>165</i>																																																																																								
E.R. van Oort	Delft University of Technology	D. Verscheure	Katholieke Universiteit Leuven																																																																																								
L. Sonneveldt	Delft University of Technology	J. Swevers	Katholieke Universiteit Leuven																																																																																								
Q.P. Chu	Delft University of Technology	J. De Schutter	Katholieke Universiteit Leuven																																																																																								
J.A. Mulder																																																																																											
ThM04-2	11:40–12:05	ThP01	Les Arcades																																																																																								
<i>Inverse Optimal Nonlinear Adaptive Control Design for a Missile Autopilot</i>	<i>158</i>	Control applications 7																																																																																									
L. Sonneveldt	Delft University of Technology	Chair: J. Anthonis	14:00–15:15																																																																																								
E.R. van Oort	Delft University of Technology	Q.P. Chu	Delft University of Technology			J.A. Mulder				ThM04-3	12:05–12:30	ThP01-1	14:00–14:25	<i>Constrained nonlinear control based on the combination of model predictive control and feedback linearization</i>	<i>159</i>	<i>Data-based velocity observer using encoder time stamping</i>	<i>166</i>	D.A. Joosten	Delft University of Technology	R.J.E. Merry	Technische Universiteit Eindhoven	T.J.J. Lombaerts	Delft University of Technology	M.J.G. van de Molengraft	Technische Universiteit Eindhoven	T.J.J. van den Boom	Delft University of Technology	M. Steinbuch	Technische Universiteit Eindhoven	ThM05	Emanuel zaal	ThP01-2	14:25–14:50	Learning 2		<i>Gain Scheduling Control for a Structural Acoustic Isolation Problem</i>	<i>167</i>	Chair: J. Suykens	11:15–12:30	B. Pajjmans	Katholieke Universiteit Leuven			J. De Caigny	Katholieke Universiteit Leuven			J. Camino	Katholieke Universiteit Leuven			J. Swevers	Katholieke Universiteit Leuven	ThM05-1	11:15–11:40	ThP01-3	14:50–15:15	<i>An Iterative Feedforward Control Design Strategy for SISO Nonlinear Minimum Phase Systems</i>	<i>160</i>	<i>Experimental Stabilization and Tracking of a Nonholonomic Control Moment Gyroscope</i>	<i>168</i>	K. Smolders	Katholieke Universiteit Leuven	J. van de Loo	Technische Universiteit Eindhoven	P. Sas	Katholieke Universiteit Leuven	H. Nijmeijer	Technische Universiteit Eindhoven	J. Swevers	Katholieke Universiteit Leuven	M. Reyhanoglu	Embry-Riddle Aeronautical University	ThM05-2	11:40–12:05	ThP02	Bloemenzaal	<i>Inferring scenario trees for stochastic programming: a machine learning perspective</i>	<i>161</i>	Circuits/Networks		B. Defourny	University of Liege	Chair: J. Suykens	14:00–15:15	R. Sepulchre	University of Liege	L. Wehenkel	University of Liege		
Q.P. Chu	Delft University of Technology																																																																																										
J.A. Mulder																																																																																											
ThM04-3	12:05–12:30	ThP01-1	14:00–14:25																																																																																								
<i>Constrained nonlinear control based on the combination of model predictive control and feedback linearization</i>	<i>159</i>	<i>Data-based velocity observer using encoder time stamping</i>	<i>166</i>																																																																																								
D.A. Joosten	Delft University of Technology	R.J.E. Merry	Technische Universiteit Eindhoven																																																																																								
T.J.J. Lombaerts	Delft University of Technology	M.J.G. van de Molengraft	Technische Universiteit Eindhoven																																																																																								
T.J.J. van den Boom	Delft University of Technology	M. Steinbuch	Technische Universiteit Eindhoven																																																																																								
ThM05	Emanuel zaal	ThP01-2	14:25–14:50																																																																																								
Learning 2		<i>Gain Scheduling Control for a Structural Acoustic Isolation Problem</i>	<i>167</i>																																																																																								
Chair: J. Suykens	11:15–12:30	B. Pajjmans	Katholieke Universiteit Leuven																																																																																								
		J. De Caigny	Katholieke Universiteit Leuven																																																																																								
		J. Camino	Katholieke Universiteit Leuven																																																																																								
		J. Swevers	Katholieke Universiteit Leuven																																																																																								
ThM05-1	11:15–11:40	ThP01-3	14:50–15:15																																																																																								
<i>An Iterative Feedforward Control Design Strategy for SISO Nonlinear Minimum Phase Systems</i>	<i>160</i>	<i>Experimental Stabilization and Tracking of a Nonholonomic Control Moment Gyroscope</i>	<i>168</i>																																																																																								
K. Smolders	Katholieke Universiteit Leuven	J. van de Loo	Technische Universiteit Eindhoven																																																																																								
P. Sas	Katholieke Universiteit Leuven	H. Nijmeijer	Technische Universiteit Eindhoven																																																																																								
J. Swevers	Katholieke Universiteit Leuven	M. Reyhanoglu	Embry-Riddle Aeronautical University																																																																																								
ThM05-2	11:40–12:05	ThP02	Bloemenzaal																																																																																								
<i>Inferring scenario trees for stochastic programming: a machine learning perspective</i>	<i>161</i>	Circuits/Networks																																																																																									
B. Defourny	University of Liege	Chair: J. Suykens	14:00–15:15																																																																																								
R. Sepulchre	University of Liege	L. Wehenkel	University of Liege																																																																																								
L. Wehenkel	University of Liege																																																																																										

ThP02-1	14:00–14:25
<i>Analysis and modelling of analog discrete-time systems using multisine excitations</i>	169
L. Bos	Vrije Universiteit Brussel
G. Vandersteen	Vrije Universiteit Brussel
Y. Rolain	Vrije Universiteit Brussel

ThP02-2	14:25–14:50
<i>Trajectory Piecewise Linear approach for nonlinear differential-algebraic equations</i>	170
T. Voß	University of Groningen

ThP02-3	14:50–15:15
<i>Discrete-time piecewise-affine models of genetic regulatory networks</i>	171
A. Meyroneinc	Centrum voor Wiskunde en Informatica
B. Fernandez	Centre de Physique Théorique
R. Lima	Centre de Physique Théorique
R. Coutinho	

ThP03	Impressario zaal
	MPC 2
Chair: R. De Keyser	14:00–15:15

ThP03-1	14:00–14:25
<i>Control of a Tubular Reactor using POD and MPC</i>	172
O.M. Agudelo	Katholieke Universiteit Leuven
J.J. Espinosa	Universidad Nacional de Colombia
B. De Moor	Katholieke Universiteit Leuven

ThP03-2	14:25–14:50
<i>Nonlinear Model Predictive Control for a DC-DC converter: A NEPSAC approach</i>	173
J. Bonilla	Ghent University
R. De Keyser	Ghent University

ThP03-3	14:50–15:15
<i>Advanced Speed Control for the Air Turbine Motor of the NLR High Temperature Seal Test Rig</i>	174
T.A. ter Meer	National Aerospace Laboratory NLR
J.D. Stigter	Wageningen University

ThP04	Western zaal
	LPV
Chair: K. Smolders	14:00–15:15

ThP04-1	14:00–14:25
<i>Robust performance of self-scheduled LPV control of doubly-fed induction generator in wind energy conversion systems</i>	175
H. Nguyen Tien	Delft University of Technology
C.W. Scherer	Delft University of Technology
J.M.A. Schepen	Delft University of Technology

ThP04-2	14:25–14:50
<i>Modeling and Control for the Air Path System of Diesel Engines by LPV Techniques</i>	176
X. Wei	Delft University of Technology
L. del Re	Johannes Kepler University of Linz

ThP04-3	14:50–15:15
<i>Comparison between gain-scheduling control and LPV control for a pick-and-place machine</i>	177
B. Pajjmans	Flanders' Mechatronic Technology Centre
W. Symens	Flanders' Mechatronic Technology Centre
J. Swevers	Katholieke Universiteit Leuven
H. Van Brussel	

ThP05	Emanuel zaal
	Optimal Control 2
Chair: C. Scherer	14:00–15:15

ThP05-1	14:00–14:25
<i>Time-optimal trajectory generation for industrial manipulators along predefined paths with kinematic constraints</i>	178
N.J.M. van Dijk	Technische Universiteit Eindhoven
N. van de Wouw	Technische Universiteit Eindhoven
W.C.M. Pancras	Bosch
H. Nijmeijer	

ThP05-2	14:25–14:50
<i>Multi-robot exploration: a novel approach</i>	179
J.A. Rogge	Ghent University
D. Aeyels	Ghent University

ThP05-3	14:50–15:15
<i>Continuous state and action space Q-leaning using interval analysis</i>	180
E. de Weerdt	Delft University of Technology
Q.P. Chu	Delft University of Technology
J.A. Mulder	Delft University of Technology

ThP06	Seaside zaal
	Observers
Chair: P. van den Hof	14:00–15:15

ThP06-1	14:00–14:25
<i>A Luenberger observer for an infinite dimensional system with disturbances at the boundary: a UV disinfection example</i>	181
D. Vries	Wageningen University
K.J. Keesman	Wageningen University
H. Zwart	University of Twente

ThP06-2	14:25–14:50
<i>Discrete-Time Interval Observers - Application to Continuous Cultures of Phytoplankton</i>	182
G. Goffaux	Faculté Polytechnique de Mons
A. Vande Wouwer	Faculté Polytechnique de Mons
O. Bernard	INRIA

ThP06-3	14:50–15:15
<i>Distributed Fuzzy Observers</i>	183
Z. Lendek	Delft University of Technology
R. Babuska	Delft University of Technology
B. De Schutter	Delft University of Technology

Les Arcades	
Best Junior Presentation Award ceremony	
Chair: P. van den Hof & J. Van Impe	15.45–16.15

Part 1: Table of Contents 3

Overview of scientific program

Part 2: Contributed Lectures 17

One-page abstracts

Part 3: Plenary Lectures 185

Presentation materials

Part 4: List of Participants 275

Alphabetical list

Part 5: Organizational Comments 277

Comments, overview program, map

Part 2

Contributed Lectures

Velocity control of a 2D dynamic walking robot

G. van Oort
 Impact institute/University of Twente
 g.vanoort@ewi.utwente.nl

S. Stramigioli
 Impact institute/University of Twente
 s.stramigioli@utwente.nl

1 Introduction

In this abstract we introduce velocity control for our 2D dynamic walking robot Dribbel [1] (figure 1) and show that, by ‘closing the loop’, this automatically leads to increased robustness. Takuma and Hosoda [2] also have used active gait adaptation by using step-by-step feedback, but their research was largely based on experimental results, whereas this research is more theoretical.

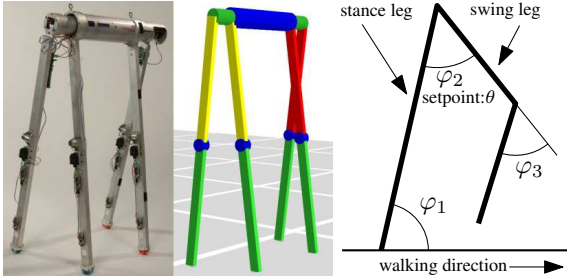


Figure 1: The dynamic walker Dribbel (left), a simulation model (middle) and the degrees of freedom (right). The hip is actuated; the knees are unactuated.

2 The walking algorithm in Dribbel

The control algorithm used in Dribbel and in the corresponding 20-sim simulations is very simple. As soon as the swing foot hits the ground, the (former) stance leg is swung forward. For this movement a very non-stiff P-controller is used in the hip. The setpoint θ can be varied.

For each θ within a certain range, a limit cycle can be found, where the walker has a certain velocity (figure 2). Each limit cycle has a basin of attraction (denoted as $BOA(\theta)$): the set of all states $x = (\varphi_1, \varphi_2, \varphi_3, \dot{\varphi}_1, \dot{\varphi}_2, \dot{\varphi}_3)^T$ for which the walker will converge back to the limit cycle (i.e. it does not fall).

3 Changing velocity

Changing the velocity of the walker can simply be done by changing the setpoint θ to a new value θ_{new} . Given a certain state x of the walker, it is interesting to know which values for θ_{new} can instantaneously be given without making the walker fall. Theoretically, this can be formulated as follows:

$$\text{find the set } \Theta(x) = \{\theta_{new} \in [0, \pi] | x \in BOA(\theta_{new})\} \quad (1)$$

such that, if the walker is in state x , choosing any $\theta_{new} \in \Theta(x)$ will *not* make the walker fall (assuming no more disturbances, of course). Similarly, a $\Theta(x^*)$ can be found for a reduced state $x^* = (\varphi_2, \dot{\varphi}_1)^T$ at the end of the step.

The algorithm for changing velocity now works as follows. If the desired θ_{new} is in $\Theta(x^*)$, directly change the setpoint

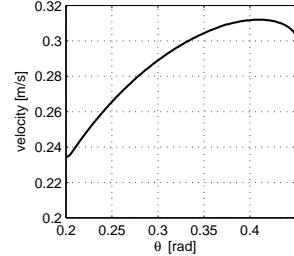


Figure 2: The limit-cycle velocity of the walker for different values of θ . This graph was obtained by simulation.

to the desired value. If not, select a temporary $\theta_{temp} \in \Theta(x^*)$ which is closest to θ_{new} and wait a few steps before changing the setpoint again.

4 Improving robustness

A nice feature of this strategy is that it automatically increases robustness. Assume that a disturbance puts the walker in a state x_{dist}^* . If $x_{dist}^* \in BOA(\theta)$, it is no problem; the walker will automatically converge back to its limit cycle again. If $x_{dist}^* \notin BOA(\theta)$, then, using the same strategy, a temporary $\theta_{temp} \in \Theta(x_{dist}^*)$ can be chosen which is close to the original θ but does not make the walker fall.

5 Implementation in Dribbel

A variant of the algorithm described above has already been implemented in Dribbel. As $\dot{\varphi}_1$ cannot be measured in Dribbel (it lacks angular sensors in the feet), the set Θ is approximated by a range $[\theta_{min}, \theta_{max}]$ which is dependent only on the walking velocity measured during the previous step $v_{last-step} = (2\ell \sin \frac{\varphi_2}{2})/t_{step}$ (note that the step time t_{step} is related to the angular velocity of the stance leg $\dot{\varphi}_1$). Tests showed that with this algorithm it is indeed possible to change the velocity without making the robot fall. Investigating how the robustness is affected is planned for the near future.

Acknowledgements

This research topic was initiated by Ester Guidi, who also implemented the velocity control algorithm in Dribbel. Thanks also to Edwin Dertien for his help on the research.

References

- [1] E. C. Dertien. “Realisation of an energy-efficient walking robot”, Master’s thesis no. 022CE2005, University of Twente, June 2005.
- [2] T. Takuma, K. Hosoda. “Controlling the walking period of a pneumatic muscle walker”, Int. J. Robotic Research, Vol. 25, No. 9, p. 861-866, 2006.

Application of Constraint-Based Task Specification and Estimation for Sensor-Based Robot Systems to a Laser Tracing Task

Tinne De Laet, Wilm Decré, Johan Rutgeerts, Herman Bruyninckx, Joris De Schutter

Dept. of Mechanical Engineering, Katholieke Universiteit Leuven

Celestijnenlaan 300B-3001 Heverlee, Belgium

Email: tinne.delaet@mech.kuleuven.be

1 Introduction

This presentation discusses the application of a generic framework for constraint-based task specification for sensor-based robot systems [1], to a laser tracing example. The work is situated in constraint-based task programming or task function approach [2] where the task is specified by imposing constraints on the modeled relative motions. The proposed approach integrates both task specification and estimation of geometric uncertainty in a unified framework. Major components are (i) the use of feature coordinates, defined with respect to object and feature frames, which facilitate the task specification, and (ii) the introduction of uncertainty coordinates to model geometric uncertainty. Simulations and real world experiments were carried out for the laser tracing example.

2 Method

The laser tracing task is geometrically complex and involves an underconstrained specification as well as estimation of uncertain geometric parameters. The goal is to trace simultaneously a path on a plane as well as on a cylindrical barrel using two lasers which are rigidly attached to the robot end effector as shown in Figure 1. Initially, the position and orientation of the plane and the position of the barrel on the ground are unknown. During task execution, the lasers measure the distance to their associated surface, enabling the on-line estimation of these unknown positions and orientation.

The generic framework introduces additional task related coordinates, denoted as *feature coordinates* χ_f , to facilitate the modeling of constraints and measurements by the user. Furthermore, *uncertainty coordinates* χ_u are introduced which represent modeling errors, uncontrolled degrees of freedom in the robot system or geometric disturbances in the robot environment. These two types of coordinates are defined in *object frames* and *feature frames* that are chosen by the task programmer in a way that simplifies the specification of the task at hand. The choice of the frames is shown in Figure 1. For each of the lasers four frames (plus the world frame) are introduced which form a kinematic chain: $w \rightarrow o1 \rightarrow f1 \rightarrow f2 \rightarrow o2 \rightarrow w$. The six degrees of freedom between $o1$ and $o2$ are distributed over three submotions: the relative motion of (I) $f1$ with respect to $o1$, (II) $f2$ with respect to $f1$, (III) $o2$ with respect to $f2$.

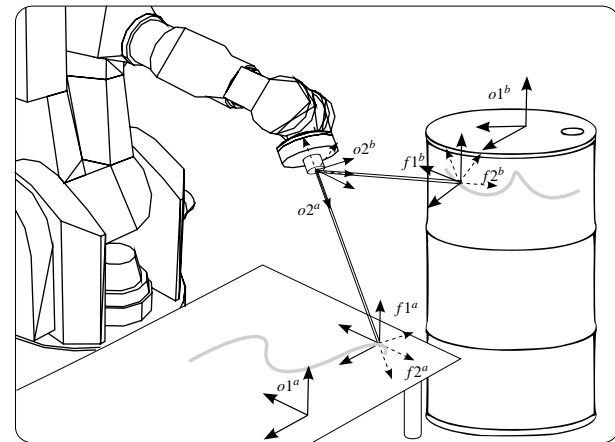


Figure 1: The object (o) and feature frames (f) for simultaneous laser tracing on a plane and a barrel.

The unknown position and orientation of the plane and the position of the barrel are modeled using χ_u coordinates.

3 Conclusion

The application of the framework to the laser tracing task shows that its specification and estimation are greatly simplified by introducing auxiliary feature coordinates. Simulations and experiments for the presented example show the validity and the potential of the approach.

4 Acknowledgements

Tinne De Laet is a Research Assistant of the Research Foundation - Flanders (FWO-Vlaanderen). Wilm Decré's research is funded by a Ph.D. grant of the Institute for the Promotion of Innovation through Science and Technology in Flanders (IWT- Vlaanderen).

References

- [1] J. De Schutter, T. De Laet, J. Rutgeerts, W. Decré, R. Smits, E. Aertbeliën, and H. Bruyninckx. Constraint-based task specification and estimation for sensor-based robot systems in the presence of geometric uncertainty. 2006. Submitted for publication.
- [2] C. Samson, M. Le Borgne, and B. Espiau. *Robot Control, the Task Function Approach*. Clarendon Press, Oxford, England, 1991.

Sensor-Based Control using The Open Robot RealTime Toolkit

Ruben Smits, Herman Bruyninckx

Department of Mechanical Engineering

Katholieke Universiteit Leuven

Celestijnenlaan 300B-3001 Leuven

Belgium

Email: ruben.smits@mech.kuleuven.be

Peter Soetens

Flanders' Mechatronics Technology Centre

Celestijnenlaan 300D-3001 Leuven

Belgium

Email: peter.soetens@fmtc.be

1 Introduction

This work deals with building different sensor-based robotic tasks using generic components using Orocous [2]. The Orocous Project contains three basic C++-libraries. The first and most important library is the RealTime Toolkit (RTT), which allows rapid development of control components guarantying threadsafe data exchange[1] and realtime execution. A second library, the Kinematic and Dynamic Library (KDL), contains kinematic objects and algorithms which can be executed in real-time applications. A third library, the Bayesian Filtering Library (BFL), provides an application independent framework for inference in Dynamic Bayesian Networks, and is used to process sensor information. Figure 1 shows how different components are linked together in a control application. The experimental environment is PC-based with Linux including RTAI and a custom made interface to a industrial robot arm. Four applications will be discussed, joint space control, Cartesian space control, force control and visual servoing in Cartesian space.

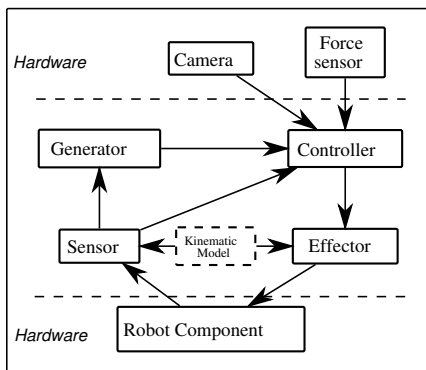


Figure 1: Overview of components for sensor based robot control, the arrows show the data-exchange.

2 Motion control of a 6 dof industrial robot.

2.1 Hardware

This component for hardware robot access supplies data-ports for reading the current joint positions and writing the desired joint velocities in realtime.

2.2 Joint space control

To control the robot in joint space a set of generic components is used. These components can be used for any number of axes and are therefor called nAxes components. Four types of components can be distinguished. The nAxesSen-

sor collects the joint positions from the hardware component. The nAxesGenerators create trajectories for positions and/or velocities. The nAxesControllers control the sensed position or velocity to the desired value in the trajectory. The nAxesEffector sends the output velocities of the controller to the hardware component. These components can be used not only for robots but for any type of machine containing any number of joints.

2.3 Cartesian space control

To control the robot in Cartesian space a kinematic model is needed. Herefor KDL is used. The same kind of components are used as in 2.2. Only now the sensor contains an kinematic algorithm to transform the joint positions to the 6D pose of the robot and the effector contains an algorithm to transform the 6D output velocity of the robot's end effector to the joint velocities.

3 Force control

For force control a hardware component is used to read the force sensor 6D forces in realtime. This force is transformed to the end effector of the robot using KDL. For force control an environment stiffness model is used to transform the force error to a velocity. This velocity in Cartesian space can be used as input for a velocity controller component of 2.3.

4 Visual servoing

For visual servoing a hardware component is used to get the images from the camera. A component containing the visual servoing algorithms is used to calculate a desired velocity in Cartesian space, this velocity can be used as input for a velocity controller in 2.3.

5 Conclusion

The Orocous Project has made it very easy to build different sensor based robot applications without having to rewrite a lot of code. Because all components have build-in XML-configuration and a realtime scripting interface, the same components can be used in different types of applications with different types of hardware.

References

- [1] J. Anderson, S. Ramamurthy, and K. Jeffay. Real-time computing with lock-free shared objects. *Proceedings of the 16th IEEE Real-Time Systems Symposium*, pages 28–37, 1995.
- [2] H. Bruyninckx. Open RObot COntrol Software. <http://www.orocos.org/>, 2001.

Image Based Robotic Apple Harvesting

Kevin Donné, Sven Boedrij, Wim Beckers, Johan Baeten, Eric Claesen
 Katholieke Hogeschool Limburg, Dep. Industriële Wetenschappen en Technologie
 Kevin.Donne@iwt.khlim.be

1 Introduction

The use of robots is no longer strictly limited to industrial environments. Also for outdoor activities, robotic systems are increasingly combined with new technologies to automate labor intensive work, such as e.g. fruit harvesting [1, 2]. This abstract describes the control aspects involved in the feasibility study and the development of an Autonomous Fruit Picking Machine (AFPM)¹.

2 Construction of AFPM

The AFPM is built on a platform mounted behind a agriculture tractor. In order to reduce the development period of the AFPM, although overkill, an industrial (Panasonic) robot is chosen as manipulator. The AFPM further consists of a tractor-driven generator for power supply, a (2D) horizontal stabilization unit, a safety scanning device, a control unit with HMI and a specially for this task designed fruit gripper with a camera mounted in the center of the gripper. The flexible gripper² guarantees a firm grip without damaging the fruit and serves in fact as the mouth of a vacuum cleaner.

Placing the camera in the center of the gripper offers numerous advantages. First of all, the gripper is always in line with the camera and thus with the image, which simplifies the (necessary) coordinate transformation from image to robot. Furthermore, the position of the camera is fully controllable. The camera can always point with its optical axis to the apple. This reduces image distortion and eliminates

the necessity for thorough calibration. A final advantage is that the camera is protected against collisions or bad weather conditions.

3 Control Structure

Figure 1 shows the global set-up and data flow. The autonomous harvesting operation is hierarchically structured. Once the AFPM is stationed in front of the tree, it scans the tree from 40 look-out positions. For each look-out position all detectable apples are listed and picked one by one in a looped task. A picking operation consists of following steps:

- The position of the apple in the image is determined. The actual image processing (including de-clustering) takes about 0.6 seconds.
- The camera rotates in order to point the optical axis straight to the apple.
- While approaching the apple, several images are processed to calculate by triangulation the exact distance to the apple.
- Once the apple is within a given range of the gripper, the vacuum suction is activated.
- The apple is picked by rotating it and tilting it softly and is then put aside.

4 Results and Conclusion

The current set-up ensures an apple picking period of 8 sec. Experiments in the field demonstrate that about 80% of the apples are detected and harvested correctly. The bottleneck in the communication lies in the connection between the PC and the central control unit. Future work will focus on improving the bandwidth of this connection, hereby reducing the picking period to about 5 seconds. In that case the AFPM will perform equivalently to about 6 workers, which makes the machine economically viable.

References

- [1] Peterson D., Bennedsen B., Anger W., Wolford S. "A Systems Approach To Robotic Bulk Harvesting Of Apples", Trans. of the ASAE, VOL. 42(4): pp. 871-876, 1999
- [2] Bulanon D.M., Kataoka T., Okamoto H., Hata S. "Feedback Control of Manipulator Using Machine Vision for Robotic Apple Harvesting" ASAE Paper No. 053114, P1-8, Tampa (USA), 2005

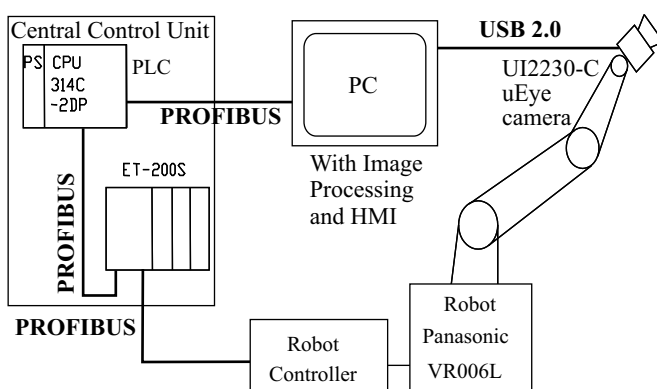


Figure 1: Control structure

Mechatronics and Control for Atomic Force Microscopy at Video-Rate

Georg Schitter
 Delft Center for Systems and Control
 Delft University of Technology
 Mekelweg 2, 2628 CD Delft
 The Netherlands
 Email: g.schitter@tudelft.nl

1 Introduction

The Atomic Force Microscope (AFM) as it has been invented by Binnig, Quate, and Gerber in 1986 [1] has evolved to an advanced instrument for imaging, material characterization and particle manipulation down to the molecular level. Although the AFM already has found a broad range of application in science and industry, AFM operation is still very time consuming (about 1 to 100 minutes per image) and imaging applications are limited to the observation of quasi-static phenomena.

2 Problem Formulation

The main limitation for AFM operation nowadays is the imaging speed [2], where the primary limiting factors are i) the dynamic behavior of the scanning unit, ii) the control bandwidth of the AFM and the speed of the data acquisition (DAQ) system, and iii) the response time of the force sensor. Piezoelectric tube scanners, as they are used in commercial AFM systems, typically have resonance frequencies in the scanning directions at about 1 kHz and in the vertical direction at about 9 kHz.

When the fundamental frequency of the triangular scanning signal is higher than about 1 percent of the scanning unit's lateral resonance frequency, the higher frequency components of the scanning signal excite the dynamics of the scanning unit, resulting in imaging artifacts and distortions of the imaged structure.

The proportional-integral (PI) feedback controller, which is standard in commercial AFMs to control the imaging force, is limited in its bandwidth by the AFM system's dynamics in the vertical direction.

3 Approach

This contribution addresses improvements in performance of a prototype AFM by re-designing the scanning unit, in order to achieve higher resonance frequencies, and by applying better control of the individual positioning axes in order to improve the imaging bandwidth and image quality at high-speed.

Mechanical Design:

High first resonance frequencies can be achieved by combining piezoelectric stack actuators to a three dimensional positioner by means of a flexure mechanism. A recent design [3] of such an implementation has its lowest resonance frequency in the scanning directions at 22 kHz at a positioning range of 13 micrometer. In the vertical direction the first resonance frequency is at 40 kHz with a positioning range of 4.3 micrometer.

Improved Control:

Better control methods allow for compensation of the scanning unit's dynamics and enable scanning at high speed with reduced imaging artifacts and imaging with minimized tip-sample interaction forces. Pre-shaping of the scanning signals minimize ringing of the scanner during high-speed imaging.

This application driven research serves as input for the development of new tools for imaging and particle-manipulation on the nanometer scale and is an important step towards imaging of chemical and biological processes on the molecular level in real-time.

4 Acknowledgements

This work has been supported by SNF-fellowship PA002-108933, by faculty 3mE grant PAL615, by a research agreement with Veeco #SB030071, and by the National Institutes of Health under Award RO1 GM 065354-05.

References

- [1] G.K. Binnig, C.F. Quate, and Ch. Gerber, "Atomic Force Microscope," *Physical Review Letters* 56(9), p. 930-933 (1986).
- [2] P.K. Hansma, G. Schitter, G.E. Fantner, and C. Prater, "High-speed atomic force microscopy," *Science* 314, p. 601-602 (2006).
- [3] G. Schitter, K.J. Åström, B. DeMartini, P.J. Thurner, K. Turner, and P.K. Hansma, "Design and modeling of a high-speed AFM-scanner," *IEEE Transactions on Control Systems Technology*, in press.

Dealing with Flexible Modes in 6 DOFs Robust Control

Tom Oomen and Okko Bosgra

Department of Mechanical Engineering, Technische Universiteit Eindhoven

P.O. Box 513, 5600 MB Eindhoven, The Netherlands

Email: T.A.E.Oomen@tue.nl, O.H.Bosgra@tue.nl

1 Introduction

New trends in lithography for IC production lead to developments in mechatronic stage designs. The trends in lithography are

- new light sources \Rightarrow operation in vacuum
- finer patterns ICs \Rightarrow higher accuracy
- increased throughput \Rightarrow aggressive movements.

In IC production, a wafer stage positions the wafer, containing the to-be-produced ICs, with respect to the imaging optics in all six degrees-of-freedom (DOFs), see Fig. 1. A contactless operation of the wafer stage is desirable both for the vacuum environment and for achieving high accuracy. The need for a gravity compensation in contactless operation and more aggressive movements motivate **lightweight** stage designs.

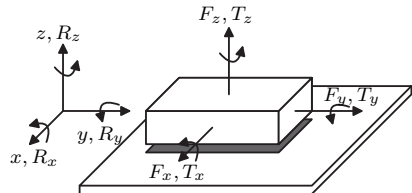


Figure 1: DOFs in a mechatronic stage.

2 Control perspective

A lightweight stage design typically results in a flexible structure. Present state-of-the-art control designs mainly address the rigid-body behaviour. Higher performance can be achieved by explicitly addressing the flexible behaviour of the plant during control design, *e.g.*, compensating the position-dependent behaviour of the structure due to movements, using inferential measurements ($z \neq y$) since the position where performance is desired is not measured, and compensating flexibilities by means of overactuation/oversensing.

3 Hypothesis

High performance flexible stages mainly exhibit linear dynamics due to an almost perfect mechatronic design. At nanometer scale, nonlinear effects will be present throughout the entire actuation chain that are largely reproducible. The flexible behaviour of the plant can be compensated for to a certain limit. In particular, the behaviour of the plant

can only be predicted to a certain extent. In this research, the limits for compensating flexible behaviour are investigated. Additionally, these limits may be relocated by increasing the number of actuators and sensors.

4 Approach

The present research, which is continuously and interactively supported by experimental results, focusses on:

1. *Experimental modeling* of mechanical systems is effective, since the measurements are reproducible, fast, and inexpensive. In a model-based control design approach, compensation of more complex dynamics requires more complex models. Present state-of-the-art tools are mainly restricted to SISO systems. The present research focusses on an experimental and closed-loop relevant identification approach that can reliably handle six degrees-of-freedom with flexibilities. Improving the numerical performance of the algorithms, *e.g.*, by using orthogonal vector polynomials or orthogonal rational functions [1], appears to be key in developing multivariable modeling tools.
2. An *experimental validation* confirms a more complex model indeed is more accurate for the desired task. Furthermore, it reveals the limits of the tools used during experimental modeling and the limit of reproducibility of the system. Similar validation experiments should be performed if position-dependent models are used, *e.g.*, those arising from interpolating several linear models. Additionally, quantification of the remaining uncertainty should be performed by means of an experimental validation-based uncertainty modeling approach.
3. A *robust control* design should be made based upon the nominal model of Step 1 and the uncertainty model of Step 2. The achieved closed-loop performance should again be validated. If the expected performance is not achieved, the nominal model or uncertainty model can be modified. Additionally, a direct controller tuning can be considered. The robust control design should reveal performance limitations due to the presence of both flexibilities and uncertainty.

References

- [1] A. Bultheel, M. Van Barel, P. Van gucht, *Orthogonal basis functions in discrete least-squares rational approximation*, J. Comp. Appl. Math. 164-165:175-197 (2004).

Multivariable Ellipsoidal Unfalsified Control

Jeroen van Helvoort, Bram de Jager and Maarten Steinbuch

Technische Universiteit Eindhoven, Mechanical Engineering, Control Systems Technology

PO Box 513, WH -1.125, 5600 MB Eindhoven, The Netherlands

Email: j.j.m.v.helvoort@tue.nl

1 Data-driven control design

“Find a controller, using only input-output data of the system, i.e., without any plant model.”

As a consequence, the approximations and assumptions introduced in the plant modeling step are avoided.

2 Ellipsoidal Unfalsified Control

The ability of candidate controllers to meet a pre-defined performance requirement is evaluated using measured data only. If the test fails, the controller is removed from the candidate set (ergo, the controller is falsified) [4].

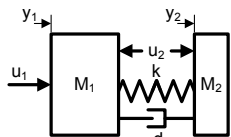
The set of candidate controllers is described by an ellipsoid \mathcal{E} . This continuous set in the controller parameter space contains infinitely many candidate controllers, nonetheless, the ellipsoidal description allows for the simultaneous evaluation of the entire set [1].

New measurement data defines a region \mathcal{U} of controllers that are unfalsified by this data. The set of candidate controllers is updated to reflect this new information. The update is a minimum-volume outer-bounding ellipsoidal approximation of the intersection $\mathcal{E} \cap \mathcal{U}$, which can be computed analytically if the performance requirement is an ℓ_∞ -bound on the tracking error and if the inverse of the controller is affine in the controller parameters [2]. This ellipsoidal approximation is computed for every time step.

3 Multivariable EUC

For a multivariable system, a region \mathcal{U}_i is constructed of controllers that is unfalsified for the i^{th} output with current measurement data. The set of candidate controllers \mathcal{E} is update with a minimum-volume outer-bounding ellipsoidal approximation of $\mathcal{E} \cap \mathcal{U}_i$ for all i outputs sequentially, similar to consecutive time steps. This procedure is repeated for every time-step. As a consequence, with a generalization of the controller structure, full-block multivariable controllers can be designed with the EUC control design framework [3].

4 Example application: Dual stage concept



The dynamics of y_1 and y_2 are highly coupled. The desired closed loop behavior incorporates decoupling and high-

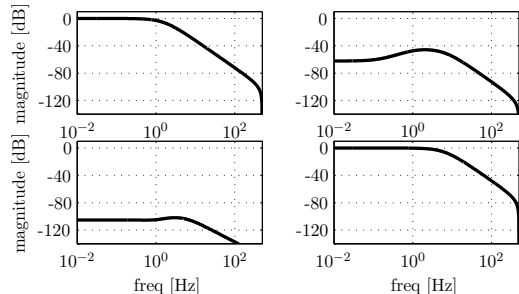
frequency roll-off:

$$G_m(s) = \begin{bmatrix} \frac{10^2}{s^2 + 2 \cdot 10s + 10^2} & 0 \\ 0 & \frac{40^2}{s^2 + 2 \cdot 40s + 40^2} \end{bmatrix}.$$

The trajectory $r(t)$ consists of two asynchronous square waves of amplitude 5 and 1 respectively. An exponential decaying bound is imposed on the tracking error:

$$|G_m(s)r(t) - \underline{y}(t)| \leq \begin{bmatrix} 0.005 + 10e^{-0.15t} \\ 0.0012 + 10e^{-0.2t} \end{bmatrix}.$$

The controllers are synthesized with input-output data only, i.e., without any plant model. However, since in this simulation the plant is known, the closed loop transfers with the controller designed with Multivariable Ellipsoidal Unfalsified Control can be derived:



The diagonal transfers are similar to the reference model $G_m(s)$. Decoupling of the dynamics is achieved of at least 40 dB for $r_2 \rightarrow y_1$, even 100 dB for $r_1 \rightarrow y_2$. The achieved specifications concur with the tracking requirements and the specific trajectories.

References

- [1] F.B. Cabral and M.G. Safonov. Unfalsified model reference adaptive control using the ellipsoid algorithm. *Internat. J. Adapt. Control Signal Process.*, 18(8):683–696, October 2004.
- [2] J.J.M. van Helvoort, B. de Jager, and M. Steinbuch. Unfalsified control using an ellipsoidal unfalsified region applied to a motion system. In *Proc. IFAC World Congress*, Prague, Czech Republic, July 2005.
- [3] J.J.M. van Helvoort, B. de Jager, and M. Steinbuch. Data-driven multivariable controller design using ellipsoidal unfalsified control. In *Proc. Amer. Contr. Conf.*, accepted, New York, July 2007.
- [4] M.G. Safonov and T.-C. Tsao. The unfalsified control concept and learning. *IEEE Trans. Automatic Control*, 42(6):843–847, June 1997.

Linear Control Design of Time-Domain Constrained Systems

Wouter Aangenent, René van de Molengraft, and Maarten Steinbuch
 Control Systems Technology, Technische Universiteit Eindhoven
 Email: w.h.t.m.aangenent@tue.nl

Introduction

The transient response to command or disturbance inputs is an important issue in many control systems. A method to enforce time-domain constraints on the in- and output of a linear control system has recently been proposed in literature, [1]. Here, we present an extension to the method suitable for complex valued closed-loop poles. We consider plants and controllers of the form

$$P(s) = \frac{b(s)}{a(s)}, \quad C(s) = \frac{d(s)}{c(s)}.$$

Method

First, a controller $C_0(s)$ is designed with the pole-placement method. It is well-known that the closed-loop poles are invariant when the Youla-Kučera parameter $q(s)$ is added to the controller

$$C(s) = \frac{d_0(s) + b(s)q(s)}{c_0(s) + a(s)q(s)}.$$

When both real and complex poles are present in the closed-loop transfer function, the systems output is described by

$$y(t) = \sum_{i=0}^{n_r} y_i e^{-p_i t} + \sum_{i=n_r+1}^{n_r+n_c/2+1} \left(a_i 2 \cos(\beta_i t) + b_i 2 \cos(\beta_i t - \frac{1}{2}\pi) \right) e^{-\alpha_i t}$$

where p_i and $\alpha_i + j\beta_i$ are the real and complex poles and y_i, a_i, b_i are corresponding coefficients, depending on $q(s)$. In case the poles are rational valued with least common multiple m , upper and lower bounds are given by

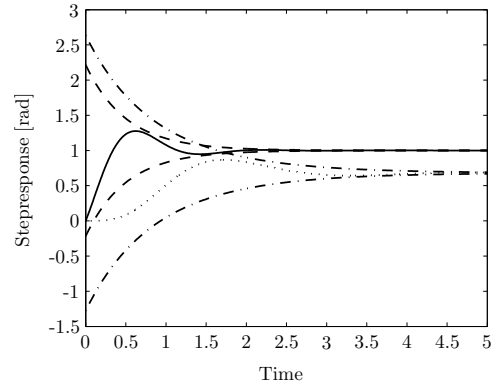
$$y_{\text{upper}}(t) = \sum_{i=0}^{n_r} y_i \lambda^{k_i} + \sum_{i=n_r+1}^{n_r+n_c/2+1} (2|a_i| + 2|b_i|) \lambda^{k_i},$$

$$y_{\text{lower}}(t) = \sum_{i=0}^{n_r} y_i \lambda^{k_i} - \sum_{i=n_r+1}^{n_r+n_c/2+1} (2|a_i| + 2|b_i|) \lambda^{k_i},$$

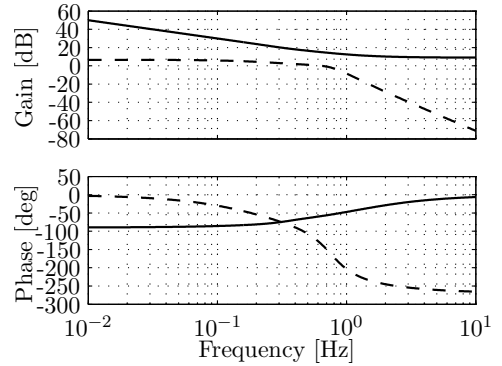
which is a polynomial in $\lambda = e^{-t/m}$. Therefore, bounds on the upper and lower bound can be expressed as positive polynomial constraints. It turns out that such a positive polynomial constraint allows for an LMI formulation, and hence computing coefficients y_i, a_i, b_i and the parameter $q(s)$ resulting in a desired time-domain response is straightforward.

Results

Consider the plant $P(s) = \frac{1}{s+1}$ for which we design the controller $C_0(s)$ such that the assigned closed-loop poles are $p_{1,2} = -1 \pm 2i$, $p_{3,4} = -2 \pm 4i$. The step response (dotted) together with the exponential bounds (dash-dot) are shown in the following figure.



The step response after optimizing the Youla-Kučera parameter is also depicted in the above figure (solid). The Bode diagrams of the corresponding controllers are depicted in the following figure.



While both the original and the new closed-loop systems have the same closed-loop poles, the extra freedom in the form of the Youla-Kučera parameter is used to shape the time-domain response. This approach has also been successfully implemented in an experimental 2-mass-spring setup.

References

[1] D. Henrion, S. Tarbouriech, and V. Kučera, “Control of linear systems subject to time-domain constraints with polynomial pole placement and LMIs”, *IEEE Trans. Autom. Cont.*, Vol. 50, No. 9, pp. 1360-1364, 2005.

Solving control-to-facet problems using output feedback

L.C.G.J.M. Habets

Technische Universiteit Eindhoven

Department of Mathematics and Computer Science

P.O. Box 513, NL-5600 MB Eindhoven

Email: l.c.g.j.m.habets@tue.nl

P.J. Collins

Centrum voor Wiskunde en Informatica

P.O. Box 94079, NL-1090 GB Amsterdam

Email: Pieter.Collins@cwi.nl

J.H. van Schuppen

Centrum voor Wiskunde en Informatica

P.O. Box 94079, NL-1090 GB Amsterdam

Email: J.H.van.Schuppen@cwi.nl

1 Piecewise-affine hybrid systems

In the study of hybrid systems, a specific subclass of so-called *piecewise-affine hybrid systems* plays an important role. These systems consist of an automaton, with at each discrete mode of the automaton an affine system on a polytope, evolving in continuous time. As soon as the continuous state reaches the boundary of the polytope, a discrete event is triggered, and the automaton switches to a new discrete mode. There the continuous state is restarted and will evolve according to the system dynamics of the affine system corresponding to the new discrete mode. In every discrete mode, the dynamics of the corresponding continuous-time affine system, and the polytope on which this system is defined, may be different.

In the literature, several approaches are proposed for the control of piecewise-affine hybrid systems. A popular one is the computational approach developed by Morari and Bemporad, in which the time is discretized, and control problems are formulated as mixed linear integer programming problems. An alternative method, really working in continuous time, has been developed by the authors in several papers ([1], [2], [3], [4]). It is based on a decomposition of the problem into two control problems, one at the continuous and one at the discrete level. In particular it focuses on the question how continuous inputs can be used for influencing the discrete switching behavior of a hybrid system.

2 Control-to-facet problems

In a piecewise-affine hybrid system, the discrete event that is triggered when the continuous state leaves the state polytope depends on the facet through which the polytope is left. So, for controlling the discrete switching using the continuous input, one has to solve the so-called *control-to-facet* problem: find a controller that guarantees that the state of a continuous system leaves the state polytope in finite time, by crossing a specific facet, without crossing other facets first. In [2], [3], necessary and sufficient conditions are obtained for solving this problem by affine state feedback. These con-

ditions are stated as linear inequalities on the input vectors at the vertices of the state polytope. Once a solution to these inequalities is obtained, one tries to realize the corresponding controller by affine state feedback.

3 Output feedback

In this talk, we present a generalization of these results to affine systems on polytopes with partial observations. So we assume that the appropriate inputs at the vertices should be realized by *output feedback*. The application of *static* output feedback leads to an additional coupling condition on the inputs at the vertices. Alternatively, dynamic output may be applied for solving the control-to-facet problem. Finally, also a combination of static and dynamic output feedback will be discussed.

References

- [1] L.C.G.J.M. Habets and J.H. van Schuppen, Control of piecewise-linear hybrid systems on simplices and rectangles. In M.D. Di Benedetto and A. Sangiovanni-Vincentelli, Eds., *Hybrid Systems: Computation and Control*, Lecture Notes in Computer Science, vol. 2034, pp. 261–274. Springer-Verlag, Berlin, 2001.
- [2] L.C.G.J.M. Habets and J.H. van Schuppen, A control problem for affine dynamical systems on a full-dimensional polytope. *Automatica*, vol. 40, pp. 21–35, 2004.
- [3] L.C.G.J.M. Habets, P.J. Collins, and J.H. van Schuppen, Reachability and control synthesis for piecewise-affine hybrid systems on simplices. *IEEE Trans. Aut. Contr.*, vol. 51, pp. 938–948, 2006.
- [4] P. Collins, L. Habets, A. Kuut, M. Nool, M. Petreczky, and J.H. van Schuppen, ConPAHS – A software package for control of piecewise-affine hybrid systems. In *Proc. 2006 IEEE Conf. on Computer Aided Control Systems Design*, Munich, 2006, pp. 76–81.

H_∞ Control for Nonlinear Systems Based on SOS Decomposition

X. Wei

Delft Center for System and Control

Delft University of Technology

Mekelweg 2, 2628 CD Delft, The Netherlands

Email:x.wei@tudelft.nl

M. Verhaegen

Delft Center for System and Control

Delft University of Technology

Mekelweg 2, 2628 CD Delft, The Netherlands

Email:M.Verhaegen@dcsc.tudelft.nl

1 Introduction

The state feedback H_∞ control for nonlinear systems has been extensively studied under state space framework. The L_2 gain can be achieved by solving the so called Hamilton-Jacobi equation or inequality (HJE/HJI)[1]. However, so far there are no efficient algorithms proposed to solve the HJE/HJI's. In this paper, an iterative synthesis algorithm for the state feedback H_∞ control for the underlying systems is proposed based on L_2 gain calculation with the help of the sum of squares (SOS) technique [3, 2].

2 Iterative H_∞ Feedback Controller Design

The system considered in this section is assumed to be of the form

$$\begin{aligned}\dot{x} &= f(x) + g_1(x)w + g_2(x)u \\ y &= h(x)\end{aligned}\quad (1)$$

where $x \in R^n$ is the system state. $u \in R^m$ is the system input. $w \in R^l$ is the exogenous disturbance. The objective is to design a state feedback law u such that the closed loop system is asymptotically stable with a minimum L_2 gain.

Theorem 2.1 Suppose there is a smooth positive semidefinite parameter dependent function $V(x)$ that satisfies

$$V_x f + \frac{1}{2} V_x \left(\frac{1}{\gamma^2} g_1 g_1^T - g_2 g_2^T \right) V_x^T + \frac{1}{2} h h^T \leq 0 \quad (2)$$

for all $x \in R^n$, where $V_x = \frac{\partial V}{\partial x}$, then the system (1) is finite-gain L_2 stable and its L_2 gain less than or equal to γ . Furthermore, $u = -g_2^T V_x^T$ is the controller.

Algorithm 2.2 Step 1: Design a state feedback controller u_0 which stabilizes system (1). With the help of the SOS-TOOLS [4] compute the L_2 gain of the closed loop system

$$\begin{aligned}\dot{x} &= (f(x) + g_2(x)u_0) + g_1(x)\omega \\ y &= h(x)\end{aligned}$$

which satisfies the Hamilton-Jacobi inequality

$$V_x^0 f_0 + \frac{1}{2\gamma_0^2} V_x^0 g_1 g_1^T (V_x^0)^T + \frac{1}{2} h h^T \leq 0$$

where $f_0 = f + g_2 u_0$.

If the L_2 gain is finite ($\gamma_0 < +\infty$) with a positive smooth function $V^0(x)$, go to step 2. Otherwise redesign the initial controller or stop if it is impossible to design such a regulator.

Step 2: Set $u_i = u_{i-1} - g_2^T V_x^{i-1}$ ($i = 1, 2, \dots, n$), calculate the L_2 gain γ_i and V^i which are the solutions of

$$V_x^i f_i + \frac{1}{2\gamma_i^2} V_x^i g_1 g_1^T (V_x^i)^T + \frac{1}{2} h h^T \leq 0$$

where $f_i = f_{i-1} + g_2 u_i$.

Step 3 Check the L_2 gain γ_i and the iteration number i . If γ_i is small enough or the iteration number is larger than the expected value, stop the algorithm. Otherwise, set $i = i + 1$, go to step 2.

3 Simulation Examples

The proposed algorithm is utilized to several nonlinear systems. The initial controller synthesis, the L_2 gain convergence procedure and phase portraits for open and closed loop systems are presented.

References

- [1] A. van der Schaft, “ L_2 -Gain and Passivity Techniques in Nonlinear Control”, Springer, Verlag London, 2000.
- [2] P. A. Parrilo, “Structured Semidefinite Programs and Semialgebraic Problems on Robustness and Optimization”, Ph.D thesis, California Institute of Technology, Pasadena, USA, 2000.
- [3] E. Pampain, “An application of the Sum of Squares Decomposition to the L_2 Gain Computation for a class of nonlinear systems”, Proceedings of 44th IEEE Conference on Decision and Control and the European Control Conference, Seville, Spain, 2005.
- [4] S. Prajna, A. Papachristodoulou, P. Seiler and P. A. Parrilo, “SOSTOOLS: Sum of Squares Optimization Toolbox for Matlab”, <http://www.cds.caltech.edu/sostools>, 2004.

Closed-Loop Oil and Gas Reservoir Management

Sippe G. Douma
 Shell SIEP-EPT - Exploratory Research
 Kesslerpark 1, 2288GS Rijswijk
 Email: sippe.douma@shell.com

Roald Brouwer
 Shell SIEP-EPT - Exploratory Research
 Kesslerpark 1, 2288GS Rijswijk
 Email: roald.brouwer@shell.com

J.D. Jansen
 Dept. of Geotechnology / Exploratory Research
 Delft University of Technology / Shell SIEP-EPT
 Email: j.d.jansen@tudelft.nl / jan-dirk.jansen@shell.com

The oil and gas industry is revealing a tendency to develop so-called "smart fields". A smart field denotes a reservoir with measurement and control facilities. One can think of continuous measurements of pressures and rates and measurements and surface-controlled valves in different segments of the wells deep below the surface. Apart from having the available technical infrastructure much research still is to be done in how to use the measurement and control capabilities to actually enhance the oil and gas recovery. To increase the recovery in a reservoir we aim at a management strategy in which optimal control theory is used to compute the control of valves in oil producers and water or gas injectors that optimizes the production over the life-time of the reservoir. The model used in this optimization is to be updated nearly continuous on the basis of measurements such as production data (rates and pressures) and 4D seismic data. This places the reservoir management in a closed-loop with a near continuous adaptation of control decisions and of the models they are based on. This is sharp contrast with the traditional campaign based reservoir management strategy, in which models are created every five years or so. In [1] the effectiveness of such a closed-loop reservoir management, using an adjoint-based gradient computation for the control strategy and the Ensemble Kalman Filter for updating the model, was successfully demonstrated on small-scale synthetic reservoir models. Since then the methodology is made applicable to realistic, large-scale models by incorporating the adjoint in the reservoir simulator of Shell. Key research issues in control of reservoir models are well location optimization, the effect of constraints during the optimization of valve settings, the balance between long-term and short-time optimization and how to optimize robustly over a set of models. Extensive research is conducted as well in the updating of models on the basis of measurement data, so-called data assimilation (system identification). Numerous techniques are available, such as gradient-based methods, the representer method, Monte Carlo Markov Chain methods, particle filters, the extended Kalman and the Ensemble Kalman Filter. While all methods have their specific issues, they all have to deal with the problems inherent to oil reservoirs. Reservoir models typically have gridblock sizes

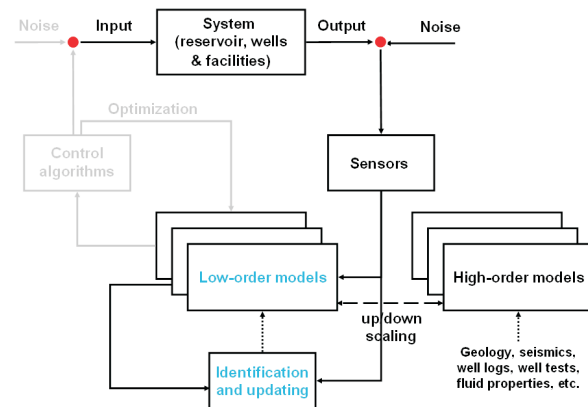


Figure 1: Closed-loop oil and gas reservoir management

ranging between $1e4$ and $1e7$ with in each gridblock two states and around four parameters to be estimated. Regularization of the estimation problem is clearly a key issue. Moreover, issues like decision-relevant modeling, controllability and observability are very crucial, though commonly not considered, in the context of reservoir management. A number of these issues and some solutions will be presented in this talk.

References

[1] Brouwer, D.R., Naevdal, G., Jansen J.D., Vefring E. and Van Kruijsdijk, C.P.W.J., "Improved reservoir management through optimal control and continuous model updating", paper SPE 90149 presented at the SPE Annual Technical Conference and Exhibition, Houston, USA (2004) September.

Real-Time Estimation of Well Inflow Parameters Using Only Pressure and Temperature Measurements

Martijn Leskens

Department of Process Modelling and Control, TNO Science and Industry
De Rondom 1, 5612 AP Eindhoven, The Netherlands
Email: martijn.leskens@tno.nl

Stefan Belfroid

Department of Flow and Structural Dynamics, TNO Science and Industry
Stieltjesweg 1, 2628 CK Delft, The Netherlands
Email: stefan.belfroid@tno.nl

Abstract

Motivated by the growing discrepancy between demand for and availability of oil and gas and by the increased availability of downhole measurement and control equipment, the upstream oil and gas industry has recently embraced the "smart wells" philosophy. The main idea of this philosophy can be stated as the improvement of current reservoir management by extending and improving current reservoir and well monitoring and control practice. By doing so, one aims at a higher yield from a given reservoir, on the short-term and/or on the long-term, while simultaneously fulfilling production constraints.

One main "smart wells" element is monitoring of downhole reservoir and well flow parameters. Here, the aim is to estimate variables that are not measured, either because that is impossible or because that is too expensive, via a model of the well and reservoir and via quantities that *are* measured. The resulting information, c.q. estimated quantities, is then used to improve well and reservoir management by feeding it either to the well operator or to a controller. Many "smart wells" monitoring (also referred to as data assimilation, soft sensing and many other names) applications focus on estimating reservoir properties, such as permeability, via the Ensemble Kalman Filter [1], one of several nonlinear extensions of the famous (linear) Kalman filter [2]: see e.g. [3]. Other applications are more focused on well monitoring and involve e.g. gas-lifting [4]. Another line that is followed uses empirical (blackbox) models as e.g. the Shell Field-Ware Production Universe tool [5].

Here, a monitoring tool is discussed for real-time estimation of downhole *well* inflow parameters, more specific of gas, water and liquid fraction and flow at some inflow point of the well. From an economic point of view, a particularly interesting such real-time estimator (RTE) is one that uses down-hole pressure and temperature measurements only as these are (relatively) cheaply available. Such a commercially attractive RTE of well inflow parameters is presented here and, by means of simulation results, shown to work well at least under the condition of no plant-model mismatch and under

both normal well operating conditions and when gas or water breakthrough occurs. The RTE is an extended Kalman filter [6] using a specific cheap Jacobian approximation to reduce the computation time to below the imposed sample time. It employs a rigorous (first-principles) dynamic well model using a two-phase drift-flux formulation [7] to account for slip between gas and liquid. Specific attention is given to modelling of the well and to the cheap Jacobian approximation.

The results discussed here have been obtained as part of an ongoing research project within the field of "smart wells" denoted as ISAPP (Integrated System Approach Petroleum Production), which is a joint research project of Shell, TNO and the Delft University of Technology.

References

- [1] G. Evensen. "The Ensemble Kalman Filter: theoretical formulation and practical implementation", *Ocean Dynamics* 53, pp. 343-367, 2003.
- [2] R.E. Kalman. "A New Approach to Linear Filtering and Prediction Problems". *Trans. ASME, Journal of Basic Engineering*, Vol. 82 (Series D), pp. 35-45, 1960.
- [3] G. Nævdal, L.M. Johnsen, S.I. Aanonsen and E.H. Vefring. "Reservoir Monitoring and Continuous Model Updating Using Ensemble Kalman Filter", *SPE paper 84372*, 2003.
- [4] H.H.J. Bloemen, S.P.C. Belfroid, W.L. Sturm and F.J.P.C.M.G. Verhelst. "Soft Sensing for Gas-Lift Wells", *SPE paper 90370*, 2004.
- [5] R. Cramer, C. Moncur and L. Berendschot. "Well-Test Optimization and Automation", *SPE paper 99971*, 2006.
- [6] A.H. Jazwinski. "Stochastic Processes and Filtering Theory", Academic Press, 1970.
- [7] J.P. Brill and H. Mukherjee. "Multiphase Flow in Wells", *SPE Monograph Vol. 17*, 1999.

Parameterization of reservoir properties for closed-loop reservoir management

Jorn van Doren

Delft Center for Systems and Control
Delft University of Technology
Mekelweg 2, 2628 CD Delft
Email: j.f.m.vandoren@tudelft.nl

P.M.J. Van den Hof and O.H. Bosgra
Delft Center for Systems and Control
Delft University of Technology
Mekelweg 2, 2628 CD Delft

Maarten Zandvliet

Delft Center for Systems and Control
Delft University of Technology
Mekelweg 2, 2628 CD Delft
Email: m.j.zandvliet@tudelft.nl

J.D. Jansen

Dept. of Geotechnology
Delft University of Technology
Mijnbouwstraat 120, 2628 RX Delft

1 Introduction

An important goal of oil companies is to maximize oil recovery over the entire life of the reservoir. One way to achieve this goal is to inject water into the reservoir via injection wells, such that the water displaces the oil to the production wells. Optimal control theory can be applied to calculate optimal well locations and optimal dynamic production and injection rates that maximize recovery [1]. This methodology needs an accurate description of the fluid flows in the reservoir. Therefore a reservoir model is built describing the physics in the reservoir. The resulting model is large-scale ($10^5 - 10^6$ states), nonlinear, discretized in time and space, and uncertain in the parameters and initial condition. Uncertainty in the model arises from the lack of information and from uncertain data sources. Due to uncertainty in the model the predicted flows and, more importantly, the resulting control strategy are prone to errors.

2 Reparameterization

Dynamic reservoir models are usually overparameterized. The discretized reservoir models can easily contain 100.000 grid blocks, where each grid block has states x and parameters θ like permeability and porosity. However, earlier work indicated that the dynamics of the reservoir flow is governed by a much smaller number of (transformed) state variables, and that therefore also the number of relevant parameters is much smaller [2]. The amount of pressure measurements that can be used to estimate the parameters is also limited and normally insufficient to estimate the parameters uniquely. This means that the parameter estimation problem is ill-posed. The parameter estimation problem is

$$\hat{\theta} := \arg \min_{\theta \in \mathbb{R}^n} V(\theta, \bar{y}), \quad (1)$$

where V is a cost function that minimizes the squared difference between the measurements \bar{y} taken from the real system and the outputs y of the model, and $\hat{\theta} \in \mathbb{R}^n$ the estimated pa-

rameter. The optimal control problem, as mentioned in the introduction, is

$$\hat{u} := \arg \max_{u \in \mathbb{R}^p} J(u, \hat{\theta}, \hat{x}_0), \quad (2)$$

where J is an economic goal function, $\hat{\theta}$ again the estimated parameter, \hat{x}_0 the initial condition (assumed as known), and \hat{u} the control calculated based on the estimated parameter. To resolve the non-uniqueness issue a parameterization matrix $\theta = P\alpha$ is introduced, where $\alpha \in \mathbb{R}^m$, $m \ll n$. The new parameter estimation problem is now defined as

$$\hat{\alpha} := \arg \min_{\alpha \in \mathbb{R}^m} V(P\alpha, \bar{y}). \quad (3)$$

The idea is to parameterize only the reservoir properties that are connected to observable and controllable states. As a first step a one-phase flow model is analyzed, which has the advantage that it is linear. The model is spatially discretized into 10x10 grid blocks and contains 2 wells. Both wells can observe pressure in the well and can inject or produce. When the observability and controllability matrix is calculated and its singular vectors are projected on the reservoir simulation grid, it can be seen that only the grid blocks near production and injection wells are observable and controllable. On the basis of several cases the connection between the parameter field and the observability and controllability of the states is shown.

References

- [1] Brouwer, D.R., Naevdal, G., Jansen, J.D., Vefring, E. and van Kruijsdijk, C.P.J.W.: "Improved reservoir management through optimal control and continuous model updating", SPE ATCE, Houston, USA (2004).
- [2] Heijn, T, Markovic, R., Jansen, J.D.: "Generation of low-order reservoir models using system-theoretical concepts", SPE Journal, June, (2004), 202-218.

Adjoint-Based Well Placement Optimization Under Production Constraints

Martijn Handels^a

m.handels@student.tudelft.nl

Jan Dirk Jansen^{a,c}

j.d.jansen@citg.tudelft.nl

Maarten Zandvliet^b

m.j.zandvliet@tudelft.nl

Roald Brouwer^c

roald.brouwer@shell.com

^a Department of Geotechnology, TU Delft.

^b Delft Center for Systems and Control, TU Delft.

^c Shell International Exploration and Production.

1 Abstract

This following is an excerpt from [1].

Determining the optimal location of wells with the aid of an automated search algorithm can significantly increase a project's Net Present Value (NPV) as modeled in a reservoir simulator. This paper has two main contributions: first to determine the effect of production constraints on optimal well locations, and second to determine optimal well locations using a gradient-based optimization method. Our approach is based on the concept of surrounding the wells whose locations have to be optimized by so-called pseudo-wells. These pseudo-wells produce or inject at a very low rate, and thus have a negligible influence on the overall flow throughout the reservoir. The gradients of NPV over the lifespan of the reservoir with respect to flow rates in pseudo-wells are computed using an adjoint model. These are subsequently used to approximate 'improving directions', *i.e.* directions in which to move the wells to achieve an increased NPV, based on which improving well positions can be determined. The main advantage over previous approaches, such as finite difference or stochastic perturbation methods, is that the method computes improving directions for all wells in only one forward and one backward (adjoint) simulation. The process is repeated until no further improvements are obtained.

2 Example

The method is illustrated by two waterflooding examples. In the first the location of a single injector is optimized to maximize NPV. Starting from four different initial injector locations the algorithm converges to four similar local optima. The second example involves optimization of the locations of 9 producers and 4 injectors in a heterogeneous field whose permeability is given in Figure 1. Starting from two different initial well configurations we obtain nearly the same (local) optimal value for NPV - see Figures 2 and 3.

References

[1] M.Handels, M.J. Zandvliet, D.R. Brouwer, and J.D. Jansen, "Adjoint-Based Well Placement Optimization Under Production Constraints", paper SPE 105797 presented at the 2007 SPE Reservoir Simulation Symposium, Houston.

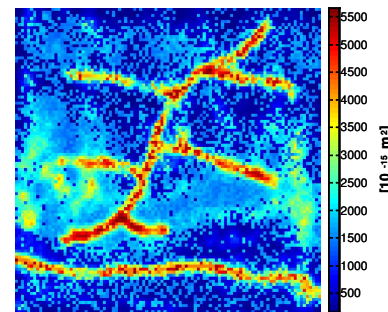


Figure 1: Absolute permeability field.

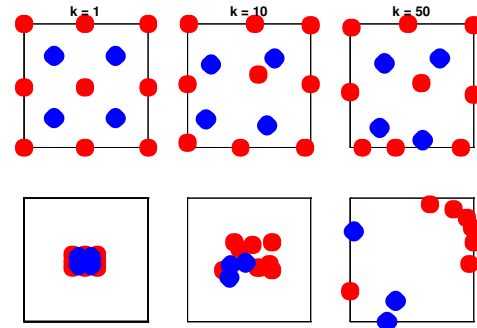


Figure 2: Well optimization path for standard initial pattern (top) and 'mini' initial pattern (bottom), with 9 producers (blue) and 4 injectors (red).

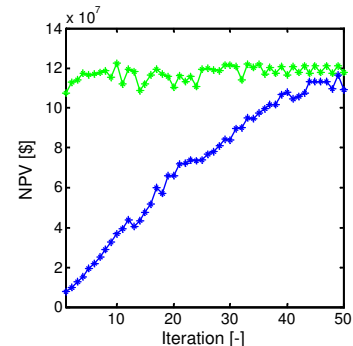


Figure 3: NPV per iteration for standard initial pattern (green) and 'mini' initial pattern (blue).

A hierarchical system approach toward improved oil reservoir management

G.M. van Essen, O.H. Bosgra

P.M.J. Van den Hof

Delft Center for Systems & Control

Delft University of Technology

Mekelweg 2, 2628 CD Delft

The Netherlands

Email: g.m.vanessen@tudelft.nl

J.D. Jansen

Department of Geotechnology

Delft University of Technology/

Shell Int. Exploration & Production

Mijnbouwstraat 120, 2628 RX Delft

The Netherlands

Email: j.d.jansen@citg.tudelft.nl

1 Introduction

Over the recent years a variety of new developments have been introduced within the field of oil recovery, with the aim to maximize production of oil and gas from petroleum reservoirs. One of these new developments is the introduction of so-called "smart wells", which are equipped with control valves to actively control the oil production. Recent studies have shown that the optimal operational strategy of these control valves can be found using a dynamic optimization procedure [1]. Generally, the objective in these optimization studies is to maximize ultimate oil recovery from the entire reservoir over its life-cycle, using reservoir models that describe the dynamic behavior of the reservoir over large time and spatial scales. The daily operation of the wells in the reservoir is driven by much faster dynamic processes, which occur in or near the well. However, to really maximize value of an oil field, economic optimization over all relevant time and spatial scales over the full life cycle is required. This work discusses the main obstacles and proposed methodology to come to an hierarchical system approach. The goal of this approach is to make the multi-scale optimization of oil recovery possible.

2 Main Obstacles

The dynamic processes that determine the daily production strategy are different from those determining the reservoir depletion strategy. The main dynamic processes in well operations involve the pressure drop and flow regime inside the well and the occurrence of fracturing of reservoir rock and gas coning near the well. On a reservoir scale the main dynamic processes involve the flow of oil, water and gas through the porous and (strongly) heterogeneous reservoir rock proportional to a pressure gradient. Besides these differences in the dominant dynamic processes, daily operation of wells is usually driven by different objectives. On a reservoir scale the objective is usually to maximize the total (cumulative) oil recovery from the reservoir. Wells however are generally operated such that the production rate is maximized. These objective do not necessarily contradict each other, but in many cases they cannot be met simultaneously.

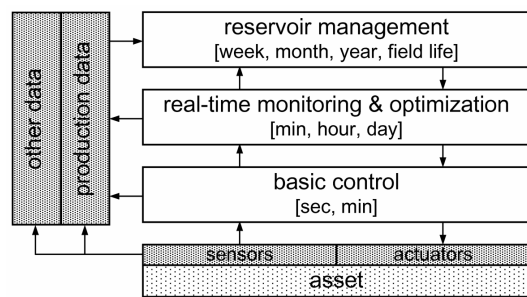


Figure 1: Proposed hierarchical model structure for reservoir management with 3 levels of control.

3 Proposed Methodology

The dynamic models used on a reservoir scale or not able to (accurately) capture the dynamics that occur in and near the wells and vice versa. A direct coupling of the dynamic models is a possible approach. However, capturing the fast dynamics would require a short time leading to (impractical) long computation time to perform just one simulation run over the entire life of the reservoir. The subdivision in multiple hierarchical layers of control, where the fast dynamics are controlled by the lower levels and the slow dynamics by the upper layers is also encountered in the process industry. Nikolaou *et.al.* describe such a hierarchical model structure for reservoir management with 5 levels of control. The structure proposed in this work creates a subdivision into 3 levels, as depicted in Figure 1. The subdivision into 3 levels is based in the current level of control and models used, and the notion that the number of levels should be confined.

References

- [1] D.R. Brouwer and J.D. Jansen, Dynamic optimization of water flooding with smart wells using optimal control theory, *SPE journal*, vol. 9, 2004, pp 391-402.
- [2] M. Nikolaou, A.S. Cullick, L. Saputelli, G. Mijares, S. Sankaran and L. Reis, A Consistent Approach Toward Reservoir Simulation at Different Time Scales, *Proceedings of the 2006 SPE Intelligent Energy Conference and Exhibition*, Amsterdam, The Netherlands, April 11-13, 2006.

(In)equivalence of Discrete Time LPV State-Space and Input/Output Representations

R. Tóth¹, P. S. C. Heuberger¹, F. Felici, and P. M. J. Van den Hof
 Delft Center for Systems and Control (DCSC)
 Delft University of Technology
 Mekelweg 2, 2628 CD Delft, The Netherlands
 email: r.toth@tudelft.nl

1 Introduction

In the past 15 years, significant research has been carried out on *Linear Parameter Varying* (LPV) systems due to the increasing demand of the industry for accurate control of nonlinear systems [2]. The reason of this enormous interest roots in the fact that the LPV framework provides a well applicable alternative to model mildly nonlinear systems or position dependent dynamics, in particular found in servomechanical applications. Moreover, by extending the results of *Linear Time Invariant* (LTI) control & system theory, recently powerful LPV control design methods have appeared through optimal control and gain scheduling control, delivering high performance and robust control solutions for several application fields ranging from aerospace to consumer electronics. Beside the progress in LPV control, also several LPV identification methods were proposed to supply control design with accurate and applicable models. However, in general these methods lack in efficiency, due to the problem of choosing appropriate LPV model structures.

2 Problem of I/O and SS representations

In the LTI case, it is well-known that for any I/O model, there exists an equivalent *State-Space* (SS) based model and vice versa. Similarly, LPV system models are also described in either a SS or an I/O representation, where the parameters are smooth and continuous functions of a time varying *scheduling parameter* vector $p(k) : \mathbb{Z} \rightarrow \mathbb{P}$, with \mathbb{P} a compact set denoting the *scheduling parameter domain*. The well known equivalence of such representations in the LTI case may be the reason why in the LPV framework often no care is taken about the domain (i.e. the state space or the I/O operator domain) where the actual system is represented or identified. However, it can be shown that model representations in the two domains with static dependence (dependence without memory) on $p(k)$ have *distinct* equivalence classes due to differences in time propagation of $p(k)$ [4]. Nevertheless, in the LPV framework the models are almost entirely considered with static dependence on $p(k)$. As a result, the inequivalence of the representations causes misuse and confusion among many authors in the literature, for

instance in [1], [3]. For details see [4].

3 Re-establishment of equivalence classes

By studying the effects causing the inequivalence and by introducing canonical forms for LPV-SS realizations, similar to the *Linear Time Varying* (LTV) framework, exact formulas for the connection between I/O and SS based LPV models can be derived. Then, equivalence classes are re-established by recasting general LPV systems to have affine dependency on an extended scheduling parameter, incorporating the required dynamic dependence (dependence with memory) of the equivalent models.

4 Consequences for LPV system identification

The inequivalence of LPV-I/O and LPV-SS models with static dependence on p has major consequences. As the introduced equivalence transformation can alter the causality of the model and increase its complexity, it is necessary to guarantee that the physical system is identified in its ‘natural’ domain. Furthermore, as today’s identification methods can only handle static dependency on p , either a separation of I/O or SS identifiable systems is needed or the methods have to be extended to handle dynamic dependence over p .

References

- [1] B. Bamieh and L. Giarré. Identification of linear parameter varying models. *Int. Journal of Robust and Nonlinear Control*, 12:841–853, 2002.
- [2] W. Rugh and J. Shamma. Research on gain scheduling. *Automatica*, 36(10):1401–1425, 2000.
- [3] M. Steinbuch, R. van de Molengraft, and A. van der Voort. Experimental modelling and LPV control of a motion system. In *Proc. of the American Control Conf.*, pages 1374–1379, Denver, CO, 2003.
- [4] R. Tóth, F. Felici, P. S. C. Heuberger, and P. M. J. Van den Hof. Discrete time LPV I/O and state space representations, differences of behavior and pitfalls of interpolation. *Submitted to the European Control Conf.*, 2007.

¹Support by the Netherlands Organization for Scientific Research (NWO) is gratefully acknowledged.

Reachability analysis and verification of hybrid systems using Ariadne

Alberto Casagrande

Department of Mathematics and Computer Science
 University of Udine
 Via delle Scienze 206
 33100 Udine, Italy
 casagrande@dimi.uniud.it

Pieter Collins

Centrum voor Wiskunde en Informatica
 Kruislaan 413, Postbus 94079
 1090 GB Amsterdam, The Netherlands
 Pieter.Collins@cwi.nl

Tiziano Villa

Department of Computer Science
 University of Verona
 Ca' Vignal 2 - strada le Grazie 15
 37134 Verona, Italy
 tiziano.villa@univr.it

The reachability problem for hybrid systems

Hybrid systems [1] are systems comprising both discrete and continuous dynamics, such as a physical plant controlled by a digital controller. Hybrid systems exhibit considerably more complexity than systems operating in discrete-time or continuous-time.

The *reachable set* of a hybrid system is the set of all points reachable by a trajectory of the system starting from a set of initial states. Computation of the reachable set is important for the verification of safety properties, such as proving that the state remains in a set of safe states.

The semantics used to define the trajectories of a hybrid system is of critical importance in determining the computability of convergent approximations, since hybrid systems exhibit discontinuous dependence on initial conditions over finite time intervals [2]. Further, the best possible computable over-approximation to the reachable set is the *chain-reachable set*, which may be much larger. However, even for nonlinear hybrid systems, it is possible to compute rigorous over-approximations to the chain-reachable set, and hence verify safety.

Computation of reachable sets using ARIADNE

ARIADNE [3] is a general-purpose open-source tool for computing properties of dynamic systems, including hybrid systems. General nonlinear systems are supported, and specialised techniques are available for certain classes of systems, such as piecewise-affine systems. The computational kernel of ARIADNE includes a *geometry module* for operating on sets of points, a *system module* for describing discrete, continuous and hybrid systems, and an *evaluation module* for solving equations, applying transformations, and integrating flows. The computational kernel is supported

by an *input module* and an *output module*. The package is written in C++ using a modular approach to facilitate third-party extinctions. A Python interface is provided and a Java/MATLAB interface is also planned.

ARIADNE supports rigorous numerical computations by implementing fundamental operations such as union and intersection of sets, evaluation of continuous functions, and integration of vector fields. These operations are implemented exactly for basic types such as rectangles, polyhedra, grid-based sets and affine maps, and as over/under approximations for more general types. Other operations, such as computing the chain-reachable set of a hybrid system, may be implemented by combining the fundamental operations.

We illustrate the use of ARIADNE on benchmark problems in automotive control and electrical power systems. These examples exhibit many of the technical challenges arising in the analysis of hybrid systems. Further optimisations to the code are required to make the package suitable for the analysis of more realistic examples.

References

- [1] Arjan van der Schaft and Hans Schumacher. *An introduction to hybrid dynamical systems*. Springer, 2000.
- [2] Pieter Collins and John Lygeros. “Computability of finite-time reachable sets for hybrid systems.” In *Proceedings of the 44th IEEE Conference on Decision and Control*, 2005.
- [3] Andrea Balluchi, Alberto Casagrande, Pieter Collins, Alberto Ferrari, Tiziano Villa, and Alberto L. Sangiovanni-Vincentelli. “Ariadne: a framework for reachability analysis of hybrid automata.” In *Proceedings of the 17th International Symposium on the Mathematical Theory of Networks and Systems*, 2006.

On a balanced canonical form for continuous-time lossless systems

Ralf Peeters
 Mathematics Department
 Universiteit Maastricht
 PO Box 616, 6200 MD Maastricht, The Netherlands
 Email: ralf.peeters@math.unimaas.nl

Bernard Hanzon
 School of Mathematical Sciences
 University College Cork
 Cork, Ireland
 Email: b.hanzon@ucc.ie

Martine Olivi
 INRIA Sophia-Antipolis
 BP 93, 06902 Sophia-Antipolis Cedex, France
 Email: olivi@sophia.inria.fr

1 Introduction

There is a rich literature on the construction of canonical forms for various classes of linear systems. It may be noticed that for balanced state-space canonical forms, the class of *lossless systems* lies at the heart of many such constructions ([8], [5]). Lossless systems are important in their own right too because of their usefulness for several other purposes: (i) to study H_2 -model approximation problems; (ii) to perform system identification by the method of separable least squares (see [2]) using output normal forms; (iii) to generate polyphase representations of orthogonal filter banks when implementing orthogonal wavelet decomposition schemes.

2 Balanced canonical forms for lossless systems

In the *continuous-time* case, a balanced canonical form for lossless systems was first presented in the work of Ober ([6], [7]). This form has a tridiagonal dynamical matrix A and the useful property that the corresponding controllability matrix K is upper triangular. To deal with the *discrete-time* case one may apply the bilinear transform, which preserves balancedness but destroys upper triangularity of K . In [3] another balanced canonical form for discrete-time lossless systems was developed directly starting from upper triangularity of K . This canonical form is conveniently parameterized with Schur parameters. In [4] this result is generalized to the multivariable case by exploiting the connection with the tangential Schur algorithm. In the discrete-time setting, the construction of such balanced canonical forms is achieved in a recursive way with unitary matrix multiplications. Each step of the recursion involves an interpolation condition at a point located either inside or outside the unit circle.

To transfer these discrete-time results back to continuous-time, the bilinear transform can again be used. As a result, unitary matrix multiplications are replaced by more general linear fractional transformations. However, it can be established that the original balanced canonical form of Ober is *not* recovered in this way.

3 Results

In the present paper we note that the canonical form of Ober involves interpolation conditions *at infinity*. We extend the work of [4] on discrete-time lossless systems to allow for interpolation conditions *on the unit circle*, using results from interpolation theory ([1]). Then the bilinear transform allows us to deal with interpolation conditions at infinity for continuous-time systems. By making appropriate choices for these conditions, we show how the balanced state-space canonical form of Ober can now be recovered. The multivariable case can be treated analogously.

References

- [1] J.A. Ball, I. Gohberg, L. Rodman, Interpolation of rational matrix functions, *Oper. Th.: Adv. Appl.*, **45**, Birkhäuser, 1990.
- [2] J. Bruls, C.T. Chou, B.R.J. Haverkamp, M. Verhaegen, Linear and non-linear system identification using separable least-squares, *Eur. J. Contr.*, **5**, 116–128, 1999.
- [3] B. Hanzon, R.L.M. Peeters, Balanced Parametrizations of Stable SISO All-Pass Systems in Discrete-Time, *MCSS*, **13**, 240–276, 2000.
- [4] B. Hanzon, M. Olivi, R.L.M. Peeters, Balanced realizations of discrete-time stable all-pass systems and the tangential Schur algorithm, *Lin. Alg. Appl.*, **418**, 793–820, 2006.
- [5] B. Hanzon, R.J. Ober, Overlapping block-balanced canonical forms for various classes of linear systems, *Lin. Alg. Appl.*, **281**, 171–225, 1998.
- [6] R.J. Ober, Balanced realizations: canonical form, parametrization, model reduction, *Int. J. Contr.*, **46**, 643–670, 1987.
- [7] R.J. Ober, Asymptotically stable allpass transfer functions: canonical form, parametrization and realization, *Proc. of the IFAC World Congress*, Munich, 1987.
- [8] R.J. Ober, Balanced parametrization of classes of linear systems, *SIAM J. Control Optim.*, **29**, 1251–1287, 1991.

Matrix Factorization and Stochastic State Representations

Bart Vanluyten Jan C. Willems Bart De Moor

Department of Electrical Engineering (ESAT), Katholieke Universiteit Leuven

Email: {bart.vanluyten, jan.willems, bart.demoor}@esat.kuleuven.be

1 Introduction

In this presentation we consider a problem which is related to the hidden Markov realization problem [1]. Given two random variables y^- and y^+ which both take values from the finite set \mathbb{Y} with probability measure $P(y^-, y^+)$, find two random variables x^- and x^+ both with values from a finite set \mathbb{X} , with $|\mathbb{X}|$ as small as possible, such that

$$P(y^-, y^+ | x^-, x^+) = P(y^- | x^-)P(y^+ | x^+),$$

and $P(y^+ | x^+) = P(y^- | x^-)$.

This problem is related to the realization problem for finite valued processes of length 2. Indeed, let $y = y(1), y(2)$ be a two-point process which is the output of a hidden Markov model, and take $y^- = y(1)$ and $y^+ = y(2)$ then the random variables x^- and x^+ can be interpreted as underlying state variables $x(1)$ and $x(2)$ respectively.

2 Hidden Markov Models (HMMs)

A finite valued process y can be represented by a HMM which assumes an underlying state process x taking values from the finite set \mathbb{X} . A Moore HMM is defined as $(\mathbb{X}, \mathbb{Y}, \Pi_{\mathbb{X}}, \beta, \pi(1))$, where

- \mathbb{X} with $|\mathbb{X}| < \infty$ is the state alphabet, and \mathbb{Y} is the output alphabet;
- $\Pi_{\mathbb{X}}$ is a matrix in $\mathbb{R}_+^{|\mathbb{X}| \times |\mathbb{X}|}$ such that $\Pi_{\mathbb{X}}e = e$, where $e := [1 \ 1 \ \dots \ 1]^\top$;
- β is a map from \mathbb{Y} to $\mathbb{R}_+^{|\mathbb{X}|}$, with $\sum_{y \in \mathbb{Y}} \beta(y) = e$;
- $\pi(1)$ is a row vector in $\mathbb{R}_+^{|\mathbb{X}|}$ with $\pi(1)e = 1$.

The matrix $\Pi_{\mathbb{X}}$ contains the state transition probabilities $(\Pi_{\mathbb{X}})_{ij} = P(x(t+1) = j | x(t) = i)$, the vectors $\beta(y)$ represent the output probabilities $\beta(y)_i = P(y(t) = y | x(t) = i)$ and π is the initial state distribution $\pi(1)_i = P(x(1) = i)$. Suppose an ordering $(y_k, k = 1, 2, \dots, |\mathbb{Y}|)$ on the set \mathbb{Y} , then $B := [\beta(y_1) \ \dots \ \beta(y_{|\mathbb{Y}|})]$.

3 State representation of two-point processes

Let P be the $|\mathbb{Y}| \times |\mathbb{Y}|$ matrix with k, l -th element $P(y_k y_l)$, where $y_k y_l$ denotes the concatenation of the symbols y_k and y_l .

If the string probabilities come from an underlying HMM, then one can easily see that

$$P = B^\top \text{diag}(\pi(1)) \Pi_{\mathbb{X}} B.$$

From this last observation, we will show that the problem of finding an underlying state process for a two point output process, can be translated in the problem of finding nonnegative matrices $V \in \mathbb{R}^{|\mathbb{Y}| \times |\mathbb{X}|}$ and $A \in \mathbb{R}^{|\mathbb{X}| \times |\mathbb{X}|}$, with $|\mathbb{X}|$ as small as possible, such that

$$P = V A V^\top.$$

4 Nonnegative Matrix Factorization

We solve the nonnegative factorization $P = V A V^\top$ by an optimization based approach (cfr [2]), i.e. we chose the inner dimension and then iteratively minimize the Kullback-Leibler divergence between P and $V A V^\top$, where the Kullback-Leibler divergence between X and Y is defined by

$$D(X||Y) = \sum_{ij} (X_{ij} \log \frac{X_{ij}}{Y_{ij}} - X_{ij} + Y_{ij}).$$

We propose the following multiplicative update formulas

$$A_{ij} \leftarrow A_{ij} \frac{\sum_{\mu} \sum_{\nu} V_{\mu i} V_{\nu j} \frac{P_{\mu \nu}}{(V A V^\top)_{\mu \nu}}}{\sum_{\mu} \sum_{\nu} V_{\mu i} V_{\nu j}},$$

$$V_{ki} \leftarrow V_{ki} \frac{\sum_{\lambda} \sum_{\nu} V_{\nu \lambda} A_{i \lambda} \frac{P_{k \nu}}{(V A V^\top)_{k \nu}} + V_{\nu \lambda} A_{i \lambda} \frac{P_{\nu k}}{(V A V^\top)_{\nu k}}}{\sum_{\lambda} \sum_{\nu} V_{\nu \lambda} A_{i \lambda} + V_{\nu \lambda} A_{i \lambda}}.$$

During the presentation, we will prove interesting properties of these formulas.

We will also give simulation examples showing the quality of the obtained models.

References

- [1] B.D.O. Anderson, The realization problem for hidden Markov models, *Mathematics of Control, Signals, and Systems*, vol. 12-1, 1999, pp 80-120.
- [2] D. Lee and S. Seung, Learning the Parts of Object by Non-Negative Matrix Factorization, *Nature*, vol. 401, 1999, pp 788-791.

Realization of Rational Systems

Jana Němcová

Centrum voor Wiskunde en Informatica
P.O. Box 94079, 1090 GB Amsterdam
The Netherlands
Email: J.Nemcova@cwi.nl

1 Introduction

The biochemical processes in a cell of any living organism are well described by rational positive dynamical systems. A detailed motivation for studying rational positive systems, the mathematical framework of these systems and the first result on realization of rational positive systems can be found in [4]. In this talk we restrict attention to rational dynamical systems. We outline our present approach to the realization of these systems.

We consider rational input-output systems as systems on real affine varieties with the dynamics defined by rational vector fields and with rational output functions. As the set of input values we take an arbitrary set U and as the space of output values we take \mathbb{R}^r . Then, by a rational input-output system we mean a triple (X, f, h) , where X is a real affine variety, f is a family $\{f_\alpha, \alpha \in U\}$ of rational vector fields on X and $h : X \rightarrow \mathbb{R}^r$ is an output function with rational components. The concept of rational reachability and observation algebra of such systems was introduced in [2]. To study the problem of realization of rational systems we use Bartosiewicz's paper [1]. This paper studies polynomial realizations by using algebraic geometry and commutative algebra. Our working hypothesis is that the same tools and ideas can be used for the study of rational systems.

A different approach for studying rational realizations (without considering the minimality problem) is presented in [5]. The next goal of our work is to compare these two theories.

2 Realization problem

We define the response map p_{x_0} of the system (X, f, h) from the initial state $x_0 \in X$ as the map producing the output value in \mathbb{R}^r after the action of the piecewise constant U -valued input for which a trajectory from x_0 is defined. We get the existence and uniqueness of trajectories of rational vector fields by applying the same reasoning as in [3].

Let \mathcal{U} be the admissible class of inputs (it is a subset of piecewise constant functions) and let $p : \mathcal{U} \rightarrow \mathbb{R}^r$ be an abstract response map. Then the realization problem can be formulated as finding a rational input-output system (X, f, h) and an initial state $x_0 \in X$ such that $p_{x_0} = p$ on the set of admissible inputs and such that the admissible class of inputs is a subset of piecewise constant functions – inputs for which the trajectory of rational vector field f from x_0 exists.

Our goal is to verify the validity of the following statements which hold for polynomial systems (see [1]) in the case of rational systems.

A sufficient and necessary condition for existence of a rational realization of a smooth abstract response map p is that the observation algebra of p is a subset of a finitely generated algebra of real functions on the admissible class of inputs stable under the derivations D_α .

There are two 'independent' sufficient and necessary conditions for existence of a minimal rational realization of a smooth abstract response map p . An abstract response map p has an algebraically minimal rational realization if and only if it has an algebraically observable rational realization if and only if the observation algebra of p is finitely generated.

After the construction of a canonical minimal rational realization we get that any two algebraically minimal realizations of the same smooth abstract response map are isomorphic.

A simple example of a realization problem of a biochemical reaction network will be presented.

3 Conclusion

Realization theory of rational systems requires further research. Once we can characterize the realization of rational dynamical systems, we want to focus our attention to the realization of rational positive dynamical systems because of its relevance for mathematical biology.

References

- [1] Z. Bartosiewicz, Minimal polynomial realizations, *Math. Control Signals Systems* 1 (1988), 227–237.
- [2] Z. Bartosiewicz, Rational systems and observation fields, *Systems & Control Letters* 9 (1987), 379–386.
- [3] Z. Bartosiewicz, Ordinary differential equations on real affine varieties, *Bulletin of the Polish academy of sciences Mathematics*, Vol. 35, No. 1-2, (1987).
- [4] J.H. van Schuppen, System theory of rational positive systems for cell reaction networks, *MTNS*, (2004).
- [5] Y. Wang, E. Sontag, Algebraic differential equations and rational control systems, *SIAM J. Control Optim.* 30, (1992), 1126–1149.

Design of an inferential sensor for a chemical batch reactor

G. Gins, I.Y. Smets and J.F. Van Impe*

BioTeC, Department of Chemical Engineering, Katholieke Universiteit Leuven,

W. de Croylaan 46, B-3001 Leuven, Belgium.

{geert.gins, ilse.smets, jan.vanimpe}@cit.kuleuven.be

* Corresponding author

B. Pluymers and W. Van Brempt

IPCOs - ISMC office,

Technologilaan 11/0101, B-3001 Leuven, Belgium.

{bert.pluymers, wim.vanbrempt}@ipcos.com

1 Introduction

Batch processes are widely used in the chemical industry for flexible manufacturing. To consistently and safely obtain a high product quality, online monitoring of these batch processes is required. Recently, multivariate statistical methods have been extended from continuous to batch processes [3, 4, 5, 6].

In this work, an inferential sensor is designed, using a *partial least squares* (PLS) model. This sensor is capable of predicting the final product quality, which cannot be measured online, well before the termination of the current batch.

2 Modelling procedure

The available data set consists of 30 measurement variables sampled over the duration of 91 batches. After performing a *derivative dynamic time warping* (DDTW) to bring all batch measurement profiles to an identical length [1, 2], the optimal input variables are selected via a *branch-and-bound* method.

In a next step, a PLS model is trained and validated (with a 10-fold cross-validation procedure) on the selected input variables, in analogy to [6]. To obtain early predictions of the final product quality, additional PLS models are trained, on the basis of partial measurement profiles as inputs.

3 Results

The developed inferential sensor gives accurate predictions of the final product quality. Even with partial batch measurement profiles, obtained after 50% and 75% of the total batch time, accurate predictions are obtained.

4 Conclusions & future work

In this work, *derivative dynamic time warping* and *partial least squares* modelling were used to develop an in-

ferential sensor capable of predicting an unmeasurable quality parameter well before the end of the batch.

Further research will consist in implementing an online version of the *derivative dynamic time warping* algorithm. This will result in the development of a true online estimator of the product's batch end-quality.

Acknowledgements. Work supported in part by IWT Project 040363 and Project OT/03/30 of the Research Council of the Katholieke Universiteit Leuven and the Belgian Program on Interuniversity Poles of Attraction, initiated by the Belgian Federal Science Policy Office. The scientific responsibility is assumed by its authors.

The authors would like to thank J. De Wilde of CYTEC (Drogenbos, Belgium) for the data sets provided for this study.

References

- [1] A. Kassidas, J.F. MacGregor, and P.A. Taylor. 1998. Synchronization of batch trajectories using dynamic time warping. *AIChE J.*, 44(4):864-875.
- [2] E.J. Keogh and M.J. Pazzani. 2001. Derivative Dynamic Time Warping. *First SIAM International Conference on Data Mining* (Chicago, IL).
- [3] J.H. Lee, and A.W. Dorsey. 2004. Monitoring of batch processes through state-space models. *AIChE J.*, 50(6):1198-1210.
- [4] N. Lu, Y. Yao, and F. Gao. 2005. Two-dimensional dynamic PCA for batch process monitoring. *AIChE J.*, 51(12):3300-3304.
- [5] P. Nomikos, and J.F. MacGregor. 1994. Monitoring batch processes using multiway principal component analysis. *AIChE J.*, 40(8):1361-1375.
- [6] P. Nomikos, and J.F. MacGregor. 1995. Multiway partial least squares in monitoring batch processes. *Chemometr Intell Lab*, 30:97-108.

Parameter Identification to Enforce Practical Observability - Application to (Fed-)batch Bioprocesses

Guillaume Goffaux¹, Levente Bodizs², Alain Vande Wouwer¹, Philippe Bogaerts³, Dominique Bonvin²

¹Service d'Automatique, Faculté Polytechnique de Mons, Belgium

¹Laboratoire d'Automatique, Ecole Polytechnique Fédérale de Lausanne, Switzerland

³Service de Chimie générale et Biosystèmes, Université Libre de Bruxelles, Belgium

Observability tests typically provide a binary yes/no answer and thus do not help assess whether practical observability problems such as slow convergence of the state estimates will occur. A study has shown that even an accurate bioprocess model can lead to poor state estimates when the sensitivity of the unmeasured states to the measurements is low [1]. To alleviate this problem, the same authors have suggested a model "falsification" procedure, in which the model parameters are identified so as to achieve a compromise between model accuracy (via the minimization of a maximum-likelihood criterion expressing the deviation between the model and plant states) and system observability (via a measure of observability based on sensitivity matrices). Consideration of system observability improves the rate of convergence by increasing the sensitivity to the measurements. Unfortunately, the combined cost function contains a weighting coefficient that is best determined via a trial-and-error procedure involving repeated optimization.

The contribution of this paper is to propose a cost function that (i) combines the two aforementioned measures, and (ii) can be determined without trial-and-error procedure. This study also compares the classical extended Kalman filter with a less classical (at least in bioprocess monitoring) particle filter [2] on two case studies, one in simulation and the other using experimental data.

It turns out that the new cost function can be formulated as the product of a measure of model accuracy and a measure of system observability rather than a weighted sum of the two. The advantage of the proposed cost function is twofold: (i) The identification process is no longer repetitive, and (ii) the cost function has a sound theoretical (less heuristic) justification. The disadvantage of the product cost function is however the existence of local minima corresponding to the sought compromise and to unbalanced situations where one of the two model measures (accuracy or observability) is pushed to the extreme at the expense of the other measure. The use of a multi-start strategy is therefore advised.

One could also argue that a "falsified" model will lead to steady-state offsets, and this might indeed be observed in practice. However, the proposed procedure is mostly intended for speeding up the convergence of state estimates in batch or fed-batch processes, i.e. where time of operation

is limited and monitoring is important from the beginning.

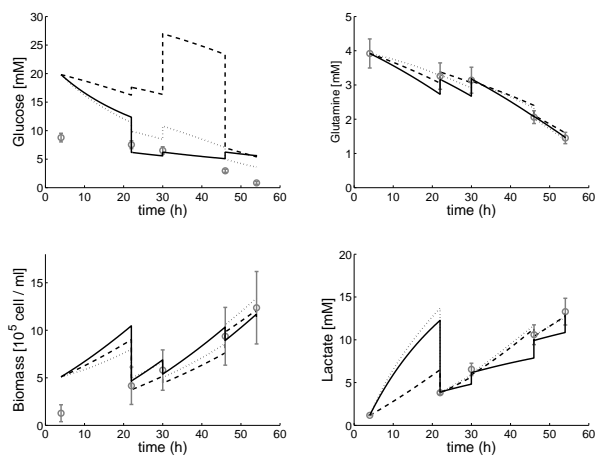


Figure 1: State estimation with a particle filter ($N = 500$) using the cost function "output error" (- -), "weighted sum" (· · ·), and "product" (-)

References

- [1] P. Bogaerts and A. Vande Wouwer. Parameter identification for state estimation – application to bioprocess software sensors. *Elsevier, Chemical Engineering Science*, 59(12):2465–2476, June 2004.
- [2] A. Doucet, N. de Freitas, and N. Gordon. *Sequential Monte Carlo Methods in Practice*. Springer-Verlag, New-York, January 2001.

State observer for fed-batch reactor with uncertain kinetics

Frédéric Sauvage and Denis Dochain
 Unité d'Ingénierie des Matériaux et Procédés
 Université catholique de Louvain
 Place Ste Barbe 2, 1348 Louvain-la-Neuve
 Belgium
 frederic.sauvage@uclouvain.be

1 Introduction

Monitoring the component concentrations is a key question for productivity and safety in the chemical industry. However it often requires very specific and expensive sensors that cannot be used in practice. Therefore the real-time estimation of component concentrations using a state observer is a very attractive option.

A major difficulty when applying state observers to real processes is to deal with model uncertainties. A common source of model uncertainties encountered in the chemical and biological industry is related to the kinetics model. This one is usually identified from experimental, often sparse results assuming a simplified reaction scheme.

In the following we focus an exothermic stirred tank reactor with an unknown kinetics model. The reactor initially contains a reactant B and a second reactant A is progressively added so that the reaction rate is controlled by the available amount of reactant A . Let us also consider that the chemical reaction is exothermic and that the reactor is coupled with a cooling system which is controlled via the temperature of a cooling fluid. The dynamical model of such a reactor can be expressed by the following differential equations:

$$\dot{T} = \frac{Q}{V}(T_{in} - T) - \frac{\Delta H}{\rho c_p} r + \frac{UA}{\rho c_p V} (T_j - T) \quad (1)$$

$$\dot{r} = \xi \quad (2)$$

$$y = T \quad (3)$$

The fed-batch operating mode allows to compute the concentration from the reaction rate without any kinetics model. As the initial concentration of reactant A is equal to zero, the concentration can be computed by the following material balance:

$$C(t) = \frac{1}{V} \left(C_{in} \int_0^t Q(\tau) d\tau - \int_0^t r(\tau) V(\tau) d\tau \right) \quad (4)$$

where C_{in} and \hat{r} are the feed concentration and the reaction rate estimate, respectively.

Here we propose a concentration estimation algorithm that proceeds in two steps. The reaction rate is firstly estimated

with a finite time converging observer. Then the concentration is computed with the reaction rate estimate. This technique has been successfully applied to the industrial production of a resin as illustrated on Figure 1.

2 Estimation algorithm

The first step of the estimation consists to estimate the reaction rate with the following finite time converging observer:

$$\begin{aligned} \dot{\hat{x}}(t) = & (e^{-F_I D} - e^{-F_{II} D})^{-1} \\ & (e^{-F_I D} \dot{z}_I(t) - \dot{z}_I(t - D) - e^{-F_{II} D} \dot{z}_{II}(t) + \dot{z}_{II}(t - D)) \end{aligned}$$

where z_I , z_{II} , F_I , F_{II} and D are two observers with linear error dynamics for the system described by (1) and (2), the matrices of the errors' dynamics and the convergence time interval.

Once the reaction rate estimate \hat{r} is obtained by the above state observer, the concentration is computed by:

$$\hat{C}(t) = \frac{1}{V} \left(C_{in} \int_0^t Q(\tau) d\tau - \int_0^t \hat{r}(\tau) V(\tau) d\tau \right) \quad (6)$$

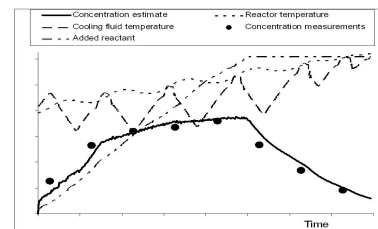


Figure 1: Experimental results

References

- [1] R. Aguilar, R. Martínez-Guerra and A. Pozniak “Reaction heat estimation in continuous chemical reactors using high gain observers,” Chemical Engineering Journal, 87, 351-356, 2002.
- [2] R. Engel, G. Kreisselmeier, “A continuous-time observer which converges in finite time”, IEEE Trans. Aut. Control, 47, 1202–1204, 2002.

Real-time Dynamic Optimization of Crystal Yield in a Fed-batch Crystallization of Ammonium Sulphate

A. Mesbah¹ and L.C.P. Spierings²

¹Delft Center for Systems and Control, Delft University of Technology
Mekelweg 2, 2628 CD Delft, the Netherlands

²Process and Energy Laboratory, Delft University of Technology
Leeghwaterstraat 44, 2628 CA Delft, the Netherlands
[E-mail: ali.mesbah@tudelft.nl](mailto:ali.mesbah@tudelft.nl)

Keywords: Fed-batch crystallization, Advanced control system, Optimizing controller, Heat input, Crystal growth.

1 Introduction

Crystallization is one of the most widely used separation and purification processes in the chemical industry. Batch crystallization from solution is often used for production of high purity, high added-value materials with tight specifications on crystal properties, i.e. size, purity and morphology. In order to meet these requirements, an effective control strategy is often needed.

In this study, the controllability of a 75-liter draft tube crystallizer was investigated by means of the real-time optimization of crystal yield in a fed-batch crystallization of ammonium sulphate.

2 Methodology

The seeded fed-batch crystallization of ammonium sulphate from an aqueous solution is represented by means of a non-linear moment model containing a calculation of leading moments of the Crystal Size Distribution (CSD), mass balance for solute and an empirical relation for crystal growth. Due to a high seed loading, supersaturation was kept at a low level at all times during the batch [1].

The abovementioned process model was used for the design of a real time optimizing controller on the basis of the sequential optimization strategy. The controller was employed to optimize the heat input trajectory in accordance with an objective function corresponding to the maximization of the crystal yield subjected to a growth-rate constraint.

The optimizing controller was then implemented in an on-line mode on a 75-liter draft tube crystallizer in the

framework of an advanced control system [2], where an extended Luenberger-type observer was used to estimate the evolution of the supersaturation during the fed-batch crystallization process.

3 Results

It was observed that the experimentally implemented heat input effectively followed the optimal heat input trajectory and the growth-rate constraint was not violated at the optimal heat input profile. Moreover, it was revealed that the optimized growth rate resulted in an increase in the slurry crystal fraction after a typical batch process of 3 hours.

In the future, a real time optimizing controller will be developed based on a different optimization strategy, namely the simultaneous approach. Furthermore, the robustness of the optimizing controllers will be compared to that of a classical model predictive controller implemented on the same crystallizer.

4 Acknowledgments

The authors would like to thank A.N. Kalbasenka and J. Landlust for their collaborations.

References

- [1] N. Doki, N. Kubota, M. Yokota, and A. Chianese (2005), Determination of Critical Seed Loading Ratio for the Production of Crystals of the Uni-Modal Size Distribution in Batch Cooling Crystallization of Potassium Alum. *J. Chem. Eng. Japan* 35, page 670-676.
- [2] A. Kalbasenka, J. Landlust, A. Huesman and H. Kramer (2005), Application of observation techniques in a model predictive control framework of fed-batch crystallization of ammonium sulphate, Delft University of Technology, Delft, The Netherlands.

Stabilization of the Optimally Scheduled Cyclic Operation of an Hybrid Chemical Plant

Iliyana Simeonova

CESAME/UCL, Av. G. Lemaître 4,
B - 1348 Louvain la Neuve, Belgium
simeonova@inma.ucl.ac.be

François Warichet

CORE/UCL
Belgium
warichet@core.ucl.ac.be

Georges Bastin

CESAME/UCL
Belgium,
bastin@inma.ucl.ac.be

Denis Dochain

CESAME/UCL
Belgium
dochain@inma.ucl.ac.be

Yves Pochet

CORE/UCL
Belgium
pochet@core.ucl.ac.be

1 Abstract

This communication presents a strategy for the feedback stabilization of the operation of an hybrid chemical plant with several parallel lines, shared resources and a continuous discharging unit at an optimal periodic scheduled operation which is open loop unstable.

2 Problem Definition

The considered hybrid plant has several batch reactors operated in parallel and limited shared resources (reactant, steam, etc.). The reactors discharge the same final product in a storage tank having a continuously discharging output. The plant is hybrid in the sense that it combines time driven and event driven processes, moreover it operates periodically. In the present study it is assumed that:

- The hybrid automaton model of the plant and its periodic open loop schedule are available [2].
- In the presence of a constant disturbance, the operation of each reactor follows its predefined sequence of modes (filling, stand-by before heating, heating, etc.) and there is a non-conflicting resources sharing. Consequently the plant production cannot be stopped due to the conflicts of resource sharing;

However due to the existing disturbance, the storage tank which is discharged continuously, can be over- or under-fed and, as a result, the production may be stopped. This shows that the state trajectory of the plant, produced by this optimal periodic schedule, is open loop unstable. Consequently we are interested in the operation of the tank. The aim of the feedback control algorithm is:

- the stabilization of the operation of the hybrid plant;
- the minimization of the instantaneous energy, of the controlled output flow rate of material leaving the

plant in order to have a smooth material transfer to the downstream processing stage, while keeping the volume of the tank in the scheduled bounds.

Our goal is to show how this stability problem of the cyclic plant operation [1] can be solved by applying a simple PI controller to the storage tank.

3 Results and Perspectives

The hybrid periodically scheduled process of the continuous discharging unit is presented not only as an hybrid automaton but also as a continuous process subject to periodic inputs. The operation of the plant under PI control with an unknown disturbance is compared to the behavior of the plant with the updated best schedule that could be computed if the disturbances were known. It is shown that by using the PI controller the best possible average plant performance, in terms of productivity, is achieved.

The closed loop performance and the controller tuning are assessed with a simulator of the hybrid plant developed in a Matlab/Simulink/Stateflow environment.

Some of the issues that are under study are to define a time varying optimal periodic output flow rate of material leaving the storage tank (here it is constant) and to study in this case the stability of the plant process under a constant disturbance as well as under a bounded - random one.

References

[1] T. Burton, "Stability and periodic solutions of ordinary and functional differential equations," Mathematics in Science and Engineering, Vol. 178, Orlando etc.: Academic Press, Inc., Harcourt Brace Jovanovich, Publishers. X, 337 p, 1985.

[2] I. Simeonova, F. Warichet, G. Bastin, D. Dochain, and Y. Pochet "Benchmark Hybrid Automaton Model of Industrial Process," <http://astwww.bci.uni-dortmund.de/hycon4b/>, 2005.

Frequency Domain Identification of Linear Slowly Time-Varying Systems

J. Lataire⁽¹⁾R. Pintelon⁽¹⁾

(1) Vrije Universiteit Brussel, Department ELEC, Pleinlaan 2, B1050 Brussels, Belgium, e-mail: jlataire@vub.ac.be

1. PROBLEM FORMULATION

The framework of LTI (Linear Time Invariant) systems has shown to provide good approximating models for a large amount of real-life dynamic systems. However, the assumption of time invariance is not always satisfied for some applications: systems with a varying set point (e.g. flight flutter analysis) or systems with varying parameters (e.g. pit corrosion or metal deposition). In this work we model linear, slowly and aperiodically time-varying (LSTV) systems via linear discrete-time models with linear time-varying coefficients. Contrary to previous work (e.g. [1]), the identification is performed in the frequency domain. This has the advantages that a non-parametric noise model can be used and that the frequency band of interest is well-defined.

2. ASSUMPTIONS

In this study the considered systems are assumed to be described by linear ordinary difference equations with parameters varying linearly in time:

$$\sum_{n=0}^{n_A} (\alpha_n t + \beta_n) y(t-n) = \sum_{n=0}^{n_B} (\gamma_n t + \delta_n) u(t-n) \quad (1)$$

with u and y respectively in- and output signals. α_n , β_n , γ_n and δ_n are constants. A motivation for this is that every linear time-varying (LTV) dynamic system can be approximated by a system with piece-wise linear parameters as long as the length of one piece is small enough w.r.t. the smallest time constants of the varying parameters. Note that, in order to be able to model the dynamics of the system under test, this assumes that the variations of the parameters are much slower than the dominant time-constant of the system.

Starting from eq. (1), it can be shown that the input $U_N(k)$ and output $Y_N(k)$ DFT spectra of N input/output samples $u(t)$, $y(t)$, ($t = 0, \dots, N-1$) satisfy exactly the following equation:

$$\begin{aligned} Y_N \sum_{n=0}^{n_A} n \alpha_n z_k^{-n} - \frac{dY_N}{dz_k} \sum_{n=0}^{n_A} \alpha_n z_k^{-n+1} + Y_N \sum_{n=0}^{n_A} \beta_n z_k^{-n} + I_y(z_k) = \\ U_N \sum_{n=0}^{n_B} n \gamma_n z_k^{-n} - \frac{dU_N}{dz_k} \sum_{n=0}^{n_B} \gamma_n z_k^{-n+1} + U_N \sum_{n=0}^{n_B} \delta_n z_k^{-n} + I_u(z_k) \end{aligned} \quad (2)$$

where $I_y(z)$ and $I_u(z)$ are polynomials of order n_A-1 and n_B-1 respectively, and with $z_k = \exp(j2\pi k/N)$. They represent so-called transient terms, caused by the windowing of the signals.

3. IDENTIFICATION OF A LSTV SYSTEM

When a measurement record of a LSTV system is available, an estimation of the parameters can be obtained. To this end the equation error $e(k)$ is calculated as the difference between the left and right hand side of

Acknowledgement: This work is sponsored by the Research Council of the VUB (HOA), the Fund for Scientific Research (FWO-Vlaanderen), the Flemish Government (GOA-ILiNoS), and the Belgian Government (IUAP VI).

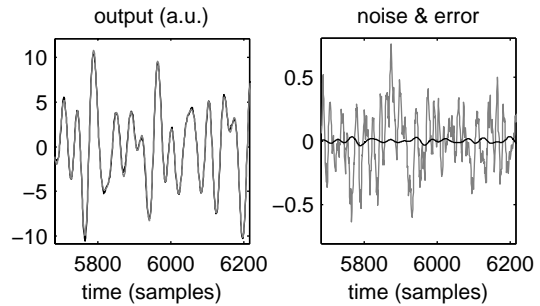


Figure 1. Time-domain signals. Left: True (black) and simulated with identified model (grey) output signals. Right: simulation error (black), noise level during identification (grey). Note the different scales between left and right figure.

(2) for every frequency line k . Assuming that the input and output noise (co-)variances are known, the maximum likelihood estimator can be derived as:

$$C = \sum_k |e(k)|^2 / \sigma_e^2(k) \quad (3)$$

where $\sigma_e^2(k)$ is the variance of $e(k)$. Minimizing this expression w.r.t. the parameters α_n , β_n , γ_n , δ_n and the coefficients of I_x and I_y results in the maximum likelihood solution.

4. DIFFICULTY WITH NOISE ESTIMATION

A major difficulty of time-varying systems is that it is often practically impossible to repeat a measurement. In addition, the “quasi steady-state” response of a time-varying system to a periodic signal is not periodic. As a consequence, the estimation of a non-parametric noise is not straightforward.

An empirical method has been elaborated to obtain this noise information by using multisine excitations as input signals. This method assumes that the power spectrum of the noise varies smoothly with the frequency and relies on information extracted from non-excited frequencies in the input and output spectra.

5. RESULTS ON SIMULATIONS

The identification method described in section 3 has been applied on a simulated, linear, third order, slowly time-varying discrete-time system. Figure 1 shows the results in time-domain. The right figure shows that the identification error is significantly lower than the noise level during the identification. The identification method is intended to be applied on measurements of real-life systems.

6. REFERENCES

[1] A.G. Pouliomenos, S.D. Fassois, Parametric time-domain methods for non-stationary random vibration modelling and analysis - A critical survey and comparison, Mechanical Systems and Signal Processing 20 (2006), pp. 763 - 816.

Estimating the power spectrum and sample variance of the Fourier coefficients using overlapping sub-records

Kurt Barbé, Johan Schoukens and Rik Pintelon
 Vrije Universiteit Brussel, Dept. ELEC, Pleinlaan 2, 1050 Brussel
 kbarbe@vub.ac.be

1 Introduction

Welch's method [3] for estimating the power spectrum based on averaging modified periodograms has been widely used. Such an estimate is based on random data and is therefore a random variable. To compute the uncertainty of the estimate one needs the probability density function (pdf) of the random variable.

In [2] the pdf for estimating the power spectrum based on data drawn from overlapping sub-records was investigated, an expression for the pdf in terms of generalized hypergeometric functions was derived. In [1] the pdf was derived in terms of Laguerre polynomials. Further, in [1] an unbiased estimate for the variance of the Fourier coefficients, at frequency bin k , of a periodic signal $u[n]$ corrupted with additive filtered Gaussian noise was constructed,

$$\hat{\sigma}_U^2(\omega_k) = \frac{1-r}{P-1} \sum_j |U_j(\omega_k) - \hat{U}(\omega_k)|^2 \quad (1)$$

where $U(\omega_k)$ denotes the fourier coefficient at frequency bin k , P the number of measured periods of the signal u , r the fraction of overlap, and with $\hat{U}(\omega_k)$ the mean Fourier coefficient at bin k .

In this paper, we study the limit distribution of the sample variance (1) as the fraction of overlap r tends to 1. Further we prove that the Errors-In-Variables (EIV) estimator for linear dynamic systems is consistent using data extracted from overlapping sub-records. Moreover, we analyze the convergence rates regarding the EIV-estimator and its cost function.

2 Main Results

It is shown that the distribution of equation (1) satisfies,

$$\hat{\sigma}_U^2(\omega_k) \stackrel{d}{=} \sigma_U^2(\omega_k) \sum_j \lambda_j G_j^2 \quad (2)$$

where $\stackrel{d}{=}$ denotes equality in distribution, λ_j are the eigenvalues of an associated bilinear form as a function of the percentage overlap r and the frequency line ω_k . The variables G_j are independent Gaussian random variables with zero mean and unit standard deviation. Therefore, we can interpret the distribution (2) as a weighted sum of chi-squared variables.

Acknowledgement: This research was supported by the FWO-Vlaanderen, The Flemish community (concerted action ILiNoS) and the Belgian Government (IUAP/V22)

Let $u(n)$ be a data stream of a periodic signal corrupted with additive Gaussian filtered noise of length $N := P \cdot L$, where P denotes the number of measured periods of the signal $u(t)$ and L the number of measured points per period. The data stream $u(n)$ is segmented in M overlapping sub-records with percentage of overlap r .

Theorem 1 For r tending to 1 the following properties hold,

- (i) The limit distribution of (2) becomes skewed and does not approach a Gaussian distribution.
- (ii) The variance of the estimator (1) is a non-increasing function of r . Moreover

$$\lim_{r \rightarrow 1} \text{Var}(\hat{\sigma}_U^2(\omega_k)) = \sigma_U^4(\omega_k) \frac{2P-3}{3(P-1)^2}.$$

Theorem 1 implies the following important result for the Errors-In-Variables estimator for linear dynamic systems,

Theorem 2 Let $Y(\omega_k) = G(\omega_k, \theta)U(\omega_k)$ a linear dynamic system with transfer function $G(\omega_k)$ parametrized in θ . If the data is drawn from at least 4 overlapping sub-records then the estimator $\hat{G}(\omega_k, \hat{\theta}_{EIV})$ is consistent.

3 Conclusions

We proved that the limiting distribution of the sample variance if the percentage of overlap tends to 1 is not Gaussian although a percentage r tending to 1 implies an infinite amount of overlapping sub-records. Secondly, we found a closed form expression for the variance of the sample variance if r tends to 1 implying that the variance of the sample variance can be reduced by introducing overlap. The study of the distribution of the sample variance allowed to prove consistency of the EIV-estimator for linear dynamic systems for data extracted from overlapping sub-records. All the theoretic results have been verified by extensive simulations.

References

- [1] K. Barbé and J. Schoukens. Non-parametric noise models extracted from overlapping sub-records. In *Proceedings of IMTC 2006- Instrumentation and measurement technology conference*, pages 1758–1763, 2006.
- [2] P. E. Johnson and D. G. Long. The probability density of spectral estimates based on modified periodogram averages. *IEEE Transactions on Signal Processing*, 47(5):1255–1261, 1999.
- [3] P. Welch. The use of fast fourier transform for the estimation of power spectra: a method based on time averaging over short, modified periodograms. *IEEE transactions on audio and electroacoustics*, 15(2):70–73, 1967.

Finite-time experiment design with multisines

X. Bombois

Delft Center for Systems and Control, Delft, The Netherlands

x.j.a.bombois@tudelft.nl

S. Taamallah

National Aerospace Laboratory (NLR), Amsterdam, The Netherlands

staamall@nlr.nl

M. Barenthin

School of Electrical Engineering, KTH, Stockholm, Sweden

marta.barenthin@ee.kth.se

1 Introduction

We consider the optimal design of the input signal of an identification experiment. The typical approach to this problem has been to maximize the accuracy of the identified model for a given experiment time and under prespecified constraints on input power (see e.g. Chapter 13 of [5]). In recent contributions this trade-off has been addressed from the dual perspective; dual perspective that we will here consider. In this novel framework, assuming that the experiment time is fixed, the optimal (open-loop) identification experiment is defined as the experiment whose input signal power is minimized under the constraint that the variance of the identified model is guaranteed to remain below some pre-specified threshold [3, 1]. In most of the contributions until now, this experiment design problem is solved by determining the power spectrum of the input signal using an expression of the variance of the identified model which is asymptotic in the number of data and assuming thus that this asymptotic expression represents a good approximation of the actual variance obtained with a finite number of data.

2 Results

In the contribution [2], restricting our attention to model structures that are linearly parametrized, we proposed a solution to the optimal experiment design problem using an expression of the variance of the identified model exact for finite data set. The optimal input signal was chosen within a relatively restricted class of input signals: the class of PRBS signals. In this contribution, we extend the results of [2] by proposing a methodology in order to determine the optimal finite-time input signal within a more extended class of signals: the class of multisines (sum of sinusoids) having a fundamental period exactly equal to the number N of data. The decision variables of the optimization problem are the amplitudes of the different sines of the multisines. In [4][Chapter 4], the same class of input signal is also considered in a finite-time experiment design framework. However, in [4], if the identification is performed using the data

from $t = 0$ to $t = N - 1$, it is assumed that the input signal has actually been applied to the true system since $t = -\infty$. In our situation, we consider the case where the input signal is zero for all time instants $t < 0$. The main difference between the two situations is that, in [4], the data are in stationary regime while, in the case considered here, the data contains transient effects.

Besides developing a methodology in order to determine the optimal finite-time multisine in the case where the multisine is only applied from $t = 0$ to $t = N - 1$, another contribution of this presentation is to show, based on an example, that transient effects are beneficial to the identification. In this example, we determine the optimal (least powerful) multisine in the case considered in [4] where the data are in stationary regime and also in the case considered in this paper i.e. where transient effects are present in the data. We observe that the required input power is significantly smaller in the case where transient are present in the data, especially when N is small. For larger N , the required input power in the two cases becomes similar.

References

- [1] M. Barenthin, H. Jansson, and H. Hjalmarsson. Applications of mixed H2 and Hinfin input design in identification. In *Proc. IFAC World Congress, Prague*, 2005.
- [2] X. Bombois and M. Gilson. Cheapest identification experiment with guaranteed accuracy in the presence of undermodeling. In *14th IFAC Symposium on System Identification, Newcastle*, 2006.
- [3] X. Bombois, G. Scorletti, M. Gevers, P. Van den Hof, and R. Hildebrand. Least costly identification experiment for control. *Automatica*, 42(10):1651–1662, 2006.
- [4] H. Jansson. *Experiment design with applications in Identification for Control*. PhD thesis, Royal Institute of Technology, Stockholm, Sweden, 2004.
- [5] L. Ljung. *System Identification: Theory for the User, 2nd Edition*. Prentice-Hall, Englewood Cliffs, NJ, 1999.

Hybrid optimization of optimal temperature inputs for the accurate estimation of microbial cardinal temperatures

Eva Van Derlinden, Kristel Bernaerts, Filip Logist and Jan F. Van Impe
 Chemical and Biochemical Process Technology and Control Section,
 W. de Crooylaan 46, B-3001 Leuven, Belgium

jan.vanimpe@cit.kuleuven.be - kristel.bernaerts@cit.kuleuven.be - eva.vanderlinden@cit.kuleuven.be

1 Introduction

Rigorous parameter estimation is enabled if highly informational experimental data are available. The technique of optimal experiment design for parameter estimation (OED/PE) is an excellent basis for the selection of experiments resulting in accurate parameter estimates with good statistical quality. In this paper, the OED/PE problem is tackled for a four-parameter model from the field of predictive microbiology, namely, the Cardinal Temperature Model with Inflection point (CTMI) [3]. This model describes the temperature dependency of the maximum specific growth rate and is here embedded in a dynamic growth model [2]. Optimal temperature profiles are designed with a deterministic, a stochastic and a hybrid optimization method and the efficiency of these approaches is compared.

2 Materials and methods

The unknown parameters are the four kinetic parameters of the CTMI, and the measured model output is the evolution of cell density in time. Optimal experiments are calculated with respect to the D-criterion, which aims at the maximization of the determinant of the Fisher information matrix. The optimization problem is reduced to a two-by-two estimation problem. For all six parameter combinations, an optimal $T(t)$ -profile is designed. Four optimal experiments will then be selected such that each parameter is considered twice. Global identification on these experiments yields a new set of parameter estimates. The $T(t)$ -input is parameterized to obtain a finite dimensional optimization problem: a period at constant temperature is followed by a linear temperature change reaching a final stage at constant temperature. Temperature profiles with either a positive or negative slope are considered. To guarantee model validity and proper measurement of growth, constraints are imposed on the design variables. Optimization programs are written in Fortran, using the NAG library. The optimization problem is solved by means of a stochastic (ICRS) [1], a deterministic (SQP in E04UCF) and a hybrid optimization (ICRS+SQP) method.

3 Results and discussion

Depending on the initialization, criterion values recovered from SQP-optimization often correspond to a local opti-

mum. Running ICRS mostly yields criterion values closer to the global optimum. Application of the hybrid algorithm generally results in the global optimum and is therefore adopted to optimize the temperature profiles.

Optimal $T(t)$ -profiles show similar characteristics for the different parameter combinations. In experiments with a linear temperature decrease, temperature starts to decline shortly after the start and is followed by a longer period at a constant, lower temperature. Experiments with a temperature increase start with an extended period at constant temperature and temperature starts to increase near the end. The most informative rate of temperature change in most cases coincides with the fastest allowable value. Initial and final temperatures are determined by the sensitivity functions. Out of the linearly decreasing $T(t)$ -profiles, a series of four optimal experiments is combined for the parameter estimation. Based on simulations, identifiability of the four parameters is evaluated.

4 Conclusion

By combining a stochastic and deterministic algorithm, a hybrid optimization method is created that outstands in convergence. D-optimal $T(t)$ -profiles are calculated for each parameter couple and a set of four informational experiments is selected for experimental validation.

5 Acknowledgements

Work supported in part by Projects OT/03/30 and EF/05/006 (Center-of-Excellence Optimization in Engineering) of the Research Council of the Katholieke Universiteit Leuven, and by the Belgian Program on Interuniversity Poles of Attraction, initiated by the Belgian Federal Science Policy Office. Kristel Bernaerts is a postdoctoral fellow with the Fund for Scientific Research - Flanders (FWO - Vlaanderen). The scientific responsibility is assumed by its authors.

References

- [1] J.R. Banga, A.A. Alonso and R.P. Singh, Stochastic dynamic optimization of batch and semicontinuous bioprocesses, *Biotechnol. Prog.*, vol. 13, 1997, pp 326-335.
- [2] J. Baranyi and T.A. Roberts, A dynamic approach to predicting bacterial growth in food, *Int. J. Food. Microbiol.*, vol. 23, 1994, pp 277-294.
- [3] L. Rosso, J.R. Lobry, S. Bajard and J.P. Flandrois, Convenient model to describe the combined effects of temperature and pH on microbial growth, *Appl. Environ. Microbiol.*, vol. 61, 1995, pp 610-616.

Stable Approximations of Unstable Models

T. D'haene, R. Pintelon

Vrije Universiteit Brussel, departement ELEC, Pleinlaan 2, B1050 Brussels, Belgium
email: Tom.Dhaene@vub.ac.be

I. INTRODUCTION

In this paper the stability enforcement algorithm of [1] is improved at several points. The original stabilisation algorithm [1] consists of a two-step method. In the first step a (high) degree model without stability constraints is estimated that passes the validation tests (analysis cost function and whiteness test of the residuals). This step suppresses in an optimal way the noise without introducing systematic errors. In the second step the constraint will be added: The (high) degree model will be approximated by a stable one. For this the weighted difference between the unconstrained model and the stable model is minimized.

$$e(s_l, \Theta) = w(s_l)(G(s_l) - \hat{G}(s_l, \Theta)) \quad (1)$$

The big advantage of the two step procedure is that it provides models with uncertainty and bias errors, which is not the case when stability is imposed during the noise removal.

II. THE ALGORITHM

Starting from stable initial values Θ_k ($k = 0$) [1], one can calculate the error (1) to calculate the step $\delta\Theta$. This results in the new values Θ_{k+1} that lower the cost function.

$$\Theta_{k+1} = \Theta_k + \delta\Theta \quad (2)$$

If $G(s, \Theta_{k+1})$ is stable we start a new iteration, if not we decrease $\delta\Theta$ with a factor (ex. 2), until $G(s, \Theta_{k+1})$ becomes stable.

The basic idea of this method is to leave some freedom to the transfer function parameters (gain, poles, zeros) to lower the cost function. The reason why this algorithm creates better models than the methods that generates the starting values, lays in the fact that the created stable models are optimized in a user-defined frequency band, while the starting values optimize a criterion over the whole frequency axis [3].

III. IMPROVEMENTS

The major drawback of this algorithm is that the poles that reach the constraint borders will prevent the model to improve further. The reason for this is that the step will be reduced till zero for every new iteration step. To overcome this problem the parameters Θ are divided in 2 groups Θ^V and Θ^F . Θ^V fulfil the constraints and are

This work is sponsored by the Research Council of the VUB (HOA), the Fund for Scientific Research (FWO-Vlaanderen), the Flemish Government (GOA-ILINoS), and the Belgian Government (IUAP VI).

allowed to be adapted by the algorithm. Θ^F contains all the parameters that violate the constraints; these will be hold fixed. Now whenever a parameter of Θ^V violate the constraints, it is moved to Θ^F , so e can be lowered by further adapting the remaining Θ^V .

An equiripple stable model can also be imposed as follows:

$$\text{minimize}_{\Theta} \max_{s_l \in \Omega} (|e(s_l, \Theta)|) \quad (3)$$

with Ω the user defined frequency band, where the user wants a good model through his/her data. To find a minimax solution for a stable model based on the existing iterative algorithm, an iterative reweighted least squares method is an obvious choice [2].

Next, a scheme to calculate high order stable approximations is proposed. There are two easy ways to increase the order of the model without violating the stability constraints. By adding or multiplying the stable transfer function $\hat{G}(s_l, \Theta)$ with an other stable transfer function $\hat{G}_{extra}(s_l, \Theta_{extra})$ that lowers the global error $e_{tot}(s_l) = w(s_l)(G(s_l) - \hat{G}_{tot}(s_l, \Theta_{tot}))$.

$$\begin{aligned} \hat{G}_{tot}(s_l, \Theta_{tot}) &= \hat{G}(s_l, \Theta) + \hat{G}_{extra}(s_l, \Theta_{extra}) \\ \hat{G}_{tot}(s_l, \Theta_{tot}) &= \hat{G}(s_l, \Theta) \cdot \hat{G}_{extra}(s_l, \Theta_{extra}) \end{aligned} \quad (4)$$

In a first step $\hat{G}_{tot}(s_l, \Theta_{tot})$ is put in the iterative algorithm described in Section II but only Θ_{extra} is allowed to adapt. This step creates optimal starting values for $\hat{G}_{extra}(s_l, \Theta_{extra})$. The second step is a final optimization of $\hat{G}_{tot}(s_l, \Theta_{tot})$ where all parameters Θ_{tot} are modified. This will further lower $|e_{tot}(s_l)|$.

IV. CONCLUSION

In this work an improved algorithm for finding stable approximations of unstable models has been presented. In addition stable minimax solutions can be generated. The performance of the improved algorithm is demonstrated on a real measurement example.

V. REFERENCES

- [1] T. D'haene R. Pintelon, G. Vandersteen, "An Iterative Method to Stabilize a Transfer Function in the s- and z-domains", *IEEE Transactions on Instrumentation and Measurement*, vol. 55, no. 4, August, 2006, pp. 1192-1196.
- [2] R. Vuerinckx, "Design of Digital Chebyshev Filters in the Complex Domain", PhD thesis, Vrije Universiteit Brussel, Brussels, February, 1998.
- [3] Mari Jorge, "Modifications of rational transfer matrices to achieve positive realness", *Signal Processing*, no. 80, 2000, pp. 615-635.

Sub Nano positioning

Jan van Hulzen
 Delft Center for Systems and Control
 Delft University of Technology Mekelweg 2 2628 CD, Delft
 j.r.vanhulzen@tudelft.nl

1 Scanning tunnel microscopy

The Scanning Tunnel Microscope was the first device requiring accuracies in the nano and sub-nano meter range. A STM uses a probe to take spatial measurements of conducting surfaces. Its main advantage is that it used elections already present in surface and probe freeing it from the wavelength restrictions imposed by illumination through external radiation. Theoretically a STM can achieve vertical resolutions up to 0.1 Å or 10 pm.

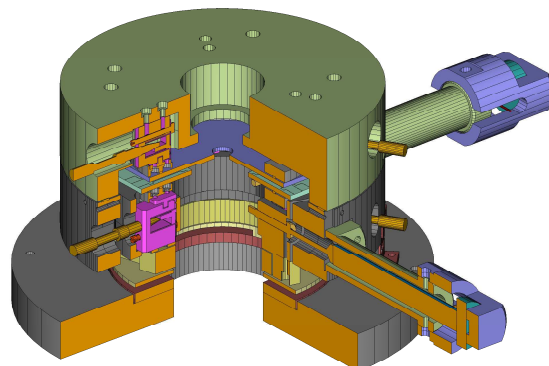
The positioning stage of the STM is the subject of this PHD project. Starting from an existing stage design, the goal is to investigate the limits of performance and improve upon them. Ultimately the positioning resolution of a stage should be around one tenth of an atom or about 30 pm with an accuracy of ± 10 pm.

2 Precision design

In the case of the STM we require control over the lateral and vertical and position of the scan tip. We are not interested in restricting the rotational degrees of freedom as long as scan tip position is not affected. In general we require the following:

- Frame design: high stiffness and damping; high degree of thermal stability and seismic isolation.
- Guidance of moving parts : (Frictionless, preferably linear and observing Abbé Principle)
- Measurement : sensors based on direct displacement measurement with a metrology frame that isolates sensors from force paths and machine distortion.
- Control and actuation : high stiffness and bandwidth with actuation through axes of reaction.

The design of the prototype is based on a guidance system consisting of three folded blade springs in combination with a rotation stop [1]. The stage is actuated by two piezos pushing the stage with a flexible strut. The scanning probe is mounted on the stage and positioned below a frame in which we place the sample. The position of the stage relative to the sample stage is measured using a capacitive sensor. The design also features a suspension which keeps the thermal center of the stage guidance and the sample frame.

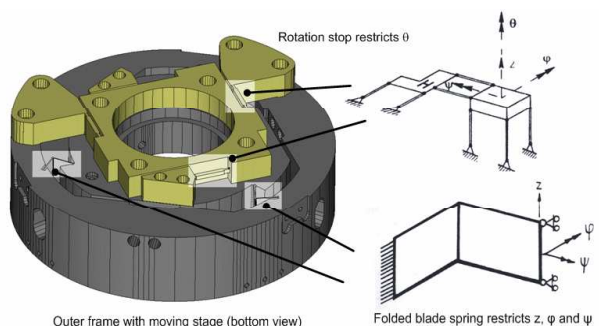


3 Modeling and and identification of stage dynamics

From a control point of view we are interested in the dynamical behavior of the system and view the quality of the guidance and thermal stability as disturbances.

⇒ to add later (this is a draft after all)

- identification of stage dynamics
- control example



References

[1] Koster M.P., Constructieprincipes voor het nauwkeurig bewegen en positioneren, 3rd edition, Twente University Press, 2000

Active Printhead Alignment

Dennis Bruijnen
 Control Systems Technology
 Technische Universiteit Eindhoven
 P.O. Box 513, 5600 MB Eindhoven
 The Netherlands
 Email: d.j.h.bruijnen@tue.nl

Introduction

To improve print quality for higher productive wide format printing systems, an active printhead alignment approach (see Fig 1.) has been investigated.

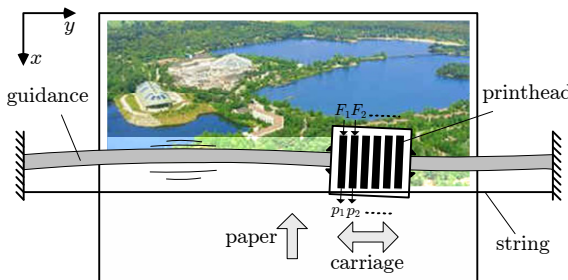


Fig 1. Active printhead alignment concept

The position of each printhead is measured with respect to a string [1]. By using two leaf-springs and a voice coil actuator, the printheads are mutually aligned [2]. The main challenges are to cope with: (i) a temperature varying environment, (ii) $< 10 \mu\text{m}$ accuracy, (iii) attenuation of parasitic dynamics such as string and guidance vibrations, (iv) cost minimization. The active printhead alignment setup is shown in Fig 2.

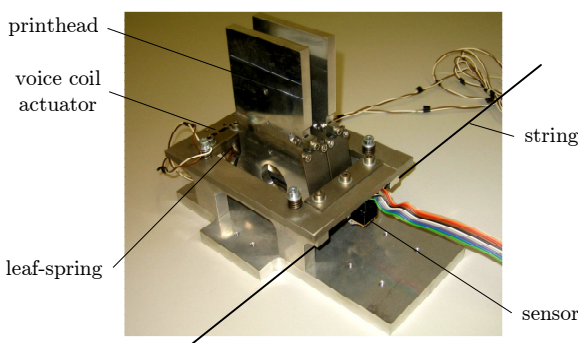


Fig 2. Active printhead alignment setup

Experiments

The regulation problem in a real printer is translated to a tracking problem for the active printhead alignment setup.

A trajectory has to be tracked while the string is excited with a pulse. The result is shown in Fig 3. The transients of the harmonics have settled 0.05 s after the pulse disturbance is applied such that an accuracy of $2 \mu\text{m}$ is again attained while the lightly damped string keeps vibrating.

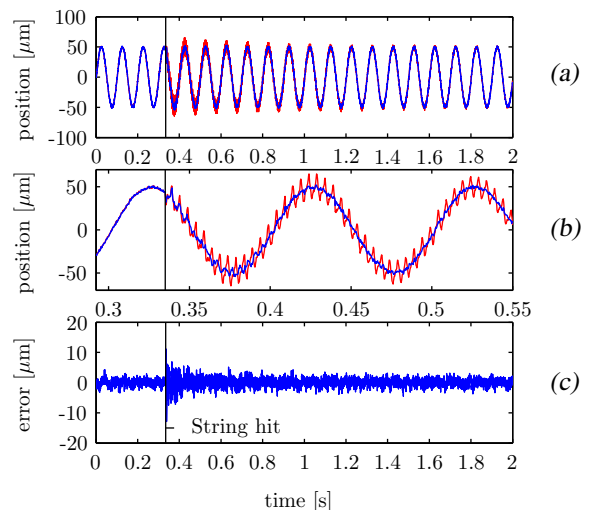


Fig 3. Tracking under string vibrations.
 (a): red line: sensor signal (p_1 in Fig. 1), blue line: p_1 filtered with a harmonics filter, (b): Close up of (a), (c): error between the trajectory and the filtered signal.

Conclusions

The active printhead alignment concept has shown to be feasible. Experiments have been carried out showing that the alignment error remains below $10 \mu\text{m}$ under disturbances.

References

- [1] D. J. H. Bruijnen, M. J. G. van de Molengraft, T. Heeren, A. A. Draad, and M. Steinbuch. Design of a printhead alignment sensor for a temperature varying environment. In *American Control Conference*, pages 388–393, Minneapolis, United states, 2006.
- [2] A.W. Notenboom, D.J.H. Bruijnen, F.G.A. Homburg, M.J.G. van de Molengraft, L.J.M. van den Bedem, and M. Steinbuch. Mechatronic design of an active printhead alignment mechanism for wide format printing systems. *Mechatronics*, page Accepted, 2006.

Dealing with Instability in Hybrid Stepper Motors

J. Stolte, A. Veltman, P.P.J. van den Bosch

Department of Electrical Engineering
Eindhoven University of Technology
P.O. Box 513, 5600 MB, Eindhoven

The Netherlands

Email: J.Stolte@tue.nl

1 Introduction

Stepper motors are widely applied as inexpensive actuators in electro-mechanical devices. Their inherent stepping behaviour means they do not need an (expensive) incremental encoder to function. However, stepper motors are notorious for their inefficiency and poor dynamical behaviour which includes resonances and even instability, as shown in figure 1. Especially the phenomenon of instability is acknowledged but not well understood, and literature on it is very poor. This contribution focusses on explaining and solving parametric instability in stepper motors.

Alternatively, open-loop current control theoretically does not suffer from instability, though it does result in very poorly damped systems. In reality however pure current control cannot be realized due to the inductive nature of the stepper motor phases. To implement pure current control the controller needs an infinitely high voltage to instantaneously track the current reference. In practice this is not available and pure current control drivers do not exist. Whether or not instability occurs in these non-perfect current controllers depends very much on the exact implementation which makes the stability of the system very unpredictable.

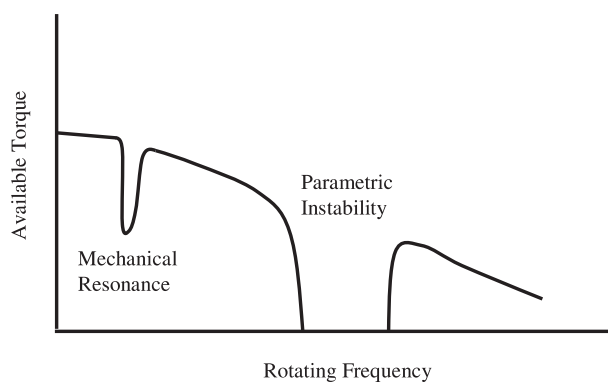


Figure 1: Stepper motors can have a frequency region in which the motor is unstable and cannot deliver any torque.

2 Stepper Motor Control & Instability

Three important methods of controlling stepper motors can be distinguished:

- Open-Loop Voltage Control
- Open-Loop Current Control
- Closed-Loop Control

Because of the cost advantage in practice most stepper motor systems are controlled in open loop. It has been shown that theoretically stepper motors only suffer from instability when they are driven in open-loop voltage control [1]. In this work a more precise frequency boundary of instability is calculated, which allows better prediction of when to expect instability in a stepper motor under voltage control.

3 Observer Based Control

Using only open-loop control it is impossible to make dynamically well behaving systems, and therefore the industry has grown accustomed to using workarounds for the problems mentioned in other ways (flexible mountings, inertial dampers, overactuation etc.). However, recently it has become possible to obtain closed loop control without the use of an incremental encoder.

Due to the ever decreasing price of processing power it is now much cheaper to use a microprocessor in the system than to have an incremental encoder. Using a microprocessor enables measurements of phase currents and voltages, and from these the angular states of the system can be estimated [2], and used for closed-loop control.

Since in reality pure current control cannot be realised the authors argue that from a stability point of view it is better to stabilize the system using voltage control. A voltage controller which stabilizes the system is developed and evaluated in this work.

References

- [1] A. Hughes and P.J. Lawrenson, "Simple theoretical stability criteria for 1.8° hybrid motors", proc. int. symp. on stepping motors and systems, University of Leeds, 1979, pp 127-135.
- [2] S-M. Yang and E-L. Kuo, "Damping a hybrid stepper motor with estimated position and velocity", IEEE Transactions on Power Electronics, 18(3), 2003, pp 880-887.

Contactless Planar Actuator with Manipulator - Experimental Setup for Control

Michal Gajdušek, Ad Damen, Paul van den Bosch

Department of Electrical Engineering
Eindhoven University of Technology
P.O.Box 513, 5600 MB Eindhoven
The Netherlands

Email: m.gajdusek@tue.nl

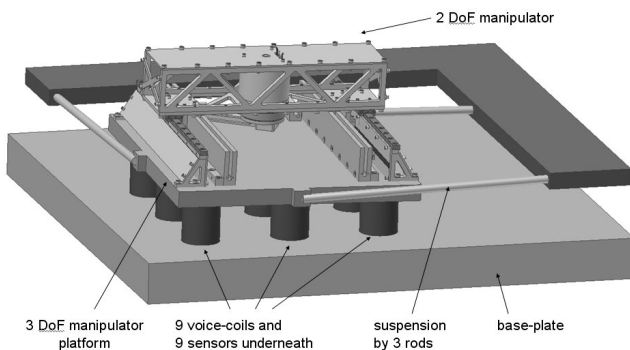
1 Introduction

The goal of this project is to control 6-DOF a magnetically levitated platform with manipulator (6 DOF CPAM) on top of it. Levitation and propulsion is provided by coils in standstill base-plate and permanent magnets in the platform. The manipulator is controlled and powered wirelessly. Such wireless system allows for combination of long-stroke with precise short-stroke movement.

The electromagnetic design and wireless power transmission will be done by research colleague J. de Boeij [1]. Apart from the design of the commutation, this project needs a number of innovations in wireless communication, real-time wireless control as well as in MIMO disturbance rejection of the mutual influence between manipulator and platform.

2 Experimental setup

In order to test and validate control design for the ultimate 6-DOF CPAM, a 3-DOF pre-prototype with 2-DOF Manipulator has been designed. The platform, that mimics the final magnetic array, is suspended such that it can only move in 3 other DOFs: vertically and two tilting angles. The 3 DOFs will be fixed by a suspension system consisting of 3 stiff rods.



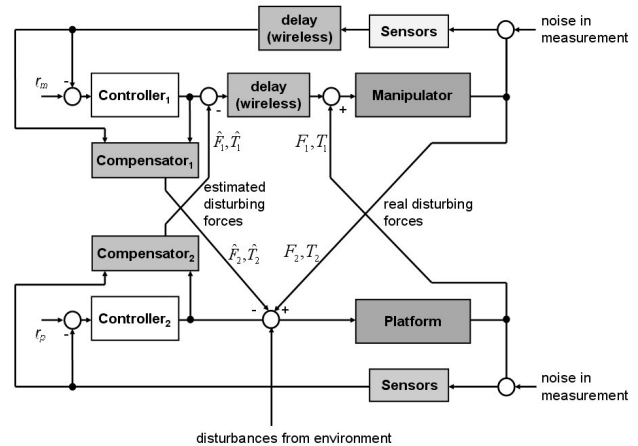
The platform is actuated by 9 voice coils underneath which are distributed into regular array to simulate the topology of the planar actuator and will be used for gravity compensa-

tion and for manipulator platform control in 3 DOF.

The manipulator on top of the platform has 2 DOF which provide precise linear and rotary movement of an end tip of the manipulator.

3 Control

The control consists of two main control loops: one for control of the platform and other for control of the manipulator. These two control loops are interconnected by force and torque disturbances acting from the manipulator on the platform and vice versa. These disturbances should be rejected by two compensators in cross link. Wireless communication in between controller and manipulator with its delays and packet losses causes an extra complication in control design [2].



References

- [1] J. de Boeij, E. A. Lomonova, A. J. A. Vandeput, "Modeling ironless permanent magnet planar actuator structures," *IEEE Trans. Magn.*, vol. 42, no. 8, 2009-2015, Aug. 2006.
- [2] N. J. Plodys, P. A. Kawka, A. A. Alleyne, "Closed-loop Control over Wireless Networks," *IEEE Control Systems Magazine*, vol. 24, no. 3, 58-71, June 2004.

Switched Linear Controller Breaks Waterbed Effect

R.A. van den Berg, A.Y. Pogromsky, J.E. Rooda

Department of Mechanical Engineering

Eindhoven University of Technology

PO Box 513, WH0.126, 5600 MB Eindhoven, The Netherlands

Email: [R.A.v.d.Berg, A.Pogromsky, J.E.Rooda]@tue.nl

1 Introduction

For the linear control system given in Figure 1, the sensitivity function is given by $S = (1 + CP)^{-1}$. According to Bode's sensitivity integral the sensitivity function of this system must satisfy

$$\int_0^\infty \ln |S(j\omega)| d\omega = 0, \quad (1)$$

whenever the system's open loop transfer function has a relative degree ≥ 2 (and some stability conditions are satisfied).

Equation (1) states that the total area of 'low' sensitivity ($\ln |S(j\omega)| < 0$) must equal the total area of 'high' sensitivity ($\ln |S(j\omega)| > 0$). Therefore, if by some control action the sensitivity can be reduced in a certain frequency range, then in another frequency range the sensitivity increases. Because of this disadvantageous property the term "waterbed effect" is often used in relation to (1).

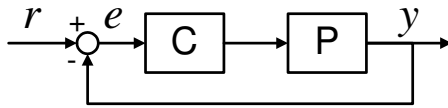


Figure 1: Block diagram of linear control system

2 Main Statement

Consider the system in Figure 1 with a plant of relative degree 2. Any physically realizable linear controller has a relative degree ≥ 0 , and therefore in combination with the mentioned plant results in an open loop transfer function that has a relative degree ≥ 2 . Thus, the Bode integral (1) is zero. On the other hand, if a switched linear controller is applied, an obvious analog of the Bode integral can become negative.

3 Switched Linear Controller causes Bode Integral < 0

Consider the system in Figure 2, which can be described by

$$\begin{aligned} \dot{x} &= Ax + B\varphi + Ew \\ \varphi &= k \cdot \text{sign}(Cx) \end{aligned} \quad (2)$$

with $x = [y \ \dot{y} \ e_1]^T$, $w = [r \ \dot{r}]$,

$$A = \begin{bmatrix} 0 & 1 & 0 \\ -ab & -(a+b) & 0 \\ -c & -1 & -c \end{bmatrix}, \quad B = \begin{bmatrix} 0 \\ 1 \\ -1 \end{bmatrix}, \quad E = \begin{bmatrix} 0 & 0 \\ 0 & 0 \\ c & 1 \end{bmatrix},$$

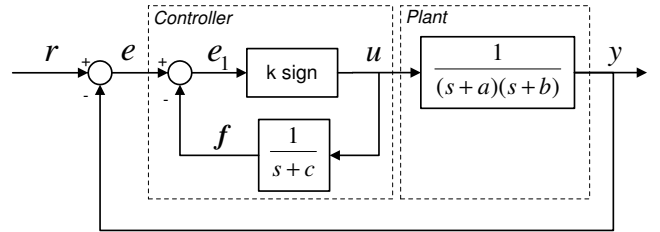


Figure 2: System with switched linear controller

and $C = [0 \ 0 \ 1]$, where a, b, c , and k are positive numbers. Note that the plant has relative degree 2. Assume the input r and its derivative are bounded. Consider these lemmata:

Lemma 1 *If there exists a matrix $P = P^T > 0$ such that $A^T P + PA < 0$ and $PB = -C^T$ hold, then system (2) is ultimately bounded, with a bound that is independent of k .*

Lemma 2 *For sufficiently large k , the sliding mode $e_1 = 0$ is globally asymptotically stable (GAS).*

The sliding mode dynamics ($\dot{e}_1 = e_1 = 0$) are given by the linear closed loop dynamics

$$\ddot{y} + (a + b + 1)\dot{y} + (ab + c)y = \dot{r} + cr. \quad (3)$$

Since the sliding mode is GAS and thus for $t \rightarrow \infty$ the system dynamics can be described by the linear dynamics (3), linear control systems theory can be used to define a sensitivity function for system (2):

$$S = \frac{(s+a)(s+b)}{s^2 + (a+b+1)s + (ab+c)}.$$

It is possible to find $a, b, c > 0$, satisfying the conditions of Lemma 1, such that for this sensitivity function the Bode integral is negative. For example, take $a = b = c = 1$, then

$$\int_0^\infty \ln |S(j\omega)| dw = -\frac{\pi}{2}.$$

4 Conclusion

The presented example shows that switched linear controllers can achieve better performance than linear controllers in terms of overall sensitivity.

References

[1] H. Bode, "Network Analysis and Feedback Amplifier Design," D. Van Nostrand, New York, 1945.

Swarm Intelligence Methods for Traffic Control

Jelmer van Ast Robert Babuška Bart De Schutter
 Delft Center for Systems and Control, Delft University of Technology
 Email: {j.m.vanast,r.babuska}@tudelft.nl, b@deschutter.info

1 Introduction

In this contribution we will review two of the most prevalent methods of Swarm Intelligence (SI) and discuss their potential for traffic control.

Swarm Intelligence (SI) is the field of Artificial Intelligence (AI) that studies the behavior and properties of swarms of interacting agents. Typically, these agents are restricted in their resources, such as computational power and communication range. While these individuals are not considered to possess any real AI power, the collection of them does. SI systems and algorithms are inspired by the behavior of social insects and animals such as foraging ants, fish schools and bird flocks. Global patterns arise through self-organization from local interaction of the individuals. SI can be applied as a heuristic to solve optimization problems. Two metaheuristics are prevalent in this field: Particle Swarm Optimization and Ant Colony Optimization.

2 Particle Swarm Optimization

Particle Swarm Optimization [1] can be used for solving nonlinear multidimensional optimization problems. The swarm consists of agents, or particles, having a state (position x_k and velocity v_k) in the search space. In each iteration, the state is updated according to:

$$v_{k+1} = wv_k + c_1r_1(P_{\text{best}} - x_k) + c_2r_2(G_{\text{best}} - x_k) \quad (1)$$

$$x_{k+1} = x_k + v_{k+1}, \quad (2)$$

where $w, c_{1,2}$ are constants tuning the behavior of the swarm, $r_{1,2}$ random variables used for exploration and $P_{\text{best}}, G_{\text{best}}$ the best position of the individual (personal) and of all the agents in the swarm (global), respectively. These 'best' positions are evaluated according to some fitness function. It has been shown that under certain conditions, the swarm converges to the optimal solution.

In traffic networks, each vehicle can be regarded as an agent in a particle swarm. Similar equations as Eq. 1 can be composed to determine the desired speed of each vehicle considering its personal best and the traffic network's global (or local) best. With each vehicle containing wireless technology, an ad-hoc network can be used to exchange information about personal best states. One of the main challenges is to ensure that the local information is sufficient to lead to convergence to satisfactory solutions. A second challenge is to design the fitness functions according to which the states are evaluated.

3 Ant Colony Optimization

Ant Colony Optimization [2] is inspired by the behavior of ants and can solve hard combinatorial optimization problems, cast in a graph. The agents, or artificial ants, move from node to node across the edges. The probability of choosing node i while being on node j is:

$$p_{ij} = \frac{\tau_{ij}^\alpha \eta_{ij}^\beta}{\sum_l \tau_{il}^\alpha \eta_{il}^\beta}, \quad (3)$$

for all nodes i that can be reached in one step from j . In Eq. 3 η_{ij} denotes some heuristic, or prior knowledge about the fitness of this edge, τ_{ij} is the local pheromone value and α and β determine the relative importance of η_{ij} and τ_{ij} . Pheromones increase the probability for other agents to take this edge and thus choosing more promising solutions. The pheromone values decay and the trail is updated in each iteration.

For traffic control, a typical application is the optimal routing problem. The traffic network must be cast into a graph, with roads as edges and interconnections as nodes. Vehicles traversing the network may leave some signal at the edges contributing to the pheromone value associated with it. The length of the road will be represented as the heuristic η . The route choice at a node is now influenced by both the road length and the recommendation by other vehicles that have recently crossed that road.

4 Conclusions and Future Research

SI methods have the potential to be applied to various traffic control problems. We will investigate to what extend this distributed approach leads to more flexible use of traffic networks. The methods discussed in this contribution must be implemented and simulated to verify the improvement.

Acknowledgements: This research is partly funded by Senter, Ministry of Economic Affairs of the Netherlands within the BSIK-ICIS project "Self Organizing Moving Agents for Distributed Sensing and Control" (grant no. BSIK03024)

References

- [1] J. Kennedy and R. Eberhart, "Particle swarm optimization.", in *Proceedings of IEEE International Conference on Neural Networks*, pp. 1942–1948, 1995.
- [2] M. Dorigo and C. Blum, "Ant colony optimization theory: A survey," *Theoretical Computer Science*, vol. 344, pp. 243–278, Nov. 2005.

Consensus problems with distributed delays, with application to traffic flow models

Wim Michiels

Department of Computer Science
K.U.Leuven

Email: Wim.Michiels@cs.kuleuven.be

Constantin Irinel Morarescu

Department of Mathematics
University “Politehnica” of Bucharest
Email: moraresco@yahoo.com

Silviu-Iulian Niculescu

Laboratoire de Signaux et Systèmes (L2S), Supélec
Email: Silviu.Niculescu@lss.supelec.fr

1 Introduction

We study consensus problems for classes of linear systems with time-delays from a stability analysis point of view, see [1] and the references therein for an introduction to consensus problems. One of the motivating applications is the stability analysis of the following differential equations, encountered in modeling traffic flow dynamics (see [2] and the references therein for the derivation of the model):

$$\dot{v}_k(t) = \sum_{i=1}^{p-1} \alpha_{k,k-i} \int_0^\infty f(\theta; n, T, \tau) (v_{k-i}(t-\theta) - v_k(t-\theta)) d\theta, \quad k = 0, \dots, p-1, \quad (1)$$

where the kernel of the distributed delay is given by

$$f(\xi; n, T, \tau) = \begin{cases} 0, & \xi < \tau \\ \frac{(\xi-\tau)^{n-1} e^{-\frac{\xi-\tau}{T}}}{T^n (n-1)!}, & \xi \geq \tau \end{cases}, \quad (2)$$

with $n \in \mathbb{N}$, $T > 0$, and $\tau \geq 0$. The indices in (1) should be interpreted modulo p . It is assumed that $\alpha_{k,l} \geq 0$ for all k and l and that $\alpha_{k,k-1} > 0$ for $k = 0, \dots, p-1$. The left hand side of (1) represents the *acceleration* of the k^{th} vehicle, and the right hand side expresses the *velocity differences* of the vehicles, which are in a ring configuration. The *distributed delay*, whose kernel is a so-called gamma-distribution with a gap, is used to model the human drivers’ behavior in the average.

We are interested in characterizing the set of parameters of the delay distribution for which the system (1) solves a consensus problem, that is, all cars eventually get the same speed (which may depend on the initial values).

Notice that (1) is a special case of the system

$$\dot{x}(t) = A \int_0^\infty f(\theta; n, T, \tau) x(t-\theta) d\theta, \quad (3)$$

where A is a p -by- p *Metzler matrix* with zero row sums.

2 Main results

Various conditions for which the system (3) reaches a consensus for all initial conditions will be discussed. For instance, we have the following result [2, Theorem 3.9]:

Theorem 1 *If $n = 1$ and all eigenvalues μ_1, \dots, μ_p of A are real, then the system (3) solves a consensus problem if and only if*

$$T \in [0, \infty), \quad \tau \in [0, \tau^*(T)),$$

where

$$\tau^*(T) = \min_{\substack{k=1, \dots, p, \\ \mu_k \neq 0}} \frac{|\angle(\mu_k)| - \angle(j\omega_k(T)(1+j\omega_k(T))^n)}{\frac{\omega_k(T)}{T}} \quad (4)$$

and $\omega_k(T)$ is the positive solution of $|\omega(1+j\omega)^n| = T|\mu_k|$. Otherwise, it solves a consensus problem if and only if

$$T \in [0, T^*), \quad \tau \in [0, \tau^*(T)),$$

where

$$T^* = \min_{\substack{k=1, \dots, p, \\ \Im(\mu_k) > 0}} \frac{\tan((\angle\mu_k - \pi/2)/n)}{|\mu_k| [\cos((\angle\mu_k - \pi/2)/n)]^n}$$

and $\tau^*(T)$ is given by (4). The consensus functional satisfies $\chi(\phi) = V_0^T \phi(0) / (V_0^T E_0)$ with (V_0, E_0) a pair of (left, right) eigenvectors of A corresponding to the zero eigenvalue.

Also the behavior of the solutions at the onset of instability will be addressed. Next, the results will be further worked out for the special case (1) and interpreted in terms of this traffic flow application.

References

- [1] R. Olfati-Saber. and R.M. Murray: “Consensus problems in networks of agents with switching topology and time-delays”. IEEE Transactions on Automatic Control, 49(9) (2004) 1520-1533.
- [2] W. Michiels, C.I. Morarescu and S.-I. Niculescu, “Consensus problems with distributed delay, with application to traffic flow problems” TW Report, Department of Computer Science, K.U.Leuven (submitted to SIAM J. Control and Optimization)

Hierarchical traffic control and management with intelligent vehicles

Lakshmi Dhevi Baskar, Bart De Schutter, Hans Hellendoorn

Delft Center for Systems and Control, Delft University of Technology, The Netherlands

l.d.baskar@tudelft.nl, b@deschutter.info, j.hellendoorn@tudelft.nl

1 Introduction

Traffic congestion is one of the main problems of today's society. Building new roads could be a way for handling the traffic congestion problem, but it is less feasible due to political and environmental concerns. An alternative could be to make efficient use of the existing transportation facilities by incorporating advanced communication and information technologies. This is the primary objective of the "Intelligent Vehicle Highway System" (IVHS) program.

The approach we propose develops IVHS-based control and management methods that integrate the additional control measures offered by intelligent vehicles with those of the roadside infrastructure to substantially improve traffic performance in terms of safety, throughput, and environment. Our approach incorporates both vehicle-vehicle and vehicle-roadside communication.

2 Intelligent Vehicles and Traffic Control

Intelligent Vehicles (IVs) aim to enhance intelligence in vehicles and driver capabilities. An IV system senses the immediate environment and strives to achieve more efficient vehicle operation either by assisting the driver (advisory) or by taking complete control of the vehicle (automation) [1].

Improving the traffic flow eventually should alleviate congestion, ameliorate safety, and maximize the use of infrastructure. Fully autonomous driving on IVHS was considered to substantially improve the traffic flow [2]. The most interesting functionality that allows hands-free operation is to arrange the vehicles in a closely spaced group called "platoons". In a platoon, the vehicles travel with high speeds and short distances. Functional areas that were found to support a combination of platooning and roadside intelligence are Cooperative Adaptive Cruise Control (CACC), Intelligent Speed Adaptation (ISA) and dynamic route guidance.

3 Proposed Control Framework

The framework we propose is inspired by the PATH AHS platoon concept [2] and uses IV-based control measures to implement a next-level traffic control and management approach. The architecture is a distributed hierarchy as shown in Figure 1 and is characterized as follows:

- Higher level controllers (area, regional, and supraregional) provide network-wide coordination of lower

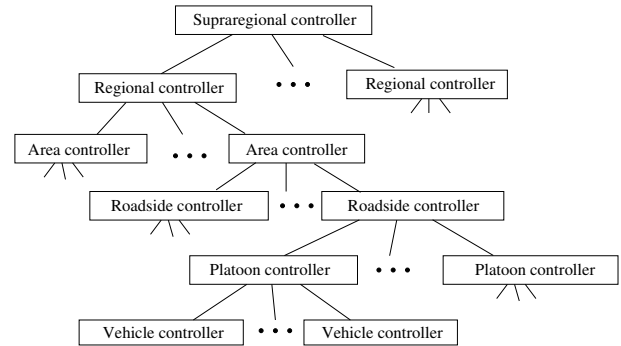


Figure 1: IV-based control framework

and middle level controllers.

- The roadside controllers use IV-based control measures. They assign desired speeds for each platoon (ISA), safe distances for platoons (CACC), provide dynamic route guidance for the platoons, and also instruct for merges, splits and lane changes of platoons.
- The platoon controllers receive commands from the roadside controllers and are concerned with executing the inter-platoon and intra-platoon maneuvers.
- The vehicle controllers receive commands from the platoon controllers and translate these commands into control signals for the vehicle actuators such as throttle, braking, and steering actions.

4 Conclusion and Future Research

We have proposed a framework that combines IV-based measures and roadside infrastructure for implementing a next-level traffic management. Future research includes determining appropriate traffic models for this IV-based framework, defining the benchmarks, and implementing this framework on a small-scale setup.

Acknowledgement: This research is supported by STW-VIDI project "Multi-Agent Control of Large-Scale Hybrid Systems", BSIK TRANSUMO, and the Transport Research Center Delft.

References

- [1] R. Bishop. *Intelligent Vehicles Technology and Trends*. Artech House, 2005.
- [2] P. Varaiya. Smart cars on smart roads. *IEEE Transactions on Automatic Control*, 38(2):195–207, February 1993.

Stabilization of Collective Motion in Three Dimensions

L. Scardovi and R. Sepulchre

Department of Electrical Engineering and Computer Science, University of Liège, Belgium

{l.scardovi, r.sepulchre}@ulg.ac.be¹

1 Introduction

In recent years particular attention has been devoted to the design of control laws for the coordination of a group of autonomous systems. Applications include sensor networks, where a group of autonomous agents has to collect information about a process by choosing maximally informative samples, and formation control of autonomous vehicles (e.g. unmanned aerial vehicles). In these contexts it is relevant to consider the case where the ambient space is the three-dimensional Euclidean space.

In this work we address the problem of designing control laws to stabilize motion patterns in a model of identical particles moving at unit speed in three-dimensional Euclidean space. If the control law is a feedback function of *shape* quantities (i.e. relative frame orientations and relative positions), the closed loop vector field is invariant under the action of the symmetry group $SE(3)$. The resulting closed loop dynamics evolve in a quotient manifold called *shape space* and the equilibria of the reduced dynamics are called *relative equilibria*. Relative equilibria of the model have been characterized in [3]. The equilibria are of three types: parallel motion, the particles move in the same direction with arbitrary relative positions; circular motion, the particles draw circles with the same radius and in planes orthogonal to the same axis of rotation; helical motion, the particles draw circular helices with the same radius, pitch, axis and axial direction of motion.

2 Contribution

This work builds on previous works on planar formation control laws [4, 5] extending the main results to the three-dimensional setting. First we consider the case of all-to-all communication among the agents, and we derive a (static) control law which uses only measurements about relative positions and orientations of the other agents. All-to-all communication is an assumption that is often unrealistic in multi-agent systems. In particular, in a network of moving agents, some of the existing communication links can fail and new links can appear when other agents enter in an effective range of detection. To adapt the all-to-all feedback design in presence of limited communication, we use the approach recently proposed in [1, 2]. We replace the average quantities often required in a collective optimization

algorithm by local estimates provided by a consensus estimator. On the bases of these results we design control laws that globally stabilize collective motion patterns under mild assumptions on the communication topology.

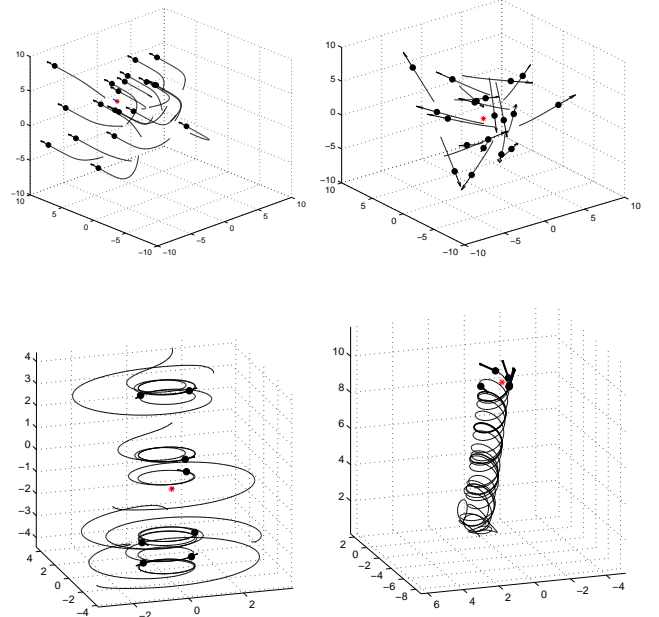


Figure 1: Formations stabilized with the proposed control laws.

References

- [1] L. Scardovi, A. Sarlette, and R. Sepulchre, “Synchronization and Balancing on the N -Torus,” to appear in *Systems and Control Letters*, 2006.
- [2] L. Scardovi and R. Sepulchre, “Collective optimization over average quantities,” to appear in *Proc. of the 45th IEEE Conference on Decision and Control*, San Diego, Ca, 2006, pp. 3369–3374.
- [3] E. W. Justh and P. S. Krishnaprasad, “Natural frames and interacting particles in three dimensions,” in *Proc. of the 44th IEEE Conference on Decision and Control and European Control Conference*, Seville, Spain, 2005, pp. 2841–2846.
- [4] R. Sepulchre, D. Paley, and N. Leonard, “Stabilization of planar collective motion with all-to-all communication,” accepted for publication in *IEEE Trans. on Automatic Control*.
- [5] ——, “Stabilization of planar collective motion with limited communication,” *IEEE Trans. on Automatic Control*, 2006, submitted.

¹This paper presents research results that are, in part, of the Belgian Programme on Interuniversity Attraction Poles, initiated by the Belgian Federal Science Policy Office. The scientific responsibility rests with its authors.

Time-varying delays in Networked Control Systems¹

Marieke Cloosterman, Nathan van de Wouw and Henk Nijmeijer
 Mechanical Engineering, Dynamics and Control
 Technische Universiteit Eindhoven
 P.O. Box 513, 5600 MB Eindhoven
 the Netherlands
 Email: m.b.g.cloosterman@tue.nl

1 Introduction

In high-tech systems design, couplings between the domains of control engineering and real-time software need to be considered. Here, we focus on the coupling between the latency and jitter in the real-time software, i.e. time-delay in control terms, and the stability of the controlled system. It is well known that time-delays can destabilize the system. In the area of Networked Control Systems (NCSs) [3] time-varying delays occur due to the use of a communication network. Here, we propose a stability test for NCSs with time-varying delays.

2 Networked Control Systems

An NCS consists of a continuous-time plant that is coupled to a discrete-time controller over a communication network:

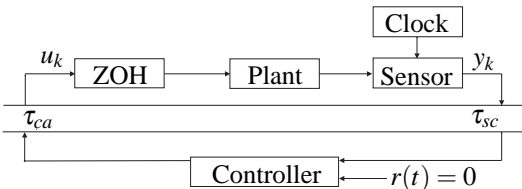


Figure 1: Schematic overview of an NCS.

The total time-delay consists of the computation time and the communication delays, i.e. the sensor-to-controller delay τ_{sc} and the controller-to-actuator τ_{ca} delay. Under the assumption that the controller and actuator act event-driven and that the sensor acts time-driven, these three time-delays can be lumped together into one delay.

The linear discrete-time model of an NCS, with a state-feedback controller $u_k = -Kx_k$, is given by $\xi_{k+1} = \tilde{A}(\tau_k)\xi_k$.

3 Robust Stability

Two different stability tests to guarantee robust asymptotic stability are proposed, based on a convex overapproximation of the matrix \tilde{A} . Method 1 [1] is based on interval matrix theorems. Method 2 [2] is based on the Jordan Canonical Form of the continuous-time system matrix A . For both cases, a set of LMIs is defined that

guarantees robust stability for time-varying delays that satisfy $\tau_k \in [0, \tau_{max}]$, with $\tau_{max} \leq h$. As an example, the following motor-pinch model is used: $\dot{x}_s = \frac{n r_P}{J_M + n^2 J_P} u$, with $J_M = 1.95 \cdot 10^{-5} \text{ kgm}^2$, $J_P = 6.5 \cdot 10^{-5} \text{ kgm}^2$ the inertia of the motor and pinch, $r_P = 14 \text{ mm}$ the radius of the pinch, $n = 0.2$ the transmission ratio between motor and pinch, x_s the sheet position and u the motor torque. The obtained stabilizing controllers for constant delays and robustly stabilizing controllers for time-varying delays are given in Figure 2 for $h = 1 \text{ ms}$ and $K = (50 \quad K_2)$. It is obvious that Method 2 is less conservative.

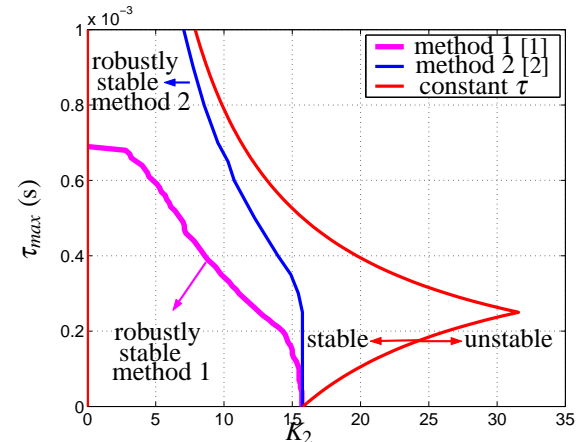


Figure 2: Stabilizing controller gains for $\tau_k \in [0, \tau_{max}]$ and constant delays τ_{max} .

References

- [1] M. Cloosterman, N. v.d. Wouw, M. Heemels and H. Nijmeijer, "Robust Stability of Networked Control Systems with Time-varying Network-induced Delays," in Proc. of the 45th Conference on Decision and Control, San Diego, USA, 2006, pp. 4980-4985.
- [2] M. Cloosterman, N. v.d. Wouw, M. Heemels and H. Nijmeijer, "Robust control of Networked Control Systems with uncertain time-varying delays", DCT internal report 2006-121, Technische Universiteit Eindhoven, the Netherlands, 2006.
- [3] B. W. Zhang, M.S. Branicky and S.M. Phillips, "Stability of Networked Control Systems," IEEE Control Systems Magazine vol. 21, pp. 84-99, 2001.

¹This work has been carried out as part of the Broderc project under the responsibility of the Embedded Systems Institute. This project is partially supported by the Netherlands Ministry of Economic Affairs under the Senter TS program.

Why must the brain take into account the eyes translations during active head movements ?

Daye Pierre
CESAME, UCL, Belgium
daye@inma.ucl.ac.be

Wertz, Vincent
CESAME, UCL, Belgium
wertz@inma.ucl.ac.be

Lefèvre, Philippe
CESAME, UCL, Belgium
Philippe.Lefevre@UCLouvain.be

1 Introduction

Depending on the size of the explored area and the oculomotor range, foveate mammals need to combine head movements with eyes movements to catch information about their surrounding environment [1].

Classically, the study of the orientation of the visual axis (i.e. gaze orientation) was first based on eye-only movements. This implies that only the eyes angular orientations were needed to characterize eyes movements. Later, studies on eye-head coordination applied the same principles of angular orientations to characterize gaze movements. However, because the eyes centers of rotation and the head center of rotation are not the same, a rotation of the head implies a translation of the eyes centers of rotation.

If \vec{H}_s corresponds to the dual-vector (see [2] for a description of dual-vector applied to kinematics calculations) representing the position and orientation of the head with respect to an inertial frame and if \vec{E}_h corresponds to the dual-vector representing the position and orientation of an eye with respect to a frame linked to the head, the gaze can be computed as in (1).

$$\vec{G} = \vec{E}_s = \vec{H}_s + \vec{E}_h \quad (1)$$

From this equation, one can see that the gaze is the position and orientation of the eye in space (\vec{E}_s).

Depending the eye position measuring apparatus, the acquired data can estimate the orientation of \vec{E}_s (with a search coil [3]) or the orientation of \vec{E}_h (for a video-based eye tracking). In the literature, the head position is represented by the movement of three non-collinear points fixed to the head [4] or with a coil firmly fixed to the head [1].

Because (1) is a dual-vector equation, the sum of the two dual-vectors can only be perform if these dual-vectors are expressed in the same frame. Nevertheless, it is common in the specialized literature to compute \vec{E}_h as a **scalar** difference between \vec{H}_s and \vec{E}_s which is an assumption equivalent to saying that there is no translation of the eyes center of rotation due to a head rotation.

Our study assessed the necessity to use a more complex model in eye-head coordination research to incorporate the eyes centers of rotation translations to be closer to a model that is used by the brain.

2 Method

Therefore, we conducted simulations to test the measurement sensitivity to the relative position of the eyes center compared to the head center when a subject fixates a stationary target and moves his/her head.

Three gaze models were used. The first is the commonly used model where the head and the eyes centers of rotation are the same and remain fixed, the second one takes into account the distance between the two centers of rotation and the third one incorporates the bending of the spine [5]. First, the gaze movement was simulated as a pure horizontal movement (like [1]). Then we simulated a vertical movement and finally the study incorporated a more complex 2D movement.

3 Results and discussion

The simulations demonstrate the importance of knowing the measuring apparatus sensitivity and give information on the precision of measures in a head free experiment.

If the gaze control system does not account for the translations of the eyes center of rotation, we show with simulations that this generates an error when pointing to an object, which is in contradiction with the observed behavior in real experiments.

References

- [1] J.S. Stahl. Amplitude of human head movements associated with horizontal saccades. *Experimental Brain Research*, 126:41–54, 1999.
- [2] I.S. Fisher. *Dual-Number methods in kinematics, statics and dynamics*. CRC Press, 1999.
- [3] D.A. Robinson. A Method of Measuring Eye Movement Using a Scleral Search Coil in a Magnetic Field. *IEEE Trans Biomed. Eng*, BME-10:137–145, 1963.
- [4] R. Ronsse, O. White, and P. Lefèvre. Computation of gaze orientation under unrestrained head movements. *Journal of Neuroscience Methods*, 159:158–169, 2007.
- [5] N. Bourdet, R. Willinger, and F. Le Gall. Analysis of the modal behavior of the head-neck system in vivo. In *Colloque TILT, Lille*, 2003.

Effects of a recently discovered voltage-dependent current on the electrical activity of midbrain dopaminergic neurons: modeling and experiments

Maxime Bonjean

Cyclotron Medical Research Center,
School of Medicine
& Systems and Modeling Research Unit
University of Liège
m.bonjean@ulg.ac.be

Olivier Waroux & Vincent Seutin

Center for Cellular and Molecular
Neurobiology Center
School of Medicine
University of Liège
v.seutin@ulg.ac.be

Rodolphe Sepulchre

Systems and Modeling Research Unit
Montefiore Institute
School of Engineering
University of Liège
r.sepulchre@ulg.ac.be

1 Introduction

The function of midbrain dopaminergic (DA) systems is implicated in various illness such as Parkinson diseases, schizophrenia and drug abuse. In physiological condition, DA neurons can switch between tonic, irregular, and burst firing. Because burst firing increases the amount of released dopamine, a lot of effort has been devoted to unraveling the mechanisms underlying the switch between these firing patterns. Both experimental and modeling approaches have suggested that burst firing requires a glutamatergic input, a reduced GABA_A input, and a reduced opening of small-conductance K⁺-activated channels [1, 2]. Very recently, a new type of K⁺-current, namely a M-type current [3] has been found in these neurons [4, 5]. However, the effect of this current on the electrical activity on DA neurons is currently unknown. In this study, we aim to address this issue using both experiments and modeling.

2 Experiments

Extracellular single-cell recordings combined with drug iontophoresis are performed on chloralhydrate anesthetized male Wistar rats. Burst firing is induced by iontophoresing a SK blocker onto dopaminergic neurons. The M-current is blocked by injected the KCNQ blocker (XE-991) intravenously.

3 Modeling

The specific anatomical morphology of DA neurons – aspiny and sparsely branched with three to six primary dendrites – is described in a realistic three-compartment model including soma, proximal, and distal dendrites. We embed the model in Fig. 1 with few modifications, where all compartments include a fast Na⁺ current, a delayed rectifier K⁺ channel, a transient outward K⁺ current, a leak current, and a sodium pump. The soma compartment is also modeled with specific Ca²⁺ currents and pump, as well as a SK channel current. Glutamatergic (AMPA and NMDA) and GABAergic synaptic currents are also included. Each spe-

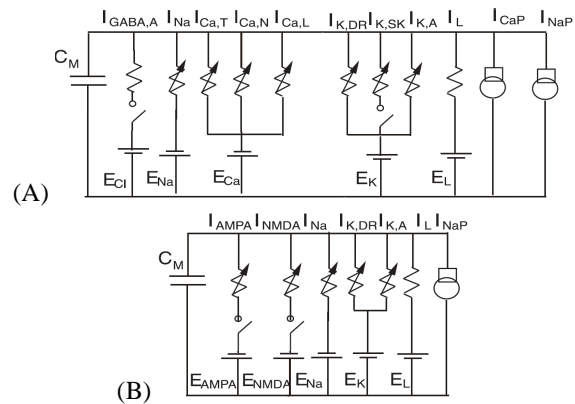


Figure 1: Schematic representation of the model (Adapt. [1]).

cific compartment is described with a set of nonlinear partial differential equations condensed in

$$C_m \frac{\partial V}{\partial t} = \left(- \sum i_m + \frac{1}{r_a} \frac{\partial^2 V}{\partial x^2} \right),$$

where C_m is the neuron membrane capacitance, $\sum i_m$ is the sum of the applicable membrane currents, and $1/r_a$ is the axial conductance.

References

- [1] C. Canavier, R. Landry *An Increase in AMPA and a Decrease in SK Conductance Increase Burst Firing by Different Mechanisms in a Model of a Dopamine Neuron In Vivo*, *J. Neurophysiol.*, 96:2549–2563, 2006.
- [2] O. Waroux, et al., *SK channels control the firing pattern of midbrain dopaminergic neurons in vivo*, *E. J. Neurosci.*, 22, 2005.
- [3] P. Delmas, D. A Brown, *Pathways Modulating Neural KCNQ/M (Kv7) Potassium Channels*, *Nature*, 6, 850–862
- [4] S. Koyama, S. Appel, *Characterization of M-current in Ventral Tegmental Area Dopamine Neurons*, *J. Neurophys.*, 96, 2006.
- [5] H. Hansen, et al., *The KCNQ Channel Opener Retigabine Inhibits the Activity of Mesencephalic Dopaminergic Systems of the Rat*, *J. Pharmacol.*, 318(3):1006–1019, 2006

Actigraphy as a way of distinguishing sleep from wake

Tilmanne Joëlle

TCTS Lab

Faculté Polytechnique de Mons, Belgium
joelle.tilmanne@fpms.ac.be

Kothare Mayuresh V.
Chemical Engineering Department
Lehigh University, Bethlehem, PA, U.S.A.

Kothare Sanjeev V.
St Christopher's Hospital for Children
Philadelphia, PA, U.S.A.

Urbain Jérôme

TCTS Lab

Faculté Polytechnique de Mons, Belgium
jerome.urbain@fpms.ac.be

Vande Wouwer Alain
Automatic Control Lab
Faculté Polytechnique de Mons, Belgium

Due to the drawbacks associated with the gold standard, polysomnography (PSG), which is used to study quality of sleep, there is a need for other tools in the sleep medicine field. Actigraphy is a very promising alternative which is made possible due to devices called actimeters. An actimeter is a device of about the size of a wrist-watch which records the patient's movements in everyday life conditions.

The objective of our work is to develop algorithms for automatic sleep/wake scoring using only the actigraphic signal. The database used is composed of 354 nights of recordings of infants aged less than one year. Those recordings have been performed between 1994 and 1998 in the context of the Collaborative Infant Home Monitoring Evaluation (CHIME) study. For each night, the actigraphic signal, the PSG recording, and the reference scoring (based on PSG and behavioral observations done by professional sleep technicians) are available. The measures used to evaluate the performance of our algorithms are the accuracy (ability to score properly each 30- second epoch), the sensitivity (ability to detect sleep) and the specificity (ability to detect wake). These performance measures have been evaluated on epochs different from those used to optimize the algorithms, according to the cross-validation principle.

First, we studied algorithms developed by Sadeh et al. [1] and by Sazonov et al. [2]. These algorithms are linear combinations of features calculated for each epoch. After optimization on the basis of our data, Sadeh's algorithm gives an accuracy of 78.9%, a sensitivity of 93.7% and a specificity of 43.8%, and the performance measures of Sazonov's algorithm are respectively 78.3%, 94.9% and 39%. At the cost of a slight diminution of accuracy, we obtain better trade-offs between sensitivity and specificity by changing the cost function used during the optimization of the algorithm (for example 75.7% of accuracy, 83.4% of sensitivity and 57.5% of specificity with Sazonov's algorithm).

Secondly, we developed two new algorithms, using methods which are very common for classification tasks but novel

in actigraphy: neural networks and decision trees. These two methods can model the optimal classification border if they are accurately trained, even if that border is non-linear. This an innovation in the actigraphic field where classification algorithms developed to-date are linear combinations of parameters, apart from one algorithm using Kohonen's self-organizing map, a special kind of neural networks [2].

In order to apply these techniques, we carried out a feature selection to choose the most discriminant ones using Fisher's discriminant analysis. These methods significantly improve the classification performance. Neural networks give an accuracy of 80.5%, a sensitivity of 92.5%, and a specificity of 52%. With decision trees, these measures respectively reach 82.1%, 92.2% and 58.1%. Once again the trade-offs between sensitivity and specificity are quite bad. To overcome this problem, we proposed to increase the proportion of epochs scored as wake in the training database, which gave among others 80.5% of accuracy, 83.9% of sensitivity, and 72.2% of specificity with decision trees.

The results obtained in this study are satisfying and promising: the recent actimeters being much more advanced compared to those used in the CHIME study, the combination of these new sensors with neural networks or decision trees gives hope for an additional improvement of the results, and may provide a new perspective for actigraphic scoring.

Acknowledgements

The authors gratefully acknowledge the support of the Belgian Program on Interuniversity Poles of Attraction, initiated by the Belgian Federal Science Policy Office.

References

- [1] A. Sadeh, K. M. Sharkey and M. A. Carskadon, "Activity-Based Sleep-Wake Identification: An Empirical Test of Methodological Issues", *Sleep*, 17(3):201-207, 1994.
- [2] E. Sazonov, N. Sazonova, S. Schuckers, M. Neuman and CHIME study group, "Activity-based sleep-wake Identification in Infants", *Physiological Measurements*, 25:1291-1304, 2004.

A System Identification Approach to Kinetic Modeling of Metabolic Networks of Eukaryotic Cells from Experimental Data

J. Shi^{1,2}, A.J. den Dekker¹, P.T.J. Verheijen², W.A. van Winden²,
M. Verhaegen¹, and J.J. Heijnen²

¹ Delft Center for Systems and Control, Delft University of Technology

² Kluyver Laboratory for Biotechnology, Delft University of Technology

Email: {jing.shi, a.j.dendekker, P.J.T.Verheijen, W.A.vanWinden, m.h.g.verhaegen, J.J.Heijnen} @tudelft.nl

1 Introduction

Over the past decades, a number of mathematical models have been published that give a detailed kinetic description of metabolic pathways. Considering the complexity of these models that only describe a very limited subset of the intracellular metabolic reactions and that do not even touch upon the genetic control structures that govern the reaction capacities *in vivo*, it is clear that a detailed modeling approach is infeasible for full-scale cell models. The Bioprocess Technology group of TU Delft has recently developed an approximate kinetic format that aims at giving a satisfactory description of cell dynamics whilst keeping the number of kinetic parameters and mathematical complexity as limited as possible. This so-called 'linear-logarithmic' (from here on: 'linlog') format [3,4], has the attractive property that its parameters are directly interpretable using the well established metabolic control analysis theory. Moreover, the uniform mathematical structure of the employed equations allows steady state solutions of the models, which allows the straightforward use of the models in microbial redesign.

2 LinLog Model

The linlog description of the dynamic behavior of a metabolic network is given by the following differential equation:

$$\frac{dx(t)}{dt} = S \cdot \text{diag}(J^0) \cdot \text{diag}\left(\frac{e(t)}{e^0}\right) \cdot \left(I + E_X \ln\left(\frac{x(t)}{x^0}\right) + E_C \ln\left(\frac{c(t)}{c^0}\right)\right),$$

where $x(t)$ is vector of concentrations of the internal metabolites at time instance t , $e(t)$ a vector of concentrations of the enzymes that catalyze the different reactions in the metabolic network, and $c(t)$ a vector of concentrations of extracellular effectors. The vectors $e(t)$,

$x(t)$ and $c(t)$ have been normalized with respect to a reference steady-state ($e^0; x^0; c^0$) with corresponding flux J^0 . And the matrix S is called the stoichiometry matrix. Typically, not all metabolite concentrations are measured during experiments. To take that into account we can add the following measurement equation:

$$y(t) = Mx(t)$$

Where the matrix M indicates which metabolite concentrations are measured.

3 Goal

Taking a closer look at these equations, we recognize a dynamical state-space model, in which the metabolite concentrations $x(t)$ form the state vector. The proposed linlog format is in fact a nonlinear state-space system with a particular structure. Thus the main goal of this research is the development of system identification techniques[1,2] for dynamical models of a metabolic network that can be described by this Linlog model.

Acknowledgements: This research is sponsored by Delft Centre for Life Science & Technology

References

- [1]V. Verdult and M. Verhaegen. "Subspace identification of multivariable linear parameter-varying systems". *Automatica*, 38(5):805–814, 2002.
- [2]V. Verdult, L. Ljung, and M. Verhaegen. "Identification of composite local linear state-space models using a projected gradient search". *International Journal of Control*, 75(16/17):1385–1398, 2002.
- [3]D. Visser and J. J. Heijnen. "Dynamic simulation and metabolic re-design of a branched pathway using linlog kinetics". *Metabolic Engineering*, 5(3):164–176, July 2003.
- [4]L. Wu, W. M. Wang, W. A. van Winden, W. M. van Gulik, and J. J. Heijnen. "A new framework for the estimation of control parameters in metabolic pathways using lin-log kinetics". *European Journal of Biochemistry*, 271(16):3348–3359, 2004.

Adaptive ‘minimal’ model for glycemia control in critically ill patients

Tom Van Herpe, Greet Van den Berghe and Bart De Moor

Katholieke Universiteit Leuven, Department of Electrical Engineering (ESAT), SCD-SISTA,

Kasteelpark Arenberg 10, B-3001 Leuven (Heverlee), Belgium

Email: {tom.vanherpe, bart.demoor}@esat.kuleuven.be,

greta.vandenbergh@med.kuleuven.be

1 Introduction

Insulin resistance and associated hyperglycemia (i.e., an increased glucose concentration in the blood) are common in critically ill patients (who are typically admitted to an intensive care unit (ICU)). It is shown that glycemia normalization (between 80 and 110 mg/dl, by means of rigorous administration of insulin) results in a spectacular mortality and morbidity rate reduction in comparison with the conventional insulin therapy in which insulin is only administered if glycemia exceeds 215 mg/dl [3, 2]. The use of a predictive control system to normalize glycemia (semi-) automatically has the potential to reduce workload for medical staff and to further reduce mortality and morbidity [4]. In this study a physical model structure used for predicting glycemia and a model re-estimation strategy are presented.

2 The ICU minimal model (ICU-MM)

The presented model structure originates from the known *minimal* model that was developed by Bergman et al. [1]. In [5] the original minimal model was extended to the ICU minimal model (ICU-MM) by taking into consideration some features typical of ICU patients. Due to the large inter and intra patient variability, the implementation of an adaptive estimation strategy is crucial for accurately predicting glycemia [4]. In this study a *relaxation* of the ICU-MM is estimated by using a real-life clinical ICU dataset (19 ventilated adult patients who were admitted to the surgical ICU). The first 24 hours are considered as initial estimation set. Next, the model is re-estimated every hour for the rest of each patient’s dataset. The number of recent data that are considered in each re-estimation process is called the Back-In-Time (BIT) number. The model performance for each patient is measured by computing the mean squared error (MSE) and the mean percentage error (MPE).

The optimal BIT is found to be 4 because of the smallest MSEs and MPEs in that case (see Figure 1). This indicates that it is advised to incorporate only the data of the last four hours in the re-estimation process of the ICU-MM. The average MSE (std-dev) and average MPE (std-dev) that is obtained when applying this ‘optimal’ re-estimation strategy to the present data are 172.3 mg²/dl² (148.2 mg²/dl²) and 8.5% (3.6%), respectively.

3 Conclusion

In this study we present an optimized adaptive ‘minimal’ modeling approach for predicting glycemia of critically ill

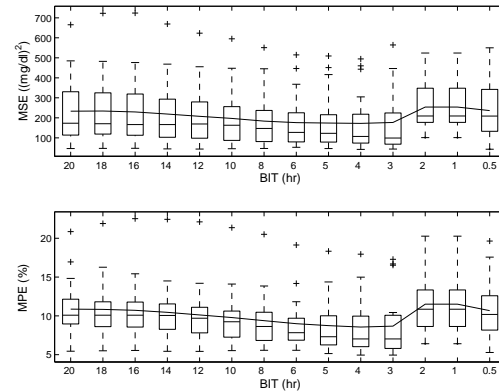


Figure 1: Distribution of the MSEs (top panel) and MPEs (bottom panel), generated for each patient and presented as a function of BIT. The ICU-MM is re-estimated every hour. The line connects the averages of the MSEs and the MPEs.

patients. The optimal size of the dataset to be considered in each re-estimation process is found to be four hours and results in clinically acceptable prediction errors. Future work is focused on the implementation of the re-estimation strategy in the design of a model based predictive controller.

References

- [1] R.N. Bergman, L.S. Phillips, and C. Cobelli. Physiologic evaluation of factors controlling glucose tolerance in man: measurement of insulin sensitivity and beta-cell glucose sensitivity from the response to intravenous glucose. *J Clin Invest*, 68(6):1456–1467, Dec 1981.
- [2] G. Van den Berghe, A. Wilmer, G. Hermans, W. Meersseman, P.J. Wouters, I. Milants, E. Van Wijngaerden, H. Bobbaers, and R. Bouillon. Intensive insulin therapy in the medical ICU. *N Engl J Med*, 354(5):449–461, Feb 2006.
- [3] G. Van den Berghe, P. Wouters, F. Weekers, C. Verwaest, F. Bruyninckx, M. Schetz, D. Vlaeselaers, P. Ferdinandse, P. Lauwers, and R. Bouillon. Intensive insulin therapy in the critically ill patients. *N Engl J Med*, 345(19):1359–1367, Nov 2001. Clinical Trial.
- [4] T. Van Herpe, M. Espinoza, B. Pluymers, I. Goethals, P. Wouters, G. Van den Berghe, and B. De Moor. An adaptive input-output modeling approach for predicting the glycemia of critically ill patients. *Physiol Meas*, 27(11):1057–1069, Nov 2006.
- [5] T. Van Herpe, B. Pluymers, M. Espinoza, G. Van den Berghe, and B. De Moor. A minimal model for glycemia control in critically ill patients. In *Proc. of the 28th IEEE EMBS Annual International Conference (EMBC 06)*, pages 5432–5435, 2006.

Acknowledgements

Tom Van Herpe is a research assistant at the Katholieke Universiteit Leuven. Greet Van den Berghe holds an unrestricted Katholieke Universiteit Leuven Novo Nordisk Chair of Research. Bart De Moor and Greet Van den Berghe are full professors at the Katholieke Universiteit Leuven, Belgium. KUL research is supported by Research Council KUL: GOA AMBioRICS, CoE EF/05/006, several PhD/postdoc & fellow grants; Flemish Government: FWO: projects, G.0407.02, G.0197.02, G.0141.03, G.0491.03, G.0120.03, G.0452.04, G.0499.04, G.0211.05, G.0226.06, G.0321.06, G.0302.07; IWT: PhD Grants, McKnow-E, Eureka-Flite2; Belgian Federal Science Policy Office: IUAP P5/22; EU: ERNSI;

Contact structures: a tool for modeling and analyzing thermodynamical systems

Audrey Favache, Denis Dochain
 IMAP, Université catholique de Louvain
 1348 Louvain-la-Neuve (Belgium)
 audrey.favache@uclouvain.be

Bernhard Maschke
 LAGEP, Université Claude Bernard, Lyon 1
 69622 Villeurbanne (France)

1 Introduction

Thermodynamical systems are a class of systems that allow to represent devices in which chemical reactions and heat exchange take place. But the dynamics of such systems are often non-linear. Abstract mathematical tools are needed to represent and analyze such non-linear systems. Those tools, like for example passivity storage functions or Lyapunov functions are abstract concepts. The aim is to link those abstract concepts to the physics of the system.

For electro-mechanical systems this has been done through their Hamiltonian formulation: total energy has been used as Lyapunov function or for passivity analysis. But in thermodynamic systems irreversible phenomena occur that prevents from extending results from electro-mechanics to thermodynamics.

Contact structures are concepts from differential geometry that allow to describe the possible states of thermodynamic systems. They are directly linked to Gibbs's relation and to the first principle of thermodynamics, i.e. the conservation of energy. The dynamics of such a system can be represented by a contact vector field. These tools have been introduced by R. Mrugała ([1]) and Chen ([2]). Eberard et al. have shown how Hamiltonian systems can also be expressed in this formalism ([3], [4]).

The aim of this work is to apply this formalism to physical systems. The link is made between the physical phenomena, and more particularly the energy and matter fluxes. This will be illustrated by some simple examples. Finally this formalism will be integrated in a network approach for the modeling and analysis of more complex systems.

2 Differential geometry for modeling thermodynamics

The state of a thermodynamic system can be represented via some physical quantities: internal energy U , volume V , entropy S , number of moles of each component n , pressure P , temperature T and chemical potential of each species μ . These quantities are not independent and have to respect Gibbs's relation which can be written on the following way:

$$dS - \frac{1}{T}dU - \frac{P}{T}dV + \frac{\mu^T}{T}dn = 0$$

This means that the possible states are on a Legendre manifold with the entropy function $S(U, V, n)$ as one of the pos-

sible generating functions.

The dynamics are expressed by a contact vector field generated by a contact Hamiltonian function. This contact Hamiltonian function can be related to the expression of the physical phenomena that are taking place. The contact Hamiltonian function of interconnected systems can be obtained directly from the contact Hamiltonian function of the more simple subsystems.

3 System analysis

All the information about the behaviour of the system are contained in two functions: the generating function of the Legendre submanifold on one hand, and the contact Hamiltonian function on the other hand. The analysis of these two functions can give us information about steady states, stability, passivity...

4 Acknowledgments

This paper presents research results of the Belgian Programme on Interuniversity Attraction Poles, initiated by the Belgian State, Prime Ministers Office for Science, Technology and Culture. The scientific responsibility rests with its authors. The work of A. Favache is funded by a grant of aspirant of Fonds National de la Recherche Scientifique (Belgium). Exchanges with the LAGEP (Université Claude Bernard, Lyon, France) have been supported by the project Tournesol of the Communauté française de Belgique.

References

- [1] R. Mrugała, "Continuous contact transformations in thermodynamics," *Reports on Mathematical Physics*, vol. 33, pp. 149–154, 1993.
- [2] M. Chen, "On the geometric structure of thermodynamics," *Journal of Mathematical Physics*, vol. 40, pp. 830–837, 1999.
- [3] D. Eberard, B. Maschke, and A. van der Schaft, "Port contact systems for irreversible thermodynamical systems," in *44th IEEE Conference on Decision and Control and European control Conference*, Sevilla, Spain, December 2005.
- [4] D. Eberard, B. Maschke, and A. van der Schaft, "On the interconnection structures of open physical systems," in *3rd IFAC Workshop on Lagrangian and Hamiltonian methods for non-linear control*, Nagoya (Japan), July 2006.

Growth rate of a switched homogeneous system

S. Emre Tuna

Montefiore Institute, University of Liege, Belgium

tuna@montefiore.ulg.ac.be

1 Switched linear systems and joint spectral radius

A discrete-time switched linear system is described by

$$x_{k+1} = A_q x_k \quad \text{for } q \in \{1, 2, \dots, \bar{q}\} \quad (1)$$

where at each time k , the switching index q arbitrarily chooses a matrix A_q from a finite set of matrices $\{A_1, A_2, \dots, A_{\bar{q}}\}$. For system (1) one can always find some $\sigma \geq 0$ and $M \geq 1$ such that all possible trajectories satisfy

$$|x_k| \leq M\sigma^k|x_0| \quad (2)$$

for all k . More interesting and significantly harder is to find the infimum of all such σ for which there exists some M and (2) is satisfied. That infimum happens to equal the joint spectral radius (JSR) of the set of matrices $\{A_1, A_2, \dots, A_{\bar{q}}\}$.

Switched linear systems appear in numerous applications and in most of those applications, essential is the following question: *Do all of the trajectories of the system converge to the origin?* The answer is affirmative if (and only if) the JSR of the set of matrices is strictly less than unity. Apart from being an indicator of asymptotic stability, JSR is still important to know since it constitutes a bound on the rate of convergence (divergence) of the trajectories.

2 Switched homogeneous systems and growth rate

A superclass of switched linear systems is the class of switched homogeneous systems, described by

$$x_{k+1} = \Lambda_q(x_k) \quad (3)$$

where each Λ_q is homogeneous, i.e. $\Lambda_q(\lambda x) = \lambda \Lambda_q(x)$ for all $\lambda \geq 0$. In addition to being interesting on their own right, homogeneous systems also may appear as better approximations to certain nonlinear systems than linear systems do. Like in linear case, one observes that the trajectories of (3) satisfy (2) for some (M, σ) pair and that all trajectories converge to the origin if (and only if) the infimum of all such σ is strictly less than unity. That infimum is called the *(maximum) growth rate* of system (3).

3 An algorithm to approximate growth rate

Most, if not all, of the algorithms approximating JSR of a switched linear system make use of the linearity in a way

that cannot be extended to the more general case of homogeneous systems. Namely, such algorithms involve computing eigenvalues or singular values of matrices generated out of A_q 's of (1). Hence a different approach is necessary to compute/approximate the growth rate of a homogeneous system. One quite beneficial aspect of homogeneous systems is that the global behaviour can trivially be reconstructed from local through scaling. To be precise, for each trajectory, there is a scaled trajectory starting on the unit ball. Using that fact along with time-invariance, one can rearrange (3) as

$$\begin{aligned} \eta_{k+1} &= \frac{\Lambda_q(\eta_k)}{|\Lambda_q(\eta_k)|}, & \eta_0 &= \frac{x_0}{|x_0|} \\ \lambda_{k+1} &= |\Lambda_q(\eta_k)|\lambda_k, & \lambda_0 &= |x_0|. \end{aligned} \quad (4)$$

Note then that $|\eta_k| = 1$ for all k and $x_k = \lambda_k \eta_k$. The key observation at this point is the following

$$\text{growth rate} = \sup_{\substack{\text{over all possible} \\ \text{sequences } \{\lambda_k\}}} \limsup_{k \rightarrow \infty} \lambda_k^{1/k}. \quad (5)$$

Eq. (5) suggests an approximation algorithm where the unit ball is discretized into a grid of finitely many points and an approximation of the system (4) that evolves on a finite graph is considered. When sequences of $\{\lambda_k\}$ are generated by this approximate system to compute the growth rate, principle of optimality can be used to prevent computing all possible sequences and only the “worst” ones can be considered instead. This means that the number of sequences of length N to be considered depends linearly on N instead of exponentially. The proposed algorithm gives an upper-bound on the growth rate of system (3). That upperbound can be shown to converge to the actual growth rate as the grid becomes finer. The algorithm also makes a new option for computing JSR of switched linear systems.

References

- [1] S.E. Tuna, “Optimal regulation of homogeneous systems,” *Automatica*, 41(11), pp. 1879-1890, 2005.
- [2] V.D. Blondel and Y. Nesterov, “Computationally efficient approximations of the joint spectral radius,” *SIAM J. Matrix Anal. Appl.*, 27(1), pp. 256-272, 2005.
- [3] D. Liberzon and A.S. Morse, “Basic problems in stability and design of switched systems,” *IEEE Control Systems Magazine* 19(10), pp. 59-70, 1999.

On the Circle Criterion for Feedback Systems with both Unbounded Observation and Control

Piotr Grabowski

Institute of Automatics, AGH University of Science and Technology, PL-30-059 Cracow, Poland
pgrab@ia.agh.edu.pl

Frank M. Callier

Department of Mathematics, University of Namur (FUNDP), B-5000 Namur, Belgium
frank.callier@fundp.ac.be

1 Abstract

A Lur'e feedback control system consisting of a linear, infinite-dimensional system of boundary control in factor form and a nonlinear static sector type controller is considered. A criterion of absolute strong asymptotic stability of the null equilibrium is obtained using a quadratic form Lyapunov functional. The construction of such a functional is reduced to solving a Lur'e system of equations. A sufficient strict circle criterion of solvability of the latter is found, which is based on results by J.C. Oostveen and R.F. Curtain [4]. The paper uses extensively the philosophy of reciprocal systems with bounded generating operators as recently studied by R.F. Curtain in e.g. [1].

2 Some More Detail

This paper reports the main results of the circle criterion paper [3]. We consider a Lur'e feedback system as in Figure 1

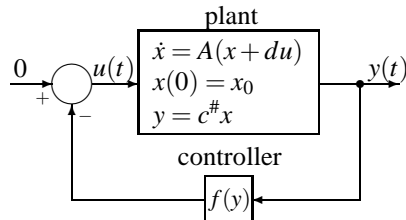


Figure 1: The Lur'e feedback system

▷ SISO linear plant described by

$$\left\{ \begin{array}{l} \dot{x}(t) = A[x(t) + du(t)] \\ y(t) = c^\#x(t) \end{array} \right\}, \quad (1)$$

▷ Static scalar controller nonlinearity described by $f(y)$.

The linear plant is subject to the following assumptions:

- $A : (\mathcal{D}(A) \subset H) \rightarrow H$ generates a linear exponentially stable (EXS), C_0 -semigroup $\{S(t)\}_{t \geq 0}$ on a Hilbert space H with a scalar product $\langle \cdot, \cdot \rangle_H$.

- y is a scalar output defined by a linear observation functional $c^\#$, with $\mathcal{D}(A) \subset \mathcal{D}(c^\#)$ which is A -bounded (i.e. bounded on \mathcal{D}_A , i.e. the space $\mathcal{D}(A)$ equipped with the graph norm of A , here equivalent to $\|x\|_A := \|Ax\|_H$). The restriction of $c^\#$ to $\mathcal{D}(A)$ is representable as $c^\#x = \langle h, Ax \rangle_H$ for every $x \in \mathcal{D}(A)$ and some $h \in H$, or shortly $c^\#|_{\mathcal{D}(A)} = h^*A$.

- $d \in \mathcal{D}(c^\#) \subset H$ is a factor control vector, $u \in L^2(0, \infty)$ is a scalar control function.

The closed-loop system is described by the abstract nonlinear differential equation

$$\dot{x}(t) = A \{x(t) - df[c^\#x(t)]\}. \quad (2)$$

We give conditions under which the state $x=0$ of (2) is strongly globally asymptotically stable: essentially a sector type condition for the nonlinearity and the satisfaction of two Lur'e operator equations for the linear part. The solution of the latter is discussed by a Kalman-Yacubovitch-Popov type result..

References

- [1] R.F. Curtain, *Regular linear systems and their reciprocals: application to Riccati equations*, Systems and Control Letters, **49** (2003), pp. 81 - 89.
- [2] P. Grabowski, F.M. Callier, *Circle criterion and boundary control systems in factor form: Input-output approach*, Int. Jour. Applied Math. and Computer Science, **11** (2001), pp. 1387 - 1403.
- [3] P. Grabowski, F.M. Callier, *On the circle criterion for boundary control systems in factor form: Lyapunov stability and Lur'e equations*. ESAIM: COCV, **12** (2006), pp.169 - 197.
- [4] J.C. Oostveen, R.F. Curtain, *Riccati equations for strongly stabilizable bounded linear systems*, Automatica **34** (1998), 953-967.

Pseudo-Gradient and Lagrangian Boundary Control Formulation of Electromagnetic Media

Dimitri Jeltsema

Delft Center for Systems and Control
Delft University of Technology

Mekelweg 2, 2628 CD, Delft
The Netherlands

Email: d.jeltsema@tudelft.nl

Arjan van der Schaft

Inst. for Mathematics and Computing Science
University of Groningen
P.O.Box 800, 9700 AV, Groningen
The Netherlands

Email: a.j.van.der.schaft@math.rug.nl

Introduction and Motivation

In the early sixties, Brayton and Moser developed a mathematical analysis to study the stability of nonlinear electrical networks [1]. Their method is based on the observation that the dynamics of a large class of RLC networks can be written in the form¹

$$\mathbf{Q}(\mathbf{u})\dot{\mathbf{u}} = \mathcal{P}_{\mathbf{u}}(\mathbf{u}), \quad (1)$$

where $\mathbf{u} \in \mathbb{R}^n$ is a vector containing the inductor currents and capacitor voltages, $\mathcal{P} : \mathbb{R}^n \rightarrow \mathbb{R}$ represents the so-called mixed-potential function describing the resistive (R) part of the network, and $\mathbf{Q}(\mathbf{u}) \in \mathbb{R}^{n \times n}$ is a block-diagonal matrix containing the inductances (L) and capacitances (C). The principal application of the concept of mixed-potential concerns its use in determining (Lyapunov-based) stability criteria for nonlinear networks. A strong feature of the method is that it can also be applied to networks with negative resistors.

During the last four decades several notable extensions and generalizations have been presented in the literature. However, to our knowledge, all these contributions deal with finite dimensional lumped-parameter networks, except for the work contained in [2]. The latter paper presents a mixed-potential-based stability theory of a single transmission line system connected to a nonlinear load. Instead of a function $\mathcal{P}(\mathbf{u})$ as in Eq. (1), the analysis starts with the construction of a functional $\mathcal{P}[\mathbf{u}]$ which involves an extended vector $[\mathbf{u}] = \text{col}(\mathbf{u}, \mathbf{u}^b)$ and the spatial derivatives of \mathbf{u} , i.e.,

$$\mathcal{P}[\mathbf{u}] = \int_{\mathbb{Z}} \overline{\mathcal{P}(\mathbf{u}, \mathbf{u}_z)} dz + \mathcal{P}^b(\mathbf{u}^b),$$

where \mathbf{u}^b denote the currents and voltages at both ends of the transmission line.

Contributions

In this presentation, we will further generalize the results of [1] and [2] by defining an electromagnetic mixed-potential that describes Maxwell's curl equations (i.e., the Ampère-Maxwell law and Faraday's law). Besides the completion of the overall Brayton-Moser picture, the construction of an

electromagnetic mixed-potential suggests some alternative variational principles that imply the existence of a family of novel Lagrangian functionals. In contrast to the existing methods in mathematical physics, these new Lagrangian functionals explicitly yield both Maxwell's curl equations without invoking the usual vector magnetic and scalar electric potentials [3]. Furthermore, a suitable extension of the functional derivative enables us to consider electromagnetic media with non-zero boundary conditions. This leads to a Lagrangian boundary control system of the form:

$$(\delta_{[\mathbf{q}_l]} \mathcal{L}[\mathbf{q}, \mathbf{q}_l]), - \delta_{[\mathbf{q}]} \mathcal{L}[\mathbf{q}, \mathbf{q}_l] = \mathbf{0},$$

where $\delta_{[\cdot]}$ denotes the extended functional derivative. In this setting, the generalized velocities \mathbf{q}_l represent the electric and magnetic field intensities, and the generalized displacements \mathbf{q} represent their respective time-integrals, i.e., the electric 'flux' and the magnetic 'displacement' density vectors. The associated (symplectic) Hamiltonian counter part is shown to coincide with the total stored energy in the fields.

Additional contributions include the generation of power-based electromagnetic storage functionals that can be used to determine stability or passivity properties of the medium along the lines of [4]. This in return enables us to construct a new family of Poynting-like conservation laws.

References

- [1] R. K. Brayton and J. K. Moser, "A theory of nonlinear networks, part I", *Quart. Appl. Math.*, Vol. 12, No. 1, pp. 1–33, 1964.
- [2] R. K. Brayton and W. L. Miranker, "A stability theory for nonlinear mixed initial boundary value problems", *Arch. Ratl. Mech. and Anal.*, Vol. 17, No. 5, pp. 358–376, 1964.
- [3] P. Bracken, "Determination of the electromagnetic Lagrangian from a system of Poisson brackets", *Int. J. Th. Phys.*, Vol. 44, No. 1, pp. 127–138, 2005.
- [4] D. Jeltsema, R. Ortega and J. M. A. Scherpen, "On passivity and power-balance inequalities of nonlinear RLC circuits", *IEEE Trans. Circ. and Syst.-I: Fund. Th. Appl.*, Vol. 50, No. 9, pp. 1174–1179, 2003.

¹The subscript notation $(\cdot)_{\mathbf{u}}$ denotes partial differentiation w.r.t. \mathbf{u} .

Observable graphs¹

Raphaël Jungers and Vincent D. Blondel

Université catholique de Louvain, Department of applied mathematics,
4 avenue Georges Lematre, B-1348 Louvain-la-Neuve, Belgium.
 {jungers, blondel}@inma.ucl.ac.be.

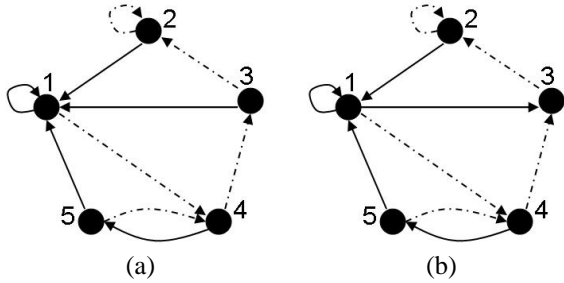


Figure 1: Two colored graphs. Are they both observable?

1 Introduction

Consider an agent moving from node to node in a directed graph whose edges are colored. The agent knows the colored graph perfectly but does not know his position in the graph, that is, the node in which he is. From the sequence of colors he observes he wants to deduce his position. We say that an edge-colored directed graph is *observable* if there is some observation time length after which, whatever the color sequence observed, the agent is able to determine his position in the graph and is able to do so for all subsequent times. Of course, if all edges are of different colors, or if edges with different end-nodes are of different colors, then an agent is always able to determine his position after a single observation. So the interesting situation is when there are fewer colors than there are nodes. Consider for instance the two graphs on Figure 1 which differ only by the edge between the nodes 1 and 3. The edges are colored with two “colors”: solid (S) and dashed (D). We claim that the graph (a) is observable but that (b) is not. In graph (a), if the observed color sequence is DDS then the agent must be at node 1, while if the sequence is SDD he must be at node 3. Actually one can show that the observation of color sequences of length three always suffices to determine the exact position of the agent in this graph. Consider now the graph (b) and assume that the observed sequence is SSDSS; after

these observations are made, the agent may either be at node 1, or at node 3. There are two paths that produce the color sequence SSDSS and these paths have different end-nodes. Sequences of increasing length and with the same property can be constructed and so graph (b) is not observable.

2 Some results about observable graphs

The concept of observable graph leads to some interesting questions: Firstly, given a sequence of colors, how to deduce from this information the possible current states of the agent? We will see that there is a straightforward algorithm that does this job, and we will put it in relation with the well known Viterbi algorithm for Hidden Markov Models. Now, if one is given a colored graph, how to check whether it is an observable graph? How to compute the length of the observation necessary to localize the agent? We will derive necessary and sufficient conditions that allow one to recognize observable graphs in polynomial time. Another interesting question is the following one: if one is given a simple (uncolored) graph, how to color it in order to have an observable graph? We will first analyse some particular graphs that appear in practice, and we will give efficient algorithms to answer to these questions for these particular graphs. For general graphs however, we prove that such questions are NP-hard to answer, and we raise then the question of the approximation of the optimum.

3 Conclusion

The aim of this talk is to be tutorial. The accent will be put on relations with other topics in systems and control: Hidden Markov Models [4], Observable Discrete Event Systems, and Trackable Networks [2] are a few of them.

References

¹The research reported here was performed while the authors were at MIT, Cambridge. It was partially supported by the “Communauté française de Belgique - Actions de Recherche Concertées”, by the EU HYCON Network of Excellence (contract number FP6-IST-511368), by the Belgian Programme on Interuniversity Attraction Poles initiated by the Belgian Federal Science Policy Office, and by the DoD AFOSR URI for “Architectures for Secure and Robust Distributed Infrastructures”, F49620-01-1-0365 (led by Stanford University). The scientific responsibility rests with its authors. Raphaël Jungers is a FNRS fellow (Belgian Fund for Scientific Research).

- [1] V. Crespi, G. V. Cybenko, and G. Jiang. The Theory of Trackability with Applications to Sensor Networks. Technical Report TR2005-555, Dartmouth College, Computer Science, Hanover, NH, August 2005.
- [2] L. R. Rabiner. A tutorial on hidden markov models and selected applications in speech recognition. In A. Waibel and K.-F. Lee, editors, *Readings in Speech Recognition*, pages 267–296. Kaufmann, San Mateo, CA, 1990.

Productivity optimization of cultures of *S. cerevisiae* through a robust control strategy

Laurent Dewasme, Frederic Renard and Alain Vande Wouwer
 Laboratoire d'Automatique, Faculté Polytechnique de Mons,
 7000 Mons, Belgium

{Laurent.Dewasme, Frederic.Renard, Alain.VandeWouwer }@fpms.ac.be

S. cerevisiae is one of the most popular host microorganism for vaccine production. The possibility to easily express a variety of different recombinant proteins explains its important role in the pharmaceutical industry. In order to maximize productivity, a common strategy is to regulate the ethanol concentration at a low value, thus ensuring an operating point close to the edge between the respiratory and respiro-fermentative regimes where the yeast respiratory capacity is exactly filled. Several applications of this principle can be found, for instance in [1, 2]. However, these control schemes all require the on-line measurement of the ethanol concentration, implying the availability of an (unfortunately quite expensive) ethanol probe. This explains that alternative strategies based on more basic measurement signals, such as the dissolved oxygen concentration, have been proposed, e.g. in [3], or that software sensors reconstructing ethanol from the measurements of basic signals have been designed [4].

Based on singular perturbation and linearization, three simple linear models are derived from Sonnleitner's model ([5]). They describe the transfer between the feed rate and the dissolved oxygen concentration or the ethanol concentration, respectively. In the latter case, two different linear models are used to describe the respiratory and respiro-fermentative mode of operation. Interestingly, these three linear models have exactly the same structure, and only differ in the values of their coefficients so that the same controller design procedure can be used.

An adaptive RST controller is then designed to regulate the dissolved oxygen or the ethanol concentrations, according to the considered model, at an imposed setpoint. This design is based on pole placement (for setpoint tracking) and the selection of an observer polynomial (for loop robustification), which can be achieved independently.

The performance of these control schemes is then assessed both in simulation and in real experimental studies with different yeast strains. Attention is focused on ethanol regulation, which leads to better biomass productivity than oxygen regulation. Ethanol can be either measured directly using an appropriate probe, or indirectly using a software sensor based on elementary signals such as base addition (for pH control), stirrer rotational speed, etc. ([4]).

In all the case studies, the controller performed well, demonstrating its reliability under various conditions. As compared to conventional open-loop operation, the application of the control schemes can lead to about 40 % productivity

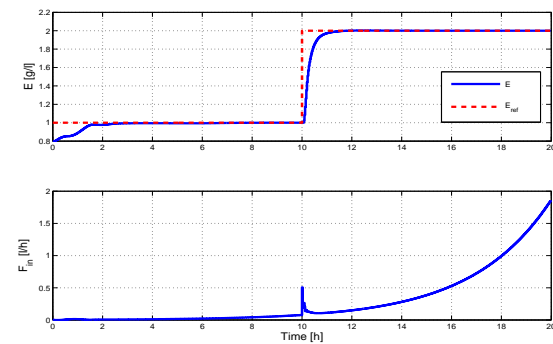


FIG. 1: Simulation results with the RST controller - Evolution of the ethanol concentration (E : continuous line and E_{ref} : dashed line) and the feed flow rate (F_{in}).

gain. As an example, the evolution of the ethanol concentration and the feed flow rate are represented in Fig. 1, following two setpoint changes, the first one starting at $t = 0$ and corresponding to 1 g/l , and the second one applied at $t = 10 \text{ h}$ and corresponding to 2 g/l .

Acknowledgements

The authors gratefully acknowledge the support of the Belgian Program on Interuniversity Poles of Attraction, initiated by the Belgian Federal Science Policy Office.

References

- [1] L. Chen, G. Bastin, and V. van Breusegem. A case study of adaptive nonlinear regulation of fed-batch biological reactors. *Automatica*, 31(1):55–65, 1995.
- [2] S. Valentiniotti, B. Srinivasan, U. Holmberg, D. Bonvin, C. Cannizzaro, M. Rhiel, and U. von Stockar. Optimal operation of fed-batch fermentations via adaptive control of overflow metabolite. *Control engineering practice*, 11:665–674, 2003.
- [3] M. Akesson. *Probing control of glucose feeding in Escherichia coli cultivations*. PhD thesis, Lund Institute of Technology, 1999.
- [4] X. Hulhoven, F. Renard, S. Dessoy, P. Dehottay, P. Bogaerts, and A. Vande Wouwer. Monitoring and control of a bioprocess for malaria vaccine production. *5th IFAC Symposium on Robust Control Design*, July 2006.
- [5] B. Sonnleitner and O. Käppeli. Growth of *Saccharomyces cerevisiae* is controlled by its limited respiratory capacity : Formulation and verification of a hypothesis. *Biotechnol. Bioeng.*, 28:927–937, 1986.

Application of Robust Control to the Activated Sludge Process

R. David, A. Vande Wouwer

Service d'Automatique, Faculté Polytechnique de Mons, 31, Boulevard Dolez, 7000, Mons, Belgium
Alain.Vandewouwer@FPMs.ac.be

J.-L. Vasel

Service Environnement, Université de Liège, 185, Avenue de Longwy, 6700, Arlon, Belgium
JLVasel@ULg.ac.be

I. Queinnec

LAAS-CNRS, 7, Avenue du Colonel Roche, 31077, Toulouse cedex 4, France
Queinnec@LAAS.fr

The Activated Sludge Model no. 1 (ASM1) [3], which is the most widely accepted model of wastewater treatment plants (WWTPs), is used to describe the biotransformation processes of nitrification-denitrification. Due to its complexity and nonlinearity, this model is however not well-suited to the design of a control structure. The objective of this work is threefold: (1) to reduce the ASM1, (2) to linearize the reduced model, and (3) to design a robust control algorithm, in order to improve the plant performance and reject perturbations. The two first points have been exposed in [1]. The control procedure is now illustrated with data from the COST benchmark [4].

Standard activated sludge processes consist of anoxic and anaerobic tanks in closed-loop with a secondary settler (see Fig. 1). Despite large variations in flow and load, together with uncertainties concerning the composition of the incoming wastewater, these plants have to be operated continuously, meeting more and more stringent norms on the quality of the effluent water.

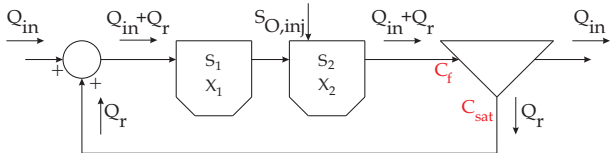


Figure 1: WWTP scheme: an anoxic tank, an aerobic one, and then a secondary settler. Q_{in} is the volumetric influent rate, Q_r is the recirculation volumetric rate, $S_{O,inj}$ is the injected dissolved oxygen, C_f is the feed concentration in particulate components, and C_{sat} is the saturation concentration at the sludge outlet

The resulting ODEs model after reduction involves 5 state variables for the anoxic tank, and 6 state variables for the aerobic one. A simple Taylor series is used for linearization, which avoids generating data sets and identifying unknown coefficients (which are relatively cumbersome tasks), and this linearization is effected around average operational values, which avoids the use of a multi-model strategy. The settler model can be reduced by considering that, in most of the operational range (despite a varying feed concentration C_f), the sludge outlet is characterized by a constant (satura-

tion) concentration C_{sat} . The reduced and linearized model satisfactorily follows the evolution of the nonlinear model.

For the purpose of our study, we consider three sets of data concerning dry, rainy and stormy weathers [4]. These data sets are used to test our reduced linear model and our control strategy in the face of realistic events and perturbations.

The reduced and linearized model serves as a basis for the design of robust H_2 controllers regulating the dissolved oxygen concentration in the aerobic tank (via $S_{O,inj}$) as well as the ammonium or nitrate/nitrite concentrations (via Q_r and Q_{in}). The robust controllers show satisfactory performance, mostly when Q_{in} can be manipulated via a retention tank. As all the wastewater treatment plants are not equipped with such a tank, an alternative is the manipulation of soluble substrate $S_{S,in}$, by modulating the outlet flow rate of a buffer tank placed at the plant inlet and containing a solution at a given concentration.

Acknowledgments. The authors gratefully acknowledge the support of the Belgian Program on Interuniversity Poles of Attraction, initiated by the Belgian Federal Science Policy Office.

References

- [1] David, R., Sol, O., Vande Wouwer, A., Queinnec, I. and Vasel, J.-L., Derivation of a reduced-order linear model from ASM1 - Control perspectives. 25th Benelux Meeting on Systems and Control, Book of Abstracts, Technische Universiteit Eindhoven, p 87, 2006.
- [2] Gomez-Quintero, C.S., Queinnec, I. and Spérando, M., A reduced linear model of an activated sludge process, 9th IFAC Symposium on Computer Applications in Biotechnology (CAB'9), Nancy (France), 28-31 March, 2004.
- [3] Henze, M., Grady, C., Gujer, W., Marais, G. and Matsuo, T., Activated sludge model no. 1. IAWQ Scientific and Technical Report No. 1. IAWQ, London, 1987.
- [4] IWA Task Group on Benchmarking of Control Strategies for WWTPs, <http://www.benchmarkwwtp.org/>.
- [5] Smets, I. Y., Haegebaert, J. V., Carrette, R. and Van Impe, J. F., Linearization of the activated sludge model ASM1 for fast and reliable predictions. Water Research, 37 (2003), 1831 - 1851.
- [6] Zhou, K., Doyle, J.C. and Glover K., *Robust and optimal Control*, Prentice Hall, New Jersey, 1996.

Asymptotic Behavior and Bistability of a Biochemical Reactor Distributed Parameter Model

A. K. DRAMÉ¹ †, D. DOCHAIN¹, J. J. WINKIN²,

¹ Université catholique de Louvain, CESAME,
4-6 av. G. Lemaître, B-1348 Louvain-La-Neuve, Belgium,
drame@inma.ucl.ac.be, dochain@csam.ucl.ac.be

† Currently : Department of Mathematical Sciences,
University of Nevada, Las Vegas, 4505 Maryland Pkwy, NV 89154 USA

² University of Namur (FUNDP), Department of Mathematics,
8 Rempart de la Vierge, B-5000 Namur, Belgium, joseph.winkin@fundp.ac.be

Key Words

Biochemical reactor, state trajectories, asymptotic behavior, multiple equilibrium profiles, bistability.

Biochemical Reactor Model

The dynamical analysis and control of tubular biochemical reactors have motivated many research activities over the last decades (see e.g. [2], [3], [5], [6], [8]). The dynamics of these reactors are described by distributed parameter systems and typically by nonlinear partial differential equations with e.g. Danckwerts type boundary conditions, (see e.g. [2], [3]).

In this presentation we consider a nonlinear dynamical model of a fixed bed tubular biochemical reactor with axial dispersion, [4]. The nonlinearity in the model arises from the substrate inhibition term in the model equations and is a specific rational function of the state components. The basis of the model under study is derived from the work performed on anaerobic digestion in the pilot fixed bed reactor of the LBE-INRA in Narbonne (France) and is mainly inspired from the dynamical models built and validated on the process ([1], [7]). This study follows and extends the preliminary one performed in [6].

Dynamical Properties

The existence and uniqueness of the state trajectories (limiting substrate and limiting biomass) as well as their asymptotic behavior are analyzed for this model. The trajectories exist on the whole (nonnegative real) time axis and the set of all physically feasible state values is invariant under the dynamical equation. This set takes into account the positivity of the state variables as well as a saturation condition on the substrate. Moreover the asymptotic behavior of the trajectories is investigated and it is reported that the trajectories converge to equilibrium solutions of the system.

In addition the existence of multiple equilibrium profiles is analyzed. The multiplicity is established together with the stability of equilibrium profiles by using phase plane analysis of ordinary differential equations. The results are illustrated by some numerical simulations.

Acknowledgments

This paper presents research results of the Belgian Programme on Inter-University Poles of Attraction initiated by the Belgian State, Prime Minister's office for Science, Technology and Culture. The scientific responsibility rests with its authors.

References

- [1] O. Bernard, Z. Hadj-Sadok, D. Dochain, A. Genovesi and J. -P. Steyer; Dynamical model development and parameter identification for an anaerobic wastewater treatment process, *Biotech. Bioeng.*, **75**, 424-438, 2001.
- [2] P. D. Christofides and P. Daoutidis; Nonlinear feedback control of parabolic PDE systems, in *Nonlinear Model Based Process Control*; R. Berber and C. Kravaris (eds), *Kluwer*, Dordrecht, 1998.
- [3] D. Dochain; Contribution to the Analysis and Control of Distributed Parameter Systems with Application to (bio)chemical Processes and Robotics, *Thèse de Doctorat d'Etat, CESAME, Université Catholique de Louvain, Belgique*, 1994.
- [4] A. K. Dramé, D. Dochain and J.J. Winkin; Asymptotic behaviour and stability for solutions of a biochemical reactor distributed parameter model, *IEEE Trans. on Automatic Control*, 2006; submitted.
- [5] M. Laabissi, M. E. Achhab, J. J. Winkin and D. Dochain; Trajectory Analysis of nonisothermal tubular reactor nonlinear models, *Systems and Control letters*, **42**, 169-184, 2001.
- [6] M. Laabissi, J. J. Winkin, D. Dochain and M. E. Achhab; Dynamical Analysis of a Tubular Biochemical Reactor Infinite-Dimensional Nonlinear Model, *Proc. 44th IEEE CDC-ECC*, 5965-5970, 2005.
- [7] O. Schoefs, D. Dochain, H. Fibrianto and J. -P. Steyer; Modelling and identification of a partial differential equation model for an anaerobic wastewater treatment process, *Proc. 10th World Congress on Anaerobic Digestion (AD01-2004)*, Montréal, Canada, 2004.
- [8] J.J. Winkin, D. Dochain and P. Ligarius; Dynamical analysis of distributed parameter tubular reactors, *Automatica*, **36**, 349-361, 2000.

The effect of feedback on the stability of biochemical reaction systems

M. Sbarciog

M. Loccufier

E. Noldus

Ghent University, Department of Electrical Energy, Systems and Automation
 Technologiepark 914, Zwijnaarde-Gent, 9052, Belgium
mihaela@autoctrl.UGent.be

1 Introduction

This paper addresses the optimization of biochemical reaction systems, operated in a continuous mode, in which an arbitrary number of components n are involved in only one reaction.

Biochemical reaction systems are complex, highly nonlinear systems. Due to the presence of reaction rate functions displaying various types of process inhibition effects, the system usually possesses at least two stable equilibrium points, one of which corresponds to the normal operating point of the process and the other one to a wash out state, where all or almost all biological activity in the reactor vessel has disappeared. In addition, there exist one or more than one unstable equilibrium. Hence, for the analysis, design and operation of biochemical engineering systems, it is essential to be able to decide from which initial states the process will converge to normal operation that provides economic benefits and which initial states will lead the system to a wash out or non-productive conditions.

Two optimization problems are solved: (i) the problem of optimal operation for maximum production in steady state, and (ii) the problem of the start-up to the optimal steady state. The effect of feedback on the stability of the set point is investigated.

2 System dynamics

The systems under investigation can generally be cast in the form [1]:

$$\dot{\xi} = cr(\xi) - D\xi + F \quad (1)$$

where $\xi \in R^{+n}$ is the vector of concentrations of the various components participating to the process (the system's state); $D \in R^{+}$ is the specific volumetric outflow rate or dilution rate; $F \in R^{+n}$, $F = \text{col}(F_i) = D \cdot \text{col}(\xi_{in_i})$, $i = 1 \dots n$ represents the vector of supply rates, eventually corrected for the rates of removal of components in gaseous form; $c \in R^n$, $c = \text{col}(c_i)$, $i = 1 \dots n$ is the vector of yield coefficients; $r(\xi) \in R^+$ is the reaction rate function. For analysis and derivation of the optimal control strategy, no analytical expression for the reaction rate function is assumed, only considerations based on biological evidence are made.

The system model (1) has bounded states and the set of equilibrium points is globally convergent [2].

3 Optimization

Optimizing the operation of a bioreactor means determining the sequence of dilution rates which maximize a certain cost index during the transient as well as in steady state. Generally the dilution rate is constrained to $D_1 \leq D \leq D_2$.

The steady state optimization consists of determining a set point $\dot{\xi}_s$ (corresponding to the dilution rate D_s) for the bioreactor operation, which ensures an optimal productivity. It is shown that such an optimal set point always exists, independent of the reaction kinetics structure.

The problem of start-up to the optimal set point is solved as a free finite time optimal control problem. The controller which ensures the optimal transient is of the bang-bang type with no singular intervals. There can only be one switching between the minimum and maximum values of the dilution rate. In order to avoid solving complicated numerical problems with split boundary conditions, the switching is chosen to take place on the system's stability boundary corresponding to the nominal operating point when $D = D_2$. This stability boundary can be accurately estimated using a trajectory reversing technique [2].

4 Conclusions

The feedback controller moves the stability boundary of the set point to the stability boundary of the uncontrolled system's operating point corresponding to the minimum dilution rate. This stability boundary defines a wide region of attraction which, depending on the system parameters and reaction kinetics, can extend to almost the entire state space.

References

- [1] G. Bastin and D. Dochain, *On-line Estimation and Adaptive Control of Bioreactors*, Amsterdam: Elsevier, 1990.
- [2] M. Sbarciog, M. Loccufier, E. Noldus, "Convergence and stability of biochemical reaction systems of rank one", In: Proceedings of *CDC-ECC'05*, Seville, pp. 5540–5545, 2005.

Analysis of nonlinear biochemical networks: the hybrid approach

Mark Musters

Department of Electrical Engineering
Eindhoven University of Technology
Den Dolech 2, 5600 MB Eindhoven
The Netherlands
Email: m.w.j.m.musters@tue.nl

Natal van Riel

Department of Biomedical Engineering
Eindhoven University of Technology
Den Dolech 2, 5600 MB Eindhoven
The Netherlands
Email: n.a.w.v.riel@tue.nl

1 Introduction

Unraveling the complexity of biology requires a thorough understanding of the biochemical networks that form the basis of life's robust dynamics. For example, the human body is composed of approximately 10^{14} cells, each including a plethora of biochemical networks, e.g. genetic networks, signal transduction pathways and metabolic processes. Simple reasoning is not sufficient to predict the dynamics. Tools from systems theory have therefore been introduced in biology, from which the field of *Systems Biology* has emerged. In biological applications, one faces a serious lack of accurate experimental data, while this is a requirement for modeling with ordinary differential equations. Moreover, biochemical networks are traditionally littered with nonlinearities that hamper analysis. We have therefore developed a procedure to analyze the biochemical networks, based on qualitative hybrid systems. This class of systems is characterized by combining both continuous and discrete aspects into one unifying framework. Since a qualitative hybrid approach was chosen, the required amount of quantitative information is limited. As application of this procedure we considered the so-called unfolded protein response (UPR), which is a biochemical network that regulates the correct folding of proteins. Studying UPR is of great importance; it has been hypothesized that misfolded proteins are involved in cardiovascular diseases and Alzheimer.

2 Methods

By means of extensive exploration in the literature, one can often derive a deterministic model of a biochemical network with the following set of ordinary differential equations (ODEs):

$$\dot{x} = Ax + f(x), \quad (1)$$

with x : state vector of the system; A : matrix with the linear part of the state equations; and $f(x)$: matrix description of nonlinear functions. This model is in general too large for analysis, since networks contain in general more than 10 substrates; thus model reduction is required. Large differences in time scales in biological processes have been observed. Therefore, singular perturbation theory can be used to reduce the model in Eq. (1). The next step is to approximate all nonlinear functions in $f(x)$ as piecewise affine

(PWA) functions $\varphi(x)$ of the form:

$$\varphi(x) = \begin{cases} h_1(x) & \text{if } g(x) \leq C, \\ h_2(x) & \text{if } g(x) > C, \end{cases} \quad (2)$$

with $h_1(x)$ and $h_2(x)$: linear functions that are valid if invariants $g(x) \leq C$ and $g(x) > C$ are satisfied, respectively; $g(x)$: linear function that describes the threshold plane between two modes; and C : constant. This divides the total phase space in various modes, depending on the number of nonlinear terms in the original model. Transitions between modes can be obtained by determining the dot product of the trajectories within the system and the normal of the boundary plane between the modes [1]. Whether mode transition is feasible and under which conditions depend on symbolic inequalities of the parameter values. As a consequence, complete analysis of the system generates several phase spaces of the system that are only valid for specific sets of parameters.

3 Results

The procedure has been applied on the UPR model. Analysis shows a single steady-state, its exact location in phase space is determined by the parameter values. Comparison with experimental data confirms this observation.

4 Discussion and Future Perspectives

We presented a qualitative method to analyze nonlinear biochemical networks. A model of UPR was taken as example. Next step is to link this analysis method to perform parameter estimation, as the symbolic restrictions on the parameter values can be implemented in nonlinear identification methods [2].

References

- [1] E. Sacks, "Automatic qualitative analysis of dynamic systems using piecewise linear approximations," *Artif Intell*, vol. 41, pp 313–364, 1990.
- [2] M. W. J. M. Musters, D. J. W. Lindenaar, A. Lj. Juloski and N. A. W. van Riel, "Hybrid identification of nonlinear biochemical processes" *IFAC SYSID*, Newcastle Australia, 2006.

Operational Acoustic Modal Analysis: Sensitivity-based mode shape normalisation

Gert De Sitter

Department of Mechanical Engineering
Vrije Universiteit Brussel
Pleinlaan 2, 1050 Brussel
Belgium

Email: gert.de.sitter@vub.ac.be

Patrick Guillaume

Department of Mechanical Engineering
Vrije Universiteit Brussel
Pleinlaan 2, 1050 Brussel
Belgium

1 Operational Acoustic Modal Analysis

Experimental acoustic modal analysis is a well known technique. However there are some difficulties. A first difficulty is the fact that the equivalent of the mechanical force in structural modal analysis is the volumetric acceleration in acoustic modal analysis. So to perform an experimental acoustic modal analysis one needs calibrated volumetric acceleration sound sources which are not widely available. Another problem concerning the sound sources is that they have to be omnidirectional. Almost all existing sound sources are directive. A third problem concerning the sources is that they always have certain dimensions. So they change the volume of the cavity altering the acoustic system [1].

Over the past years, a modal identification technique that uses output-only data has been developed: operational modal analysis (OMA). It typically uses auto- and cross-power spectra in stead of frequency response functions [2]. The big advantage of operational modal analysis in the acoustic domain is that one does not need any volume sources anymore. The background noise is sufficient to estimate the modal parameters. The only disadvantages of OMA is that the mode shapes are not correctly scaled and that the background noise is not perfectly white.

2 Sensitivity-based rescaling method

In structural Modal Analysis, one has shown that it is possible to estimate the correctly scaled mode shapes by combining two operational modal analyses [3]. In this contribution it will be shown that there exists an acoustic equivalent. After doing a first operational modal analysis one has to change the cavity in some points and perform a second measurement. The first measurement results in n resonance frequencies (ω_n) and n operational mode shapes ($\Psi_{i,n}$). If one now changes the acoustic system with known local volume changes at a set of known locations ΔV_i ($i = 1 \dots N_c$) one can calculate a scaling factor for each mode n :

$$\alpha_n = \sqrt{\frac{-2 \cdot \Delta \omega_n}{\omega_n \cdot \left(\sum_{i=1}^{N_c} \Psi_{i,n}^2 \cdot \Delta V_i \right)}} \quad (1)$$



Figure 1: Experimental set-up

Multiplying the operational mode shape with this scaling factor results in the volume-normalised mode shapes. Note that this calculation is based on a linearisation of a sensitivity analysis. As a rule of thumb one can assume that this linearisation is valid if the percentage of volume change is lower than 5 percent of the volume of the cavity.

3 Experiments

The proposed technique has been experimentally validated on a box with dimensions $1.24m \times 0.3m \times 0.36m$.

References

- [1] Wyckaert, K. and Meulewaeter, L., On the Influence of Finite Acoustic Source Dimensions on Acoustical Frequency Response Functions inside an Enclosed Cavity, *Proceedings of the International Conference on Noise and Vibration Engineering (ISMA-21)*, Leuven (Belgium), 1996.
- [2] Guillaume, P., Hermans, L. and Van der Auweraer, H., Maximum Likelihood Identification of Modal Parameters from Operational Data, *Proceedings of the 17th International Modal Analysis Conference*, 1999, p. 1887-1893.
- [3] Parloo, E., Guillaume, P., Van Overmeire, M. and Verboven, P., Sensitivity-based operational mode shape normalization, *Mechanical Systems and Signal Processing*, 16, p. 757-767, 2002.

Operational Modal Analysis Using Transmissibility Measurements

Christof Devriendt

Department of Mechanical Engineering
Acoustics and Vibration Research Group
Vrije Universiteit Brussel (VUB)
Pleinlaan 2, B-1050 Brussels, Belgium
Email: cdevrien@vub.ac.be

Patrick Guillaume

Department of Mechanical Engineering
Acoustics and Vibration Research Group
Vrije Universiteit Brussel (VUB)
Pleinlaan 2, B-1050 Brussels, Belgium
Email: paguilla@vub.ac.be

1 Introduction

Recently a new technique for Operational Modal Analysis was proposed and validated. This technique makes use of transmissibility measurements only. In general, the poles that are identified from transmissibility measurements do not correspond with the system's poles. However, by combining transmissibility measurements under different loading conditions, it is shown that the model parameters still can be identified. The advantage of the recently proposed technique is that the operational forces are no longer assumed to be white noise. They can be arbitrary (colored noise, swept sine, impact ...) as long as they are persistently exciting in the frequency band of interest.

2 Theoretical results

Transmissibilities are obtained by taking the ratio of two response spectra, i.e. $T_{ij}(\omega) = \frac{X_i(\omega)}{X_j(\omega)}$. By assuming a single force that is located in, say, the input degree of freedom (DOF) k , it is readily verified that the transmissibility reduces to

$$T_{ij}(\omega) = \frac{X_i(\omega)}{X_j(\omega)} = \frac{H_{ik}(\omega)F_k(\omega)}{H_{jk}(\omega)F_k(\omega)} = \frac{N_{ik}(\omega)}{N_{jk}(\omega)} \triangleq T_{ij}^k(\omega) \quad (1)$$

with $N_{ik}(\omega)$ and $N_{jk}(\omega)$ the numerator polynomials occurring in the transfer-function models $H_{ik} = \frac{N_{ik}(\omega)}{D(\omega)}$ and $H_{jk} = \frac{N_{jk}(\omega)}{D(\omega)}$. Note that the common-denominator polynomial, $D(\omega)$, which roots are the system's poles, λ_m , disappears by taking the ratio of the two response spectra. Consequently, the poles of the transmissibility function (1) equal the zeroes of transfer function $H_{jk}(\omega)$, i.e. the roots of the numerator polynomial $N_{jk}(\omega)$. So, in general, the peaks in the magnitude of a transmissibility function do not at all coincide with the resonances of the system.

It is known that transmissibility function depends on the location of the force, however by making use of the modal model between input DOF, k , and, say, output DOF, i ,

$$H_{ik}(\omega) = \sum_{m=1}^{N_m} \frac{\phi_{im}L_{km}}{i\omega - \lambda_m} + \frac{\phi_{im}^*L_{km}^*}{i\omega - \lambda_m^*} \quad (2)$$

one concludes that the limit value of the transmissibility function (1) for $i\omega$ going to the system's poles, λ_m , con-

verges to model that the limit value of the transmissibility function (1) for $i\omega$ going to the system's poles, λ_m , converges to

$$\lim_{i\omega \rightarrow \lambda_m} T_{ij}^k(\omega) = \frac{\phi_{im}L_{km}}{\phi_{jm}L_{km}} = \frac{\phi_{im}}{\phi_{jm}} \quad (3)$$

and is independent of the (unknown) force at input DOF k . Consequently, the subtraction of two transmissibility functions with the same output DOFs, (i, j) , but with different input DOFs, (k, l) satisfies

$$\lim_{i\omega \rightarrow \lambda_m} (T_{ij}^k(\omega) - T_{ij}^l(\omega)) = \frac{\phi_{im}}{\phi_{jm}} - \frac{\phi_{im}}{\phi_{jm}} = 0 \quad (4)$$

To sum up, the system's poles, λ_m , are zeroes of the rational function $\Delta T_{ij}^{kl}(\omega) \triangleq T_{ij}^k(\omega) - T_{ij}^l(\omega)$, and, consequently, poles of its inverse, i.e.

$$\Delta^{-1} T_{ij}^{kl}(\omega) \triangleq \frac{1}{\Delta T_{ij}^{kl}(\omega)} = \frac{1}{T_{ij}^k(\omega) - T_{ij}^l(\omega)} \quad (5)$$

In a next step the modal parameters can easily be identified by directly applying a frequency-domain estimator to the transmissibility-based $\Delta^{-1} T_{ij}^{kl}(\omega)$ functions. One can readily understand that above results do not depend on the nature of the unknown input forces and therefore the proposed method reduces the danger to identify force contributions as true physical poles.

References

- [1] P. Guillaume, C. Devriendt, G. De Sitter; Identification of Modal Parameters from Transmissibility Measurements; 1st International Operational Modal Analysis Conference, April 2005; Copenhagen, Denmark.
- [2] C. Devriendt, P. Guillaume, G. De Sitter; Identification of modal parameters from transmissibility measurements with multiple loads, Twelfth International Congress on Sound and Vibration (ICSV12); July 2005; Lisbon, Portugal.
- [3] C. Devriendt, P. Guillaume, Operational Modal Analysis in the Presence of Unknown Arbitrary Loads Using Transmissibility Measurements, Thirteenth International Congress on Sound and Vibration (ICSV13); July 2006; Vienna, Austria.

Reference-based combined deterministic-stochastic subspace identification for modal analysis applications

Edwin Reynders and Guido De Roeck

Dept. of Civil Engineering

Katholieke Universiteit Leuven

Kasteelpark Arenberg 40, B-3001 Leuven

Belgium

Email: edwin.reynders@bwk.kuleuven.be

1 Introduction

The reference-based combined deterministic-stochastic subspace identification (CSI/ref) [2] is a generalization of the robust CSI algorithm [3] which is especially suited for the modal analysis of large mechanical structures with artificial (measured) excitation. CSI/(ref) yields estimates for the system matrices of the combined deterministic-stochastic state-space description of the linear system:

$$\begin{aligned} x_{k+1} &= Ax_k + Bu_k + w_k \\ y_k &= Cx_k + Du_kv_k \end{aligned}$$

A modal analysis of this state-space system description yields the structure's modal parameters.

2 The CSI/ref algorithm

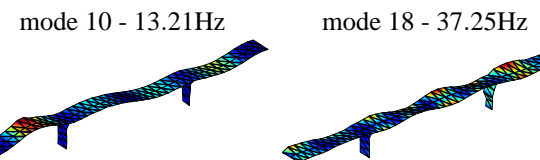
For large mechanical structures on which a large number of outputs n is measured in one setup, the classical CSI algorithm has 2 disadvantages:

1. As the number of block rows in the Hankel matrix that is built from the measured data needs to be large enough to get accurate results, the total number of rows is large if n is large which slows down the algorithm;
2. If n is large, it often happens that some output signals are of clearly less quality than others, which can deteriorate the accuracy of the identified system.

As in modal analysis, all channels contain almost the same modal information (frequencies, damping ratios), only the modal amplitudes differ, a solution to these disadvantages is to make use of some *reference* output signal only to built the row space of past output data in the data block Hankel matrix. If the number of reference outputs is small, this results in a large data reduction. If the reference outputs contain the less noisy channels, this results in an increase of accuracy. This is precisely what is done in the CSI/ref algorithm. The theoretical proof for this algorithm can be constructed for the proof of CSI [3], where now the non-stationary Kalman filter has to be replaced by a Kalman filter that makes use of the reference outputs only.

3 Application: modal analysis of the Z24 bridge

The CSI/ref algorithm has been applied to the Z24 bridge data, which have been proposed as a benchmark for the comparison of system identification algorithms for the modal analysis of large structures [1]. The bridge was measured in 9 setups, in which 2 inputs (forces provided by hydraulic shakers) and between 28 and 33 outputs (accelerations) were measured at once. Using CSI/ref, the best benchmark results reported so far are obtained (18 modes, 15 of which have high quality mode shapes). Two of the identified modes are shown below.



4 Conclusions

The CSI/ref algorithm is a very powerful system identification algorithm for the modal analysis of large mechanical structures. If the reference outputs are well chosen, the algorithm is faster and more accurate than CSI. Using CSI/ref, the best benchmark results reported so far for the Z24 bridge have been obtained.

References

- [1] B. Peeters and C. Ventura. Comparative study of modal analysis techniques for bridge dynamic characteristics. *Mechanical systems and signal processing*, 17(5):965–988, 2003.
- [2] E. Reynders and G. De Roeck. Reference-based combined deterministic-stochastic subspace identification for experimental and operational modal analysis. *Mechanical Systems and Signal Processing*, submitted for publication.
- [3] P. van Overschee and B. De Moor. *Subspace identification for linear systems*. Kluwer Academic Publishers, Dordrecht, The Netherlands, 1996.

Disturbance Accommodated Control

Matthijs Boerlage, Bram de Jager, Maarten Steinbuch

Department of Mechanical Engineering

Technische Universiteit Eindhoven

P.O.Box 513, 5600MB Eindhoven, The Netherlands

Email: M.L.G.Boerlage@tue.nl, A.G.de.Jager@tue.nl

Scope of the work

Multivariable feedback control design faces fundamental algebraic and analytical limitations, [1]. Within these limitations, tradeoffs must be made. Algebraic tradeoffs are tradeoffs between different transfer function matrices ($S + T = I$). Analytical tradeoffs are dictated by the multivariable Bode sensitivity integral,

$$\sum_i \int_0^\infty \ln \sigma_i(S_o) d\omega = 0. \quad (1)$$

Herein, tradeoffs can be made spatially, i.e., per direction. In the case that disturbances act in a particular direction, attenuation in that direction can be increased while attenuation is decreased in other directions. When, in a certain frequency band, the nett effect on the Bode sensitivity integral is zero, other frequency bands are not influenced, Figure 1. Spatial

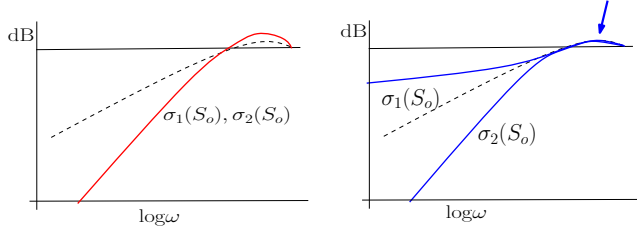


Figure 1: Initial design (dashed). Left: Design for a disturbance in all directions (thick). Right: design for disturbance in one fixed direction (thick).

shaping of transfer functions requires knowledge about the multivariable aspects of disturbances. Therefore, methods are studied to analyse and model multivariable disturbances.

Blind identification

The challenge in modeling disturbances $d(t)$ is that one has no measurements from the physical sources $s(t)$ causing the disturbances. This leads to a *blind* identification problem. In the signal model, $d(t) = Hs(t)$, only $d(t)$ is known. Using independent component analysis (ICA), one can recover both H and $s(t)$, see Figure 2, up to some indeterminancies. From ICA, the physical location of disturbances can be derived.

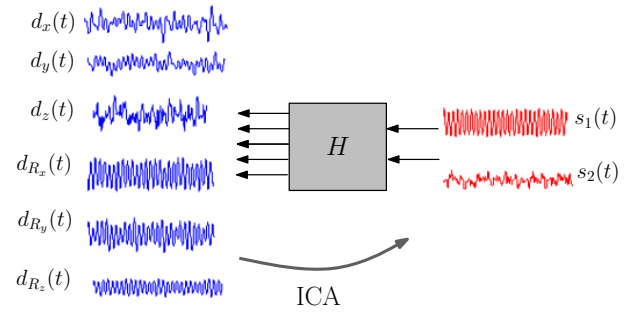


Figure 2: Reconstruction of components $s(t)$ and matrix H from observations, $d(t)$

Experimental setup

The problem is illustrated with the active vibration isolation platform depicted in Figure 3. Six degrees of freedom can be controlled individually, but all degrees of freedom suffer from unknown (possibly artificially added) disturbances. The challenge is to identify the disturbances blindly so that spatial shaping of multivariable transfer functions is facilitated. Hence, multivariable control design freedom can be exploited.

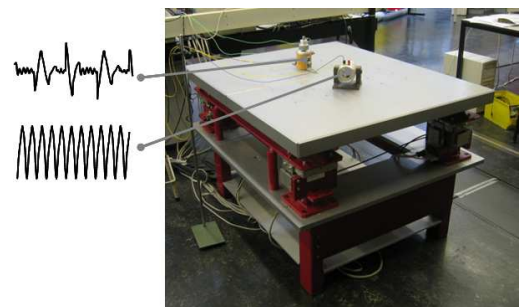


Figure 3: Active vibration isolation platform.

References

[1] J.S. Freudenberg, D.P. Looze, "Frequency domain properties of Scalar and Multivariable Feedback Systems", Lecture Notes in Control and Information Sciences, Springer Verlag, Vol. 104, 1988.

Variance calculation of covariance-driven stochastic subspace identification estimates

Edwin Reynders and Guido De Roeck
 Dept. of Civil Engineering
 Katholieke Universiteit Leuven
 Kasteelpark Arenberg 40, B-3001 Leuven
 Belgium

Email: edwin.reynders@bwk.kuleuven.be

Rik Pintelon
 Dept. ELEC
 Vrije Universiteit Brussel
 Pleinlaan 2, B-1050 Brussels
 Belgium

Email: rik.pintelon@vub.ac.be

1 Introduction

Stochastic Subspace Identification (SSI) [3] is today recognized as one of the most accurate and robust methods for the identification of linear systems from output-only measurement data. SSI yields estimates for the system matrices A and C of the stochastic state-space description of the linear system:

$$\begin{aligned} x_{k+1} &= Ax_k + w_k \\ y_k &= Cx_k + v_k \end{aligned}$$

However, one of the drawbacks of this method is that, till now, no information about the accuracy of the identified system parameters was available from the algorithm.

2 Covariance-driven Stochastic Subspace Identification

In [3], Van Overschee and De Moor indicate that, with a particular choice of weighting matrices, the Stochastic Subspace algorithm reduces to the Principal Component algorithm [1] on which this paper focuses. This algorithm starts with the construction of a block Toeplitz matrix of output covariances $\Lambda_j^{ref} = E[y_{k+j}y_k^{refT}]$ (the subscript ref stands for reference sensors):

$$L_{1|i}^{ref} = \begin{bmatrix} \Lambda_i^{ref} & \dots & \Lambda_1^{ref} \\ \dots & \dots & \dots \\ \Lambda_{2i-1}^{ref} & \dots & \Lambda_i^{ref} \end{bmatrix}$$

A singular value decomposition of $L_{1|i}^{ref}$ yields the extended observability matrix O_i , of which the first rows are equal to the matrix C and from which the matrix A is determined as:

$$L_{1|i}^{ref} = U\Sigma V^T \quad O_i = U\Sigma^{1/2} \quad A = \underline{O_i}^\dagger \overline{O_i}$$

3 Covariances on the system parameter estimates

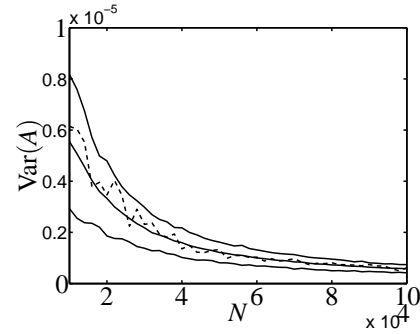
In [2], a new sensitivity-based formula for the covariances on the identified system matrices is derived:

$$\text{Cov} \left(\text{vec} \left(\begin{bmatrix} A \\ C \end{bmatrix} \right) \right) = \begin{bmatrix} \mathcal{A}_1 \\ \mathcal{A}_2 \end{bmatrix} (\mathcal{B} + \mathcal{C}) \text{Cov} \left(\text{vec} (\Delta L_{1|i}^{ref}) \right) (\mathcal{B} + \mathcal{C})^T \begin{bmatrix} \mathcal{A}_1 \\ \mathcal{A}_2 \end{bmatrix}^T$$

where $\text{Cov} \left(\text{vec} (\Delta L_{1|i}^{ref}) \right)$ is estimated with statistical techniques and $\mathcal{A}_1, \mathcal{A}_2, \mathcal{B}$ and \mathcal{C} are calculated from matrices that are determined during the identification procedure.

4 Simulation example

Consider the SISO system $A = 0.98$, $C = 0.25$, $\text{Cov} \left([w_k^T \ v_k^T]^T \right) = \text{diag} \left([1 \ 0.01]^T \right)$. The influence of the number of samples N on the accuracy of the identified system pole A is investigated by means of Monte-Carlo simulations. For each value of N , the sample variance calculated from 200 numerical simulations (dashed line) is compared to the sample mean and the 2σ uncertainty bound of the variance estimates of A computed with the covariance formula (full lines):



5 Conclusion

From the figure it can clearly be observed that the variance estimation procedure presented in this paper yields not only *unbiased*, but also *accurate* estimates of the variance on system parameters identified with reference-based covariance-driven stochastic subspace identification.

References

- [1] M. Aoki. *State space modeling of time series*. Springer Verlag, Berlin, 1987.
- [2] E. Reynders, R. Pintelon, and G. De Roeck. Variance calculation of covariance-driven stochastic subspace identification estimates. In *Proceedings of the IMAC XXV International Modal Analysis Conference*, 2007.
- [3] P. van Overschee and B. De Moor. *Subspace identification for linear systems*. Kluwer Academic Publishers, Dordrecht, The Netherlands, 1996.

Global chassis control under varying road conditions

Mathieu GERARD

Delft Center for Systems and Control - Delft University of Technology

Mekelweg 2 - 2628 CD Delft - The Netherlands

m.p.gerard@tudelft.nl

Michel VERHAEGEN

m.verhaegen@moesp.org

1 Project Goal

The number of active systems in a car is rapidly increasing. So far, each actuator is controlled independently. Therefore, undesired coupling between the different control schemes may lead to severe loss of performance. By designing a global nonlinear MIMO controller and integrating all the available actuators into a common strategy, the global performance and safety of the vehicle will be optimized.

2 Active systems

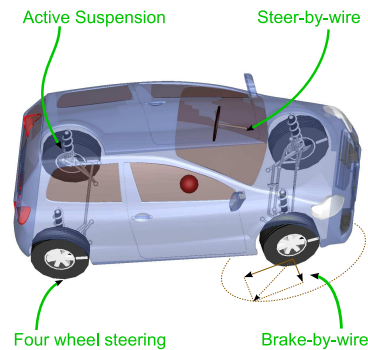
In the near future, most cars will be equipped with four types of active systems which will all have specific capabilities. Active suspension can increase the roll control capacity, reduce the risk of roll-over and improve the load transfer and distribution of braking forces. Thanks to a Steer-by-Wire system (i.e., electronic control of the steering angle) the car can have a more predictable (linear) behaviour, even in case of large steering commands. Also the lateral performance and stability can be well improved close to the friction limit. Using a Four Wheel Steering vehicle, where we have the ability to steer the rear wheels, it becomes possible to decouple lateral forces and yaw moments which can provide more accurate and consistent behaviour as well as better disturbance rejection(such as from side winds). Finally, the implementation of a Brake-by-Wire system (i.e., electronic control of the brakes) allows for a more efficient distribution of the tyre forces on the friction ellipse, especially in case of low friction.

3 Control objectives

Our objective is to integrate and optimally control all the active systems previously described to ultimately make the vehicle behaviour more consistent and predictable and improve simultaneously the handling and ride performance, the disturbance behaviour, the handling at the friction limit and the comfort. Furthermore, the redundancy in the actuators enables closed loop system fault-tolerance, which is extremely critical.

4 The problem of friction

The problem is even more complex when many parameters are *a priori* unknown. In particular the road conditions, together with the friction characteristics, can change drasti-



cally during driving. Basically, the tyre friction curve has a maximum for some normalized speed at the contact point. To reach the best performance, the maximum is targeted. However, the peak introduces an unstable region that should be avoided at any cost. The maximum available friction is so different when driving on snow or on dry asphalt that just making the system robust would lower the performance too much due to the associated conservatism. This means there is a need for adaptation and therefore the friction has to be estimated. Nevertheless such estimation is still very complicated to get even if research has been going on for decades. One promising solution is the estimation of the friction in parallel with the tyre forces using a nonlinear Kalman filter.

5 Results

The challenges for the car industry for the next generation of cars and the problems related to the varying shape of the tyre friction curve are formulated. The estimation of the friction is then analyzed making use of an Unscented Kalman Filter. Finally, the impact of nonlinear control methods for a global control strategy is explained. Simulations using the Vehicle Dynamics Library for Modelica - Dymola provide better insight about the global problem and support the friction estimator.

References

- [1] J. Andreasson, C. Knobel, T. Bünte, "On Road Vehicle Motion Control - striving towards synergy", Proceedings of AVEC'06, Taipei, Taiwan, aug. 2006.
- [2] M. Gerard, "Tire-Road Friction Estimation Using Slip-based Observers", Master Thesis, Lund University of Technology, Sweden, 2006.

Hydraulic CVT Slip Control: New Challenges

Stan van der Meulen, Bram de Jager, Maarten Steinbuch, and Bram Veenhuizen
 Eindhoven University of Technology, Mechanical Engineering, Control Systems Technology
 PO Box 513, 5600 MB Eindhoven, The Netherlands
 {S.H.v.d.Meulen,A.G.de.Jager,M.Steinbuch,P.A.Veenhuizen}@tue.nl

1 Introduction

A pushbelt continuously variable transmission (CVT) is a stepless power transmission device with infinitely many transmission ratios within a certain range. This is enabled by the variator, which consists of a segmented steel V-belt that is clamped in between two pairs of conical sheaves, see Figure 1. High clamping forces are exerted by a hydraulic actuation system to prevent global slip of the belt at all times, which leads to increased hydraulic pump losses and increased friction losses.



Figure 1: Pushbelt CVT variator

2 Variator Slip Control

2.1 Why?

One way to reduce these losses and to improve the variator efficiency is to lower the clamping forces to a level that is sufficient to transfer the torque. This implies that global slip of the belt is allowed to a limited extent. However, in the presence of driveline disturbances this strategy possibly results in excessive slip of the belt and severe damage of the variator. Hence, it is necessary to control the slip in the variator [1].

2.2 How?

The desired slip region is based on Figure 2. For each of three transmission ratios, the desired slip region is different, since it changes in accordance with the maximum variator efficiency. A slip controller is applied to keep the slip in the desired slip region for each transmission ratio.

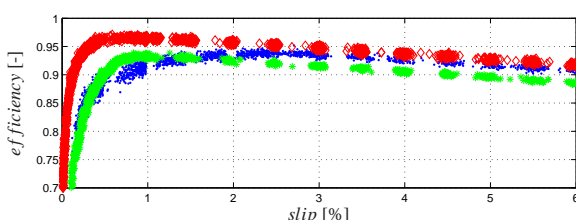


Figure 2: Experimental variator efficiency as a function of slip

(·: low; ◇: medium; *: overdrive).

2.3 When not?

At present, the application of slip control is not feasible in several situations, due to possible unstable behaviour. These situations concern, for example, extreme driveline disturbances and fast transmission ratio changes, *e.g.*, kickdowns and emergency stops.

3 Project Objective

Demonstrate the fuel-saving potential of slip control with a vehicle implementation for all driving conditions.

4 Approach and New Challenges

The approach to achieve this objective consists of an iterative analysis / synthesis cycle between theory and experiments, see Figure 3. Relevant research questions are:

Modeling for Control: What are the characteristics of the transmission ratio dynamics and the slip dynamics in the applicable slip range?

Control Design: What are the possibilities of linear parameter varying control and extremum seeking control?

Slip Estimation: What are the possibilities of a slip observer design in comparison with a cheap, reliable, and accurate slip sensor design?

Driveline Disturbances: What are the consequences of driveline disturbances, *e.g.*, torque converter and road disturbances, for slip control?

Driveability: What are the implications of the perception of the driver for slip control?

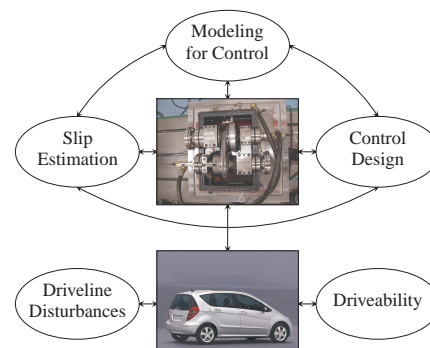


Figure 3: Interaction between theory, test rig experiments, and vehicle experiments.

References

[1] B. Bonsen, T. W. G. L. Klaassen, R. J. Pulles, S. W. H. Simons, M. Steinbuch, and P. A. Veenhuizen. Performance optimisation of the push-belt CVT by variator slip control. *Int. J. Vehicle Design*, 39(3):232–256, 2005.

Controller design for the active control of gearbox noise: preliminary results

Bert Stallaert, Simon Hill, Wim Symens, Jan Swevers, Paul Sas

Department of Mechanical Engineering, Division PMA

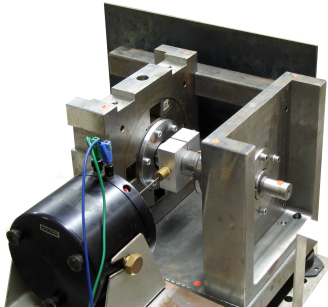
Katholieke Universiteit Leuven

Celestijnenlaan 300B, 3001 Heverlee, Belgium

Email: Bert.Stallaert@mech.kuleuven.be

1 Introduction

Active Structural Acoustic Control (ASAC) tries to reduce the radiated sound by actively influencing the dynamics of a structure. The main idea behind this research is to apply ASAC by acting on the structure as close as possible to the noise source, in order to cancel the vibration energy as soon as possible in the transfer path. For the considered application of gear noise, an experimental set-up has been built, as discussed in [1]. The set-up (see figure below) consists of a shaft supported by two bearings, of which one is made "active" by mounting piezo-actuators around it, to influence the vibration transfer in the bearings. Sound is radiated by a flexible panel mounted on the set-up.



The presentation first discusses briefly a first attempt to reduce the radiated noise by increasing the transmission loss with collocated integral force feedback [2]. Then it focusses on the design of a feedforward controller to directly influence the radiated noise [3]. The design is preceded by a modal analysis in order to be able to carefully analyse the set-up's dynamics.

2 Dynamic characterization of the set-up

Efficient ASAC requires the knowledge of the important noise radiating modes, and how they are excited by the disturbance. Furthermore, the controllability and observability of these modes should be assessed. For a mechanical structure, a modal analysis is a powerful tool to help answering these questions; by exciting the system and measuring the dynamic response in several points, the vibration patterns are identified and modal participation factors are calculated.

The modal participation factors indicate how well the modes are excited by each actuator. Therefore, the system is excited by an external electrodynamic shaker and by the control actuators which are present in the system. The shaker simulates the disturbance introduced by gear forces. The modes with a high modal participation factor for the shaker input will be best excited by the disturbance and need to be targeted by controller. The controller can only be efficient when these modes are controllable. This can be checked by looking at their modal participation factors for the control actuators. This information, combined with sound pressure measurements, leads to the selection of two noise radiating modes that will be addressed by the controller.

3 Controller design

First control experiments show that collocated integral force feedback control is able to reduce the transmitted force through the bearings, but the effect on noise radiation is limited [2]. When using a collocated force sensor, the observability of the panel modes is very limited, because they are local modes. Therefore, an alternative feedforward approach is developed and implemented, using the rotational speed as reference signal, and using pressure sensors or accelerometers as error signals.

Acknowledgment

Research funded by a Ph.D grant of the Institute for the Promotion of Innovation through Science and Technology in Flanders (IWT-Vlaanderen).

References

- [1] B. Stallaert, S.G. Hill, J. Swevers, P.Sas, "Design of active bearings for gearbox noise control," *26th Benelux meeting on systems and control*, Heeze, The Netherlands, 2006.
- [2] S.G. Hill, B. Stallaert, W. Symens, P.Sas, "Force transmission loss as a mechanism for the active control of noise using an active bearing: preliminary results," *Proceedings of the International Conference on Noise and Vibration Engineering, ISMA2006*, Leuven, Belgium, 2006.
- [3] S.J. Elliott, "Signal processing for active control," Academic Press, London, 2001.

Special Session: A round-robin benchmark for the Large Signal Network Analyzer

Y. Rolain¹, W. Van Moer¹, C. Gaquière², D. Ducateau², M. Fernandez Barciela³, D. Schreurs⁴, M. Vanden Bossche⁵ and F. Verbeyst⁵

¹Vrije Universiteit Brussel (Dept. ELEC/TW); Pleinlaan 2; B-1050 Brussels (Belgium)

²Université des Sciences et Technologies de Lille, SUAIO Avenue Carl Gauss, 59655 Villeneuve d'Ascq Cedex (France)

³Universidad de Vigo. Lagoas-Marcosende. E-36200-Vigo(Spain)

⁴ESAT - TELEMIC; Kasteelpark Arenberg 10; B-3001 Heverlee (Belgium)

⁵NMDG Engineering; Fountain Business Center - Building 5;Cesar van Kerckhovenstraat 110;B-2880 Bornem (Belgium)

Abstract - The importance of traceability of nonlinear measurements increases as the techniques start to be used in industrial applications. An intercomparison between a number of Large Signal Network Analysis (LSNA) architectures and setups is proposed here as a first step towards standardisation for nonlinear microwave measurements

I. INTRODUCTION

The measurement of the behaviour of nonlinear systems operating at microwave and RF frequencies is one of the emerging topics in RF and microwave measurements. Several measurement prototypes and a few commercial products are available by now, and the field has matured sufficiently to start spreading the instrumentation setups to a wider application community.

From a metrology point of view, the time has now come to start an inter-comparison effort to prepare for the traceability of the instruments to a common standard. This work is a first step towards such a standardization. It is performed in the context of the NOE Target, whose goal is the design of power amplifiers at RF frequencies. There have been earlier attempts for an inter-laboratory comparison campaign, one hosted by the NIST [1,2], and a second one hosted by the Target network. This work builds on the experience that has been gathered during this prior research.

II. PROPOSED METHOD

One of the cornerstones of existing inter-comparison measurements for other quantities is that the characteristic of the device under test (DUT) can be traced to one of the fundamental quantities, (such as a length, a voltage,). Unfortunately, there is no known nonlinear device that meets this requirement, and hence the 'exact' value of the DUT remains unknown.

In the earlier NIST [1,2] study, a black-box neural net model is used as an 'exact' reference value. The major problem is that this model is also to be extracted based on measurements, and cannot be validated by an independent test. Here, the choice has been made to avoid the use of such device models. The proposed alternative is to use a stochastic test to determine whether or not the signals measured by the different partners were generated by the same device, given that the excitation conditions match. This removes the problem of the determination of the "true" device model.

III. PROPOSED DEVICE

The DUT as a whole needs to be stable over a long period of time and has to be isolated as much as possible from small non-idealities of the measurement setup.

In this work, a custom developed HEMT transistor is used as the nonlinear element. It was developed and characterized by the USTL-Lille partner. The main problem to characterise such a device is that its nonlinear response depends on the impedance presented at the ports and the spectrum generated by the signal source. As the instruments are different, this dependence complicates the comparison a lot.

To isolate the nonlinearity from the small differences in impedance and spectral content, the nonlinear element is connected in tandem with a lowpass filter at the input side and an isolation amplifier at the output side. This reduces both the impedance and the spectral dependence of the response of the DUT by an order of magnitude. It leaves the device with a nearly perfectly reproducible excitation signal and isolates the output of the device from load variations at the output, up the 15 GHz bandwidth of the isolation amplifier.

Note that this isolation is obtained even when the brand of the components of the instrument differ. This is a very important feature, as the hardware of the prototypes is scattered over different brands and models.

IV. MEASUREMENT CAMPAIGN

The device is circulated between the 5 partners. After each measurement, the device is returned to the organizing lab (VUB-ELEC) and is re-measured to avoid the effect of wear-out and drift on the obtained results.

V. CONCLUSION

A preliminary 2-node comparison shows that the final round robin can be started. The device will be sent to all labs starting begin of January 2007.

VI. REFERENCES

[1] R. B. Marks, J. A. Jargon, and J. R. Juroshek, "Calibration comparison method for vector network analyzers" 48th ARFTG Conference Digest, pp. 38-45, November, 1996.

[2] D. C. DeGroot, R. B. Marks, and J. A. Jargon. "A Method for Comparing Vector Network Analyzers," 50th ARFTG Conference Digest, pp. 107-115, 1997

Multiple-objective optimisation of jacketed tubular reactors

Peter Van Erdeghem, Filip Logist, Ilse Y. Smets and Jan F. Van Impe

BioTeC, Department of Chemical Engineering

Katholieke Universiteit Leuven

W. de Crooylaan 46, B-3001 Leuven

Belgium

Email: {peter.vanderdeghem, filip.logist, ilse.smets, jan.vanimpe}@cit.kuleuven.be

1 Introduction

Due to market saturation and global competition, today's chemical industry strives for more efficient processes to reduce the production costs. Mathematical process models have proven over the past decades to be extremely valuable tools for optimising the operation and control of chemical processes, resulting in the desired profit improvement. Application of these model based techniques to jacketed tubular reactors, still important workhorses in process industry, paves the way to improved operation policies.

In this study a set of optimal temperature profiles are derived for the optimal and safe operation of a tubular reactor in the presence of multiple and conflicting objectives. The reactor under study is a classic tubular reactor in which an exothermic, irreversible, first-order reaction takes place. To remove the heat of reaction a surrounding jacket is used. Under the assumptions of (i) plug flow, (ii) steady-state conditions and (iii) an Arrhenius law dependence of the reaction rate on the temperature, the reactor can be described by a 1D-model yielding a set of first-order differential equations with respect to the spatial coordinate z . As mentioned before the optimal control problems include multiple and conflicting objectives, i.e., maximising a reactant conversion and minimising an energy cost [3].

2 Optimisation procedure

The entire set of optimal solutions, i.e., the Pareto front, is obtained based on a linear weighted sum of the conversion and energy cost. In order to calculate the Pareto front efficiently a four step procedure of indirect, analytical and direct numerical optimal control techniques is proposed. First, the analytical expressions for all possible arcs are computed based on Pontryagin's Minimum Principle, an *indirect optimal control technique* [1]. Second, by implementing a *direct optimal control method*, i.e., *control vector parametrisation* (CVP) [5], the optimal control profiles are determined numerically for a coarse grid of weights A . In the third step the optimal sequence of the arcs present in the numerically obtained control profiles is identified. Finally, the *analytical parametrisation* (AP) [4], based on the identified optimal sequence (*step three*) and analytical expressions

(*step one*) of the arcs, is applied. These low dimensional analytical optimisation problems with mainly the switching points between the arcs as decision variables are numerically solved for a refined grid of trade-off coefficients.

3 Results and future work

Optimal control profiles based on both the reactor and the jacket fluid temperature are derived for the entire range of trade-off values. Additionally, characteristic features of the temperature profiles are identified and explained chemically [2]. Future work will exploit the here developed techniques in order to optimise tubular reactor processes in which diffusive phenomena are explicitly taken into account.

4 Acknowledgments

Work supported in part by Projects OT/03/30 and EF/05/006 (Center-of-Excellence Optimization in Engineering) of the Research Council of the Katholieke Universiteit Leuven, and by the Belgian Program on Interuniversity Poles of Attraction, initiated by the Belgian Federal Science Policy Office. The scientific responsibility is assumed by its authors.

References

- [1] A.E. Bryson and Y.-C. Ho. *Applied Optimal Control*. Hemisphere, Washington D.C., 1975.
- [2] F. Logist, P. Van Erdeghem, I.Y. Smets, and J.F. Van Impe. Multiple-objective optimization of a jacketed tubular reactor. In *submitted*, 2007.
- [3] I.Y. Smets, D. Dochain, and J.F. Van Impe. Optimal temperature control of a steady-state exothermic plug flow reactor. *AICHE Journal*, 48(2):279–286, 2002.
- [4] B. Srinivasan, S. Palanki, and D. Bonvin. Dynamic optimization of batch processes I. Characterization of the nominal solution. *Computers and Chemical Engineering*, 27:1–26, 2003.
- [5] V.S. Vassiliadis, R.W.H. Sargent, and C.C. Pantelides. Solution of a class of multistage dynamic optimization problems. 1. Problems without path constraints. *Industrial and Engineering Chemistry Research*, 33:2111–2122, 1994.

Classic vs. flow reversal operation of jacketed tubular reactors

F. Logist, I.Y. Smets, J.F. Van Impe

BioTeC, Dept. of Chemical Engineering, K.U.Leuven

W. de Croylaan 46, B-3001 Leuven, Belgium

Email: {filip.logist, ilse.smets, jan.vanimpe}@cit.kuleuven.be

A. Vande Wouwer

Service d'Automatique, Faculté Polytechnique de Mons,

Boulevard Dolez 31, B-7000 Mons, Belgium

Email: alain.vandewouwer@fpmms.ac.be

1 Introduction

For classic *jacketed tubular reactors* optimal temperature profiles often exhibit a trapezoidal shape, i.e., increasing until a certain reactor temperature is reached, keeping that temperature constant over an interval, and decreasing the temperature towards the end [5, 7]. However, inducing the constant temperature part via the jacket is difficult for an exothermic reaction, because a spatially varying jacket fluid temperature profile is required. The flow reversal or *reverse flow reactor* is an alternative configuration. Periodically reversing the flow causes the fixed bed inside the reactor to act as a regenerative heat exchanger, typically yielding trapezoidal temperature profiles [1, 4]. A quantitative comparison between the classic and the reverse flow reactor has been reported for the adiabatic case [2]. However, a cooling jacket is required when certain temperature limits must not be exceeded or when the constant temperature level has to be controlled [3, 6]. A comparison for this nonadiabatic case is still lacking.

2 Procedure

This study focusses on the performance comparison of two practically feasible jacketed reactor configurations, which lead to (near-)optimal temperature profiles. First, a classic tubular reactor with a finite number of isothermal jacket zones is selected. As second option a cooled reverse flow reactor is studied. Both configurations involve a simple 1D model and an exothermic irreversible first-order reaction with Arrhenius kinetics enabling a fair comparison between the (cyclic) steady-state performance. Two cost criteria are studied which involve an inherent trade-off between conversion and energy costs. To ensure a safe operation an upper limit is imposed for the reactor temperature. Additionally, the start-up procedure is checked to ensure a safe convergence to the desired (cyclic) steady-state.

3 Results and discussion

For both configurations and for both cost criteria a reasonable approximation of the optimal steady-state profiles and

a safe convergence during start-up has been obtained. The classic configuration outperforms the reverse flow reactor, when a sufficient number of isothermal intervals is installed. However, the more isothermal intervals, the more complex the control scheme will be. The flow reversal strategy, however, requires more equipment.

Acknowledgments

Work supported in part by Projects OT/03/30 and EF/05/006 (Center-of-Excellence Optimization in Engineering) of the Research Council of the Katholieke Universiteit Leuven, and by the Belgian Program on Interuniversity Poles of Attraction, initiated by the Belgian Federal Science Policy Office. The scientific responsibility is assumed by its authors.

References

- [1] G. Eigenberger and U. Nieken. Catalytic combustion with periodic flow reversal. *Chemical Engineering Science*, 43(8):2109–2115, 1988.
- [2] A. Gawdzik and L. Rakowski. Dynamic properties of the adiabatic tubular reactor with switch flow. *Chemical Engineering Science*, 43(11):3023–3030, 1988.
- [3] J. Khinast, A. Gurumoothy, and D. Luss. Complex dynamic features of a cooled reverse-flow reactor. *AIChE Journal*, 44(5):1128–1140, 1998.
- [4] G. Kolios, J. Frauhammer, and G. Eigenberger. Autothermal fixed-bed reactor concepts. *Chemical Engineering Science*, 55:5945–5967, 2000.
- [5] F. Logist, I.Y. Smets, and J.F. Van Impe. Operational performance of jacketed tubular reactors: exploiting optimal control theory results in controller setpoint selection. *submitted*, 2006.
- [6] F. Logist, A. Vande Wouwer, I.Y. Smets, and J.F. Van Impe. Optimal temperature profiles for tubular reactors implemented through a flow reversal strategy. *revised version submitted*, 2006.
- [7] I.Y. Smets, D. Dochain, and J.F. Van Impe. Optimal temperature control of a steady-state exothermic plug flow reactor. *AIChE Journal*, 48(2):279–286, 2002.

Solving large-scale Lyapunov equations with multigrid

Bart Vandereycken, Stefan Vandewalle

Department of Computer Science, Katholieke Universiteit Leuven

Celestijnenlaan 200A, 3001 Leuven, Belgium

{bart.vandereycken, stefan.vandewalle}@cs.kuleuven.be

1 Motivation

We consider the numerical solution of Lyapunov matrix differential equations with multigrid. Such equations have many applications, for example, in the field of numerical control, model reduction and for the computation of second moments (variance) in systems modeled by differential equations with stochastic coefficients.

A wide range of problems can be (approximately) modeled by a linear system subject to gaussian input

$$\dot{x} = Ax + Bu.$$

To study the open-loop stability of such systems, we can directly compute the covariance matrix of the state x by

$$\dot{P} = AP + PA^T + BB^T.$$

This can be used to determine the influence of random parameters in the model, e.g. for the conservation of food [1]. Other applications include model reduction by balanced truncation [2] where the gramians obey two Lyapunov equations

$$AP + PA^T + BB^T = 0.$$

2 Multigrid

If the dynamical system is a PDE, we can discretise this PDE in space and end up with a linear dynamical system. However, the number of states N is very large, e.g. 10^6 is not uncommon. To solve the states of this PDE for a given input, we can use existing solvers like multigrid. They usually rely on the sparse structure of the matrix A but the large number of unknowns do not pose a practical problem, as long as the solution can be stored in memory.

A major problem in solving the Lyapunov equation for a PDE is the size of the solution matrix P . Even at moderate mesh-sizes the number of unknowns becomes very large, e.g. 10^{12} unknowns for 3D problems. In [3] the optimal cooling of steel bars in a rolling mill is solved by a LQR problem. The resulting heat equation is discretised by a FEM of the steel bar.

We will show how the solution can be computed in a compressed format, namely a low rank approximation

$$P \simeq UV^T,$$

with U and V tall matrices of dimension $N \times k$, $k \ll N$. When this low-rank compression is used throughout the multigrid cycle, a significant reduction of the solution time and memory requirements can be achieved. While a standard multigrid method would require $O(N^2)$ computations, we need only $O(N \log^c N)$, with c a small number. This is an extension of [4] to the time-dependent case and to more robust solvers.

References

- [1] B. Nicolaï, P. Verboven, N. Scheerlinck and J. De Baerdemaeker, *Numerical Analysis of the Propagation of Random Parameter Fluctuations in Time and Space During Thermal Food Processes*, Journal of Food Engineering, 38: 259–278, 1998
- [2] A. Antoulas, *Approximation of Large-Scale Dynamical Systems*, SIAM, 2006
- [3] P. Benner, *Solving Large-Scale Control Problems*, IEEE Control Systems Magazine, 24(1):44-59, 2004
- [4] L. Grasedyck and W. Hackbusch, *A Multigrid Method to Solve Large Scale Sylvester Equations*, MIS Preprint 48, 2004

Playing Clobber on a Cycle¹

Vincent D. Blondel, Cristobald de Kerchove, Julien M. Hendrickx and Raphaël Jungers
 Dpt of mathematical engineering, Université catholique de Louvain

{blondel, dekerchove, hendrickx, jungers}@inma.ucl.ac.be

Abstract We present the combinatorial 2-player game clobber and its 1-player version solitaire clobber. We present some old and recent results on both games.

1 What is Clobber?

The combinatorial game clobber was introduced by Albert, Grossman, Nowakowski and Wolfe in 2002 [1]. It is played with black and white pawns as in the game of Draughts. White begins and moves a white pawn onto an adjacent black pawn and removes this black pawn from the game. The place formerly occupied by the white pawn is then empty and cannot be occupied anymore. Then Black plays similarly with the black pawns, etc. The player making the last move wins the game. As this game admits no draw and only a bounded number of moves, it can be proved that for any initial position there exists a winning strategy for either White or Black. The following initial position (where pawns lie on a line) is for instance winning for White $\circ\bullet\circ\bullet\bullet\bullet\bullet\bullet$, and the first play could be $\circ\bullet\circ\bullet\bullet\bullet$ \circ . Clobber is usually played on $n \times m$ grids with alternated \circ and \bullet , but it can be generalized on any graph, locating the pawns on the nodes. A 1-player version of the game was proposed in [2], Solitaire clobber (see also [3, 4]). In this game, the goal is to remove as many pawns as possible by moving black or white pawns in the same way as in the usual clobber but without necessarily alternating black moves and white moves. We analyze clobber and solitaire clobber in the particular case where pawns lie on a cycle.

2 Previous and new results on Clobber

Consider first the solitaire game. The *reducibility value* of an initial conformation is the minimal possible number of remaining pawns at the end of the game [2, 3]. A conformation allowing one to remove all pawns but one has for example a reducibility value of one. The case where pawns lie on a line has already been studied relatively deeply. It has been proved that the reducibility value is at most $\lceil n/2 \rceil$ (n being the initial number of pawns), and an initial conformation has been found where this bound is tight [2]. We focus on another particular graph, the cycle. It has been recently asked whether the maximal reducibility value on the

¹This research was supported by the Concerted Research Action (ARC) “Large Graphs and Networks” of the French Community of Belgium and by the Belgian Programme on Interuniversity Attraction Poles initiated by the Belgian Federal Science Policy Office. The scientific responsibility rests with its authors. J.M. Hendrickx and R. Jungers hold a FNRS fellowship (Belgian Fund for Scientific Research)

cycle is $\simeq n/4^1$. This value is obtained on a cycle of length $n = 4k$ by taking k repetitions of the pattern $\circ\bullet\circ\bullet$ as initial conformation. Indeed, an optimal strategy for the solitaire on this conformation can be proved to be the following: reduce each pattern $\circ\bullet\circ\bullet$ to a simple \circ by first moving the leftmost pawn to the right, then the rightmost pawn to the left, and finally the leftmost one to the right. We answer the question negatively by presenting a conformation on the cycle for which the reducibility value is $k = n/3$, and consisting in k repetitions of the pattern $\circ\bullet\circ$. Moreover we show that this is the the worst conformation, closing the question of general bounds on the reducibility value on the cycle. We also analyze the original (two players) clobber game. Some initial conformations have already been studied, many of which leading to interesting open questions. It has for instance been conjectured that the line $(\circ\bullet)^k$ (that is, k repetitions of $\circ\bullet$) always admits a winning strategy for the first player except for $k = 3$. We propose a general strategy for 2-players clobber that leads to victory in an infinite class of initial conformations. Roughly speaking, one puts the game in a symmetric conformation so that for any move of the opposite player, there exists a symmetric move restoring this symmetry. Therefore, the opposite player can only lose since every one of its moves is followed by another one. This strategy is applied to show that the second player can always win a game on the cycle if the original conformation is $2k + 1$ repetitions of the pattern $\circ\bullet$.

Acknowledgment: The authors wish to thank Eric Duchêne for having made them discover this interesting topic and for his suggestions of open issues.

References

- [1] M ALBERT, JP GROSSMAN, RJ NOWAKOWSKI, D WOLFE, *An introduction to Clobber*, *INTEGERS: The Electronic Journal of Combinatorial Number Theory* 5(2), 2005.
- [2] ED DEMAINE, ML DEMAINE AND R FLEISCHER, *Solitaire Clobber*, *Theoretical Computer Science*, 313(3):325338, 2004.
- [3] L BEAUDOU, E DUCHENE, L FARIA AND S GRAVIER, *Solitaire Clobber 2 played on graphs*, *Submitted for publication*.
- [4] P DORBEC, E DUCHENE, AND S GRAVIER, *Solitaire Clobber 2 on Hamming graphs*, *Submitted for publication*.

¹E-mail communication with Eric Duchêne

Adaptive Missile Guidance Laws using Game Theoretic Equilibria

E. J. Trottemant

Delft Center for Systems and Control (DCSC)

Delft University of Technology, Mekelweg 2, 2628 CD Delft

Email: e.j.trottemant@tudelft.nl

1 Introduction

The nature of the interception problem with 2 non-cooperative players, namely a missile and target, leads to the field of differential games. In general game-theoretic approaches to missile guidance design are based on the zero-sum Nash equilibrium [1]. The interesting differential games are the so-called pursuit-evasion games formulated with 2 players, one being the pursuer and the other being the evader. The pursuer and evader are not cooperating as both have a different objective. In real-life the strategy of the evader is never known a priori, and furthermore constraints, imperfect state measurements and inaccurate system parameter estimations make that it is rather difficult to choose the optimal weighting parameters at the beginning of the pursuit-evasion engagement. Therefore one should like to adapt the choice of weighting parameters during the engagement. Such a dynamical adjusting of the weight parameters at discrete time intervals will lead to an adaptive guidance law, which is presented in this paper.

2 Problem definition

The conflicting interest of both players can be captured in one performance index, which the pursuer tries to minimize while the evader tries to maximize it. The general performance index, with state x and commanded lateral acceleration of pursuer a_p and evader a_e , is given as:

$$J(x_0, a_p, a_e) = \frac{1}{2} x(t_F)^T Q_F x(t_F) + \frac{1}{2} \int_{t_0}^{t_F} R_p a_p(t)^2 - R_e a_e(t)^2 dt \quad (1)$$

The values of R_p and R_e and the bounds on the controls determine whether the problem is, soft-constrained ($R_p, R_e > 0$), semi soft-constrained ($R_p > 0, R_e = 0$) or hard-constrained ($R_p = R_e = 0$). All resulting differential games can be reformulated as a Two-Point Boundary Value Problem (TPBVP). In case of the (semi) soft-constrained problems one can manipulate the TPBVP and obtain a Riccati Differential Equation (RDE), which needs to be solved.

3 Approach

In case of a (semi) soft-constrained problem no guarantee of meeting the bounds on the controls is obtained. These bounds can be respected by tuning the weighting parameters

in the performance index. The choice of weighting parameters R_p, R_e together with the initial condition x_0 and given weight matrix Q_F define the strategies and thus also the state trajectory and therefore:

$$J(x_0, a_p^*, a_e^*) = J(x_0, R_p, R_e) \quad (2)$$

The saddle points strategies are optimal in the Nash formulation (denoted with $*$) in case the performance index truly represents the actual physical goals. However, this engineering information is in most cases not available. One can now imagine to apply dynamic programming principles [2] for the on-line tuning of the weighting parameters at discrete time (update) intervals, $t_k \in [t_0, t_F], k = 0, \dots, k_{max}$. Once the optimal weighting parameters are obtained, the associated Riccati Differential Equations will be recalculated and the feedback implementation of the open-loop solutions will be used for the remaining of the intercept.

4 Results

The results will be included in the final version.

5 Acknowledgements

This research project is a cooperation between 1) Delft University of Technology, 2) TNO Defence, Safety and Security and 3) NLDA, Netherlands Defence Academy.

References

- [1] T. Basar, and G. J. Olsder, "Dynamic Noncooperative Game Theory," Society for Industrial and Applied mathematics, 1999.
- [2] D. P. Bertsekas, "Dynamic Programming and Optimal Control," Athena Scientific, 2005.

Computability of solutions of dynamical games

Pieter Collins

Centrum voor Wiskunde en Informatica
Kruislaan 413, P.O. Box 94079
1090 GB Amsterdam, The Netherlands
Pieter.Collins@cwi.nl

Lorenzo Sella

Centrum voor Wiskunde en Informatica
Kruislaan 413, P.O. Box 94079
1090 GB Amsterdam, The Netherlands
Lorenzo.Sella@cwi.nl

1 The problem

An important problem in nonlinear control theory is the computation of a feedback controller satisfying some control objective in the presence of noise. While the noise may be modelled by a stochastic process, we may not have sufficient information to be able to construct a realistic stochastic model, and instead consider a worst-case nondeterministic noise. Worst-case noise may also be used if it is critical that the controller satisfy the control objectives under all possible conditions.

The assumption of nondeterministic noise leads naturally to the formulation of the problem as a *dynamical game*, which in discrete-time can be written

$$x_{n+1} = f(x_n, u_n, v_n) \quad (1)$$

and in continuous time

$$\dot{x}(t) = f(x(t), u(t), v(t)), \quad (2)$$

where $x \in X$ is the *state*, $u \in U$ is the *input* and $v \in V$ is the *noise*. In discrete-time, we assume that u_n must be chosen without knowledge of v_n , and in continuous time, we assume that $u(t)$ is subject to some “infinitesimal” delay, giving rise to a δ -game [1].

We consider the problem of controlling the system such that any trajectory starting in some initial set X_0 eventually reaches some target set A , and remains in A for all subsequent times. That is,

$$\forall x_0 \in X_0, \exists T \geq 0 \text{ s.t. } x(t) \in A \forall t \geq T. \quad (3)$$

We are interested in computing the *controllable set*, that is, the set of initial conditions for which (3) has a solution, and further, computing a *feedback controller* implementing the control.

2 Main results

There is a vast body of literature on dynamical games, and related problems in optimal control theory, see [2]. However, much of this literature contains theoretical results which cannot be directly implemented, or approximate numerical algorithms for which it is not always clear if the computed controller satisfies the control objectives. Indeed,

since the problem is formulated in terms of arbitrary sets and functions, it is not even clear how to represent the problem data and solution on a digital computer. We therefore use the framework of computable analysis developed in [3], which provides a rigorous theory for effective computations involving sets, maps and flows using Turing machines. This framework also allows much simpler proofs than those based on explicit discretization methods such as [4].

In discrete-time, we show that under certain semicontinuity requirements on the system behaviour, we can rigorously compute convergent under-approximations to the controllable set. Since it may not be possible to find a continuous controller, we discuss the existence of minimally-restrictive semicontinuous multivalued controllers. We then consider optimal over-approximations to the controllable set, and show that these need not converge to the controllable set itself.

In continuous time, we use sample-and-hold control to reduce the problem to discrete-time, and we consider the relation between instantaneous feedback control, sample-and-hold control, and feedback control with delays.

3 Summary

We consider the effective computation of control strategies for dynamical games in discrete and continuous time. We show that under certain conditions, it is possible to compute feedback controllers and the controllable set. We use the framework of computable analysis, which gives a simple, natural and rigorous theory for effective numerical computation in the continuous setting.

References

- [1] Avner Friedman. *Differential games*. Wiley, 1971.
- [2] N. N. Krasovskii and A. I. Subbotin. *Game-theoretical control problems*. Springer, 1988.
- [3] Klaus Weihrauch. *Computable analysis - An introduction*. Springer, 2000.
- [4] Lars Grüne. *Asymptotic behavior of dynamical and control systems under perturbation and discretization*. Springer, 2002.

Application of a Weibull-type model to *Listeria innocua* inactivation at dynamic conditions of lactic acid and pH

A. Verhulst¹, M. Janssen¹, A.H. Geeraerd², F. Devlieghere³, J.F. Van Impe¹

¹Chemical and Biochemical Process Technology and Control, Dept. of Chemical Engineering,

Katholieke Universiteit Leuven, W. de Crooylaan 46, B-3001 Leuven (Belgium)

anke.verhulst@cit.kuleuven.be - jan.vanimpe@cit.kuleuven.be

²Mechatronics, Biostatistics and Sensors, Dept. of Biosystems, Katholieke Universiteit Leuven, W. de Crooylaan 42, B-3001 Leuven (Belgium)

³ Laboratory of Food Microbiology and Food Preservation, Dept. of Food Safety and Food Quality, Ghent University, Coupure Links 653, B-9000 Ghent (Belgium)

1 Introduction

Lactic acid is a popular preservative in the food industry because of its activity against a broad spectrum of pathogenic and spoilage microorganisms. The lactic acid antimicrobial activity is twofold: (i) release of protons at dissociation lowers the extracellular pH, and (ii) the undissociated form of the acid is able to diffuse into the cell, affecting the cell metabolism.

In the field of predictive microbiology, mathematical models are developed and analyzed to characterize the microbial evolution in response to environmental factors. Recently, a combined primary and secondary model for the inactivation of *L. innocua* under controlled initial conditions of undissociated lactic acid [*LaH*] and pH was presented [2]. The so-called primary model for the description of the cell concentration *N* [cfu/mL] as function of time is a Weibull-type model, which can be written as follows [3]:

$$N(t) = N_0 \cdot 10^{-\left(\frac{t}{\delta}\right)^p} \quad (1)$$

The secondary model describing the variation of the shape factor *p* and the time for the first decimal reduction *δ* [h] as a function of [*LaH*] and pH, was subsequently developed.

The aim of this study is to evaluate the predictive power of this model, created for static conditions, under dynamic conditions of [*LaH*] and pH. Herein, the basic hypothesis is made that the microbial cells react immediately on the instantaneous pH and [*LaH*] conditions and thereby are physiologically independent of preceding pH and [*LaH*] conditions.

2 Materials and methods

Experiments Two dynamic experiments were performed in 1 L erlenmeyer flasks filled with a rich, modified Brain Heart Infusion medium. For both experiments, the initial and final (pH;[*LaH*]) conditions were equal to (4.5;0.01M) and (3.5;0.05M), respectively. A peristaltic pump was used to transfer medium with (pH;[*LaH*]) equal to (3;0.08M), from a reservoir to the erlenmeyer flask in which the *L. innocua* was inoculated. For first experiment the flow rate was set at 0.02 mL/min. The rate in the second experiment was set at

0.04 mL/min.

Modelling approach The inactivation under dynamic conditions is simulated by means of both the static form [Eq. (1)] and the (non-autonomous) dynamic form [Eq. (2)] of the Weibull equation [1], combined with the secondary model.

$$\frac{dN}{dt} = -\frac{\ln(10)}{\delta^p} p t^{p-1} N \quad (2)$$

Two approaches were used during the simulation. In the first approach, for every simulated time interval, *N*₀ was set at the last value of the previous interval and *t* was reset to zero. pH and [*LaH*] measurements were used to calculate *δ* and *p*. The second approach calculated *N* from pH and [*LaH*] measurements and a momentary time, based on [4].

3 Results

A slower inactivation of *L. innocua* than predicted by the simulation, was observed. This means that the working hypothesis is not correct, i.e., the physiology of the microbial cells does depend on preceding conditions.

4 Conclusions

A model developed for the *L. innocua* inactivation at static conditions of pH and [*LaH*] was used to describe inactivation at dynamic conditions. The results indicate that the microbial cells were able to develop an induced stress resistance at increasing [*LaH*] and decreasing pH conditions.

References

- [1] I. Albert, P. Mafart (2005). A modified Weibull model for bacterial inactivation. *Int. J. Food Microbiol.* **100**:111-117.
- [2] M. Janssen, A.H. Geeraerd, A. Cappuyns, L. Garcia-Gonzalez, G. Schockaert, N. Van Houteghem, K.M. Vereecken, J. Debevere, F. Devlieghere and J.F. Van Impe (2006). Individual and Combined Effects of pH and Lactic Acid Concentration on *Listeria innocua* Inactivation: Development of a Predictive Model and Assessment of Experimental Variability. *Under revision*.
- [3] P. Mafart, O. Couvert, S. Gaillard, I. Leguerinel (2002). On calculating sterility in thermal preservation methods: application of the Weibull frequency distribution model. *Int. J. Food Microbiol.* **72**:107-113.
- [4] M. Peleg and C.M. Penchini (2000). Modeling Microbial Survival during Exposure to a Lethal Agent with Varying Intensity. *Crit. Rev. Food Sc. Nutr.* **40**:159-172.

NN-based Software Sensors in Yeast and Bacteria Fed-Batch Processes

Laurent Dewasme, Alain Vande Wouwer, Laboratoire d'Automatique, Faculté Polytechnique de Mons, Belgium
 {Laurent.Dewasme, Alain.VandeWouwer }@fpms.ac.be
 X. Hulhoven and P. Bogaerts
 Service de Chimie Générale et Biosystèmes, Université Libre de Bruxelles, Belgium
 {Xavier.Hulhoven, Philippe.Bogaerts }@ulb.ac.be

In recent years, the economical ascent of biotechnology has urged bioprocess industry to improve culture productivity. Even though a wide range of state estimation algorithms are readily available for on-line process monitoring ([1]; [2]; [3]), their practical use is still relatively limited. The main reasons are : (a) many state estimation algorithms require a dynamic model of the bioprocess, involving a macroscopic reaction scheme and kinetics, which are difficult to establish from prior process knowledge and available measurement data ; (b) state estimation algorithms usually rely on some hardware sensors, which are expensive and not always fully reliable ; (c) manual operation has a long history in the bio-process industry and advanced monitoring and control are currently emerging techniques.

This study aims at assessing the potentialities of NN software sensors for estimating on-line the time-evolution of some key components of interest (in the case studies described in this paper, biomass estimation is considered) in yeast and bacteria batch and fed-batch cultures. The underlying idea is to use the information contained in signals which are routinely measured in industrial plants. These signals are usually involved in basic regulations (pH, stirrer speed, dissolved oxygen, feed flowrate) and carry over information on cell growth. In order to discriminate among these signals, a principal component analysis is first achieved. Then, a feed-forward RBF NN, whose architecture has proved quite useful in modeling bioprocesses (see, e.g., [4]), is trained using the most informative signals (or a combination of them as provided in the main PCs).

This straightforward approach is tested with a large set of experimental results corresponding to various yeast and bacteria strains, the expression of different recombinant proteins and different bioreactor scales. These tests demonstrate that a small number of experiments (between 2 and 4) are sufficient for NN training, and that the NN software sensor has good generalization properties (with respect to reactor scale, and to some extent, to the product of interest).

As an example, Figure 1 shows the time-evolution of the four input signals and the estimation of the biomass concentration by a RBF NN trained with 4 data sets corresponding to cultures of bacteria in 20 l-reactor where a recombinant protein RP_1 is expressed. This NN software sensor is then tested with independent data, where another recombinant protein RP_2 is expressed.

The main drawback of this approach is that it is based on a static map, and as such, it is unable to provide a prediction of the biomass (or of another component) evolution (as a conventional observer, based on a dynamic model of the bioprocess, would do). The main advantage is that a mathematical (biological) model of the cell culture is not required, and that biomass estimation can be obtained at a fast rate, based on fast-sampled basic signals.

Acknowledgements

The authors gratefully acknowledge the support of the Belgian Program on Interuniversity Poles of Attraction, initiated by the Belgian Federal Science Policy Office.

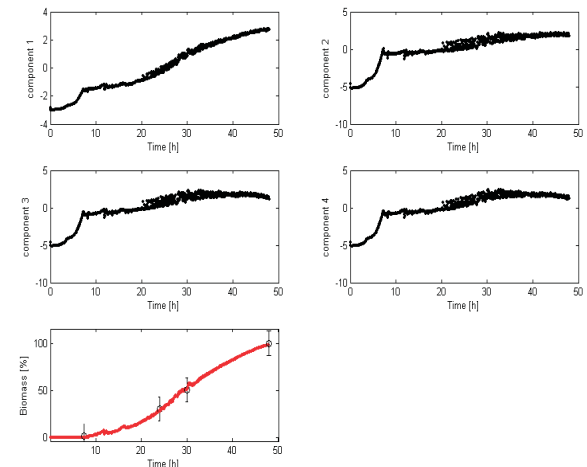


FIG. 1: Biomass estimation in 20l scale fed-batch culture of *E. coli* (expression of RP_2)

References

- [1] G. Bastin and D. Dochain. *On-line Estimation and Adaptive Control of Bioreactors*. Elsevier Science Publishers B.V., 1990.
- [2] Ph. Bogaerts and A. Vande Wouwer. Software sensors for bioprocesses. *ISA Transactions*, 42 :547–558, 2003.
- [3] G. Goffaux and A. Vande Wouwer. Bioprocess state estimation : Some classical and less classical approaches. *Symposium on Nonlinear Control and Observer Design - Stuttgart 2005*, September 2005.
- [4] A. Vande Wouwer, C. Renotte, and P. Bogaerts. Biological reaction modeling using radial basis function networks. *Computers and Chemical Engineering*, 28 :2157–2164, May 2004.

Modeling AI-2 type quorum sensing in *Salmonella Typhimurium*

A.M. Cappuyns¹, K. Bernaerts¹, S.C. De Keersmaecker², J. Vanderleyden², J.F. Van Impe¹

¹ Chemical and Biochemical Process Technology and Control Section, K.U.Leuven
W. de Crooylaan 46, B-3001 Leuven (Belgium)

astrid.cappuyns@cit.kuleuven.be - kristel.bernaerts@cit.kuleuven.be - jan.vanimpe@cit.kuleuven.be

²Centre of Microbial and Plant Genetics, K.U.Leuven
Kasteelpark Arenberg 20, B-3001 Leuven (Belgium)

1 Introduction

Bacteria communicate through production, release and detection of signaling molecules. This so-called quorum sensing or cell-cell communication plays a crucial role in important bacterial functions, e.g., virulence, survival, pathogen-host interactions. Among the different quorum-sensing systems, the only one shared by Gram-positive and Gram-negative bacteria involves the production of autoinducer-2 or AI-2. LuxS, the AI-2 synthase, is widely spread, suggesting that AI-2 is a common language for interspecies communication. In this study, the production and uptake of the AI-2 signalling molecule by *Salmonella Typhimurium* is studied in controlled bioreactor environments. The experimental results are used to build a macroscopic model that describes AI-2 quorum sensing by the food pathogen *Salmonella Typhimurium*.

2 Results and discussion

Both batch and continuous bioreactor experiments were performed to study the production and uptake of AI-2 by *Salmonella Typhimurium*.

Batch data confirm that AI-2 is produced during exponential growth (see [1]), but only during growth on a preferential substrate, i.e., in this case galactose. During a second growth phase on acetate, no AI-2 is produced.

At a constant dilution rate, a certain specific growth rate is maintained when a steady state is reached. During different steady states realized at different dilution rates (within a single experimental run), steady states were also reached for the AI-2 metabolism [2]. For each steady state, the level of AI-2 concentration positively correlates with the specific growth rate. When feeding stops and all galactose is depleted, the AI-2 concentration in the medium decreases. These results suggest that AI-2 production is strongly correlated with preferential substrate metabolism.

The dynamics of the bioreactor experiments are described by mass balance type equations [3]. Based on the experimental observations described above and information obtained from literature, the following equation is proposed to

describe the AI-2 production and uptake:

$$\frac{dC_{AI2}}{dt} = \underbrace{\frac{\sigma_{C_S}}{Y_{AI2}} \cdot C_X}_{\text{production}} - \underbrace{\sigma_{AI2} \cdot \frac{C_{AI2}}{C_{AI2} + \epsilon} \cdot C_X - D \cdot C_{AI2}}_{\text{uptake}}$$

with $\epsilon = 10^{-3}$ and C_{AI2} [-] the AI-2 concentration, C_X [OD₅₉₅] the cell density, σ_{C_S} [g/L · h⁻¹] the specific galactose consumption rate, σ_{AI2} [(1/OD) · h⁻¹] the coefficient for the specific consumption rate of AI-2 and Y_{AI2} [(g/L)⁻¹] is the yield coefficient for AI-2 production. The Monod-term with C_{AI2} reflects the fact that AI-2 is needed to suspend the repression of LsrR on the AI-2 transporter and by doing so, to regulate its own uptake.

3 Conclusions

The results confirm that AI-2 production is correlated with preferential substrate metabolism. Experimental observations together with knowledge from literature, are combined in a macroscopic model describing the AI-2 production and uptake by *Salmonella Typhimurium*. The predictions of the models were compared with experimental data for different modes of operation and delivered satisfying results.

Acknowledgements

Work supported in part by the IWT-GBOU-20160 project, OT/03/30 of the Research Council of the Katholieke Universiteit Leuven, the Belgian Program on Interuniversity Poles of Attraction, initiated by the Belgian Federal Science Policy Office and by the K.U.Leuven-BOF EF/05/006 Center-of-Excellence Optimization in Engineering. K. Bernaerts is Postdoctoral Fellow with the Fund for Scientific Research Flanders (FWO).

References

- [1] Surette, M.G. and Bassler, B.L. (1998). Quorum sensing in *Escherichia coli* and *Salmonella typhimurium*. *Proceedings of the National Academy of Science, U.S.A.* **95**, 7046-7050.
- [2] De Lisa, M.P., Valdes, J.J. and Bentley, W.E. (2001). Mapping stress-induced changes in autoinducer AI-2 production in chemostat- cultivated *Escherichia coli* K-12. *Journal of Bacteriology* **183**(9), 2918-2928.
- [3] Bastin, G. and Dochain, D (1990). *On-line estimation and adaptive control of bioreactors*. Elsevier Science Publishing Co., Amsterdam.

Computer Based Real Time Aircraft Model Identification

Thomas Lombaerts, Ping Chu and Bob Mulder

Faculty of Aerospace Engineering

Delft University of Technology

Kluyverweg 1, 2629 HS Delft

the Netherlands

e-mail: {t.j.j.lombaerts, q.p.chu, j.a.mulder}@tudelft.nl

1 Introduction

Current automatic flight control systems of aircraft (AFCS) are implemented with a high degree of redundancy regarding actuators, sensors, computer hardware, hydraulic pipelines, etc. As a consequence, today's research efforts are gradually shifting from correcting additive failures (sensors and actuators) towards dealing with parametric failures (structural and engine). This last principle is called fault tolerant flight control (FTFC). One possible option for a satisfactorily performing FTFC strategy is using a model based control routine. In this setup, not only a reconfiguring controller is needed, but also a suitable FDI/identification strategy. This publication will focus on the latter component.

2 Two Step Method

The identification routine which is used for the above mentioned reconfiguring control purpose is the so-called two step method, which has been continuously under development at Delft University of Technology over the last 20 years, the last major milestones in this development process can be found in ref. [2] and [3]. Key concept of the two step method, is that the identification procedure has been split into two consecutive steps, as substantiated in ref. [1]. The aim is to update an a priori aerodynamic model (obtained by means of windtunnel tests and CFD calculations) by means of on line flight data. The first step is called the Aircraft State Estimation phase, where the second one is the Aerodynamic Model Identification step. In the Aircraft State Estimation procedure, an Iterated Extended Kalman Filter is used to determine the aircraft states, the measurement equipment properties (sensor biases) and the wind components by making use of the nonlinear kinematic and observation models, based upon redundant but contaminated information from all sensors (air data, inertial, magnetic and GPS measurements). By means of this state information, input signals of the pilot and the earlier measurements, it is possible to construct the combined aerodynamic and thrust forces and moments acting on the aircraft, and by means of a recursive least squares operation, finally the aerodynamic derivatives can be deduced from this information. Validation tests by means of batch process identification, least squares innovation analysis and reconstruction of velocity and angular rate components using these aerodynamic derivatives has

shown that this method is very accurate. Finally this recursive method has been implemented in Simulink and combined with the conventional sensor output of a Boeing 747 simulator from the Dutch Aerospace Laboratory (NLR), together with connecting a joystick as input. This allows performing real time computer based identification calculations while performing flight manoeuvres by hand in a Simulink aircraft simulator. The progress of the identification process is continuously visualised on the computer display. The development of the aerodynamic derivatives is shown in a real time developing box plot like representation, while also the time varying covariance of the aerodynamic derivatives is shown. The latter information provides some indication to the user if it is needed to adapt his manual input signal in order to reduce the uncertainty of the identification results.

3 Future research

In the next phase of this research project, the above mentioned procedure will be extended to include identification capabilities for damaged aircraft models. First of all the robustness of this procedure for variations in mass, inertia and center of gravity must be analysed and improved if necessary. Moreover, the model structure in the second phase must be adapted so that it is representative for the damaged aircraft model. Therefore, information can be used from the least squares innovation signal. Finally, the obtained model is only locally valid. It can be rendered globally valid by the process of fuzzy clustering of the local identified models over the flight envelope hyperboxes.

References

- [1] Q.P. Chu, J.A. Mulder, and J.K. Sridhar. Decomposition of Aircraft State and Parameter Estimation Problems. *Proceedings of the 10th IFAC Symposium on System Identification*, Vol. 3, pp. 61-66, 1994.
- [2] M. Laban. On-Line Aircraft Aerodynamic Model Identification. Ph.D. thesis, Delft University of Technology, May 1994.
- [3] J.C. van Tooren. Fuzzy Aerodynamic Model Identification. MSc. thesis, Delft University of Technology, June 2005.

A Frequency Domain Identification Algorithm for Single-Ended Line Measurements

Carine Neus, Patrick Boets, Leo Van Biesen

Vrije Universiteit Brussel, Pleinlaan 2, 1050 Brussels, Belgium
 Department of Fundamental Electricity and Instrumentation (ELEC),
 Email: cneus@vub.ac.be

1 Introduction

In order to identify whether a subscriber loop is suitable for a certain Digital Subscriber Line (DSL) service, the transfer function of the loop has to be estimated. Several measurement techniques exist, however Single-Ended Line Testing (SELT) is often preferred by the telecom operators because all necessary measurements are done at the central office, in contrast to Dual-Ended Line Testing (DELT), where a technician needs to be dispatched to the customer's site.

2 Measurement vs. identification domain

SELT measurements can be performed in time or frequency domain. Both domains are also suited for identification. All four combinations of measurement and identification domain are possible, with the use of a direct or inverse Fourier transform where necessary. Till now measurements have mainly been performed by measuring the one-port scattering parameter in the frequency domain ($S_{11}(f)$) but identification has mainly been attempted in the time domain [1, 2]. This paper proposes a new approach by doing the identification in the frequency domain.

3 Frequency domain identification algorithm

The main idea is to exploit the information in the periodicity of $S_{11}(f)$, which is present due to constructive and destructive interference of the waves propagating along the line under test. The following processing steps are performed:

- Change of impedance base when the measurement device is not matched to the line under test.
- Using only the reliable frequency band. Otherwise applying an inverse Fourier-transform will lead to a distorted time-domain signal.
- Using the real or complex part of $S_{11}(f)$ instead of the classical polar representation (abs and phase). As shown in Figure 1, the real and complex part contain the same amount of information.
- Windowing the frequency domain signal in order to reduce time-domain leakage.
- Zero-padding the frequency domain data to improve resolution. This is important especially when only a small frequency band is reliable, resulting in few measurement points.

Subsequently an FFT-operation is applied to reveal the present periodicities. Each periodicity results in a peak, giving us information about the loop make-up. In the example of Figure 1, the line segments of 1000 m and 1500 m can clearly be recognized. It is important to mention that the obtained signal is again in the time-domain but has lost its physical meaning due to the performed processing steps.

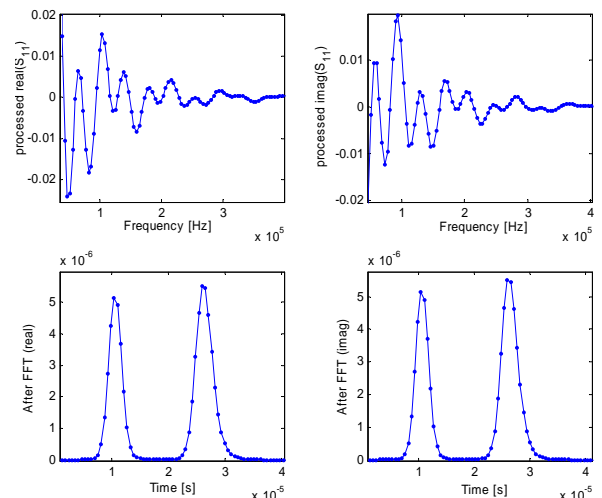


Figure 1 The periodicity of the processed data is extracted by the FFT; loop make-up: 1000 m in cascade with 1500 m

4 Conclusions

A measurement campaign confirms that the new algorithm leads to good loop identification. Once the loop make-up is known, the transfer function can be calculated. This is important for telephone companies providing DSL services, in order to have a tool to characterize and evaluate the capability of a subscriber local loop in carrying DSL services.

References

- [1] P. Boets, T. Bostoen, L. Van Biesen and T. Pollet, "Pre-Processing of Signals for Single-Ended Subscriber Line Testing", IEEE Trans. Instrum. and Meas., Vol. 55, No. 5, October 2006, pp.1509-1518
- [2] S. Galli and K. Kerpez, "Single-Ended Loop Make-Up Identification - Part I: A Method of Analyzing TDR Measurements", IEEE Trans. Instrum. and Meas., Vol. 55, No. 2, April 2006, pp528-537.

Transmission line modelling exploiting ‘common-mode’ signals

Wim Foubert, Patrick Boets, Leo Van Biesen

Vrije Universiteit Brussel, Pleinlaan 2, 1050 Brussels, Belgium
 Department of Fundamental Electricity and Instrumentation (ELEC),
 Email: wfoubert@vub.ac.be

1 Introduction

Digital Subscriber Line (DSL) technology provides broadband service over ‘twisted pair’ copper wires of the existing telephone network. The inherent structure of this network causes crosstalk, which significantly reduces the achievable bit rate for each user. The exploitation of ‘common-mode’ signals could compensate for the performance reduction and lead to a significant increase in capacity.

2 ‘Differential-Mode’ vs ‘Common-Mode’ signals

Data transmission over copper ‘twisted pair’ (TP) cables is accomplished by sending and receiving ‘differential-mode’ (DM) signals. As can be seen in Figure 1, DM signals appear as a voltage difference $d(t)$ measured between the two wires, or equivalently as a current within the loop formed by the TP and the termination impedances

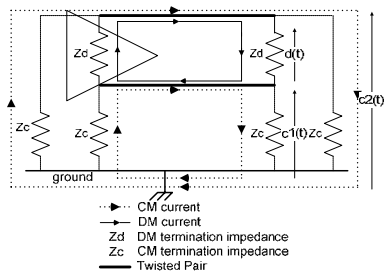


Figure 1: Differential-mode (DM) and common-mode (CM) current and voltage

The ‘common-mode’ (CM) signal, in contrast, is the arithmetic mean of the voltages $c_1(t)$ en $c_2(t)$, measured between each wire and ground. The corresponding CM currents appear in the loops formed by each wire, the CM termination impedances and ground [1]. This CM signal contains useful information about the interference signals and therefore can be used to reduce degradation caused by crosstalk. For this, we have to model and characterize the transmission channel.

3 Channel modelling

Parametric and tabulated line models are frequently used in the study of new telecommunications systems in order to describe the transfer function and the crosstalk behavior. However, the existing models are only

applicable when using the line pairs in differential mode. New models are under development, describing besides the differential mode also the common mode load, propagation and crosstalk. These models are operative for a bundle of line pairs where signal transfer exists from the differential mode to the common mode and vice versa. The multi-conductor transmission lines theory forms the base to formulate the cable characteristics. A frequency dependent multi-port matrix will describe the cables installed in the field by means of geometrical and physical cable properties. The current theory is only valid for uniform line systems. However, the cable, which can attain a total length of several kilometers, is non-uniform due to the twisting of the line pairs and the rotation of groups of line pairs. As can be seen in Figure 2, the system can be split up in very short line segments to overcome this problem.

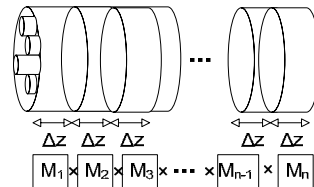


Figure 2: Working method for multi-port description

Each line segment is considered to be uniform and is represented by a transmission matrix. The multi-port description is obtained by multiplication of the different matrices.

Future work will focus on the design of parametric models and on the modelling of crosstalk.

4 Conclusions

Improved DSL can be designed, by exploiting ‘common-mode’ signals to reduce crosstalk. Therefore, we first have to set up reliable transmission channel models, in particular models between ‘common-mode’ signal paths and between ‘common-mode’ and ‘differential-mode’ signal paths.

References

[1] T. Magesacher, P. Ödling, P. O. Börjesson, W. Henkel, T. Nordström, R. Zukunft, S. Haar, “On the Capacity of the Copper Cable Channel Using the Common Mode”, Proceedings IEEE GLOBECOM-02, November 2002, Taipei, Taiwan.

State feedback control of switching server flowline with setups

J.A.W.M. van Eekelen · E. Lefeber · J.E. Rooda
 Technische Universiteit Eindhoven, Systems Engineering Group
 {j.a.w.m.v.eekelen, a.a.j.lefeber, j.e.rooda}@tue.nl

1 Introduction

We consider the control of flowlines consisting of switching servers, through which different types of jobs flow. Switching from one job type to an other takes time. Examples of such flowlines can be found in manufacturing industry, food processing industry, communication networks, data flow and traffic flow.

The optimal process cycle with respect to work in process (wip) levels for a single switching server with two job types is known from previous work, [1]. This optimal wip level value is an absolute lower bound on average wip levels for flowlines with more than one workstation, since upstream workstation only move wip to downstream workstations, without reducing it. In this study we derive conditions for workstations in a flowline that have to be met in order to achieve the minimal wip level of an isolated workstation for the whole flowline. Based on these conditions, the class of flowlines is characterized that can behave as if it were a single switching server. For an introduction to the topic in more detail, the reader is referred to [2].

2 Example of switching server flowline

Consider the flowline as shown in Figure 1, consisting of two workstations. The workstations process two different job types, which are stored in separate buffers with length x_i^j with $i \in \{1, 2\}$ the job type and $j \in \{A, B\}$ the workstation identifier. Jobs arrive with constant arrival rate λ_i and are processed by the servers with maximum rate μ_i^j . Switching from one job type to another job type takes time: σ_{12}^j or σ_{21}^j time units. A process cycle of a server always has the following operations: setup to type 1, process type 1 jobs, setup to type 2, process type 2 jobs, setup to type 1, etc.

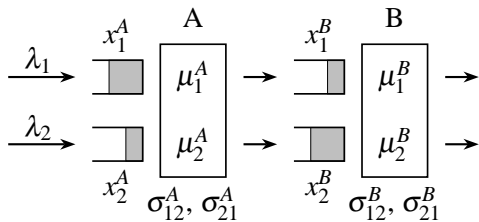


Figure 1: Flowline of 2 switching servers with 2 job types.

3 Desired periodic behavior

From [1] we know the optimal process cycle with respect to time averaged wip levels of a single switching server with two job types and setup times. If it is possible to treat a flowline of such switching servers as a black box which as a whole behaves like the optimal process cycle for a single switching server, then the flowline also has a cycle with this minimal mean wip level. Each server in the flowline has to meet conditions to fulfill this desired behavior:

- All servers have the same period length of a cycle.
- Buffers may never become negative.
- If the most downstream workstation has an empty buffer, all buffers of that type have to be empty.
- All servers process the same number of jobs of each type during a process cycle.

These conditions yield mathematical conditions which have to be fulfilled to make a switching server flowline behave like a single stand-alone switching server. These mathematical conditions completely characterize the class of flowlines for which this is possible.

4 State feedback controller

A state feedback controller is proposed that steers a trajectory to the desired trajectories for all servers in the flowline, from any arbitrary start point (buffer levels and current mode of operation of a workstation). Convergence to the desired process cycles is proven mathematically. Although the analysis is performed with a hybrid fluid model, the controller can successfully be implemented in a (stochastic) discrete event case study.

5 Conclusion

We have derived conditions for flowlines of switching servers with two job types and setup times to behave as if it were a single switching server. A state feedback controller has been proposed, which has been proven mathematically.

References

- [1] J.A.W.M. van Eekelen, E. Lefeber, J.E. Rooda, *Feedback control of 2-product server with setups and bounded buffers*, in Proceedings of the 2006 American Control Conference; Minneapolis, United States, 544–549, 2006.
- [2] J.A.W.M. van Eekelen, E. Lefeber, J.E. Rooda, *State feedback control of switching server flowline with setups*, accepted for the 2007 American Control Conference, New York, United States, 2007.

Model and actuator improvements for surge control

Jan van Helvoirt*, Bram de Jager, Maarten Steinbuch

Control Systems Technology Group

Department of Mechanical Engineering

Technische Universiteit Eindhoven

P.O. Box 513, 5600 MB Eindhoven

The Netherlands

E-mail: *J.v.Helvoirt@tue.nl

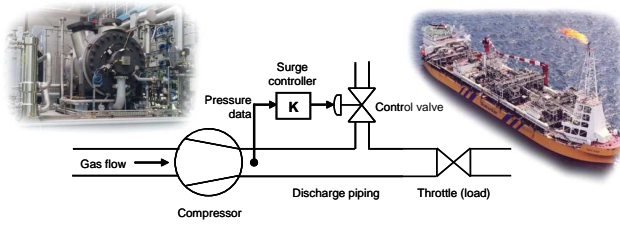


Figure 1: Active surge control of industrial compressors.

1 Introduction

The performance and operating range of centrifugal compressors is limited by the occurrence of an aerodynamic instability called *surge*. Moreover, the large thermal and mechanical loads involved can severely damage the compression system. Till now a breakthrough in compressor stabilization by means of active control has not been made [1]. Our research focusses on modeling and identification for the control of centrifugal compressors. Furthermore, we aim at removing the technological barriers for successful surge control of an industrial compression system.

2 Compressor modeling

Experiments on an industrial test compressor revealed the presence of acoustic phenomena in the discharge piping system. These effects were not captured by the widely used Greitzer compressor model. In order to investigate the influence on surge control performance, we developed a nonlinear transmission line model for these piping acoustics.



Figure 2: Centrifugal compressor test rig.

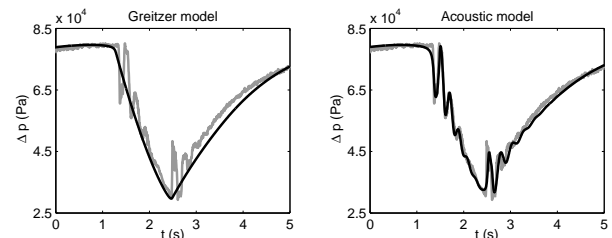


Figure 3: Surge measurement (gray) and simulation (black).

3 Surge control actuator

After modeling and identification of the compressor dynamics, we confirmed that successful surge control was hampered by the limited actuator performance. Therefore, we developed a high-speed control valve prototype that meets the requirements for stabilization of the system.

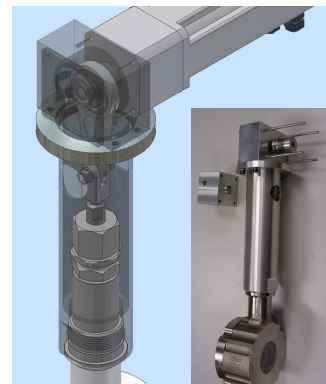


Figure 4: Prototype of high-speed (25 Hz) control valve.

4 Future work

Research will now focus on the application of a surge control strategy to the experimental compression system. Furthermore, attention will be paid to improve the robustness of the controller with respect to model uncertainties and noise.

References

[1] J.D. Paduano, E.M. Greitzer and A.H. Epstein, "Compression system stability and active control," *Ann. Rev. Fluid Mechanics*, vol. 33, pp. 491–517, 2001.

A four-channel adaptive structure for high friction teleoperation systems in contact with soft environments

Thomas Delwiche

Université Libre de Bruxelles
Control Engineering Department
CP 165/55, Av. F.D.Roosevelt, 50
1050 Brussels, Belgium
thomas.delwiche@ulb.ac.be

Michel Kinnaert

Université Libre de Bruxelles
Control Engineering Department
CP 165/55, Av. F.D.Roosevelt, 50
1050 Brussels, Belgium
michel.kinnaert@ulb.ac.be

Introduction and background

Teleoperation consists in performing a remote task with an electromechanical master-slave device. The master part of the system is manipulated by the human operator while the slave part, which is located remotely, tries to perform the task imposed by the master. When force feedback is present at the master side to make the user feel the interaction force between the slave and its environment, one talks about bilateral teleoperation.

The four-channel (4C) structure is a bilateral teleoperation control scheme depicted in figure 1 in the case of a one degree of freedom device. This scheme was first introduced in [2] and later improved by adding local force loops in [1]. The associated notations are: F_e (F_h), the net force exerted on the environment (the master) by the slave (the user), F_e^* , the active force exerted by the environment on the slave as opposed to a reaction force, F_h^* , the muscular force of the user, X_s (X_m), the position of the slave (the master), F_m (F_s), the sum of F_h ($-F_e$) and the force provided by the actuator of the master, $F_{m,actuator}$ (of the slave, $F_{s,actuator}$). The different impedances (Z_i , $i \in \{m, h, s, e\}$) are defined as follows: $F_e + F_e^* = Z_e X_s$, $F_h^* - F_h = Z_h X_m$, $F_s = Z_s X_s$, $F_m = Z_m X_m$. With this scheme, both position and force are fed back from the master to the slave and vice-versa. One can show that under ideal conditions (perfectly linear and perfectly known system), this scheme allows perfect transparency which can be defined as perfect force and position tracking between the master and the slave.

Adaptive structure: modeling and experiments

An adaptive structure based on a modified 4C scheme is proposed in order to keep suitable performance with high friction devices, i.e. non-ideal devices.

First, the adaptive approach is motivated based on practical considerations. Next, a more detailed representation of the 4C structure is proposed. This model makes explicit some conversion ratios, which are hidden in Z_h and Z_e in the model of figure 1. These coefficients, aimed at reducing the external forces (F_h and F_e) to the actuator axes, appear to be significant when studying the influence of friction on performance. Indeed, it is shown that some of these

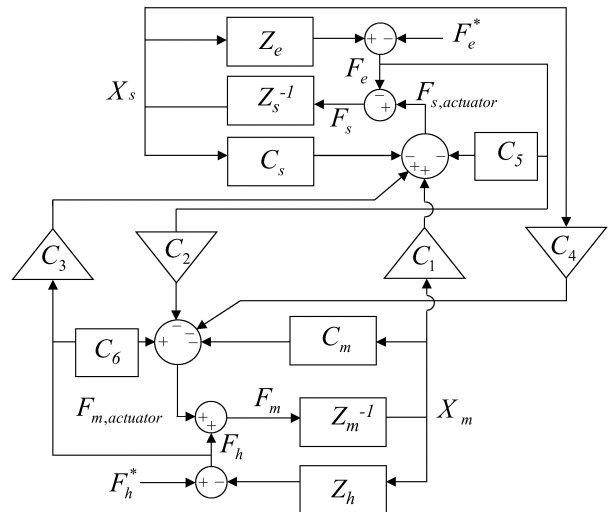


Figure 1: Four channel control architecture including local force loops (C_5 and C_6).

ratios are time-varying. So, in order to cope with this variation, an adaptive structure is defined. A preliminary study of stability is made for the obtained adaptive structure which was implemented on a one degree of freedom device. Although some vibrations were felt by the user, both force and position tracking were improved.

Acknowledgements

The work of T. Delwiche is supported by a FRIA grant.

References

[1] Hashtrudi-Zaad,K. and Salcudean,S.E. On the use of local force feedback for transparent teleoperation. *Proceedings of the IEEE International Conference on Robotics and Automation*, 1999.

[2] Lawrence,D.A. Stability and transparency in bilateral teleoperation. *IEEE Transactions on Robotics and Automation*, 9(5), 1993.

Real-time Optimal Power Balance Control Using Nodal Prices

A. Jokic, P.P.J. van den Bosch and M. Lazar

Department of Electrical Engineering¹

Eindhoven University of Technology

P.O. Box 513, 5600 MB Eindhoven

The Netherlands

Email: a.jokic@tue.nl

1 Introduction

Electrical power systems have certain unique properties, which often make the control of those systems a challenging task. For example, electrical energy cannot be efficiently stored in large amounts, which implies that production has to meet rapidly changing demands in real-time, making electricity a commodity with fast changing production costs. Furthermore, unlike other transportation systems, which assume a free choice among alternative paths between source and destination, the flow of power in electrical energy distribution networks is governed by physical laws and, for some fixed pattern of power injections, it can be influenced only to a certain degree. Therefore, physical and security limits on the maximal power flow in the lines of electrical energy distribution networks represent crucial system constraints, which cannot be neglected. The common characteristic of virtually all existing approaches is that the congestion management problem is treated in a *static manner*, while for real-time control of power flow in the lines the AGC (Automatic Generation Control) [1] scheme is utilized. In the talk, we present an *explicit, price-based, dynamic* controller for real-time optimal power balancing and congestion management [2]. Here, by *explicit* we mean that the controller is not based on solving on-line an optimization problem, as it is for instance the case of the model predictive control (MPC) framework.

2 Control problem

In a rather general form, the optimal power balance problem is formulated as follows. Consider an LTI system Σ , given by its state-space realization with the state vector $x = \text{col}(x_1, x_2)$, the input vector $w = \text{col}(d, u)$, the output vector y , and consider a strictly convex optimization problem

$$\min_{x_1} \{J(x_1) \mid H \text{col}(x_1, d) = h, G \text{col}(x_1, d) \leq g\}, \quad (1)$$

associated with the state vector x_1 . Here, H, G, h and g are suitably defined constant matrices and vectors. We are con-

cerned with the following control problem: Design an explicit controller, which has y as input and u as output, such that for any constant value of the exogenous input d , the system settles in a steady-state point, which is such that the value of the state vector x_1 coincides with the solution of the optimization problem (1).

For electrical power systems control, the above stated problem has the following interpretation. Dynamical system Σ represents the power system and includes appropriate models of its generators. Vector x_1 collects the network power injections [MW] of all generators in the system. Output vector y consists of the measured network frequency and the measured power flows in the lines. Input vector u is a set of nodal prices for electrical power. Nodal price is a price of electrical power at specific node in the network. The objective function in (1) is a negated sum of the production costs for all generators in the network. Exogenous input d represents the loads in the power system. Equality constraint in (1) represents the power balance constraint, while the inequality in (1) represents the limits on the maximal power flow in the lines.

3 Controller design

The main idea in the controller design is to ensure that the closed-loop steady-state relations satisfy the Karush-Kuhn-Tucker optimality conditions for the optimization problem (1). Due to the inequality constraints representing the line flow limits, the controller has a piecewise affine structure. In the talk, we will present a distributed implementation of the developed controller.

References

- [1] P. Kundur, "Power System Stability and Control," McGraw-Hill, 1994.
- [2] A. Jokic, M. Lazar, and P.P.J. van den Bosch, "Price-based Optimal Control of Power Flow in Electrical Energy Distribution Networks," Proceedings of the Hybrid Systems: Computation and Control conference, 2007, to appear.

¹This research has been performed within the framework of the research program "Intelligent Power Systems" that is sponsored financially by SenterNovem. SenterNovem is an agency of the Dutch Ministry of Economic Affairs.

Control Issues in Rotor-Bearing Interactions

H. M. N. K. Balini and Carsten W. Scherer

Delft Center for Systems and Control, Delft University of Technology, Mekelweg 2, 2628 CD, Delft.

email address corresponding author: h.m.n.k.balini@tudelft.nl

Keywords: Lateral Rotor dynamics, μ -Synthesis, LPV Control, Robust Estimation

Introduction: The present exposition is aimed at reporting current research issues in relation to control of high speed rotor-bearing systems. A wealth of literature exists citing successful applications ranging from hard-disk drive systems to turbo machinery. Interaction of rotor with Active Magnetic Bearings and Air Bearings presents considerable challenge in achieving desired machine performance. A major area of concern is the lateral vibrations of the system because of disastrous consequences. Hence, our approach consists of techniques for accurate modeling, analysis and appropriate control strategies.

Lateral Vibrations in Rotors: Lateral vibrations primarily occur due to interaction forces from rotor surrounding (bearings) and/or due to mass imbalance. In air bearings, these interaction forces are modeled to be generated from a spring damper system. A reasonable description of the dynamics can be obtained by accurate estimation of the stiffness and damping constants. Various techniques for estimating these constants are given in the literature. Further, they depend on the operating speeds. In magnetic bearings, the interaction forces depend on the current supplied, which acts as a control variable.

An imbalance force is generated when the center of mass does not lie on the axis of rotation. This acts as a periodic excitation for the lateral dynamics, and hence, needs to be accounted for in the model or regarded as disturbances/uncertainties for control. In the first case, determination of the amount of imbalance and its eccentricity is posed as an estimation problem. This enables balancing procedures to be applied as a corrective measure.

Air Bearings: Fluid properties between the journal and bearing govern the lateral/axial dynam-

ics and are obtained as solutions to the Reynolds' equation. These are obtained by means of iterative schemes and influence the load capacity, rotational speeds and fluid film thickness. They aid in stability analysis. Extensive literature is devoted to the study of precession motion in air bearings. Influencing the fluid properties by means of mass flow control at the feed-through in externally pressurized bearings is a yet to be explored area. Hence, our research efforts are focussed on this area.

Magnetic Bearings: Active Magnetic Bearings have grown to be a mature technology incorporating a variety of control concepts. Control is primarily aimed at countering the imbalance response at various operating conditions. Controllers based on μ -synthesis regard these imbalances as uncertainties in the plant model and give robust performance at the particular operating speeds. By solving a series of H-infinity control problems at different operating speeds, self scheduled H-infinity controllers can be obtained as functions of linear combinations of the speeds. An attractive feature is that the linear dependence of the system matrix on rotational speed renders the controller to be solved by a set of Linear Matrix Inequalities. Literature exists for designing refined LPV controllers with reduced conservatism (in terms of arbitrarily fast parameter variations). We would like to consider application of these concepts to hybrid air-magnetic bearings for further research.

S. Zhou and J. Shi, "Active Balancing and Vibration Control of Rotating Machiner: A Survey," *The Shock and Vibration Digest*, vol. 33, no. 4, pp. 361-371, July 2001.

F. Matsumura, T. Namerikawa, K. Hagiwara and M. Fujita, "Application of Gain Scheduled H_∞ Robust Controllers to a Magnetic Bearing," *IEEE Trans. Contr. Syst. Technol.*, vol. 4, no. 5, September 1996.

Modelling and identification of a SMB process

V. Grosfils, M. Kinnaert,
 Service d'Automatique et d'Analyse des Systèmes,
 Université Libre de Bruxelles,
 CP 165/55, 50, Av. F. D. Roosevelt, B-1050 Brussels,
 Belgium
 Email : valerie.grosfils@ulb.ac.be

Chromatographic separation processes are based on the differential adsorption of the components of a mixture. The Simulated Moving Bed (SMB) process, made of a series of chromatographic columns, allows a counter-current movement of the solid phase and the liquid phase, which contains the mixture to be separated, by periodically switching inlet and outlet valves in the direction of the liquid flow. The design and the control of SMB units require the use of a process model and the estimation of the model parameters.

SMB models are based on the differential fluid and solid mass balances in the columns. The following equation is obtained for the component i of a binary mixture in one column in the SMB process:

$$\frac{\partial c_i}{\partial t} = -v \frac{\partial c_i}{\partial z} + D \frac{\partial^2 c_i}{\partial z^2} - \frac{1-\varepsilon}{\varepsilon} \frac{\partial q_i}{\partial t} \quad (1)$$

with c_i , the fluid concentration, q_i , the solid concentration, v , the fluid velocity, D , the diffusion coefficient, ε , the porosity. t denotes the time and z , the axial coordinate. The last term of the equation characterizes the mass transfer between the solid and the liquid phase and depends on the adsorbed equilibrium concentration, q_i^{eq} . The latter is here described by the Langmuir isotherm:

$$q_i^{eq} = \frac{q_{Si} b_i c_i}{1 + b_1 c_1 + b_2 c_2} \quad (2)$$

where q_{Si} and b_i are respectively the saturation capacity and the equilibrium constant of component i .

The model complexity can be modified by neglecting diffusion or by modifying the shape of transfer term. In this study, three models have been taken into account:

- the linear driving force model, that considers linear driving force for the mass transfer:

$$\frac{\partial q_i}{\partial t} = k(q_i^{eq} - q_i) \quad (3)$$

with k the mass transfer resistance.

- the equilibrium dispersive model, which considers equilibrium between solid and fluid phase:

$$q_i = q_i^{eq} \quad (4)$$

- the kinetic model that considers linear driving force for the mass transfer (Eq. 3) but neglects axial diffusion ($D = 0$ in Eq.1).

The parameters to be estimated are the isotherm parameters, the mass transfer resistance and/or the diffusion coefficient.

C. Levrie, A. Vande Wouwer
 Service d'Automatique,
 Faculté Polytechnique de Mons,
 Boulevard Dolez, 31, 7000 Mons,
 Belgium

The aim of this paper is to validate on experimental SMB data the systematic approach to SMB processes model identification presented in (Grosfils et al., 2006). Parameters are first estimated from experiments performed on one SMB column (elution peaks) by minimizing a cost function characterizing the difference between measured and simulated elution peaks using a numerical optimization. Then the cross-validation is performed with SMB experiments so as to assess whether the parameters identified from batch experiments may be used in a SMB model.

The parameter estimation procedure has been developed after a systematic study of parameter identifiability. Thanks to a sensitivity analysis, the experiment design has been performed. Moreover, from a systematic comparison of the identifiability of the parameters of the 3 models, together with the evaluation of the computational load associated to these models, it follows that a kinetic model yields an appropriate compromise between these criteria. Because of the presence of local minima, it turns out that a multi-start procedure is advisable. It consists in performing several identifications from different initial values of the parameters. Besides, confidence intervals for the estimated parameters and for the simulation errors are computed.

The second step is the cross-validation with SMB experiments performed on a preparative SMB unit. As pumps and detectors are introduced between the columns of this SMB process, it turns out that the extra-column dead volume can not be neglected. In this study, the dead volume model developed in (Migliorini et al., 1999) is adapted to the considered SMB plant. Good cross-validation results are obtained on SMB experiments.

Acknowledgement

This work has been performed in the framework of Movidia project (contracts n°0114843 and 0114961) funded by the Walloon Region (Belgium).

References

Grosfils V., L. Levrie, M. Kinnaert, A. Vande Wouwer (2006). A systematic approach to SMB processes model identification from batch experiments, submitted to Chemical Engineering Science

Migliorini C., Mazzoti M. and M. Morbidelli, (1999), Simulated Moving-Bed Units with extra-Column Dead Volume, AIChE Journal, vol.45, n° 7

Model Approximation for Distributed Parameter Systems

S.K.Wattamwar¹Dr. Siep Weiland¹Dr. Leyla Özkan²

1 Introduction

Phenomenon in Fluid Dynamics are usually modeled by partial differential equations which are solved by discretization of the spatial domain. Such discretization leads to a high order systems. Despite the currently available computing power, it is difficult to use such high order models for online control and optimization applications. This motivates the search for lower dimensional models which could approximate the original high dimensional models without much loss of the original information. Such low dimensional (reduced) models should satisfy various criteria like a smaller dimension, an accurate prediction, faster computability, stability and good performance in closed loop. The problem of finding of suitable substitute model is usually referred to as model reduction.

2 Glass Manufacturing

To investigate novel model reduction ideas we are working on a Cathode Ray Tube (CRT) glass manufacturing process. This process is highly energy intensive and involves many complex phenomena. In this process raw material is fed into a melter containing molten glass. A batch blanket is formed which is heated from the top by oil/gas fired burners and by molten glass from the bottom. This process is roughly divided into four sub-processes which are melting, fining, homogenization and refining. Inhomogeneous supply of heat to the glass induces a convective flow pattern of glass in the tank which in-turn has effect on each of these sub processes. The Glass flow pattern in the tank is laminar and temperature varies between 1500-1800 K. Glass quality is highly dependent on how well each of the sub processes is carried, on the flow pattern and on the temperature distribution in the tank. Dynamic behaviour of the glass tank depends on the heat input to the tank and heat exchange within the tank. Control of temperature distribution in the tank is the main control task which is very difficult due to long thermal response time of the glass. Hence it is tried to run the tank as stationary and stable as possible. A proper selection of inputs that define bubbling, electrical boosting, stirring are used to ensure proper operating conditions.

3 Research focus

In this presentation we consider the problem of model reduction for a CRT glass manufacturing process which is

¹Department of Electrical Engineering, Eindhoven University of Technology, P.O. Box 513, 5600 MB Eindhoven, The Netherlands, E-mail: s.wattamwar@tue.nl.

²IPCOS, Bosscheweg 143, 5282 WV Boxtel, The Netherlands.

modeled semi-empirically. This means that the model consists of two parts: a mechanistic one and an empirical one. The mechanistic part comes from first principle modeling techniques consisting of a basic set of equations (PDE) which comes from conservation of mass, momentum and heat transfer. For a laminar flow, these are described by Navier-Stokes equations. Computational Fluid Dynamics (CFD) tools which are used to model these equations. A second part that is defined in an empirical manner comes from observed data or uncertain parameters. Many involved phenomena like radiation, glass melting and bubbling are modeled empirically. Such a complex model results into a system of dimension of thousands of order. Due to its very high dimensions, choice of the model reduction methods is limited. Our research is focused on Proper Orthogonal Decomposition (POD) or Karhunen-Loeve expansion method which is based on the system simulation data. The POD method searches for coherent patterns in the observed data and uses these patterns to define low dimensional projection spaces for reduced order models. This method is therefore data dependent. Although the POD method gives reduced models, the involved computational time for such models is still large. Typically, this is due to a loss of sparsity structure in the original model. We want to investigate into a decomposition technique that uses the POD method but leaves this sparsity structure invariant. On the application side we are trying to capture the complex phenomena of corroding glass tank walls, glass batch melting and radiation effects. We also want to look into the theoretical aspects of the POD like error analysis, adaptation of the POD basis functions and closed loop model reduction. In brief, research focus is to get reduced models that are computationally faster.

Acknowledgement

This work has been supported by the European union within the Marie-Curie Training Network PROMATCH under the grant number MRTN-CT-2004-512441

References

- [1] NCNG course on glass manufacturing 1997.
- [2] R. Romijn, L. Özkan, S. Weiland, W. Marquardt, J. Ludlage “Hybrid Modeling approach for the reduction of nonlinear systems”, DYCOPS 2007.
- [3] P. Astrid, “Reduction of process simulation models”, Phd thesis 2004.
- [4] L. Huisman, “Control of glass melting processes based on reduced CFD models”,PhD thesis 2005.

Mathematical performance analysis of a temperature controlled bulk storage room

Simon van Mourik and Hans Zwart

Department of Applied Mathematics, University of Twente, The Netherlands,
e-mail: s.vanmourik@utwente.nl

Karel Keesman

Systems & Control Group, Wageningen University, The Netherlands,
email: Karel.Keesman@wur.nl

1 Introduction

We consider a bulk storage room for agricultural food products. A ventilator enforces the air circulation, and the air is cooled down by a cooling device, see Figure 1. Cold air flows usually upwards through the bulk. Inside

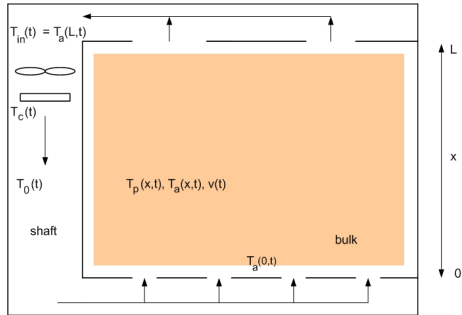


Figure 1: Schematic representation of a bulk storage room.

the bulk, the air warms up and consequently the products at the top will be some degrees warmer than those at the bottom, see [1]. A larger airflow will decrease these spatial variations, but will be costly. Model-based control design is a nontrivial task, since a standard model that describes the time- and spatially dependent temperatures will consist of a set of nonlinear partial differential equations.

Systems design is strongly correlated to controller design. The controller adds dynamics to the system, causing it to behave differently than the uncontrolled system. For storage room design, it is therefore desirable to design the plant and controller simultaneously, instead of separately.

2 Method

We started with the results in [2], where a basic physical model was derived and validated with experimental results. An open loop control law, which explicitly depends on all the physical model parameters, was successfully constructed. The controller determines the times when to switch between two discrete inputs. This input switching is realistic since often in practice the ventilator is switched on and off

on a regular basis. Then we defined two criteria that indicate the performance of the system. The performance criteria are the total energy usage by the cooling device and the ventilator, and the temperature difference between the products at the top and at the bottom of the bulk. The controller as well as the performance criteria are closed expressions that contain all the prior physical knowledge. The relationship between each design criterium and the design parameters consists of a single expression and is therefore easily computed. Since some analytical relations could not be found in the literature, they are identified experimentally. These relations describe the energy usage of the ventilator, and the effectiveness of the heat exchanger, both as functions of the airflow.

3 Results

The following design tradeoffs were observed. The total energy usage is minimized by a low temperature of the cooling device, but the temperature difference over the bulk is minimized by a high temperature of the cooling device. Further, the temperature difference is decreased by a more powerful ventilator. However, the tradeoff here is that such a ventilator will be more expensive in purchase. The energy usage is decreased by a lower bulk. The tradeoff is that for a fixed bulk volume, a lower bulk means a larger floor area, which is usually more expensive than a higher roof.

4 Acknowledgement

This work was supported by the Technology foundation STW under project number WWI.6345.

References

- [1] A. Rastovski and A. van Es et al. *Storage of potatoes, Post-harvest behaviour, store design, storage practice, handling*. Pudoc Wageningen, 1987.
- [2] S. Van Mourik, H.J. Zwart, and K.J. Keesman. Analytic control law for a food storage room. *Submitted*, 2006.

An algebraic approach to control theory for PDE

Harry Trentelman
 University of Groningen
 H.L.Trentelman@math.rug.nl

Diego Napp
 University of Groningen
 diego@math.rug.nl

1 Introduction

In this talk, we give a very general overview of the theory of multidimensional systems using a behavioral framework. This framework relies on the idea that control systems are described by equations, but their properties of interest are most naturally expressed in terms of the set of all solutions to the equations. This is formalized by the relatively new notion of the system behaviour (denoted by \mathfrak{B}), due to Willems. We will focus our attention on systems described by partial differential equations with constant coefficients and in the relation between finitely generated modules and these behaviours. This enables the application of the huge and powerful machine of commutative algebra to problems in multidimensional linear systems theory. The main difficulty in using this relation is that it is highly abstract. However we will see how it is possible to give interpretation of some algebraic theory. We will explain the mathematical background needed and show how structural properties such as controllability or autonomy can be described in terms of some algebraic properties.

In particular I will investigate in some detail the decomposition of a given behavior into the sum of finer components. It is immediately apparent that decomposition is a powerful tool for the analysis of the system properties. It is, indeed, of particular interest, the case of multidimensional systems where a description of the nD systems trajectories is quite complicate and decomposing the original behavior into smaller components seems to be an effective way for simplifying the systems analysis.

Another motivation for considering this problem is that the problem is also an interesting question from a purely mathematical point of view and allows different approaches.

The autonomous-controllable decomposition has played a significant role in the theory of linear time-invariant systems. Such decomposition expresses the idea that every trajectory of the behavior can be thought of as the sum of two components: a free evolution, only depending on the set of initial conditions, and a force evolution, due to the presence of a soliciting input. In the case of $1D$ systems, this sum is direct, i.e.

$$\mathfrak{B} = \mathfrak{B}_{cont} + \mathfrak{B}_{aut} \text{ and } \mathfrak{B}_{cont} \cap \mathfrak{B}_{aut} = 0.$$

where \mathfrak{B}_{cont} and \mathfrak{B}_{aut} represent the controllable and autonomous part of \mathfrak{B} respectively.

However, this decomposition is, in general, not longer direct for $n \geq 2$, and we may have that the controllable part of \mathfrak{B} , (which is uniquely defined for a given \mathfrak{B}) intersects all possible autonomous parts involved in the controllable-autonomous decomposition [5, 6, 7].

Some of the results I will give are already known, and my main contribution will be a completely new approach to the problem using algebraic geometry, which hopefully opens new ways to tackle open problems in multidimensional systems theory.

Finally we provide an algorithm to effectively solve our problem.

References

- [1] J. Wood, E. Rogers, and D. H. Owens, 'Modules and Behaviours in nD Systems Theory' *Mult. Systems and Signal Processing*, 2000.
- [2] J. C. Willems, 'On Interconnections, Control, and Feedback', *IEEE Trans. on Auto. Contr.*,
- [3] U. Oberst, 'Multidimensional Constant Linear Systems', *Acta Applicandae Mathematicae*, vol. 20, 1990.
- [4] H. Pillai and S. Shankar, 'A Behavioural Approach to Control of Distributed Systems', *SIAM Journal on Control and Optimization*, vol. 37, 1999.
- [5] Wood, Jeffrey and Rogers, Eric and Owens, David H., 'Controllable and autonomous nD linear systems,' *Multidimens. Systems Signal Process.*, vol. 10, 1999.
- [6] Valcher, Maria Elena, 'On the decomposition of two-dimensional behaviors,' *Multidimens. Systems Signal Process.*, vol. 11, 2000.
- [7] Bisiacco, Mauro and Valcher, Maria Elena, 'Two-dimensional behavior decompositions with finite-dimensional intersection: a complete characterization,' *Multidimens. Systems Signal Process.*, vol. 16, 2005.

Distributed wavefront reconstruction for Adaptive Optics

Rogier Ellenbroek

Delft Center for Systems and Control,

Faculty of Mechanical, Maritime and Materials Engineering, Delft University of Technology
r.m.l.ellenbroek@tudelft.nl

Michel Verhaegen

Delft Center for Systems and Control,

Faculty of Mechanical, Maritime and Materials Engineering, Delft University of Technology
m.verhaegen@moesp.org

Niek Doelman

TNO Science and Industry

niek.doelman@tno.nl

1 Introduction

In the world of astronomers, bigger does not automatically mean better. A bigger telescope is not always a better telescope – at least when “bigger” means “larger than about one meter”. This is because the image resolution of telescopes is limited by atmospheric turbulence. When a star emits light, its wavefront is an expanding sphere that is so big when it reaches the earth, that its surface is assumed to be flat. While traveling through the earth’s turbulent atmosphere this is significantly distorted, but can be corrected by reflecting the light on a mirror that has a shape equal to half the negative of the distortion.

The Real-Time Controller (RTC) of an AO system processes the wavefront non-flatness measurements to obtain suitable actuator signals for a Deformable Mirror (DM) to correct the atmospheric disturbance. However, as telescope sizes keep growing, so must the number of actuators of the DM, which may be in the order of many thousands. This poses a problem for the design of both the DM and the RTC.

In this collaboration project, an extendible DM is being designed at the TU Eindhoven [2] together with an extendible control system at the TU Delft [1]. For the RTC a distributed design is foreseen, which – apart from the distributed structure – needs to be able to work with low signal to noise ratios, one to three kHz sampling frequency and at least a few samples loop delay.

2 Distributed control

In the context of AO, a distributed controller satisfies the following four properties:

1. each actuator has its own controller,
2. controllers receive a small set of local measurements,
3. controllers communicate with only a few neighbors,
4. calculation time of individual controllers is independent of the total number of actuators.

The main challenge in the design of a distributed controller arises from the fact that the sensor measures the wavefront

indirectly in terms of spatial gradients. Therefore, classical and even current \mathcal{H}_2 optimal controllers contain a reconstructor to obtain the real wavefront shape, which doesn’t easily fit the distributed framework.

3 Distributed wavefront reconstruction

To overcome this, several options were explored, starting with iterative solvers. These can be tailored to fit a distributed communication structure, but the number of iterations they require grows with the number of actuators, violating the 4th property of a distributed controller. By adding a predictor filter to exploit spatio-temporal correlation in the disturbance, this can be significantly reduced but not completely resolved.

However, by limiting the reconstructor to a distributed structure, a loss of performance may be expected. In this work we want to quantify relation between computational and communications complexity on one hand and the resulting performance loss on the other. This is done by posing the wavefront reconstruction as a state estimation problem of a dynamical turbulence model that is identified from measurement data. The structure and complexity of the model then determine the complexity and performance of the reconstructor.

References

- [1] Rogier Ellenbroek, Michel Verhaegen, Roger Hamelinck, Niek Doelman, Maarten Steinbuch, and Nick Rosielle. Distributed control in adaptive optics – deformable mirror and turbulence modeling. In *Proceedings of the SPIE conference on astronomical telescopes and instrumentation*, page 62723K. SPIE, May 2006.
- [2] Roger Hamelinck, Nick Rosielle, Maarten Steinbuch, Rogier Ellenbroek, Michel Verhaegen, and Niek Doelman. Actuator tests for a large deformable membrane mirror. In *Proceedings of the SPIE conference on astronomical telescopes and instrumentation- advances in adaptive optics*, page 627225. SPIE, May 2006.

Efficient Numerical Solution of SDPs Derived from the Generalized KYP Lemma

G. Pipeleers ^a, L. Vandenberghe ^b, B. Demeulenaere ^a, J. Swevers ^a, J. De Schutter ^a

(a) K.U.Leuven, Dept. of Mechanical Engineering

Celestijnenlaan 300B, B-3001 Heverlee, Belgium

(b) UCLA, Electrical Engineering Department

Engineering IV, Los Angeles, CA 90095

Email: goele.pipeleers@mech.kuleuven.be

1 Introduction

The KYP lemma is the basis of some important applications of semidefinite programming problems (SDPs) in control. However, due to the high number of optimization variables, the corresponding SDPs are often difficult to solve using general-purpose SDP software packages. Recently, an extension of the KYP lemma has been proposed [1, 2], called the generalized KYP lemma. While having promising control applications, even more auxiliary variables are introduced in the corresponding SDPs. This paper proposes a strategy to reduce the computational cost of solving these SDPs. This technique extends the results of [3], valid for the (regular) KYP lemma.

2 SDPs from the Generalized KYP Lemma

The generalized KYP lemma gives rise to SDPs of the following form:

$$\begin{aligned} \text{minimize} \quad & r^T x \\ \text{subject to} \quad & Q \succeq 0 \\ & \mathcal{K}(P) + \mathcal{L}(Q) + \mathcal{M}(x) + N \preceq 0, \end{aligned}$$

where

$$\begin{aligned} \mathcal{K}(P) &= \begin{bmatrix} A & B \\ I & 0 \end{bmatrix}^T (\Phi \otimes P) \begin{bmatrix} A & B \\ I & 0 \end{bmatrix}, \\ \mathcal{L}(Q) &= \begin{bmatrix} A & B \\ I & 0 \end{bmatrix}^T (\Psi \otimes Q) \begin{bmatrix} A & B \\ I & 0 \end{bmatrix}, \\ \mathcal{M}(x) &= \sum_{i=1}^p x_i M_i. \end{aligned}$$

\otimes denotes the matrix Kronecker product. The optimization variables are $x \in \mathbf{R}^p$, $P \in \mathbf{H}^n$ and $Q \in \mathbf{H}^n$, where \mathbf{H}^n denotes the space of $n \times n$ Hermitian matrices. The problem data are $r \in \mathbf{R}^p$, $A \in \mathbf{R}^{n \times n}$, $B \in \mathbf{R}^n$, $M \in \mathbf{H}^{n+1}$, $N \in \mathbf{H}^{n+1}$, $\Phi \in \mathbf{H}^2$ and $\Psi \in \mathbf{H}^2$. The pair (A, B) is assumed to be controllable. Compared to SDPs arising from the (regular) KYP lemma two differences are observed which substantially increase the computational cost: (i) the matrix variable P is Hermitian instead of symmetric and (ii) an additional auxiliary Hermitian matrix variable, Q , is introduced.

3 Efficient Numerical Solution

Solving this SDP using general purpose software comes at a computational cost of $O(n^6)$. To obtain a more efficient implementation, this SDP is first transformed to its dual form:

$$\begin{aligned} \text{maximize} \quad & \Re\{\text{Tr}(ZN)\} \\ \text{subject to} \quad & \mathcal{L}^{\text{adj}}(Z) \succeq 0 \\ & \mathcal{K}^{\text{adj}}(Z) = 0 \\ & \mathcal{M}^{\text{adj}}(Z) = -r, \end{aligned} \quad (1)$$

where \mathcal{K}^{adj} , \mathcal{L}^{adj} and \mathcal{M}^{adj} are the adjoint mappings of \mathcal{K} , \mathcal{L} and \mathcal{M} , respectively. Subsequently, the dual optimization variable $Z \in \mathbf{H}^{n+1}$ is eliminated based on constraint (1). The computational cost hereby decreases to $O(n^4)$.

Both the theoretical details and numerical results illustrating the computational efficiency of this strategy will be presented.

Acknowledgement

Goele Pipeleers is a Research Assistant of the Research Foundation - Flanders (FWO-Vlaanderen) and Bram Demeulenaere is a Postdoctoral Fellow of the Research Foundation - Flanders. This work has been carried out within the framework of projects G.0528.04 and G.0446.06 of the Research Foundation - Flanders and also benefits from K.U.Leuven-BOF EF/05/006 Center-of-Excellence Optimization in Engineering.

References

- [1] T. Iwasaki, and S. Hara, "Generalized KYP lemma: unified frequency domain inequalities with design applications," *IEEE Transactions on Automatic Control*, 50(1): 41-59, 2005.
- [2] C. W. Scherer, "LMI relaxations in control," *European Journal of Control*, 12(1): 3-29, 2006.
- [3] L. Vandenberghe, V. R. Balakrishnan, R. Wallin, A. Hansson, and T. Roh, "Interior-Point Algorithms for Semidefinite Programming Problems Derived from the KYP lemma."

Efficient dynamic optimization for Nonlinear Moving Horizon Estimation

Niels Haverbeke, Moritz Diehl, Bart De Moor

K.U.Leuven, ESAT-SCD-SISTA and OPTEC

Kasteelpark 10, B-3001 Heverlee-Leuven, Belgium

{niels.haverbeke,moritz.diehl,bart.demoor}@esat.kuleuven.be

Abstract

In this presentation a Gauss-Newton approach with structure exploitation is proposed for nonlinear moving horizon estimation (NMHE). The dynamic optimization problem is solved as a nonlinear least squares problem using a constrained Gauss-Newton (CGN) approach. The proposed algorithm exploits the sparse structure of the KKT-matrix that arises from NMHE. In particular ideas of square root covariance Kalman filtering are proposed in order to efficiently update covariance matrices occurring in the factorization of the KKT-matrix. The algorithm is able to compute - without any additional costs - the covariance of the last estimate within the horizon, which reflects the accuracy of the estimate.

1 Introduction

The basic strategy of moving horizon estimation is to estimate the state using a moving and fixed-size window of data. When a new measurement becomes available, the oldest measurement is discarded and the new measurement is added. The philosophy is to penalize deviations between measurement data and predicted outputs. In addition - for theoretical reasons - a regularization term on the initial state estimate (the so-called *arrival cost*) is added to the objective function. In nonlinear moving horizon estimation a fixed-size nonlinear least squares optimization problem (NLSQ) is solved in each time step. The Kalman filter can be interpreted as a recursive least square minimizer that delivers an optimal estimator gain for the linearized system. Schemes for NMHE were investigated first in [1] and a detailed analysis of its stability properties was given in [2]. More recently a real-time iteration scheme for NMHE was proposed in [4].

2 Efficient MHE algorithm

The optimization problem considered in this presentation is represented as:

$$\begin{aligned} \min_{x_k, w_k} & \|P(x_0 - \bar{x}_0)\|_2^2 + \sum_{k=0}^T \|w_k\|_2^2 + \|\eta_k - h(x_k)\|_2^2, \\ \text{s.t.} & \quad x_{k+1} = f(x_k, w_k), \quad k = 0, \dots, T-1. \end{aligned}$$

Here we define the states $x_k \in \mathbb{R}^n$, disturbances $w_k \in \mathbb{R}^m$ and outputs $\eta_k \in \mathbb{R}^p$. The prior data is summarized by the initial state estimate \bar{x}_0 and corresponding covariance matrix P^{-2} . Using a constrained Gauss-Newton method we obtain

a linearized least squares problem (L-LSQ). It can be observed that the KKT-matrix for this problem is highly structured. The proposed algorithm exploits this sparse structure by performing a forward block matrix recursion inspired by Kalman Filtering, and a backwards vector recursion to obtain the CGN step. Using two QR-factorizations it is possible to express square root covariances for intermediate points within the horizon. In this way, an efficient algorithm with linear complexity in the horizon length is obtained. As a by-product, the covariance matrix of the last estimate within the horizon can be obtained without any additional computations.

3 Applications

The presented algorithm can be applied to systems with fast sampling times. This could open up new opportunities for nonlinear moving horizon estimation.

Acknowledgements

Niels Haverbeke is a research assistant supported by IWT-Vlaanderen. Dr. Moritz Diehl is an associate professor at the COE Optimization in Engineering (OPTEC) of the Katholieke Universiteit Leuven, Belgium. Dr. Bart De Moor is a full professor at the Katholieke Universiteit Leuven. Research supported by Research Council KUL: GOA AMBioRICS, CoE EF/05/006 Optimization in Engineering; FWO: PhD/postdoc grants, projects, G.0407.02, G.0197.02, G.0141.03, G.0491.03, G.0120.03, G.0452.04, G.0499.04, G.0211.05, G.0226.06, G.0321.06, G.0553.06, research communities; IWT: PhD grants, GBOU, Eureka-Flite2; IUAP P5/22; PODO-II; EU: FP5-Quprodis; ERNSI; Contract Research/agreements: ISMC/IPCOS, Data4s, TML, Elia, LMS, Mastercard.

References

- [1] K.R. Muske and J.B. Rawlings, *Nonlinear moving horizon state estimation*, in Methods of Model Based Process Control, R. Berber, Kluwer, 1995, pp. 349-365.
- [2] C.V. Rao, J.B. Rawlings and D. Mayne, *Constrained State Estimation for Nonlinear Discrete-time systems: Stability and Moving Horizon Approximations*, IEEE Transactions on Automatic Control, 2003, vol. 48 pages 246-258.
- [3] M. Verhaegen and P. Van Dooren, *An efficient implementation of square root filtering : error analysis, complexity and simulations on flight-path reconstruction*, Proceedings 6th Int. Conf. System Analysis and Optimization, 63:250-267, 1984.
- [4] M. Diehl, P. Kuhl, H.G. Bock and J.P. Schloeder, *Fast algorithms for state and parameter estimation on moving horizons*, Automatisierungstechnik 54 (2006) 12.

Design of dynamically optimal B-spline motion inputs: Experimental results.

Jan De Caigny, Bram Demeulenaere, Jan Swevers, Joris De Schutter

Department of Mechanical Engineering

Katholieke Universiteit Leuven

Celestijnenlaan 300B, B-3001 Heverlee, Belgium

Email: jan.decaigny@mech.kuleuven.be

1 Introduction

This work considers the design of point to point motion inputs for flexible positioning systems. The key issue is to design motion inputs that excite the system's flexibilities as little as possible during the point to point motion, such that little or no residual vibrations occur after the motion. This results in a significant decrease of the settling time. Since designing the motion input is an open-loop technique, robustness against both variation of the system's parameters as well as unmodeled dynamics has to be taken into account.

In the proposed framework, the motion input is parameterized using B-splines of a user-defined degree N . The chosen parametrization guarantees continuity of the motion input up to derivative $N - 2$ and is inspired by [1]. The B-splines are optimized in a large linear optimization such that they minimize the residual vibrations after system motion, subject to boundary and other constraints, for example maximum velocity and acceleration of the system.

2 Experimental test set-up

As a case-study, the motion inputs for a two Degree-Of-Freedom mass-spring-damper system are optimized. Fig. 1 shows a picture of the set-up as well as a schematic drawing. In this case the goal is to design the input $u(t)$, such that the outputs $x_1(t)$ (upper mass) and $x_2(t)$ (lower mass) perform a fast point to point motion without residual vibration. Robustness against uncertainty on the system's resonances is taken into account.

The system is identified using frequency domain identification tools. The identified models for $X_1(s)/U(s)$ and $X_2(s)/U(s)$ have two resonances and in addition, $X_2(s)/U(s)$ has one anti-resonance (see Table 1).

	Frequency [Hz]	Damping [%]
resonance 1	2.6	1.55
resonance 2	7.8	3.06
anti-resonance	4.2	2.31

Table 1: Identified (anti-)resonances of the test set-up.

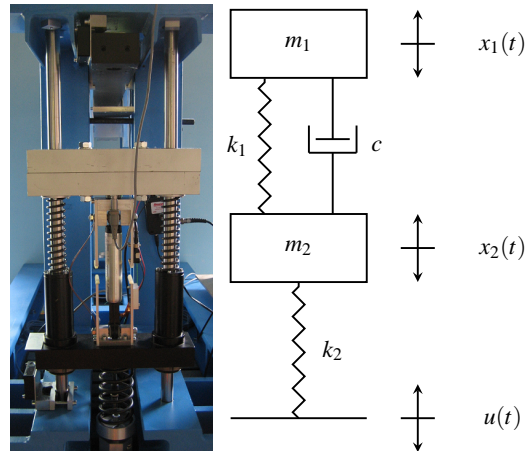


Figure 1: Picture and schematic drawing of the test set-up.

3 Results

Both numerical and experimental results are presented for the considered case-study using the proposed framework. Results presented in [2] and [3] are reproduced for the test set-up and are used as a benchmark. The two Degree-Of-Freedom set-up is of particular interest since it allows analysis of the effect of unmodeled higher dynamics; i.e. how well are the residual vibrations reduced if only the first resonance is taken into account and how much can be gained in performance by taking the second resonance into account?

4 Acknowledgements

This work has been carried out within the framework of projects G.0446.06 and G.0462.05 of the Research Foundation - Flanders (FWO - Vlaanderen). Bram Demeulenaere is a Postdoctoral Fellow of the Research Foundation - Flanders. This work also benefits from K.U.Leuven-BOF EF/05/006 Center-of-Excellence Optimization in Engineering.

References

- [1] H. Kwakernaak and J. Smit, "Minimum Vibration Cam Profiles," *Journal of Mechanical Engineering Science*, 10(3):219–227, 1968.
- [2] N. C. Singer and W. P. Seering, "Preshaping command inputs to reduce system vibration," *Transactions of the ASME, Journal of Dynamic Systems, Measurement and Control*, 112:76–82, 1990.
- [3] L. N. Srinivasan and Q. J. Ge, "Designing dynamically compensated and robust cam profiles with bernstein-bézier harmonic curves," *Transactions of the ASME, Journal of Mechanical Design*, 120:40–45, 1998.

Optimising the robust stability of time-delay systems via nonsmooth eigenvalue optimisation

Joris Vanbiervliet, Wim Michiels

Department of Computer Science, Katholieke Universiteit Leuven,
Celestijnenlaan 200A, 3001 Leuven, Belgium

{joris.vanbiervliet, wim.michiels}@cs.kuleuven.be

1 Introduction

The stabilisation of a system with a finite number of free parameters is a problem that typically arises in the design of fixed-order controllers. Most methods attempt to solve this stabilisation problem by trying to satisfy certain types of stabilisability conditions. The drawback of such methods is that these conditions are in general sufficient, but not necessary. Therefore, the system may be stabilisable although the stabilisability conditions cannot be satisfied. Our approach is to directly act on the spectrum of the system to optimise the corresponding stability. We will first consider a nonsmooth optimisation method that maximises the exponential decay of the system trajectories. Since this commonly yields unrobust solutions, we will also apply this method to the optimisation of the robustness of a system against perturbations.

2 Spectral abscissa minimisation

A straightforward method to solve the stabilisation problem is to minimise the largest real part of the eigenvalues, also called spectral abscissa α , in function of the optimisation parameters. Asymptotic stability is then achieved as soon as this objective function becomes negative, because the trajectories are bounded by an exponential decay that lies below e^α . However, the spectral abscissa is in general a nonsmooth and nonconvex function, precluding the use of standard optimisation methods. Instead, we use a recently developed bundle gradient optimisation algorithm, namely the gradient sampling algorithm [1], which has already been successfully applied to fixed-order controller design problems for systems of ordinary differential equations.

We apply this approach to the stabilisation of systems of time-delay type. As the linearisation of such systems has in general an infinite number of eigenvalues, a direct pole placement is indeed not possible. In dealing with these time-delay systems, we thus extend the use of the gradient sampling algorithm to infinite-dimensional systems. This is realised by combining the optimisation method with advanced numerical algorithms that are able to efficiently and accurately compute the rightmost eigenvalues of time-delay systems with the use of linear multistep techniques.

A problem with the minimisation of the spectral abscissa is that it commonly results in a spectrum for which the eigen-

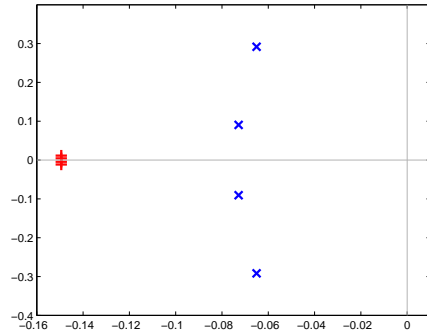


Figure 1: The spectrum of the optimised system w.r.t. exponential decay (+) and w.r.t. robust stability (x)

values are of higher multiplicity. Such eigenvalues are very sensitive with respect to small changes of the parameters or of the system's definition. This means that a tiny error in the system model may in practice lead to a huge increase of the spectral abscissa or may even result in the loss of stability. Thus, although it provides an optimal stability, the solution of a spectral abscissa minimisation is often accompanied by a very bad robustness w.r.t. stability against perturbations.

3 Robust stability

In [2], it is shown that the robustness of a system can be optimised by maximising the complex stability radius, measuring the smallest perturbation which would lead to instability. Since a point for which $\alpha < 0$ suffices to guarantee stability, we can use this point as a starting value for the robustification process. Fig. 1 depicts the spectra as a result of a spectral abscissa minimisation as compared to a complex stability radius maximisation, showing that the robustness is indeed improved, at the cost of a lower spectral abscissa.

References

- [1] J.V. Burke, A.S. Lewis, and M.L. Overton, *A robust gradient sampling algorithm for nonsmooth, nonconvex optimization*, SIAM J. Optimization, 15 (2005), pp. 751-779.
- [2] W. Michiels, D. Roose, *An eigenvalue based approach for the robust stabilization of linear time-delay systems*, Int. J. Control, 76 (2003), pp. 678-686.

Young's Modulus Reconstruction Using a Constrained Gauss-Newton Method

Juan F. Camino and Mauro Sette

Department of Mechanical Engineering

Katholieke Universiteit Leuven

Celestijnenlaan 300B, B3001 Heverlee, Belgium

{Juan.Camino,Mauro.Sette}@mech.kuleuven.be

1 Abstract

We present an ongoing work on the application of the Gauss-Newton method for solving an inverse elasticity problem. The motivation is to provide an inverse reconstruction technique for computing the spatial distribution of Young's modulus within human tissues. The idea consist on deriving a model of the tissue using the finite element method, affine on the Young's modulus, and finally solving a nonlinearly constrained least squares problem that includes the measured forces and displacements from experimental data.

2 Introduction

In clinical practice, palpation is one of the main diagnostic tools. This procedure is based on identifying the tissue characteristics as being hard or soft, since most of the diseases harden the tissue. For instance, a tumor can be identified as a hard ball embedded inside a volume. In this context, research has recently been conducted to provide a human independent probing tool that is able to quantify the stiffness of tissues.

To determine the Young's modulus of a volume which is directly related to the stiffness, the solution of an inverse elasticity problem (IEP) is needed, where the material properties are calculated for given applied forces and displacements. For a volume under a prescribed static load, the displacement field can be determined using an elastography technique (Doyley et al., 2000), that gives information about the displacement field. The applied load used to deform the volume can be acquired by a force sensor.

3 Nonlinear Least Squares Problem Formulation

Once these data are collected, the goal is to solve the corresponding IEP, or equivalently, to fit to the data a finite element (FEM) model of the soft tissue considered as a linear, isotropic and incompressible medium. For this FEM model, the stiffness matrix, affine in the Young's modulus, is calculated using a Poisson ratio of $\nu = 0.495$. For this purpose, the optimization problem is posed as follows: find a set of Young's modulus $\alpha = \{E_1, E_2, \dots, E_m\}$ such that it solves

Moritz Diehl

Department of Electrical Engineering

Katholieke Universiteit Leuven

KastelparkArenberg 10, B3000 Leuven, Belgium

Moritz.Diehl@esat.kuleuven.be

$$\min_{\alpha, x} \frac{1}{2} \|Cx - \bar{x}\|_2^2, \quad \text{s. t.} \quad (K_0 + \sum_{i=1}^m \alpha_i K_i)x = f$$

for a given measured displacement vector $\bar{x} \in R^q$, force vector $f \in R^n$, matrices $K_i = K_i^T \geq 0$, $i = 1, \dots, m$, and correspondence matrix $C \in R^{q \times n}$. This is a nonlinearly constrained least squares problem which can be efficiently solved using a constrained Gauss-Newton (CGN) method.

4 Constrained Gauss-Newton Scheme

The idea behind the constrained Gauss-Newton method (Bock, 1987) is to iterate on a linear least squares subproblem originating from the linearization of the objective and the equality constraints. We can show that the Karush-Kuhn-Tucker (KKT) conditions for this subproblem are given by

$$\begin{pmatrix} C^T C & A_x^T & 0 \\ A_x & 0 & A_\alpha \\ 0 & A_\alpha^T & 0 \end{pmatrix} \begin{pmatrix} \delta_x \\ -\lambda \\ \delta_\alpha \end{pmatrix} = - \begin{pmatrix} Cx - \bar{x} \\ (K_0 + \sum_{i=1}^m \alpha_i K_i)x - f \\ 0 \end{pmatrix}$$

with $A_x = K_0 + \sum_{i=1}^m \alpha_i K_i$ and $A_\alpha = [K_1 x \dots K_m x]$. The steps are taken as $x_{k+1} = x_k + \delta_x$ and $\alpha_{k+1} = \alpha_k + \delta_\alpha$.

5 Numerical Results

Numerical results show that the possibility to use the measured data \bar{x} as the initialization for x makes the method very insensitive to the initial guess for α , thus being more attractive than sequential Newton-Raphson methods commonly used in elastography.

6 Acknowledgments

K. U. Leuven BOF EF/05/006 Center of Excellence: Optimization in Engineering and ARIS*ER European Network.

References

H.G. Bock. Randwertproblemmethoden zur parameteridentifizierung in systemen nichtlinearer differentialgleichungen. *Bonner Mathematische Schriften* 183, 1987.

M. M. Doyley et al. Evaluation of an iterative reconstruction method for quantitative elastography. *Phys. Med. Bio.*, 45:1521–1540, 2000.

Time Averaging in solid substrates

Veerle Beelaerts, Fjo De Ridder, Rik Pintelon, Johan Schoukens
 Vrije Universiteit Brussel, Dept. ELEC, Pleinlaan 2, 1050 Brussel
 and Frank Dehairs
 Vrije Universiteit Brussel, Dept. ANCH, Pleinlaan 2, 1050 Brussel
 vbeelaer@vub.ac.be

1. Introduction

Nature provides us with several proxy recordings of Earth's climate (sources of climate information from natural archives), i.e. preserved in rock and in sediment layers on the ocean floor [1]; even in some organisms like sponges and bivalves [2], which store environmental information during their life.

Processing the collected substrates, to obtain the proxies which are incorporated involves sampling solid substrate. Whether sampling means drilling a hole or counting a proxy per square meter, the sample always has a certain dimension (the dimension of the drill hole or of the count area). In most cases the dimension of the sample is neglected. This is allowed when the width of the sample is small compared to the variation of interest. Nevertheless, if the sample width spans a considerable part of this variation, the amplitude of the signal will be averaged out and will result in an underestimation.

In this work a method is presented to propose a correction for this underestimation, based on advanced signal processing tools and standard filtering techniques.

2. Approach

In a first approach the sample (drill hole or count area) is rectangular and has two negligible dimensions (i.e.: height and depth), and one non negligible dimension (i.e. width). For simplicity reasons the problem was explored by means of a simulation.

This averaging effect behaves like a filter as a multiplication of the ideal frequency plot with a sinc-function (with zeros at frequencies where a sample exactly overlaps one period). For that reason, the amplitude loss is studied in the frequency domain: eg. see Figure 1.

This is logical as the samples in these solid substrates are not points (dirac train), but samples over a certain non negligible sample width (block train).

In a next stage other sample shapes will be studied, like Gaussians mimicking bioperturbations.

3. Results

With a constant accretion rate the correction for a sample width which is 40% of the variation of interest, the error is 25%; after correction more than 99.9% of the

amplitude is recovered.

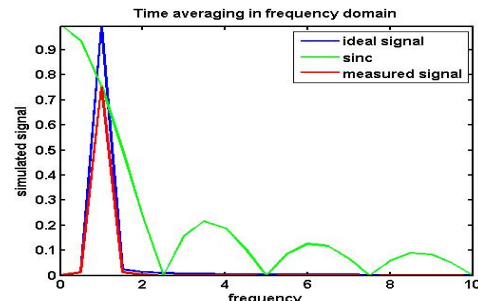


Figure 1: Time averaging in frequency domain

In reality, the accretion rate often changes with time. Such a signal is shown in figure 2.

When the accretion rate is decreasing with time or distance, the best result is shown in Figure 2. The amplitude of the measured signal decreases with the

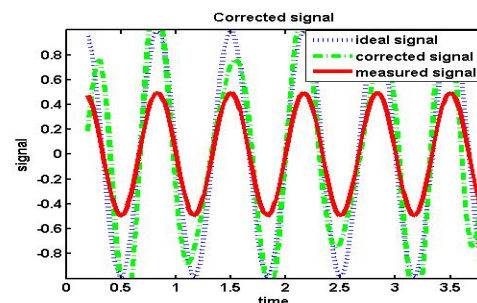


Figure 2: Best results for a decreasing accretion rate

time and the correction of the signal is dependent on that amplitude. For measured amplitudes which are too small the correction still does not produce good values.

References

- [1] Huang S., Pollack N. H., Shen P., 2000. Temperature trends over the past five centuries from reconstructed borehole temperatures. *Nature* 403: 765-758.
- [2] Lazareth C.E., Willenz P., Navez J., Keppens E., Dehairs F., André L., 2000. Sclerosponges as a new potential recorder of environmental changes: Lead in *Ceratoporella nicholsoni*. *Geology* 28: 515-518.

An estimation approach to system inversion

Steven Gillijns and Bart De Moor

ESAT – SCD – SISTA

Katholieke Universiteit Leuven

Kasteelpark Arenberg 10

3001 Leuven, Belgium

Email: {steven.gillijns,bart.demoor}@esat.kuleuven.be

1 Introduction

The concept of system inversion has received a lot of attention due to its applications in control, estimation and coding theory. A distinction must be made between two classes of inversion problems. A left inverse of a system S is a system S_L which computes the input signal applied to S from knowledge of its output. A right inverse, on the other hand, is a system S_R which computes an input signal such that S has a desired output. The left inverse S_L can thus be interpreted as an estimator, whereas S_R can be seen as a controller. In this presentation, we consider left invertibility of linear time-invariant (LTI) discrete-time system. We develop an optimal input estimator and derive the general form of the left inverse based on this estimator.

2 Invertibility criteria

Consider the LTI system

$$x_{k+1} = Ax_k + Bu_k, \quad (1a)$$

$$y_k = Cx_k + Du_k, \quad (1b)$$

where x_k is the state vector, u_k is an unknown input vector and y_k is the output vector. An important issue in system inversion is the condition under which an inverse of (1) exists. Simple and elegant invertibility criteria can be found in [1, 2, 3]. The approach taken by Sain and Massey [1] is of particular importance for this presentation because they introduce the concept of L -delay left invertibility. In short, the system (1) is said to be L -delay left invertible if u_k can be uniquely determined from the knowledge of x_k and $y_{[k,k+L]} := [y_k^T \ y_{k+1}^T \ \dots \ y_{k+L}^T]^T$. In the next section, we derive an L -delay left inverse of (1).

3 System inversion

We propose a new approach to system inversion based on joint input and state estimation. Consider an estimator of the form

$$\hat{x}_{k+1} = A\hat{x}_k + K(y_{[k,k+L]} - \bar{y}_{[k,k+L]}), \quad (2a)$$

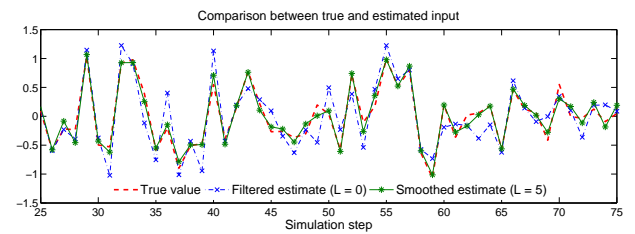
$$\hat{u}_k = M(y_{[k,k+L]} - \bar{y}_{[k,k+L]}), \quad (2b)$$

where $\bar{y}_{[k,k+L]} := O_L \hat{x}_k$ with $O_L := [C^T \ (CA)^T \ \dots \ (CA^L)^T]^T$. Let $\mathbb{E}[\hat{x}_0] = x_0$, then we show that the matrices K and M can

be computed such that $\mathbb{E}[\hat{x}_k] = x_k$ and $\mathbb{E}[\hat{u}_k] = u_k$ if and only if the system (1) is L -delay left invertible. Also, we establish conditions under which the estimation error converges asymptotically to zero for $k \rightarrow \infty$. Note that the estimator (2) is a LTI discrete-time system with input $y_{[k,k+L]}$ and output \hat{u}_k . We show that an L -delay left inverse of (1), i.e. a system with input y_k and output u_{k-L} , follows almost immediately from the estimator (2). This L -delay left inverse system has a very general form which consists of two matrix parameters which can be freely chosen. We show that the choice of these parameters influences the stability, observability, ... of the inverse system. The construction of stable inverse systems has also been addressed in e.g. [3, 2].

4 Application to filtering and smoothing

Finally, we consider the case where the system is subject to process and measurement noise. We show how time-varying matrix parameters K_k and M_k can be computed so that \hat{x}_k and \hat{u}_k are minimum-variance unbiased. Note that (2a) is a one step ahead predictor for $L = 0$, a filter for $L = 1$ and a smoother for $L > 1$. Similarly, (2b) is a filter for $L = 0$ and a smoother for $L > 0$. Filtered and smoothed estimates of the input of a 0-delay left invertible system subject to process and measurement noise are show in the figure below. Note that smoothing strongly increases estimation accuracy.



References

- [1] M.K. Sain and J.L. Massey. Invertibility of linear time-invariant dynamical systems. *IEEE Trans. Autom. Control*, 14(2):141–149, 1969.
- [2] L.M. Silverman. Inversion of multivariable linear systems. *IEEE Trans. Autom. Control*, 14(3):270–276, 1969.
- [3] P.J. Moylan. Stable inversion of linear systems. *IEEE Trans. Autom. Control*, 22(1):74–78, 1977.

Bayesian filtering and smoothing techniques in gait analysis

Friedl De Groote[†], Tinne De Laet[†], Ilse Jonkers[‡], Joris De Schutter[†]

[†]Department of Mechanical Engineering
Katholieke Universiteit Leuven
Celestijnenlaan 300B-3001 Leuven
Belgium

Email: friedl.degroot@mech.kuleuven.be

[‡]Department of Kinesiology
Katholieke Universiteit Leuven
Tervuursevest 101-3001 Leuven
Belgium

1 Introduction

This research deals with determining the joint kinematics from measured body-surface marker positions during human motion, a first and essential preprocessing step in gait analysis. Applications of gait analysis include the treatment of gait pathologies, rehabilitation, prosthesis design, ergonomics and sports. It is shown that the use of Bayesian filtering and smoothing techniques substantially improves the estimate of joint kinematics as compared to the currently used techniques.

2 Current approach

During gait analysis data is acquired using a photogrammetric system to measure the position of body-surface markers and a force plate to measure the 3D ground reaction forces. Usually this setup is supplemented with external electrodes to measure EMG. The two most important sources of measurement errors are noise and soft tissue artifacts caused by the relative motion between the markers and the bone. A generic model, scaled to the subject's dimensions using marker information collected during a static trial, underlies the data processing. The degrees of freedom of the model are represented by the generalized coordinates, q . An estimate of q is obtained by a nonlinear least squares fit between the model and the measurements for each time instant separately, referred to as inverse kinematics. The generalized coordinates are numerically derived to obtain the generalized speeds, \dot{q} , and accelerations, \ddot{q} . Joint reaction moments and forces are calculated from the ground reaction forces and the generalized coordinates and its derivatives. These joint reaction moments and forces are input to a dynamic musculoskeletal analysis to determine the muscle forces.

3 Contribution

It is known that the movement of the human body is smooth. Since in this approach to estimate the joint kinematics each time step is considered separately, this knowledge can not be included. Furthermore numerical differentiation of q leads to exploding errors on \dot{q} and \ddot{q} , severely compromising the quality of the dynamic musculoskeletal analysis. Bayesian filtering and smoothing techniques allow to use the knowledge about the movement and to estimate \dot{q} and \ddot{q} along with q . Therefore gait analysis can benefit from the use of these techniques.

4 Simulation

In the current study, multiple aspects of the use of Bayesian filtering and smoothing techniques in gait analysis are explored in simulation:

- Different filtering and smoothing techniques, for example extended Kalman, unscented Kalman, non-minimal Kalman, etc. are compared and evaluated against the state of the art nonlinear least squares methods.
- Different underlying joint movement models, e.g. constant velocity, constant acceleration, periodic movement, etc. are studied in order to obtain the model that gives the best estimate of the joint accelerations.
- The influence of skin artefacts is examined along with the possibility to include these artefacts in the underlying model.
- Extra features offered by the Bayesian framework are explored: model prediction and interpolation in the case of temporarily incomplete measurements and the detection of marker detachment.

The simulations are based on the musculoskeletal model provided in SIMM (Delp, 1990), although the approach allows the use of any musculoskeletal model. Marker positions are simulated based on filtered joint kinematics obtained from a gait trial to guarantee realistic input data.

5 Conclusion

A good choice of Bayesian filtering and smoothing techniques together with the underlying movement model substantially improves the estimate of joint kinematics under the ideal conditions of a simulation environment. The developed framework is now ready for application on real movement data.

6 Acknowledgements

Friedl De Groote and Tinne De Laet are Research Assistants of the Research Foundation - Flanders (FWO-Vlaanderen). Ilse Jonkers is Postdoctoral Fellow of the Research Foundation - Flanders. Ilse Jonkers receives additional funding from the Belgian Educational Foundation and the Koning Boudewijn Fonds. This work is also supported by BOF EF/05/006 Center-of-Excellence Optimization in Engineering.

Review of filtering methods for removal of resuscitation artifacts from human ECG signals

Ivan Markovsky Sabine Van Huffel

K.U.Leuven, ESAT-SCD, Kasteelpark Arenberg 10, B-3001 Leuven, Belgium
 {Ivan.Markovsky, Sabine.VanHuffel}@esat.kuleuven.be

Anton Amann

Innsbruck Medical University, Anichstr 35, A-6020 Innsbruck
 Anton.Amann@uibk.ac.at

1 Introduction

We are dealing with a particular filtering problem that arises in a biomedical signal processing application—removal of resuscitation artifacts from ventricular fibrillation ECG signals. The measured ECG signal y is the sum of two components: the ventricular fibrillation ECG signal v , which is the useful signal, and the resuscitation artifacts c , which is the disturbance. The goal is to extract the unknown signal v from the given signal y . Our study is empirical and is based on a database of separately recorded resuscitation artifacts and ventricular fibrillation ECG signals.

The bandpass, Kalman, and adaptive filtering methods rely on different type of prior knowledge that allows to make the separation of the useful signal from the disturbance. In the particular application at hand, we are given a third signal, the arterial blood pressure u , that is correlated with the artifact c . This information is used by the Kalman and adaptive filters.

2 Compared methods

1. Low-pass filter (ad-hoc selected cut-off frequency)
2. Kalman filter (model identified from observations)
3. Kalman filter (model identified from true data)
4. Normalized LMS adaptive filter (ad-hoc selected number of lags and step size)

The third method is called the “reference method” because theoretically it achieves optimal performance (assuming that the true data satisfies an LTI model). The reference method is of course not practical. Note that the second and the third methods lead to noncausal data processing because on the identification step all the data is used in batch.

3 Results

For validation of the methods we construct an artificial “measured” signal $y := v + \alpha c$, where the scaling factor α is chosen according to the desired signal-to-noise ratio

$\text{SNR}(y) := \|v\|_2^2 / \|y - v\|_2^2$. The methods are evaluated on the basis of the SNR of the restored signal \hat{v} .

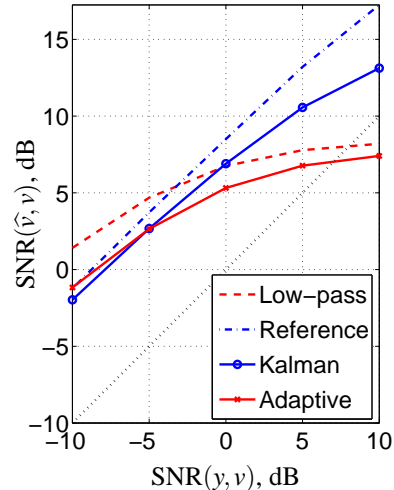


Figure 1: SNR improvements for the compared methods.

The obtained results show that for low SNR of the given signal, the simplest low-pass filtering method achieves the best performance. The reason for this might be the good robustness of the low-pass filtering method.

References

- [1] J. Husøy, J. Eilevstrønn, T. Eftestøl, S. Aase, H. Myklebust, and P. Steen. Removal of cardiopulmonary resuscitation artifacts from human ECG using an efficient matching pursuit-like algorithm. *IEEE Trans. Biomed. Eng.*, 49:1287–1298, 2002.
- [2] I. Markovsky, A. Amann, and S. Van Huffel. Application of filtering methods for removal of resuscitation artifacts from human ECG signals. Technical Report 06–212, Dept. EE, K.U.Leuven, 2006.
- [3] K. Rheinberger, T. Steinberger, K. Unterkofler, M. Baubin, and A. Amann. Removal of CPR artifacts from the ventricular fibrillation ECG by adaptive regression on lagged reference signals. Draft, 2006.

A positioning technique for GSM, using the signal strengths of one antenna site

Nico Deblauwe, Leo Van Biesen

Vrije Universiteit Brussel, Pleinlaan 2, 1050 Brussels, Belgium
 Department of Fundamental Electricity and Instrumentation (ELEC),
 Email: nico.deblauw@vub.ac.be

1 Introduction

Mobile location estimation gained recently much attention, both scientifically and commercially. Based upon the usage expectations and profit projections of LBS (Location Based Services), there is a high plausibility that future mobile communication systems, 4th generation (4G) and onwards, will include high precision positioning requirements already in their design phase [1]. Until then, for the current 2G and 3G networks, a positioning solution needs to be found. To provide an overview in the numerous studies that have been examining the possibilities for mobile location estimation, we would advocate a division into four categories: 1) GPS-aided, 2) proximity sensing, and lateration or angulation 3) with additional hardware in the network or 4) by using the received signal strengths. In this abstract, we take a closer look at a method that fits in the latter category.

2 Positioning technique basics

The path loss PL relates the transmitted power at the base station (BS) to the received signal strength at the mobile phone, and accounts for the signal attenuation caused by the distance d_i and shadow fading (modelled as a zero mean Gaussian distributed random variable X):

$$PL(d_i) = a_i + b_i \log_{10} d_i + X \quad (1)$$

The coefficients a_i and b_i are determined by the clutter type (\approx classification for propagation environment, e.g. urban, open land...) and are rather independent of the antenna. Because of the antenna gain pattern, the transmitted power is also dependent of the angle α_i under which the mobile phone is seen. We have modelled this as a polynomial function $G(\alpha_i)$, having values between 0 and 1, to be multiplied with the amplifier output power P_i , known per antenna. Figure 1 shows how these antenna patterns look like. The received signal strength A_i from BS_i can thus be written as

$$A_i [dBm] = P_i \cdot G(\alpha_i - \theta_i) - (a_i + b_i \log_{10} d_i) \quad (2)$$

In this formula, θ_i accounts for the azimuth (=direction).

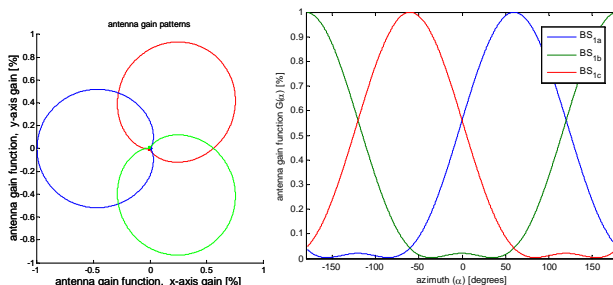


Figure 1: Antenna gain patterns. The $G(\alpha)$ function is a polynomial of the 10th order in α . The azimuth angles are respectively: $\pi/3$, π , and $-\pi/3$.

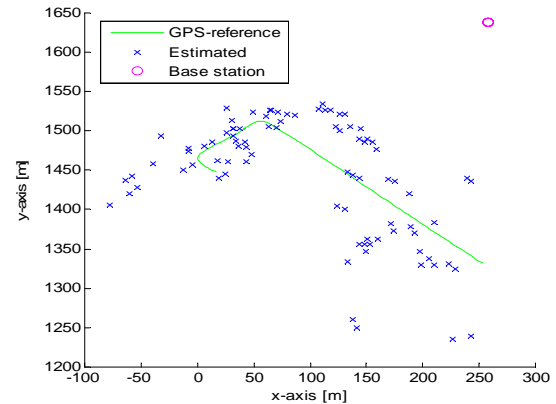


Figure 2: Simulation results of the positioning technique, using realistic noise parameters for the 900 MHz beacon signal.

By combining the signal strengths of the three antennas located at the same BS location, the first term of formula 2 can be isolated. Due to the correlated nature of the noise, the angle α_i can be determined rather accurately. Simulations have shown that the error is a zero mean process with a standard deviation of 5 degrees for realistic fading noise parameters. The distance can be determined with formula 2 once the angle is known. By performing a LS optimisation over the three received signal strengths, the error on the position decreases to about 50 m. Combining the angle and distance information finally leads to a position estimate. Figure 2 shows the results of a realisation.

3. Conclusion and future work

The presented method clearly shows some potential. Based on the received signal strengths of as few as one base station, it is possible to determine the position of a mobile phone within reasonable error limits: an average position error of 50m. The full potential of this technique lays in its combination with extra information sources (e.g. the received signal strengths of other BSs, a road database...) in order to decrease the error. As well, some extra tests with real network measurements need to be made in order to confirm the current results.

References

- [1] Y. Zhao, "Standardization of Mobile Phone Positioning for 3G Systems", IEEE comm. Mag, vol 40, issue 7, pp. 108-116, July 02
- [2] J. N. Ash and L.C. Potter, "Sensor network localization via received signal strength measurements with directional antennas", Proc. 2004 Allerton Conference Communication, Control, and Computing, 2004, pp. 1861-1870

Optimal control in a data-based context

Arjen den Hamer¹ Rene v.d. Molengraft¹
 a.j.d.hamer@tue.nl m.j.g.v.d.Molengraft@tue.nl

¹ Control Systems Technology group
 Department of Mechanical Engineering
 Technische Universiteit Eindhoven

Georgo Angelis² Maarten Steinbuch¹
 georgo.angelis@philips.com m.steinbuch@tue.nl

² Philips Applied Technologies
 High Tech Campus Eindhoven

Introduction

Acquiring parametric models for advanced controller design, e.g. \mathcal{H}_2 and \mathcal{H}_∞ , is non-trivial in practical applications. Within this research it is explored whether such a parametrization of the plant can be omitted while exploiting the benefits of optimal controller synthesis tools. This naturally may lead to a controller of limited complexity.

Approach

Synthesis of optimal controllers in a non-parametric way, e.g. computing the Frequency Response Data (FRD) of the optimal controller, is explored in order to omit parametrization of the plant. By parameterizing the controller after the synthesis step, knowledge is present about the relation between parametrization error and performance/stability. This is an advantage over the conventional approach where the fitting error can not be directly linked to closed-loop performance loss such that iterative approaches are required to obtain this data after the synthesis step (see Fig.1).

Since the trade-off between controller order and performance is embedded in the controller parametrization step naturally, the approach can be extended towards low-order controller synthesis.

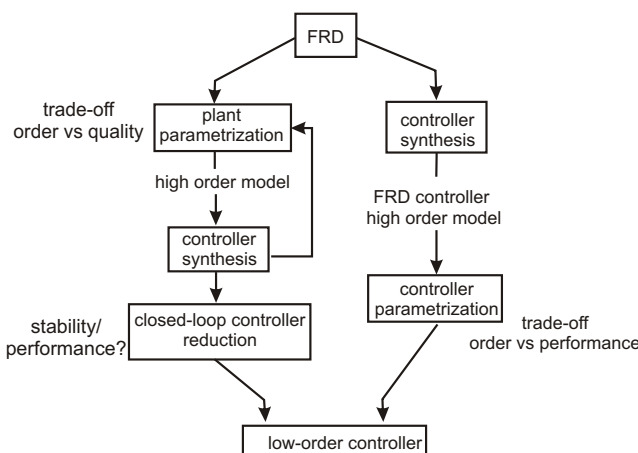


Fig.1: Overview of common (left) and proposed controller synthesis path (right)

Synthesis algorithm for the SISO case

An algorithm is developed that deduces the FRF of the \mathcal{H}_∞ optimal controller directly from non-parametric plant data for the SISO case. This is achieved by rewriting the \mathcal{H}_∞ problem as a specific model-matching problem [2]:

$$\|W_1 S|^2 + |W_2 T|^2\|_\infty = \|T_1 - T_2 Q\|_\infty \leq 1$$

By appropriate factorization, it can be shown by Nevanlinna-Pick interpolation theory [1] that the zeros of the plant are the only required parametric data to acquire the Youla parameter Q . Combining the plant FRD and the Youla parameter gives the optimal controller FRD:

$$C(\omega_j) = \frac{Q(\omega_j)}{(1 - P(\omega_j)Q(\omega_j))}$$

As a natural extension, the set of allowable FRD for suboptimal controllers can be obtained on the given frequency grid for a given $\gamma > \gamma_{opt}$ (see Fig.2). This can be of great value to fit low-order suboptimal controllers or guarantee robust performance over a set of plant FRD's.

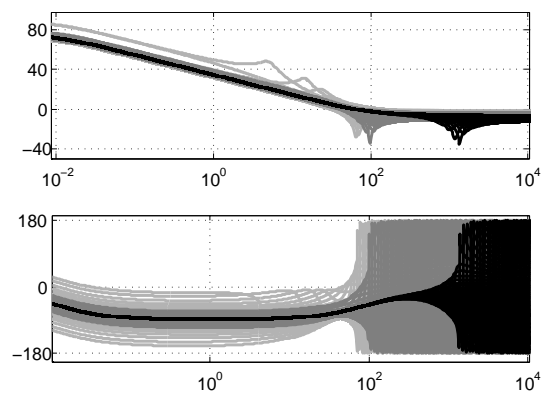


Fig.2: Open-loop using the set of (sub)optimal controllers for $(-)\gamma = 2$, $(-)\gamma = 1.5$ and $(-)\gamma = 1$

References

- [1] J.A. Ball, I. Gohberg, and L. Rodman, (1990), 'Interpolation of rational matrix functions', Birkhauser
- [2] J. Doyle, B. Francis, and A. Tannenbaum, (1992), 'Feedback control theory', McMillan

Design of Robust Optimal Feedback Controllers for Periodic Disturbances

Goele Pipeleers, Bram Demeulenaere, Jan Swevers, Joris De Schutter
 Dept. of Mechanical Engineering
 Katholieke Universiteit Leuven
 Celestijnenlaan 300B, B-3001 Heverlee, Belgium
 Email: goele.pipeleers@mech.kuleuven.be

1 Introduction

In many control applications the dominant disturbances are periodic, for instance, in the track-following servo system of optical disk drives, active noise control and robotized laparoscopic surgery. Furthermore, disturbances due to rotating unbalances or nearby combustion engines are dominantly periodic.

In the presence of periodic disturbances, repetitive control [1] is a commonly used control design strategy. Based on the internal model principle, repetitive control explicitly includes the disturbance dynamics in the feedback controller, yielding an infinite loop gain at the harmonics of the disturbance. Although this strategy guarantees perfect disturbance rejection, it makes the closed-loop stability highly sensitive to unmodelled dynamics. Hence, a trade-off between disturbance attenuation and closed-loop stability has to be made. Recently, Steinbuch [2] proposed an extension of the classical repetitive control scheme to increase the robustness of the performance to uncertainty on the period of the disturbance.

2 Methodology

The present paper proposes an alternative controller design strategy based on the Youla-parametrization. For any control problem, the set of closed loop transfer matrices $H(z)$ achievable by an internally stabilizing controller is given by:

$$H(z) = T_1(z) + T_2(z)Q(z)T_3(z).$$

$T_1(z)$, $T_2(z)$ and $T_3(z)$ are transfer matrices determined by the plant while $Q(z)$ is a free stable transfer matrix, called the Youla-parameter of $H(z)$, [3]. Once $Q(z)$ is known, the corresponding controller can be calculated. In this paper a FIR-model is proposed for $Q(z)$.

Using this parametrization the design of a controller that optimally attenuates periodic disturbances with a given period T_0 is transformed into a convex optimization problem. If additionally uncertainty on T_0 is considered, the controller design amounts to a robust convex program. While being still convex, this optimization problem has infinitely many constraints. However, by the use of the generalized KYP

lemma [4] this optimization problem is transformed into a finite-dimensional semidefinite program. In addition to uncertainty on the period of the disturbance, both parametric and dynamic plant uncertainties are considered as well. These uncertainties are accounted for while preserving the convexity of the corresponding optimization problem.

3 Results

The developed design strategy is validated on simulation for the design of a track-following controller for optical disk drives. Trade-off curves between conflicting control specifications are computed and the developed controller design is compared to the design of [2].

Acknowledgement

Goele Pipeleers is a Research Assistant of the Research Foundation - Flanders (FWO-Vlaanderen) and Bram Demeulenaere is a Postdoctoral Fellow of the Research Foundation - Flanders. This work has been carried out within the framework of projects G.0528.04 and G.0446.06 of the Research Foundation - Flanders and also benefits from K.U.Leuven-BOF EF/05/006 Center-of-Excellence Optimization in Engineering. The authors wish to acknowledge Dr. J. Camino (Universidade Estadual de Campinas, Brazil; visiting fellow (2006-2007) at K.U. Leuven) for his remarks on the subject of this paper.

References

- [1] G. Hillerstrom, and K. Walgama, "Repetitive control theory and applications - a survey," Proc. of the 13th IFAC World Congress, Vol. D, 1996.
- [2] M. Steinbuch, "Repetitive control for systems with uncertain period-time," Automatica, 38: 2103-2109, 2002.
- [3] S. Boyd, and C. Barratt, "Linear Controller Design: Limits of Performance," Prentice-Hall, 1991.
- [4] T. Iwasaki, and S. Hara, "Generalized KYP lemma: unified frequency domain inequalities with design applications," IEEE Transactions on Automatic Control, 50(1): 41-59, 2005.

Multi Objective Optimization for Dynamic Baking Processes

Hadiyanto*, D.C. Esveld** and R Boom**, G. van Straten* and A.J.B. van Boxtel*
 *System and Control group, **Food Process Engineering Group Wageningen University
 P.O. Box 17, 6700 AA Wageningen, The Netherlands
 Email: hady.hadiyanto@wur.nl

1. Introduction

The development of dynamic operations for food processes with product quality as a central criterion deals with multi criteria for optimization. These criteria are often conflicting, which means that improving one objective will cause worsening at least one of other objective functions. For example, for baking processes the level of brownness may conflict with the degree of crispness. It is hardly possible to solve such multi objective optimization (MOO) problem in a single optimization. Therefore, finding a set of feasible solutions is more relevant than one single optimum solution. The set of feasible solution is described with Pareto line.

2. Normal Boundary Intersection (NBI)

MOO is formulated as:

$$\min F(x) = [f_1(x) \ f_2(x) \ \dots \ f_n(x)]^T, \text{ with } n \geq 2.$$

x^* is Pareto optimum if and only if there is no x , such that $f_i(x) \leq f_i(x^*)$ for all i , with at least one strict inequality. To generate the Pareto line, the Normal Boundary Intersection (NBI) method is used (Fig. 1). NBI is a multi objective optimization method which has been developed recently [1] to generate an even distribution of Pareto line.

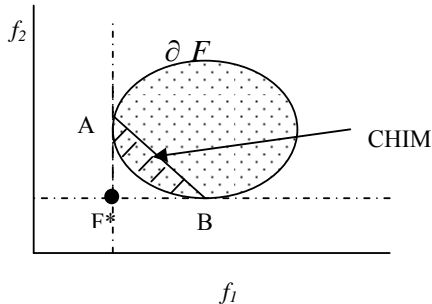


Figure 1 NBI method to generate Pareto optimal solution for two objective functions

The principle of this methodology is that the intersection point between the boundary ∂F and the normal pointing towards the origin from any point at the CHIM (Convex Hull Individual Minima) is the

part of ∂F containing the efficient points which is guaranteed to be a Pareto optimal point. Let, x^* be the respective global minimiser $f_i(x)$, $F_i^* = F(x^*)$ and Φ is pay-off matrix ($n \times n$) whose i^{th} column is $F_i^* - F_i$ then a set points that are convex combinations of $F_i^* - F_i$; i.e. $\left\{ \Phi w : \sum_{i=1}^n w_i = 1, w_i \geq 0 \right\}$ is referred to CHIM.

3. Case Study

The MOO problem was applied to bread baking with the two objective functions:

$$f_1 = (brown(t_f) - 0.8)^2, \ f_2 = (crispness(t_f) - 0.95)^2$$

The final temperature of product is expected to be 40°C since it is considered as eating temperature. **Fig 2a** shows a set of feasible solutions for control trajectories of this case study. The variation of control inputs in **Fig 2a** corresponds to each point in the Pareto line as depicted in Fig 2b.

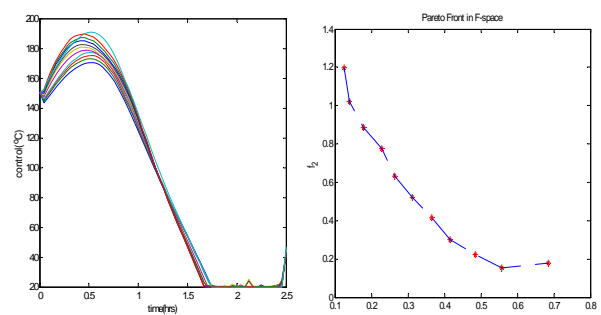


Figure 2 The set of optimum heating trajectories (a) and Pareto line(b)

References

- [1]. Das and Dennis, 1998, Normal-Boundary intersection : An alternate Method for Generating Pareto Optimal points in multi criteria Optimization Problems, *ICASE Report 92-296*;
- [2]. Hadiyanto, A. Asselman, G. van Straten, R.M. Boom, D.C. Esveld and A.J.B. van Boxtel, 2007, Quality Prediction of Bakery Products in the Initial Phase of Process Design, *submitted to IFSET Journal*

Towards economic optimal dynamic plantwide operation

A.E.M. Huesman

Delft Center for Systems and Control
Delft University of Technology
Mekelweg 2, 2628 CD Delft
The Netherlands

Email: a.e.m.huesman@tudelft.nl

O.H. Bosgra

Delft Center for Systems and Control
Delft University of Technology
Mekelweg 2, 2628 CD Delft
The Netherlands

Email: o.h.bosgra@tue.nl

1 Introduction

Due to globalization the process industry is faced with increased competition. This has resulted in pressure on the margins and the process industry has to find ways to improve its economic performance. This can be done by changing the design, the operation or a combination of both. Certainly for existing plants improving the operation is an attractive “low-cost” option.

Economic optimization in the process industry already dates back nearly 50 years. The current state of the art is Real Time Optimization (RTO). Since RTO is in fact steady state optimization it is not compatible with batch operation. It has been recognized that RTO is slow since each optimization has to be proceeded by a steady state. The last two decades there has been a substantial amount of work on dynamic optimization. However the main focus has been on how to perform dynamic optimization. The same is true for batch optimization. To bridge the gap between economic performance and dynamic optimization the presentation focuses on the following question:

How to frame dynamic optimization such that we can expect optimal operation in an economic sense?

2 Framework

In the presentation a general framework will be proposed. The framework adopts a *plantwide system boundary*. In this way there is no need to know intermediate prices. The system boundary *includes product tank(s)*. This allows for more flexibility in the sense that at least the production rate is allowed to vary. As a result the framework supports any kind including continuous and batch operation.

Within this framework optimal plantwide operation can be formulated as a dynamic optimization problem:

$$\min \int_0^{t_f} \text{operating costs}(t) dt \quad (1)$$

$$\text{s.t.} \left\{ \begin{array}{l} \text{plant behaviour} \\ \text{required quantity and quality} \\ \text{operational constraints} \end{array} \right. \quad (2)$$

The variable t_f denotes the *finite horizon*. The horizon as well as the required quantity and quality are supplied by

scheduling. This facilitates integration with scheduling but it also means that the product is handled as a constraint rather than as a part of the economic objective.

Often the objective is linear, the same goes for the required quantity and quality and the operational constraints. However the plant behaviour is normally non-linear and for that reason problem (1) - (2) is a non-linear optimization problem.

3 Experiments

The framework is subjected in an off-line setting to two numerical experiments; a Stirred Tank Reactor (STR) and a Distillation Column (DC). The off-line setting has to do with separation of the benefits. The off-line benefits are associated with the type of operation, the on-line benefits with the way disturbances are handled. Applying the framework to the STR results in batch operation while in the DC case it results in continuous operation.

Some results related to the STR case seem arbitrary in the sense that a change in the initial guess for the decision variables leads to a different solution for the decision variables. However the different solutions have the same objective value. From an optimization point of view these results can be explained as “multiple solutions”; there is an optimal subspace rather than a single optimal point. In control terms it means that not all degrees of freedom are fixed. The occurrence of multiple solutions can be understood from a geometrical perspective. It is desirable to avoid multiple solutions since in a on-line setting it can lead to “jumping around solutions”.

4 Conclusions

A general framework has been formulated that can determine economic optimal dynamic plantwide operation. This framework supports any kind of operation and can easily be integrated with scheduling.

Currently the framework allows for multiple solutions. The future research will focus on multiple solutions; can they be avoided? If the answer is yes then the next question is how? If the answer is no then the next question is why not?

A Note on cooperative Linear Quadratic Control

J.C. Engwerda
 Tilburg University
 e-mail: engwerda@uvt.nl

1 Abstract

In this note we consider the cooperative linear quadratic control problem. That is, the problem where a number of players, all facing a (different) linear quadratic control problem, decide to cooperate in order to optimize their performance. It is well-known, in case the performance criteria are positive definite, how one can determine the set of Pareto efficient equilibria for these games. In this note we generalize this result for indefinite criteria.

Keywords: LQ theory; Convexity; Riccati equations; Cooperative differential games; Pareto frontier.

game with nontransferable payoffs, *Journal of Optimization Theory and Applications*, vol.124, pp.701-724.

References

- [1] Engwerda J.C., 2005, *LQ Dynamic Optimization and Differential Games*, Chichester, Wiley.
- [2] Engwerda J.C., 2006, A note on cooperative linear quadratic control, Internal Report, Tilburg University.
- [3] Fan K., Glicksberg I. and Hoffman A.J., 1957, Systems of inequalities involving convex functions, *American Mathematical Society Proceedings*, Vol.8.
- [4] Geerts T., 1991, A priori results in linear-quadratic optimal control theory, *Kybernetika*, vol.27, pp.446-457.
- [5] Leitmann G., 1974, *Cooperative and Non-cooperative Many Players Differential Games*, Springer Verlag, Berlin.
- [6] Molinari B.P., 1977, The time-invariant linear-quadratic optimal control problem, *Automatica*, vol.13, pp.347-357.
- [7] Takayama A., 1985, *Mathematical Economics*, Cambridge University Press, Cambridge.
- [8] Trentelman H.L., 1989, The regular free-endpoint linear quadratic problem with indefinite cost, *SIAM J. Control and Optimization*, vol.27, pp.27-42.
- [9] Trentelman H.L. and Willems J.C., 1991, The dissipation inequality and the algebraic Riccati equation. In S. Bittanti, A.J. Laub and J.C. Willems (Eds.), *The Riccati Equation*, Springer Verlag, Berlin, pp.197-242.
- [10] Willems J.C., 1971, Least squares stationary optimal control and the algebraic Riccati equation, *IEEE Transactions on Automatic Control*, vol.16, pp.641-634.
- [11] Yeung D.W.K and Petrosyan L.A., 2005, Subgame consistent solutions of a cooperative stochastic differential

Some Practical Applications of a Nonlinear Block Structure Identification Procedure

Lieve Lauwers, Johan Schoukens and Rik Pintelon
 Vrije Universiteit Brussel, dep. ELEC, Pleinlaan 2, 1050 Brussel, BELGIUM
 email: lieve.lauwers@vub.ac.be

Abstract - A structure identification method based upon the Best Linear Approximation is applied to three different physical systems: the silverbox, a crystal detector and an RF amplifier.

I. INTRODUCTION

In nonlinear system identification, the selection of an appropriate nonlinear model structure is a first critical step. If no prior knowledge is available, it might be hard for the user to know whether the selected model structure is appropriate for modelling the system due to the large variety among nonlinear model structures. Therefore, a method is required that gives the user some guidance in his/her choice of nonlinear model structures.

II. THE NONLINEAR BLOCK STRUCTURE IDENTIFICATION PROCEDURE

In [1], we proposed a method to discriminate between different nonlinear block oriented model structures. This structure identification method is based upon the Best Linear Approximation (BLA) of the nonlinear system [2],[3]. For random excitation signals, a nonlinear system can be represented by its Best Linear Approximation followed by a noise source representing the unmodelled nonlinear contributions of the system [4]. These nonlinear contributions depend on the particular realization of the input signal and they exhibit a stochastic behaviour. In practice, this BLA can be estimated by averaging the measured Frequency Response Functions (FRFs) for different input realizations.

The approach of this method is to apply a Gaussian-like input signal and to vary in a first experiment the root mean square (rms) value of this signal while maintaining the shape of the power spectrum, and to vary in a second experiment the shape of the power spectrum while keeping the rms value constant. According to the resulting changes (a vertical shift or a shape change) of the amplitude and phase characteristics of the Best Linear Approximation, a distinction can be made between candidate nonlinear block structures for approximating the real system.

III. PRACTICAL ILLUSTRATIONS

To illustrate its user friendliness, ease and wide scope, this structure identification method will be applied to three physical systems in various domains. The first system is an electrical circuit simulating the behaviour of

This work was supported by the FWO-Vlaanderen, the Flemish community (Concerted action ILiNoS), the Belgian government (IUAP-VI/22), the TARGET Network ("Top Amplifier Research Groups in a European Team") and the Information Society Technologies Programme of the EU under contract IST-1-507893-NOE - www.target-net.org.

	Gaussian excitation signals			
	changing rms value		changing shape power spectrum	
	$ G_{BLA} $	$\angle G_{BLA}$	$ G_{BLA} $	$\angle G_{BLA}$
Wiener-Hammerstein (WH)	↗	=	↗	=
Wiener (W)	↗	=	↗	=
Hammerstein (H)	↗	=	=	=
(W)H-polyNFIR	↗	=	Δ	Δ
WH-NFIRsum	Δ	Δ	Δ	Δ
H-NFIRsum	Δ	Δ	=	=
NonLinearFeedBack (NLFB)	Δ	Δ	Δ	Δ

Table I: General behaviour of the BLA of some nonlinear systems (NFIR: Nonlinear Finite Impulse Response). Symbol \nearrow stands for a vertical shift; = means that nothing changes; and Δ denotes a frequency dependent change.

a nonlinear mass-spring-damper system, also known as the 'Silverbox' [5]. The second system is an Agilent-HP420C crystal detector, a device used for microwave power measurements, and the third system is an RF amplifier. By comparing the experimental results of the system's BLA with the theoretical results (see Table I), an analysis can be made about the appropriateness or ability of some nonlinear block structures concerning the identification of the system under test [1].

IV. CONCLUSION

A structure identification procedure based upon the Best Linear Approximation is illustrated. We showed that this method is applicable in various fields and easy to implement since the user only needs to carry out FRF measurements together with a variance analysis.

References

- [1] L. Lauwers, J. Schoukens, R. Pintelon, M. Enqvist. Nonlinear Structure Analysis Using the Best Linear Approximation. *Proceedings of the International Conference on Noise and Vibration Engineering*, pp. 2751-2760, 2006.
- [2] R. Pintelon, J. Schoukens (2001). *System Identification. A Frequency domain approach*. IEEE Press, New Jersey.
- [3] M. Enqvist, Linear Models of Nonlinear Systems. PhD thesis, Linköping University, Linköping, Sweden, 2005.
- [4] J. Schoukens, R. Pintelon, T. Dobrowiecki, Y. Rolain. Identification of linear systems with nonlinear distortions. *Automatica*, Vol. 41, No. 3, pp. 491-504, 2005.
- [5] J. Schoukens, J. G. Nemeth, P. Crama, Y. Rolain, R. Pintelon. Fast approximate identification of nonlinear systems. *Automatica*, Vol. 39, No. 7, pp. 1267-1274, 2003.

Detection of Nonlinearities when Measuring Respiratory Impedance

C. Ionescu, A. Caicedo, M. Gallego, R. De Keyser

Department of Electrical energy, Systems and Automation
Ghent University, Technologiepark 913, Gent B9052, Belgium
Email: clara@autoctrl.UGent.be

1 Introduction

The forced oscillation technique (FOT) is a non-invasive method which is commonly used to measure respiratory mechanics [1] using the device schematically represented in figure 1. FOT employs small-amplitude pressure oscillations superimposed on the normal breathing. Although it is more interesting to study the respiratory system closer to the breathing frequency ($\approx 0.3\text{Hz}$), distortions may corrupt the measurements. Identifying the best linear approximation of the human respiratory system impedance, results in minimizing the influence of the nonlinearities (NL) coming from the device.

2 Detection of Nonlinearities

Due to limitations of the loudspeaker in the low frequency range, the input signal has to be amplified in order to obtain a good signal-to-noise-ratio at frequencies lower than 4Hz. This amplification can lead to NL effects. Using a method for input signal optimization described in [2], these NL from the device can be quantified and are depicted in figure 2. In order to identify the NL coming from the respiratory system, the pressure and the flow in the input at the mouth were measured. The corrected results are depicted in figure 3. It can be observed that the NL effects are stronger at frequencies closer to the breathing frequency. Using the methods described in [2], the linear and nonlinear behavior of the patient can be extracted from these results. Once the nonlinear effects introduced by the device are separated from the measured signals, only the NL coming from the patient remains. This will include effect of both the breathing signal, as well as effects from the geometrical structure of the respiratory tree itself. Characterizing the diagnostic capacity of these nonlinear effects is ongoing research.

References

- [1] E. Oostveen, D. Macleod, H. Lorino, R. Farré, Z. Hantos, K. Desager, F. Marchal, "The forced oscillation technique in clinical practice: methodology, recommendations and future developments", *Eur Respir J*, **22**, 1026-1041, (2003)
- [2] J. Schoukens, R. Pintelon, T. Dobrowiecki, Y. Rolain, "Identification of linear systems with nonlinear distortions", *Automatica*, **41**, 491-504, (2005)

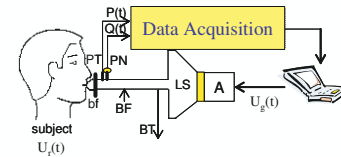


Figure 1: FOT measurement setup. Notations apply: A - amplifier; LS - loudspeaker; BT - bias-tube; BF - bias-flow; PN - pneumotachograph; BF - antibacterial filter; PT - pressure transducer; $Q(t)$ - measured flow; $P(t)$ - measured pressure; $U_g(t)$ - driving signal; $U_r(t)$ - breathing

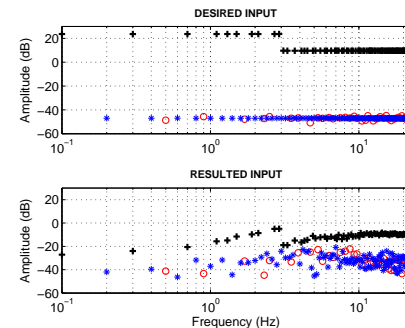


Figure 2: NL from the device without the patient: original (desired) signal (+); odd NL (o); even NL (*).

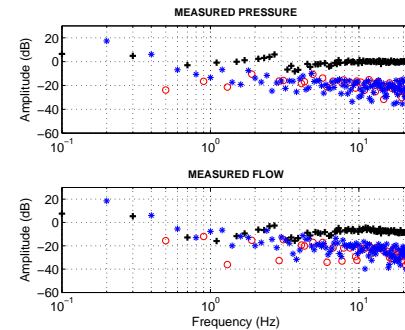


Figure 3: NL from the device and the patient: original signal (+); odd NL (o); even NL (*).

Estimating the FRF Matrix and the Level of Nonlinearity for Multivariable Systems using a Single Periodic Broadband Excitation

Kris Smolders, Jan Swevers

Katholieke Universiteit Leuven – Department of Mechanical Engineering, PMA

Celestijnenlaan 300B, B3001 Heverlee, Belgium

{kris.smolders, jan.swevers}@mech.kuleuven.be

Abstract

For a LTI multivariable (MIMO) system with p inputs and q outputs the dynamic relationship between the inputs $u \in \mathbb{R}^p$ and the outputs $y \in \mathbb{R}^q$ is given in the frequency domain by the $q \times p$ MIMO FRF matrix $G(j\omega)$ according to:

$$\underbrace{\begin{bmatrix} Y^{[1]} \\ \dots \\ Y^{[q]} \end{bmatrix}}_{Y(j\omega)} = \underbrace{\begin{bmatrix} G^{[1,1]} & G^{[1,p]} \\ \dots & \dots \\ G^{[q,1]} & G^{[q,p]} \end{bmatrix}}_{G(j\omega)} \underbrace{\begin{bmatrix} U^{[1]} \\ \dots \\ U^{[p]} \end{bmatrix}}_{U(j\omega)}. \quad (1)$$

$G(j\omega)$ is estimated as $\hat{G}(j\omega)$ from input-output data measured during system excitation. Accurate FRF estimation requires the selection of appropriate excitation signals. It is shown [2] that periodic broadband excitation has several advantages. For a single excitation signal this corresponds to:

$$u(kT) = \sum_{n=n_l}^{n_h} U_n \cos(n\omega_0 kT + \phi_n). \quad (2)$$

$u(kT)$ is the k th time sample of a periodic broadband excitation signal with ground pulsation ω_0 [rad/s] and k going from 1 to $N - 1$. N is the number of samples present in one period. T [s] indicates the sample period. The overall period of the excitation is $T_0 = NT = 2\pi/\omega_0$ [s]. Due to the periodic nature of the signal the spectrum is discrete. n indicates the spectral component corresponding to frequency $\omega_n = n\omega_0$ [rad/s]. U_n is the amplitude of the n th spectral component and ϕ_n the corresponding phase. The lowest frequency present in u is $n_l\omega_0$ [rad/s], the highest is $n_h\omega_0$ [rad/s]. The advantages of using periodic broadband excitation are explained in detail in [1, 2, 3]. Random phase indicates that ϕ_n is sampled from a uniform random distribution $[0, 2\pi]$, while the user is free to design U_n at will (e.g. to have a certain power spectrum for the excitation).

In this presentation it is assumed that the system is time-invariant but not necessarily linear because in practice no system is truly linear. This yields that the estimation of the FRF matrix is disturbed by (internal) nonlinear system characteristics (called nonlinear disturbances) in addition to the omnipresent (external) noise sources (called a-periodic disturbances) acting on the system. In this presentation it is also assumed that the input is exactly known, as is the case for most control applications, such that all external disturbances are assumed at the output. The systems considered

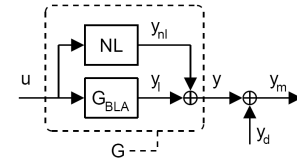


Figure 1: Schematic representation of the considered systems G .

in this presentation can be represented as in figure 1: G is the system with inputs u and outputs y . The outputs y consist of a linear contribution y_l coming from the so-called best linear approximation G_{BLA} of G under the considered excitation u [2], and a nonlinear contribution y_{nl} which can be thought of as an input driven noise source [3]. The measured outputs y_m are disturbed by external noise sources y_d . The assumptions under which a system can be represented as in figure 1 are given in [3, 4].

This presentation extends an existing method [3] for estimating the level of the nonlinear disturbances y_{nl} and a-periodic disturbances y_d for SISO systems to MIMO systems. It is shown how to obtain an estimate of the additive uncertainty based on the estimated level of nonlinear disturbances, both in the SISO and in the MIMO case. Furthermore the method presented in this presentation estimates all this information together with an estimate of the MIMO FRF matrix from one single experiment using specially designed broadband excitation signals. Experimental results of the method on a half car test setup are presented.

Acknowledgements

This work has been performed in the framework of project G.0528 ‘Accurate tracking control for nonlinear multi-variable systems based on experimentally identified general block-oriented models’ of the Fund for Scientific Research - Flanders (FWO).

References

- [1] P. Guillaume, R. Pintelon, J. Schoukens; *Accurate Estimation of Multivariable Frequency Response Functions*; Proceedings of the 13th Triennial World Congress, San Francisco; 1996, pp. 423-428.
- [2] R. Pintelon, J. Schoukens; *System Identification - a Frequency Domain Approach*; IEEE Press, 2001.
- [3] J. Schoukens, T. Dobrowiecki, R. Pintelon; *Parametric and Nonparametric Identification of Linear Systems in the Presence of Nonlinear Distortions - a Frequency Domain Approach*; IEEE Transactions on Automatic Control, vol. 43, 1998, pp. 176-190.
- [4] J. Schoukens, R. Pintelon, Y. Rolain, T. Dobrowiecki; *Frequency Response Function Measurements in the Presence of nonlinear Distortions*; Automatica, vol. 37, 2001, pp. 939-946.

Extending the Best Linear Approximation for Frequency Translating Systems

Koen Vandermot, Wendy Van Moer, Yves Rolain and Rik Pintelon

Vrije Universiteit Brussel, dep. ELEC, Pleinlaan 2, 1050 Brussels, BELGIUM
e-mail: koen.vandermot@vub.ac.be

Abstract - The concept of a Best Linear Approximation (BLA) will be introduced for frequency translating devices, such as mixers.

I. INTRODUCTION

A mixer is frequently used in all kinds of telecommunication applications [1]. Besides the ideal frequency translation, a real mixer produces a lot of additional linear and nonlinear disturbances: e.g. isolation effects, intermodulation products,... To obtain a simple model for this important system function, the Frequency Response Function (FRF) is no longer useful because the output at one frequency is no longer only dependent on the input at the same frequency.

To generate a simple model for a real mixer, we will follow the lines of the Best Linear Approximation (BLA) reasoning [2]. First an ideal mixer is defined as a perfect frequency translating device. It converts the input signal to the output by an ideal frequency translation and a complex frequency dependent gain. All the remaining effects will be grouped and modelled as a perturbation source with a frequency dependent Power Spectral Density (PSD).

II. EXTENDING THE BLA TO THE BEST MIXER APPROXIMATION (BMA)

A. An ideal mixer [1]

An ideal mixer is a three-port system consisting of two input ports (U, LO) and one output port (Y), where $y(t) = u(t).lo(t)$. In the ideal case, the local oscillator port (LO) is excited with a pure sinewave signal of frequency f_{LO} , which plays the role of the pump. As a consequence, the LO signal is always a large signal compared to the signal at port U. When the mixer is observed as an upconvertor, the partial ideal mixer model becomes:

$$Y(\omega_k + \omega_{LO}) = U(\omega_k)LO(\omega_{LO}) \quad (1)$$

B. A real mixer - Definition of the BMA

A real mixer produces a lot of additional linear and nonlinear disturbances. Bringing into account these disturbances results in the Best Mixer Approximation (BMA). The response of the upconverted frequency

band of the real mixer can be written as [3]:

$$\begin{aligned} Y(\omega_{LO} + \omega_k) &= G_0(\omega_{LO} + \omega_k)U(\omega_k)LO(\omega_{LO}) \\ &+ G_B(\omega_{LO} + \omega_k)U(\omega_k)LO(\omega_{LO}) \\ &+ \sum_{n_k} G_S^{n_k}(\omega_{LO} + \omega_k) \prod_{i=1}^{n_k} U(\omega_{k_i}) \end{aligned} \quad (2)$$

where $\sum_i \omega_{k_i} = \omega_k$. $G_S^{n_k}(\omega_{LO} + \omega_k)$ includes the higher order terms in LO. The sum of the first two terms is called the Best Mixer Approximation (BMA):

$$G_{BMA}(\omega) = G_0(\omega) + G_B(\omega) \quad (3)$$

The BMA captures both the ideal mixer contributions and the nonlinear systematic contributions which are always phase coherent to U , independent of the realization of the phase spectrum of this signal. The last terms in equation (2) are the “noise” contributions. Herein, G_S represents the additional noise source created by the nonlinear perturbation which is random with respect to the phase realizations of U . As a conclusion, the model for the mixer can now be written as follows:

$$\begin{aligned} G(\omega_{LO} + \omega_k) &= \frac{Y(\omega_{LO} + \omega_k)}{U(\omega_k)LO(\omega_{LO})} \\ &= G_{BMA}(\omega_{LO} + \omega_k) + G_S(\omega_{LO} + \omega_k) \end{aligned} \quad (4)$$

Measurement experiments confirm this theory.

III. CONCLUSION

The BLA has been extended for frequency translating systems, also called the Best Mixer Approximation (BMA). It is now possible to classify the impact of nonlinear perturbations in systematic (bias) and stochastic (nonlinear noise) contributions.

IV. REFERENCES

- [1] S.A. Maas. *Nonlinear Microwave Circuits*, John Wiley & Sons, USA, 1988.
- [2] R. Pintelon, J. Schoukens (2001). *System Identification. A frequency domain approach*. IEEE Press, New Jersey.
- [3] K. Vandermot. Internal note: Derivation of the BMA, 2006. (koen.vandermot@vub.ac.be).

This work was fund by a grant of the Flemish Institute for improvement of the scientific-technological research in industry (IWT), the Fund for scientific Research (FWO - Concerted action ILiNoS), and the Belgian government (IUAP-V/22). Research reported here was also performed in the context of the network TARGET and supported by the Information Society Technologies Programme of the EU under contract IST-1-507893-NOE, www.target-net.org.

Experimental stability analysis of nonlinear feedback systems

L. Vanbeylen, J. Schoukens

Vrije Universiteit Brussel, dept. ELEC, Pleinlaan 2, B1050 Brussels, BELGIUM
e-mail: laurent.vanbeylen@vub.ac.be

1 Introduction

It is well known that nonlinear modelling is a very hard task. First, the model selection is problematic. But especially the validation of nonlinear models is time consuming, extremely difficult, and hence expensive; there is no guarantee that the model is good everywhere, and consequently there is a large risk for remaining model errors. When a nonlinear plant has to be controlled, the best one can do is to use the available plant model to design the controller, and hope that the remaining model errors will not drive the real life feedback-controlled nonlinear system (RLFCNS) into an unstable mode. Indeed, even if the controlled model performs well (stably), nothing can be guaranteed about the stability of the RLFCNS; there still remains a risk that the RLFCNS behaves unstably, due to the remaining model errors. As supported by simulation studies, it appears that under certain circumstances (properties of the input signal, e.g. the rms-level), certain nonlinear feedback loops behave stably, while under other circumstances, the same loop behaves occasionally unstably, or even highly unstably, while the analysis of the control loop on the basis of the model guaranteed the stability.

The current problem has only been investigated in [1]; that relies on the framework of the best linear approximations, and on the small gain theorem. In this contribution, using extreme value statistics, we aim to get more information about the instability of a nonlinear feedback loop, starting from experimental data on the physical feedback system, without building an additional model.

2 The idea

We will call a system stable, if an input with bounded variance results in an output with bounded variance.

The idea is to split the nonlinear feedback system in two parts: (i) a (known) stable part and (ii) another (possibly unstable) remaining part, which accounts for all unmodelled effects, both connected in parallel (sum). The output of the latter will be called residual.

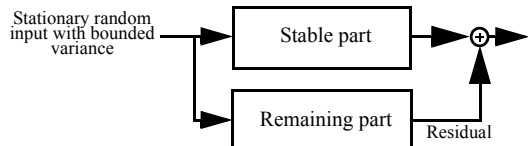


Fig. 1. Block schematic representation of the equivalent model

This work was supported by the FWO-Vlaanderen, the Flemish community (Concerted action ILiNoS), and the Belgian government (IUAP-V/22).

At this moment, the first part is chosen as the best linear approximation (residual minimal in least-squares sense) [2]; this provides the advantage that the maximum amount of coherent power between input and output is extracted. If the excitation has a bounded variance, the variance of the output of the first part will be finite, even when instability occurs in the nonlinear feedback system. Therefore, in that case, the residual will have an infinite variance. Hence, a statistical description of the residual is crucial.

3 Extreme value model

For many natural phenomena (waves, wind speed, temperature, floods, earthquakes, rainfall) and in financial applications, extreme value statistics are a standard tool for statistical modeling of extreme events. It has been shown that for a very wide class of distributions (the so-called maximum-domain of attraction), the excesses over a sufficiently high threshold are generalised-Pareto distributed [3]. For this distribution, a maximum likelihood estimator (MLE) is available for estimating its parameters and their asymptotic covariance matrix. It is also known from this generalised-Pareto distribution, that the variance is infinite for shape parameters ξ beyond 0.5.

4 Proposed algorithm

1. Estimate the stable part of the model and its output.
2. Compute the absolute values of the residuals.
3. Estimate the parameters (and asymptotic covariance matrix) of the generalised-Pareto model on the tails (extreme values) of the residuals.
4. After this step, we are able to predict the probability that a certain value of the residual is exceeded in magnitude.

The closer the estimated shape parameter comes to 0.5, the higher the variance of the residual, and the higher the probability of instability.

This has been verified via numerical Monte-Carlo simulations, showing that the shape parameter estimates shift to the right with increasing probability of instability.

References

- [1] Schoukens J., Dobrowiecki T., Pintelon R. (2004), Estimation of the risk for an unstable behaviour of feedback systems in the presence of nonlinear distortions. *Automatica* (40) 1275-1279.
- [2] Pintelon R., Schoukens J. (2001), *System identification, a frequency domain approach*. New York: IEEE Press.
- [3] Coles S. (2001), *An introduction to statistical modeling of extreme values*. London: Springer.

Overview of the Control Architecture used for the Biped Lucy

Bram Vanderborght, Ronald Van Ham, Björn Verrelst, Michaël Van Damme & Dirk Lefeber
 Robotics & Multibody Mechanics Research Group
 Vrije Universiteit Brussel, Pleinlaan 2, B-1050 Brussels, Belgium
 Email: bram.vanderborght@vub.ac.be URL: <http://lucy.vub.ac.be>

1 Biped Lucy

The bipedal walking robot Lucy (Fig 1, [1]) has 12 pleated pneumatic artificial muscles to actuate 6 degrees of freedom (hip, knee and ankle of both legs). The motion of Lucy is restricted to the sagittal plane by a guiding mechanism. The guiding mechanism, which prevents the robot from falling sideways, has limited length, so a treadmill is used to be able to walk longer distances. The robot's total mass is about 33 kg and it is 150 cm tall. The global control architecture consists of a trajectory generator, and a joint trajectory tracking controller.

2 Trajectory Generator

The trajectory generator calculates trajectories for the different joints so that the robot can walk from a certain position to another while keeping the Zero Moment Point (ZMP) in the stability region, thus ensuring dynamic balance of the robot. For each step the objective locomotion parameters (step length λ , intermediate foot lift κ and speed v) can be chosen. The main idea of the trajectory generator is to plan the motion of the CoG, represented by the waist motion, in function of desired ZMP trajectories determined by the foothold sequences. The problem is regarded as a ZMP servo control implementation, trying to track the ZMP by servo control of the horizontal acceleration. Because often the hip has to move before the ZMP path changes, information about desired position of the ZMP in the future is needed, hence the use of a preview control method as proposed by Kajita [2]. The dynamics are simplified to a cart-table model, a cart that represents the global COG of the robot moving on a horizontally positioned pedestal table with negligible mass. Since the true robot is a multibody system the real and desired position of the ZMP will differ. In order to solve this issue the error is presented to a second stage of the preview control.

3 Joint Trajectory Tracking Controller

The joint trajectory tracking controller is divided into a computed torque controller, a delta-p unit and a pressure bang-bang controller. The computed torque controller calculates the required joint torques based on the robot dynamics. This dynamic model is different for single and double support phase because during single support the robot has 6 DOF and during double support the number of DOF is reduced



Figure 1: Photograph of the robot Lucy

to 3, which makes the system over-actuated. For each joint a delta-p unit translates the calculated torques into desired pressure levels for the two muscles of the antagonistic set-up. Finally a bang-bang controller determines the necessary valve signals to control the actions of the on-off valves to set the correct pressures in the muscles. The trajectory generator, computed torque and delta-p units are implemented on a central PC, the bang-bang controller is locally implemented on micro-controller units. Currently the robot is able to walk with a speed up to $0.15m/s$.

Acknowledgements

The author B. Vanderborght is Phd student with a grant from the Fund for Scientific Research-Flanders (Belgium)(FWO). Lucy has been built with the financial support of the Research Council (OZR) of the Vrije Universiteit Brussel

References

- [1] B. Verrelst, R. Van Ham, B. Vanderborght, F. Daerden, and D. Lefeber, "The pneumatic biped LUCY actuated with pleated pneumatic artificial muscles," *Autonomous Robots*, vol. 18, pp. 201–213, 2005.
- [2] S. Kajita, F. Kanehiro, K. Kaneko, K. Fujiwara, K. Harada, K. Yokoi, and H. Hirukawa, "Biped walking pattern generation by using preview control of zero-moment point," in *IEEE International Conference on Robotics and Automation (ICRA03)*, vol. 2, 2003, pp. 1620 – 1626.

Design and control of Pneumatic Artificial Muscle actuators for fatigue testing

Kristel Deckers, Patrick Guillaume and Dirk Lefeber

Department of Mechanical Engineering, Vrije Universiteit Brussel, Pleinlaan 2 1050 Brussel, Belgium
kristel.deckers@vub.ac.be, patrick.guillaume@vub.ac.be and dirk.lefeber@vub.ac.be

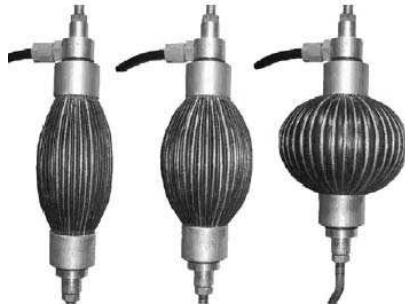


Figure 1: Picture of the PPAM [2].

1 Introduction

Nowadays test rigs, like the ones used for fatigue testing, are often hydraulically driven. The hydraulic supply system operates at high pressures which can cause safety problems when e.g. leaks occur. The maintenance of such systems is often outsourced which leads to high maintenance costs. Moreover, changing the oil and the occurrence of leaks strains the environment.

Possible alternatives to hydraulic actuation may be delivered by the Pleated Pneumatic Artificial Muscles (PPAM), developed by the Robotics and Multibody Mechanics research department at the Vrije Universiteit Brussel or the pneumatic muscles of Festo.

2 Pneumatic Muscles

Pneumatic muscles have some interesting advantages like e.g. a high force weight ratio, a low pressure operation which delivers fairly high forces and a more environment-friendly usage than the hydraulic systems. Because these muscles operate at low pressures and in the presence of leaks, they are safe. The most important disadvantage of the muscles is the non-linear link between the pressure in the muscle and the resulting force applied by the muscle (Figure 2).

3 Control of the muscles

Since we want to use the muscles in fatigue testing, the input signals will be applied iteratively. This implies the use of an adaptive controller which adapts the input signal of

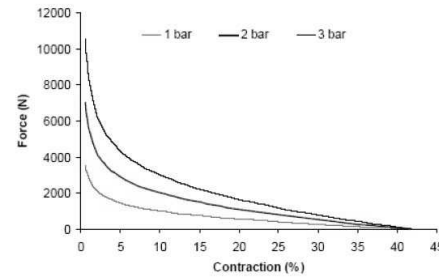


Figure 2: Pulling force versus contraction of a PPAM [2].

the current iteration according to the output of the previous one.

Using Iterative Learning Control (ICL) and more specifically Time Waveform Replication (TWR), a feedforward control that tracks a specific reference is created. The advantage of this type of control is that the information from the previous iterations is used to eliminate the influence of repeating disturbances in advance [3]. This offers a lot of possibilities to increase the bandwidth of the proposed actuators [4].

Furthermore the Time Waveform Replication algorithm will be adapted to continuously estimate the systems behavior and update the system model at each iteration. The goal of the project is to develop the adapted algorithm using a specific case-study: the fatigue testing of slat tracks.

References

- [1] F. Daerden, Conception and realization of pleated pneumatic artificial muscles and their use as compliant actuation elements, PhD Thesis, Vrije Universiteit Brussel, July 1999
- [2] B. Verrelst, A dynamic walking biped actuated by pleated pneumatic artificial muscles: Basic concepts and control issues, PhD Thesis, Vrije Universiteit Brussel, February 2005
- [3] D.A. Bristow, M. Tharayil, A.G. Alleyne, A survey of iterative learning control: A learning-based method for high-performance tracking control, IEEE Control Systems Magazine, June 2006
- [4] J. De Cuyper, Linear feedback control for durability test rigs in the automotive industry, PhD Thesis, K.U. Leuven, 2006

Proxy-Based Sliding Mode Control of a 2-DOF Pneumatic Manipulator

M. Van Damme, B. Vanderborght, R. Van Ham, F. Daerden, D. Lefeber
 Robotics and Multibody Mechanics Research Group
 Department of Mechanical Engineering
 Vrije Universiteit Brussel
 michael.vandamme@vub.ac.be

1 Introduction

In [1], Kikuwe and Fujimoto have introduced Proxy-Based Sliding Mode Control. It combines responsive and accurate tracking during normal operation with smooth, slow recovery from large position errors that can sometimes occur after abnormal events. The method can be seen as an extension to both conventional PID control and sliding mode control.

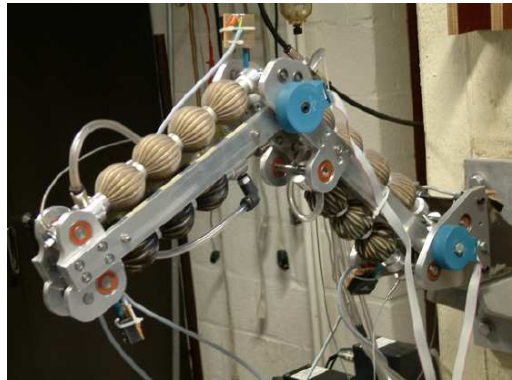


Figure 1: 2-DOF planar manipulator actuated bij Pleated Pneumatic Artificial Muscles.

Here Proxy-Based Sliding Mode Control is used to control a 2-DOF planar manipulator actuated by Pleated Pneumatic Artificial Muscles (PPAMs, [2]), shown in figure 1. The principal advantage of this control method is increased safety for people interacting with the manipulator.

2 Proxy-Based Sliding Mode Control

The basic idea behind Proxy-Based Sliding Mode Control for robotics is to attach an imaginary, virtual object, called proxy, to the robot's end effector by means of an imaginary, somewhat spring-like virtual coupling. This is illustrated in figure 2 for a 2-DOF robot in the horizontal plane.

The proxy's trajectory is controlled by a sliding mode controller which exerts the force F_a . Depending on their relative positions, the PID-type virtual coupling will cause an interaction force F_c between end effector and proxy.

The (statical) torques that would be produced in the robot

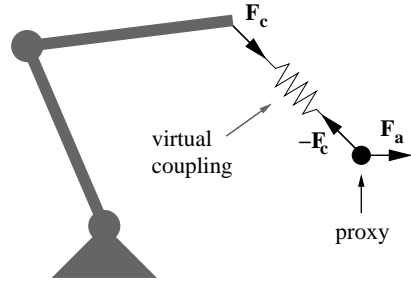


Figure 2: Idea behind Proxy-Based Sliding Mode Control.

joints if F_c were physically present are given by the well-known relation

$$\tau = J^T F_c$$

(with J the the robot's Jacobian matrix). Actually applying these torques will cause the end effector's position to be servo-controlled to follow the proxy's position. By limiting the maximum value of F_a , the controller behaves as a PID controller for small errors, while exhibiting safe, smooth sliding-mode based recovery from large positional errors. The disadvantage of limiting F_a is that it also limits the maximum disturbance force that can be tolerated.

Using a discrete-time approach, Kikuwe and Fujimoto [1] have devised a chattering-free controller based on this idea.

Both the original and a modified version of this Proxy-Based Sliding Mode Controller were implemented and tested on the system, and their performance was experimentally evaluated. Both forms performed very well with respect to safety. Good tracking was also obtained, especially with the modified version.

References

- [1] Ryo Kikuwe and Hideo Fujimoto, *Proxy-Based Sliding Mode Control For Accurate and Safe Position Control*, Proceedings of the 2006 IEEE International Conference on Robotics and Automation, pp 25-30, 2006 (Orlando, USA)
- [2] F. Daerden and D. Lefeber, *The concept and design of pleated pneumatic artificial muscles*, International Journal of Fluid Power, 2(3):41-50, 2001

Long-Stroke Six Degree of Freedom Planar Actuator Topology

C.M.M. van Lierop, J.W. Jansen, A.A.H. Damen, P.P.J. van den Bosch

Department of Electrical Engineering¹

Eindhoven University of Technology

P.O.Box 513

5600 MB Eindhoven

The Netherlands

Email: c.m.m.v.lierop@tue.nl

1 Introduction

In recent years, magnetically levitated planar actuators have been developed as an alternative to xy -drives constructed of stacked linear actuators. Although the translator of these actuators can only move over relatively large distances in the xy -plane, it has to be controlled in six degrees-of-freedom (DOF) because of the active magnetic bearing. These actuators have either moving coils and stationary magnets [1] or moving magnets and stationary coils [2] [3]. The coils in the actuator are simultaneously used for propulsion in the xy -plane as well as for the 4-DOF active magnetic bearing.

2 Contribution

To integrate long-stroke propulsion and active magnetic bearing of a moving-magnet actuator, new design and control methods have been developed [4] [5] [6]. The new methods directly decouple the force and torque. The decoupling can be achieved using either Lagrange multipliers [6] or weighted 2-norm optimization [4]. Moreover, there are similarities with the dq0-transformation which allow for a structured design of the planar actuator with respect to the controllability and power consumption.

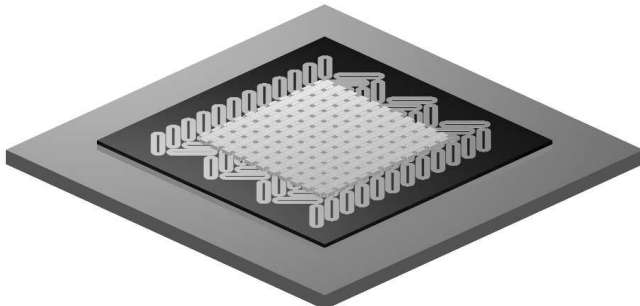


Figure 1: new 6-DOF planar actuator topology.

3 Results

The controllability and the power consumption of various planar actuator topologies have been investigated using the theory derived in [4]. Fig. 1 shows an actuator topology which is currently being manufactured at the Eindhoven University of Technology. The coils are spaced according to a three-phase system and they are placed in a herringbone structure. Each coil is individually controlled using 84 amplifiers. During the presentation theoretical and practical results will be compared.

References

- [1] J.C. Compter, "Electro-dynamic planar motor," *Precision Engineering*, vol. 28, no. 2, pp. 171-180, Apr 2004.
- [2] J.C. Compter, P.C.M. Frissen, and J. van Eijk, "Displacement device," WO patent application 2006/075291 A2, publ. date July 20, 2006
- [3] A.J. Hazelton, M.B. Binnard, and J.M. Gery, "Electric motors and positioning devices having moving magnet arrays and six degrees of freedom," US patent 6,208,045, March 27, 2001
- [4] C.M.M. van Lierop, J.W. Jansen, A.A.H. Damen, P.P.J. van den Bosch, "Control of Multi-degree-of-freedom planar actuators," in *Proc. of the 2006 IEEE International Conference on Control Applications (CCA)*, Munich, Germany, pp 2516-2521, 4-6 October 2006.
- [5] C.M.M. van Lierop, J.W. Jansen, A.A.H. Damen, E.A. Lomonova, P.P.J. van den Bosch, A.J.A. Vandenput, "Model based commutation of a long-stroke magnetically levitated linear actuator," *Conference record of the 2006 IEEE Industry Applications Conference 41st Annual Meeting*, Tampa, Florida, 8-12 October 2006.
- [6] W. Potze, and P.C.M. Frissen, "Method for controlling an electric motor, control unit and electric motor," WO patent application 2006/054243 A2, publ. date May 26, 2006

¹This IOP-EMVT project is funded by SenterNovem. SenterNovem is an agency of the Dutch Ministry of Economical Affairs.

Vibration reduction using dynamic absorbers

Frits Petit and Mia Loccufier
 SYSTeMS Research Group, Ghent University
 Frits.Petit@ugent.be

1 Introduction

Reducing vibrations is an important objective encountered in many areas of engineering. A technique frequently used (easy to attach and not expensive) is the local addition of a dynamic absorber to the main system. Basically the absorber consists of an inertia (m_h) connected to the structure with a spring (k_h) and a damper (c_h) (Fig. 1). The founders

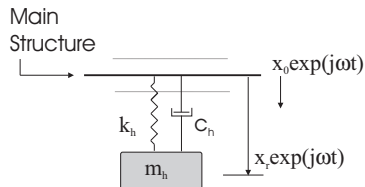


Figure 1: Basic dynamic absorber.

of this technique are Frahm [1] and Den Hartog [2]. The main structure is represented as a lumped parameter model (linear and undamped) consisting of mass and spring elements. The equations of motion of the main structure become:

$$M\ddot{q} + Kq = F \quad (1)$$

with $M = M' \in R^{m \times m}$ the mass matrix, $K = K' \in R^{m \times m}$ the stiffness matrix, $F \in R^m$ the excitation force and $q \in R^m$ the coordinate vector representing m degrees of freedom. We consider resonance conditions, i.e. the excitation is harmonic and its frequency (ω_a) equals one of the eigenfrequencies (ω_i) of the structure. As a result high vibration amplitudes will almost certainly damage the structure.

To avoid this resonance phenomenon the eigenfrequency of the absorber is tuned to the excitation frequency ω_a : $\sqrt{\frac{k_h}{m_h}} = \omega_a = \omega_i$. The effect of attaching an undamped dynamic absorber can be seen in figure 2. Taken into account model mismatch and changes in the excitation frequency, a robust design requires effectiveness over a wider frequency band. Therefore, replacing the simple dynamic absorber by more complex absorbers (e.g. adding nonlinearities) will be analyzed. This requires a perfect understanding of the simple dynamic absorber.

2 Problems with the classical absorber

A lot of design methods are available to derive the optimal stiffness k_h and damping c_h in function of the mass m_h of the dynamic absorber [3]. However they do not justify the value of the mass, nor the location of the absorber. Here we

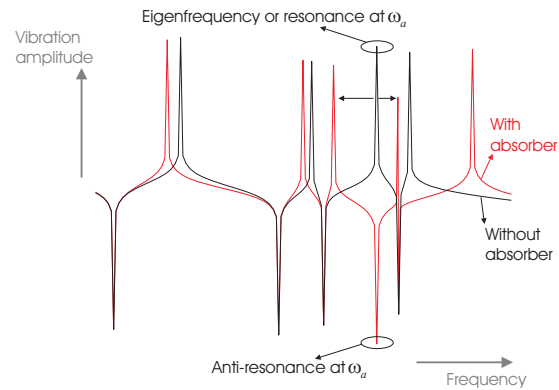


Figure 2: Attaching a dynamic absorber introduces a shift of the eigenfrequencies together with an anti-resonance (high vibration reduction) at frequency ω_a .

analyze both choices as they will be vital to design the more complex absorbers. To achieve vibration reduction over a wide frequency band, we try to maximize the shift of the eigenfrequencies near ω_a (Figure 2) using an undamped dynamic absorber.

3 Results

Combining simulation results with a mathematical approach yields an interesting theorem. We prove that the eigenfrequencies cannot shift further than the neighboring anti-resonances. These anti-resonances are different for each location, such that an optimal location for the absorber can be derived. Further more, we analyze the dependence of the amount of shift of the eigenfrequencies on the absolute value of the absorber mass. Combining both will optimize the absorber design with respect to relocating eigenfrequencies and clear the way for the analysis of more complex absorbers.

References

- [1] H. Frahm *Device for Damping Vibrations of Bodies*, U.S. Patent 989,958 (1911).
- [2] J.P. Den Hartog *Mechanical Vibrations*, McGraw-Hill, New York (1956).
- [3] M.B. Ozer and T.J. Royston *Extending Den Hartog's Vibration Absorber Technique to Multi-Degree-Of-Freedom Systems*, Journal of Vibration and Acoustics, Vol.127/341-350 (2005).

Observer design for real-time controlled restraint systems

Ewout van der Laan

Email: e.p.v.d.laan@tue.nl

Technische Universiteit Eindhoven, The Netherlands

1 Motivation

In the field of automotive engineering, restraint systems refer to the safety devices in a vehicle that assist in restraining the occupant during a crash. The design and development of these safety devices is largely oriented at car occupants of average height and weight and at a set of standardized and legislated (high speed) crashes. Since restraint systems in general are not able to adjust their performance characteristics during a crash event, an occupant will not be optimally protected in every crash scenario. A huge step in injury reduction will be made when the restraint systems can continuously be manipulated as a function of measured signals. This kind of systems is not yet available for today's passenger vehicles, but simulation results with a controlled seat-belt and airbag show a significant injury reduction [1]. Therefore, this class of systems is a main focus of current state-of-the-art restraint system development [2].

2 Problem definition

There is a number of issues that need to be solved before the next generation passenger vehicles can be equipped with a controlled restraint system. Important problems concern (i) the required restraint actuators, (ii) the sensors to determine the injury measures, (iii) the development of control algorithms and (iv) pre-crash information on the upcoming crash, since this sets the performance criteria. These implementation issues are sketched in Fig. 1. In this paper, the main focus is on injury measures, e.g. chest acceleration and chest deflection. Not all of the required sensors to measure the occupant's movement do yet exist, whereas many of the available sensors are too expensive, too inaccurate or have too low a bandwidth. So automotive safety engineering will largely benefit from alternative techniques in spatial occupant sensing.

3 Project aim

It is proposed here that filtering of one or more observable signals offers the possibility to estimate the injury measures. A typical restraint control algorithm aims at lowering the chest acceleration a_{chest} . However, sensors to obtain a_{chest} are not yet implementable. It is therefore investigated whether measurement of the belt displacement x_{belt} at the belt outlet can be used to estimate a_{chest} by means of an observer.

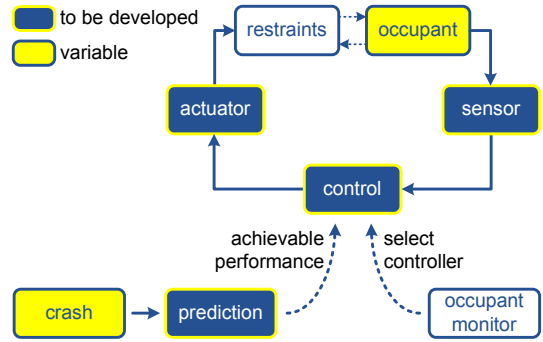


Figure 1: Principle of controlled restraint systems

4 Approach

In the observer design, a low order input-state-output model has to be constructed of the occupant and restraints. This has led to an approach that is referred to as *multi-fidelity modeling*. Accurate and hence complex, high order models are employed to derive less complex models, dedicated to the scope of the control problem. Subsequently, these models are transformed to linear (time-invariant) models which have the lowest fidelity. With these latter models, observer and control algorithms are developed.

5 Results

A low order multi-body model is constructed, based on a complex, high order model with 37 bodies. It represents the dummy, confined by a seat, the vehicle interior and a belt system. Although the low order model consists of only 9 bodies, it is able to accurately map the belt force to the chest acceleration and belt displacement in a standard crash scenario. The observer is derived from a linearization of the low order model. Simulation results show that this observer may be a useful alternative to direct sensor methods for spatial occupant sensing. The estimation accuracy however will always be limited by the low order model accuracy.

References

- [1] R. J. Hesseling. *Active restraint systems; feedback control of occupant motion*. PhD thesis, TU Eindhoven, 2004.
- [2] J.S.H.M. Wismans. State-of-the-art report: Smart restraint systems. Task 5 report, European Vehicle Passive Safety Network, January 2003.

Robust low-complexity controller design applied to integrated clutch control

Gerrit Naus, René van de Molengraft

Department of Mechanical Engineering, Control Systems Technology group,

Technische Universiteit Eindhoven, Eindhoven, The Netherlands

g.j.l.naus@tue.nl, m.j.g.v.d.molengraft@tue.nl

Rudolf Huisman

Product Development, Technical Analysis Group,

DAF Trucks N.V., Eindhoven, The Netherlands

rudolf.huisman@daftrucks.com

1 Introduction

Control systems in the automotive industry become increasingly complex due to the rising amount of electronic and software components. The corresponding performance improvements and extra features are often realized by specialized suppliers. This has led to systems that are more or less black boxes to the Original Equipment Manufacturers (OEMs). Today, the automotive industry exploits the potential benefits of integrated control strategies combining functionality of several systems. The OEMs are challenged with the integration of all subsystems, leading to significantly increased tuning effort [1]. The Automated Manual Transmission (AMT) incorporating the clutch control system is a typical example of a system OEMs buy from specialized suppliers.

2 Integrated Clutch Control

This paper presents the first results of a model-based, robust low-complexity design technique, applied to the controller for the clutch engagement process of an AMT clutch system (see Figure 1).

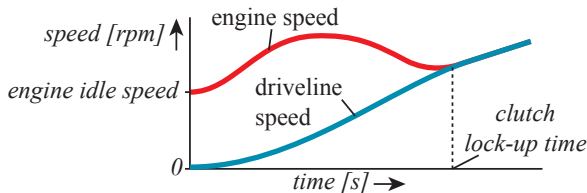


Figure 1: Illustrative example of the clutch engagement process from standstill.

Focus lies on the integration of engine and clutch control. In a general integrated automotive control system, this is indicated by the upper control level (see Figure 2). Currently, both control systems are developed and tuned separately. However, they both influence the engagement process, and the performance of the engagement process may thus be improved by an integrated controller design. Literature already shows the potential benefits of an integrated

clutch engagement control design. The Integrated Clutch Control (ICC) strategy developed in this work provides improved coordination between the Engine Management System (EMS) and the AMT control system. Aiming firstly at damping and minimizing induction of undesired driveline oscillations, comfort is increased by robust adaptation to changing situations, e.g. road slope and vehicle configuration.

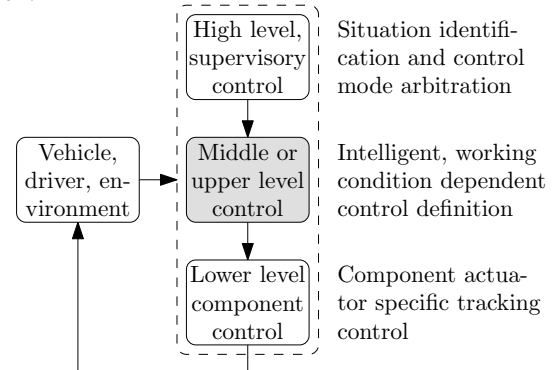


Figure 2: General representation of integrated automotive control systems.

3 Future research

The adopted approach has the potential of resolving tuning problems OEMs currently have when integrating systems. Research will target at the development of methods for robust low-complexity controller design such as presented here, and algorithms and software tools for automatic tuning of controller parameters. Focus lies on integrated control systems in the field of commercial vehicles. Within this framework, several case studies will be executed, e.g. the design and tuning of an Adaptive Cruise Controller (ACC) in cooperation with TNO Automotive, Helmond, The Netherlands.

References

[1] Richter, K. and Ernst, R. (2006), 'How OEMs and suppliers can face the network integration challenges', *EDAA06*

Symmetric Non-negative Matrix Factorization

Ngoc-Diep Ho, Paul Van Dooren
 Department of Applied Mathematics
 Universit catholique de Louvain
 Avenue G. Lemaître, 4
 B-1348 Louvain-la-Neuve, Belgium
 Email: {ho, vdooren}@inma.ucl.ac.be

1 Introduction

The Non-negative Matrix Factorization problem is to find a low-rank approximation with non-negativity conditions imposed on the factors (i.e. $A \approx \sum_{i=1}^k u_i v_i^T$, $u_i, v_i \geq 0$) and can be stated as follows:

NNMF: *Given a non-negative matrix $A_{m \times n}$, find two non-negative matrices $U_{m \times p}$ and $V_{n \times p}$ that minimize $\|A - UV^T\|_2^2$, where $p \ll m, n$.*

For this problem, an iterative method was introduced in [3] using the following multiplicative rules:

$$V \leftarrow V \circ \frac{[U^T A]}{[U^T U V]}, \quad U \leftarrow U \circ \frac{[A V^T]}{[U V V^T]}. \quad (1)$$

This method and its variations for the NMF problem has been extensively used in many fields, including image representation and recognition, document clustering, etc.

In some applications, the input matrix A is found to be symmetric, for example the adjacency matrix of a graph [2] and the correlation matrix used in finance [4]. In those application, it is required that the approximation is symmetric and that the two factors are equal (i.e. $A \approx UU^T$).

When the non-negativity constraint is not applied to the factors, one can find the optimal solution with the Singular Value Decomposition (SVD). But when it is, the problem becomes the Symmetric Non-negative Matrix Factorization (SNMF).

In fact, non-negative matrices that can be written as UU^T ($U \geq 0$) are *Completely Positive* (*cp*) matrices [1]. Hence, the SNMF can be restated as: *finding a rank p cp-matrix that approximates the input symmetric matrix A* .

One also can find in [1] that the smallest number of columns of $U \geq 0$ such that $A = UU^T$ is called the *completely positive rank* (*cp-rank*) of A . And there is no simple algorithm known yet to answer the following questions: *Is a given matrix completely positive?* and *What is the cp-rank of a given matrix?*

Therefore, it is not realistic to solve the true SNNMF problem but one needs to consider a relaxed version of it. Our

approach is to use the NNMF problem to produce acceptable results for the SNNMF problem.

2 Contributions

We will briefly report variations of the mentioned algorithm to deal with the Symmetric Non-negative Matrix Factorization problem and its use in the applications of Graph Clustering [2] and Risk Modelling [4].

Acknowledgements

This paper presents research supported by the Concerted Research Action (ARC) "Large Graphs and Networks" of the French Community of Belgium, and by the Belgian Programme on Inter-university Poles of Attraction, initiated by the Belgian State, Prime Minister's Office for Science, Technology and Culture. The scientific responsibility rests with the authors.

A research fellowship from FRIA is also gratefully acknowledged by the second author Ngoc-Diep Ho.

References

- [1] A. BERMAN AND N. SHAKED-MONDERER, *Completely Positive Matrices*, World Scientific Publishing Co., New Jersey, 2003.
- [2] V. BLONDEL, N. D. HO AND P. VAN DOOREN, *Non-negative Matrix Factorization - Extensions and Applications*, Internal report 005-35, Cesame, Universit catholique de Louvain, 2005.
- [3] D. D. Lee and H. S. Seung (1999). Learning the parts of objects by nonnegative matrix factorization. *Nature*, 401, 788-791.
- [4] A. VANDENDORPE, N.D. HO, S. VANDUFFEL AND P. VAN DOOREN, *The Parameterization of the CreditRisk⁺ Model for estimating Credit Portfolio Risk*. In preparation, 2006.

Maximizing PageRank via outlinks

Cristobald de Kerchove, Laure Ninove and Paul Van Dooren

Dpt. of Applied Math. Univ. cath. of Louvain

dekerchove, ninove, vandooren@inma.ucl.ac.be

1 Motivations

Google's well-known PageRank, introduced by Page and Brin in [1], classifies the pages of the World Wide Web by allocating a score to each of them. A page with a high PageRank will appear among the first items in the list of pages corresponding to a particular query. No surprise then that one normally wishes to maximize its own PageRank [2, 3, 4]. However, the only control the user has on its own page or site is the outlinks pointing to some external pages. Modifying these outlinks leads to perturbations in the PageRank and therefore one wants to study the sensitivity of the PageRank [5, 6, 7]. Ipse-Wills [7] report that new inlinks to some page u always increase the PageRank of u , but that adding new outlinks from u does not necessarily decrease its PageRank. Sydow [8] shows via some simulations that well chosen outlinks may increase ones own PageRank. All this motivates the question of finding an optimal linkage strategies for one or several pages.

2 PageRank Equations

Let $\mathcal{G} = (\mathcal{N}, \mathcal{E})$ be a directed webgraph, with a set of nodes $\mathcal{N} = \{1, 2, \dots, n\}$. From [5], the adjacency matrix A of \mathcal{G} has no zero row and a zero diagonal. Let $P = D^{-1}A$ be the stochastic $n \times n$ matrix which is obtained by scaling the adjacency matrix A with the inverse of the diagonal matrix D of outdegrees of all nodes. Let also $c \in [0, 1]$ be a *damping factor*, and z be a stochastic *personalization vector*, i.e. $z^T 1 = 1$. The *Google matrix* G is then defined as $G = cP + (1 - c)1z^T$, where 1 denotes the vector of all ones, its dimension usually follows from the context. We suppose that G is irreducible, which is the case as soon as A is irreducible, or $c < 1$ and $z > 0$. The *PageRank vector* π is then defined by

$$\pi^T G = \pi^T, \quad \pi^T 1 = 1, \quad (1)$$

and is usually interpreted as the stationary distribution of a random surfer using hyperlinks between pages with a probability c and jumping to some new page according to the personalization vector with a probability $(1 - c)$.

3 Optimal outlink structure

We are interested in how a set \mathcal{I} of given pages can modify their PageRank by changing their outlink structure. We consider two cases: first, a single page wants to maximize its PageRank, and second, a set of $n_{\mathcal{I}}$ pages wants to maximize the sum of the PageRanks of its pages. In these two

cases, the only variables are the links from \mathcal{I} to the rest of the graph.

We make the assumption that there exists at least one outlink from the considered set of pages \mathcal{I} to the rest of the graph. Otherwise Google could penalize that set of pages in the context of detecting spam alliances [3].

The adjacency matrix A of the webgraph can therefore be written as

$$A = \begin{pmatrix} A_{\mathcal{I}} & A_{\text{out}(\mathcal{I})} \\ A_{\text{in}(\mathcal{I})} & A_{\bar{\mathcal{I}}} \end{pmatrix},$$

where $A_{\mathcal{I}}$, $A_{\text{in}(\mathcal{I})}$ and $A_{\bar{\mathcal{I}}}$ are given, and $A_{\text{out}(\mathcal{I})} \in \{0, 1\}^{n_{\mathcal{I}} \times n_{\bar{\mathcal{I}}}}$, $A_{\text{out}(\mathcal{I})} \neq 0$ has to be determined.

We prove that in any case, the optimal linkage strategy is reached when the set of pages \mathcal{I} points to one page not in \mathcal{I} via one outlink, i.e. $A_{\text{out}(\mathcal{I})}$ has one non-zero entry.

References

- [1] L. PAGE AND S. BRIN AND R. MOTWANI AND T. WINOGRAD, *The PageRank Citation Ranking: Bringing Order to the Web*, Stanford Digital Library Technologies Project, 1998.
- [2] K. AVRACHENKOV AND N. LITVAK, *The effect of new links on Google pagerank*, Sto. Models vol 22, 319–331, 2006.
- [3] Z. GYONGYI AND H. GARCIA-MOLINA, *Link spam alliances*, VLDB '05: Proc. of the 31st int. conf. on Very large data bases, 2005.
- [4] R. BAEZA-YATES AND C. CASTILLO ET AL., *PageRank Increase under Different Collusion Topologies*, Proc. of the 1st Int. Workshop on Adversarial Information Retrieval on the Web, 2005.
- [5] M. BIANCHINI AND M. GORI AND F. SCARSELLI, *Inside PageRank*, ACM Trans. Inter. Tech. vol 5, 92–128, 2005.
- [6] A. N. LANGVILLE AND C. D. MEYER, *Deeper inside PageRank*, Internet Math. vol 1, 335–380, 2004.
- [7] I. C. F. IPSE AND R. S. WILLS, *Mathematical Properties and Analysis of Google's PageRank*, Bol. Soc. Esp. Mat. Apl. vol 34, 191–196, 2006.
- [8] M. SYDOW, *Can One Out-Link Change Your PageRank?*, Lecture Notes in Computer Science vol 3528, 408–414, 2005.

Optimization of the RADICAL contrast for ICA

M. Journée*, P.-A. Absil[†] and R. Sepulchre*

*University of Liège, Department of Electrical Engineering and Computer Science, Belgium

[†]Université Catholique de Louvain, Department of Mathematical Engineering, Belgium

Abstract

This paper indicates that Independent Component Analysis (ICA) fits perfectly within the framework of optimization over matrix manifolds [1]. All optimization algorithms resulting from that theory can be particularized to ICA, such that a whole range of new methods is available.

1 Introduction

Each ICA algorithm consists in the optimization of a particular contrast on a matrix space [2]. The contrast is a statistically motivated function that measures the statistical independence between some random variables. The diagonality of the cumulant tensor, the joint diagonality of a set of matrices, the constraint covariance and the mutual information are typical examples.

Let γ be a such contrast function, so that $\gamma(W)$ expresses the quality of the demixing matrix W . This function is defined for a matrix W of the matrix manifold \mathcal{M} . Since the independent nature of random variables is neither altered by a scaling nor by a permutation of these variables, the contrast presents some inherent symmetries. Optimizing functions with symmetries is usually awkward unless some constraints are introduced. In case of ICA, the matrix W is usually assumed to be orthogonal, i.e., $W^T W = I$. Two options are conceivable to deal with such constraints. First is to perform constrained optimization over a Euclidean space, i.e.,

$$\min_{W \in \mathbb{R}^{n \times n}} \gamma(W) \quad \text{s.t.} \quad W^T W = I,$$

where a square problem of dimension n is assumed. This paper favors the second alternative which incorporates the constraints directly into the search space and performs unconstrained optimization over a nonlinear matrix manifold, i.e.,

$$\min_{W \in \mathcal{M}} \gamma(W) \quad \text{with} \quad \mathcal{M} = \{W \in \mathbb{R}^{n \times n} \mid W^T W = I\}.$$

Most classical unconstrained optimization methods have been generalized to the optimization over matrix manifolds. This is in particular the case of the gradient-descent, Newton, trust-region and conjugate gradient methods [1].

2 Optimization of the RADICAL contrast

The mutual information is a straightforward mean to characterize statistical independence. It is nevertheless extremely complex to evaluate. The RADICAL algorithm [3] computes an approximation to the mutual information that is

based on order statistics and spacings. It first decomposes that quantity in a sum of differential entropies,

$$\gamma_{\text{RADICAL}}(W) = \sum_{i=1}^n H_i(W),$$

and then estimates each $H_i(W)$ in an accurate and computationally efficient way as follows,

$$\hat{H}_i(W) = \frac{1}{N-m} \sum_{j=1}^{N-m} \log \left(\frac{N+1}{m} (e_i^T W^T (x^{(k_{j+m})} - x^{(k_j)})) \right),$$

where $x^{(j)}$ denotes the j th column of the observation matrix $X \in \mathbb{R}^{n \times N}$, n is the dimension of the problem, N is the number of samples, e_i is the i th basis vector and m is typically set to \sqrt{N} . The indices k_{j+m} and k_j result from the order statistics. We refer to [3] for more details about this contrast.

In its original implementation, the RADICAL contrast is optimized by means of Jacobi rotations [3]. Only one parameter is varying at each iteration and minimization is accomplished by exhaustive search over that parameter.

In this work, we propose new algorithms for ICA. These are based on the RADICAL contrast but differ on the method that is used to perform the optimization. Once analytical expressions to the gradient and the Hessian of that contrast are established, all the optimization algorithms described in [1] are available. We focus in particular on gradient-descent and trust-region optimizations. Comparisons with the original implementation indicate that the new algorithms require much less computational effort by preserving the strengths of the RADICAL contrast.

References

- [1] P.-A. Absil, R. Mahony, and R. Sepulchre, “Optimization Algorithms on Matrix Manifolds”, Princeton University Press, to appear.
- [2] P. Comon, “Independent component analysis, A new concept?”, *Signal Processing*, vol. 36, 1994.
- [3] E.G. Learned-Miller and J. W. Fisher III, “ICA using spacings estimates of entropy,” *Journal of Machine Learning Research*, vol. 4, pp. 1271–1295, 2003.

Acknowledgments

This work was supported by the Belgian National Fund for Scientific Research (FNRS) through a Research Fellowship at the University of Liège and by Microsoft Research through a Research Fellowship at Peterhouse, Cambridge. This paper presents research results of the Belgian Programme on Interuniversity Attraction Poles, initiated by the Belgian Federal Science Policy Office. The scientific responsibility rests with its authors.

Comparative analysis of genome-scale expression data using a new extension of the singular value decomposition

Xander Warnez
ESAT-SCD
xander.warnez@esat.kuleuven.be

Lieven De Lathauwer
CNRS - Lab. ETIS
delathau@ensea.fr

Bart De Moor
ESAT-SCD
bart.demoor@esat.kuleuven.be

1 General outline

Some years ago the concept of the singular value decomposition (SVD) has been extended towards a simultaneous decomposition of two matrices. This new decomposition was then later on extended towards multiple matrices. These extensions of the (regular) SVD are called generalized singular value decompositions (GSVD). Looking at the enormous success of the SVD over the last few years, it is clear that those generalizations offer a huge amount of potential for the future. Provided with the necessary amount of theoretical founding they can with out a doubt lead to new insights and applications. However, at this time a large piece of the theoretical founding and insight that is needed for the successful application of this technique in fields such as bio-informatics and text mining is missing.

2 The simultaneous SVD

The SVD of a matrix A , $A = U\Sigma V^T$, decomposes the matrix into 2 orthogonal matrices, U and V , and a pseudo-diagonal matrix Σ , consisting of non-negative elements. Several extensions to this concept were already designed. In its most simple form these extensions result into a decomposition of two matrices with one common dimension, $A(m \times n)$ and $B(p \times n)$, called the quotient-SVD (QSVD): $A = U_A S_A Q$, $B = U_B S_B Q$. Both matrices U_A and U_B are orthogonal, both matrices S_A and S_B are quasi-diagonal, and the matrix Q is a regular matrix, common to both decompositions. A similar decomposition exists for the production of two matrices, called the product-SVD (PSVD): $A = U_A S_A P^{-1}$, $B = U_B S_B P$.

This concept has been further extended to multiple matrices, where a cross-wise equality in matrix dimensions is required. These generalizations of the SVD, i.e. the GSVD, are in fact a subclass of a broad family of matrix decompositions, called the simultaneous matrix decompositions. A well known subclass of this family of simultaneous matrix decompositions, simultaneous decompositions for matrices of equal dimensions, is commonly used in the field of signal processing for what is called blind source separation algorithms.

This concept of simultaneous matrix decompositions is a powerful tool: by calculating a simultaneous decomposition of the data matrices a common structure is enforced upon those matrices, revealing the shared characteristics of the

underlying data.

We will extend the SVD to a subclass of those simultaneous matrix decompositions, but unlike the GSVD, the matrices will all have the same dimension in common. In its simplest form this results into a QSVD. More generally, the decomposition for multiple matrices $A_1(n_1 \times m), A_2(n_2 \times m), \dots, A_k(n_k \times m)$, this yields: $A_1 = U_1 D_1 M^T, A_2 = U_2 D_2 M^T, \dots, A_k = U_k D_k M^T$, where the matrices U_i are orthogonal, matrices D_i quasi-diagonal, and the matrix M^T is common for all decompositions. This new extension to the SVD is called the simultaneous SVD (SSVD). The new decomposition has the major advantage that the problem becomes overdetermined, which allows us to compute the results in a least squares sense, leading to a stable solution.

3 Comparative analysis of genome-scale expression data

The use of the SVD and the GSVD in the field of bio-informatics to deal with data-integration has only been recently studied by O. Alter et al. [1, 2]. Her research shows the great potential of these techniques in the bio-informatics division for e.g. the analysis of genome-scale expression data. We will extend this research, that has been applied to one and two organisms, towards multiple organisms using the newly developed extension to the SVD, the SSVD (see figure 1).

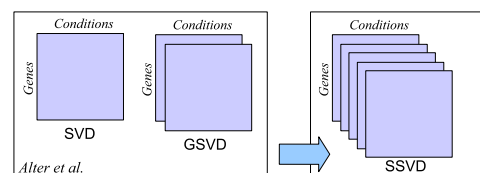


Figure 1: Extension of the research of Alter et al. to multiple organisms using the SSVD.

References

- [1] O. Alter, P. O. Brown, and D. Botstein - Singular value decomposition for genome-wide expression data processing and modeling.
- [2] O. Alter, P. O. Brown, and D. Botstein - Generalized singular value decomposition for comparative analysis of genome-scale expression data sets of two different organisms.

Phase feedback in MEMS resonators

R. M. C. Mestrom*, R. H. B. Fey, H. Nijmeijer

Department of Mechanical Engineering, Eindhoven University of Technology

P.O. Box 513, WH -1.144, 5600 MB, Eindhoven, The Netherlands

Email: *r.m.c.mestrom@tue.nl

1 Introduction

Micro-electromechanical silicon resonators provide an interesting alternative for quartz crystals as accurate timing devices in oscillator circuits for modern data and communication applications [1]. Their compact size, feasibility of integration with IC technology and low cost are major advantages. In oscillator circuits, nonlinearities in resonators influence oscillator performance (e.g. S/N-ratio) (see [2]). MEMS resonators inherently can store less energy than quartz crystals, due to their smaller size. For this reason, they have to be driven into nonlinear regimes. Here, an approach for coping with nonlinearities of MEMS resonators in oscillator circuits will be investigated.

2 Oscillator circuits

An oscillator circuit produces a periodic output signal with a high spectral purity. A schematic representation of an oscillator is depicted in figure 1. Oscillators consist of two

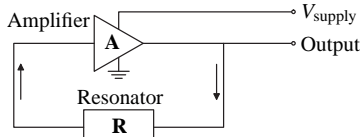


Figure 1: Schematic representation of an oscillator circuit.

essential parts: an active amplifier (or gain circuit) and a resonator, which acts as a passive frequency selective network. The latter determines the frequency and stability of the generated signal. From figure 1, it can be seen that the output of the resonator is fed back into the amplifier. If this happens with the correct amplitude and phase, sustained oscillations may occur.

Two oscillation conditions (for amplitude and phase) for the circuit can be written in terms of the amplifier gain $A = Ae^{j\phi_A}$ and resonator voltage ratio $R = Re^{j\phi_R}$, which are complex functions of the oscillation frequency Ω :

$$AR \geq 1 \quad \text{and} \quad \phi_A + \phi_R = 2n\pi, \quad n = 0, 1, 2, \dots,$$

where A and R denote the amplitude and ϕ_A and ϕ_R denote the phase shift of the amplifier and resonator, respectively.

3 Phase feedback

For a nonlinear oscillator, linear approximations to the amplitude-frequency and phase-frequency curve can be cal-

culated for varying excitation frequencies Ω . These nonlinear equivalents to the bode diagram are depicted in figure 2 in non-dimensional form. It can be seen that both the ampli-

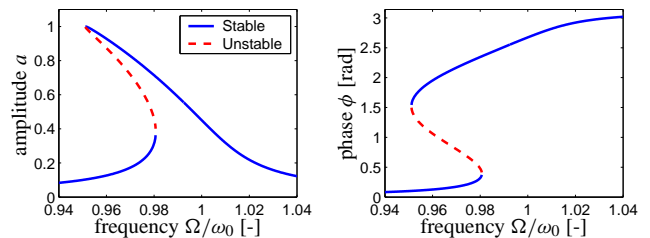


Figure 2: Amplitude-frequency and phase-frequency curve for a nonlinear resonator (linear natural frequency is ω_0).

tude a and the phase ψ are not single-valued functions of the phase. This would normally limit oscillator performance.

A technique to cope with resonator nonlinearities in a feedback circuit is described in [3] and makes use of the fact that frequency is a single-valued function of phase. By means of so-called phase feedback, the amplifier phase is set to $\phi_A = 2\pi - \phi_R$ in order to force the resonator to operate at a frequency that corresponds to a phase shift of ϕ_R .

4 Results

Simulation results show that phase feedback works very well for nonlinear MEMS resonators. On simulation level, closed-loop phase feedback yields an increase in S/N-ratio of several decades compared to open-loop. Furthermore, useful means for selecting optimal operation points for oscillator circuits can be defined. In the near future, the approach will be verified experimentally and the effect of the electrical circuit on the gain in S/N-ratio will be investigated.

References

- [1] C. T.-C. Nguyen, "MEMS Technology for Timing and Frequency Control", *Proc. Joint IEEE Int. Frequency Control/Precision Time & Time Interval Symposium, Vancouver, Canada, Aug. 29–31, pp. 1–11, 2005.*
- [2] V. Kaajakari, T. Mattila, A. Oja, and H. Seppä, "Nonlinear Limits for Single-Crystal Silicon Microresonators", *J. Microelectromechanical Systems*, 13(5):715–724, 2004.
- [3] D. S. Greywall, B. Yurke, P. A. Busch, A. N. Pargellis, R. L. Willett, "Evading Amplifier Noise in Nonlinear Oscillators" *Physical Review Letters*, 72(19):2992–2995, 1994.

Modelling the dynamics of cluster formation

Dirk Aeyels and Filip De Smet

SYSTeMS Research Group, Dept. of Electrical Energy, Systems and Automation,
Ghent University, Technologiepark-Zwijnaarde 914, 9052 Zwijnaarde, Belgium.
E-mail: Dirk.Aeyels@UGent.be, Filip.DeSmet@UGent.be

1 Introduction and motivation

The clustering phenomenon is observed in fields ranging from the exact sciences to social and life sciences; consider e.g. swarm behavior of animals or social insects, opinion formation or the clusters in the frequency space for synchronized coupled oscillators as a model for heart cells. We present a model that captures this phenomenon and at the same time allows a mathematical analysis. We also describe some applications.

2 The dynamics

The differential equations for the model consisting of N agents ($N > 1$) are

$$\dot{x}_i(t) = b_i + \frac{1}{N} \sum_{j=1}^N f(x_j(t) - x_i(t)), \quad (1)$$

$\forall t \in \mathbb{R}, \forall i \in \{1, \dots, N\}$. The function $f : \mathbb{R} \rightarrow \mathbb{R}$ is Lipschitz continuous, odd, non-decreasing and attains a saturation value: $\exists d > 0 : f(x) = F, \forall x \geq d$.

For convenience we will restrict to the model (1), but an extension to more general interaction structures is possible [1].

3 Analysis and results

Assume that, for a particular solution of (1), the behavior of the agents can be characterized as follows by an ordered set of *clusters* (G_1, \dots, G_M) defining a partition of $\{1, \dots, N\}$:

- The distances between agents in the same cluster remain bounded (i.e. $|x_i(t) - x_j(t)|$ is bounded for all $i, j \in G_k$, for any $k \in \{1, \dots, M\}$, for $t \geq 0$).
- After some positive time T , the distances between agents in different clusters are at least d and grow unbounded with time.
- The agents are ordered by their membership to a cluster: $k < l \Rightarrow x_i(t) < x_j(t), \forall i \in G_k, \forall j \in G_l, \forall t \geq T$.

We will refer to this behavior as *clustering behavior*.

In [1] we derive a set of *necessary and sufficient* conditions for clustering behavior of *all* solutions of the system (1),

with the cluster structure (G_1, \dots, G_M) independent of the initial condition. We also show that for every given set of parameters b_i and F there exists a *unique* ordered partition (G_1, \dots, G_M) of clusters satisfying these conditions. In general there exist $N - 1$ *bifurcation* values for the intensity of attraction F , defining N intervals for F ; each interval corresponds to a particular cluster configuration, and transitions to new cluster configurations take place at these bifurcation points.

4 Applications

4.1 The Kuramoto model

The Kuramoto model [2] is a mathematical model describing systems of coupled oscillators, which also exhibits clustering behavior. Simulations indicate that the clustering behavior is independent of the initial condition, as in the model (1), and also the transitions between the different clusters for varying coupling strength are similar.

4.2 Compartmental systems

Consider N different basins connected by horizontal pipes, each basin furthermore subject to either a constant external inflow or outflow of water, with the total inflow equal to the total outflow. Assuming that the pipes have a maximal throughput, the system is described by an extended version of the model (1). The objective is to prevent the existence of multiple clusters, since otherwise there would be at least one cluster of basins flooding and at least one cluster of basins running empty.

Acknowledgments

This paper presents research results of the Belgian Programme on Interuniversity Attraction Poles, initiated by the Belgian Federal Science Policy Office. The scientific responsibility rests with its authors.

Filip De Smet is a Research Assistant of the Research Foundation - Flanders (FWO - Vlaanderen).

References

- [1] D. Aeyels and F. De Smet. Clustering in a network of non-identical and attractive agents. In preparation, 2006.
- [2] Y. Kuramoto. Cooperative dynamics of oscillator community. *Prog. Theoret. Phys. Suppl.*, 79:223–240, 1984.

Rigid body attitude synchronization: a consensus approach

A.Sarlette

University of Liège

alain.sarlette@ulg.ac.be

R.Sepulchre

University of Liège

r.sepulchre@ulg.ac.be

N.Leonard

Princeton University

naomi@princeton.edu

1 Context

The distributed synchronization of a set of agents - *i.e.* driving all the agents to a common position and orientation without referring to a leader or external reference - is an ubiquitous task in current engineering problems. Practical applications include autonomous swarm/formation operation, distributed decision making, and many algorithmical problems involving “dynamical average computations”. In a modeling framework, the understanding of swarm behavior has also led to many important studies.

Synchronization is well understood in Euclidean space. However, many interesting applications involve manifolds that are not homeomorphic to an Euclidean space. The most important case is maybe the group $SO(3)$, representing the orientations of 3-dimensional rigid bodies. For example, several modern space mission concepts involve the use of multiple satellites flying in formation. Many interesting studies are devoted to *position* synchronization in \mathbb{R}^3 , but *attitude* synchronization in $SO(3)$ is less understood.

In [1], we study the problem of decentralized consensus in a swarm of agents evolving on a compact, connected homogeneous manifold. A simple integrator model is assumed for each individual agent. Restricted inter-agent communication links are represented by the edges of a graph. For undirected, time-invariant and (hence inevitably) connected communication graphs, we define a cost function P whose global maximum occurs at synchronization. We derive gradient control laws that only use relative positions available through the communication links and asymptotically stabilize the synchronized state. For directed and time-varying communication graphs, we introduce auxiliary variables that communicating agents exchange as sets of scalars. Almost-global asymptotic synchronization is achieved whenever the communication graphs are uniformly connected.

2 Contributions

In the present paper, we specialize the study of [1] to the manifold $SO(3)$ characterizing the orientation of identical rigid bodies.

In a first approach, we show how the consensus strategies developed in [1] for simple integrators can be implemented when considering the actual second-order rigid body dynamics (forced Euler equations). We use the kinematic controls of [1] as desired rotation rates. Making the actual rota-

tion rates track the desired ones, we present control torques that drive all the rigid bodies towards a common, constant (or predefinedly rotating) orientation.

In a second approach, inspired by the work of [2], we directly consider the dynamical setting and use the cost function P as an artificial potential in order to stabilize the synchronized state for fixed, undirected communication graphs. The difficulty of this approach is to properly introduce “inter-agent artificial dissipation”, without referring to an external reference or simply slowing down the motion of each individual rigid body. The advantages of this approach are first that the control does not have to counteract the free rigid body motion, and second that proper “inter-agent artificial dissipation” can lead to synchronized states where the rigid bodies are still rotating freely. In particular, any free motion of the synchronized rigid bodies is an equilibrium trajectory for these control laws.

3 Acknowledgments

This paper presents research results of the Belgian Programme on Interuniversity Attraction Poles, initiated by the Belgian Federal Science Policy Office. The scientific responsibility rests with its authors. Alain Sarlette is supported as an FNRS fellow (Belgian Fund for Scientific Research). Most of this work was achieved while he was a Visiting Student Research Collaborator at the MAE department of Princeton University, whose hospitality and intellectually inspiring environment are gratefully acknowledged; financial support for this visit was partly provided through the 1st Odissea prize 2005 initiated by the Belgian Senate.

References

- [1] A. Sarlette and R. Sepulchre. Consensus optimization on manifolds. *Submitted to SICON special issue on Control and Optimization in Cooperative Networks*, 2006.
- [2] S. Nair and N.E. Leonard. Stabilization of a coordinated network of rotating rigid bodies. *Proc. 43rd IEEE Conf. on Decision and Control*, pages 4690–4695, 2004.

Opinion dynamic models: on the $2R$ conjecture.¹

Vincent D. Blondel

Dept of Math. Engineering, UCLouvain
blondel@inma.ucl.ac.be

Julien M. Hendrickx

Dept of Math. Engineering, UCLouvain
hendrickx@inma.ucl.ac.be

John N. Tsitsiklis

Lab. for Information and Decision Systems, Massachusetts Institute of Technology
jnt@mit.edu

Abstract We consider an opinion dynamic model and study its convergence and the properties of the equilibria to which it converges. We attempt to explain why the observed distances between opinions at equilibrium are typically larger than what one could expect, an observation captured in the so-called $2R$ conjecture.

1 Krause opinion dynamic model

We consider a simple dynamical model of agents distributed on the real line. The agents have a limited vision range R and they synchronously update their positions by moving to the average position of the agents that are within their vision range (i.e. those that are separated from them by a distance smaller than or equal to R). This dynamical model was initially introduced in the social science literature as an opinion dynamic model and is known there as the “Krause model” [1].

2 Observations, conjectures and results

The model gives rise to surprising and partly unexplained dynamics. One of the central observations is the $2R$ conjecture: when sufficiently many agents are distributed on the real line and have their position evolve according to the above dynamics, the agents eventually merge into clusters that have inter-cluster distances roughly equal to $2R$ as shown in Figure 1. This observation is supported by extensive numerical evidence and is robust under various modifications of the model. It is easy to see that clusters need to be separated by at least R [2, 3]. On the other hand, the unproved bound $2R$ that is observed in practice can probably only be obtained by taking into account the specifics of the model’s dynamics. We study these dynamics and consider a number of issues related to the $2R$ conjecture that explicitly uses the model dynamic. In particular, we provide bounds for the vision range that lead all agents to merge into only one cluster, we analyze the relations between agents on finite

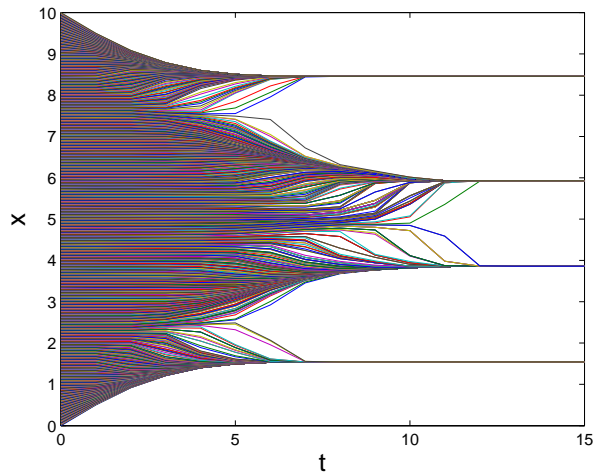


Figure 1: Evolution for 15 time steps of 1000 agent opinions initially equidistantly located on an interval of length 10. The observed inter-cluster distances are much larger than the vision range ($R = 1$) of the agents.

and infinite intervals, and we introduce a notion of equilibrium stability for which clusters of equal weights need to be separated by at least $2R$ to be stable. These results, however, do not prove the conjecture. To understand the system behavior for a large agent density, we also consider a version of the model that involves a continuum of agents. We study properties of this continuous model and of its equilibria, and investigate the connections between the discrete and continuous models.

References

- [1] U. Krause. Soziale dynamiken mit vielen interakteuren. eine problemskizze. In *Modellierung und Simulation von Dynamiken mit vielen interagierenden Akteuren*, pages 37–51. 1997.
- [2] U. Krause. A discrete nonlinear and non-autonomous model of consensus formation. *Communications in Difference Equations*, pages 227–236, 2000.
- [3] J. Lorenz. A stabilization theorem for continuous opinion dynamics. *Physica A*, 355(1):217–223, 2005.

¹This research was supported by the National Science Foundation under grant ECS-0426453, by the Concerted Research Action (ARC) “Large Graphs and Networks” of the French Community of Belgium and by the Belgian Programme on Interuniversity Attraction Poles initiated by the Belgian Federal Science Policy Office. The scientific responsibility rests with its authors. Julien Hendrickx holds a FNRS fellowship (Belgian Fund for Scientific Research).

Iterative learning control with an identified time-varying robot model

W.B.J. Hakvoort

Netherlands Institute for Metals Research
University of Twente
P.O. Box 217, 7500 AE Enschede
The Netherlands
w.hakvoort@nimr.nl

R.G.K.M. Aarts, J. van Dijk and J.B. Jonker

Laboratory of Mechanical Automation
University of Twente
P.O. Box 217, 7500 AE Enschede
The Netherlands
{r.g.k.m.aarts, j.vandijk, j.b.jonker}@utwente.nl

1 Introduction

Demanding applications require the tip of an industrial robot to move with an accuracy of ± 0.1 mm at speeds beyond 100 mm/s. This is not feasible using standard industrial controllers. Since industrial robots have a good repeatability, the use of Iterative Learning Control (ILC) is investigated.

2 Method

Previously a model-based ILC algorithm was developed for linear time-varying systems and it was applied successfully to reduce the low-frequency tracking error of an industrial robot [1]. Compensation for the high-frequency tracking error requires adequate modelling of the configuration dependent high-frequency robot dynamics.

It is proposed to model the configuration dependent robot dynamics as a linear time-varying (LTV) system by interpolating several autoregressive models with external inputs (ARX) along the trajectory:

$$y(t) = \sum_{i=1}^{N_i} p_i(t) \left(\sum_{\tau=N_k}^{N_p} b_{i,\tau} u(t-\tau) - \sum_{\tau=1}^{N_a} a_{i,\tau} y(t-\tau) \right) + v(t),$$

where $u(t)$ is the input, $y(t)$ is the output and $v(t)$ is noise. Parameters $p_i(t)$ are predefined parameters that interpolate the parameters $a_{i,\tau}, b_{i,\tau}$ of the N_i ARX-models. The parameters $a_{i,\tau}, b_{i,\tau}$ can be estimated using linear regression [2].

3 Results

The performance of ILC with the LTV-ARX model is tested for the setup shown in figure 1. The robot tip moves with a speed of 200 mm/s from the initial position in the picture towards the robot's base. Perpendicular to this main motion the robot tracks the saw-tooth profile of a metal strip. An optical sensor measures the position of the metal strip relative



Figure 1: Stäubli RX90 robot at the start of the trajectory

to the robot tip [1]. The LTV-ARX model structure is used to describe the relation between the commanded motion and the measured motion perpendicular to the main motion. Parameter identification yields a model with varying local frequency response as shown in figure 2. Figure 3 shows the tracking error reduction of ILC with the LTV-ARX model.

4 Conclusions

The tracking accuracy of an industrial robot can be improved in a wide frequency band using model-based ILC and an ARX-LTV model. Model structure selection and estimation of the model accuracy are subject of ongoing research.

References

- [1] W.B.J. Hakvoort et al., 2006. Iterative Learning Control for Linear Time-Varying systems with application to an industrial robot. In: Book of Abstracts 25th Benelux Meeting on Systems and Control. Page 32.
- [2] L. Ljung, 1999. System Identification - Theory For the User, 2nd ed, Prentice Hall, Upper Saddle River, N.J.

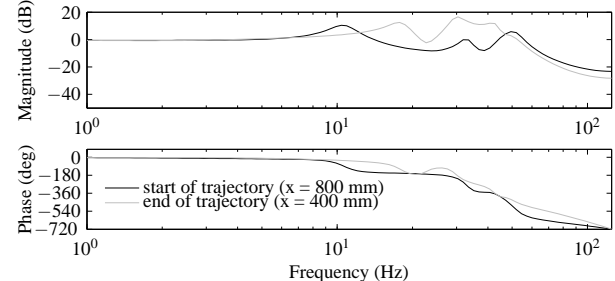


Figure 2: Local frequency responses of the robot model

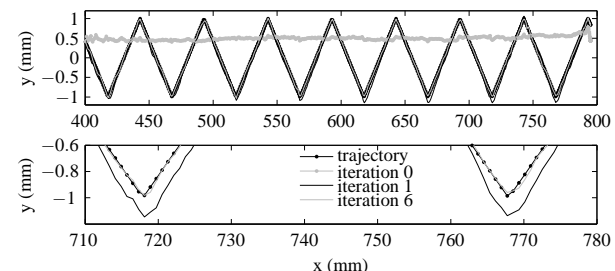


Figure 3: Trajectory and motion of the robot tip

Robust Iterative Learning Control

Jeroen van de Wijdeven

Department of Mechanical Engineering
Technische Universiteit Eindhoven
P.O. Box 513, 5600 MB Eindhoven
The Netherlands
Email: J.J.M.v.d.Wijdeven@tue.nl

Okko Bosgra

Department of Mechanical Engineering
Technische Universiteit Eindhoven
P.O. Box 513, 5600 MB Eindhoven
The Netherlands
Email: O.H.Bosgra@tue.nl

Introduction

To improve robustness properties of controllers, knowledge about model uncertainties can be included in the controller design. Here, we use results of robust control techniques in the design of a new robust control strategy in Iterative Learning Control (ILC).

ILC is a control strategy used to iteratively improve the performance of a batch repetitive process by updating the command signal from one experiment (trial) to the next, using signal information of the previous trials.

Robust ILC

Currently, robust ILC control design often follows standard robust control techniques, [1, 2] (Figure 1): Given a system, possibly in frequency domain, an ILC controller $L(z)$ is calculated using H_∞ synthesis. The main drawback of this approach is that the obtained ILC controllers are causal, while the strength of ILC is related to the non-causality of its controllers, [3].

In our approach, a non-causal finite time domain ILC controller is designed using the original Hamiltonian system solution of the H_∞ control problem, instead of a steady state approximation (Figure 1). The final robust ILC controller consists of this Hamiltonian system together with a set boundary conditions related to the finite time interval of an experiment.

The properties of the new robust ILC control strategy will be discussed, and compared to current robust ILC controllers.

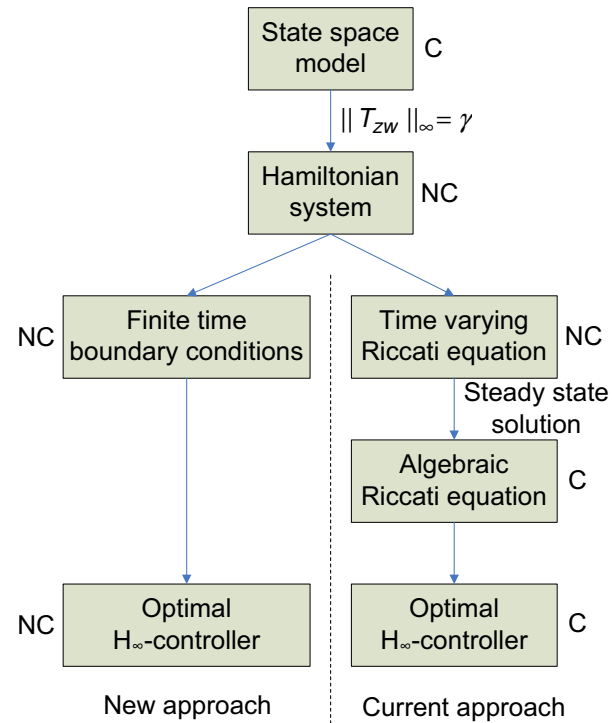


Figure 1: Figure 1, From initial model to H_∞ controller, for both the current (right) and new (left) approaches. C: causal; NC: non-causal.

References

- [1] D. de Rover. Synthesis of a robust Iterative Learning Controller using an H_∞ approach. In *Proc. of the 35th Conference on Decision and Control*, pages 3044–3049, Kobe, Japan, December 1996.
- [2] T.-Y. Doh and J.-H. Moon. Feedback-based iterative learning control for uncertain linear MIMO systems. In *5th Asian Control Conference*, pages 198–203, Melbourne, Australia, July 20–23 2004.
- [3] M. Norrlöf and S. Gunnarsson. A note on causal and CITE iterative learning control algorithms. *Automatica*, 41:345–350, 2005.
- [4] K.L. Moore, Y.-Q. Chen, and H.-S. Ahn. Algebraic h_∞ design of higher-order Iterative Learning Controllers. In *Proc. of the 2005 IEEE International symposium on intelligent control*, pages 1213–1218, Limassol, Cyprus, June 27–29 2005.

Reinforcement Learning for Aerospace Control

E. van Kampen, Q. P. Chu, J. A. Mulder

Delft University of Technology, Department of Control and Simulation

P.O. Box 5058, 3600 GB Delft, The Netherlands

E.vanKampen@TUDelft.nl, Q.P.Chu@TUDelft.nl, J.A.Mulder@TUDelft.nl

1 Introduction

Reinforcement Learning (RL), also called neuro-dynamic programming, is a control method based on human learning, where a reward signal is used to learn which actions lead to favourable states [1]. The first applications of RL were for discrete systems with a limited number of possible states and actions, such as simple games or decision making processes. However, when the number of states in the system increases, the discrete implementation of RL becomes impossible due to the ‘curse of dimensionality’, i.e. the number of combinations of states and actions becomes too large to store. The solution to this problem is to generalize the state and action spaces, using function approximators such as artificial neural networks.

2 Application of RL in aerospace systems

When function approximators are used to generalize the states and actions RL can be applied to more complex continuous systems and several RL controllers have been designed for aerospace applications. Enns and Si, with their model-free controller for the AH-64 Apache helicopter, were one of the first to systematically design a RL-controller for a nonlinear MIMO system [2][3]. Ferrari and Stengel used a fixed model-based RL approach to design a controller for a six-degree-of-freedom business jet [4]. Van Kampen, Chu and Mulder designed an adaptive model-based RL-controller for the General Dynamics F-16 which is capable of adapting to changes in the dynamics of the aircraft [5]. The addition of an online adapting model of the system shows increased performance and adaptability compared to the model-free RL-controller.

3 Future of RL

One of the most important drawbacks of RL-controllers for the continuous domain (with the function approximators), is that it is very hard to guarantee stability during the learning process. If this problem could be solved systematically, such that it holds for any implementation, the future for RL-based controllers in complex systems will be ensured. One of the ideas posed to solve this problem is to combine RL with robust control. When the changes in the neural networks during learning are considered as uncertainties in the system, robust control techniques can be used to limit the amount and direction of learning in such a way that the total

system stability is guaranteed [6].

Based on the concept that a combination of RL with existing control or optimization techniques could lead to guaranteed stability, a completely new idea of combining RL with interval analysis is considered. Interval analysis can be used to find global minima/maxima of sets of nonlinear equations [7]. In the current RL-controllers, some sets of initial neural network weights will converge to the correct solution, while other sets do not. The same pattern can be discerned for the learning rate and other training parameters. By combining RL with interval analysis it may be possible to get a better idea of how the learning parameters influence the stability and performance of the controller.

This work is performed as a part of the MicroNed-MISAT project.

References

- [1] Richard S. Sutton and Andrew G. Barto. *Reinforcement Learning, An Introduction*. Adaptive Computation and Machine Learning series. A Bradford Book, The MIT Press, 1998.
- [2] R. Enns and J. Si. Helicopter trimming and tracking control using direct neural dynamic programming. *Neural Networks, IEEE Transactions on*, 14:929–939, 2003.
- [3] J. Si and J. Wang. On-line learning control by association and reinforcement. *Neural Networks, IEEE Transactions on*, 12:264–276, 2001.
- [4] S. Ferrari and R.F. Stengel. Online adaptive critic flight control. *Journal of Guidance, Control, and Dynamics*, 27:777–786, 2004.
- [5] E. van Kampen, Q.P. Chu, and J.A. Mulder. Continuous adaptive critic flight control aided with approximated flight dynamics. *AIAA Guidance, Navigation, and Control Conference and Exhibit, Keystone, Colorado, Aug. 21-24, 2006*, 2006.
- [6] Robert Matthew Kretchmar. *A synthesis of reinforcement learning and robust control theory*. PhD thesis, 2000. Adviser-Steven Seidman.
- [7] Ramon E. Moore. *Interval Analysis*. Series in Automatic Computation. Prentice-Hall, Inc., 1966.

Fuzzy Approximation in Continuous-Space Reinforcement Learning

Lucian Buşoniu

Bart De Schutter

Robert Babuška

Delft Center for Systems and Control, Delft University of Technology, Mekelweg 2, 2628CD Delft, The Netherlands
Email: i.l.busoniu@tudelft.nl, b@deschutter.info, r.babuska@tudelft.nl

1 Introduction

In reinforcement learning (RL) control, the task is to find a state-feedback control law for a dynamical system, using a scalar reward signal, such that control performance is maximized [1]. The control performance measure is the discounted return $\sum_{k=1}^{\infty} \gamma^{k-1} r_k$, with r_k the instantaneous reward and $0 < \gamma < 1$ the discount factor. Well-understood algorithms are available to solve the RL task for discrete-valued states and actions, both when the system dynamics and reward function are known and when they are not.

However, many problems of interest have continuous states and actions, in general requiring approximate algorithms. Convergence guarantees and bounds on suboptimality cannot easily be derived for approximate RL. In this presentation, an algorithm relying on a fuzzy partition of the state space is introduced and its results illustrated in simulation.

2 Fuzzy Q-iteration

A normal fuzzy partition $\{\mathcal{X}_1, \dots, \mathcal{X}_N\}$ is defined on the state space X : a state x belongs to each fuzzy set \mathcal{X}_i with a membership degree $\mu_i(x) \in [0, 1]$. Normality requires that $\forall x, \sum_{i=1}^N \mu_i(x) = 1$. Center values x_i are associated with \mathcal{X}_i . A discrete subset of command values $\{u_1, \dots, u_M\}$ is chosen from the command space U .

Fuzzy Q-iteration maintains a matrix $q \in \mathbb{R}^{N \times M}$, containing one value for each fuzzy set-discrete action combination. The algorithm starts with an arbitrary q_0 and uses an approximate form of value iteration [1]:

$$q_{\ell+1}(i, j) = \rho(x_i, u_j) + \gamma \max_{\substack{j=1, \dots, M \\ i=1, \dots, N}} \sum_{i=1}^N \mu_i(f(x_i, u_j)) \cdot q_{\ell}(i, j), \\ i = 1, \dots, N, \quad j = 1, \dots, M \quad (1)$$

where f is the system dynamics and ρ the reward function. Here, $\sum_{i=1}^N \mu_i(x) q(i, j)$ approximates the action-value $Q(x, u_j)$, defined as the expected return after applying action u_j in state x .

Due to the normality of the fuzzy partition, (1) is a contraction with factor γ and therefore converges to a unique fixed point q^* as $\ell \rightarrow \infty$. The approximately optimal command for each center x_i is u_{j^*} where $j^* = \arg \max_j q^*(i, j)$. For x between the centers, the command is interpolated between the local commands using the membership degrees as weights.

3 Illustration: a two-link manipulator

A two-link manipulator operating in a horizontal plane (Figure 1) has two control inputs, the torques in the two joints,

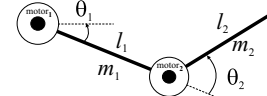


Figure 1: Two-link manipulator.

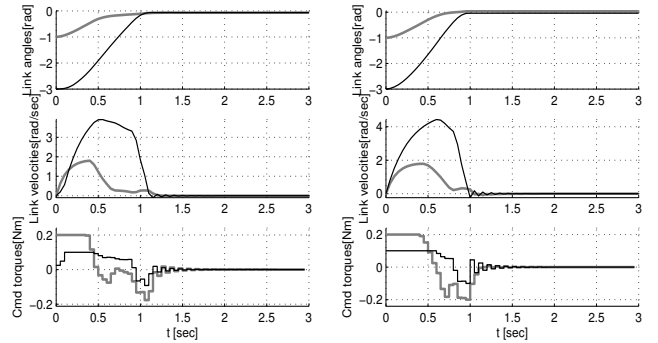


Figure 2: RL control for $\theta_0 = [-1, -3]$ rad. Left: centralized RL, right: decentralized RL. (Gray: link 1, black: link 2.)

and four states, the angles and angular speeds of the two links. Fuzzy Q-iteration was used to compute first a centralized control policy, and then separate decentralized policies for the two joints. The control goal is the stabilization of the two links in minimum time.¹ An example controlled trajectory of the manipulator is given in Figure 2.

Discussion. Both centralized and decentralized RL control successfully stabilize the system in slightly over 1 second. Coordination between the two links is visible around $t = 1$ s (left), $t = 0.8$ s (right), when link 1 is pushed counter-clockwise ('up') due to the negative acceleration in link 2. The controller of link 1 counters this effect by accelerating clockwise ('down').

Because the command is discretized and interpolated between the centers x_i , the control law will in general be suboptimal. Determining the distance to the optimal control law, and choosing \mathcal{X}_i and u_j to minimize this distance, are open problems.

Acknowledgement: This research is financially supported by Senter, Ministry of Economic Affairs of the Netherlands within the BSIK-ICIS project (grant no. BSIK03024).

References

- [1] R. S. Sutton and A. G. Barto, *Reinforcement Learning: An Introduction*. Cambridge, US: MIT Press, 1998.
- [2] L. Buşoniu, B. De Schutter, and R. Babuška, "Decentralized reinforcement learning control of a robotic manipulator," in *Proc. ICARCV 2006* (Singapore), pp. 1347–1352, 5–8 December.

¹For details on the model and the setup of the RL algorithm, see [2].

On the Equivalence between some Block Oriented Nonlinear Models and the Nonlinear Polynomial State Space Model

Johan Paduart, Johan Schoukens and Liesbeth Gommé
 Vrije Universiteit Brussel, dep. ELEC, Pleinlaan 2, 1050 Brussel, BELGIUM
 email: johan.paduart@vub.ac.be

Abstract - A comparison is made between block-oriented nonlinear models and nonlinear polynomial state space models in order to determine which classes of nonlinear systems can be modeled using the nonlinear state space approach. Some standard block-oriented models are discussed and the results are applied to measurements from two physical setups.

I. INTRODUCTION

Over the last decades, research on the modeling of nonlinear systems has narrowed down to specific classes of nonlinear systems. Simple block-oriented models, like the Hammerstein, Wiener, Wiener-Hammerstein and the Nonlinear-Feedback model have been used extensively to model nonlinear systems, e.g. in [1]. On the other hand, the NonLinear polynomial State Space model (NLSS) has been applied successfully to model several nonlinear systems, such as a combine harvester, a quarter car, and the Silverbox, which is an electronic circuit that emulates the behaviour of a mass-spring-damper system with a nonlinear spring [2]. In this work we establish a link between the NLSS and some standard block-oriented models.

II. NLSS VS. BLOCK-ORIENTED MODELING

The idea behind the NLSS model is to extend the linear discrete time state space model such that it can approximate the behaviour of the nonlinear system to be modeled. In (1), $\bar{u}(k)$ is the input vector, $\bar{y}(k)$ is the output vector and $\bar{x}(k)$ is the state vector at time instant k . The approximate behaviour of NLSS is accomplished by adding static nonlinear vector functions to the linear state equations, in the form of a product of a coefficient matrix (E, F) multiplied with a vector of polynomial functions ($\bar{\xi}(k), \bar{\eta}(k)$). The standard choice is to take $\bar{\xi}(k)$ and $\bar{\eta}(k)$ equal to $\bar{\xi}(k)_{(r)}$ which denotes the vector of all nonlinear combinations of the elements of $\bar{u}(k)$ and $\bar{x}(k)$.

$$\begin{cases} \bar{x}(k+1) = A\bar{x}(k) + B\bar{u}(k) + E\bar{\xi}(k) \\ \bar{y}(k) = C\bar{x}(k) + D\bar{u}(k) + F\bar{\eta}(k) \end{cases} \quad (1)$$

The next step is to see if the block-oriented models fit into this model class. By parametrizing the linear parts of the block-oriented models (shown in Fig. 1. and Fig. 2.) in state space form, and parametrizing the nonlinear blocks as polynomials, it can be shown that the input/output behaviour of these systems is identical to the behaviour of (1) for a well chosen A, B, C, D, E and F as a function of the parameters of the block-oriented

This work was supported by the FWO-Vlaanderen, the Flemish community (Concerted action ILiNoS), the Belgian government (IUAP-V/22), the TARGET Network ("Top Amplifier Research Groups in a European Team") and the Information Society Technologies Programme of the EU under contract IST-1-507893-NOE - www.target-net.org.

systems. This also holds for Hammerstein and Wiener models, which are special cases of the W.-H. model.

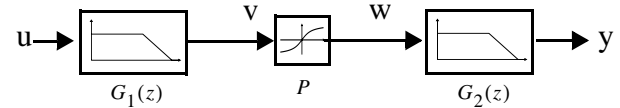


Fig. 1. Wiener-Hammerstein System

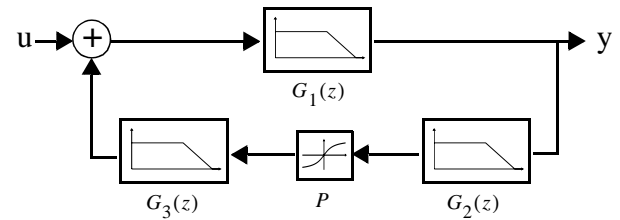


Fig. 2. Nonlinear-Feedback System

III. EXPERIMENTAL RESULTS

The results were verified on measurements from two experimental setups: an electrical circuit with a Wiener-Hammerstein structure [3] and a Agilent-HP420C Crystal detector for which it has been shown that it has a Nonlinear-Feedback structure [4]. Both systems were modeled using two different approaches: first the NLSS approach, and secondly a method which explicitly uses a priori knowledge of the system's structure. Both methods showed comparable results, and a significant improvement compared to linear modeling.

IV. CONCLUSION

It has been shown that block-oriented models form a subclass of NLSS. Both block-oriented modeling and NLSS modeling have some pros and cons. These are summarized in the following table:

	Block-Oriented	State Space
Physical interpretation	⊕	⊖
Number of parameters	⊕	⊖
Flexibility of the model	⊖	⊕
Model initialization	⊖	⊕
MIMO systems	⊖	⊕

REFERENCES

- [1] R. K. Pearson, M. Pottmann. Gray-box identification of block-oriented nonlinear models. *Journal of Process Control*, Vol. 10, Issue 4, Aug. 2000, pp. 301-315
- [2] J. Paduart, J. Schoukens, R. Pintelon, T. Coen. Nonlinear State Space Modelling of Multivariable Systems. *Proceedings of the 14th IFAC Symposium on System Identification*, 2006.
- [3] Vandersteen G. Identification of linear and nonlinear systems in an errors-in-variables least squares and total least squares framework. Ph.D. Thesis, Vrije Universiteit Brussel (1997).
- [4] J. Schoukens, L. Gommé, W. Van Moer, Y. Rolain. Identification of a crystal detector using a block structured nonlinear feedback model. Accepted for IMTC 2007.

Identification of Linear and Nonlinear Systems using Signal Processing Techniques

G. Kerschen, F. Poncelet, J.C. Golinval

Aerospace and Mechanical Engineering Department, University of Liège, Belgium
g.kerschen,fponcelet.jc.golinval@ulg.ac.be

A.F. Vakakis

Division of Mechanics, National Technical University of Athens, Greece
vakakis@central.ntua.gr

L.A. Bergman

Department of Aerospace Engineering, University of Illinois at Urbana-Champaign, USA
lbergman@uiuc.edu

Identification of linear and nonlinear mechanical systems is achieved using two signal processing techniques, namely the second-order blind identification (SOBI) method and the Hilbert-Huang transform (HHT). Although unrelated, these techniques share the common feature of decomposing a measured signal in terms of elemental components.

1 Blind Source Separation

Recovering unobserved source signals from their observed mixtures is a generic problem in many domains and is referred to as blind source separation (BSS) in the literature [1]. One well-known example is the cocktail-party problem, the objective of which is to retrieve the speech signals emitted by several persons speaking simultaneously in a room using only the signals recorded by a set of microphones located in the room. BSS techniques proved useful for the analysis of multivariate data sets such as financial time series, astrophysical data sets, electrical and hemodynamic recordings from the human brain, and digitized natural images. In this presentation, we show that the SOBI method, which belongs to the class of BSS techniques, may be useful in linear structural dynamics. Specifically, for free and random vibrations, a one-to-one relationship between the vibration modes and the mixing matrix computed through SOBI is demonstrated using the concept of virtual source. Based on this theoretical link, a new method for the extraction of the mode shapes, natural frequencies and damping ratios directly from the measured system response (i.e., operational modal analysis) is proposed. The method is then validated using numerical and experimental applications. In particular, modal analysis of a compressor blade of a turbojet engine is carried out [2, 3].

2 Hilbert-Huang Transform

The HHT has been shown to be effective for characterizing a wide range of nonstationary signals in terms of elemen-

tal components through what has been called the empirical mode decomposition (EMD) [4]. It has been utilized extensively despite the absence of a serious analytical foundation, as it provides a concise basis for the analysis of strongly nonlinear systems. In this presentation, we attempt to provide the missing theoretical link, showing the relationship between the EMD and the slow-flow equations of a system. The slow-flow reduced-order model is established by performing a partition between slow and fast dynamics using the complexification-averaging technique in order to derive a dynamical system described by slowly-varying amplitudes and phases. These slow-flow variables can also be extracted directly from the experimental measurements using the Hilbert transform coupled with the EMD. The comparison between the experimental and analytical results forms the basis of a novel nonlinear system identification method, termed the slow-flow model identification (SFMI) method. Through application examples, we demonstrate that the proposed method is effective for characterization and parameter estimation of nonlinear systems [5].

References

- [1] P. Comon, Independent component analysis: a new concept ?, *Signal processing* 36 (1994), 287-314.
- [2] G. Kerschen, F. Poncelet, J.C. Golinval, Physical interpretation of ind. component analysis in structural dynamics, *Mechanical Systems and Signal Processing*, in press.
- [3] F. Poncelet, G. Kerschen, J.C. Golinval, D. Verhelst, Output-only modal analysis using blind source separation, *Mechanical Systems and Signal Processing*, in press.
- [4] N.E. Huang, M.L. Wu, W.D. Qu, S.R. Long, S.S.P. Shen, *Hilbert-Huang Transform and Its Applications*, World Scientific, Singapore, 2003.
- [5] G. Kerschen, A.F. Vakakis, Y.S. Lee, D.M. McFarland, L.A. Bergman, Toward a fundamental understanding of the Hilbert-Huang transform in nonlinear dynamics, *Journal of Vibration and Control*, in press.

Crystal detector as calibration standard for Large Signal Analysis

Liesbeth Gommé, Johan Schoukens, Yves Rolain, Wendy Van Moer

Vrije Universiteit Brussel (Dept. ELEC/IW), Pleinlaan 2, B-1050 Brussels (Belgium)
Phone: +32.2.629.28.68 Fax: +32.2.629.28.50 Email: lgommé@vub.ac.be

Abstract - The aim of this paper is to estimate and validate a parametric black-box model for a crystal detector. This detector is used as a reference element to calibrate the phase distortion of a LSNA, [1], operating under narrow band modulated excitation.

Index Terms - Squared crystal detector, feedback model, phase calibration.

I. INTRODUCTION

One of the challenges in modulated measurements resides in the calibration of the instrument's phase distortion for such signals. The calibration of continuous wave (CW) carriers and their harmonics relies on the well-established step recovery diode (SRD) method [1]. This method cannot be used for spectra containing lines that do not lie on the harmonic grid ($f_0, 2f_0, \dots$). As a consequence, it cannot be used to calibrate a narrow band modulated signal.

The crystal detector (HP 420C) will be used as a reference element, because it translates the envelope of the RF signal to IF frequencies [2].

II. THE DETECTOR AS CALIBRATION STANDARD

Observe an amplitude modulated signal, $x_{AM}(t)$ as shown in figure 1. The carrier frequency is chosen on the coarse frequency grid, imposed by the SRD-method, while the modulation tones determine the fine grid. If $x_{AM}(t)$ is now exciting an uncalibrated instrument, the modulated signal will be distorted by the linear dynamics of the channel. (fig.1) In order to quantify the phase distortion induced by the LSNA, the phase relations between the tones in the excitation signal ought to be known exactly.

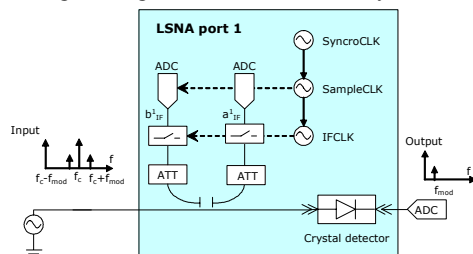


Figure 1 : Fine frequency phase calibration setup

This can be achieved by measuring the response of the detector and, indirectly, the applied modulated tone. To this end, we have modelled the crystal detector and this model will be used to retrieve the modulated input signal by measurement of the detector's response.

III. MODEL ESTIMATION AND VALIDATION

As we have verified in [3] that downconversion of the detector is independent of the RF carrier frequency, it is

The work was supported by the Belgian government (IUAP-V/22) and the Flemish government (GOA-ILiNoS), the TARGET-network and the Information Society Technologies Programme of the EU under contract IST-1-507893-NOE, www.target-net.org,

allowed to perform low frequency measurements to extract a baseband block oriented nonlinear feedback model, [4], for the nonlinear detector. High frequency validation measurements have been performed to confirm the model prediction capability at RF. The model consists of a linear direct path and a nonlinearity in the feedback path, as is shown in fig.2a. This baseband model has been validated using the setup in fig.1. The RF input, x , is measured and fed to the model to predict the low frequency envelope, \hat{y} . This modelled envelope is then compared to the ADC-measured low frequency output, y . The measured (black) and modelled (red) output envelopes are shown in fig.2b.

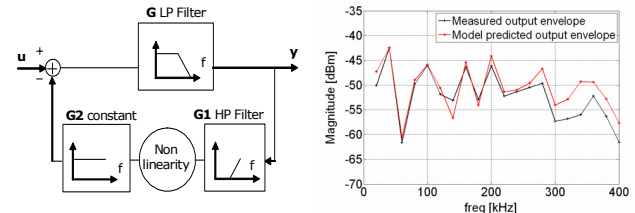


Figure 2 : a) Detector model, b) Validation measurements

The mean deviation between the modelled and measured envelope is relatively small compared to the measurement uncertainty. The difference in the beginning of the spectral band of interest equals 1dBm, as can be seen from figure 2b. The spectral behaviour of the modelled output coincides less with the measured output envelope for higher frequency modulation tones.

IV. CONCLUSION

This work presents a new calibration standard, the crystal detector. The device has been identified as a nonlinear feedback block oriented model. The comparison between measured envelope and modelled envelope by performing RF validation measurements shows good results.

REFERENCES

- [1] W.Van Moer, Y.Rolain, *A Large-Signal Network Analyzer: Why is it needed?* IEEE Microwave Magazine, Vol. 7, No. 6, pp. 46-62, 2006.
- [2] A.Barel, Y.Rolain. *A microwave multisine with known phase for the calibration of narrowbanded nonlinear vectorial network analyzer measurements.* IEEE MTT-S Int. Microwave Symp., Vol.3, pp. 1499-1502, 1998.
- [3] L.Gommé, A.Barel, Y.Rolain and F.Verbeyst. *Fine frequency grid phase calibration for the Large Signal Network Analyser.* IEEE MTT-S Int. Microwave Symp., pp. 1444-1447, 2006.
- [4] S.Billings, S.Fakhouri, *Identification of systems containing linear dynamic and static nonlinear elements,* Automatica, 18, pp. 15-26, 1982.

Online Identification of a Nonlinear Battery Model for Hybrid Electrical Vehicles

P.J. van Bree, A. Veltman, P.P.J. van den Bosch, W.H.A. Hendrix

Department of Electrical Engineering
Technische Universiteit Eindhoven
P.O. Box 513, 5600 MB Eindhoven
The Netherlands

Email: P.J.v.Bree@tue.nl

1 Battery Model

An online procedure to estimate the parameters of a nonlinear lead acid battery model, meant for prediction, is developed and validated.

The parameters of a nonlinear grey-box battery model are estimated using several minutes of high-rate vehicle current-voltage data. The developed model is based on a simulation model established using electrochemical impedance spectroscopy applied to lead acid batteries [1]. The nonlinear behavior of a battery along with the high rate excitation excludes the use of linear models and corresponding identification techniques.

By adapting the model to the present battery behavior (e.g. every ten minutes, dependent on availability of suitable identification data), it adapts to changing battery conditions (temperature, State-of-charge (SoC) or State-of-health (SoH)) and is able to predict dynamic battery behavior tens of minutes ahead.

2 Identification

Parameter estimation is based on minimizing the sum of squares of the error between measured and model voltage. Levenberg Marquardt, an iterative nonlinear least squares optimization method is used. The defined model structure allows for an analytical expression of the Jacobian matrix of the error function, which considerably speeds up the identification procedure (required for online implementation of the procedure).

3 Verification

The procedure is validated using real-life vehicle data, obtained using a micro-hybrid electrical vehicle (Ford Fiesta technology demonstrator) which has a single battery power-net topology (14V), and features regenerative braking and engine stop/start operation. No electric propulsion is involved. Test-drives took place on similar routes (≈ 45 min.) through and around the city of Aachen, involving both city and highway driving.

Figure 1 shows the result when 200s of data (sampled at 100Hz) is used for identification, and the voltage course of 300s is predicted.

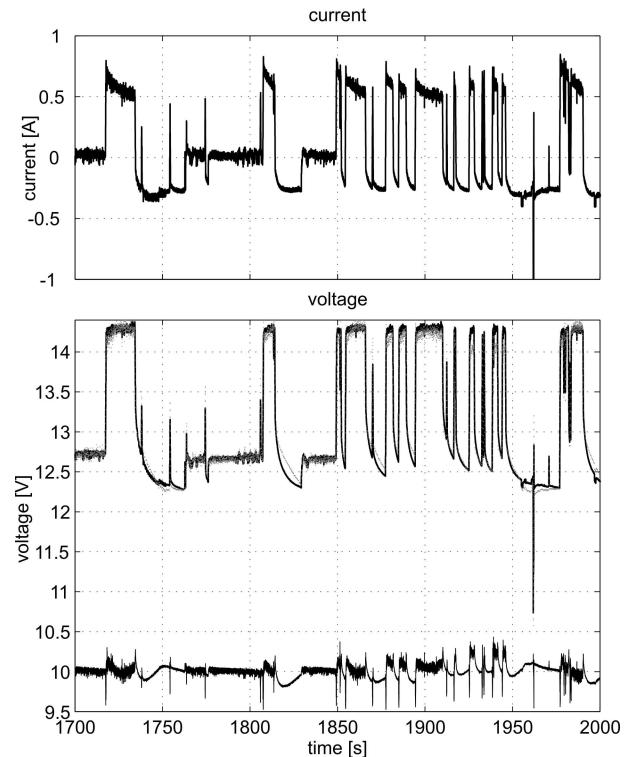


Figure 1: Result of prediction for 300s [1700, 2000s]. Identification took place on 200s of data [1400, 1600s]. The upper plot shows the (normalized) input current. The lower plot contains three lines, the measured battery voltage (black) and the model output gray. The difference between measurement and model (black) is plotted at 10V.

References

[1] Buller, S. (2002) *Impedance-Based Simulation Models for Energy Storage Devices in Advanced Automotive Power Systems*, dissertation thesis, RWTH Aachen University. ISBN 3-8322-1225-6.

Mathematical performance analysis of a temperature controlled bulk storage room

Simon van Mourik and Hans Zwart

Department of Applied Mathematics, University of Twente, The Netherlands,
e-mail: s.vanmourik@utwente.nl

Karel Keesman

Systems & Control Group, Wageningen University, The Netherlands,
email: Karel.Keesman@wur.nl

1 Introduction

We consider a bulk storage room for agricultural food products. A ventilator enforces the air circulation, and the air is cooled down by a cooling device, see Figure 1. Cold air flows usually upwards through the bulk. Inside

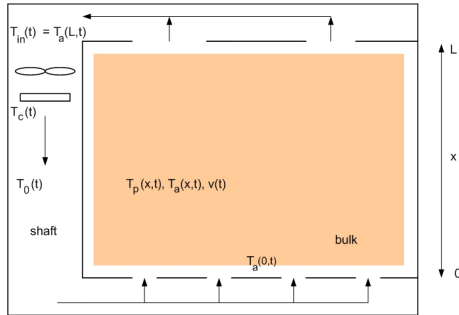


Figure 1: Schematic representation of a bulk storage room.

the bulk, the air warms up and consequently the products at the top will be some degrees warmer than those at the bottom, see [1]. A larger airflow will decrease these spatial variations, but will be costly. Model-based control design is a nontrivial task, since a standard model that describes the time- and spatially dependent temperatures will consist of a set of nonlinear partial differential equations.

Systems design is strongly correlated to controller design. The controller adds dynamics to the system, causing it to behave differently than the uncontrolled system. For storage room design, it is therefore desirable to design the plant and controller simultaneously, instead of separately.

2 Method

We started with the results in [2], where a basic physical model was derived and validated with experimental results. An open loop control law, which explicitly depends on all the physical model parameters, was successfully constructed. The controller determines the times when to switch between two discrete inputs. This input switching is realistic since often in practice the ventilator is switched on and off

on a regular basis. Then we defined two criteria that indicate the performance of the system. The performance criteria are the total energy usage by the cooling device and the ventilator, and the temperature difference between the products at the top and at the bottom of the bulk. The controller as well as the performance criteria are closed expressions that contain all the prior physical knowledge. The relationship between each design criterium and the design parameters consists of a single expression and is therefore easily computed. Since some analytical relations could not be found in the literature, they are identified experimentally. These relations describe the energy usage of the ventilator, and the effectiveness of the heat exchanger, both as functions of the airflow.

3 Results

The following design tradeoffs were observed. The total energy usage is minimized by a low temperature of the cooling device, but the temperature difference over the bulk is minimized by a high temperature of the cooling device. Further, the temperature difference is decreased by a more powerful ventilator. However, the tradeoff here is that such a ventilator will be more expensive in purchase. The energy usage is decreased by a lower bulk. The tradeoff is that for a fixed bulk volume, a lower bulk means a larger floor area, which is usually more expensive than a higher roof.

4 Acknowledgement

This work was supported by the Technology foundation STW under project number WWI.6345.

References

- [1] A. Rastovski and A. van Es et al. *Storage of potatoes, Post-harvest behaviour, store design, storage practice, handling*. Pudoc Wageningen, 1987.
- [2] S. Van Mourik, H.J. Zwart, and K.J. Keesman. Analytic control law for a food storage room. *Submitted*, 2006.

Optimal control design for a solar greenhouse

R.J.C. van Ooteghem
 Wageningen University
 Rachel.vanOoteghem@wur.nl

Keywords: greenhouse, solar greenhouse, greenhouse model, model validation, optimal control, crop biophysics

1 Introduction

The research of my Ph.D.-thesis was part of a larger project aiming at the design of a greenhouse and an associated climate control that achieves optimal crop production with sustainable instead of fossil energy. This so called solar greenhouse design extends a conventional greenhouse with an improved roof cover, ventilation with heat recovery, a heat pump, a heat exchanger and an aquifer. The thesis describes the design of an optimal control strategy for the solar greenhouse, to ensure that the benefits of this innovative greenhouse are exploited in the best possible way.

The ingredients of an optimal control design are a dynamic model for greenhouse and crop, an explicitly formulated cost function, and a solution method. The advantages of this systematic approach are that scientific knowledge concerning the greenhouse and the crop is fully exploited, and with a goal that is stated in clear and transparent quantitative terms, it computes the best possible control. Furthermore it gives flexibility because the control is automatically adjusted when economic or other factors determining the cost function are changed. The control objectives used here are: minimize gas use and maximize crop yield, development and quality. Since the optimal control fully relies on the cost function and the dynamic model, this model must give a good description of the system response for a wide range of temperature and humidity conditions.

2 Contribution

The first major contribution of the thesis is the development of a comprehensive, science-based, dynamic model of the greenhouse-with-crop system in a form that is suitable for optimal control purposes. The model describes the temperature, the carbon dioxide balance and the water vapour balance in the greenhouse, as a function of the external inputs (i.e. the outdoor weather conditions) and the control inputs (e.g. valve positions and window apertures). This model has been validated with data, and was found to give a good description of reality.

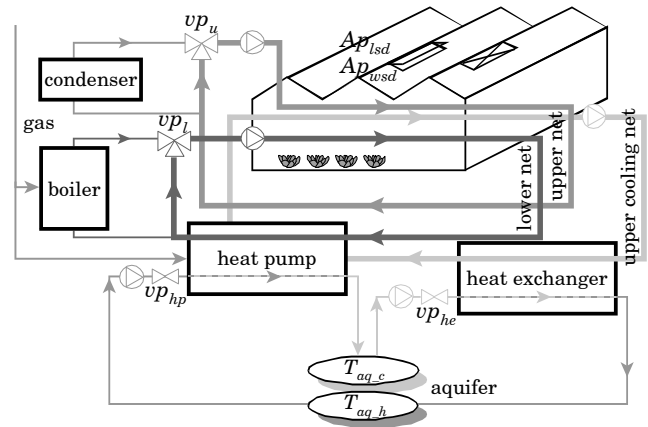


Figure 1: Greenhouse configuration

The second major contribution of the thesis is the design of the optimal controller, including an efficient solution technique. A conjugate gradient search is used as the ultimate fine-tuning method, but it has the risk of achieving local minima, and it is time consuming. Therefore, a grid search method has been designed to provide a good initial guess for the gradient search method. This method uses only a small number of discrete constant control trajectories, which are then modified with rule based state dependent control input bounds to obtain initial control trajectories.

3 Results

Receding horizon optimal control has been used for year-round computations of the solar greenhouse with crop. Extensive analyses have been made of the effect of various components of the solar greenhouse system and of the uncertainty in weather. Growers should be aware that setting tighter humidity bounds increases energy use. It was found that in the optimally controlled solar greenhouse, gas use can be seriously reduced (by 52%), while the crop production is significantly increased (by 39%), as compared to an optimally controlled conventional greenhouse without the solar greenhouse elements.

References

R.J.C. van Ooteghem (2007). *Optimal control design for a solar greenhouse* Ph.D. thesis, Wageningen University, Wageningen, The Netherlands. 304 p.

Control-oriented model of a dwelling coupled to a water-to-water heat pump system

R. Lepore, S. Nourricier, F. Renard, H. Diricq, M.-E. Duprez, E. Dumont, C. Renotte, V. Feldheim, M. Frère
 Pole Energie, Faculté Polytechnique de Mons, Belgium
 renato.lepore@fpms.ac.be

1 Introduction

The consumption of primary energy (mainly from fossil origin) has two major drawbacks: first, its increasing cost and scarcity, second, the production of undesirable carbon dioxide. As the domestic and tertiary sectors are responsible for around 30 % of the total primary energy consumption, reducing this consumption in buildings is nowadays of major concern (note the appearance of more severe standards concerning insulation and energy savings). To achieve these goals, various sources of renewable energy (solar, wind, biomass, geothermy,...) can be exploited. Among several techniques, heat pumps use the refrigeration thermodynamic cycle to extract heat from a colder outside air/ground and deliver it to the house, at higher temperature. This operation can be advantageously performed a priori at any time (in contrast with solar or wind energy). A description of this technique and its utilization is summarized in [1].

In this work, as depicted in figure 1, we consider a real one-family house, which uses a water-to-water heat pump as a heating system (Leuze, Belgium). The heat pump cold source and hot sink are the outside ambiance and a radiant floor, respectively.

2 Contribution and results

We adopt a reduced-order modelling as well as a unique programming language, namely Matlab®. This way, we intend to alleviate interfacing problems which arise when mixing different softwares and to better address model-based control in later stages of the study (e.g., if estimation-adaptation of time-varying parameters is required):

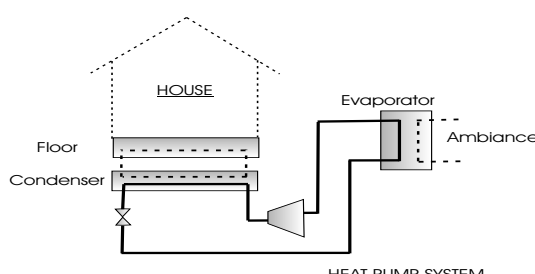


Figure 1: Principle of a dwelling coupled to the heat pump system using air as cold source.

- The house model is of the one-zone type and is based on a standard method describing the temperature nodes and the related heat fluxes. A small number of layers describes the walls and the floor (maximum three layers), all radiation and convection phenomena are lumped into global coefficients. This results into a set of nine Ordinary Differential Equations (ODEs).

- The heat pump is described by a set of Algebraic Equations (AEs), which is in agreement due to its high dynamics. The thermal phenomena in the heat exchangers (evaporator and condenser) are expressed using global transmission coefficients. The fluid properties and the calculation of the thermodynamic cycle are achieved using the NIST Refprop7® property database and the related access libraries.

- The radiant floor is described according to a one-dimensional model of piped thermo-active elements.

The model is validated in two ways:

- first, against a previously-developed model containing accurate descriptions of the house (Trnsys Type56® model) and of the heat pump;
- second, against the experimental data collected for several months, which are related to the house thermal phenomena as well as to the heat pump behaviour.

If model-based control strategies are to be addressed, computational performance is a nonnegligible aspect. In this case, it is noted that a great computational burden is due to the nested sets of algebraic equations to solve (in fact, REPROP7 functions solve AEs). The computational performance decreases particularly when mixtures are used as fluids, as is often the case. The problem of accelerating this calculation step is also particularly addressed.

References

[1] Natural Resources Canada's Office of Energy Efficiency (EnerGuide team). (2004). Heating and cooling with a heat pump, see <http://oee.nrcan.gc.ca/publications/>.

An efficient Gaussian proposal in SMC methods

Saikat Saha¹

Department of Applied Mathematics, University of Twente
PO Box 217, 7500 NB Enschede, The Netherlands
Email: s.saha@ewi.utwente.nl

1 Introduction

Consider a nonlinear dynamic system given by

$$x_k = f(x_{k-1}) + w_k, \quad w_k \sim \mathcal{N}(0, Q) \quad (1)$$

$$y_k = h(x_k) + v_k, \quad v_k \sim \mathcal{N}(0, R), \quad k = 1, 2, \dots \quad (2)$$

where (x_k) are the state with prior $p(x_0) \equiv p(x_0|x_{-1})$ and (y_k) are the measurements. Furthermore, the process noises (w_k) are assumed to be independent of the measurement noises (v_k) . The main statistical problem here is to estimate (filter) the unobserved x_n in some optimal manner from all the observations $y_{1:n} \equiv (y_1, y_2, \dots, y_n)$. However, except in a few special cases such as when both the system and observation equation (1)–(2) are linear (Kalman filter), it is not possible to obtain an analytical solution. As a result, many analytical approximations such as Extended Kalman filter, Unscented Kalman filter and Gaussian sum filter are developed. The sequential Monte Carlo (SMC) methods, also referred to as Particle Filters (PF's), on the other hand, use simulation technique to reach a solution.

The biggest advantage of SMC is that, it can easily adapt to the nonlinearity in the model and/or non-Gaussian noises. The estimate is centered on describing $p(x_n|y_{1:n})$ by a cloud of particles. The particles are generated from a so called importance function, $\pi(\cdot)$, also known as proposal distribution. Furthermore, each particle receives an importance weight depending on the likelihood and the proposal density used. Although the resulting distributions do converge to the true filtered density as the Monte Carlo sample size tends to infinity, for finite sample size the efficiency of the SMC method depends heavily on the proposal density used. Usually the ‘naive’ proposal $p(x_k|x_{k-1})$ is used as the importance function, mainly due to the ease of drawing samples from this Gaussian distribution and the simplicity of weight update equations. However, if the measurement is very informative, a lot of samples are wasted. To make the method more effective, importance functions of the form $\pi = p(x_k|x_{k-1}, y_k)$, i.e., the one which incorporates both the system and observation processes is suggested in [1]. There are two major, practical drawbacks for using this type of importance function. First, drawing samples according to $p(x_k|x_{k-1}, y_k)$ is, in general, difficult. Secondly, it is also difficult to get an analytical expression for the proposal density needed to update the importance weights. To circumvent

that, the authors in [1] approximate the observation model (2) with a linearized version so that $p(x_k|x_{k-1}, y_k)$ becomes Gaussian and subsequently uses that as the importance function.

2 Contributions and results

We propose another Gaussian importance function ([3]) that is built by first approximating the conditional distribution of (x_k, y_k) given x_{k-1} , by a Gaussian distribution whose moments are matched exactly to the theoretical moments obtained from the dynamic system equations (1)–(2). Subsequently, an extension is suggested for more general case. This in essence, extends the method in [1]. Recently, other Gaussian importance functions have been proposed ([2]). Although these methods also perform better (in term of root mean squared error (RMSE)) than the linearization method in [1], the improvement is at comparable level with our proposed method. However, our method is computationally less demanding than that in [2].

Another issue is the use of RMSE as a criterion of comparison. In RMSE, true x_k is compared with the mean of the posterior density $p(x_k|y_{1:k})$. However, this is not a good criterion as the filtered densities obtained by different methods may be quite different but having the same mean and thus would lead to the same RMSE. Better criterion would be to compare directly the estimated densities with the true posterior. Here, we envisage the Kullback-Leibler Distance (KLD) measure for comparing densities. Since in most cases, true posterior is not known, we approximate it by the density obtained from PF using a large number of samples. We use the kernel density estimation method to obtain the density function from particle clouds and KLD is estimated subsequently using the Monte Carlo Integration technique. We also show that our proposal performs better when compared with those in [2] in terms of KLD.

References

- [1] A. Doucet, S. Godsill, and C. Andrieu, *On sequential Monte Carlo sampling methods for Bayesian filtering*, Statistics and Computing **10** (2000), 197–208.
- [2] D. Guo, X. Wang, and R. Chen, *New sequential Monte Carlo methods for nonlinear dynamic systems*, Statistics and Computing **15** (2005), no. 2, 135–147.
- [3] S. Saha, P.K. Mandal, Y. Boers, and H. Driessens, *Exact moment matching for efficient importance functions in SMC methods*, Proceedings of NSSPW 2006, Cambridge.

¹This research was made possible by a research grant from THALES Nederland B.V.

Model Reduction Based On A Cross-Energy Function For Nonlinear Systems

T. C. Ionescu

Rijksuniversiteit Groningen

t.c.ionescu@tudelft.nl, t.c.ionescu@rug.nl

J. M. A. Scherpen

Rijksuniversiteit Groningen

j.m.a.scherpen@rug.nl

1 Introduction

We extend the method presented in [7, 1] to nonlinear systems. The method presented there is for linear symmetric systems and it consists of solving a Sylvester equation. The solution of this equation is called cross-Gramian (e.g. see [2]) and its eigenvalues are the Hankel singular values of the system, the same that can be obtained using the well-known balancing procedure. The advantages of this method are that it requires solving only one Sylvester equation and that it avoids the balancing procedure, being more efficient from computational point of view.

2 Balanced truncation for nonlinear symmetric systems

Defining $\mathcal{S} : U \rightarrow Y$, we have the Hankel operator of the system defined as $\mathcal{H} = \mathcal{O}\mathcal{C}$, where \mathcal{C} is the controllability operator and \mathcal{O} is the observability operator of \mathcal{S} . The operator corresponding to the cross-Gramian is $\mathcal{X} = \mathcal{C}\mathcal{O}$. For square systems it is immediate that the nonzero eigenvalues of \mathcal{X} are the eigenvalues of \mathcal{H} , in accordance with [7]. However, the singular value problem is not the same and there is a majorization relation between the Hankel singular values and the singular values of the \mathcal{H} operator. We prove that for a symmetric linear system, $\lambda(\mathcal{X}^* \mathcal{X}) = \lambda(\mathcal{H}^* \mathcal{H})$. For nonlinear systems, first, we introduce the concept of symmetry, in the sense of [7, 2] which is related to the duality of nonlinear systems. This latter concept is presented in [6]. A square nonlinear system is called symmetric if it is equivalent to its dual via a change of coordinates. The duality and symmetry of nonlinear systems are studied here in the context of a non-trivial extension of the results in [1, 2]. Starting from the nonlinear balancing technique for nonlinear asymptotically stable systems presented in [3, 4], we study the problem of differential eigenstructure of the operator \mathcal{X} , of a symmetric system, in relation with the differential eigenstructure problem $(d\mathcal{H})^* \mathcal{H}$. We aim at a direct relation between the solutions of the two problems and as in [1, 2, 7] to find an energy function (Gramian), related to the \mathcal{X} operator, solution of the nonlinear version of the Sylvester equation. It will be called cross-energy and will simultaneously depend on the controllability and observability functions of the system and its singular values are the Hankel singular values of the system. The advantage is that a direct diagonalization of this cross-energy function gives the squared values of the Hankel singular values of the

system, thus avoiding the balancing procedure and simplifying the computations, like in the linear case. We make non-trivial steps towards this extension.

Finally, the truncation of the less important singular value functions is performed, obtaining a reduced system which is asymptotically stable too.

3 Remarks and future work

The difficulty of the problem resides in the fact that the adjoint of a nonlinear operator is more involved and not so straightforward as in the linear case, which makes the relations between the controllability and observability operators and their symmetric counterparts for a nonlinear symmetric system quite tedious.

The developments in this paper are the first steps towards easier computations for the nonlinear passive systems case, starting from positive real balancing, see [5].

References

- [1] R. W. Aldaheri, "Model order reduction via real Schur-form decomposition", *Int. J. Control.*, vol. 53, no. 3, p. 709-716, 1991.
- [2] K. V. Fernando, H. Nicholson, "On the structure of balanced and other principal representations of SISO systems", *IEEE Trans. Automat. Contr.*, vol. 28, no. 2, p. 228-231, 1983.
- [3] K. Fujimoto, J. M. A. Scherpen, "Singular Value Analysis of Hankel Operators for General Nonlinear Systems", *Proceedings of ECC*, 2003.
- [4] K. Fujimoto, J. M. A. Scherpen, "Nonlinear Input-Normal Realizations Based on the Differential Eigenstructure of Hankel Operators", *IEEE Trans. On Aut. Control*, vol. 50, 2005.
- [5] T. C. Ionescu, J. M. A. Scherpen, "Positive Real Balancing For Nonlinear Systems", *SCEE06 Conference*, 2006.
- [6] J. M. A. Scherpen, "Duality and singular value functions of the nonlinear normalized right and left coprime factorizations.", *Proceedings of the 44th IEEE CDC-ECC*, p. 2254-2259, 2005.
- [7] D. C. Sorensen, A. C. Antoulas, "The Sylvester equation and approximate balanced truncation", *Linear Algebra and Its Applications*, vol. 351-352, p. 671-700, 2002.

Model Reduction through Proper Orthogonal Decompositions for Multidimensional systems

Femke van Belzen

Department of Electrical Engineering
Technische Universiteit Eindhoven
PO Box 513, 5600 MB Eindhoven
The Netherlands
Email: f.v.belzen@tue.nl

1 Introduction

Systems in which variables have both space and time as independent variables occur in a large variety of applications. First principle modeling of spatial-temporal systems usually involves partial differential equations, whose solutions are numerically computed by finite element methods. The large scale nature of these models causes excessive computation and simulation time. This makes it desirable to find approximations to these models that offer an accurate description of the process and allow for faster computations. The method of Proper Orthogonal Decompositions (POD) is suitable for both nonlinear as well as large scale systems [1]. POD is a data-driven method, where spectral decompositions are used to approximate the solution of the model equations. The first step in POD is the computation of coherent patterns from a representative set of measurement data of the process, thus defining a projection for the model equations.

Problem formulation and results

Suitable basis functions for multidimensional systems are currently determined by stacking the elements of a discretized domain, i.e. collecting suitable measurement data in a matrix W . The left singular vectors of the singular value decomposition of W define suitable basis functions. However, computing the singular value decomposition can be problematic, especially when the dimensions of the spatial coordinates are large. We propose an alternative way to define spectral expansions which is relevant for reduced order modeling. This takes into account the multidimensional nature of the spatial coordinates. Consider the following two-dimensional heat transfer process:

$$\rho c_p \frac{\partial w}{\partial t} = \kappa_x \frac{\partial^2 w}{\partial x^2} + \kappa_y \frac{\partial^2 w}{\partial y^2} + u \quad (1)$$

One time sample of the simulation of this process is displayed in Figure 1. To approximate the solution of the PDE (1) we propose the following spectral expansion:

$$w_{nm}(x, y, t) = \sum_{k=1}^n \sum_{l=1}^m a_{kl}(t) \varphi_k(x) \psi_l(y) \quad (2)$$

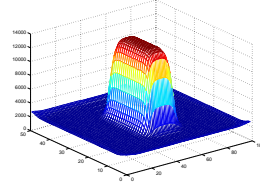


Figure 1: One time sample from the simulation data.

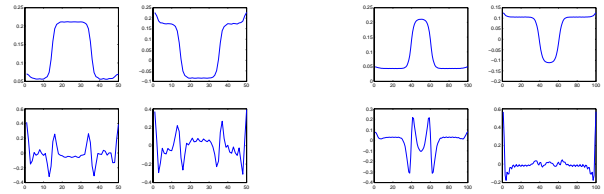


Figure 2: First basis functions for \mathcal{X} (left) and \mathcal{Y} (right)

where $\{\varphi_k\}$ is an orthonormal basis for \mathcal{X} and $\{\psi_l\}$ is an orthonormal basis for \mathcal{Y} . $\{\varphi_k\}$ and $\{\psi_l\}$ are computed using the Higher-Order Singular Value Decomposition (HOSVD) [2], see Figure 2. The approximation of the measurement is not optimal, an upper bound to the approximation error is given [2], but there is no lower bound, see also [3].

References

- [1] P. Astrid, "Reduction of process simulation models: a proper orthogonal decomposition approach," Techn. Univ. Eindhoven, 2004.
- [2] L. de Lathauwer et al., "A Multilinear Singular Value Decomposition," SIAM J. Matrix Anal. Appl., vol. 21 (4), 2000.
- [3] Weiland, S. and Belzen, F. van, "Model reduction through multi-linear singular value decompositions", EC-COMAS CFD, 2006.

Flood prevention combining model predictive control with expert knowledge

Toni Barjas Blanco, Bart De Moor
 K.U. Leuven, ESAT-SCD-SISTA Kasteelpark 10
 B-3001 Heverlee-Leuven, Belgium
 toni.barjas-blanco@esat.kuleuven.be, bart.demoor@esat.kuleuven.be

Patrick Willems, Jean Berlamont
 Kasteelpark Arenberg 1, 3001 Leuven (Heverlee)
 Patrick.Willems@bwk.kuleuven.be, Jean.Berlamont@bwk.kuleuven.be

1 Abstract

In this presentation an implementation is discussed concerning river flood prevention of the river Demer using a nonlinear model predictive controller (NMPC). The main goal of this controller is not only to prevent flooding but to also take some predefined rules into account. The predefined rules are imposed by the local water management and can be considered as expert knowledge. Some results on historical data and fictitious data show the improvement obtained by the NMPC strategy.

2 Problem setting

The Demer is a river located in Belgium, more specifically in Flanders, that has caused lots of damage to its surroundings in the past. In periods of heavy rainfall the demer caused widespread flooding affecting many fields, streets and houses. In order to reduce the amount of flooding the local water management AMINAL has provided the river with some hydraulical structures and reservoirs making it possible to influence the water levels of the Demer bassin. These hydraulical structures are controlled manually based on experience and some simple rules. Although this actions have led to a reduction in flooding, tests on historical data have shown that flooding could have been reduced even more if was opted for a different control action. Therefore the purpose of this investigation is to design a control strategy able to generate a more optimal control action in order to further reduce flooding and if possible to prevent it. The control strategy for which is opted in this research is nonlinear model predictive control (NMPC) because this strategy allows to cope with all the challenges concerning river control. The discussed algorithm also takes expert knowledge from the local water management into account. This knowledge is based on experience of the operators controlling the Demer bassin for years and can add very usefull information with respect to the control of the system.

Model Predictive Control is a control strategy typically used in process industry to control relatively slow processes. This strategy basically consists of calculating an optimal control

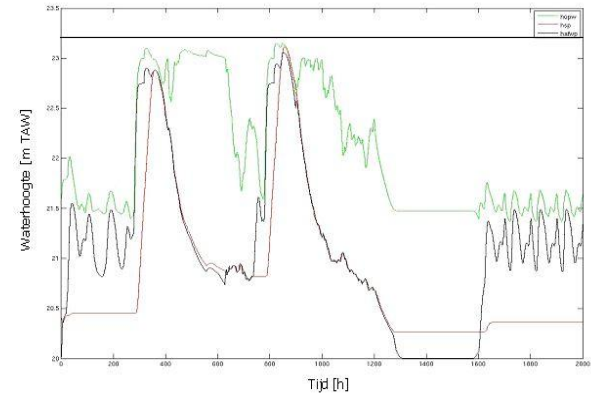


Figure 1: MPC control on historical data

action such that the future states of the system reach the desired values. This strategy seems suitable to control river systems because of their relatively slow dynamics and the amount of constraints that have to be satisfied when controlling them. Furthermore, MPC makes it possible to take rain predictions into account. The simulations in this work are based on both historical and fictitious data.

3 Results

Acknowledgements Research Council KUL: GOA AMBioRICS, CoE EF/05/006 Optimization in Engineering, CoE EF/05/007 SymBioSys, IDO (Genetic networks), several PhD/postdoc and fellow grants; Flemish Government: FWO: PhD/postdoc grants, projects, G.0407.02 , G.0197.02 , G.0141.03 , G.0491.03 , G.0120.03 , G.0413.03 , G.0388.03 , G.0229.03 , G.0452.04 , G.0499.04 , G.0499.04 , G.0232.05 , G.0318.05 , G.0211.05 , G.0226.06 , G.0321.06 , research communities (ICCoS, AN-MMM, MLDM); AWI: Bil. Int. Collaboration Hungary/ Poland; IWT: PhD Grants, GBOU-McKnow , GBOU-SQUAD , GBOU-ANA , Eureka-Flite2, TAD-BioScope, Silicos; Belgian Federal Science Policy Office: IUAP P5/22 ; PODO-II ; EU-RTD: FP5-CAGE (Compendium of Arabidopsis Gene Expression); ERNSI; FP6-NoE Biopattern; FP6-IP , FP6-MC-EST , FP5-Quprodis; Contract Research/agreements: ISMC/IPCOS, Data4s, TML, Elia, LMS, Mastercard

References

- [1] J.A. Rossiter, Model-Based Predictive Control - A Practical Approach, CRC Press, Boca Raton, FL, 2003.
- [2] Ruiz-Carmona, V. M., Clemmens, A. J., and Schuurmans, J., Canal control algorithms formulations. Journal of Irrigation and Drainage Engineering 124(1):31-39, 1998

Model Based Controllers for a Solar Power Plant

Manuel Gálvez-Carrillo*, R. De Keyser, C. Ionescu

*Department of Control Engineering and System Analysis

*Université Libre de Bruxelles, Av. F. D. Roosevelt 50 - CP165/55, B1050 Brussels, Belgium

*Email: mgalvezc@ulb.ac.be

Department Electrical energy, Systems and Automation

Ghent University, Technologiepark 913, B9052 Gent-Zwijnaarde, Belgium

Email: rdk@autoctrl.UGent.be

The concern about renewable energies is growing around the world due to their economical and environmental impact. Converting these clean sources of energy in other types that can account for human and industrial use is now of global interest [1]. Therefore, it is necessary not only to adequately design the conversion processes, but also to ensure their optimal technical and economical operation by means of good control strategies. The present work studies the distributed solar collector field ACUREX of the *Plataforma Solar de Almería*, located in the southern Spain. The parabolic-through technology of this plant is the only type of solar plant with existing commercial operating systems [2]. In such a system, a fluid (oil) is heated while travelling in the field, using the energy of the solar radiation concentrated by parabolic mirrors.

Our control objective is that the fluid outlet temperature follows the reference signal, by varying the inlet oil-flow. Notice that the main source of energy, the solar irradiation, cannot be manipulated [3] and constitute the main disturbance of the process. The process is also challenging because of the presence of variable time delay. A schematic of the process can be seen in Figure 1.

In this work, nonlinear and linear models have been obtained in order to replicate the process and disturbances, with emphasis of the adequate election of the variable time delay model. A nonlinear model based predictive control (MPC), the Nonlinear EPSAC (Extended Prediction Self-Adaptive Controller) [4], has been implemented with a modified Smith Predictor in order to overcome the fact of the presence of the variable time delay. This control strategy has been tested and compared with other two strategies: a linear MPC, the EPSAC; and a modified PI controller (Filtered Predictive PI, FPPI), that is designed based on a model of the plant. Both strategies are also combined with a Smith Predictor algorithm. The results are presented in Figure 2 for the output (outlet oil temperature). The nonlinear EPSAC controller behaves better than the other two linear ones, the linear EPSAC reacts faster the FPPI, but the latter is more robust when high changes in reference occur.

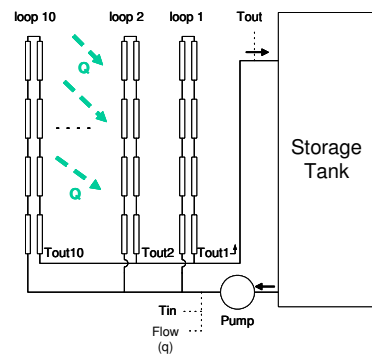


Figure 1: Schematic representation of the solar power plant.

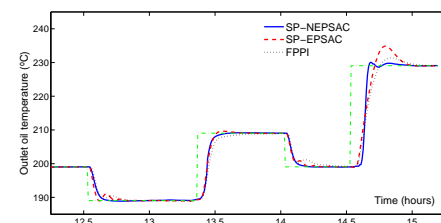


Figure 2: Comparison of Output Temperature for the designed controllers.

References

- [1] A. Woloski, "Fuel of the Future: A Global Push Toward New Energy", *Harvard International Review*, vol.27, no.4, 40-43, (2006)
- [2] V. Quaschnig, M. Blanco, "Solar Power - Photovoltaics or Solar Thermal Power Plants?", *VGB Congress Power Plants*, Brussels, (2001)
- [3] E. F. Camacho, M. Berenguel, F. Rubio, "Advanced Control of Solar Power Plants", *Springer-Verlag*, (1997)
- [4] R. De Keyser, "Model Based Predictive Control", *Invited Chapter in UNESCO Encyclopedia of Life Support Systems (EoLSS)*, article 6.43.16.1, Eolss Publishers Co Ltd, 30p, ISBN 0 9542 989 18-26-34 (2003)

Multi-Agent Control for Large-Scale Transportation Systems

Alina Tarău Bart De Schutter Hans Hellendoorn
 Delft Center for Systems and Control, Delft University of Technology
 Mekelweg 2, 2628 CD Delft, The Netherlands
 Email: {a.n.tara, j.hellendoorn}@tudelft.nl, b@deschutter.info

1 Introduction

We focus on a specific class of transportation systems, characterized by materials being processed while they are transported by conveyor systems e.g. sorting machines, baggage handling, distribution systems. During the last decades, these transportation systems have encountered increasing demands and the focus has shifted to quality, reliability, and throughput maximization. The throughput of these automated transporting machines is limited by mechanical capabilities and also by the performance of the process devices (surface scanners, address reading devices, bar-code reading devices, etc.).

Typical issues of this class of transportation systems are: coordination of the processing units, task allocation, time scheduling, prevention of jams and deadlocks, buffer overflows, avoiding damage of the goods, maximization of the throughput, cost minimization. In this presentation we will take automated sorting machines as an example of a transportation system.

2 Control problems

The throughput of a postal sorting machine is limited by physical and operational constraints. Therefore, the feeding rate has to be set as high as possible (in order to maximize the throughput), and low enough in order to avoid unprocessed items reaching the end of the delay line (buffer overflow). We consider flats sorting systems. By flats we understand large letters (A4 size envelopes), plastic-wrapped mail items, magazines, catalogs, etc. They are inserted into transport boxes by a feeder device. The boxes carry the pieces with constant speed and sort them into destination trays according to the selected sorting scheme.

The throughput of a basic system sketched above can be augmented by adding a second feeder device and designing a system which moves the trays to the right, to the left or not move at all. The new design is illustrated in Figure 1.

3 Framework

In order to control the system described in Figure 1, model-based predictive control with dynamic operational constraints is used. The system presented in Figure 1 will be modeled and analyzed, and the obtained results will be compared to the experimental results.

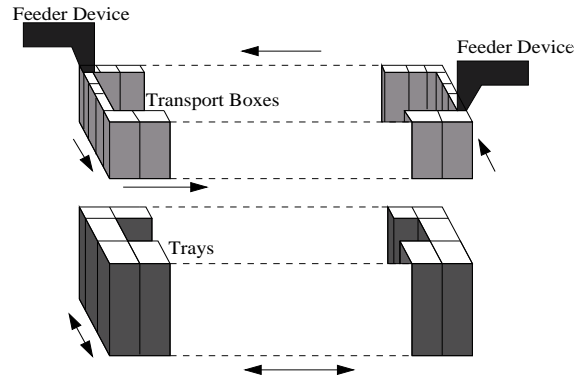


Figure 1: Flats sorting machine - a new design

For a stand-alone sorting machine, centralized control is suitable. However, when considering large-scale sorting systems, we will deal e.g. with a large number of coupled postal sorting machines, each of which may have more than one feeder device. Due to computational complexity, necessity of communication and scalability, we propose to use a multi-agent approach, see e.g. [2], combined with distributed model predictive control, see e.g. [1].

4 Conclusions and future work

Typical issues and control problems of a specific class of transportation systems have been considered, together with a solution for a flats sorting machine. In future work, the proposed algorithm will be extended to baggage handling and other sorting systems.

Acknowledgments: This research is financially supported by the STW-VIDI project Multi-Agent Control of Large-Scale Hybrid Systems' (DWV.6188), the BSIK project Next Generation Infrastructures (NGI)", and by the Transport Research Centre Delft.

References

- [1] E. Camponogara, D. Jia, B. H. Krogh, and S. Talukdar. Distributed model predictive control. *IEEE Control Systems Magazine*, 22(1):44–52, 2002.
- [2] G. Weiss. *Multiagent Systems*. London, UK: The MIT Press Cambridge, 1999.

Modular Reconfigurable Flight Control Design

E.R. van Oort, L. Sonneveldt, Q.P. Chu, J.A. Mulder

Aerospace Software and Technologies Institute

Delft University of Technology

e.r.vanoort@tudelft.nl, l.sonneveldt@tudelft.nl, q.p.chu@tudelft.nl, j.a.mulder@tudelft.nl

1 Introduction

The implementation of electronic flight control systems (FCS) and the increase of computational power on-board has opened the door to Reconfigurable and Flight Tolerant Control. The goal of the current project is to design an adaptive control scheme applicable to agile aircraft with highly nonlinear dynamics, based on a combination of separately designed modules.

2 Modular Adaptive Control

In the modular adaptive control approach the system model is parameterized with respect to an unknown vector θ . An on-line parameter estimator generates an estimate $\hat{\theta}$ at each time instant by processing the plant input and output. This estimate specifies a system model, which is treated as the “true” model for the control design: the certainty equivalence principle. An illustration of the modular approach is shown in Figure 1.

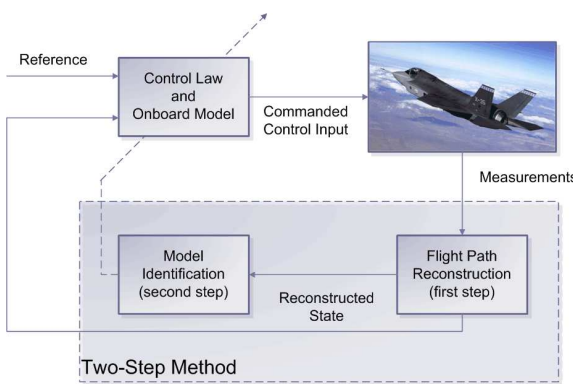


Figure 1: The modular adaptive flight control approach

One of the main advantage of such a modular control scheme is that the estimated parameters converge to their true values, if the model structure has been chosen adequately. Such knowledge can, for instance, be used for on-line health monitoring of the aircraft systems and allows for a change of control strategy based on the remaining control authority over the aircraft. Another important advantage of the modular adaptive control approach is that the parameter identifier and control law can be designed separately.

3 Control Law

The modular approach allows us to separate the control law design from the identifier design. Unfortunately, a major obstacle in such designs is the weakness of certainty equivalence controllers in the case of nonlinear systems: nonlinearities have to be severely restricted in order to achieve controller-identifier separation [1]. This weakness can be overcome by applying controllers with strong parametric robustness characteristics: achieving boundedness without adaptation. Such a design can for instance be based on a robust backstepping scheme, for which any standard gradient or least-squares identifier can be employed.

4 Parameter Estimation

An interesting approach to the parameter estimation problem is the “Two Step Method” (TSM) developed at the Delft University of Technology [2]. In this method, the state trajectory is reconstructed in the first step, while the parameters of the aerodynamic model are estimated in the second step. The first step can be based on an Extended-Kalman Filter (EKF), while simple regression methods such as recursive least squares can be used for the parameter estimation. This approach allows us not only to identify actuator failures, but also changes of the dynamics related to structural damage can be identified.

The aerodynamic parameters are varying as a (nonlinear) function of, for example, the angle of attack and the Mach number. To avoid unlearning, the flight envelope is partitioned into a certain number of clusters with similar aircraft behavior. In each of these clusters, the aerodynamic parameters are estimated and stored.

References

- [1] Miroslav Krstić, Ioannis Kanellakopoulos, and Petar V. Kokotović. *Nonlinear and Adaptive Control Design*. John Wiley & Sons, 1995.
- [2] J. A. Mulder, H. L. Jonkers, J. J. Horsten, J. H. Bree-
man, and J. L. Simons. Analysis of Aircraft Performance,
Stability and Control Measurements. *AGARD Lecture series*, (104):5–1 – 5–87, 1979.

Inverse Optimal Nonlinear Adaptive Control Design for a Missile Autopilot

L. Sonneveldt, E. R. van Oort

Aerospace Software and Technologies Institute (ASTI), Delft University of Technology

l.sonneveldt@tudelft.nl, e.r.vanoort@tudelft.nl

Q. P. Chu, J. A. Mulder

Delft University of Technology

j.a.mulder@tudelft.nl, q.p.chu@tudelft.nl

1 Introduction

The introduction of the adaptive backstepping approach [1, 2] in the beginning of the 90's led to a lot of interest in the flight control design community, mainly due to its strong convergence and stability properties and due to the fact that the method could be applied to a broad class of nonlinear systems. In this study, the control of a the nonlinear model of an aerodynamically controlled generic surface-to-air missile in the pitch plane is considered. Since the missile model is highly nonlinear and suffers from uncertainties in the aerodynamics, classical gain-scheduling control techniques are very difficult to apply. Adaptive backstepping techniques have been applied successfully in the last few years to solve the missile control problem, see e.g. [3, 4]. However, these adaptive control laws are all focussed on achieving stability and convergence rather than performance or optimality, as is the case with most adaptive backstepping designs. The transient performance results achieved by the most widely used adaptive backstepping variant, the tuning functions approach[2], only provide performance estimates on the tracking error [5], not on the control effort. The problem is that the direct optimal control problem for nonlinear systems requires the solving of a Hamilton-Jacobi-Bellman (HJB) equation which is in general not feasible.

2 Inverse Optimal Nonlinear Adaptive Control

This motivated the development of inverse optimal nonlinear control design methods [6]. In the inverse approach a Lyapunov function $V(x)$ is given and the task is to determine whether a control law minimizes some meaningful cost functional, i.e. a cost that imposes a penalty on the tracking errors and the control effort. The term inverse refers to the fact that the cost functional is determined after the design of the stabilizing feedback control law, instead of being selected beforehand by the designer. In [7] an inverse optimal adaptive backstepping control design for a general class of nonlinear systems has been derived.

In this study, an inverse optimal approach is applied to the autopilot design for the pitch control of the longitudinal missile model based on the design of [7]. The parameter

update laws of the controller have been augmented with e -modification terms and dead-zones to prevent parameter drift. A second control law is designed by means of the well known tuning functions adaptive backstepping technique, so that a comparison of both approaches can be made when applied to a practical control design problem. The stability, convergence and transient performance of both approaches are evaluated by numerical simulations with several levels of uncertainty in the aerodynamics and the control effectiveness of the missile model. The robustness of the control laws to sensor noise and (unmodeled) actuator dynamics including rate, magnitude and bandwidth limits is also examined.

References

- [1] I. Kanellakopoulos, P. V. Kokotović, and A. S. Morse, "Systematic design of adaptive controllers for feedback linearizable systems," *IEEE Transactions on Automatic Control*, vol. 36, Nov. 1991.
- [2] M. Krstić, I. Kanellakopoulos, and P. V. Kokotović, "Adaptive nonlinear control without overparametrization," *Systems and Control Letters*, vol. 19, pp. 177–185, 1992.
- [3] H. S. Ju, C. C. Tsai, and S. W. Liu, "Design of longitudinal axis full envelope control law by adaptive backstepping," in *IEEE International Conference on Networking, Sensing & Control*, 2004.
- [4] S. H. Kim, Y. S. Kim, and C. Song, "A robust adaptive nonlinear control approach to missile autopilot design," *Control Engineering Practice* 12, pp. 149–154, 2004.
- [5] M. Krstić, P. V. Kokotović, and I. Kanellakopoulos, "Transient performance improvement with a new class of adaptive controllers," *Systems and Control Letters*, vol. 21, pp. 451–461, 1993.
- [6] R. A. Freeman and P. V. Kokotović, "Inverse optimality in robust stabilization," *SIAM J. Control and Optimization*, vol. 34, pp. 1365–1391, july 1996.
- [7] Z. H. Li and M. Krstić, "Optimal design of adaptive tracking controllers for nonlinear systems," *Automatica*, vol. 33, pp. 1459–1473, 1997.

Constrained nonlinear control based on the combination of model predictive control and feedback linearization

D.A. Joosten*, T.J.J. Lombaerts[†], T.J.J. van den Boom*

*Delft Center for Systems and Control, faculty 3ME

[†]Control and Simulation Division, faculty of Aerospace Engineering

Delft University of Technology, Delft, The Netherlands

{d.a.joosten, t.j.j.lombaerts, a.j.j.vandenboom}@tudelft.nl

1 Introduction

This paper offers a discussion of the combination of feedback linearization (FBL) and linear model predictive control (MPC) to obtain a constrained and globally valid nonlinear controller. The combination of feedback linearization and linear controllers has received significant attention within the domain of aerospace engineering. The rationale for the combination of both control methods lies in the fact that a FBL controller linearizes the behavior of a nonlinear plant such that the closed loop can be controlled by a predictive controller, which is suitable for linear and time-invariant plants only.

Van Soest et al [3], for instance, show that the combination of both methods can lead to a controller for a reentry vehicle that is globally valid. The method presented in this paper differs from commonly applied methods in the sense that a control allocation step is added to the method in order to simplify the feedback linearization. Figure 1 provides a schematic of the control setup that is presented here and sections 2 and 3 present the method in more detail.

2 Control allocation and feedback linearization

The system type under consideration has the following input affine structure

$$\dot{x} = f(x) + g(x)u \quad (1)$$

$$y = h(x) \quad (2)$$

where $x \in \mathbb{R}^n$ is the state vector, $u \in \mathbb{R}^m$ are the inputs and where $y \in \mathbb{R}^p$ is the vector of outputs. It is assumed that $m \geq p$ and therefore common feedback linearization techniques [1] do not automatically apply. For ease of notation it is also assumed that $y = x$ (or $h(x) = x$), hence $p = n$. In order to resolve this issue it is possible to apply a control allocation method that maps u to a virtual input $z \in \mathbb{R}^n$ such that $z = g(x)u$. This allocation can be performed through minimization of $\|u\|^2$ subject to the constraint $z = g(x)u$ and subject to the original constraints on u .

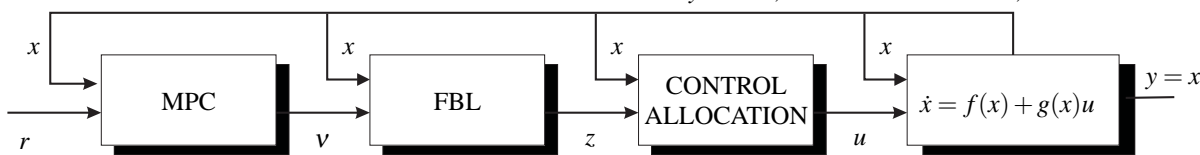


Figure 1: Overview of the complete setup of system and controller

With this choice of a virtual input z the feedback linearization problem reduces to choosing $z = -f(x) + v$ with $v \in \mathbb{R}^n$ such that the closed loop equals $\dot{x} = v$ which shows that the closed loop is linear and decoupled.

3 Model predictive control and constraint mapping

Now that the plant has been linearized it is possible to apply model predictive control to achieve reference tracking subject to constraints (see [2] for details w.r.t. MPC methods). The applied MPC method is based on quadratic programming and can take constraints into account.

Constraints on the input u , however, first need to be reformulated in terms of the input v of the feedback linearized loop. This relationship between v and u is $v = f(x) + g(x)u$ and can be used to determine the constraints on v . It is easy to see that if u has convex constraints as in $Au \leq b$, that the previous relationship denotes nothing more than the projection, albeit a time-varying one, of the original constraints into \mathbb{R}^n which itself defines a set of convex constraints on v . An issue that follows from the latter is that the constraints become state-dependent, which is impractical for MPC where constraints are assumed to be constant. Pragmatic, but conservative, solutions to this problem exist.

4 Conclusion

The presented method leads to a constrained controller for nonlinear systems (1) that is valid provided that the (failed) system is controllable. Currently, this theory is being applied in a setting of reconfigurable flight control for failed or crippled aircraft.

References

- [1] A. Isidori. *Nonlinear control systems*. Springer, 1995.
- [2] J.M. Maciejowski. *Predictive control: with constraints*. Harlow: Pearson Education, 2002.
- [3] W.R. van Soest, Q.P. Chu, and J.A. Mulder. Combined feedback linearization and constrained model predictive control for entry flight. *Journal of Guidance, Control and Dynamics*, 29 number 2:427–434, 2006.

An Iterative Feedforward Control Design Strategy for SISO Nonlinear Minimum Phase Systems

Kris Smolders, Paul Sas, Jan Swevers

Katholieke Universiteit Leuven – Department of Mechanical Engineering, PMA

Celestijnenlaan 300B, B3001 Heverlee, Belgium

{kris.smolders,paul.sas,jan.swevers}@mech.kuleuven.be

Abstract

For accurate tracking of a desired trajectory a good feedforward control is required. Based on a model this feedforward control can be obtained by inverting the model and applying the desired trajectory to the inverse. For linear time invariant (lti) systems, numerous approaches exist to invert, or approximately invert, the model (e.g.: [3]). For some applications linear approaches yield large tracking errors, usually due to the presence of nonlinear system characteristics. To improve the tracking accuracy a linear iterative learning feedforward design can be used, for example [1]:

$$u_{FF}^{[k]} = u_{FF}^{[k-1]} + \alpha^{[k]} \hat{G}^{-1} (y_r - y^{[k-1]}) ; y^{[k]} = G(u_{FF}^{[k]}).$$

$u_{FF}^{[k]}$ is the k th update of the feedforward signal to obtain the desired output y_r . \hat{G}^{-1} is a linear model of the inverse of the actual system G . In the work of De Cuyper e.a. [1] G is assumed to be lti and \hat{G}^{-1} is determined based on a measured FRF of the system. The iterative procedure is initialized by setting $u_{FF}^{[0]} = \hat{G}^{-1}(y_r)$. $\alpha^{[k]}$ is a weighting factor to improve convergence. Ideally $\alpha^{[k]} = 1$, but if the system is nonlinear one has to set $\alpha^{[k]} < 1$ to improve convergence. It has been observed that even for $\alpha^{[k]} < 1$ convergence is not guaranteed if the system is nonlinear.

This presentation discusses the combination of the iterative scheme with a novel nonlinear model structure, and presents an experimental validation of this combination. The novel nonlinear state space model structure equals:

$$\begin{aligned} \dot{x} &= Ax + Wz(x, V, G) + Bu \\ y &= Cx + Tz(x, V, G) + Du. \end{aligned} \quad (1)$$

$u \in \mathbb{R}^p$ are the inputs, $y \in \mathbb{R}^q$ are the outputs and $x \in \mathbb{R}^n$ are the states. The model combines a linear part ($Ax + Bu$, $Cx + Du$) and a nonlinear part ($Wz(x, V, G)$, $Tz(x, V, G)$). The linear part is related to the best linear approximation. For the nonlinear part general features $z(x, V, G)$ are chosen to approximate the unknown nonlinear characteristics. The features are function of the states x and parameterized by the elements of the model matrices V and G . For the considered model structure the features are $z_j(x, V_j, g_j) = 1/(1 + e^{-V_j x - g_j}) - 1/(1 + e^{-g_j})$. The combination of the nonlinear model with the iterative learning feedforward approach yields:

$$u_{FF}^{[k]} = u_{FF}^{[k-1]} + \alpha^{[k]} \left(u_{FF}^{[0]} + \hat{G}^{-1} \left[y^{[k-1]} \right] \right) ; y^{[k]} = G \left[u_{FF}^{[k]} \right].$$

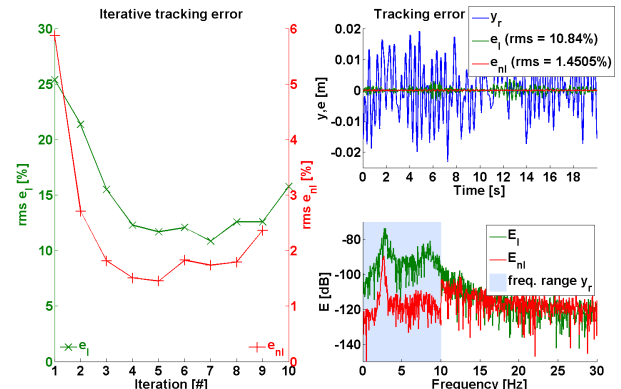


Figure 1: Iterative feedforward design on a quarter car test setup.

The brackets $[\cdot]$ indicate that the operator is nonlinear. The calculation of $\hat{G}^{-1} [\cdot]$ is the tricky part of this approach. The presentation discusses how feedback linearization [2] is applied to invert the presented nonlinear model structure (1). Due to the use of feedback linearization only minimum phase models can be used.

Experimental validation on a quarter car test setup are presented. First the identification of the model structure (1) is discussed. An iterative identification procedure is presented to identify the set of model matrices $\Theta = \{A, B, C, D, W, T, V, G\}$ under the assumption that the states x and their time derivatives \dot{x} can be determined. Then the nonlinear iterative learning feedforward design approach is applied and compared with the linear iterative learning feedforward design. Figure 1 shows the iteration results with remaining tracking error using the nonlinear model (e_{nl}) compared to the one using a linear model (e_I).

Acknowledgements

This work has been performed in the framework of project G.0528 'Accurate tracking control for nonlinear multi-variable systems based on experimentally identified general block-oriented models' of the Fund for Scientific Research - Flanders (FWO).

References

- [1] J. De Cuyper, D. Coppens, C. Liefooghe, J. Swevers, M. Verhaegen; *Advanced Drive File Development Methods for Improved Service Load Simulation on Multi Axial Durability Test Rigs*; Proc. of the International Acoustics and Vibration Asia Conference, Singapore, 1998; pp. 339-354,
- [2] H.J. Marquez; *Nonlinear Control Systems: Analysis and Design*, Wiley, 2003.
- [3] D. Torfs, J. De Schutter, J. Swevers; *Extended Bandwidth Zero Phase Error Tracking Control of Nonminimal Phase Systems*; Journal of Dynamic Systems, Measurement, and Control; September 1992, vol. 114; pp. 347-351.

Inferring scenario trees for stochastic programming: A machine learning perspective

Boris Defourny, Rodolphe Sepulchre, Louis Wehenkel
Systems and Modeling Research Unit

University of Liège, Montefiore Institute, Grande Traverse 10, B-4000 Liège, Belgium
Email: bdf@montefiore.ulg.ac.be, R.Sepulchre@ulg.ac.be, L.Wehenkel@ulg.ac.be

Abstract

We advocate the use of machine learning techniques to build scenario trees and show the interest of the approach on a two-stage decision problem under uncertainty relevant in the electric power generation industry.

1 Scenario trees as a representation of uncertainty

Optimization problems under uncertainty (see [1] for an excellent introduction) such as planning or portfolio optimization often involve time and thus require an adequate representation of the possible futures, e.g. by scenarios. In the context of stochastic programming, an approach consists in representing uncertainty in the form of a scenario tree — see for example [2]. Such a tree structure allows to model how our information about the future may evolve with time. In this talk, we consider the problem of building a tree T from a set of realizations ω_i of the uncertain process. The quality of the tree depends on the performance of the decision policy π_T obtained from the subsequent optimization problem under uncertainty $\mathcal{P}(T)$.

2 Distance between scenarios

The definition of a measure of distance between scenarios appears as a critical issue as soon as one tries to organize scenarios according to a tree structure. We propose to cast this problem as the definition of kernels between scenarios. A kernel gives the inner product between induced features of two objects. Kernels lie at the heart of many successful algorithms in machine learning.

A natural choice of scenario feature appears to be an estimate of the value of the objective function of \mathcal{P} , should this scenario occur and an optimal (but yet unknown) policy be used.

In addition, we propose to consider as features estimates of optimal actions under a (yet unknown) optimal policy, should the scenario occur. Indeed, it might be unnecessary to distinguish in the policy optimization stage scenarios for which optimal decisions will be close.

3 Tree building algorithms

We propose two scenario clustering algorithms for tree inference.

The first algorithm adopts a splitting scheme. At time 0 the scenarios are put in a same cluster. Then we increase the time index, and the divergence between scenarios appears. We define a prototype scenario for the cluster, using the kernelized distance measure. The construction of the prototype corresponds to the growing of a branch in the tree. Moreover the kernels allow us to compute a variance among the scenarios for each time step. As soon as that variance exceeds a certain threshold, the scenarios are partitioned into two clusters. The algorithm is then applied recursively to each new cluster, starting new branches in the tree. The resulting tree is guaranteed to contain branches of bounded variance. Its complexity depends on the value of the threshold.

The second algorithm projects the scenarios on a specified tree structure. Segments of prototype scenarios associated to branches are tuned such that replacing each scenario by its best prototype induced by a path in the tree incurs a low distortion. A shortest-path formulation of the problem allows close scenarios to share a same path even if they diverge temporarily — a property not shared by the first algorithm.

4 Application to energy reserves management

We consider the problem of meeting an uncertain electricity demand with minimal expected cost. The decision at time t consists in fractioning the production between a costly gas turbine and a hydraulic power plant limited by a reservoir subject to uncertain water supplies. We compare different kernels between scenarios. From the assessment of the found policies we show that considering features based on estimates of optimal decisions leads to trees that perform well.

References

- [1] R. T. Rockafellar, *Optimization under uncertainty*, Lecture notes, University of Washington.
- [2] J. Dupacova, N. Gowe-Kuska and W. Romisch, *Scenario reduction in stochastic programming : an approach using probability metrics*, Mathematical Programming, Series A 95 :493–511, 2003.

Automatic classification of primary frequency control behavior

B. Cornélusse

Montefiore Institute¹

cornelusse@montefiore.ulg.ac.be

C. Wéra

Elia System Operator, Brussels (Be)

claude.wera@elia.be

L. Wehenkel

Montefiore Institute

L.Wehenkel@ulg.ac.be

1 Motivation

In Europe, the transmission system operator (TSO) is responsible for operating, maintaining and developing the high voltage grid. The liberalization of the electric sector means that the transmission system operator should leave maximum freedom to the transactions, while ensuring system security and providing access to the grid in a non-discriminatory way. At the same time each TSO is asked to minimise his own costs and to justify them in a transparent way. In this context, the system operator is responsible of various ancillary services, such as active and reactive load balancing, which generally must be supplied by generators in order to warrant secure operation and maintain voltages, frequency, active and reactive power exchanges within prescribed bounds. Depending on the typical regulatory framework, these services are purchased beforehand through bilateral contracts or through various ancillary service markets. Afterwards, the system operator verifies whether the services have indeed been delivered so as to determine the corresponding financial transactions. In this paper, we consider the particular case of primary frequency control in the Belgian power system. The UCTE rules impose that the participation of the Belgian system to the overall frequency control of the European interconnection is approximately equal to 700 MW/Hz, and is entirely delivered within 30 seconds after a frequency drop [1, 2]. Note that the recent near-blackout [3] of November 4 2006, has shown how important it is that the primary frequency control devices have adequate performance to avoid frequency collapse in the case of system islanding. Adequate responsiveness is also mandatory in more normal conditions, to avoid large frequency deviations upon generator tripping or tariff changes inducing significant load variations on a day by day fashion.

2 Methodology

The methodology of the Belgian TSO in matters of primary frequency control consists in establishing direct contracts with the generators connected to the system for participation. After the fact, on a monthly basis, the TSO identifies the most important events in terms of frequency dips or peaks, and analyses how each one of the contracted units actually behaved under these circumstances. The goal of this analysis is to classify each unit into a number of a priori defined performance classes (satisfactory operation, ramping, pumping, oscillating, no response etc.). This information is then used to determine appropriate feedback to the generators, in order to encourage them to provide appropriate primary frequency performance. While currently these analyses are carried out in a more or less manual fashion by experts looking at power/frequency curves of all generators, the goal of our work is to develop an automatic method

based on automatic learning to carry out the performance classification. More precisely, the proposed approach uses a training set of pre-analysed power/frequency curves, for a large number of generators and frequency events, and applies to this training set machine learning techniques in order to build a classifier which mimics at best the expert classification given in the training set and generalises well to unseen scenarios [4]. From a methodological point of view, this is a time-series classification problem: for each event and each generator, the input data is composed of two time series (of 900 time-steps of 2s duration), describing the frequency and active power evolution over a 30 minutes interval centred around the frequency event. The output is the label of the performance class determined by the expert for this particular event/generator combination. Machine learning algorithms can be applied to a training set composed of a representative number of such input-output combinations, in order to automatically construct a performance classifier. This latter may then be applied to new cases, to automatically predict the performance class.

3 Results

In the paper, we will report on the results obtained on a set of 652 scenarios corresponding to different frequency events and to the generators agreed by the Belgian TSO to take part in the primary control. These scenarios were gathered from real-time recordings in the Belgian system over the 2003 to 2005 period. We have applied various state-of-the-art machine learning algorithms (tree-based ensemble methods, support vector machines) and preprocessing steps (Fourier and wavelet analyses, signal features, time-domain sampling, normalisations etc.), in order to identify the best way to handle such complex and noisy data sets. This analysis revealed that a classifier obtained by machine learning can classify generator performance with a error rate of about 10% with respect to the manual expert classification. We will discuss how this classifier may be used in practice to identify with high reliability a reduced number of curves for further analysis by the experts, thus significantly reducing the burden of human analysis.

References

- [1] UCTE Operation handbook. *Policy 1: Load-Frequency Control and Performance*.
- [2] UCTE Operation handbook. *Appendix 1: Load-Frequency Control and Performance*.
- [3] UCTE. Interim Report, System Disturbance on 4 November 2006. Technical report, 2006.
- [4] Louis Wehenkel. *Automatic learning techniques in power systems*. Kluwer Academic, Boston, 1998.

¹Department of Electrical Engineering & Computer Science, ULg (Be)

State estimation for distributed control of a semi-active suspension system for a passenger car

Maarten Witters (maarten.witters@mech.kuleuven.be), Jan Swevers, Paul Sas
K.U.Leuven, Department of Mechanical Engineering, PMA - Celestijnenlaan 300B, B-3001 Heverlee

1 Introduction

The first results of a research project are presented that investigates distributed control of semi-active suspension systems for a passenger car. The starting point is the centralized model free controller developed in a previous project [1]. This control algorithm uses estimates of modal velocities: heave, roll and pitch, which are calculated from corner acceleration measurements.

In the distributed control architecture, each shock absorber is equipped with its own control unit. For estimating the modal velocities, the units have to exchange sensor measurements over a communication network. This introduces a variable delay on the available data. The presented work discusses the development of a state estimator for the modal velocities that can cope with these delays. Some simulation results are presented to validate the state estimator.

2 The system model

A car can be simplified to a system consisting of five masses: four wheels and the car body. The suspension system is modelled as a spring and a damper in parallel, the tyre is reduced to a single spring. The system model used in the state estimator only describes the movement of the car body and uses the rattle velocities¹ as input, instead of the road profile which can not be measured. Assuming linear springs and dampers, the system can be represented with a discrete, linear time invariant state space model:

$$x(t_{n+1}) = Ax(t_n) + Bu(t_n). \quad (1)$$

The used sampling time is 0.01 s. The state vector, x , contains the heave, roll and pitch velocities, while the input vector, u , consists of the rattle velocities. The system matrices A and B are estimated with a MIMO identification procedure based on data obtained from a non-linear multibody simulation model of the car, using broadband road excitation.

3 The state estimator

The developed state estimator for the modal velocities is based on the filter proposed in [2]. The measurements that are distributed over the network experience an unknown delay. Experimental analysis of this communication showed that this delay will not be larger than the sampling time of

¹The rattle velocity is the relative velocity between the carbody corner and the wheel.

the estimator. So the sensor measurements produced at time t_n will be available at each of the control units at time t_{n+1} . Based on this knowledge, the following state estimator can be formulated:

$$\hat{x}(t_{n+1}|t_{n+1}) = A\hat{x}(t_n|t_n) + Bu(t_n) + K(t_{n+1})[y(t_n) - \hat{y}(t_n|t_n)] \quad (2)$$

where: $\hat{y}(t_n|t_n)$ the estimated output at time t_n ,
 $K(t_{n+1})$ the filter gain.

As in a normal Kalman filter, the filter gain depends on the system matrix A and the covariance matrices of the measurements and the model errors (see [2]).

4 Results and conclusions

Figure 1 shows the error on the estimated heave velocity. The estimation errors for the roll and pitch velocities are comparable in magnitude. In the next phase of the project, the described approach will be validated on a real vehicle, equipped with a semi-active suspension system.

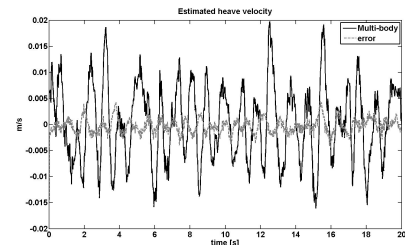


Figure 1: The estimation error for the heave velocity.

5 Acknowledgements

This work is a joint project between Tenneco Automotive Europe, Flanders Mechatronic Technology Centre (FMTc) and K.U.Leuven. The project is funded by the Institute for Promotion of Innovation by Science and Technology in Flanders (IWT).

References

- [1] C. Lauwerys (2005), *Control of active and semi-active suspension systems for passenger cars*, (PhD) K.U.Leuven, Department of Mechanical Engineering, Heverlee (Belgium).
- [2] A. Matveev, A. Savkin (2003), *The problem of state estimation via asynchronous communication channels with irregular transmission times*, IEEE Trans Automat. Contr., Vol 48(4), 670-676.

Interval Estimation with Confidence Degree - Application to AUV Positioning

G. Goffaux, A. Vande Wouwer, M. Remy

Service d'Automatique

Faculté Polytechnique de Mons

Boulevard Dolez 31, B-7000 Mons

Guillaume.Goffaux, Alain.VandeWouwer, Marcel.Remy@fpms.ac.be

State estimation techniques are commonly applied to vehicle positioning problems, in which position and velocity have to be reconstructed in real-time. Accuracy is of course desirable, but in some applications, security can be even more important. For instance, aircraft or train positioning requires a very high level of security so as to avoid collisions which could cause human and material loss.

In these applications, positioning information is usually given in the form of intervals bounding variables and parameters with some degree of confidence. In this context, interval algebra [4] has been used to build guaranteed intervals. However, guaranteed intervals can be a too idealistic assumption in some applications with critical security requirements, and some recent works report on optimal interval fusion [2, 6].

The objective of this study is to develop a confidence interval algorithm based on a dynamic model and sensors. First, a predictor is designed following the line of thoughts in [3]. This predictor is based on a nonlinear dynamic model of the vehicle, in order to estimate bounds on state variables with lower bounded integrity. Then, at each measurement time, intervals from sensors and the predictor are combined by union and intersection operations [1]. Every possible combinations are investigated such that the derived integrity satisfies the integrity objective. Then, the shortest non-empty interval is chosen among the safe intervals.

The proposed algorithm is illustrated with a positioning problem related to an autonomous underwater vehicle taken from the Marine GNC Matlab© Toolbox [5].

The developed method performs well and allows to satisfy security demand in critical applications (figure 1). This method is general and can be applied to various problems characterized by uncertainties on the initial state, inputs and parameters. Furthermore, it can handle any kind of statistical distribution.

Acknowledgements

This work is performed in the framework of the **PIST** project funded by the Walloon Region - DGTR (Belgium).

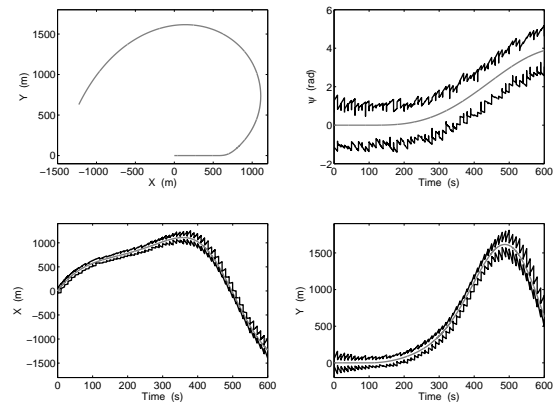


Figure 1: Confidence interval estimation for AUV positioning.

References

- [1] O. Bilenne. Integrity-directed sensor fusion by robust risk assessment of fault-tolerant interval functions. In *Proceedings of the 9th International Conference on Information Fusion*, 2006.
- [2] E. Druet, O. Bilenne, M. Massar, F. Meers, and F. Lefèvre. Interval-based state estimation for safe train positioning. In *7th World Congress on Railway Research*, 2006.
- [3] M. Z. Hadj-Sadok and J.-L. Gouzé. Estimation of uncertain models of activated sludge process with interval observers. *Journal of Process Control*, 11(3):299–310, 2001.
- [4] L. Jaulin, M. Kieffer, O. Didrit, and E. Walter. *Applied Interval Analysis*. Springer, London, England, 2001.
- [5] Marine Systems Simulator. *Norwegian University of Science and Technology*. Trondheim, Norway, 2005. <www.cesos.ntnu.no/mss>.
- [6] Y. Zhu and B. Li. Optimal interval estimation fusion based on sensor interval estimates with confidence degrees. *Automatica*, 42:101–108, 2006.

Constrained estimation with truncated Gaussians

Diederik Verscheure

K.U.Leuven, Dept. of Mech. Eng.

diederik.verscheure@mech.kuleuven.be

Jan Swevers

K.U.Leuven, Dept. of Mech. Eng.

jan.swevers@mech.kuleuven.be

Joris De Schutter

K.U.Leuven, Dept. of Mech. Eng.

jan.swevers@mech.kuleuven.be

1 Introduction

The state estimation problem consists of estimating the hidden state of a dynamic system, governed by a stochastic linear or nonlinear process model, from a set of noisy observations, which depend on the hidden state by a stochastic linear or nonlinear observation model. This problem is often solved recursively using Bayesian filtering. In the recursive Bayesian filtering approach, a new state estimate is determined at every time-step, given the latest measurement and some knowledge of the state at the previous time-step. However, incorporating a priori knowledge in the form of equality or inequality constraints on the states proves to be difficult and is still a topic of ongoing research [1, 2].

Another popular approach to on-line state estimation, is moving horizon estimation (MHE) [3], which can be considered to be a modified batch method. An important advantage of MHE over the Gaussian filter variants [6] is that it is quite natural to take into account a priori knowledge in the form of inequality constraints [4]. However, in the general nonlinear case, the MHE approach requires solving a constrained nonlinear program at every time-step, which may prove to be difficult and computationally expensive.

2 Method

Instead of turning to MHE for constrained estimation, a novel idea is introduced based on modified recursive Gaussian filters for constrained estimation by considering the class of truncated Gaussians [2]. By considering this class of distributions, prior knowledge or considerations based on physical insight can be taken into account in the form of inequality constraints on the states. Specifically, we discuss the class of Gaussians truncated outside hyperrectangles. A constrained recursive estimation algorithm is developed, based on modified Gauss-Hermite quadrature rules [6] to evaluate integrals numerically over bounded hyperrectangles. The methodology is not limited to linear systems and is easily applicable to one-dimensional systems, but extension to more-dimensional problems poses some problems. An approximate extension for more-dimensional is presented. Simulation results are presented which indicate the benefit of the proposed method both in the one-dimensional and

more-dimensional case.

3 Conclusions and future work

It is shown that the class of truncated Gaussians proves to be very useful for constrained estimation. Applications include constrained estimation for use in closed-loop, a better calculation of the arrival cost in MHE and the possibility to include inequality constraints based on physical insight or a priori knowledge. Future work includes extension to domains more general than hyperrectangles.

4 Acknowledgements

The authors gratefully acknowledge the financial support by K.U.Leuven's Concerted Research Action GOA/05/10.

References

- [1] D. Simon and D. Simon, "Kalman filtering with inequality constraints for turbofan engine health estimation," *IEE Proceedings Control Theory & Applications*, vol. 153, no. 3, pp. 371–378, 2006.
- [2] D. Simon and D. L. Simon, "Constrained kalman filtering via density function truncation for turbofan engine health estimation," National Aeronautics and Space Administration, Washington, DC, Technical report NASA TM-2006-214129, 2006.
- [3] D. G. Robertson, J. H. Lee, and J. B. Rawlings, "A moving horizon-based approach for least-squares estimation," *AICHE Journal*, vol. 42, no. 8, pp. 1547–15905, 1996.
- [4] C. Rao and J. Rawlings, "Constrained process monitoring: moving horizon approach," *AICHE Journal*, vol. 48, no. 1, pp. 97–109, 2002.
- [5] C. Rao, J. Rawlings, , and D. Mayne, "Constrained state estimation for nonlinear discrete-time systems," *IEEE Transactions on Automatic Control*, vol. 48, no. 2, pp. 246–258, 2003.
- [6] K. Ito and K. Xiong, "Gaussian filters for nonlinear filtering problems," *IEEE Transactions on Automatic Control*, vol. 45, pp. 910–927, 2000.

Data-based velocity observer using encoder time stamping

Roel Merry [§], René van de Molengraft, and Maarten Steinbuch
 Technische Universiteit Eindhoven, Department of Mechanical Engineering
 P.O. Box 513, 5600 MB Eindhoven, The Netherlands
 Email: [§]R.J.E.Merry@tue.nl

1 Introduction

In motion systems, position measurements are often obtained using optical incremental encoders. The position accuracy is limited by the quantized position measurement of the encoder. Velocity and acceleration signals obtained by numerical differentiation are dominated by high-frequency content due to the quantization. In literature, several methods have been proposed to improve the position and velocity estimations using position measurements at irregular time instants [1, 2]. These methods often require a system model to be available or are not applicable in real-time experiments.

The research focusses on the development of a fully data based observer. The observer can be applied in real-time and is based on the time stamping concept.

2 Time stamping

The time stamping concept uses the time instants of encoder transitions t_i together with their position x_i as shown in Fig. 1.

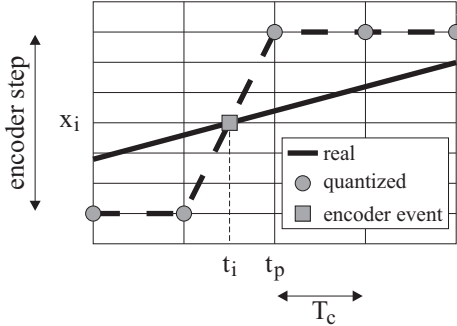


Figure 1: The time stamping concept.

The pair (t_i, x_i) is called an encoder event. The proposed observer uses a number of stored encoder events to estimate the position, the velocity and the acceleration signals.

3 Signal estimation

The position estimation is performed by fitting a polynomial of order m through n encoder events by the least squares method ($m < n$). Extrapolation of the fitted polynomial with

coefficients $p_{0,\dots,m}$ at time instant t_e results in the estimated position $\tilde{x}_e(t_e)$

$$\tilde{x}_e|_{t=t_e} = \sum_{j=1}^m p_j t_e^j + p_0. \quad (1)$$

The estimated velocity $\dot{\tilde{x}}_e$ and acceleration $\ddot{\tilde{x}}_e$ at time t_e are obtained by differentiation of the polynomial (1).

4 Experimental results

The estimated position \tilde{x}_e does not exhibit quantization effects. The estimated velocity and acceleration signals of the time stamping concept are much smoother than the differentiated encoder measurements, see Fig. 2.

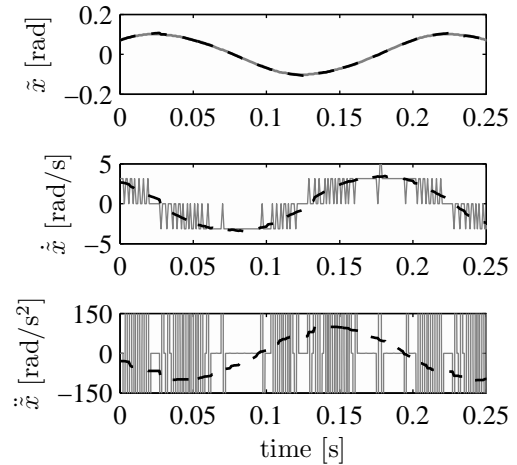


Figure 2: Position, velocity and acceleration signals obtained by the quantized and differentiated encoder measurements (solid) and by the time stamping concept (dashed).

References

- [1] R.H. Brown, S.C. Schneider, and M.G. Mulligan. Analysis of algorithms for velocity estimation from discrete position versus time data. *IEEE Transactions on Industrial Electronics*, 39(1):11–19, 1992.
- [2] P.S. Carpenter, R.H. Brown, J.A. Heinen, and S.C. Schneider. On algorithms for velocity estimation using discrete position encoders. *IEEE conf. on Industrial Electronics, Control, and Instrumentation*, 2:844–849, 1995.

Gain Scheduling Control for a Structural Acoustic Isolation Problem

Bart Paijmans, Jan De Caigny, Juan F. Camino, and Jan Swevers

Department of Mechanical Engineering

Katholieke Universiteit Leuven

Celestijnenlaan 300B, B3001 Heverlee, Belgium

juan.camino@mech.kuleuven.be

1 Abstract

This work investigates the performance of an \mathcal{H}_2 interpolating gain scheduling (IGS) controller for a structural acoustic isolation problem, for which the dynamics are highly sensitive to changes in the temperature. The proposed controller is required to attenuate the sound pressure transmitted through a plate under structural vibration. It is shown that the proposed IGS controller can achieve satisfactory performance with guaranteed closed-loop stability. The IGS controller is also compared to an LPV controller designed considering that the system varies inside a polytope where the vertices are described by four local models of the plant.

2 Introduction

A main source of noise inside aircraft cabins is the so called structural noise, generated by the vibration of the surrounding structure. In recent years, a significant amount of research in the area of acoustics has been carried out, showing that the active control strategies in many practical applications are effective in reducing low frequency noise.

It is also well known that the trade-off between performance and robustness plays an important role in the control design. Thus, when one is faced with a time-varying system, the nominal model and the uncertainty bounds should be appropriately determined. However, for most practical applications, this is a difficult task, and the final estimated uncertainty set is in general too conservative.

3 Experimental Test Setup

In many aerospace applications, the structure is subject to extreme temperature changes. In a smaller scale, this characteristic is captured by the Lexan plate used in our setup, since the material is highly sensitive to temperature changes. Consequently, the dynamics of the system also changes according to the temperature. This is illustrated in Figure 1 that shows the frequency response functions (FRF) from the control actuator to the error sensor for a grid of ten temperatures T ranging from 22.9 to 25.5 degrees Celsius.

4 Interpolating Gain Scheduling Design

In the IGS approach [3], the controllers designed for fixed operating points are interpolated to construct a gain scheduling

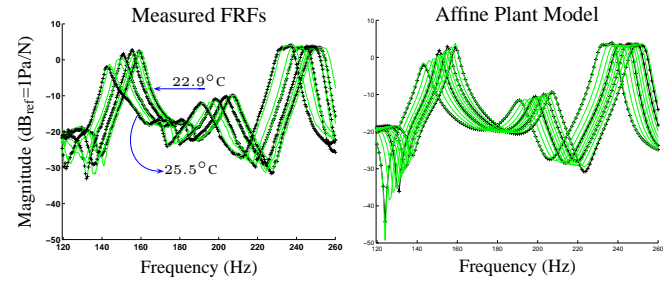


Figure 1: Experimental FRFs and the affine model.

ing controller with the following affine representation:

$$\begin{aligned} \dot{x}_c &= (A_0 + P(T)A_1)x_c + By \\ u &= (C_0 + P(T)C_1)x_c + Dy \end{aligned} \quad (1)$$

where $P(T)$ is a polynomial on T . For that purpose, we first split the ten measured FRF data presented in Figure 1 into four groups. For each group, we select a nominal FRF, and for each of these nominal FRFs, we design an \mathcal{H}_2 controller [1] using an 10th-order estimated model. To obtain the global controller (1), we apply an affine interpolating procedure between the poles, zeros and gains of the four local controllers as a function of the temperature T .

5 Numerical Results

Since the IGS approach does not guarantee stability, we use the robust stability criteria given in [2] to check if the closed-loop system is asymptotically stable. For this purpose, we also derive an affine model for the open-loop plant using the IGS approach. This is illustrated in Figure 1. The resulting final closed-loop system using the gain-scheduling controller (1) is also affine on $P(T)$. Using the LMI condition from [2], we found that the closed-loop system was stable.

References

- [1] Lazaro V. Donadon et al. Comparing a filtered-X LMS and an \mathcal{H}_2 controller for the attenuation of the sound radiated by a panel. In *Proc. of the ISMA*, Leuven, September 2006. (cdrom).
- [2] R. C. L. F. Oliveira et al. LMI conditions for robust stability analysis based on polynomially parameter-dependent lyapunov functions. *Syst. & Contr. Letters*, 55(1):52–61, 2006.
- [3] B. Paijmans et al. Gain-scheduling control for mechatronic systems with position dependent dynamics. In *Proc. of the ISMA*, Leuven, September 2006. (cdrom).

Experimental Stabilization and Tracking of a Nonholonomic Control Moment Gyroscope

J. van de Loo*, H. Nijmeijer

Department of Mechanical Engineering, Eindhoven University of Technology,
P.O. Box 513, 5600 MB, Eindhoven, The Netherlands; Email: *j.v.d.loo@student.tue.nl

M. Reyhanoglu

Department of Physical Sciences, Embry-Riddle Aeronautical University, Daytona Beach, Florida, USA

1 Introduction

A restricted Control Moment Gyroscope (CMG) is studied, which constitutes a remarkable example of a nonholonomic system (see e.g. [1]), where the nonholonomy arises as a consequence of its symmetry properties. The CMG, as depicted in Figure 1, is used to experimentally validate two different control strategies already available in the literature. The geometric phase technique [2] is used first to design a feedback control algorithm for the control of the CMG system to a desired equilibrium. Secondly a cascaded backstepping approach [2] is followed to develop a state feedback control law for the tracking of the CMG. To be able to design and validate the control strategies by means of simulations, a nonholonomic control system formulation is made for the restricted CMG dynamics. The results from the numerical simulations are compared with experimental results to illustrate the effectiveness of the controllers.

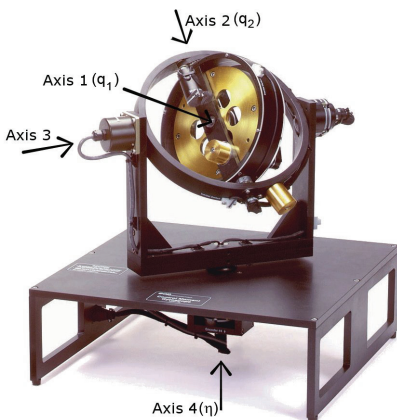


Figure 1: Control Moment Gyroscope (CMG).

2 Mathematical Model CMG

The CMG has four degrees of freedom (DOF) of which only two are actuated. To reduce the complexity of the system one DOF (axis 3 in Fig. 1) is locked, which results in a system with three DOF of which two are actuated (axis 1 and 2). This underactuated nonholonomic system can be described, after partial state feedback linearization and conversion to the chained form, as

$$\dot{z}_1 = v_1,$$

$$\dot{z}_2 = v_2,$$

$$\dot{z}_3 = z_1 v_2,$$

where z_i , $i = 1, 2, 3$ are the states and v_1 , v_2 the inputs after coordinate transformation to the chained form.

3 Geometric Phase Method

The first control strategy implemented on the CMG is based on the geometric phase method. This technique can be used to transfer the system from any initial rest configuration to the origin using specific properties from nonholonomic systems. The results from a simulation and an experiment are depicted in Figure 2.

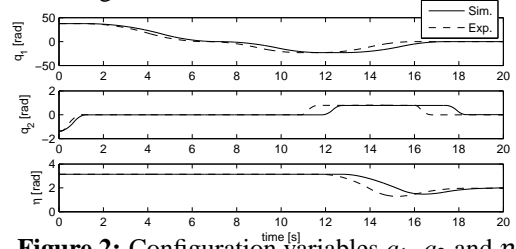


Figure 2: Configuration variables q_1 , q_2 and η .

4 State Feedback Tracking

The second controller tested on the CMG is a state feedback tracking controller based on a cascaded backstepping approach. The results from both a simulation and an experiment are depicted in Figure 3.

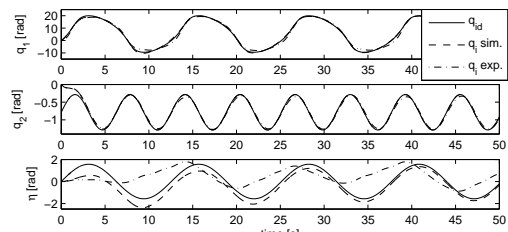


Figure 3: Configuration variables q_1 , q_2 and η .

5 Results

The results from the stabilizing controller based on the geometric phase method show that it works well in both simulations and experiments although friction is causing problems, so multiple geometric phase paths were needed to reach the origin. The tracking controller performs well in simulations without friction, but friction in the unactuated DOF causes a significant tracking error in the experiments. It can be concluded that both algorithms work well, but results can be improved by some sort of friction compensation.

References

[1] A.M. Bloch, *Nonholonomic Mechanics and Control*, Springer, New York, NY, 2003.
 168 [2] J. van de Loo, M. Reyhanoglu and H. Nijmeijer, "Experimental Stabilization and Tracking of a Nonholonomic Control Moment Gyroscope", Submitted for publication.

Analysis and modelling of analog discrete-time systems using multisine excitations

Lynn Bos, Gerd Vandersteen and Yves Rolain
 Vrije Universiteit Brussel, dep. ELEC, Pleinlaan 2, 1050 Brussel, BELGIUM
 email: lynn.bos@vub.ac.be

I. INTRODUCTION

Analog discrete-time systems are becoming more important in deep-submicron CMOS technologies [1]. These systems are based on switched-capacitor (SC) technologies where the sampling switches, driven by a periodic clock, make the overall system periodic time-varying (PTV). The PTV behaviour results into the frequency folding of frequency components higher than the Nyquist frequency.

The nonlinear distortion of nonlinear time-invariant systems can be quantified and qualified using a random phase multisine (MS) with a user defined amplitude spectrum [2]. A random phase MS is a sum of harmonically related sines with each a random phase between $[0, 2\pi]$. A random odd MS is an odd MS where 1 random odd frequency line in a group of consecutive odd lines is not excited. This enables the measurement of the even and odd nonlinearities (NL) on the respectively even and non-excited odd lines in the output spectrum. These non-excited lines are the so-called detection lines [1].

Random odd MS can't be used straightaway for PTV systems. The non-excited detection lines of a random odd MS do not only contain the nonlinear contributes, but also the aliasing components due to the frequency folding introduced by the PTV behaviour of the system.

This paper introduces an analysis with a specially designed MS for PTV systems in Section II which enables the separation of the different linear and nonlinear contributions. The concept of the best linear approximation is extended towards PTV systems in Section III. This makes it possible to determine the conversion matrix of the best linear PTV approximation of the circuit. The technique is illustrated using transistor-level simulations on a 5th order SC filter.

II. SPECIAL MS FOR PTV SYSTEMS

The separation of the nonlinear distortions and the aliasing components of the PTV system is done by exciting with $2m+1$ periods (with $m \in \mathbb{N}$) of a random odd MS with fundamental frequency f_0 . This fundamental frequency is chosen such that the periodicity T_c of the LTV system satisfies $\frac{1}{T_c} = f_c = \left(k + \frac{1}{2m+1}\right)f_0$ with $k \in \mathbb{N}$. This input spectrum guarantees that only the even and the odd nonlinear distortions are respectively on the even and the odd non-excited multiples of f_0 . If the input spectrum is limited up to $(2m+1)f_c/2$, then the aliasing components between $[f_c/2, (2m+1)f_c/2]$ lay on the frequencies which are multiples of $\frac{f_0}{2m+1}$ and which are no multiples of f_0 . This is illustrated in Figure 1. The special designed MS excitation is applied to SPICE-simulations of a 5-pole elliptic biquadratic SC filter. The output spectrum in Figure 2 shows the linear (.), the even NL (*), the odd NL (o) and the

aliasing linear (+), even NL (x), and odd NL (●) contributions. Although the signal at the input is continuous in time, the signal at the output is considered discrete-time. This output spectrum is unfolded to ease the interpretation of the plot.

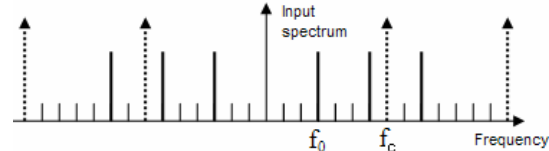


Figure 1: Input spectrum indicating the excited lines for $m=1$ and $k=2$

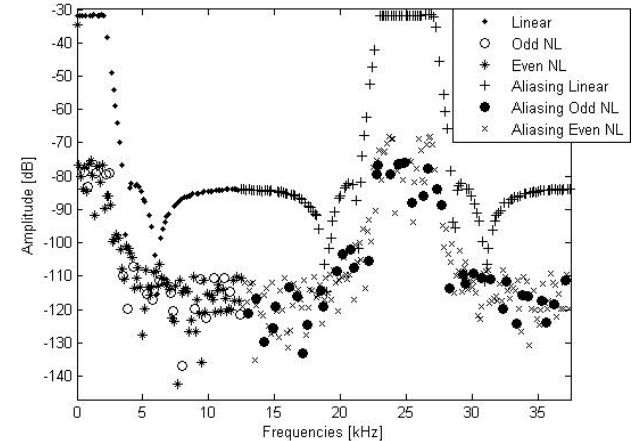


Figure 2: Unfolded output spectrum of SC filter using the proposed MS with $m=1$, $k=333$, $f_c=25\text{kHz}$, $f_0=75\text{Hz}$, $\text{RMS}_{\text{in}}=0.5\text{V}$

III. MODELLING OF PTV SYSTEMS

Analog nonlinear time-invariant systems like OPAMPS and power amplifiers were already modelled by the best linear approximation (BLA) by using random phase MS [3]. An extension of this model towards best linear PTV systems will be presented. This requires the extension from transfer functions (used for the BLA) towards conversion matrices. All components in this matrix can be extracted out of simulation results of Figure 2.

IV. CONCLUSION

The proposed MS excitation allows the analysis and modelling of PTV systems using a best linear PTV approximation. The method is illustrated using transistor level simulations of a SC filter, showing the ability of separating the linear, PTV behaviour and the nonlinear distortions.

References

- [1] R. B. Staszewski, K. Muhammad, D. Leipold et al. *All-Digital TX Frequency Synthesizer and Discrete-Time Receiver for Bluetooth Radio in 130-nm CMOS*. ISSC, Vol. 39, No.12, pp. 2278-2291, 2004
- [2] J. Schoukens, R. Pintelon, T. Dobrowiecki, Y. Rolain. *Identification of linear systems with nonlinear distortions*. Automatica, Vol. 41, No. 3, pp. 491-504, 2005
- [3] L. De Locht, G. Vandersteen, P. Wambacq, Y. Rolain et al. *Identifying the main nonlinear contributions: use of multisine excitations during circuit design*. ARFTG, pp. 74-84, 2004

Trajectory Piecewise Linear approach for nonlinear differential-algebraic equations in circuit simulation

Thomas Voß

University of Groningen, Faculty of Mathematics & Natural Sciences,
Nijenborgh 4, 9747 AG Groningen, The Netherlands
t.voss@tudelft.nl

1 Introduction

Nowadays a lot of nonlinear circuits which are used in many fields are a mixture of analogue and digital parts. The digital parts contain several sub-circuits, that have the same dynamics and only have different inputs. So simplifying these parts gives a good speed up for the transient analysis.

In this paper we present a Trajectory Piecewise Linear (TPWL) approach for nonlinear differential algebraic equations (DAE) which is based on [1]. The difference between an ordinary differential equation and a DAE is that for DAE we have additional algebraic constraints which introduce problems in the TPWL method¹.

2 Trajectory Piecewise Linear Model Order Reduction

The idea behind the TPWL method is to linearise the system several times along a typical trajectory. Then we use the local linearised systems to create a global reduced subspace and project each of them into this global reduced subspace. The final TPWL model is then a weighted sum of all local linearised reduced systems. In the following subsections we show how we apply the described steps.

2.1 Creating the local linearised models

The disadvantage of the standard linearisation methods is that the solution is only trustable if it stays close to the linearisation tuple (LT). To overcome this disadvantage the idea is to take several linearised models to create the TPWL model. Then we can trust in the results as long as the solution stays close to one of the LT.

2.2 Creating the global reduced subspace

Next we construct the global subspace. The idea is to merge all local reduced subspace to get the global reduced subspaces. To do this we create $\tilde{P} := [P_1, \dots, P_p] \in \mathbb{R}^{n \times rp}$ which spans then the union of all local reduced subspaces. Then we use a singular value decomposition (SVD) to create the final global subspace $P = U(:, 1:r)$ with $\tilde{P} = U\Sigma V^T$.

2.3 Creating the TPWL model by weighting

Now we need to combine the local linearised reduced systems to get the global TPWL model. We do this by a

¹The creation of the linearisation tuples and the linear model order reduction are more difficult

weighted sum of local models

$$\sum_{i=1}^p w_i (C_{ir} \dot{\mathbf{y}} + G_{ir} \mathbf{y} + B_i \mathbf{u}(t)) = 0.$$

The weights w_i represent the influence of the i -th local system to the global system. A way of choosing the weights is to make them distance depending.

3 Example

To show the performance of TPWL in practice we have chosen as a test circuit a chain of inverters, which consists of 100 inverters which are connected in series. The DAE which is describing the dynamics of the circuit has 104 states. For selecting the LTs we have used a distance depending method, the linear model reduction technique we used is 'Poor Mans' TBR [2]. The resulting speed up is between 5.4 and 8.3 compared to a backward differential formula method.

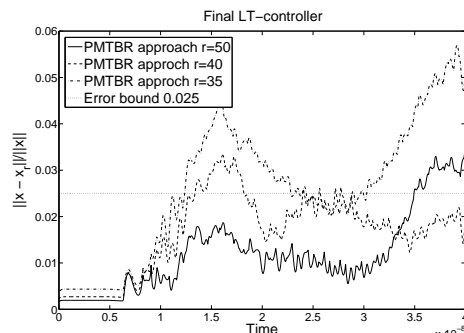


Figure 1: Relative error of the TPWL method for different orders

4 Conclusion

The TPWL method applied to nonlinear DAEs is a promising technique to reduce the simulation time. It has several advantages compared to other methods. We can get a big speed up in simulation time and we can use the well-developed linear model reduction techniques.

References

- [1] M.J. REWIĘŃSKI, *A trajectory piecewise-linear approach to model order reduction of nonlinear dynamical systems*, PhD Thesis, Massachusetts Institute of Technology, 2003
- [2] J. PHILLIPS, L.M. SILVERA, *Poor Man's TBR: A simple model reduction scheme*, IEEE transactions on computer-aided design of integrated circuits and systems. Vol. 14 No. 1, January 2005

Discrete-time piecewise-affine models of genetic regulatory networks

Arnaud Meyroneinc

Centrum voor Wiskunde en Informatica

P.O. Box 94079, 1090 GB Amsterdam, The Netherlands

A.Meyroneinc@cwi.nl

Bastien Fernandez and Ricardo Lima

Centre de Physique Théorique

13288 Marseille CEDEX 09, France

bastien,lima@cpt.univ-mrs.fr

Ricardo Coutinho

Instituto Superior Técnico

1096 Lisboa Codex, Portugal

Ricardo.Coutinho@math.ist.utl.pt

1 Modelling genetic regulatory networks

Basic models of genetic regulatory mechanisms governing genes expression simplify to networks of interacting genes where each gene is submitted both to a self-degradation and to (inter)actions with other genes. The main interaction features are their inhibiting/activating nature, their intensities and their non-linearities [1].

2 The hybrid models

In [2] we present a class of models for genetic (expression) regulatory networks (GRN) that are discrete time dynamical systems generated by piecewise affine contracting mappings whose variables represent gene expression levels.

The dynamics is defined by the relation $x^{t+1} = F(x^t)$ with

$$F_i(x) = ax_i + (1-a) \sum_{j \in I(i)} K_{ij} H(s_{ij}(x_j - T_{ij})), \quad i = 1, N \quad (1)$$

where $x^t = \{x_i^t\}_{i=1,N}$ is the local variable vector at time $t \in \mathbb{Z}$ and $F_i(x)$ is the i th component of the mapping F defined from the phase space \mathbb{R}^N into itself. In expression (1), the subscript i labels a gene (N denotes the number of genes involved in the network). The graph supporting the network (the arrows between genes) is implicitly given by the sets $I(i) \subset \{1, \dots, N\}$. For each i the set $I(i)$ consists of the set of genes which have an action on i . In particular, a self-interaction (loop) occurs when some set $I(i)$ contains i . The $a \in [0, 1]$ accounts for degradation rate, the K_{ij} for the interaction intensities, H denotes the Heaviside function, the s_{ij} account for the interaction signs and the T_{ij} for the interaction thresholds. See [2] for a more detailed description.

These models reduce to boolean networks in one limiting case of the a parameter, and their asymptotic dynamics approaches that of a differential equation in another limiting case of this parameter. For intermediate values, the models present an original phenomenology which is argued to be due to delay effects. This phenomenology is not limited to piecewise affine models but extends to smooth nonlinear discrete time models of regulatory networks.

General properties of the dynamics on arbitrary graphs

(characterisation of the attractor, symbolic dynamics, Lyapunov stability, structural stability, symmetries, etc), are obtained. But the main interest of these models lies in the ability to proceed to the fine mathematical analysis of their dynamics using symbolic dynamics, admissibility conditions (for a symbolic sequence to code for a genuine orbit point) and (semi)conjugacy of the dynamics on some components of the attractor with simpler dynamical systems such as rotations of the circle. It allows to describe the attractors and their changes with parameters. For instance, in the positive (two mutual activations) and negative (an activation and an inhibition) circuit of 2 genes, a thorough study is presented which concern stable (quasi-)periodic oscillations (depending on initial conditions for the positive circuit) governed by rotations on the unit circle – with a rotation number depending continuously and monotonically on threshold parameters. In [3, 4], dynamics in such low dimensional systems have been shown to be the most significant in large networks with the scale-free topology of GRN.

References

- [1] Hidde de Jong. Modeling and simulation of genetic regulatory systems: a literature review, *Journal of Computational Biology* 9:69-105, 2002
- [2] R. Coutinho, B. Fernandez, R. Lima and A. Meyroneinc. Discrete time piecewise affine models of genetic regulatory networks, *Journal of Mathematical Biology* 52: 547-570, 2006
- [3] R. Lima and E. Ugalde. Dynamical complexity of discrete time regulatory networks, *Nonlinearity* 19: 237-259, 2006
- [4] R. Lima and D. Volchenkov. Homogeneous and scalable gene expression regulatory networks with random layout of switching parameters, *Stochastics and Dynamics* 5:1-21, 2005
- [5] C. Aguirre, J. Martins and R. Vilela Mendes. Dynamics and coding of biologically motivated networks, *International Journal of Bifurcations and Chaos* 16(2):383-394, 2006

Control of a Tubular Reactor using POD and MPC

Oscar Mauricio Agudelo, Bart De Moor

Katholieke Universiteit Leuven, Department of Electrical Engineering, SCD-SISTA

Kasteelpark Arenberg 10, B-3001 Heverlee, Belgium

mauricio.agudelo@esat.kuleuven.be, bart.demoor@esat.kuleuven.be

Jairo José Espinosa

Universidad Nacional de Colombia, Facultad de Minas

Carrera 80 No. 65-223, Medellín, Colombia

jairo.espinosa@ipcos.com

1 Introduction

The dynamics of tubular reactors are typically described by nonlinear PDEs (Partial Differential Equations) which are derived from mass and energy balance principles. The control of such systems can be addressed by transforming the PDEs and the boundary conditions into a set of ODEs (Ordinary Differential Equations), which would make possible the application of the control theory developed for lumped parameter systems. However, the design of the controllers would be very difficult or practically impossible due to the high order models obtained of discretizing the PDEs. Therefore, it is necessary to find reduced-order models that make possible the design of the control schemes. This can be done by means of a Proper Orthogonal Decomposition (POD) and Galerkin projection. This is the approach followed in this work.

2 Control of the Reactor

Proper Orthogonal Decomposition is a technique that has been applied in many physical systems governed by PDEs for deriving reduced order models. The advantage of applying this technique is the incorporation of simulation or experimental data as well as the existing physical relationships (when the Galerkin projection is used) from the original model [1]. This work presents the application of POD and Predictive control techniques to the control of the temperature and concentration profiles of a non-isothermal tubular reactor. The control goal is to keep the operation of the reactor around a desired operating concentration and temperature profiles in spite of the disturbances that affect the reactor, that is the changes in the temperature and concentration of the feeding flow. The manipulated variables of the control system are the temperature of the jacket sections that wrap the tubular reactor. The model on which the MPC is based was derived as it is explained in the following lines. Around the operating profiles (concentration and temperature) the nonlinear PDEs that model the reactor are linearized, and afterwards the resulting linear PDEs are discretized in space giving as result a high order linear model (600 states). Then

a reduced order model of only 20 states is found by means of the POD technique. Finally a discrete-time version of the linear POD model is derived.

3 Results and Future research

Typically the variations in the temperature and concentration of the feeding flow of a tubular reactor are $\pm 10^\circ\text{K}$ for the temperature and $\pm 5\%$ of the nominal value for the concentration. Keeping in mind these magnitudes, two disturbance rejections tests were carried out. In spite of the spatial discretization of the nonlinear PDEs that model the reactor, the linearization and discretization in time of the equations, and the dramatic reduction of model order by means of POD (from 600 states to 20 states), on which the controller is based, the controller performed well. However, if larger disturbances are applied to the tubular chemical reactor, the behavior of the MPC controller would not be as good as it was during the tests, since the differences between the nonlinear model and the linear model and consequently the linear POD model would be more significant. Therefore in future work, the nonlinear characteristics of the process should be taken into account in order to design controllers with a higher degree of robustness.

Acknowledgments. This research was supported by: • Research Council KUL: GOA AMBioRICS, CoE EF/05/006 Optimization in Engineering, several PhD/postdoc & fellow grants; • Flemish Government: ◦ FWO: PhD/postdoc grants, projects, G.0407.02 (support vector machines), G.0197.02 (power islands), G.0141.03 (Identification and cryptography), G.0491.03 (control for intensive care glycemia), G.0120.03 (QIT), G.0452.04 (new quantum algorithms), G.0499.04 (Statistics), G.0211.05 (Nonlinear), G.0226.06 (cooperative systems and optimization), G.0321.06 (Tensors), G.0302.07 (SVM/Kernel), research communities (ICCoS, AN-MMM, MLDM); ◦ IWT: PhD Grants, McKnow-E, Eureka-Flite2 • Belgian Federal Science Policy Office: IUAP P5/22 ('Dynamical Systems and Control: Computation, Identification and Modelling', 2002-2006) ; • EU: ERNSI. Dr. Bart De Moor is a full professor at the Katholieke Universiteit Leuven, Belgium.

References

[1] M. Hazenberg, P. Astrid and S. Weiland, "Low order modeling and optimal control design of a heated plate", in *Proceedings of the 5th European Control Conference*, Cambridge, 2003.

Nonlinear Model Predictive Control for a DC-DC converter: A NEPSAC approach

J. Bonilla
 EeSA Department
 Ghent University
 Technologiepark 913, Zwijnaarde 9052
 Belgium
 Email: julian@autoctrl.ugent.be

R. De Keyser
 EeSA Department
 Ghent University
 Technologiepark 913, Zwijnaarde 9052
 Belgium
 Email: rdk@autoctrl.ugent.be

Power electronics (PE) devices are nowadays applied to different areas, from power generation and distribution to embedded solutions for communication, automotive and computers industries. This wide range of applications has motivated this field to be an active research area where several topologies and control strategies have been investigated. Among the possible topologies for power electronics drives, especial attention has been made to the boost DC-DC converter due to its advantages for power factor correction (PFC) tasks or low harmonics rectifiers.

The evaluated topology is illustrated in figure 1 where the goal is to control the output voltage despite the uncertainty in parameters and the disturbances coming from the input source [1]. This devices are in general quite complex from the control point of view. It presents a non-linear, hybrid behavior (including continuous and logical variables), non-minimum phase and additionally, very short time responses requiring nonlinear and fast control strategies which have to be implemented in real-time.

This work presents the results of linear and non-linear control techniques applied to a DC-DC boost converter. A *Non-linear Extended Prediction Self-Adaptive Controller (NEPSAC)* [2] is designed for this particular system. The results are compared to those of a PID which is usually applied to commercial converters. The PID is tuned using a frequency domain approach by means of a *Frequency Domain Toolbox-FRTool* [3]. The upper part of figure 2 shows a voltage tracking test over the converter operating range for both controllers, on the other hand, the robustness is evaluated by disturbing the system sequentially with an operating point change, an input voltage drop and a load change as shown in the lower part of the same figure.

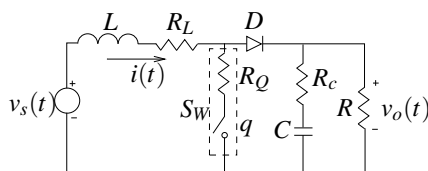


Figure 1: Boost converter circuit

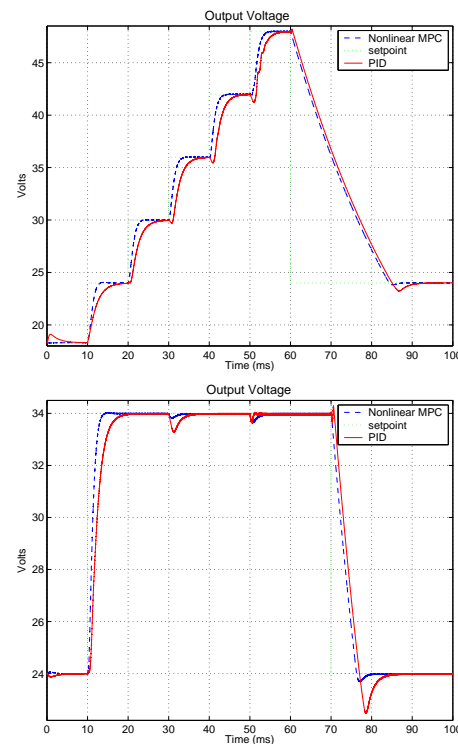


Figure 2: Voltage response for the tracking (upper) and disturbance (lower) tests

References

- [1] R. Erickson and D. Maksimovic, *Fundamental of Power Electronics*, Kluwer Academic Publishers, USA, 2001.
- [2] R. De Keyser, "Model Based Predictive Control". *Invited Chapter in UNESCO Encyclopaedia of Life Support Systems (EoLSS) contribution 6.43.16.1*, EoLSS Publishers Co. Ltda, Oxford, 2003, 30p.
- [3] R. De Keyser and C. Ionescu. "FRtool: A Frequency Response Tool for CACSD in Matlab", in proc. of the IEEE International Symposium on Computer-Aided Control Systems Design, Munchen-Germany, 2006, pp 2275-2280

Advanced Speed Control for the Air Turbine Motor of the NLR High Temperature Seal Test Rig

ing. T.A. ter Meer, MSc
Avionics Systems & Applications Division
National Aerospace Laboratory NLR
P.O. Box 153
8300 AD Emmeloord
The Netherlands
termeer@nlr.nl

dr. ir. J.D. Stigter
Systems and Control Group
Wageningen University & Research Center
P.O. Box 17
6700 AA Wageningen
The Netherlands
hans.stigter@wur.nl

1 Introduction

The NLR High Temperature Seal Test Rig is employed for the testing of seals for aircraft gas turbines. These seals are intended to prevent unintentional air flows between the primary and secondary air flows in the engine. The rotating part of this facility is driven by an air turbine motor. At the moment, a PID controller is used to keep the motor input pressure at a stable value. This method has a number of drawbacks, but many years of experience in wind tunnel models have proven that it is basically a safe and accurate way to control these types of motors. In order to overcome the disadvantages and to optimize the operation of the Seal Test Rig, a more advanced method for the motor control has been devised.

2 Control objectives

The fact that an operator has to adjust the input pressure setpoint, based on the reading of the motor speed from a display, has a number of drawbacks. First, the motor speed is dependent on a number of factors, in particular the load on the shaft and the upstream supply pressure. Second, the experience of the operator is critical in the operation of the facility. To further automate the operation and to improve the performance of the Seal Test Rig a more advanced speed control algorithm must be developed. It must not rely on controlling the motor input pressure but directly on the motor speed. Moreover, it must be able to increase the number of ‘measurement points’ per day and to keep the motor speed constant between such points. Finally, the amount of the required compressed dry air must be minimized as much as possible.

3 System description

The Seal Test Rig is a complex installation, where a number of parameters that are important for the testing of the seals can be adjusted independently. Including the control of the motor speed, a total of seven control

loops are implemented, which all interfere with each other. These parameters consist of upstream and downstream pressures, temperatures, clearances and the radial velocity.

The most important factor that influences the air turbine motor speed is a phenomenon called windage heating. The windage effect is the viscous air drag on rotating components in e.g. gas turbine engines. It both represents direct power loss and adds energy to the air in the form of heat [1]. The equation for windage heating however has an inaccuracy of 25%, but more important is that not all relevant variables can be measured.

4 The control algorithm

Model Predictive Control has been selected as the most appropriate method for the control of the air turbine motor. In this case it has a number of advantages above other control methods. First, it has knowledge of the system by using a mathematical process model. Second, it is able to handle unmeasured disturbances such as the windage effect. Finally, constraints can be put on MPC variables. Latter is particularly important for optimal use of the compressed dry air, but also to protect the aluminum motor blades motor against input pressure gradients. A Kalman filter was developed to further increase the performance in the noisy industrial environment of the facility. A mathematical model was obtained of the air turbine motor and for all relevant parts that contribute to its operation. This nonlinear model could however only be tested qualitatively. Simulations have shown that this virtual model behaves as expected. Linearized versions of the model were subsequently used to develop the MPC controller and the Kalman filter. The controller has not been implemented yet.

References

[1] J.A. Millward, M.F. Edwards, “Windage Heating of Air Passing Through Labyrinth Seals”, Transactions of the ASME, Vol. 118, April 1996, pp. 414-419.

Robust performance of self-scheduled LPV control of doubly-fed induction generator in wind energy conversion systems

H. Nguyen Tien*

Email: h.nguyentien@desc.tudelft.nl

C. W. Scherer*

Email: c.w.scherer@tudelft.nl

J. M. A. Schepen*

Email: j.m.a.schepen@tudelft.nl

* Delft Center for systems and Control
Delft University of Technology
2628 CA, Delft, The Netherlands

1 Abstract

This presentation describes a new current control design for doubly-fed induction generators in wind turbine systems. The design is based on the linear parameter varying (LPV) systems approach. Robust performance for the closed-loop system is achieved based on the design. Furthermore, robust performance of the controlled LPV system with respect to other machine parameter variations and the impact of a stator voltage dip are investigated. They show that a large performance improvement can be achieved in comparison to more classical controller designs.

2 Summary

Doubly fed induction machines (DFIMs) recently are considered to be an attractive solution for wind energy conversion systems (WECS). In the literature, the classical approach for DFIM vector control [3] allows one to achieve decoupled control of active and reactive power in both generator and motor operations. In some literature, the difficulties of the nonlinear dynamics of the doubly-fed induction generator (DFIG) are not taken into account, i.e., the model of the machine is linearized and it is assumed that both the machine parameters required by the control algorithm and the grid voltage are precisely known. Clearly, such controller design results in a closed-loop behavior that is highly sensitive to a change in conditions and/or parameters.

In order to improve the system performance against changes in the machine parameters and exogenous inputs, a control approach for an induction generator in windmill power system is proposed in [6] and for induction motor control in [1]. Recently, the LPV current control approach, which takes the parameter variations into account directly in the control design, is applied for an induction motor in [2, 5].

Our paper presents an alternative control strategy for DFIMs. The controller objective is to track references for the electrical torque and the power factor. The mechanical angular speed is considered as a time varying parameter. This particular choice is motivated by the fact that it causes the system to be nonlinear and that it can be measured online. Up to our best knowledge, this paper presents the first self-scheduled LPV control designed for DFIMs in wind tur-

bine systems.

A self-scheduled controller is designed for the inner current control loop in order to ensure that the controlled system satisfies the desired objectives for all admissible trajectories of the rotor speed in the operating range. The self-scheduled controller design guarantees the decoupling of torque and power factor and achieves high robust dynamic performance over the operating range. Furthermore, it is shown that the closed loop system performance is also fulfilled if the system is under the influence of disturbances such as machine parameter variations and/or grid voltage oscillations.

Two complete simulation models, one based on a conventional control scheme that is called dead-beat control (similar to that in [4]) and the other based on the described LPV framework are developed for the control of the electrical torque and the power factor on the rotor side in order to compare the performance of the closed loop systems. Under disadvantageous conditions of machine parameter variations and a stator voltage dip, simulation results show that the designed LPV controller is far more robust than the dead-beat controller. Oscillations in the stator and rotor currents are considerably reduced during the grid voltage faults, and the closed loop system recovers from the faults much faster than in the conventional case. Hence, the new control scheme improves the performance of the closed-loop DFIM considerably.

References

- [1] D. Diallo N. E. Bouguechal A. Makouf, M. E. H. Benbouzid. Induction motor robust control: an h_∞ control approach with field orientation and input-output linearizing. *The 17th annual conference of the IEEE industrial electronics society*, 2:1406 – 1411, 2001.
- [2] K. Trangbæk J. D. Bendtsen. Discrete-time lpv current control of an induction motor. *42nd IEEE Conference on Decision and Control*, 6:5903–5908, 2003.
- [3] W. Leonhard. *Control of electrical drives*. Springer, 1996.
- [4] Thieme A Quang N. P., Dittrich A. Doubly-fed induction machine as generator: control algorithms with decoupling of torque and power factor. *Electrical Engineering (Archiv fur Elektrotechnik)*, 80:325–325, 1997.
- [5] Klaus Trangbæk. *Linear Parameter Varying Control of Induction Motors*. PhD thesis, Aalborg University, Denmark, 2001.
- [6] H. Miyagi Y. Long and K. Yamashita. Windmill power systems controller design using h_∞ theory. *IEEE International Conference on Systems, Man, and Cybernetics*, 5:3490–3495, 2000.

Modeling and Control for the Air Path System of Diesel Engines by LPV techniques

X. Wei

Delft Center for System and Control

Delft University of Technology

Mekelweg 2, 2628 CD Delft, The Netherlands

Email:x.wei@tudelft.nl

L. del Re

The Institute for Design and Control

Johannes Kepler University of Linz

Altenberger Strae 69, A-4040 Linz, Austria

Email:luigi.delre@jku.at

1 Introduction

Under the new stringent emission regulations, NOx emission of diesel engines must be attenuated to a much lower level than today. However, up to now, the controllers in the production electric control units (ECU) are mainly gain scheduling PID controllers whose control performance leaves a lot to be desired [1]. Additionally, the parameter calibration of these controllers is a time consuming and tough work. In this work we propose to approximate the inherent nonlinear dynamics of the air path system by the quasi-LPV model. The gain scheduled H_∞ control in [3] is further applied on the regulation issue of the air path system.

2 The Air Path System of Diesel Engines

The schematic diagram of a diesel engine with turbo charger is shown in Fig. 1. The compressor pumps the fresh air into the inlet manifold to boost the pressure. The fuel is directly sprayed into the combustion and is burnt with the delivered air. Part of the exhaust gas is recirculated into the inlet manifold that is used to reduce the NOx emission. The VGT absorbs the heat energy from the exhaust gas and propels the compressor. Inter cooler is used to lower the fresh air temperature and EGR cooler to lower the recirculated gas temperature respectively. The modeling target is the dynamical relation between the system inputs, which are the VGT vane position, the fuel injection and the EGR valve rate, and the outputs which are the fresh air mass flow and the boost pressure.

3 Modeling and Control for the Air Path System

In this work, we divided the modeling problem of the air path system into three subsystem modeling issues: the inlet manifold pressure dynamics modeling, the exhaust manifold pressure modeling and the air mass flow modeling. The main LPV modeling technique can be found in [2]. The entire air path system model can be achieved by combining the subsystem models together based on their physical connections. The final model is a Hammerstein quasi-LPV model where the boost pressure, the engine speed and the VGT vane position are the scheduling variables. The entire model of the air path system is validated by the input steps.

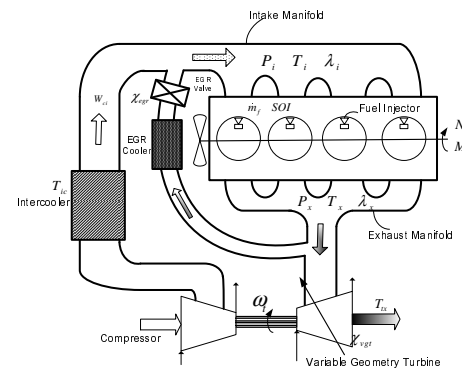


Figure 1: Turbo charged Diesel Engine System

The identified quasi-LPV model is used to synthesis the controller for the air path system. In this work, two approaches of gain schedules H_∞ control strategy are investigated for the air path tracking issue.

4 Simulation and Experimental Results

The gain scheduled LPV controller has been studied by simulation and tested on the test cell. The controller is implemented in the dSPACE environment by C-coded S functions. The controller is tested in a large scope to include many possible working scenarios. Adequately tracking performance is achieved by the designed LPV controller.

References

- [1] M. Jung and K. Glover, "Control-oriented linear parameter varying modelling of a turbocharged diesel engine," in *Proceedings of the IEEE Conference on Control Applications*, pp. 155-160, 2003.
- [2] X. Wei and L. del Re, "On persistent excitation for parameter estimation of Quasi-LPV Systems and its application in modeling of diesel engine torque," in *14th IFAC Symposium on System Identification*, pp. 517-522, 2006.
- [3] P. Apkarian and R. J. Adams, "Advanced gain-scheduling techniques for uncertain systems," *IEEE Trans. Contr. Syst. Technol.*, vol. 6, no. 1, pp. 21 - 32, 1998.

Comparison between gain-scheduling control and LPV control for a pick-and-place machine with position-dependent dynamics

Paijmans Bart, Symens Wim
 Flanders Mechatronics Technology Center
 Celestijnenlaan 300B, 3001 Heverlee
 Email: bart.paijmans@fmtc.be

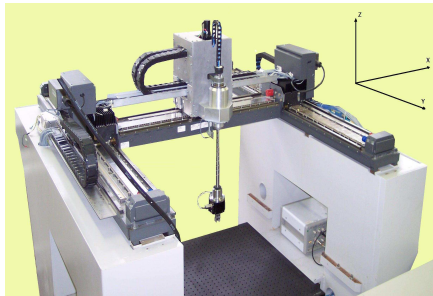


Figure 1: Picture of the setup

1 Introduction

This presentation discusses the control of a machine tool of which the dynamics change significantly with the position of the tool in the workspace. Maximal performance can only be achieved if the coefficients of the controller are also explicitly dependent on the instantaneous position of the machine-tool. Two control design approaches for systems with varying dynamics are compared. The first one is Linear Parameter Varying (LPV) control, an analytical design approach that guarantees the stability of the closed loop for all possible parameter variations. Efficient algorithms with good numerical stability exist if the LPV model has an affine parameter dependence. The second approach is traditional gain-scheduling control, where several controllers designed for fixed operating points are interpolated to construct a global gain-scheduling controller. The traditional gain-scheduling controller outperforms the LPV controller.

2 Setup

The considered test-case is an industrial 3-axis pick-and place machine shown in Fig. 1. The objective is to move the end point of the beam as accurately and fast as possible along a prescribed trajectory in the X-Z plane. Fast movements of the linear motor will excite the eigenfrequencies of the flexible beam. During motion, the length of the beam is continuously changed, giving rise to varying resonance frequencies.

3 LPV modelling and control

The setup is identified for 4 different lengths of the beam. An LPV model is fitted on the data using a grey-box ap-

Swevers Jan, Van Brussel Hendrik
 Mechanical Engineering Department
 Katholieke universiteit Leuven, 3001 Heverlee

proach: first an analytical model of the setup is derived that qualitatively describes the dynamic behavior of the system and then the unknown parameters of this analytical model are optimised. This LPV model has an affine parameter-dependence. Optimal controllers are then designed using LPV- H_∞ techniques [1].

The performance of the resulting controller is poor. This is due to the fact that the LPV controller guarantees the stability of the closed loop for the worst-case parameter variation. In this case, the worst-case parameter variation is a sinusoidal variation of the length of the vertical beam on a critical frequency with an amplitude equal to the range of the parameter variation. This critical frequency is for our setup far above the maximal bandwidth of the Z-axis.

4 Traditional gain-scheduling control

A traditional gain-scheduling controller is designed by making an interpolation between the poles and zeros of four local controllers. These local controllers are designed with the same weighting functions as the ones used to design the LPV controller [2].

5 Conclusion

An LPV controller designed for the whole parameter range is stable, but has low performance. However, the worst-case parameter variation is unrealistic for our setup. Traditional gain-scheduling control is therefore a better approach for this setup. Although LPV control is suggested as a more standardized approach than the 'pragmatic' traditional gain-scheduling approach, it is experienced that there are still cumbersome steps in the design procedure that limit the applicability to industrial applications.

References

- [1] P. Gahinet, A. Nemirovsky, A.J. Laub and M. Chi-lali, LMI Control Toolbox, The MathWorks, Inc., 1995, edition 1
- [2] B. Paijmans, W. Symens, H. Van Brussel and J. Swevers, A gain-scheduling-control technique for mechatronic systems with position-dependent dynamics, American Control Conference 2006

Time-optimal trajectory generation for industrial manipulators along predefined paths with kinematic constraints

Niels van Dijk^{*,a}, Nathan van de Wouw^a, Wilco Pancras^b and Henk Nijmeijer^a

^a Technische Universiteit Eindhoven
Department of Mechanical Engineering
P.O. Box 513, 5600 MB Eindhoven
The Netherlands
Email: ^{*}N.J.M.v.Dijk@tue.nl

^b Bosch Rexroth Electric Drives and Controls B.V.
Product area semiconductor and medical
P.O. Box 7170, 5605 JD Eindhoven
The Netherlands

1 Introduction

The research discussed here presents a method for determining time-optimal trajectories for industrial manipulators along a pre-defined path [1]. Instead of taking into account dynamic equations of a manipulator with actuator torque limits and possible torque-rate limits [2], we only require knowledge on the kinematics of a manipulator together with actuator velocity, acceleration and jerk limits. In this way, the industrial applicability of the method is highly increased. Furthermore, constraints acting on actuator level as well as process level can be taken into account.

2 Problem statement

The overall problem is to find time-optimal trajectories, i.e. to minimize the time span $T = t_f - t_0$ of the motion, i.e. $\min T = \min \int_{t_0}^{t_f} dt$, subjected to manipulators kinematics, $\underline{P} = \underline{R}(\underline{q}(t))$, constraints on the path, $\underline{P} = \underline{P}(s)$, with s the so-called path parameter; actuator constraints,

$$\begin{aligned} |\dot{q}_i| &\leq \dot{q}_{i,max}, \text{ for } i = 1, \dots, n, \\ |\ddot{q}_i| &\leq \ddot{q}_{i,max}, \text{ for } i = 1, \dots, n, \\ |\dddot{q}_i| &\leq \dddot{q}_{i,max}, \text{ for } i = 1, \dots, n, \end{aligned} \quad (1)$$

and process constraints,

$$\begin{aligned} |\dot{X}_i| &\leq \dot{X}_{i,max}, \text{ for } i = 1, \dots, 6, \\ |\ddot{X}_i| &\leq \ddot{X}_{i,max}, \text{ for } i = 1, \dots, 6, \\ |\dddot{X}_i| &\leq \dddot{X}_{i,max}, \text{ for } i = 1, \dots, 6. \end{aligned} \quad (2)$$

Herein, the path, that must be followed by the manipulator's end-effector, is represented by a six-dimensional vector \underline{P} , q_i is the displacement of joint i and n the number of joints ($\underline{q}^T = (q_1, \dots, q_n)$), X_i component i of the end-effector's pose vector \underline{X} and $\underline{R}(\underline{q}(t))$ represents the manipulator's forward kinematics. Since the total motion time is unknown, the problem is to find a mapping from time onto the path parameter (i.e. $s(t)$), while respecting the constraints as defined above. Constraints are given as function of time. So a transformation from time to the path parameter and its derivatives is defined.

The work presented here is part of the NewMotion project, that is supported by Stimulus.

3 Optimization strategy

An overview of the optimization strategy for solving the problem stated in the previous section is depicted in Figure 1. As can be seen from this figure, the chosen optimization strategy is a hybrid optimization strategy that determines points in the (s, \dot{s}) -plane which are interpolated using cubic splines. Such strategy is chosen since the solution space may be non-convex. A global optimization strategy (genetic algorithm) is proposed. The global optimization strategy is followed by a local optimization strategy (Nelder-Mead's method) to obtain a more accurate optimum solution.

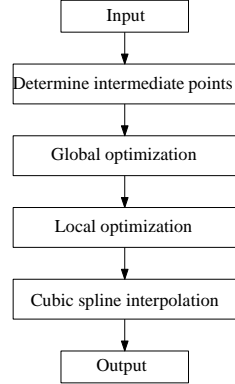


Figure 1: Optimization strategy.

4 Results

From simulation results performed on a Puma 560 manipulator, it can be concluded that for a proper choice of the kinematic constraints results can be obtained that match the quality of those obtained using the torque and torque-rate constraint approach. However, where the dynamic constraint approach asks for a specific knowledge on multi-body dynamics, the 'tuning' of the kinematic constraints may take some time.

References

- [1] N.J.M. van Dijk et al., "Time-optimal trajectory generation for industrial manipulators along predefined paths with kinematic constraints", IEEE Transactions on Robotics, 2006, *Submitted*.
- [2] D. Constantinescu and E. A. Croft, "Smooth and time-optimal trajectory planning for industrial manipulators along specified paths", Journal of robotic systems, 17(5), 233-249, 2006.

Multi-robot exploration: a novel approach

Jonathan Rogge and Dirk Aeyels
 SYSTeMS Research Group, Ghent University
 Technologiepark Zwijnaarde 914, 9052 Zwijnaarde, Belgium
 Email:jonathan.rogge@ugent.be, dirk.aeyels@ugent.be

1 Problem Statement

Nowadays multi agent robot systems are designed to take over human tasks in hazardous situations, reducing the probability of human loss. Examples include mine field clearance and exploration tasks in areas with life-endangering situations (e.g., with the presence of biohazard). Two important subdomains of multi-robot systems research are *exploration* and *complete coverage*. The exploration task orders a group of robots to explore and map an unknown area [1]. In the complete coverage task, the robots have to physically move over all of the free surface in configuration space [2].

The problem statement of the present paper is a combination of the common exploration/mapping task and the complete coverage problem. It is required that all of the free space is *sensed* by the robots; information on the shape of the explored area is not demanded. Our aim is to locate several unknown targets within the free space. Moreover, similar to the complete coverage setting we demand a 100% certainty that *all free space* has been covered by the sensors at the end of the exploration procedure, implying that all targets have been found. It is assumed that the space to be explored is an open space with convex obstacles sparsely spread throughout. We develop a novel algorithm tackling this problem, with the specific application of mine field clearance in mind.

2 An algorithm for complete sensor coverage

Consider a population of N identical robots. Each robot is equipped with two types of sensors. One type detects the goal targets to be located, e.g. landmines; the other type detects and locates other robots and obstacles in the neighborhood of the robot. Both sensors have a maximum detection range. We impose a preferred formation on the robot group with zigzag shape, as shown in Figure 1. We ensure that the areas sensed for goal targets of neighboring robots partially overlap. Once the preferred formation is attained the scanning algorithm is started. Assume for simplicity that the area S to be explored is rectangular. Divide the set S into parallel (scanning) strips. The main idea of the algorithm is to let the group of robots sweep the area S strip after strip in a zigzag-like pattern. The two robots at the extremities of the formation are allocated the task to follow the boundaries of the strip at a constant distance at a constant velocity v . These two (leader) robots do not try to stay in the preferred formation and do not maintain a fixed interdis-

tance with their neighbors. The remaining robots, however, still maintain the preferred formation. When no obstacles are present in the strip, the robots scan the strip for goal targets in the above defined preferred (rigid) formation moving at a velocity v .

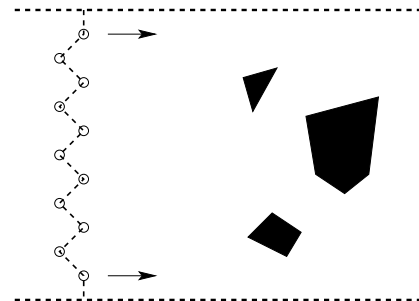


Figure 1: A depiction of the algorithm

When an obstacle is encountered the algorithm guides the robot group past it in a time-optimal way. The leader robots keep driving at the constant velocity v ; the group is split into two subgroups in order to move around to obstacle. The subgroups rejoin after passing the obstacle to resume the preferred formation structure.

The combination of exploration and complete coverage in the proposed algorithm is designed to result in a faster scanning of the area with a smaller number of robots, compared to previously published algorithms. Moreover, the algorithm can easily be adapted to tasks where a robot formation has to cross a terrain containing sparsely spread obstacles. There is a natural trade-off between coherence of the formation and avoidance of the obstacles. The robot group is allowed to split in order to pass the obstacles, resulting in faster progress of the group across the terrain.

Future work will treat the extension of the algorithm to spaces with non-convex obstacles.

References

- [1] W. Burgard, M. Moors, C. Stachniss, and F. Schneider. Coordinated multi-robot exploration. *IEEE Transactions on Robotics*, 21(3):376–386, 2005.
- [2] H. Choset. Coverage for robotics – a survey of recent results. *Annals of Mathematics and Artificial Intelligence*, 31:113–126, 2001.

Continuous State And Action Space Q-Learning Using Interval Analysis

E. de Weerdt, Q.P. Chu, J.A. Mulder

Delft University of Technology, Department of Control and Simulation

P.O. Box 5058, 3600 GB Delft, The Netherlands

E.deWeerdt@TUDelft.nl, Q.P.Chu@TUDelft.nl, J.A.Mulder@TUDelft.nl

1 Introduction

Reinforcement Learning (RL) theory can be used to incorporate automated adaptation in agents. Through interaction with the environment, a RL agent can learn to act within that environment such that it will reach its goal [1]. For each action and/or state the agent visits it will receive a reward or penalty (negative reward). The designer of the system translates the task the agent has to perform into the reward function. The agent will try to maximize the (possibly discounted) future rewards such that the task is automatically fulfilled. There are different methods to derive the optimal policy and we will focus on Q-learning. We will solve the implementation problems when dealing with a continuous state and action space.

2 Q-learning

With Q-learning the agent will store its experience in the so-called state-action value function (the Q-function). This Q-function assigns a value to each state-action (s, a) pair. The higher the value the more desirable it is for the agent to be in that state and then choose that action. Learning comprises of updating the Q-function such that it will approach the optimal Q-function. The update rule is given by [1]:

$$Q(s_t, a_t) \leftarrow Q(s_t, a_t) + \alpha \left[r_{t+1} + \gamma \max_a Q(s_{t+1}, a) - Q(s_t, a_t) \right]$$

We will now consider a continuous state and action space. Tabular storage methods are not applicable in this framework due to the ‘curse of dimensionality’ [1]. Neural networks offer the solution as they are universal non-linear function approximators, optimal in the sense of number of parameters. The problem now is to extract the action for which the maximal Q-value for the next state, i.e. $\max_a Q(s_{t+1}, a)$, is obtained. Many simple and elegant solutions exist when the action space is discrete, e.g. [2] [3], but not for continuous action spaces. We will solve this problem with interval analysis which guarantees convergence to the optimal action \bar{a}_{t+1} .

3 Interval analysis

Interval mathematics and analysis is a generalization of standard mathematics and analysis [4],[5]. Instead of using

real/imaginary numbers an interval of real/imaginary numbers is used. Interval analysis can provide upper and lower bounds on mathematical and numerical computation problem solutions. Through interval computations these bounds can be reduced to a minimum. One of the problems interval analysis can solve is root finding of non-linear (differential) equations. The most important characteristic is that interval analysis converges to the minimal bound solutions and finds all solutions with probability one. Searching for maxima is equal to the root finding problem of the derivative while taking into account that the second derivatives must be negative. The global maxima can be selected from the set of solutions found through interval analysis. We can apply this to our problem of finding \bar{a}_{t+1} by first reducing the input space of the neural network by supplying the next state s_{t+1} . Thereafter we search for all global maxima by applying interval analysis.

4 Ongoing research

The Q-learning agent using interval analysis will be applied to benchmark problems which have continuous state and action space, e.g. inverted pendulum control. We will present the results during the meeting. This work is performed as part of the MicroNed MISAT project.

References

- [1] Richard S. Sutton and Andrew G. Barto. *Reinforcement Learning, An Introduction*. The MIT Press, third printing (2000) edition, 1998.
- [2] X. Wang and T.G. Dietterich. Efficient value function approximation using regression trees. *Proceedings of: IJCAI-99 Workshop on Statistical Machine Learning for Large-Scale Optimization*, July 1999.
- [3] S.H.G. ten Hagen and B.J.A. Kroese. Pseudo-parametric q-learning using feedforward neural networks. *Proceedings of the 8th ICANN*, pages 449–454, September 1998.
- [4] R.E. Moore. *Interval Analysis*. Prentice-Hall, Inc., 1966.
- [5] E. Hansen and G.W. Walster. *Global Optimization Using Interval Analysis*. Marcel Dekker, Inc. and Sum Microsystems, Inc., 2 edition, 2004.

A Luenberger observer for an infinite dimensional system with disturbances at the boundary: a UV disinfection example

Dirk Vries, Karel J. Keesman

Dept. of Agrotechnology and Food Sc.

Systems and Control Group

Wageningen University, Wageningen, The Netherlands

Email: dirk.vries@wur.nl, karel.keesman@wur.nl

Hans Zwart

Dept. of Applied Mathematics

Systems Signals and Control Group

University of Twente, The Netherlands

Email: h.j.zwart@ewi.tu.nl

Abstract - Inspired by a convection-diffusion process in industry, we design an asymptotic strong Luenberger-like observer which is dependent on boundary observations. The observer is constructed using the theory of boundary control systems [2], instead of following the route of Bounit and Hammouri [1]. A disinfection process in an annular reactor is used as an inspiring example and further worked out. In this example, it is also shown that the performance of the boundary observer is very sensitive to the change of the diffusion-convection ratio.

1 Case Study: a UV disinfection process

In greenhouse drain water infestation and disinfection of fluid food products, *annular* tube reactors are the most commonly applied reactor types to reduce pathogenic bacteria or viruses by UV light disinfection. In annular photoreactors the lamp tube is placed along the flow direction. We take an annular reactor as our model system, with output boundary observations $y(t)$ of the active biomass concentration $w(x, t)$, as input the fluence intensity of the lamp and a measured boundary disturbance $u_d(t) = w(0, t)$. We consider (i) the modeling of dispersion phenomena by diffusion-advection laws and (ii) biomass deactivation by ultraviolet irradiation obeying first order kinetics with constant lamp input. This, along with some other (simplifying) assumptions lead to,

$$\Sigma_M := \begin{cases} \frac{\partial}{\partial t} w(x, t) = \alpha \frac{\partial^2}{\partial x^2} w(x, t) - v \frac{\partial}{\partial x} w(x, t) \dots \\ -\beta w(x, t), \quad w(x, 0) = w_0(x) \\ w(0, t) = \bar{u}_d(t), \quad \frac{\partial w}{\partial x} \Big|_{x=1} = 0 \\ y(t) = w(1, t) \end{cases} \quad (1)$$

with α the diffusion constant, v the convective flow velocity and β the degree of inactivation.

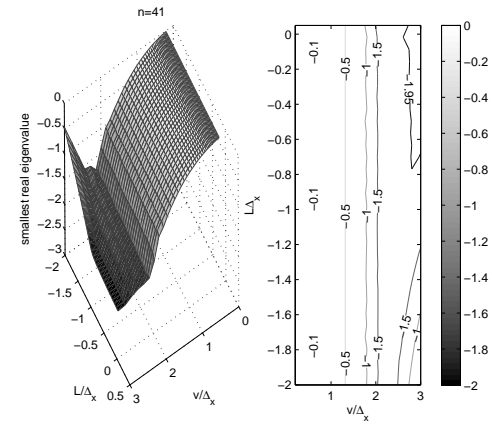
2 Theory and Results

We propose the following observer with asymptotic decreasing error $\varepsilon = w - \hat{w}$ as $t \rightarrow 0$,

$$\begin{aligned} \dot{\hat{w}}(t) &= A\hat{w}(t) \\ \mathfrak{B}_1^{\text{obs}}\hat{z}(t) &= \mathfrak{B}_1\hat{w}(t) \\ \mathfrak{B}_2^{\text{obs}}\hat{z}(t) &= \mathfrak{B}_2\hat{w}(t) + L(\hat{y}(t) - y(t)) \\ \mathfrak{C}\hat{w}(t) &= \hat{y}(t) \end{aligned} \quad (2)$$

where $(A, D(A))$ is an infinitesimal generator of a contraction C_0 -semigroup on a Hilbert space Z , $\mathfrak{B}_i^{\text{obs}}$, $i = 1, 2$ and \mathfrak{C} are boundary operators.

With finite differences, the influence of the observer gain on the system matrix is inspected and depicted in the following figure ($\alpha = 1$, $\beta = 1$):



For low Peclet numbers (low velocity - diffusion ratio) and mild inactivation, the sensitivity of the smallest real eigenvalue of the error dynamics of the observer system to the gain L is strongest.

3 Future work

Currently, system (1) in connection with a boundary observer is investigated in the bilinear setting, *i.e.*, where the lamp fluence rate is considered as a control variable, hence $\beta(t) := k_1 u(t)$, with k_1 a susceptibility constant.

References

- [1] H. Bounit and H. Hammouri. Observers for infinite dimensional bilinear systems. *European Journal of Control*, 3(1):325–339, 1997.
- [2] R.F. Curtain and H. Zwart. *An Introduction to Infinite Dimensional Linear Systems Theory*. Springer-Verlag, New York, 1995.

Discrete-Time Interval Observers - Application to Continuous Cultures of Phytoplankton

G. Goffaux, A. Vande Wouwer
 Service d'Automatique
 Faculté Polytechnique de Mons
 Boulevard Dolez 31, B-7000 Mons
 Guillaume.Goffaux, Alain.VandeWouwer@fpms.ac.be

O. Bernard
 INRIA Comore
 2004 route des lucioles - BP 93
 06902 Sophia-Antipolis, France
 Olivier.Bernard@inria.fr

State estimation of biological systems is essential for monitoring and control purposes [1]. The design of a state observer requires a process model and the availability of on-line measurements. These requirements can be difficult to fulfil in bioprocess applications, since the models are often uncertain and there is a scarcity of reliable on-line sensors.

Rather than providing an estimate of the state trajectory, it is appealing to reconstruct guaranteed intervals for this trajectory. Based on intervals bounding the uncertain initial conditions, inputs, model parameters and measurements, state estimation techniques using interval algebra have been developed in e.g. [2, 5, 6]. Most of the proposed algorithms are dedicated to situations where measurements are available continuously in time or with a fast sampling rate, which is often not the case in real-life applications. The objective of this study is therefore to tackle the problem of interval estimation in the context of discrete-time, and possibly rare, measurements. Following the work initiated in [4], our angle of attack is the use of model transformations in order to reduce the rate of increase of the interval size in the interval between two measurement times, where the only source of information is the uncertain model. In this context, two interval observers are developed and analysed :

- an interval observer using the complete model to define the predictor;
- an interval observer combining the previous predictor with another predictor obtained through a nonlinear transformation which allows part of the kinetic model to be eliminated (here, the growth rate is eliminated).

These methods are tested in simulation and with experimental data collected from cultures of phytoplankton in a chemostat. This biological system is described by Droop model [3], which has been identified based on experimental data (this identification procedure allows bounds on the uncertain parameters, inputs and initial conditions to be defined). The multi-predictor interval observer performs well, even though data are available at low sampling rate only (the sampling interval can be up to several days in this application), and opens the perspectives of combining (intersecting) more predictors through the definition of suitable state transformations.



Figure 1: Phytoplankton trail in the North Sea - Aqua Satellite.

Acknowledgment

The authors gratefully acknowledge the Laboratoire d'Océanographie in Villefranche-sur-Mer (France) for providing the experimental data.

References

- [1] G. Bastin and D. Dochain. *On-Line Estimation and Adaptive Control of Bioreactors*, volume 1 of *Process Measurement and Control*. Elsevier, Amsterdam, 1990.
- [2] O. Bernard and J.-L. Gouzé. Closed loop observers bundle for uncertain biotechnological models. *Journal of Process Control*, 14(7):765–774, 2004.
- [3] M. Droop. Vitamin B12 and marine ecology IV : The kinetics of uptake growth and inhibition in monochloris lutheri. *Journal of the Marine Biological Association*, 48(3):689–733, 1968.
- [4] J.E. Haag. *Dynamic Modelling and State Estimation of Complex Bioprocesses - Theoretical Issues and Applications*. PhD thesis, Faculté Polytechnique de Mons, 2003.
- [5] M. Z. Hadj-Sadok and J.-L. Gouzé. Estimation of uncertain models of activated sludge process with interval observers. *Journal of Process Control*, 11(3):299–310, 2001.
- [6] M. Kieffer and E. Walter. Guaranteed nonlinear state estimator for cooperative systems. *Numerical Algorithms*, 37(1):187–198, 2004.

Distributed Fuzzy Observers

Zsofia Lendek Robert Babuška Bart De Schutter
 Delft Center for Systems and Control, Delft University of Technology
 Mekelweg 2, 2628 CD Delft, The Netherlands
 Email: zs.lendek@tudelft.nl

1 Introduction

State estimation in nonlinear systems is important in applications like monitoring, fault diagnosis and nonlinear control. However, for large-scale systems, or naturally distributed applications, the construction and tuning of a centralized observer may present difficulties. Therefore, we propose the decomposition of the model into simpler subsystems.

A large class of nonlinear systems can be well represented or approximated by Takagi-Sugeno type fuzzy models [1]. We consider the case when the plant model is represented in such a form and use fuzzy observers to estimate the states of the system.

2 Cascaded Subsystems

Consider a general, observable nonlinear system, that can be partitioned into subsystems. For the ease of notation, consider only two subsystems:

$$\begin{aligned}\dot{x}^1 &= f^1(x^1) & \dot{x}^2 &= f^2(x^1, x^2) \\ y^1 &= h^1(x^1) & y^2 &= h^2(x^1, x^2)\end{aligned}$$

Assume that the subsystems are observable.

Given the above partitioning, observers can be designed for the two subsystems independently, with the second observer using the estimate of the first observer (see Figure 1). Currently, a general analysis of the joint performance (convergence, convergence speed, optimality) of the two (or more) observers with regard to a centralized observer for the joint system is missing. We study the conditions under which fuzzy observers can be designed for the subsystems, so that the convergence speed of the cascaded observers is the same as that of a single fuzzy observer.

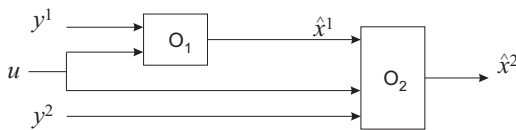


Figure 1: Cascaded observers.

3 Stability of Cascaded Systems

In general, global asymptotic stability (GAS) of the subsystems is not sufficient to prove stability of the cascade. A study of general cascades in which the subsystems are nonlinear and conditions to ensure overall stability can be found

in [2]. Assuming that the system can be expressed as:

$$\begin{aligned}\dot{x}^1 &= f_1(x^1) \\ \dot{x}^2 &= f_2(x^2) + g(x^1, x^2),\end{aligned}\tag{1}$$

under certain boundedness assumptions for f_1 , f_2 and g , a sufficient condition for the stability of the system (1) is that both subsystems $\dot{x}^1 = f_1(x^1)$ and $\dot{x}^2 = f_2(x^2)$ are uniformly GAS and the trajectories of the first subsystem are bounded.

4 Stability of Cascaded Fuzzy Observers

In the literature, several sufficient stability conditions have been derived for fuzzy systems and fuzzy observers [1,3,4]. Since the fuzzy observers are in general expressed as

$$\begin{aligned}\hat{x} &= \sum_{i=1}^m w_i(z)(A_i \hat{x} + B_i u + a_i + L_i(y - \hat{y})) \\ \hat{y} &= \sum_{i=1}^m w_i(z)(C_i \hat{x} + d_i),\end{aligned}\tag{2}$$

the stability conditions rely on the feasibility of a derived LMI problem. Two cases can be distinguished: the scheduling vector z does or does not depend on the states to be estimated. In the first case, the stability conditions for cascaded systems can be directly applied to cascaded fuzzy observers. We prove, that even if the scheduling vector depends on states to be estimated, the cascaded observer system is stable, given that the individual observers are stable. Moreover, our simulation results suggest that, in certain cases, it is possible to achieve better performance with cascaded observers.

Acknowledgement: This research is partly funded by Senter, Ministry of Economic Affairs of the Netherlands within the BSIK-ICIS project “Interactive Collaborative Information Systems” (grant no. BSIK03024).

References

- [1] K. Tanaka, T. Ikeda, and H. Wang, “Fuzzy regulators and fuzzy observers: relaxed stability conditions and LMI-based designs,” *IEEE Trans. on Fuzzy Systems*, vol. 6, pp. 250–265, 1998.
- [2] A. Loria and E. Panteley, *Advanced Topics in Control Systems Theory*, ch. Cascaded nonlinear time-varying systems: Analysis and design, pp. 23–64. Springer Berlin / Heidelberg, 2005.
- [3] M. Johansson, A. Rantzer, and K. Arzen, “Piecewise quadratic stability of fuzzy systems,” *IEEE Trans. on Fuzzy Systems*, vol. 7, pp. 713–722, 1999.
- [4] P. Bergsten, *Observers and controllers for Takagi-Sugeno fuzzy systems*. PhD thesis, Örebro University, 2001.

Part 3

Plenary Lectures

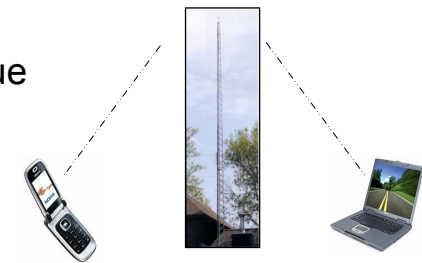
Sampling and Quantization in Signal Processing, Control and System Identification

by
 Graham C. Goodwin
 University of Newcastle
 Australia

Lecture 1
 Presented at Benelux Meeting on Systems and Control
 March 13th – 15th, 2007

1

- Most signals are analogue in nature, and
- Most systems operate in continuous time



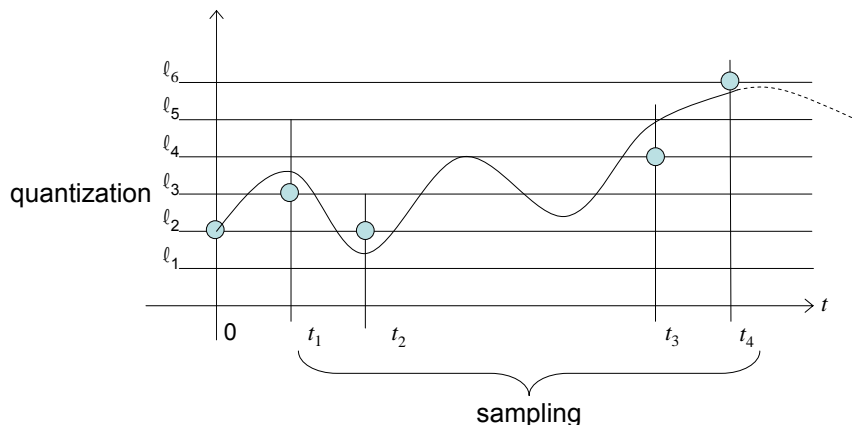
However, to store, transmit or manipulate signals, they first must be digitized.

Two aspects

- Temporal/Spatial Sampling
- Amplitude Quantization

2

Illustration of Basic Idea



3

Associated Questions

$$a(t) \in H \quad [c_1, c_2, \dots, c_N] \in A^N \quad \Psi_1(t) \quad \Psi_N(t)$$

Bases Function for Reconstruction Space
 $W \subset H$

Questions:

1. Given $a(t), \{\Psi_i(t)\}$ choose $c_i \in A$ to minimize reconstruction error?
2. If $c_1 \dots c_N$ are generated by a given sampling strategy what is the best choice for $\{\Psi_i(t)\}$?
3. Say we have already chosen $c_1 \dots c_i$, then what is the best choice for c_{i+1} ?
4. Should we pre-process $a(t)$ before sampling?

4

Series of Three Lectures

- **Lecture 1:** Sampling in Signal Processing
- **Lecture 2:** Quantization in Signal Processing and Control
- **Lecture 3:** Sampling and Quantization in Modelling and System Identification

Multidisciplinary: Combines ideas from Signal Processing, Control and Telecommunications

Lectures will take everybody (including the lecturer) out of their 'comfort zone' and introduce you to new ideas.

5

Lecture 1 Sampling in Signal Processing

Core ideas to be covered

- Nonuniform sampling patterns
- Sampling of multivariable signals
- Perfect reconstruction
- Applications to Video Compression

6

Outline

➡ 1. One Dimensional Sampling
 2. Multidimensional Sampling
 3. Sampling and Reciprocal Lattices
 4. Undersampled Signals
 5. Filter Banks
 6. Generalized Sampling Expansion (GSE)
 7. Recurrent Sampling
 8. Application: Video Compression at Source
 9. Conclusions

7

Sampling - Assume amplitude quantization sufficiently fine to be negligible.

Later we will turn to quantization issues.

Question: Say we are given

$$f(t_i); i \in \mathbb{Z}$$

Under what conditions can we recover $f(t); t \in \mathbb{R}$ from the samples?

8

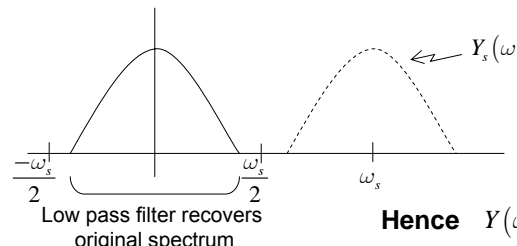
A Well Known Result (Shannon's Reconstruction Theorem) [Uniform Sampling]

Consider a scalar signal $f(t)$ consisting of frequency components in the range $(-\frac{\omega_s}{2}, \frac{\omega_s}{2})$. If this signal is sampled at period $\Delta < \frac{2\pi}{\omega_s}$, then the signal can be perfectly reconstructed from the samples using:

$$y(t) = \sum_{k=-\infty}^{\infty} y[k] \frac{\sin\left[\left(\frac{\omega_s}{2}\right)(t - k\Delta)\right]}{\left(\frac{\omega_s}{2}\right)(t - k\Delta)}$$

9

Proof: Sampling produces folding



Hence $Y(\omega) = H_s(\omega)Y_s(\omega)$

$$H_s(\omega) = 1 \quad \left(\frac{-\omega_s}{2} \leq \omega \leq \frac{\omega_s}{2} \right)$$

$$= 0 \quad \text{otherwise}$$

or $y(t) = \int_{-\infty}^{\infty} h_s(\sigma) y^s(t - \sigma) d\sigma$

$$= \int_{-\infty}^{\infty} h_s(\sigma) \sum_{k=-\infty}^{\infty} y[k] \delta(t - \sigma - k\Delta) d\sigma$$

$$= \sum_{k=-\infty}^{\infty} y[k] h_s(t - k\Delta)$$

10

189

A Simple (but surprising) Extension [Recurrent Sampling]

$$\Delta_k = M_k \Delta$$

where

$\{M_k\}$ is a periodic sequence of integers; i.e., $M_{k+N} = M_k$

Let $\sum_{k=1}^N M_k = K$

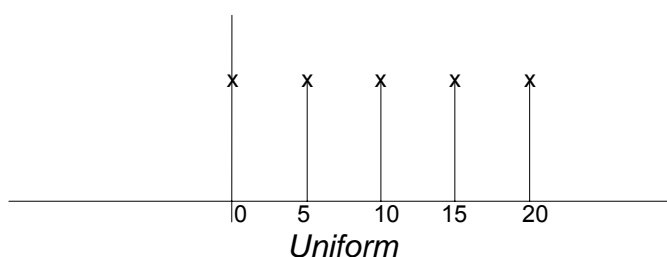
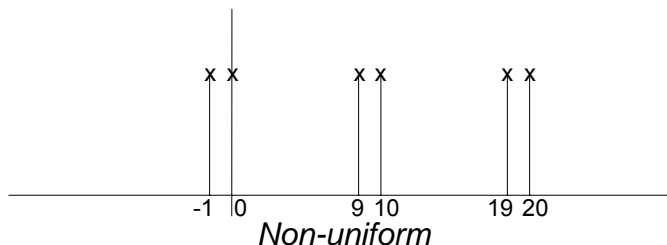
$$T = K\Delta$$

Note that the average sampling period is $\frac{K\Delta}{N} = \bar{\Delta}$

e.g.

$$\left. \begin{array}{l} \Delta_1 = 9 \\ \Delta_2 = 1 \\ \Delta_3 = 9 \\ \Delta_4 = 1 \end{array} \right\} \text{average 5}$$

11



12

Claim:

Provided the signal is bandlimited to $(-\omega_s/2, \omega_s/2)$ where $\omega_s = 2\pi/\bar{\Delta}$, then the signal can be perfectly reconstructed from the periodic sampling pattern.

where $\bar{\Delta}$ = average sampling period

Proof:

We will defer the proof to later when we will use it as an illustration of Generalized Sampling Expansion (GSE) Theorem.

13

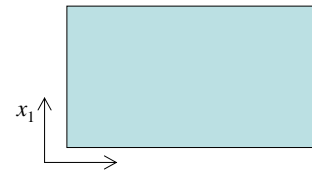
Outline

1. One Dimensional Sampling
2. Multidimensional Sampling
3. Sampling and Reciprocal Lattices
4. Undersampled Signals
5. Filter Banks
6. Generalized Sampling Expansion (GSE)
7. Recurrent Sampling
8. Application: Video Compression at Source
9. Conclusions

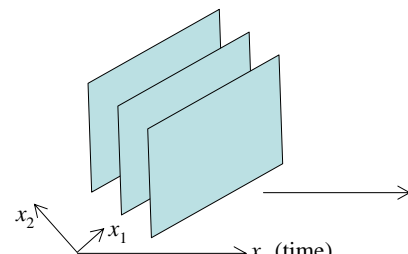
14

Multidimensional Signals

Digital Photography



Digital Video



15

Outline

1. One Dimensional Sampling
2. Multidimensional Sampling
3. Sampling and Reciprocal Lattices
4. Undersampled Signals
5. Filter Banks
6. Generalized Sampling Expansion (GSE)
7. Recurrent Sampling
8. Application: Video Compression at Source
9. Conclusions

16

How should we define sampling for multi-dimensional signals?

Utilize idea of Sampling Lattice

$$T \text{ nonsingular matrix } \in \mathbb{R}^D \times \mathbb{R}^D$$

Sampling Lattice

$$\Lambda = \text{Lat}(T) = \{Tn : n \in \mathbb{Z}^D\}$$

17

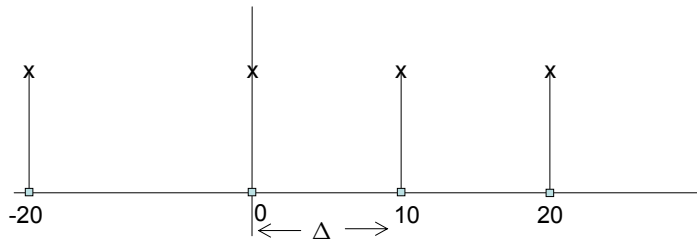
Also, need multivariable **frequency** domain concepts.

These are captured by two ideas

- i. Reciprocal Lattice
- ii. Unit Cell

18

One Dimensional Example



Reciprocal Lattice

$$\Lambda^* = \text{Lat}\{2\pi T^{-1}\} = \{2\pi T^{-1}n : n \in \mathbb{Z}^D\}$$

Unit Cell $UC(\Lambda^*)$ (Non-unique)

$$\text{i. } \{UC(\Lambda^*) + 2\pi T^{-1}n_1\} \cap \{UC(\Lambda^*) + 2\pi T^{-1}n_2\} = \emptyset$$

$$n_1, n_2 \in \mathbb{Z}^D \quad n_1 \neq n_2$$

$$\text{ii. } \bigcup_{n \in \mathbb{Z}^D} \{UC(\Lambda^*) + 2\pi T^{-1}n\} = \mathbb{R}^D$$

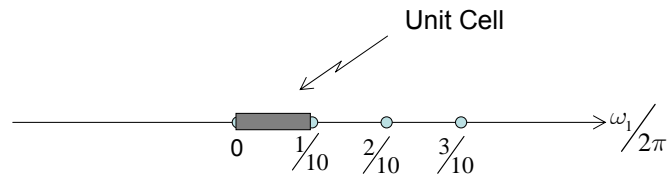
19

Sampling Lattice

$$\Lambda = \{\Delta n : n \in \mathbb{Z}\}$$

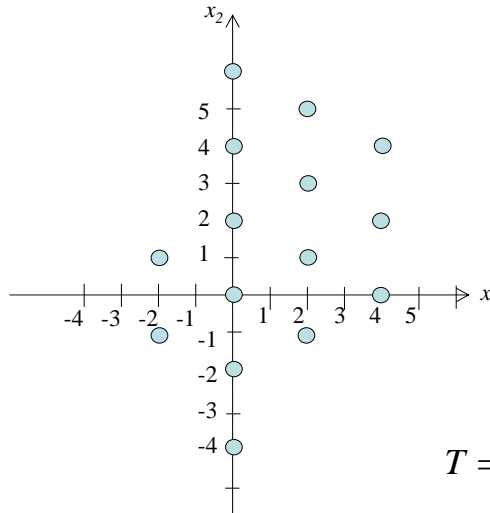
20

Reciprocal Lattice and Unit Cell



21

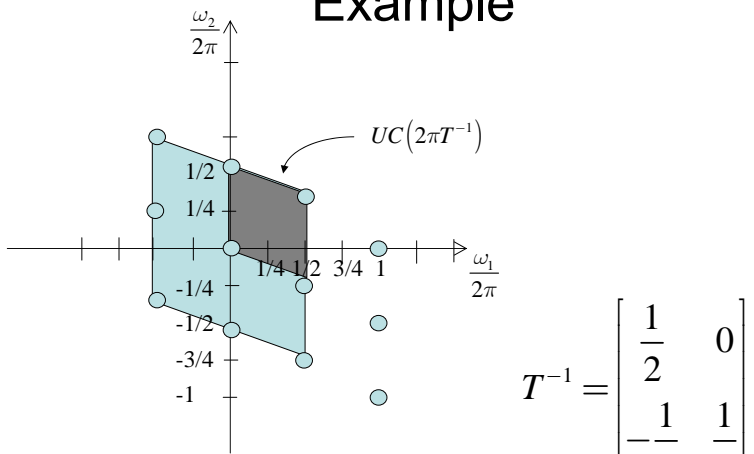
Multidimensional Example



$$T = \begin{bmatrix} 2 & 0 \\ 1 & 2 \end{bmatrix}$$

22

Reciprocal Lattice and Unit Cell for Example



$$T^{-1} = \begin{bmatrix} 1 & 0 \\ 2 & 1 \\ -1/4 & 1/2 \end{bmatrix}$$

23

Outline

1. One Dimensional Sampling
2. Multidimensional Sampling
3. Sampling and Reciprocal Lattices
4. Undersampled Signals
5. Filter Banks
6. Generalized Sampling Expansion (GSE)
7. Recurrent Sampling
8. Application: Video Compression at Source
9. Conclusions

24

We will be interested here in the situation where the Sampling Lattice is **not** a Nyquist Lattice for the signal (i.e., the signal cannot be perfectly reconstructed from the original pattern!)

Strategy:

We will generate other samples by ‘filtering’ or ‘shifting’ operations on the original pattern.

25

Consider a bandlimited signal $f(x)$, $x \in \mathbb{R}^D$.

Assume the D -dimension Fourier transform has finite support, S .

Then for given D -dimensional lattice T , there always exists a finite set $\{\omega_m\}_1^P \in \Lambda^*$, such that support

$$(\hat{f}(\omega)) \subseteq S = \bigcup_{m=1}^P (UC(\Lambda^*) + \omega_m).$$

Heuristically: The idea of “Tiling” the area of interest in the frequency domain

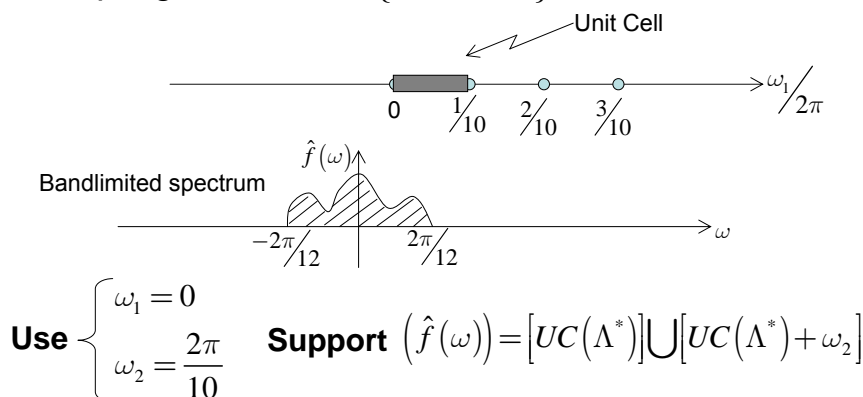
26

193

One Dimensional Example

Our one dimensional example continued.

Sampling Lattice $\Lambda = \{k\Delta; k \in \mathbb{Z}\}$



27

Outline

1. One Dimensional Sampling
2. Multidimensional Sampling
3. Sampling and Reciprocal Lattices
4. Undersampled Signals
5. Filter Banks
6. Generalized Sampling Expansion (GSE)
7. Recurrent Sampling
8. Application: Video Compression at Source
9. Conclusions

28

Generation of Extra Samples

Suppose now we generate a data set

$$\left\{ \left\{ g_m(Tn) \right\}_{m=1}^Q \right\}_{n \in \mathbb{Z}^P}$$

as shown in below ($Q \geq P$)

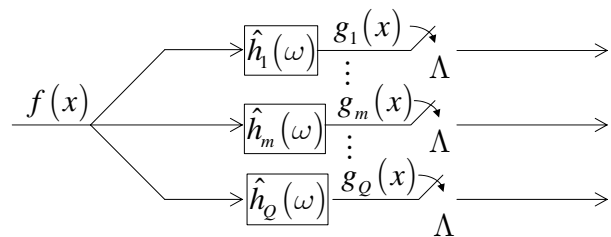


Figure: Q – Channel Configuration

29

Outline

1. One Dimensional Sampling
2. Multidimensional Sampling
3. Sampling and Reciprocal Lattices
4. Undersampled Signals
5. Filter Banks
6. Generalized Sampling Expansion (GSE) 
7. Recurrent Sampling
8. Application: Video Compression at Source
9. Conclusions

30

194

Define $H(\omega) = \begin{bmatrix} \hat{h}_1(\omega + \omega_1) & \hat{h}_2(\omega + \omega_1) & \dots & \hat{h}_Q(\omega + \omega_1) \\ \hat{h}_1(\omega + \omega_2) \\ \vdots \\ \hat{h}_1(\omega + \omega_P) & & & \hat{h}_Q(\omega + \omega_P) \end{bmatrix}$

Let $\Phi(\omega, x) = \begin{bmatrix} \Phi_1(\omega, x) \\ \vdots \\ \Phi_Q(\omega, x) \end{bmatrix}$

be the solution (if it exists) of

for $\omega \in UC(\Lambda^*)$

$$H(\omega)\Phi(\omega, x) = \begin{bmatrix} e^{j\omega_1^T x} \\ \vdots \\ e^{j\omega_Q^T x} \end{bmatrix}$$

31

Conditions for Perfect Reconstruction

Theorem:

$f(x)$ can be reconstructed from

$$f(x) = \sum_{M=1}^Q \sum_{k \in \mathbb{Z}^P} g_m(Tk) \phi_m(x - U k)$$

if and only if $H(\omega)$ has full row rank

where $\phi_m(x) = \int_{UC} \phi_m(\omega, x) e^{j\omega^T x} d\omega$

32

Proof: $\Phi_q(\omega, x) e^{j\omega^T x} = \sum_{k \in \mathbb{Z}^D} \phi_q(x - Tk) e^{-j\omega^T Tk}; \omega \in UC(\Lambda^*)$

Multiply both sides by $\hat{h}_q(\omega + \omega_p)$ and sum over 'q'

$$\begin{aligned} & \sum_{q=1}^Q \sum_{k \in \mathbb{Z}^D} \hat{h}_q(\omega + \omega_p) \phi_q(x - Tk) e^{-j\omega^T Tk} \\ &= \sum_{q=1}^Q \hat{h}_q(\omega + \omega_p) \Phi_q(\omega, x) e^{j\omega^T x} \\ &= e^{j\omega^T x} \text{ from Matrix result} \end{aligned}$$

Now using tiling property to extend from $UC(\Lambda^*)$ to S

Finally $f(x) = \int_s \hat{f}(\omega) e^{j\omega^T x} d\omega$

$$= \int_s \underline{\hat{f}(\omega)} \sum_{q=1}^Q \sum_{k \in \mathbb{Z}^D} \underline{\hat{h}_q(\omega)} \underline{\phi_q(x - Tk)} e^{j\omega^T \underline{T_k}} d\omega$$

33

Outline

1. One Dimensional Sampling
2. Multidimensional Sampling
3. Sampling and Reciprocal Lattices
4. Undersampled Signals
5. Filter Banks
6. Generalized Sampling Expansion (GSE)
7. Recurrent Sampling
8. Application: Video Compression at Source
9. Conclusions

→ 7. Recurrent Sampling

34

195

Special Case: Recurrent Sampling

$$\Psi = \bigcap_{q=1}^Q \{Lat(T) + x_q\}$$

where w.l.o.g. $\{x_q\} \in UC(T)$

Now, given the samples $\{f(\tilde{x})\}_{\tilde{x} \in \Psi}$, our goal is to perfectly reconstruct $f(x)$.

35

Define $\hat{h}_q(\omega) = e^{j\omega^T x_q}$, then $f_q(x) = f(x + x_q)$

and $\{f_q(Tn)\}_{n \in \mathbb{Z}^P, q=1, \dots, Q} = \{f(\tilde{x})\}_{\tilde{x} \in \Psi}$

Then apply GSE where

$$\begin{aligned} H(\omega) &= \begin{bmatrix} e^{j(\omega + \omega_1)^T x_1} & \dots & e^{j(\omega + \omega_1)^T x_Q} \\ e^{j(\omega + \omega_P)^T x_1} & \dots & e^{j(\omega + \omega_P)^T x_Q} \end{bmatrix} \\ &= \underbrace{\begin{bmatrix} e^{j\omega_1^T x_1} & e^{j\omega_1^T x_Q} \\ e^{j\omega_P^T x_1} & e^{j\omega_P^T x_Q} \end{bmatrix}}_{\text{Nonsingular}} \begin{bmatrix} e^{j\omega_1^T x_1} & 0 \\ 0 & e^{j\omega_P^T x_Q} \end{bmatrix} \end{aligned}$$

36

Return to our one-dimensional example

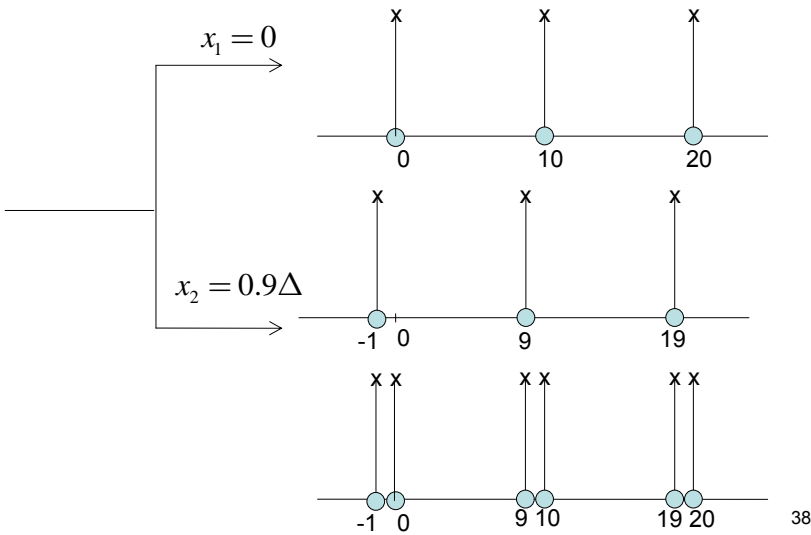
Recall that we had $\omega_1 = 0$
so that $\omega_2 = \frac{2\pi}{\Delta}$

support $\hat{f}(\omega) = [UC(\Lambda^*)] \cup [UC(\Lambda^*) + \omega_2]$

Say we use recurrent sampling with

$$x_1 = 0 \\ x_2 = 0.9\Delta$$

37



38

196

Condition for Perfect Reconstruction is

$$\begin{bmatrix} e^{j\omega_1 x_1} & e^{j\omega_1 x_2} \\ e^{j\omega_2 x_1} & e^{j\omega_2 x_2} \end{bmatrix} \text{ nonsingular} \\ = \begin{bmatrix} 1 & 1 \\ 1 & e^{j(0.9)(2\pi)} \end{bmatrix}$$

39

Outline

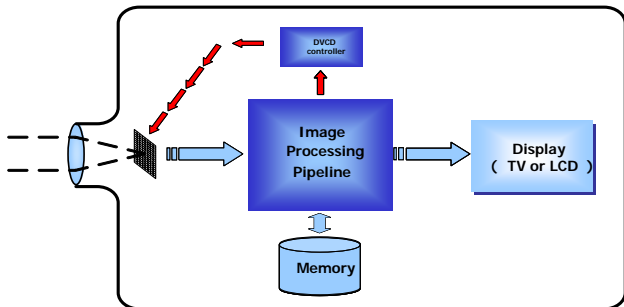
1. One Dimensional Sampling
2. Multidimensional Sampling
3. Sampling and Reciprocal Lattices
4. Undersampled Signals
5. Filter Banks
6. Generalized Sampling Expansion (GSE)
7. Recurrent Sampling
8. Application: Video Compression at Source
9. Conclusions

40

Application: Video Compression Source

Introduction to video cameras

- Instead of tape, digital cameras use 2D sensor array (CCD or CMOS)



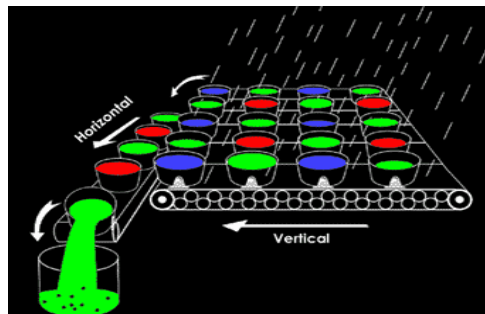
41

Image Sensor

- A 2D array of sensors replaces the traditional tape
- Each sensor records a 'point' of the continuous image
- The whole array records the continuous image at a particular time instant

42

2D Colours Sensor Array



Data transfer from array is sequential and has a maximal rate of Q .

* Based on <http://www.dpreview.com/learn/>

43

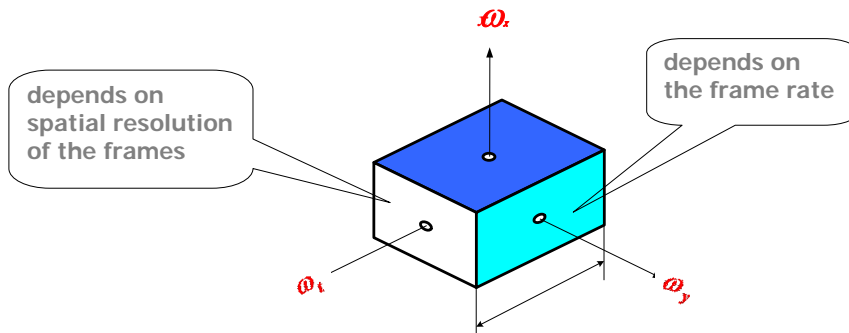
Current Technology

Uniform 3D sampling

- a sequence of identical frames equally spaced in time

44

Video Bandwidth



The volume of 'box' depends on the capacity:
pixel rate = (frame rate) x (spatial resolution)

45

BUT...

Generally

$$Q \ll RF$$

Need:

$$R_1 < R \quad F_1 < F$$

s.t.

$$R_1 F_1 = Q$$

Compromise:

- *spatial resolution* $R_1 < R$
- *temporal resolution* $F_1 < F$

47

Hard Constraints

1. Data recording on sensor:

- Sensor array density
- for spatial resolution

$$R \left[\frac{\text{pixels}}{\text{frame}} \right]$$

- Sensor exposure time
- for frame rate

$$F \left[\frac{\text{frames}}{\text{sec.}} \right]$$

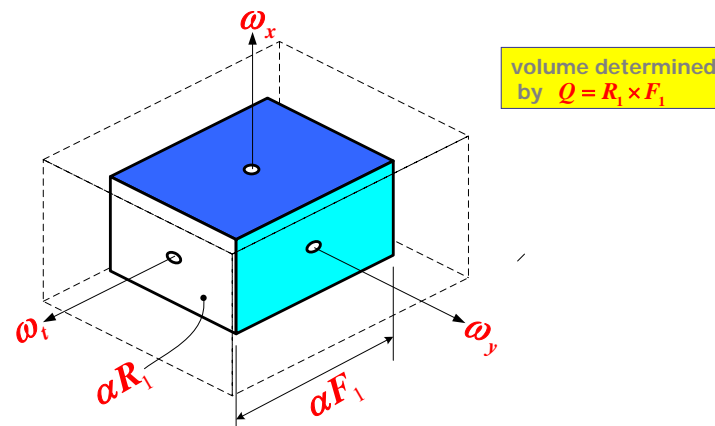
2. Data reading from sensor:

- Data readout time
- for pixel rate

$$Q \left[\frac{\text{pixels}}{\text{sec.}} \right]$$

46

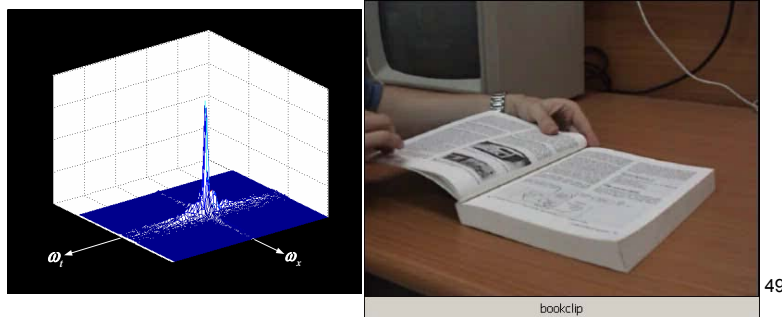
Actual Capacity (Data Readout)



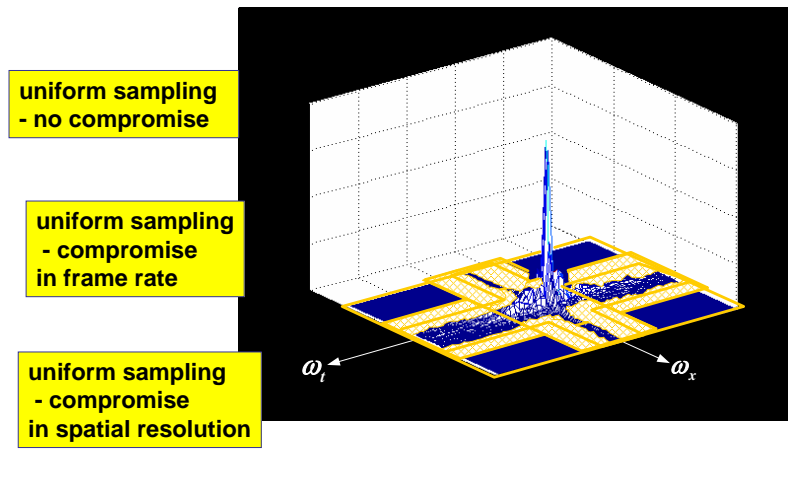
48

Observation

Most energy of typical video scene is concentrated around the (ω_x, ω_y) plane and the ω_t axis.



The Spectrum of this Video Clip



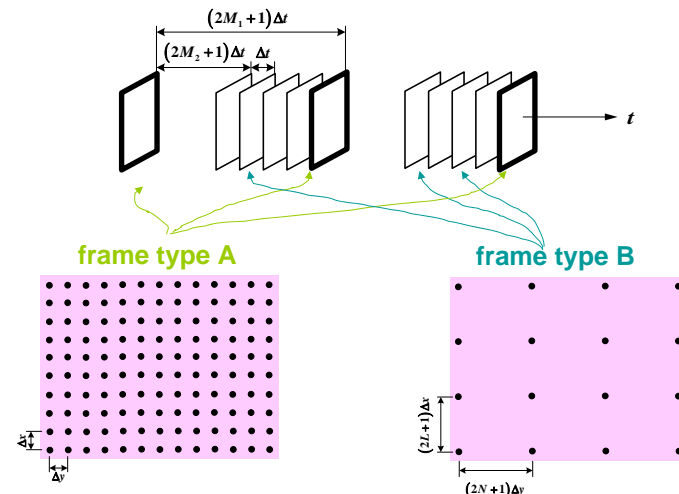
199

New Idea

- Idea is to deviate from constant resolutions in a **recorded** video clip. This means that sampling patterns within the video clip will not be **uniform**.
- Specifically, the idea is to have, within the recorded video clip, a combination of fast frames with low spatial resolution and slow frames with high spatial resolution.

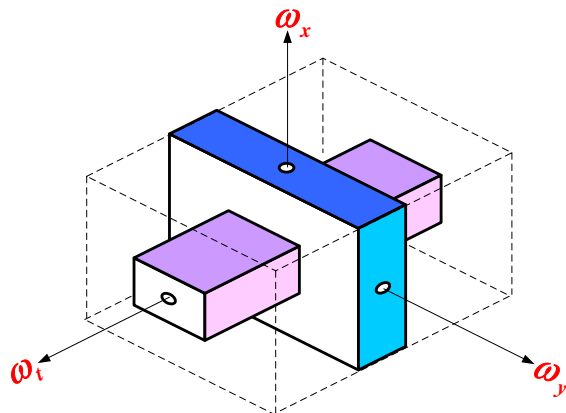
51

Recurrent Non-Uniform Sampling



52

What Does it Buy?



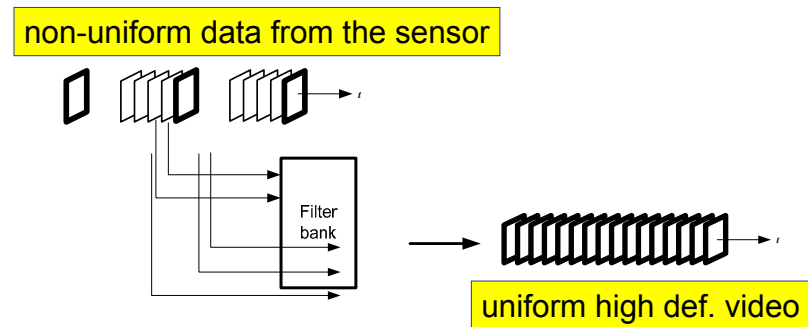
200

Recurrent Non-Uniform Sampling

A special case of
Generalized Sampling Expansion Theorem

53

Schematic Implementation



'compression at the source'

54

Sampling Pattern

The resulting sampling pattern is given by:

$$\Psi = LAT(U) \bigcup_{l=1}^{2L} \left\{ LAT(U) + \begin{bmatrix} l\Delta x \\ 0 \end{bmatrix} \right\} \bigcup_{m=2M_2+1}^{2M_1} \left\{ LAT(U) + \begin{bmatrix} 0 \\ m\Delta t \end{bmatrix} \right\}$$

$$\Psi = \bigcup_{s=1}^{2(L+M)+1} \{ LAT(U) + x_s \}$$

55

56

Frequency Domain

$$S = \bigcup_{r=1}^{2(L+M)+1} \{UC(2\Delta U^{-T}) + \omega_r\}$$

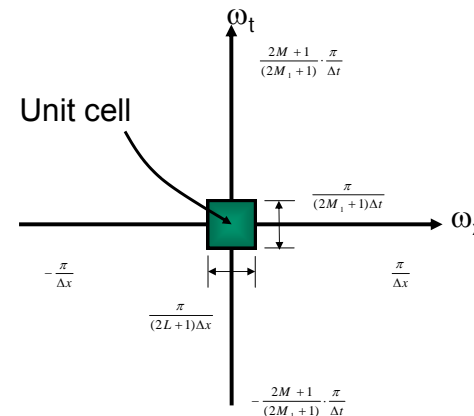
where: $UC(2\pi U^{-T}) = \left\{ \omega = \begin{bmatrix} \omega_x \\ \omega_t \end{bmatrix} : |\omega_x| < \frac{\pi}{(2L+1)\Delta x}, |\omega_t| < \frac{\pi}{(2M_1+1)\Delta t} \right\}$

is the unit cell of the reciprocal lattice

$$LAT(2\pi U^{-T}) = \left\{ \begin{bmatrix} \frac{\pi}{(2L+1)\Delta x} & 0 \\ 0 & \frac{\pi}{(2M_1+1)\Delta t} \end{bmatrix} n : n \in \mathbb{Z}^2 \right\}$$

57

Reciprocal Lattice



58

201

Apply the GSE Theorem

$$H(\omega) \begin{bmatrix} \Phi_1 \\ \Phi_2 \\ \vdots \\ \Phi_{2(L+M)+1} \end{bmatrix} = \gamma(x)$$

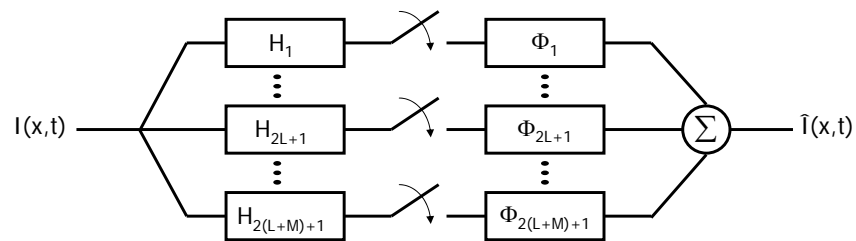
Where: $H(\omega)$ is uniquely defined by $H_1 \dots H_2 \dots$
 γ is a set of $2(L+M)+1$ constraints

If H^{-1} exists, we can find the reconstruction function

$$\Phi(\omega, x) = H^{-1}(\omega) \gamma(x)$$

59

Reconstruction Scheme



$$H_{r,s} = e^{j\omega_r^T \begin{bmatrix} x_r \\ t_r \end{bmatrix}}$$

The sub-sampled frequency of each filter H is: $\frac{\text{Nyquist frequency}}{2(L+M)+1}$

60

Reconstruction functions

$$\varphi_r(x, t) = (2L+1)\Delta x \Delta t \frac{\sin\left(\frac{\pi}{\Delta x}(x - (r-1)\Delta x)\right) \sin\left(\frac{\pi}{(2M+1)\Delta t}\right)}{\pi(x - (r-1)\Delta x)} \quad \text{for } r = 2, 3, \dots, 2L+1$$

$$\varphi_r(x, t) = (2M+1)\Delta x \Delta t \frac{\sin\left(\frac{\pi}{(2L+1)\Delta x}\right) \sin\left(\frac{\pi}{\Delta t}(t - (r-2L-1)\Delta t)\right)}{\pi x} \quad \text{for } r = 2(L+1), \dots, 2(L+M)+1$$

Multidimensional 'sinc like' functions

61

Demo

Full resolution sequence



Reconstructed sequence

Temporal decimation



Spacial decimation

62

202

Outline

1. One Dimensional Sampling
2. Multidimensional Sampling
3. Sampling and Reciprocal Lattices
4. Undersampled Signals
5. Filter Banks
6. Generalized Sampling Expansion (GSE)
7. Recurrent Sampling
8. Application: Video Compression at Source
9. Conclusions



63

This lecture has covered

- Nonuniform sampling of scalar signals
- Nonuniform sampling of multidimensional signals
- Generalized sampling expansion
- Application to video compression

64

Open Problems?

- Many!
- Example: Given a fixed bit rate what is the best combined sampling and quantization strategy?
- Current work uses 'Nyquist' sampling but a guess is that the errors due to sampling and quantization should be of the same magnitude for optimality.

Tomorrow's Lecture – Quantization!

65

References

• One Dimensional Sampling

- A. Feuer and G.C. Goodwin, *Sampling in Digital Signal Processing and Control*. Birkhäuser, 1996.
- R.J. Marks II, Ed., *Advanced Topics in Shannon Sampling and Interpolation Theory*. New York: Springer-Verlag, 1993.

• Multidimensional Sampling

- W.K. Pratt, *Digital Image Processing*, 3rd ed: John Wiley & Sons, 2001.
- B.L. Evans, "Designing commutative cascades of multidimensional upsamplers and downsamplers," *IEEE Signal Process Letters*, Vol4, No.11, pp.313-316, 1997.

• Sampling and Reciprocal Lattices, Undersampled Signals

- A. Feuer, G.C. Goodwin, 'Reconstruction of Multidimensional Bandlimited Signals for Uniform and Generalized Samples,' *IEEE Transactions on Signal Processing*, Vol.53, No.11, 2005.
- A.K. Jain, *Fundamentals of Digital Image Processing*, Englewood Cliffs, NJ: Prentice-Hall, 1989.

66

References

• Filter Banks

- Y.C. Eldar and A.V. Oppenheim, 'Filterbank reconstruction of bandlimited signals from nonuniform and generalized samples,' *IEEE Transactions on Signal Processing*, Vol.48, No.10, pp.2864-2875, 2000.
- P.P. Vaidyanathan, *Multirate Systems and Filter Banks*. Englewood Cliffs, NJ: Prentice-Hall, 1993.
- H. Böleskei, F. Hlawatsch and H.G. Feichtinger, 'Frame-theoretic analysis of oversampled filter banks,' *IEEE Transactions on Signal Processing*, Vol.46, No.12, pp.3256-3268, 1998.
- M. Vetterli and J. Kovacević, *Wavelets and Subband Coding*, Englewood Cliffs, NJ: Prentice Hall, 1995.

67

References

• Generalized Sampling Expansions, Recurrent Sampling

- A. Papoulis, 'Generalized sampling expansion,' *IEEE Transaction on Circuits and Systems*, Vol.CAS-24, No.11, pp.652-654, 1977.
- A. Feuer, 'On the necessity of Papoulis result for multidimensional (GSE),' *IEEE Signal Processing Letters*, Vol.11, No.4, pp.420-422, 2004.
- K.F.Cheung, 'A multidimensional extension of Papoulis' generalized sampling expansion with application in minimum density sampling,' in *Advanced Topics in Shannon Sampling and Interpolation Theory*, R.J. Marks II. Ed., New York: Springer-Verlag, pp.86-119, 1993.

• Video Compression at Source

- E. Shechtman, Y. Caspi and M. Irani, 'Increasing space-time resolution in video', *European Conference on Computer Vision (ECCV)*, 2002.
- N. Maor, A. Feuer and G.C. Goodwin, 'Compression at the source of digital video,' Technical Report, School of Electrical Engineering, Technion, Israel, 2006.

68

Lecture 2

Quantization in Signal Processing and Control

by
Graham C. Goodwin
University of Newcastle
Australia

Presented at Benelux Meeting on Systems and Control
March 13th – 15th, 2007

Topics to be covered include: signal quantization, predictive and noise shaping quantizers, networked control, signal coding in networked control, channel capacity issues in networked control, applications in audio compression and control over communication channels.

1

2

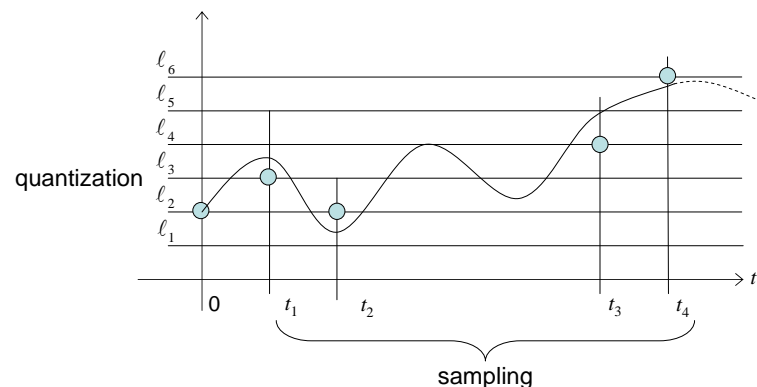
204

Outline

- ➡ 1. Quantization
- 2. Predictive and Noise Shaping Quantizers
- 3. Application to Audio Compression
- 4. Networked Control
- 5. Modelling Communication Link
- 6. Predictive and Noise Shaping Coding
- 7. Experimental Results
- 8. Conclusions

3

Recall Basic Idea of Sampling and Quantization



4

Quantization

Here: Fix the sampling pattern (say uniform for simplicity) and examine the quantization problem.

Approaches

1. Nonlinear – quantization is an inherently nonlinear process.
2. Linear – approximate quantization errors as noise.

To illustrate ideas we will follow route 2.
(*Generally gives design insights.*)

5

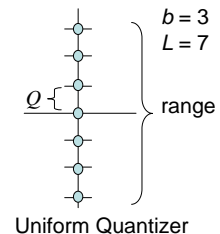
Signal to Noise Ratio Model for Quantization

b bit quantizer

$$L = [2^b - 1] \text{ levels}$$

Assume quantization errors are white noise uniformly distributed $[-\frac{Q}{2}, \frac{Q}{2}]$

$$\sigma_q^2 = \frac{Q^2}{12}$$



Uniform Quantizer

We want small probability that signal amplitude exceeds the range of the quantizer. Assume variance of signal is σ_v^2 , then e.g. 4 s.d. rule says that $4\sigma_v = \frac{1}{2}Q$.

$$\text{Hence } \sigma_q^2 = k\sigma_u^2; \quad k = \frac{16}{3}L^2 = \frac{16}{3}[2^b - 1]^2 [6\text{dB/bit}]$$

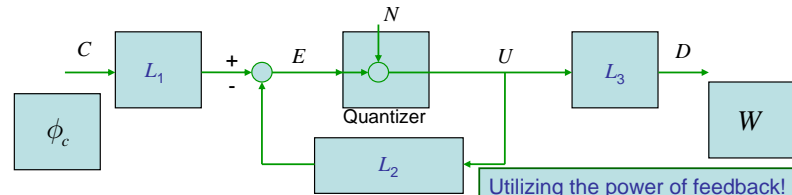
6

Outline

1. Quantization
2. Predictive and Noise Shaping Quantizers
3. Application to Audio Compression
4. Networked Control
5. Modelling Communication Link
6. Predictive and Noise Shaping Coding
7. Experimental Results
8. Conclusions

7

Predictive and Noise Shaping Quantizers (Quantization errors modeled as additive white noise)



$$D = \left\{ \frac{L_1 L_3}{1 + L_2} \right\} C + \left\{ \frac{L_3}{1 + L_2} \right\} N$$

$$E = \left\{ \frac{L_1}{1 + L_2} \right\} C + \left\{ \frac{L_2}{1 + L_2} \right\} N$$

$$= \left\{ \frac{L_1}{1 + L_2} \right\} C \quad (\text{We will return to this approximation later!})$$

8

Focus on Frequency Weighted (W) Noise Power in D

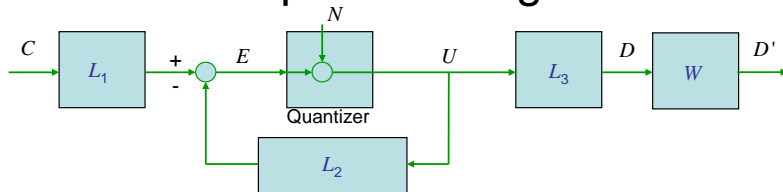
$$\begin{aligned}\{\text{Noise Power in } WD\} &= \sigma_N^2 \int \left| \frac{WL_3}{1+L_2} \right|^2 dw \\ &= (kP_E) \int \left| \frac{WL_3}{1+L_2} \right|^2 dw \\ &= k \int \left| \frac{L_1}{1+L_2} \right|^2 \phi_c dw \int \left| \frac{WL_3}{1+L_2} \right|^2 dw\end{aligned}$$

where ϕ_c is the input signal spectrum

Use normalized transfer functions; $G(0) = 1$

9

Heuristic Explanation of the Optimal Design



- Spectrum of C and characteristics of W are known.
- We have 3 filters to design.
- One degree of freedom removed by "Perfect Reconstruction" requirement i.e., $\frac{L_1 L_3}{1+L_2} = 1$
- With remaining 2 degrees of freedom can (i) shape E to have minimal variance (prediction) and (ii) shape component of D' due to N to have minimal variance (noise shaping).

10

- Perfect Reconstruction Constraint

$$\frac{L_1 L_3}{1+L_2} = 1$$

- Minimizing variance of E

$$\frac{L_1}{1+L_2} = \phi_c^{1/2} \quad (\text{Whitening Filter: Predictive coding})$$

- Minimize variance of WD due to N

$$\frac{WL_3}{1+L_2} = 1 \quad (\text{Noise shaping})$$

- Solution:**

$$\begin{aligned}L_1 &= W \\ L_2 &= \phi_c^{1/2} W - 1 \\ L_3 &= \phi_c^{1/2}\end{aligned}$$

11

Predictive Coder

Choose $W = 1$

$$\begin{aligned}\text{Optimal choices are} \quad L_3 &= \phi_c^{1/2} \\ 1+L_2 &= \phi_c^{1/2} \\ L_1 &= 1\end{aligned}$$

This solution corresponds to Minimum Variance Control

12

Noise Shaping Quantizer (Sigma-delta)

Add extra constraint $L_3 = 1$

Optimal Choices: $L_1 = W$
 $L_2 = W - 1$

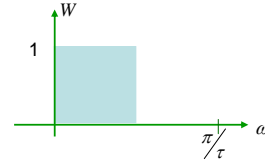
Then $D = C + \left[\frac{1}{W} \right] N$ (Noise Shaping)

$WD = W \{C\} + N$ (Achieved Performance)

13

The Role of Oversampling

Say we choose $L_3 = 1$ and W as ideal low pass filter



Then apparently, all we need do is make $\frac{1}{1+L_2}$ an ideal high pass filter to "push" "quantization noise" outside the band of interest.

Does this make sense?

14

Insights from Feedback Theory

$\frac{1}{1+L_2}$ is a sensitivity function.

We know from Bode integral that

$$\int \ln \left| \frac{1}{1+L_2} \right| = 0 \quad (\text{Water Bed Effect})$$

Thus making the sensitivity arbitrarily small in some frequency range automatically means that it will be arbitrarily large somewhere else!

15

Indeed, this goes back to the early simplifying assumption that

$$E = \left\{ \frac{L_1}{1+L_2} \right\} C$$

In fact it should have been

$$E = \left\{ \frac{L_1}{1+L_2} \right\} C + \left\{ \frac{L_2}{1+L_2} \right\} N$$

and

$$\text{Noise Power in } WD = \frac{k \int \left| \frac{L_1}{1+L_2} \right|^2 \phi_c dw \int \left| \frac{WL_3}{1+L_2} \right|^2 dw}{1 - k \int \left| \frac{L_2}{1+L_2} \right|^2 dw}$$

More Complex (but more realistic) optimization problem.

It turns out to be convex!

16

In summary – we can design an “optimal” quantizer which:

- (i) minimizes the impact of quantization noise on the output, and
- (ii) takes account of the fact that quantization errors ultimately need themselves to be quantized due to the feed back structure.

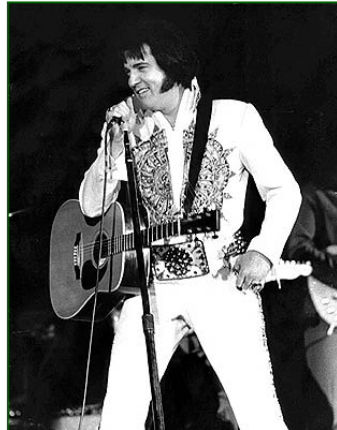
Application : Audio Compression

Original

$N=0$

$N=1$

$N=2$



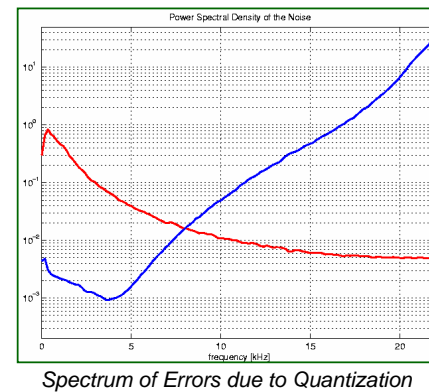
Elvis Presley

Outline

1. Quantization
2. Predictive and Noise Shaping Quantizers
3. Application to Audio Compression
4. Networked Control
5. Modelling Communication Link
6. Predictive and Noise Shaping Coding
7. Experimental Results
8. Conclusions

Other Insights From Control Theory

(i) Bode integral



Outline

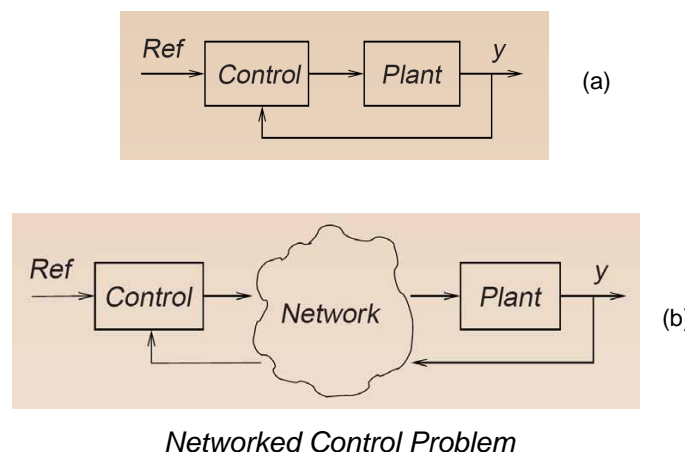
1. Quantization
2. Predictive and Noise Shaping Quantizers
3. Application to Audio Compression
4. Networked Control
5. Modelling Communication Link
6. Predictive and Noise Shaping Coding
7. Experimental Results
8. Conclusions

21

Network Control Systems

- In a Networked Control System (NCS) controller and plant are connected via a **communication link**.
- Therefore, signals transmitted:
 - Have to be quantized
 - May be delayed
 - May get lost
- The communication link constitutes a performance bottleneck.
- When designing NCS's the characteristics of the network should be accounted for to ensure acceptable performance levels.
- When comparing to traditional control loops, in NCS's there exist additional degrees of freedom to be designed.
- It is useful to investigate:
 - Architectural issues
 - Signal coding methods

22



23

Useful analog to think about:



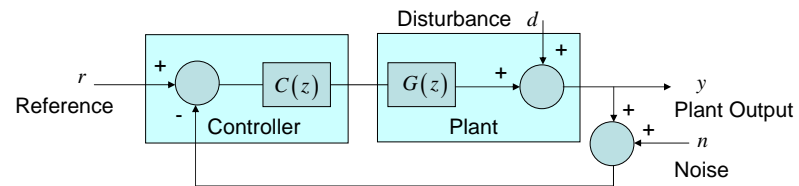
24

Nominal Control Design

- We will consider the situation where an LTI controller has already been designed for a SISO LTI plant model.
- We will refer to this design as the ***nominal design*** and we will assume that it gives satisfactory performance in a non-networked setting.
- We will show how to minimize the impact of the communication link on closed loop performance.

25

Design Relations



The tracking error is given by:

$$e \triangleq r - y = S(z)r - S(z)d + T(z)n$$

where

$$T_0(z) \triangleq \frac{G(z)C(z)}{1+G(z)C(z)}, \quad S_0(z) \triangleq \frac{1}{1+G(z)C(z)}$$

are the loop sensitivity functions.

26

Design Relationships

In non-networked situation we have:

$$e = \frac{1}{1+G(z)C(z)}r - \frac{1}{1+G(z)C(z)}d + \frac{G(z)C(z)}{1+G(z)C(z)}n$$

- To achieve good reference following and disturbance attenuation, $C(z)$ is typically chosen such that the open loop gain, $|G(e^{j\omega})C(e^{j\omega})|$ is large at frequencies where $|R(e^{j\omega})|$ and $|D(e^{j\omega})|$ are significant.
- To handle measurement noise and plant model inaccuracies, the open loop gain should be reduced at appropriate frequencies.

27

Outline

1. Quantization
2. Predictive and Noise Shaping Quantizers
3. Application to Audio Compression
4. Networked Control
5. Modelling Communication Link
6. Predictive and Noise Shaping Coding
7. Experimental Results
8. Conclusions

28

The Communication Link

- The novel ingredient in an NCS, when compared to a traditional control loop, is the communication link.
- It constitutes a significant bottleneck in the achievable performance.
- From a design perspective, this opens the possibility of investigating:

NCS Architectures

Where do I place the processing power?

Signal Coding

What information do I send?

29

211

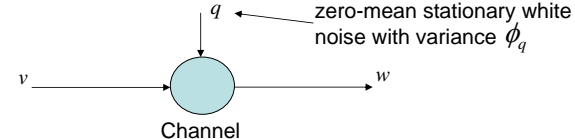
Outline

1. Quantization
2. Predictive and Noise Shaping Quantizers
3. Application to Audio Compression
4. Networked Control
5. Modelling Communication Link
6. Predictive and Noise Shaping Coding
7. Experimental Results
8. Conclusions

31

Channel Model

- We will consider an additive Noise model:



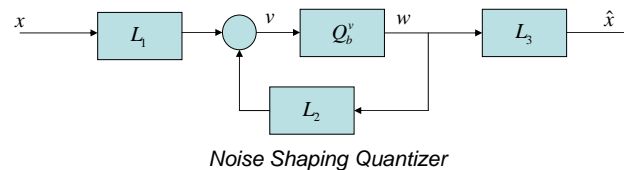
- The channel has a given signal-to-noise ratio, say SNR:

$$\text{SNR} = \left(\frac{\phi_v}{\phi_q} \right) = \frac{3}{16} \cdot 2^{2b}; \quad b : \text{number of bits/sample.}$$

- The above characterization encompasses, e.g.,
 - AWGN channels
 - Bit-rate limited channels (networks), where transmitted signals are passed through an appropriately scaled memoryless quantizer.

30

Recall Predictive and Noise shaping quantizer



Use this idea in Channel Coding

- L_1 & L_2 become part of channel **coder**
- L_3 becomes part of the channel **decoder**

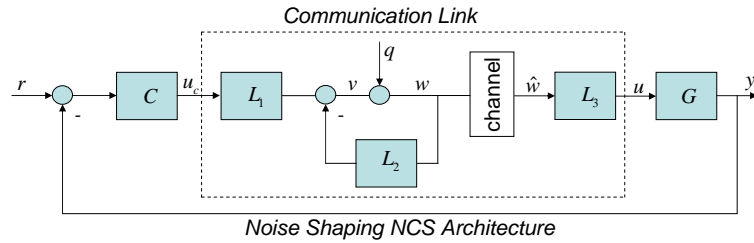
Make transparent to
nominal control loop
(i.e., Perfect Reconstruction)

$$L_1 \left(\frac{1}{1 + L_2} \right) L_3 = 1$$

32

Illustration

Channel in the Downlink



$$S_0 = \frac{1}{1+GC}$$

$$S_2 = \frac{1}{1+L_2}$$

Constraint: $L_1 S_2 L_3 = 1$

33

Analysis

$$e = r - y = S_0 G L_3 S_2 q + S_0 r$$

Hence, variance of output error due to quantization errors is

$$\sigma_{eq}^2 = \sigma_q^2 \|S_0 G L_3 S_2\|_2^2 \quad (a)$$

However, from SNR model

$$\sigma_q^2 = \frac{\sigma_v^2}{SNR} \quad (b)$$

Now

$$v = L_3^{-1} C S_0 r - (L_3^{-1} C S_0 G L_1^{-1} + T_2) q$$

$$\text{with } T_2 = (1 - S_2) \text{ and using } S_2 = T_1^{-1} T_3^{-1} \quad (c)$$

$$\sigma_v^2 = \|L_3^{-1} C S_0 \Omega_r\|_2^2 + \sigma_q^2 \|L_3^{-1} C S_0 G L_1^{-1} + T_2\|_2^2$$

34

From (a), (b), (c)

$$\sigma_{eq}^2 = \frac{\|L_3^{-1} C S_0 \Omega_r\|_2^2 \|S_0 G L_3 S_2\|_2^2}{SNR - \|1 - S_2 S_0\|_2^2}$$

35

- Expression is essentially as for the Predictive and Noise Shaping Quantizer Design save that now the Weighting Function is determined by the Nominal Loop Sensitivity.
- Hence can readily determine optimal values of L_1 , L_2 and L_3 as before!

36

Special Case (Predictive Coding) (PCM)

Fix $L_2 = 0$

Then

$$\sigma_{eq}^2 = \frac{\|L_3^{-1}CS_0\Omega_r\|_2^2 \|S_0GL_3\|_2^2}{SNR - \|T_0\|_2^2}$$

$$T_0 = 1 - S_0$$

37

Relationship to Channel Capacity Constraints

- The theory shows that for stability when deploying an AWGN channel, one needs:

$$SNR \geq \|T_0\|_2^2$$

- On the other hand, the channel capacity of an AWGN channel is:

$$C = \frac{1}{2} \log(1 + SNR)$$

- Therefore, if we redesign the controller, the smallest channel capacity consistent with stability is:

$$C = \frac{1}{2} \log\left(1 + \|T_0\|_2^2\right) \geq \sum_{i=1}^{n_p} \log|p_i|$$

where $\{p_i\}$ are the unstable poles of the plant.

38

213

Optimal Results 1: PCM Coder in Downlink

Optimal performance for the down-link architecture

- The minimum loss function is given by:

$$J_D^{opt} \triangleq \left(\frac{1}{SNR - \|T\|_2^2} \right) \left(\frac{1}{2\pi} \int_{-\pi}^{\pi} \left| S_0(e^{j\omega}) T_0(e^{j\omega}) \Omega_D(e^{j\omega}) \right|^2 d\omega \right)^2$$

- The optimal encoder satisfies:

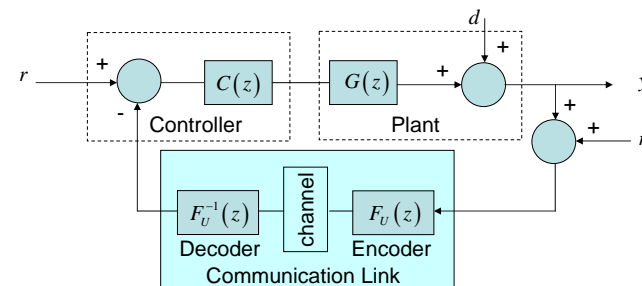
$$\left| L_3^{opt}(e^{j\omega}) \right|^2 = k_D \left| \frac{G(e^{j\omega})}{C(e^{j\omega}) \Omega_D(e^{j\omega})} \right|^2, \quad \forall \omega \in [-\pi, \pi]$$

where k_D is any positive (fixed) real number.

39

Optimal Results 2: Up-Link NCS Architecture

- For alternative architecture where the communication system is located in the up-link, i.e., between plant output and controller input.



40

Optimal Coding

- Proceeding as before, we can characterize optimal coders via:

$$|F_U^{opt}(e^{j\omega})|^2 = k_U \left| \frac{G(e^{j\omega})C(e^{j\omega})}{\Omega_U(e^{j\omega})} \right|^2, \quad \forall \omega \in [-\pi, \pi]$$

where $|\Omega_U(e^{j\omega})|^2$ is the power spectral density of the signal

$$d + n + G(z)C(z)r$$

- The corresponding optimal loss function is:

$$J_U^{opt} \triangleq \left(\frac{1}{SNR - \|T\|^2} \right) \left(\frac{1}{2\pi} \int_{-\pi}^{\pi} |S_0(e^{j\omega})T_0(e^{j\omega})\Omega_U(e^{j\omega})|^2 d\omega \right)^2$$

41

Special Case

- Internal Model Control
Choose C such that $GC = \frac{k}{(z-1)}$

- Random Walk disturbances

$$\Omega_u = \frac{k_2}{(z-1)}$$

Then

$$F_u^{opt} = \text{constant}$$

i.e., no need for coding in this special case.

42

214

Optimal Results 3: Predictive and Noise Shaping Coder in Downlink

- The optimal noise shaping parameters are given by

$$\hat{L}_{1opt}(z) = \frac{\zeta_2(z)S_0(z)G(z)}{\{\zeta_2(z)S_0(z)G(z)\}|_{z=\infty}}$$

$$\hat{L}_{3opt}(z) = \frac{\zeta_1(z)C(z)S_0(z)\Omega_r(z)}{\{\zeta_1(z)C(z)S_0(z)\Omega_r(z)\}|_{z=\infty}}$$

$$\hat{L}_{2opt}(z) = \hat{L}_{3opt}(z)\hat{L}_{1opt}(z) - 1$$

where $\zeta_1(z), \zeta_2(z)$ are generalized Blaschke products for $C(z)S_0(z)\Omega_r(z)$ and $S_0(z)G(z)$, respectively.

43

- The corresponding optimal loss function is given by

$$\hat{J}_{opt} = \frac{1}{SNR} \left(\{\zeta_1(z)\zeta_2(z)T_0(z)S_0(z)\Omega_r(z)\}|_{z=\infty} \right)^2$$

44

Some Observations

1. For PCM coding, if disturbances dominate ($r = 0$), then up-link and down-link architectures give same **optimal** performance.
2. For PCM coding, if $|GC| = |D|$ then optimal coder for **up-link** case is unity (i.e., no need for coding).
3. If $|T_0 S_0 \Omega_r|$ approximately constant as a function of frequency, then $L_2^* = 0$ (i.e., PCM optimal), otherwise 'Predictive Noise Shaping Coding' necessary to achieve optimal performance.

45

Outline

1. Quantization
2. Predictive and Noise Shaping Quantizers
3. Application to Audio Compression
4. Networked Control
5. Modelling Communication Link
6. Predictive and Noise Shaping Coding
7. Experimental Results
8. Conclusions

46

1. Simulated Example

We consider a continuous time plant given by $G_0 = 2(5s+1)^{-1}$, sampled every $T = 1[s]$ using a zero order hold at its input. The corresponding discrete time transfer function is

$$G(z) = \frac{0.36254}{(z - 0.8187)}$$

We will consider two different reference signals, r_1 and r_2 with PSD's given by

$$\begin{aligned} |\Omega_{r_1}(e^{j\omega})|^2 &= \left| \frac{0.02}{e^{j\omega} - 1} \right|^2 \\ |\Omega_{r_2}(e^{j\omega})|^2 &= \left| \frac{0.03}{(e^{j\omega} - 0.9)(e^{j\omega} - 0.7)} \right|^2 \end{aligned}$$

For the control of $G(z)$ we choose the PI controller

$$C(z) = \frac{2.44(z - 0.4871)}{(z - 1)}$$

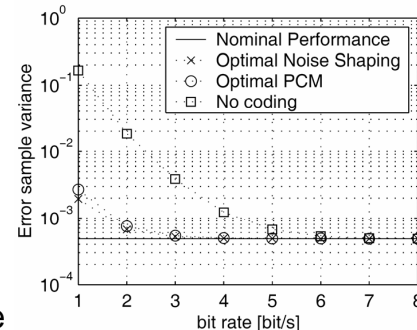
47

The Case of r_1

In this case,

$$T_0(e^{j\omega}) S_0(e^{j\omega}) \Omega_{r_1}(e^{j\omega})$$

is approximately constant for all ω . Then, the PCM based scheme should have a performance which is close to that of the noise shaping based scheme.

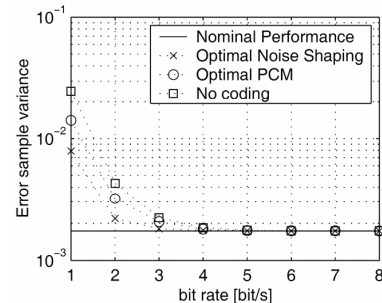


Tracking error sample variance as a function of the channel bit-rate ($r = r_1$).

48

The Case of r_2

In this case, $T_0(e^{j\omega})S_0(e^{j\omega})\Omega_{r_2}(e^{j\omega})$ is far from being constant. Therefore, the noise shaping coder system should outperform PCM.

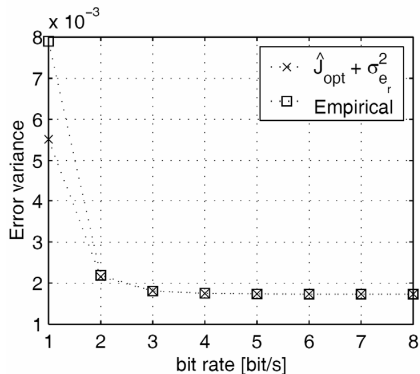


49

Finally, you may wonder about the simplification made by approximating the channel quantization errors (a nonlinear phenomenon) by a SNR constrained noise source.

The following figure compares the theoretical tracking error (using the 'noise model' expressions) with the practical (empirical) errors.

50



Comparison between theoretical variance of the tracking error as given by Theorem 1 and empirical tracking error sample variation with $r = r_2$ and optimal noise shaping coding.

51

2. Laboratory Results



52

Details

Communications:

IEEE 802.3 Ethernet

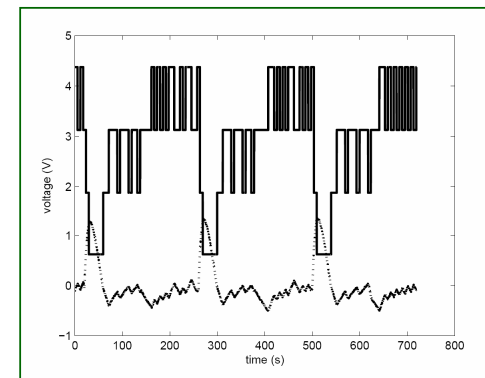
TCP/IP protocol

Process ACT

6 second sampling interval – word length 2 bits

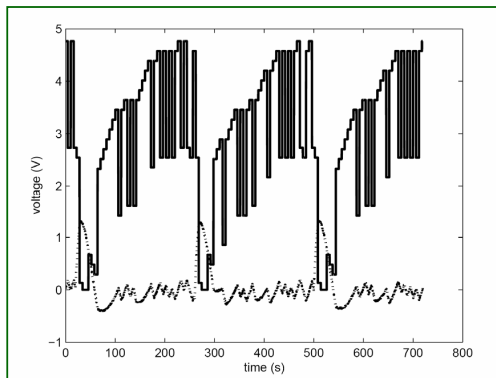
$$= \frac{1}{3} \text{ bits/second.}$$

53



Measured response when the channel is in the down-link: measured plant output (with respect to the operating point – dotted line) and plant input (solid line).

54



Measured response when the channel is in the up-link: measured plant output (with respect to the operating point – dotted line) and plant input (solid line).

55

Table: $\int |e(t)| dt$ for the proposed loops.

	non ideal down-link	non ideal up-link
without disturbance	7.2	5.5
with disturbance	194	162

As predicted by the theory: In the absence of coder/decoder- better to put channel in up-link (i.e., controller immediately before plant).

56

Outline

1. Quantization
2. Predictive and Noise Shaping Quantizers
3. Application to Audio Compression
4. Networked Control
5. Modelling Communication Link
6. Predictive and Noise Shaping Coding
7. Experimental Results
8. Conclusions



57

Conclusions

- This lecture has focused on quantization.
- Key Tool – Predictive and Noise Shaping Quantizers – widely used in Signal Processing and Telecommunication, and very recently in control and other areas e.g. Power Electronics (State of the Art).
- Applications to Audio Compression and Networked Control.

58

Open Problems

- More realistic channel models – lost packets etc
- Multivariable systems
- Decentralized architectures
- What happens if signals have very well defined spectrum
 - Can we exploit ideas of GSE
 - Filter Banks
 - etc
- Remove Perfect Reconstruction constraint and account for total errors including linear distortion

59

References

- **Quantization**
 - R.M. Gray and D.L. Neuhoff, 'Quantization', *IEEE Transactions on Information Theory*, Vol.44, No.6, pp.2325-2383, 1998.
 - M. Fu and L. Xie, 'The sector bound approach to quantized feedback control', *IEEE Transactions on Automatic Control*, Vol.50, No.11, pp.1698-1711, 2005.
 - A. Gersho and R.M. Gray, *Vector Quantization and Signal Compression*, Boston, MA:Kluwer Academic, 1992.
- **Predictive and Noise Shaping Quantizers**
 - S.R. Norsworthy, R. Schreier and G.C. Temes, Eds, *Delta-Sigma Data Converters: Theory, Design and Simulation*. Piscataway, NJ: IEEE Press, 1997.
 - S.K. Tewksbury and R.W. Hallock, 'Oversampled, linear predictive and noise-shaping coders of order N>1', *IEEE Transaction on Circuits and Systems*, Vol.25, No.7, pp.436-447, 1978.
- **Audio Compression**
 - G.C. Goodwin, D.E. Quevedo and D. McGrath, 'Moving-horizon optimal quantizer for audio signals', *Journal Audio Engineering Society*, Vol.51, No.3, pp.138-149, 2003.
 - D.E. Quevedo and G.C. Goodwin, 'Multistep optimal analog-to-digital conversion', *IEEE Transactions on Circuits and Systems I*, Vol.52, No.4, pp.503-515, 2005.
 - N. Gilchrist and C. Grewin, Eds., *Collected Papers on Digital Audio Bit-rate Reduction*. New York: Audio Engineering Society, 1996.

60

References

•Networked Control

- D. Hristu-Varsakelis and W. Levine (Eds), *Handbook of Networked and Embedded Systems*. Boston:Birkhäuser 2005.
- ‘Special Issue on networked control systems’, *IEEE Transactions on Automatic Control*, Vol.49, No.9, 2004.
- H. Ishii and B.A. Francis, *Limited Data Rate in Control Systems with Networks*, Springer, 2002.
- N. Elia and S. Mitter, ‘Stabilization of linear systems with limited information’, *IEEE Transactions on Automatic Control*, Vol.46, No.9, pp.1384-1400, 2001.
- W.S. Wong and R.W. Brockett, ‘Systems with finite communication bandwidth constraints –II: Stabilization with limited information feedback,’ *IEEE Transactions on Automatic Control*, Vol.44, No.5, pp.1049-1053, 1999.
- G. Nair and R. Evans, ‘Stabilizability of stochastic linear systems with finite feedback data rates,’ *SIAM Journal on Control and Optimization*, Vol.43, No.2, pp.413-436, 2004.
- S. Tatikonda and S. Mitter, ‘Control under communication constraints,’ *IEEE Transactions on Automatic Control*, Vol.49, No.7, pp.1056-1068, 2004.

61

References

•Modelling Communication Links

- J.H. Braslavsky, R.H. Middleton and J.S. Freudenberg, ‘Feedback stabilization over signal-to-noise ratio constrained channels,’ in *Proceedings of the 2004 American Control Conference*, Boston, USA, July 2004.
- D. Tse and P. Viswanath, *Fundamentals of Wireless Communication*, Cambridge University Press, 2005.

•Predictive and Noise Shaping Coding

- G.C. Goodwin, D.E. Quevedo and E.I. Silva, ‘Architectures and coder design for networked control systems,’ *Technical Report, School of Electrical Engineering and Computer Science*, University of Newcastle, Australia, 2006.
- E.I. Silva, G.C. Goodwin, D.E. Quevedo and M.S. Derpich, ‘Optimal noise shaping for networked control systems’, *European Control Conference*, Kos, Greece 2-5 July 2007.

62

Lecture 3

Sampling and Quantization in Modelling and Identification

Graham C. Goodwin

Centre for Complex Dynamics Systems and Control
School of Electrical Engineering



Presented at Benelux Meeting on Systems and Control
March 13th - 15th, 2007



Topics to be covered include: sampled data models, coefficient quantization and delta models, sampling zero dynamics for linear deterministic and stochastic systems, implications in robust identification from sampled data, sampling zero dynamics for nonlinear systems, applications in system identification.



220

Content

- ▶ **Interaction between Sampled Signals and Analogue Systems**
- ▶ Sampled Data Models for Linear Deterministic Systems
- ▶ Coefficient Quantization Issues
- ▶ Delta Operator
- ▶ Exploiting Connections between Continuous and Discrete Time Models
- ▶ Re-evaluation
- ▶ Sampling Zeros for Linear Systems
- ▶ Asymptotic Sampling Zeros
- ▶ Robustness Issues in System Identification arising from use of Sampled Data Models
- ▶ Sampled Data Models for Nonlinear Systems
- ▶ Conclusions



Question:

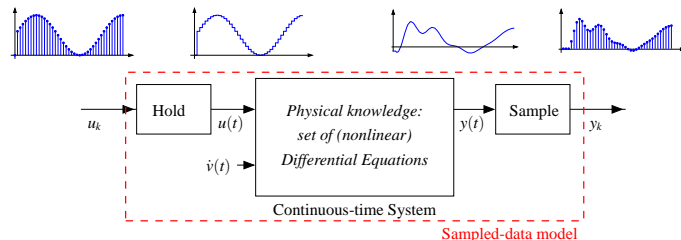
How do *sampled signals* interact with an *analogue* physical system?

Two Issues:

- (i) D/A conversion at input side (usually via some form of hold)
- (ii) A/D conversion at output side (usually including anti-aliasing filtering)



The Elements of the Sampling Process



- ▶ Sampled-data models depend upon:
 - ▶ The physical system,
 - ▶ The hold device (ZOH, FOH, ...)
 - ▶ The sampling device (anti-aliasing filters, ...)

Content

- ▶ Interaction between Sampled Signals and Analogue Systems
- ▶ **Sampled Data Models for Linear Deterministic Systems**
- ▶ Coefficient Quantization Issues
- ▶ Delta Operator
- ▶ Exploiting Connections between Continuous and Discrete Time Models
- ▶ Re-evaluation
- ▶ Sampling Zeros for Linear Systems
- ▶ Asymptotic Sampling Zeros
- ▶ Robustness Issues in System Identification arising from use of Sampled Data Models
- ▶ Sampled Data Models for Nonlinear Systems
- ▶ Conclusions



221

Deterministic Linear Systems

Once the hold and samples have been specified it is easy to obtain sampled data models for linear case.

- ▶ Continuous-time description:

$$\left. \begin{array}{l} \frac{d}{dt}x(t) = Ax(t) + Bu(t) \\ y(t) = Cx(t) \end{array} \right\} Y(s) = \underbrace{C(sI_n - A)^{-1}B}_{G(s)} U(s)$$

- ▶ Discrete-time model:

$$\left. \begin{array}{l} x_{k+1} = A_q x_k + B_q u_k \\ y_k = C_q x_k \end{array} \right\} Y(z) = \underbrace{C_q(zI_n - A_q)^{-1}B_q}_{G_q(z)} U(z)$$

$$\left\{ \begin{array}{l} A_q = e^{A\Delta} \\ B_q = \int_0^{\Delta} e^{A\eta} B d\eta \\ C_q = C \end{array} \right. \quad \text{and} \quad \left\{ \begin{array}{l} u(t) = u_k \\ t \in [k\Delta, k\Delta + \Delta) \end{array} \right. \text{ZOH input}$$

This SD model is **exact**, i.e.:

$$y_k = y(k\Delta)$$

Write in terms of the shift operator

$$\boxed{\begin{aligned} qx_k &= A_q x_k + B_q u_k \\ y_k &= C_q x_k \end{aligned}}$$

where 'q' is the forward shift operator

$$qx_k = x_{k+1}$$



Content

- ▶ Interaction between Sampled Signals and Analogue Systems
- ▶ Sampled Data Models for Linear Deterministic Systems
- ▶ **Coefficient Quantization Issues**
- ▶ Delta Operator
- ▶ Exploiting Connections between Continuous and Discrete Time Models
- ▶ Re-evaluation
- ▶ Sampling Zeros for Linear Systems
- ▶ Asymptotic Sampling Zeros
- ▶ Robustness Issues in System Identification arising from use of Sampled Data Models
- ▶ Sampled Data Models for Nonlinear Systems
- ▶ Conclusions



Illustration

Consider the following 2 Models

$$(a) \quad (q^2 - 1.9q + 0.9025) y[k] = 0$$

$$(b) \quad (q^2 - 1.9q + 0.8925) y[k] = 0$$

Note that the coefficients differ by 1%.

Hence if the coefficients were to be quantized (say to 6 bits) then the models would be identical.

Question: Does this really matter?

Maybe the systems are very similar?



A major difficulty with shift operator models is that, with fast sampling, a near perfect model is

$$y_{k+1} = y_k$$

Thus, if we consider a model such as

$$y_{k+1} = ay_k + bu_k$$

Then the behaviour depends on the difference of function from 1!

More generally, if we consider

$$y_{k+n} = a_{n-1}y_{k+n-1} + \dots + a_0y_k = bu_k$$

Then behaviour depends on difference of coefficients from the Binomial Coefficients.



Surprising Fact:

$$(a) \quad (q^2 - 1.9q + 0.9025) y[k] = 0$$

$$(b) \quad (q^2 - 1.9q + 0.8925) y[k] = 0$$

- ▶ Coefficients differ by 1% yet (a) is stable (b) is unstable.



How can we better represent the system?

Idea: Instead of modelling the next value, i.e.,

$$y_{k+1} = f(y_k)$$

How about we model the difference

$$y_{k+1} - y_k = f'(y_k)$$

This is the core idea in Delta domain models.

Content

- ▶ Interaction between Sampled Signals and Analogue Systems
- ▶ Sampled Data Models for Linear Deterministic Systems
- ▶ Coefficient Quantization Issues
- ▶ **Delta Operator**
- ▶ Exploiting Connections between Continuous and Discrete Time Models
- ▶ Re-evaluation
- ▶ Sampling Zeros for Linear Systems
- ▶ Asymptotic Sampling Zeros
- ▶ Robustness Issues in System Identification arising from use of Sampled Data Models
- ▶ Sampled Data Models for Nonlinear Systems
- ▶ Conclusions



Delta Operator

$$\left[\frac{x(t + \Delta) - x(t)}{\Delta} \right] \triangleq \delta x(t)$$

Core attributes

- ▶ Subtract what is already known (e.g. previous state) then add on later
- ▶ This **centers** the calculation
- ▶ The same idea is used in many areas:
 - ▶ Sigma Delta Modulator
 - ▶ Predictive Coding
 - ▶ Optimal Noise Shaping Quantization etc

Coefficient Quantization Revisted

- ▶ Recall shift operator example:

$$(a) \quad (q^2 - 1.9q + 0.9025) y[k] = 0$$

$$(b) \quad (q^2 - 1.9q + 0.8925) y[k] = 0$$

- ▶ Coefficients differ by 1% yet (a) is stable (b) is unstable.
- ▶ Equivalent delta operator models (assuming $\Delta = 0.1$)

$$(c) \quad (\delta^2 + \delta + 0.25) y[k] = 0$$

$$(d) \quad (\delta^2 + \delta - 0.75) y[k] = 0$$

- ▶ Coefficients differ by 400%. Stability obvious by analogy with continuous time.



Some History of Delta Operator

- ▶ 17th Century Numerical Analysis.
- ▶ Harriot (teacher of Sir Walter Raleigh) developed accurate interpolation formulae based on finite differences.
- ▶ Newton and Stirling in 18th Century developed formal calculus of differences.
- ▶ Lagrange and Laplace studied relationships between linear difference equations in shift and delta form.
- ▶ Cauchy (1827) developed operational calculus for finite differences.
- ▶ Finite difference central to numerical analysis.



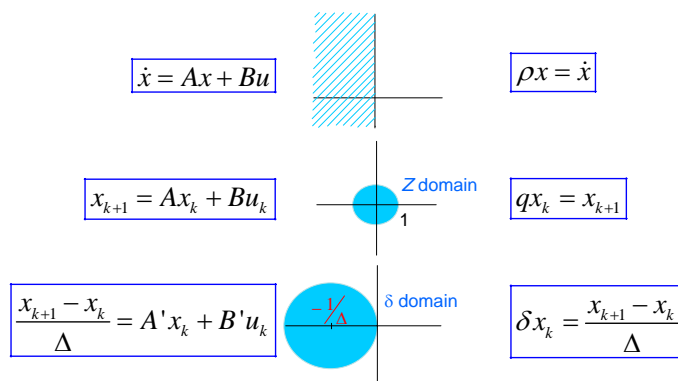
Discrete Delta Transform

$f[k] \quad (k \geq 0)$	$\mathcal{D}f[k]$	Region of Convergence
1	$\frac{1 + \Delta\gamma}{\gamma}$	$ \gamma + \frac{1}{\Delta} > \frac{1}{\Delta}$
$\frac{1}{\Delta}\delta_K[k]$	1	$ \gamma < \infty$
$\mu[k] - \mu[k - 1]$	$\frac{1}{\Delta}$	$ \gamma < \infty$
k	$\frac{1 + \Delta\gamma}{\Delta\gamma^2}$	$ \gamma + \frac{1}{\Delta} > \frac{1}{\Delta}$
k^2	$\frac{(1 + \Delta\gamma)(2 + \Delta\gamma)}{\Delta^2\gamma^3}$	$ \gamma + \frac{1}{\Delta} > \frac{1}{\Delta}$
$e^{\alpha\Delta k} \quad \alpha \in \mathbb{C}$	$\frac{1 + \Delta\gamma}{\gamma - \frac{e^{\alpha\Delta} - 1}{\Delta}}$	$ \gamma + \frac{1}{\Delta} > \frac{e^{\alpha\Delta}}{\Delta}$



224

Illustration: Stability



Some Advantages of δ Models

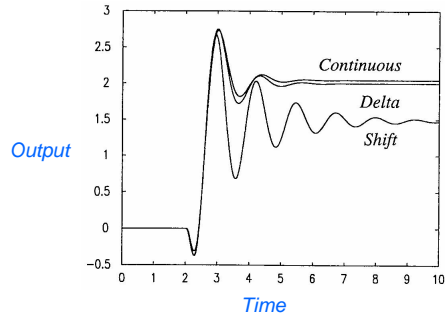
- Numerical properties
- Unification
- Insight



225

(i) Numerical Properties

Shift operator models often fail to give valid results especially when relatively small word lengths used; e.g., in Power Electronics.



Comparison of step response of continuous-time systems to the step responses of discrete-time approximation systems using shift and operator implementations.



Discrete Riccati Equation

$$\rho P = \Omega + PA^T + AP + \Delta APA^T - H [\Gamma + \Delta CPC^T] H^T$$

$$H = [(\Delta A + I)PC^T + S] [\Gamma + \Delta CPC^T]^{-1}$$



(ii) Unification

$$\begin{array}{ccc} \text{Jury Stability} & \longrightarrow & \text{Routh Stability} \\ \text{Discrete Riccati} & \longrightarrow & \text{Continuous Riccati} \\ \text{etc} & & \end{array}$$

Continuous Riccati equation

$$\rho P = \Omega + PA^T + AP - H [\Gamma - H^T] H^T$$

$$H = [PC^T + S] [\Gamma - H^T]^{-1}$$

(iii) Insights - Generally results expressed in terms of delta operator converge to the continuous time result as $\Delta \rightarrow 0$.

Example: State Space Models expressed using δ -operator rather than q -operator

► Rewriting in terms of δ -operator: $\delta = \frac{q-1}{\Delta}$

$$\begin{cases} \delta x_k = A_\delta x_k + B_\delta u_k \\ y_k = C x_k \end{cases} \quad \text{where} \quad \begin{cases} A_\delta = \frac{e^{A\Delta} - I_n}{\Delta} \\ B_\delta = \frac{1}{\Delta} \int_0^{\Delta} e^{A\eta} B d\eta \end{cases}$$

Then, as $\Delta \rightarrow 0$

$$\delta \rightarrow \frac{d}{dt} \quad A_\delta \rightarrow A \quad B_\delta \rightarrow B$$

i.e., the underlying CT system representation is recovered

► Indeed, if we use continuous-time A, B this gives a SD model of accuracy $\mathcal{O}(\Delta)$



Content

- ▶ Interaction between Sampled Signals and Analogue Systems
- ▶ Sampled Data Models for Linear Deterministic Systems
- ▶ Coefficient Quantization Issues
- ▶ Delta Operator
- ▶ **Exploiting Connections between Continuous and Discrete Time Models**
- ▶ Re-evaluation
- ▶ Sampling Zeros for Linear Systems
- ▶ Asymptotic Sampling Zeros
- ▶ Robustness Issues in System Identification arising from use of Sampled Data Models
- ▶ Sampled Data Models for Nonlinear Systems
- ▶ Conclusions



Content

- ▶ Interaction between Sampled Signals and Analogue Systems
- ▶ Sampled Data Models for Linear Deterministic Systems
- ▶ Coefficient Quantization Issues
- ▶ Delta Operator
- ▶ Exploiting Connections between Continuous and Discrete Time Models
- ▶ **Re-evaluation**
- ▶ Sampling Zeros for Linear Systems
- ▶ Asymptotic Sampling Zeros
- ▶ Robustness Issues in System Identification arising from use of Sampled Data Models
- ▶ Sampled Data Models for Nonlinear Systems
- ▶ Conclusions



Content

- ▶ Many results are available, *e.g.*
- ▶ Checking discrete stability — Jury type testing in delta domain converges to Routh-Hurwitz as $\Delta \rightarrow 0$ (Jury, Premaratne, ...)
- ▶ Discrete-time Riccati equations for $\mathcal{H}_2/\mathcal{H}_\infty$ optimization converge to Continuous-time Riccati equations as $\Delta \rightarrow 0$ (Middleton, Salgado, ...)
- ▶ Constrained Linear-Quadratic optimal control (Feuer, Yuz)



Illustration

- ▶ Continuous-time Auto-Regressive (CAR) identification:

$$\frac{d^n y}{dt^n} + a_{n-1} \frac{d^{n-1} y}{dt^{n-1}} + \dots + a_0 y = \dot{v}$$

where \dot{v} : continuous-time white noise

- ▶ It is tempting to think that, for $\Delta \rightarrow 0$, we could think of the sampled-data model as

$$\delta^n y_k + a_{n-1} \delta^{n-1} y_k + \dots + a_0 y_k = w_k$$

with w_k : discrete-time white noise

- ▶ Then we could use ordinary least squares to estimate

$$\theta = [a_{n-1}, a_{n-2}, \dots, a_0]$$



► WARNING!

$$\frac{d^2 y}{dt^2} + a_1 \frac{dy}{dt} + a_0 y = \dot{v}$$

Using hypothetical SD model:

$$\delta^2 y_k + \hat{a}_1 \delta y_k + \hat{a}_0 y_k = w_k$$

and L.S. with sampled-data gives

$$\hat{a}_1 \xrightarrow{\Delta \rightarrow 0} \frac{2}{3} a_1$$



227

► What has gone wrong?

It turns out that we need a **more accurate** representation than $\mathcal{O}(\Delta)$

- ▶ We will next find models that are of order $\mathcal{O}(\Delta^r)$ where r is the **relative degree**!
- ▶ The source of the difficulty is not the use of the delta operator but a problem due to relative degree.



Content

- ▶ Interaction between Sampled Signals and Analogue Systems
- ▶ Sampled Data Models for Linear Deterministic Systems
- ▶ Coefficient Quantization Issues
- ▶ Delta Operator
- ▶ Exploiting Connections between Continuous and Discrete Time Models
- ▶ Re-evaluation
- ▶ **Sampling Zeros for Linear Systems**
- ▶ Asymptotic Sampling Zeros
- ▶ Robustness Issues in System Identification arising from use of Sampled Data Models
- ▶ Sampled Data Models for Nonlinear Systems
- ▶ Conclusions



- ▶ (Åström, Hagander, and Sternby, 1984) For ZOH input, the sampled-data model for $G(s) = s^{-n}$ is given by:

$$G_q(z) = \frac{\Delta^n (b_{n-1}z^{n-1} + \dots + b_1z + b_0)}{n! (z-1)^n} = \frac{\Delta^n}{n!} \frac{B_n(z)}{(z-1)^n}$$

where $B_n(z)$ are the **Euler-Fröbenius polynomials**.

- ▶ In δ -operator form (Yuz and Goodwin, 2005):

$$G_\delta(\gamma) = \frac{p_n(\Delta\gamma)}{\gamma^n}$$

where $p_n(\Delta\gamma) = \det \begin{bmatrix} 1 & \frac{\Delta}{2!} & \dots & \frac{\Delta^{n-1}}{n!} \\ -\gamma & 1 & \dots & \frac{\Delta^{n-2}}{(n-1)!} \\ \vdots & \ddots & \ddots & \vdots \\ 0 & \dots & -\gamma & 1 \end{bmatrix}$

This will
reappear
later



Similar Ideas apply to Stochastic Linear Systems

- ▶ Stochastic system or *noise models*:

$$y(t) = H(\rho)\dot{v}(t) \quad \begin{cases} \frac{d}{dt}x(t) = Ax(t) + B\dot{v}(t) \\ y(t) = Cx(t) \end{cases}$$

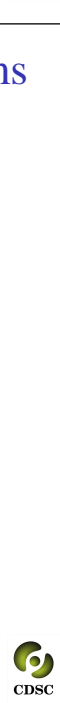
where $\dot{v}(t)$ is *CT white noise*: $E\{\dot{v}(t)\dot{v}(s)\} = \sigma_v^2 \delta(t-s)$

- ▶ Discrete-time model:

$$\begin{cases} x_{k+1} = A_q x_k + \tilde{V}_k \\ y_k = C_q x_k \end{cases} \quad \text{where } \begin{cases} A_q = e^{A\Delta} \\ \tilde{V}_k: \text{DT white noise} \\ E\{\tilde{V}_k \tilde{V}_\ell^T\} = \Omega_q \delta_K[k-\ell] \\ \Omega_q = \sigma_v^2 \int_0^\Delta e^{A\eta} B B^T e^{A^T \eta} d\eta \end{cases}$$

This model is **exact** in the sense that the 2nd order properties of the output are the same, *i.e.*:

$$r_y^d[k] = r_y(k\Delta)$$



The key observation is that we need to include additional zero dynamics!

(The, so called, Sampling Zeros)

- ▶ Some polynomials:

$$p_1(\Delta\gamma) = 1$$

$$p_2(\Delta\gamma) = 1 + \frac{1}{2}\Delta\gamma \equiv \frac{1}{2}(z+1)$$

$$p_3(\Delta\gamma) = 1 + \Delta\gamma + \frac{1}{6}(\Delta\gamma)^2 \equiv \frac{1}{6}(z^2 + 4z + 1)$$

- ▶ The sampled-data model of a general system

$$G(s) = \frac{K \prod_{\ell=1}^m (s - \beta_\ell)}{\prod_{\ell=1}^n (s - \alpha_\ell)} = \frac{F(s)}{E(s)}$$

is given by: $G_\delta(\gamma) = \frac{F_\delta(\gamma)}{E_\delta(\gamma)}$

where, as $\Delta \approx 0$: $E_\delta(\gamma) \rightarrow E(\gamma)$
 $F_\delta(\gamma) \rightarrow F(\gamma)$ $\text{p}_{n-m}(\Delta\gamma)$



- ▶ Again, rewriting in terms of δ -operator: $\delta = \frac{q-1}{\Delta}$

$$\begin{cases} \delta x_k = A_\delta x_k + V_k \\ y_k = C x_k \end{cases} \quad \text{where } \begin{cases} A_\delta = \frac{e^{A\Delta} - I_n}{\Delta} \\ V_k = \frac{1}{\Delta} V_k \\ E\{V_k V_\ell^T\} = \frac{\Omega_q}{\Delta^2} \delta_K[k-\ell] \end{cases}$$

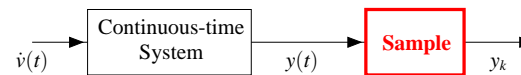
Then, as $\Delta \rightarrow 0$

$$\delta \rightarrow \frac{d}{dt}; A_\delta \rightarrow A; \frac{1}{\Delta} \Omega_q \rightarrow \sigma_v^2 B B^T; \frac{1}{\Delta} \delta_K[k-\ell] \rightarrow \delta(t_k - t_\ell)$$

i.e., the underlying CT system representation is **recovered**

- ▶ However, the sampled output spectrum contains **more** zeros than the CT output spectrum

- ▶ These **stochastic sampling zeros** depend on the sampling device



Sampling Zeros of Stochastic Linear Systems

- ▶ Let $\Phi_y(\omega)$ be the CT output spectrum with zeros $\pm z_i$, $i = 1, \dots, m$ and poles $\pm p_i$, $i = 1, \dots, n$
- ▶ Let $\Phi_y^d(\omega)$ be the instantaneously sampled output spectrum:
 - ▶ The $2n$ poles of $\Phi_y^d(z)$ equal $e^{\pm p_i \Delta} \rightarrow 1$
 - ▶ $2m$ zeros of $\Phi_y^d(z)$ will converge to 1 as $e^{\pm z_i \Delta}$, and
 - ▶ The remaining $2(n - m) - 1$ **stochastic sampling zeros** converge to the zeros of $zB_{2(n-m)-1}(z)$
- ▶ If the output is *averaged* before sampling:

$$\bar{y}(t) = \frac{1}{\Delta} \int_{t-\Delta}^t y(\tau) d\tau$$

- ▶ Then $2(n - m)$ **stochastic sampling zeros** of $\Phi_y^d(z)$ converge to the zeros of $B_{2(n-m)}(z)$



Content

- ▶ Interaction between Sampled Signals and Analogue Systems
- ▶ Sampled Data Models for Linear Deterministic Systems
- ▶ Coefficient Quantization Issues
- ▶ Delta Operator
- ▶ Exploiting Connections between Continuous and Discrete Time Models
- ▶ Re-evaluation
- ▶ Sampling Zeros for Linear Systems
- ▶ **Asymptotic Sampling Zeros**
- ▶ Robustness Issues in System Identification arising from use of Sampled Data Models
- ▶ Sampled Data Models for Nonlinear Systems
- ▶ Conclusions



Facts

An interesting question is the following:

We know that the stochastic sampling zeros have asymptotic values?

- ▶ What is the 'relative' error induced by ignoring these zeros?
- ▶ What is the 'relative' error induced by replacing the true zeros by their asymptotic values?

- ▶ Relative Error if sampling zeros ignored $\mathcal{O}(1)$ (Model is essentially useless at high frequencies)
- ▶ Relative Error if sampling zeros replaced by asymptotic values $\mathcal{O}(\Delta^r)$ (Model has good accuracy over all frequencies as $\Delta \rightarrow 0$)



CAR Identification Revisited

► Recall

$$\frac{d^2y}{dt^2} + a_1 \frac{dy}{dt} + a_0 y = \dot{v}$$

⇒? $\delta^2 y_k + \hat{a}_1 \delta y_k + \hat{a}_0 y_k = w_k$

But LS gives $\hat{a}_1 \xrightarrow{\Delta \rightarrow 0} \frac{2}{3} a_1$

► Solutions:

1. Use asymptotic sampling zeros

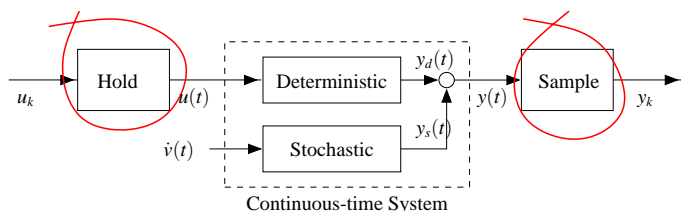
$$\delta^2 y_k + a_1 \delta y_k + a_0 y_k = \left(1 + \frac{1}{3-\sqrt{3}} \Delta \delta\right) w_k$$



230

► Characteristics of sampled-data model depend on the *details* of the sampling process

- The **hold device**: ZOH, FOH, ...
- The **sampling device**: instantaneous, averaging, ...



► Should use Filtered Least Squares

$$J = \sum \left[\frac{1}{H(\delta)} (\delta^2 y + a_1 \delta y + a_0 y) \right]^2$$

Then $\hat{a}_1 \rightarrow a_1$ and $\hat{a}_0 \rightarrow a_0$



Content

- Interaction between Sampled Signals and Analogue Systems
- Sampled Data Models for Linear Deterministic Systems
- Coefficient Quantization Issues
- Delta Operator
- Exploiting Connections between Continuous and Discrete Time Models
- Re-evaluation
- Sampling Zeros for Linear Systems
- Asymptotic Sampling Zeros
- **Robustness Issues in System Identification arising from use of Sampled Data Models**
- Sampled Data Models for Nonlinear Systems
- Conclusions



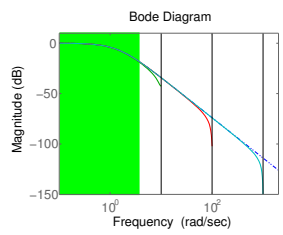
- ▶ Note that the extra *sampling zeros* arise from folding due to aliasing
- ▶ We can, indeed, exactly characterize them asymptotically and/or shift them to *benign* locations, but ...
- ▶ However, note that we are trading information derived from the data for information provided by **prior assumptions** (relative degree, *white noise*, ...)
- ▶ Hence, be careful of taking assumptions too literally
 - ▶ It is **never** a good idea to take $\Delta \rightarrow 0$ (assumptions hold at ∞ frequency)
 - ▶ Indeed, a **sensible sampling period** is probably always better than an arbitrary small sampling period!



How to achieve Robustness?

Restrict Bandwidth

- ▶ Fast sampling assumption suggests $\frac{d}{dt} \approx \delta = \frac{q-1}{\Delta}$
- ▶ For example: $\ddot{y}(t) + \alpha_1 \dot{y}(t) + \alpha_0 y(t) = \dot{v}(t)$
 - ▶ Approximate DT model: $\delta^2 y_k + a_1 \delta y_k + a_0 y_k = w_k$
 - ▶ The **exact** DT model: $\delta^2 y_k + a_1 \delta y_k + a_0 y_k = b_0 w_k + b_1 \delta w_k$
 - ▶ For $\Delta \approx 0 \dots \delta^2 y_k + a_1 \delta y_k + a_0 y_k = (1 + \frac{\Delta}{3-\sqrt{3}} \delta) w_k$

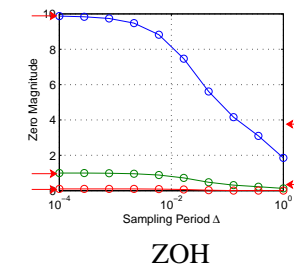


Continuous-Time System Identification:

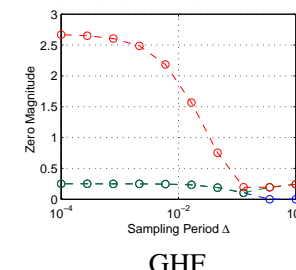
- ▶ Any method that relies on HF system characteristics will be inherently **non robust**.
- ▶ Models should be considered within a **bandwidth of validity**

Bandwidth of Validity

- ▶ GHF and GSF design procedure rely on *knowledge of system relative degree*.
- ▶ Sensitivity to **undermodelling**:
 - ▶ High frequency poles or zeros
 - ▶ CT white noise assumption
- ▶ **Bandwidth of validity** for CT models
- ▶ In the GHF example ... $G(s) = \frac{1}{(s+1)^3(0.01s+1)}$



ZOH



GHF



CT system identification from sampled data

Example: CAR Identification

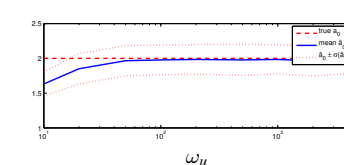
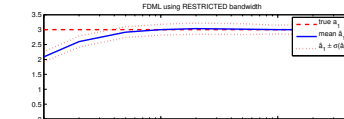
$$A_c(\rho)y(t) = (\rho^2 + 3\rho + 2) \left(\frac{1}{\omega_u} \rho + 1 \right) y(t) = \dot{v}(t)$$

- ▶ Consider the (approximate) DT model:

$$A_\delta(\delta)y_k = (\delta^2 + \hat{a}_1 \delta + \hat{a}_0)y_k = w_k$$

- ▶ DT undermodelling: sampling zeros
- ▶ CT undermodelling: fast pole / wideband noise

- ▶ Using **restricted bandwidth** $\omega_{\max} = 20[\text{rad/s}]$:



- ▶ Assume that the sampled data $\{y_k = y(k\Delta), u_k = u(k\Delta)\}$, $k = 0, \dots, N$ is generated by:

$$y_k = G_d(q, \theta)u_k + H_d(q, \theta)w_k \quad \begin{cases} w_k : \text{Gaussian DTWN} \\ w_k \sim N(0, \sigma_w^2) \end{cases}$$

- ▶ In the Frequency Domain:

$$Y_\ell = G_d(e^{j\omega_\ell \Delta}, \theta)U_\ell + H_d(e^{j\omega_\ell \Delta}, \theta)W_\ell$$

- ▶ W_ℓ are independent and (complex) Gaussian distributed:
 $W_\ell \sim N(0, N\sigma_w^2)$
- ▶ Therefore, Y_ℓ is also complex Gaussian:

$$Y_\ell \sim N(G_d(e^{j\omega_\ell \Delta}, \theta)U_\ell, N\sigma_w^2|H_d(e^{j\omega_\ell \Delta}, \theta)|^2)$$

$$p(Y_\ell) = \frac{1}{\pi N\sigma_w^2|H_d(e^{j\omega_\ell \Delta}, \theta)|^2} \exp \left\{ -\frac{|Y_\ell - G_d(e^{j\omega_\ell \Delta}, \theta)U_\ell|^2}{N\sigma_w^2|H_d(e^{j\omega_\ell \Delta}, \theta)|^2} \right\}$$



Frequency Domain Maximum Likelihood

- ▶ Considering **limited-bandwidth**, $n_{\max} \sim \omega_{\max} < \frac{\omega_s}{2}$, the log-likelihood function to minimise is:

$$L(\theta) = -\log p(Y_0, \dots, Y_{n_{\max}}) = -\log \prod_{\ell=0}^{n_{\max}} p(Y_\ell)$$

$$= \sum_{\ell=0}^{n_{\max}} \frac{|Y_\ell - G_d(e^{j\omega_\ell \Delta}, \theta)U_\ell|^2}{N\sigma_w^2|H_d(e^{j\omega_\ell \Delta}, \theta)|^2} + \log(\pi N\sigma_w^2|H_d(e^{j\omega_\ell \Delta}, \theta)|^2)$$

- ▶ The last term can be neglected **only** if (Ljung, 1993):

- ▶ H_d does NOT depend on θ ; or
- ▶ FULL bandwidth is considered, i.e., $n_{\max} = \frac{N}{2}$ (or N)
- ▶ This approach allow us to achieve robustness to
 - ▶ Effects of sampling (e.g., sampling zeros)



232

Example

$$A_c(\rho)y(t) = (\rho^2 + 3\rho + 2)y(t) = \dot{v}(t)$$

- ▶ The *exact* sampled model contains one *sampling zero*:

$$\delta^2 y_k + a_1 \delta y_k + a_0 y_k = w_k + b_1 \delta w_k \quad b_1 \xrightarrow{\Delta \approx 0} \frac{\Delta}{3 - \sqrt{3}}$$

- ▶ Consider the (approximate) DT model:

$$A_\delta(\delta)y_k = (\delta^2 + \hat{a}_1 \delta + \hat{a}_0)y_k = w_k$$

$$L = \sum_{\ell=0}^{n_{\max}} \frac{|A_d(e^{j\omega_\ell \Delta})Y(e^{j\omega_\ell \Delta})|^2}{N\sigma_w^2} - \log \frac{|A_d(e^{j\omega_\ell \Delta})|^2}{\sigma_w^2}$$

- ▶ **Full bandwidth**

0 to $\frac{\pi}{\Delta} = 125$ [rad/s]

$$\begin{bmatrix} \hat{a}_1 \\ \hat{a}_0 \end{bmatrix} = \begin{bmatrix} 4.5584 \\ 1.9655 \end{bmatrix}$$

- ▶ **Restricted bandwidth:**

0 to 20 [rad/s] *Bw of validity*

$$\begin{bmatrix} \hat{a}_1 \\ \hat{a}_0 \end{bmatrix} = \begin{bmatrix} 3.0143 \\ 1.9701 \end{bmatrix} \quad \text{unbiased!}$$



Content

- ▶ Interaction between Sampled Signals and Analogue Systems
- ▶ Sampled Data Models for Linear Deterministic Systems
- ▶ Coefficient Quantization Issues
- ▶ Delta Operator
- ▶ Exploiting Connections between Continuous and Discrete Time Models
- ▶ Re-evaluation
- ▶ Sampling Zeros for Linear Systems
- ▶ Asymptotic Sampling Zeros
- ▶ Robustness Issues in System Identification arising from use of Sampled Data Models
- ▶ **Sampled Data Models for Nonlinear Systems**
- ▶ Conclusions



- ▶ Continuous-time nonlinear systems are described by differential equations
- ▶ In general, sampled-data models are hard/impossible to obtain explicitly for nonlinear case
- ▶ However, approximate discrete-time descriptions can be obtained
- ▶ We consider:
 - ▶ **Deterministic** nonlinear systems
 - ▶ **Stochastic** nonlinear systems
- ▶ We will derive
 - ▶ Sampled-data models that are **accurate** in a *well defined* sense
 - ▶ Specify the additional zero dynamics arising from sampling (as in the linear case)



- ▶ We perform *Taylor series expansion* for each state:

$$z_1(k\Delta + \Delta) = z_1(k\Delta) + \Delta z_2(k\Delta) + \frac{\Delta^2}{2} z_3(k\Delta) + \dots + \frac{\Delta^r}{r!} [b(\zeta, \eta) + a(\zeta, \eta)u]_{t=\xi_1}$$

$$z_2(k\Delta + \Delta) = z_2(k\Delta) + \Delta z_3(k\Delta) + \dots + \frac{\Delta^{r-1}}{(r-1)!} [b(\zeta, \eta) + a(\zeta, \eta)u]_{t=\xi_2}$$

$$\vdots$$

$$z_r(k\Delta + \Delta) = z_r(k\Delta) + \Delta [b(\zeta, \eta) + a(\zeta, \eta)u]_{t=\xi_r}$$

$$\eta(k\Delta + \Delta) = \eta(k\Delta) + \Delta [q(\zeta, \eta)]_{t=\xi_{r+1}}$$

This is **exact** for some *unknown* time instants ξ_ℓ

- ▶ Thus, we obtain the δ -form **approximate** DT model:

$$\delta\zeta^S = \begin{bmatrix} 0 & 1 & \frac{\Delta}{2} & \dots & \frac{\Delta^{r-2}}{(r-1)!} \\ 0 & 0 & 1 & \dots & \frac{\Delta^{r-3}}{(r-2)!} \\ \vdots & \ddots & \ddots & \ddots & \vdots \\ 0 & \dots & 0 & 1 & 0 \\ 0 & 0 & \dots & 0 & 0 \end{bmatrix} \zeta^S + \begin{bmatrix} \frac{\Delta^{r-1}}{r!} \\ \frac{\Delta^{r-2}}{(r-1)!} \\ \vdots \\ \frac{\Delta}{2} \\ 1 \end{bmatrix} (b(\zeta^S, \eta^S) + a(\zeta^S, \eta^S)u)$$

$$\delta\eta^S = q(\zeta^S, \eta^S)$$



(a) Deterministic nonlinear systems

- ▶ We consider a class of nonlinear systems (Isidori, 1995):

$$\dot{x}(t) = f(x(t)) + g(x(t))u(t)$$

$$y(t) = h(x(t))$$

- ▶ The system has **nonlinear relative degree** r at a point x_o if:

- (i) $L_g L_f^k h(x) = 0$ for $k = 0, \dots, r-2$, and
- (ii) $L_g L_f^{r-1} h(x_o) \neq 0$.

- ▶ The system can be expressed in the **normal form**:

$$\dot{z}_1 = z_2$$

$$\vdots$$

$$\dot{z}_{r-1} = z_r$$

$$\dot{z}_r = b(\zeta, \eta) + a(\zeta, \eta)u$$

$$\dot{\eta} = q(\zeta, \eta)$$

$$\text{where } y = h(x) = z_1 \text{ and } \begin{cases} \zeta = [z_1, z_2, \dots, z_r]^T \\ \eta = [z_{r+1}, z_{r+2}, \dots, z_n]^T \end{cases}$$



Accuracy

- ▶ The **local truncation error** is of order Δ^{r+1} , i.e.:

$$|y(k\Delta + \Delta) - q y^S| < C \cdot \Delta^{r+1} \quad \text{for some constant } C$$

Links to the linear case

- ▶ The sampled-data model has nonlinear relative degree 1
- ▶ The DT nonlinear *zero dynamics* are given by:
 - ▶ The sampled counterpart of the CT zero dynamics:

$$\delta\eta^S = q(0, \tilde{z}_{2:r}^S, \eta^S)$$

$$\text{where } \tilde{z}_{2:r}^S = [\tilde{z}_2^S, \dots, \tilde{z}_r^S]^T, \text{ and}$$

- ▶ A *linear* subsystem of dimension $r-1$:

$$\delta \tilde{z}_{2:r}^S = Q_{22} \tilde{z}_{2:r}^S$$



Links to the linear case

- Moreover, the eigenvalues of the *linear* subsystem of dimension $r - 1$:

$$\delta \tilde{z}_{2:r}^S = Q_{22} \tilde{z}_{2:r}^S$$

are given by $\det(\gamma I_{r-1} - Q_{22}) = \frac{r!}{\Delta^{r-1}} p_r(\Delta \gamma)$

Note that

$$p_r(\Delta \gamma) = \det \begin{bmatrix} 1 & \frac{\Delta}{2!} & \dots & \frac{\Delta^{r-1}}{r!} \\ -\gamma & 1 & \dots & \frac{\Delta^{r-2}}{(r-1)!} \\ \vdots & \ddots & \ddots & \vdots \\ 0 & \dots & -\gamma & 1 \end{bmatrix}$$

Exactly as seen before in the linear case!

That is we have the same (asymptotic) sampling zeros as for a linear system of relative degree r

(b) Stochastic Nonlinear Systems

- We extend the results to stochastic (nonlinear) systems:

$$\begin{aligned} \frac{dx(t)}{dt} &= a(t, x) + b(t, x) \dot{v}(t) & \dot{v}(t) : \text{CTWN} \\ y(t) &= c(t, x) \end{aligned}$$

- For a proper mathematical treatment we use SDE:

$$\begin{aligned} dx_t &= a(t, x_t) dt + b(t, x) dv_t \\ x_t &= x_0 + \underbrace{\int_0^t a(\tau, x_\tau) d\tau}_{\text{drift}} + \underbrace{\int_0^t b(\tau, x_\tau) dv_\tau}_{\text{diffusion}} \end{aligned}$$

where dv_t are **increments** of a Wiener process

- The **diffusion term** integral cannot be interpreted in the *usual* Riemann-Stieljes sense.



234

- To perform *Taylor's series -like expansions* we need to consider the **Ito rule** of stochastic calculus: Given

$$dx_t = a(t, x_t) dt + b(t, x) dv_t$$

and $y = g(t, x)$, the *usual* chain rule has to be modified:

$$dy = \frac{\partial g}{\partial t} dt + \frac{\partial g}{\partial x} dx + \frac{1}{2} \frac{\partial^2 g}{\partial x^2} (dx)^2$$

- We can then apply the Ito rule to the process:

$$x_t = x_0 + \int_0^t a(\tau, x_\tau) d\tau + \int_0^t b(\tau, x_\tau) dv_\tau$$

- Doing this, we obtain Ito-Taylor series expansion:

$$x_t = x_0 + a(x_0) \int_0^t d\tau + b(x_0) \int_0^t dv_\tau + R_2^s$$

where R_2^s depends on double stochastic integrals



- Higher order Ito-Taylor expansions become increasingly involved. For example (Kloeden and Platen, 1992):

$$\begin{aligned} x_t &= x_0 + a \mathbf{I}_{(0)} + b \mathbf{I}_{(1)} + (aa' + \frac{1}{2} b^2 a'') \mathbf{I}_{(0,0)} \\ &\quad + (ab' + \frac{1}{2} b^2 b'') \mathbf{I}_{(0,1)} + ba' \mathbf{I}_{(1,0)} + bb' \mathbf{I}_{(1,1)} + R_3^s \end{aligned}$$

where $a' = \frac{\partial a}{\partial x}$, $a'' = \frac{\partial^2 a}{\partial x^2}$, $b' = \frac{\partial b}{\partial x}$, and:

$$\begin{aligned} \mathbf{I}_{(0)} &= \int_0^t d\tau_1 & \mathbf{I}_{(0,0)} &= \int_0^t \int_0^{\tau_1} d\tau_2 d\tau_1 & \mathbf{I}_{(1,0)} &= \int_0^t \int_0^{\tau_1} dv_{\tau_2} d\tau_1 \\ \mathbf{I}_{(1)} &= \int_0^t dv_{\tau_1} & \mathbf{I}_{(0,1)} &= \int_0^t \int_0^{\tau_1} d\tau_2 dv_{\tau_1} & \mathbf{I}_{(1,1)} &= \int_0^t \int_0^{\tau_1} dv_{\tau_2} dv_{\tau_1} \end{aligned}$$

- Ito-Taylor expansions can be used to derive *discrete-time approximations* to solve SDEs.



- The simplest is the **Euler-Maruyama** approximation:

$$\bar{x}_{k+1} = \bar{x}_k + a(\bar{x}_k)\Delta + b(\bar{x}_k)\Delta v_k$$

where $\bar{x}_k = \bar{x}(k\Delta)$ and:

$$\Delta v_k = \int_{k\Delta}^{k\Delta+\Delta} dv_\tau \quad \begin{cases} E\{\Delta v_k\} = 0 \\ E\{(\Delta v_k)^2\} = \Delta \end{cases}$$

- **Strong convergence of order** $\gamma > 0$, if there exists a constant $C > 0$ and a sampling period $\Delta_o > 0$ such that:

$$E\{|\bar{x}(k\Delta) - x_{k\Delta}|\} \leq C\Delta^\gamma \quad ; \quad \forall \Delta < \Delta_o$$

- The **Euler-Maruyama** expansion contains only the time and Wiener integrals of multiplicity 1, Thus, it can be interpreted as an order 0.5 strong Ito-Taylor approximation



Re-examine multiple integrator via numerical integration

- Consider the **linear** integrator $y^{(n)}(t) = \dot{v}(t)$:

$$dy = dx_1 = x_2 dt$$

⋮

$$dx_{n-1} = x_n dt$$

$$dx_n = dv_t$$



- Next consider the class of nonlinear systems expressed by:

$$dy = dx_1 = x_2 dt$$

⋮

$$dx_{n-1} = x_n dt$$

$$dx_n = a(X)dt + b(X)dv_t$$

- Expanding as before, we obtain the SD model:

$$\bar{X}_{k+1} = \begin{bmatrix} 1 & \Delta & \dots & \frac{\Delta^{n-1}}{(n-1)!} \\ 0 & \ddots & \ddots & \vdots \\ \vdots & \ddots & 1 & \Delta \\ 0 & \dots & 0 & 1 \end{bmatrix} \bar{X}_k + \begin{bmatrix} \frac{\Delta^n}{n!} \\ \vdots \\ \frac{\Delta^2}{2} \\ \Delta \end{bmatrix} a(\bar{X}_k) + b(\bar{X}_k) \tilde{V}_k$$

Theorem:

The output $\bar{y}(k\Delta) = \bar{x}_1(k\Delta)$ converges strongly to the true output with order $\gamma = n/2$

- Solving the equations:

$$y(\Delta) = x_1(\Delta) = x_1(0) + \dots + \int_0^\Delta \int_0^{\tau_1} \dots \int_0^{\tau_{n-1}} dv_{\tau_n} d\tau_{n-1} \dots d\tau_1$$

⋮

$$x_{n-1}(\Delta) = x_{n-1}(0) + x_n(0)\Delta + \int_0^\Delta \int_0^{\tau_{n-1}} dv_{\tau_n} d\tau_{n-1}$$

$$x_n(\Delta) = x_n(0) + \int_0^\Delta dv_{\tau_n} \quad (\text{exact!})$$

- This is an **exact** model, *i.e.*, converges strongly to the true solution with order $\gamma = \infty$.



- The model can be rewritten in matrix form:

$$X_{\Delta} = \underbrace{\begin{bmatrix} 1 & \Delta & \cdots & \frac{\Delta^{n-1}}{(n-1)!} \\ 0 & \ddots & \ddots & \vdots \\ \vdots & \ddots & 1 & \Delta \\ 0 & \cdots & 0 & 1 \end{bmatrix}}_{A_q = e^{A\Delta}} X_0 + \begin{bmatrix} I_{(1,0,\dots,0,0)} \\ I_{(1,0,\dots,0)} \\ \vdots \\ I_{(1)} \end{bmatrix}$$

where $I_{(1,0,\dots,0)} = \underbrace{\int_0^{\Delta} \int_0^{\tau_1} \cdots \int_0^{\tau_m}}_{m \text{ zeros}} dv_{\tau_{m+1}} d\tau_m \dots d\tau_1$

- It can also be obtained using *deterministic* transition equation:

$$X_{\Delta} = e^{A\Delta} X_0 + \int_0^{\Delta} e^{A(\Delta-\tau)} B d\tau = A_q X_0 + \tilde{V}$$

$$E\{\tilde{V}\tilde{V}^T\} = \int_0^{\Delta} e^{A\eta} B B^T e^{A^T \eta} d\eta = \left[\frac{\Delta^{2n-i-j+1}}{(n-i)!(n-j)!(2n-i-j+1)} \right]$$



Content

- Interaction between Sampled Signals and Analogue Systems
- Sampled Data Models for Linear Deterministic Systems
- Coefficient Quantization Issues
- Delta Operator
- Exploiting Connections between Continuous and Discrete Time Models
- Re-evaluation
- Sampling Zeros for Linear Systems
- Asymptotic Sampling Zeros
- Robustness Issues in System Identification arising from use of Sampled Data Models
- Sampled Data Models for Nonlinear Systems
- **Conclusions**



236

Conclusions

- We have seen that *coefficient quantization* can be an issue with sampled data models expressed in terms of shift operator
- Usually preferable to use Delta operator
- Delta operator gives improved numerical properties, unification and better insights
- Sampled Data models generally contain extra sampling zero dynamics
- Zero Dynamics can be easily quantified in Linear case
- We have issued warnings about potential robustness issues
- A special class of nonlinear sampled data models has been described having easily quantified zero dynamics

Open Problems

Again there are many, e.g.,

- Establishing *relative error* results for nonlinear sampled data models
- Robust algorithms for identifying nonlinear system from sampled data (cannot use frequency domain)
- Use of non-uniformly sampled data
- Effect of data quantization



References

- ▶ Interaction between Sampled Signals and Analogue Systems
 - ▶ R.H. Middleton and G.C. Goodwin, Digital Control and Estimation, Prentice Hall, Englewood Cliffs, 1990.
- ▶ Sampled Data Models for Linear Deterministic Systems
 - ▶ A. Feuer and G.C. Goodwin, Sampling in Digital Signal Processing and Control, Birkhäuser, Boston, 1996.
- ▶ Coefficient Quantization Issues
 - ▶ R.H. Middleton and G.C. Goodwin, 'Improved finite word length characteristics in digital control using delta operators', IEEE Transactions on Automatic Control, Vol.31, No.11, pp.1015-1021, 1986.
- ▶ Delta Operator
 - ▶ R.M. Goodall and Donoghue, 'Very high sample rate digital filters using the delta operator', Proceedings of IEE, G, Vol.140, No.3, pp.199, 1993.
 - ▶ G.C. Goodwin, R.G. Middleton and H.V. Poor, 'High-speed digital signal processing and control', Proceedings of IEEE, Vol.80, No.2, pp.240-259, 1992.
 - ▶ M.J. Newman and D.G. Holmes, 'Delta operator digital filter for high performance inverter applications', IEEE Transactions on Power Electronics, Vol.18, No.1, Part 2, 2003.
 - ▶ K. Premaratne and E.I. Jury, 'Tabular method for determining root distribution of delta operator formulated real polynomials', IEEE Transactions on Automatic Control, Vol.39, No.2, pp.352-355, 1994.



References

- ▶ Asymptotic Sampling Zeros
 - ▶ B. Wahlberg, 'Limit results for sampled systems', International Journal of Control, Vol.48, No.3, pp.1267-1283, 1988.
 - ▶ S. Weller, W. Moran, B. Ninness and A. Pollington, 'Sampling zeros and the Euler-Fröbenius polynomials', IEEE Transactions on Automatic Control, Vol.46, No.2, pp.340-343, 2001.
- ▶ Robustness Issues in System Identification arising from use of Sampled Data Models
 - ▶ G.C. Goodwin, J.I. Yuz and H. Garnier, 'Robustness issues in continuous-time system identification from sampled data', in Proceedings of 16th IFAC World Congress, Prague, Czech Republic, 2005.
 - ▶ G.C. Goodwin, J.I. Yuz and H. Garnier, 'Robustness issues in continuous-time system identification from sampled data', IFAC World Congress, Prague, 2005.
 - ▶ T. Söderström, H. Fan, B. Carlsson and S. Bigi, 'Least squares parameter estimation of continuous-time ARX models from discrete-time data', IEEE Transactions on Automatic Control, Vol.42, No.5, pp.959-673, 1997.



References

- ▶ Delta Operator Cont.
 - ▶ K. Premaratne and E.I. Jury, 'Application of polynomial array methods to discrete time system stability', Proceedings of IEE, D, Vol.140, No.3, pp.198-204, 1993.
 - ▶ K. Premaratne, S. Touset and E.I. Jury, 'Root distribution of delta operator formulated polynomials', Proceedings of IEE, D, Vol.147, No.1, pp.1-12, 2000.
 - ▶ M.E. Salgado, R.H. Middleton and G.C. Goodwin, 'Connections between continuous and discrete Riccati equation with applications to Kalman filtering', Proceedings of IEE, D, Vol.135, pp.28-34, 1988.
- ▶ Exploiting Connections between Continuous and Discrete Time Models
 - ▶ H.H. Fan, 'Efficient zero location tests for delta operator based polynomials', IEEE Transactions on Automatic Control, Vol.42, No.5, pp.722-727, 1997.
- ▶ Re-evaluation
 - ▶ E.K. Larsson and T. Söderström, 'Continuous-time AR parameter estimation using properties of sampled systems', Proceedings of IFAC World Congress, Barcelona, 2002.
- ▶ Sampling Zeros for Linear Systems
 - ▶ K.J. Åström, P. Hagander, and J. Sternby, 'Zeros of sampled systems', Automatica, Vol.29, No.1, pp. 31-38, 1984.

References

- ▶ Sampled Data Models for Nonlinear Systems
 - ▶ J.I. Yuz and G.C. Goodwin, 'On sampled data models for nonlinear systems', IEEE Transactions on Automatic Control, Vol.50, No.10, pp.1477-1489, 2005.
 - ▶ J.I. Yuz and G.C. Goodwin, 'Sampled data models for nonlinear stochastic systems', IFAC Symposium on System Identification, Newcastle, Australia, 2006.
 - ▶ S. Monaco and D. Normand-Cyrot, 'Zero dynamics of sampled nonlinear systems', Systems and Control Letters, Vol.11, pp.229-234, 1988.
 - ▶ S. Monaco and D. Normand-Cyrot, 'A unified representation for nonlinear discrete-time and sampled dynamics', Journal of Mathematics Systems, Estimation, and Control, Vol.7, No.4, pp.477-503, 1997.
 - ▶ N. Kazantzis and C. Kravaris, 'System-theoretic properties of sampled-data representations of nonlinear systems obtained via taylor-lie series', International Journal of Control, Vol.67, No.9, pp. 997-1020, 1997.
 - ▶ G.C. Goodwin, J.I. Yuz and M.E. Salgado, 'Insights into the zero dynamics of sampled-data models for linear and nonlinear stochastic systems', European Control Conference, Greece, 2-5 July, 2007.

PARAMETRIC TIME-DOMAIN METHODS FOR NON-STATIONARY RANDOM VIBRATION IDENTIFICATION: AN OVERVIEW OF METHODS AND APPLICATIONS

S.D. Fassois

STOCHASTIC MECHANICAL SYSTEMS & AUTOMATION (SMSA) LABORATORY
DEPARTMENT OF MECHANICAL & AERONAUTICAL ENGINEERING
UNIVERSITY OF PATRAS, GR 265 00 PATRAS, GREECE
fassois@mech.upatras.gr
<http://www.mech.upatras.gr/~sms>

Benelux Meeting on Systems and Control
Lommel, Belgium, March 13-15, 2007

TALK OUTLINE

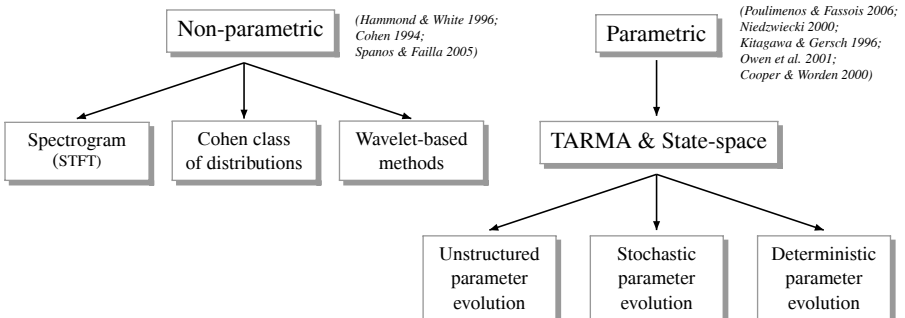
1. INTRODUCTION
2. TARMA MODEL REPRESENTATIONS
3. TARMA MODEL PARAMETER ESTIMATION
4. ASYMPTOTIC ANALYSIS FOR FS-TARMA ESTIMATORS
5. MODEL STRUCTURE ESTIMATION & VALIDATION
6. MODEL BASED ANALYSIS
7. A COMPARATIVE STUDY BASED ON MONTE CARLO EXPERIMENTS
8. APPLICATION EXAMPLES
9. CONCLUDING REMARKS & OUTLOOK

Problem Significance

Non-stationary random vibration is commonly encountered in practice:

- ◊ Seismic & structural systems
- ◊ Sea vessels
- ◊ Rotating machinery
- ◊ Automotive & aircraft systems
- ◊ Robotic devices
- ◊ Railway bridges

Methods for Non-stationary Random Vibration Modelling and Analysis



1. INTRODUCTION

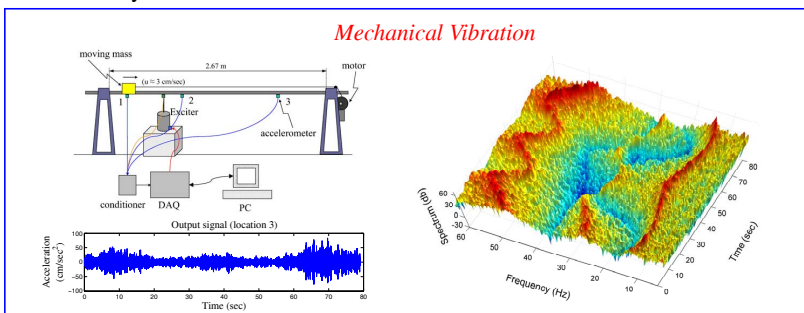
The General Problem

Modelling and analysis of non-stationary vibration.

Problem Characteristics

- Non-stationary stochastic signals are characterized by time-varying statistics
- require time-frequency methods for their analysis.

Mean: $\mu[t] = E\{x[t]\}$
 Autocovariance: $\gamma[t_1, t_2] = E\{(x[t_1] - \mu[t_1]) \cdot (x[t_2] - \mu[t_2])\}$



PARAMETRIC TIME-DOMAIN METHODS FOR NON-STATIONARY RANDOM VIBRATION IDENTIFICATION _____ 5

Why Parametric Methods?

They offer a number of advantages over non-parametric counterparts:

- ✓ Representation parsimony
- ✓ Improved accuracy and resolution
- ✓ Improved tracking of the time-varying dynamics
- ✓ Flexibility in analysis

Aims of the Presentation

1. Critical overview of parametric time-domain methods for non-stationary random vibration modelling and analysis.
2. Comparative assessment and applications.

STOCHASTIC MECHANICAL SYSTEMS & AUTOMATION (SMSA) LABORATORY UNIVERSITY OF PATRAS

PARAMETRIC TIME-DOMAIN METHODS FOR NON-STATIONARY RANDOM VIBRATION IDENTIFICATION _____ 7

The Minimum Mean Square Error (MMSE) one-step ahead prediction $\hat{x}[t|t-1]$ of $x[t]$ is:

$$\hat{x}[t|t-1] = - \sum_{i=1}^{n_a} a_i[t] \cdot x[t-i] + \sum_{i=1}^{n_c} c_i[t] \cdot e[t-i]$$

Hence: $\hat{e}[t|t-1] \triangleq x[t] - \hat{x}[t|t-1] = e[t]$, one-step-ahead prediction error or residual

Polynomial operator form

A TARMA(n_a, n_c) model may expressed in the following polynomial operator form:

$$\underbrace{\left(1 + \sum_{i=1}^{n_a} a_i[t] \cdot \mathcal{B}^i\right)}_{A[\mathcal{B}, t]} \cdot x[t] = \underbrace{\left(1 + \sum_{i=1}^{n_c} c_i[t] \cdot \mathcal{B}^i\right)}_{C[\mathcal{B}, t]} \cdot e[t]$$

\mathcal{B}^i : i -step backshift operator ($\mathcal{B}^i \cdot x[t] = x[t-i]$)
 $A[\mathcal{B}, t], C[\mathcal{B}, t]$: AR/MA time varying polynomial operators

STOCHASTIC MECHANICAL SYSTEMS & AUTOMATION (SMSA) LABORATORY UNIVERSITY OF PATRAS

PARAMETRIC TIME-DOMAIN METHODS FOR NON-STATIONARY RANDOM VIBRATION IDENTIFICATION _____ 6

2. TARMA MODEL REPRESENTATIONS

A TARMA(n_a, n_c) model is of the form:

$$x[t] + \underbrace{\sum_{i=1}^{n_a} a_i[t] \cdot x[t-i]}_{\text{AR part}} = e[t] + \underbrace{\sum_{i=1}^{n_c} c_i[t] \cdot e[t-i]}_{\text{MA part}}, \quad t \geq t_0, \quad e[t] \sim \text{NID}(0, \sigma_e^2[t])$$

t : normalized discrete time n_a, n_c : orders of the AR/MA polynomials
 $x[t]$: the non-stationary response signal $a_i[t], c_i[t]$: AR/MA time-varying parameters
 $e[t]$: innovations (residual) sequence NID : Normally Independently Distributed

Classes of Parametric Models

Parameter evolution	Representation parsimony	Dynamics evolution
UNSTRUCTURED	low	slow
STOCHASTIC	low	slow/medium
DETERMINISTIC	high	slow/medium/fast

STOCHASTIC MECHANICAL SYSTEMS & AUTOMATION (SMSA) LABORATORY UNIVERSITY OF PATRAS

PARAMETRIC TIME-DOMAIN METHODS FOR NON-STATIONARY RANDOM VIBRATION IDENTIFICATION _____ 8

Unlike in the stationary case, the backshift operator has to obey a non-commutative (“skew”) multiplication operator “ \circ ” defined as:

$$\mathcal{B}^i \circ \mathcal{B}^j = \mathcal{B}^{i+j}, \quad \mathcal{B}^i \circ x[t] = x[t-i] \cdot \mathcal{B}^i$$

To see the reason consider:

$$\{(1 - p_1[t]\mathcal{B}) \circ (1 - p_2[t]\mathcal{B})\}x[t] = (1 - p_1[t]\mathcal{B})\{(1 - p_2[t]\mathcal{B})x[t]\} \quad \forall x[t] \Leftrightarrow$$

$$\Leftrightarrow \{1 - (p_1[t] + p_2[t])\mathcal{B} + p_1[t]\mathcal{B} \circ (p_2[t]\mathcal{B})\}x[t] = x[t] - (p_1[t] + p_2[t])x[t-1] + p_1[t]p_2[t-1]x[t-2]$$

$\underbrace{p_1[t]p_2[t-1]\mathcal{B}^2}_{\text{must equal}}$

STOCHASTIC MECHANICAL SYSTEMS & AUTOMATION (SMSA) LABORATORY UNIVERSITY OF PATRAS

The Wold-type Representation of a TARMA Model (Crámer 1961)

Pre-multiplying the TARMA model equation by $A^{-1}[\mathcal{B}, t]$ yields:

$$x[t] = \underbrace{A^{-1}[\mathcal{B}, t] \circ C[\mathcal{B}, t]}_{H[\mathcal{B}, t]} \cdot e[t] \Rightarrow x[t] = \sum_{\tau=-\infty}^t \underbrace{h[t, \tau]}_{\substack{\text{impulse} \\ \text{response function}}} \cdot e[\tau], \quad (h[t, t] \equiv 1)$$

The Inverse Function Representation of a TARMA Model

Pre-multiplying the TARMA model equation by $C^{-1}[\mathcal{B}, t]$ yields:

$$\underbrace{C^{-1}[\mathcal{B}, t] \circ A[\mathcal{B}, t]}_{I[\mathcal{B}, t]} \cdot x[t] = e[t] \Rightarrow \sum_{\tau=-\infty}^t \underbrace{i[t, \tau]}_{\substack{\text{inverse} \\ \text{function}}} \cdot x[\tau] = e[t], \quad (i[t, t] \equiv 1)$$

3. TARMA MODEL PARAMETER ESTIMATION

The **complete TARMA identification** problem consists of estimating the **model parameters** (AR, MA, innovations variance) and **structure** (model orders, other structural parameters) based upon an observed data record:

$$x^N = \{x[t], \quad t = 1, 2, \dots, N\}$$

For convenience the identification problem is usually separated into the **parameter estimation** and **structure estimation** subproblems.

“Estimation of the AR, MA parameter vector and the residual variance at all time instants for a selected model form and structure”

$$\boldsymbol{\theta}[t] \stackrel{\Delta}{=} \left[\underbrace{a_1[t] \dots a_{n_a}[t]}_{\text{AR parameters}} : \underbrace{c_1[t] \dots c_{n_c}[t]}_{\text{MA parameters}} \right]^T, \quad \hat{\sigma}_e^2[t], \quad (t = 1, \dots, N)$$

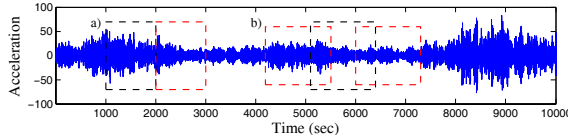
3.a Unstructured Parameter Evolution Representations

The **AR/MA** parameters do not have a “structured” time-dependency and may “freely” change with time.

Their estimation may be achieved either by **locally stationary** or **recursive** methods.

Locally stationary methods [Short Time ARMA (ST-ARMA) estimation]

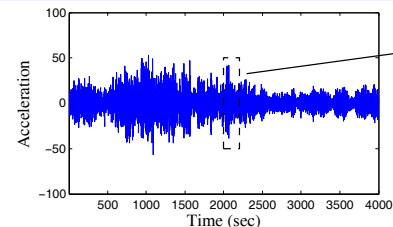
Conventional, **stationary** ARMA modelling applied to successive, “short” (approx. stationary), time segments.



Recursive methods

The AR/MA parameter vector estimate $\boldsymbol{\theta}[t]$ at each time instant t is **recursively updated** at the time instant $t+1$ that the next signal sample becomes available.

Recursive methods



$$\hat{\boldsymbol{\theta}}[t] = \hat{\boldsymbol{\theta}}[t-1] + k[t] \cdot \hat{e}[t|t-1]$$

$k[t]$: adaptation gain

Exponentially Weighted Prediction Error identification criterion:

$$\hat{\boldsymbol{\theta}}[t] = \arg \min_{\boldsymbol{\theta}[t]} \sum_{\tau=1}^t \lambda^{t-\tau} \cdot e^2[\tau, \boldsymbol{\theta}^{\tau-1}]$$

λ : forgetting factor $(0 < \lambda < 1)$

Innovations Variance Estimation → The innovations variance $\hat{\sigma}_e^2[t]$ is estimated via a moving average filter (sliding window) that slides over the prediction error sequence:

$$\hat{\sigma}_e^2[t] = \frac{1}{2M+1} \sum_{\tau=t-M}^{t+M} \hat{e}^2[\tau|t-1]$$

PAGE NUMBER: 13

RML-TARMA Estimation

Estimator update: $\hat{\theta}[t] = \hat{\theta}[t-1] + \mathbf{k}[t]\hat{e}[t|t-1]$

Prediction error: $\hat{e}[t|t-1] = x[t] - \hat{x}[t|t-1] = x[t] - \phi^T[t]\hat{\theta}[t-1]$

Gain: $\mathbf{k}[t] = \frac{\mathbf{P}[t-1]\psi[t]}{\lambda + \psi^T[t]\mathbf{P}[t-1]\psi[t]}$

“Covariance” update: $\mathbf{P}[t] = \frac{1}{\lambda} \left(\mathbf{P}[t-1] - \frac{\mathbf{P}[t-1]\psi[t]\psi^T[t]\mathbf{P}[t-1]}{\lambda + \psi^T[t]\mathbf{P}[t-1]\psi[t]} \right)$

Filtering: $\psi[t] + \hat{c}_1[t-1]\psi[t-1] + \dots + \hat{c}_{n_c}[t-1]\psi[t-n_c] = \phi[t]$

A-posteriori error: $\hat{e}[t|t] = x[t] - \phi^T[t]\hat{\theta}[t]$

$\phi[t] \triangleq \begin{bmatrix} -x[t-1] & \dots & -x[t-n_a] : \hat{e}[t-1|t-1] & \dots & \hat{e}[t-n_c|t-n_c] \end{bmatrix}^T$

Initialization: $\hat{\theta}[0] = \mathbf{0}$, $\mathbf{P}[0] = \alpha\mathbf{I}$ with α designating a “large” positive number. The signal and a-posteriori error initial values are set to zero.

PAGE NUMBER: 14

3.b Stochastic Parameter Evolution (SP-TARMA) Representations

(Kitagawa & Gersch 1996)

The AR/MA parameters are modelled as **random variables** allowed to change with time. Their evolution is subject to **stochastic smoothness constraints**:

$\Delta^\kappa a_i[t] = w_{a_i}[t] \quad \Delta^\kappa c_i[t] = w_{c_i}[t], \quad (\Delta \triangleq 1 - \mathcal{B})$

κ : constraint order $w_{a_i}[t], w_{c_i}[t]$: zero-mean white sequences

TAR(n_a)_($\kappa=2$): $\Delta^2 a_i[t] = w_{a_i}[t] \iff a_i[t] = 2 \cdot a_i[t-1] - a_i[t-2] + w_{a_i}[t], \quad (i = 1, \dots, n_a)$

$$\begin{bmatrix} a_1[t] \\ \vdots \\ a_{n_a}[t] \end{bmatrix} = \begin{bmatrix} 2 & \dots & 0 & -1 & \dots & 0 \\ \vdots & \ddots & \vdots & \vdots & \ddots & \vdots \\ 0 & \dots & 2 & 0 & \dots & -1 \end{bmatrix} \cdot \begin{bmatrix} a_1[t-1] \\ \vdots \\ a_{n_a}[t-1] \\ a_1[t-2] \\ \vdots \\ a_{n_a}[t-2] \end{bmatrix} + \begin{bmatrix} 1 & \dots & 0 \\ \vdots & \ddots & \vdots \\ 0 & \dots & 1 \end{bmatrix} \cdot \begin{bmatrix} w_{a_1}[t] \\ \vdots \\ w_{a_{n_a}}[t] \end{bmatrix} \iff$$

$$\iff \begin{bmatrix} a_1[t] \\ \vdots \\ a_{n_a}[t] \\ a_1[t-1] \\ \vdots \\ a_{n_a}[t-1] \end{bmatrix} = \begin{bmatrix} 2 & \dots & 0 & -1 & \dots & 0 \\ \vdots & \ddots & \vdots & \vdots & \ddots & \vdots \\ 0 & \dots & 2 & 0 & \dots & -1 \\ 1 & \dots & 0 & 0 & \dots & 0 \\ \vdots & \ddots & \vdots & \vdots & \ddots & \vdots \\ 0 & \dots & 1 & 0 & \dots & 0 \end{bmatrix} \cdot \begin{bmatrix} a_1[t-1] \\ \vdots \\ a_{n_a}[t-1] \\ a_1[t-2] \\ \vdots \\ a_{n_a}[t-2] \end{bmatrix} + \begin{bmatrix} 1 & \dots & 0 \\ \vdots & \ddots & \vdots \\ 0 & \dots & 1 \\ 0 & \dots & 0 \\ \vdots & \ddots & \vdots \\ 0 & \dots & 0 \end{bmatrix} \cdot \begin{bmatrix} w_{a_1}[t] \\ \vdots \\ w_{a_{n_a}}[t] \\ w[t] \end{bmatrix}$$

PAGE 17

Kalman Filter and Backward Smoothing for the Estimation of SP-TARMA Models (normalized form)

Time update (prediction)

State prediction: $\hat{z}[t|t-1] = F\hat{z}[t-1|t-1]$

Prediction error: $\hat{e}[t|t-1] = x[t] - h^T[t]\hat{z}[t|t-1]$

“Covariance” update: $\tilde{P}[t|t-1] = F\tilde{P}[t-1|t-1]F^T + G\tilde{Q}[t]G^T$

Observation update (filtering)

Gain: $k[t] = \tilde{P}[t|t-1]h[t] \left(h^T[t]\tilde{P}[t|t-1]h[t] + 1 \right)^{-1}$

State update: $\hat{z}[t|t] = \hat{z}[t|t-1] + k[t]\hat{e}[t|t-1]$

“Covariance” update: $\tilde{P}[t|t] = (I - k[t]h^T[t])\tilde{P}[t|t-1]$

Smoothing:

$A[t] = \tilde{P}[t|t]F^T\tilde{P}^{-1}[t+1|t]$

$\hat{z}[t|N] = \hat{z}[t|t] + A[t](\hat{z}[t+1|N] - \hat{z}[t+1|t])$

$\tilde{P}[t|N] = \tilde{P}[t|t] + A[t](\tilde{P}[t+1|N] - \tilde{P}[t+1|t])A^T[t]$

$\tilde{P}[t|t] \triangleq \frac{P[t|t]}{\sigma_e^2[t]}, \quad \tilde{P}[t|t-1] \triangleq \frac{P[t|t-1]}{\sigma_e^2[t]}, \quad \tilde{Q}[t] \triangleq \frac{Q[t]}{\sigma_e^2[t]} = \underbrace{\frac{\sigma_e^2[t]}{\nu[t]}}_{\nu[t]} I_{n_a}$

Initialization: $\hat{z}[0|0] = 0, \tilde{P}[0|0] = \alpha I$ with α designating a “large” positive number.

STOCHASTIC MECHANICAL SYSTEMS & AUTOMATION (SMSA) LABORATORY UNIVERSITY OF PATRAS

PAGE 18

3.c Deterministic Parameter Evolution (FS-TARMA) Representations

(Grenier 1989, Poulimenos & Fassois 2006)

The AR/MA time-varying parameters and the innovations standard deviation $\sigma_e[t]$ are expanded on functional subspaces:

$\mathcal{F}_{AR} \triangleq \{G_{ba(1)}[t], \dots, G_{ba(p_a)}[t]\}, \quad \mathcal{F}_{MA} \triangleq \{G_{bc(1)}[t], \dots, G_{bc(p_c)}[t]\}$

$\mathcal{F}_{\sigma_e[t]} \triangleq \{G_{bs(1)}[t], \dots, G_{bs(p_s)}[t]\}$

$G_j[t]$: basis functions

$b_a(i), b_c(i), b_s(i)$: AR/MA and innovations standard deviation basis function indices

$a_i[t] \triangleq \sum_{j=1}^{p_a} a_{i,j} \cdot G_{ba(j)}[t], \quad c_i[t] \triangleq \sum_{j=1}^{p_c} c_{i,j} \cdot G_{bc(j)}[t], \quad \sigma_e[t] \triangleq \sum_{j=1}^{p_s} s_j \cdot G_{bs(j)}[t]$

~ Estimation of the projection coefficient vectors:

$\vartheta \triangleq \begin{bmatrix} \underbrace{a^T}_{\text{AR vector}} & \vdots & \underbrace{c^T}_{\text{MA vector}} \end{bmatrix}^T, \quad \underbrace{s \triangleq [s_1, \dots, s_{p_s}]^T}_{\text{innovations standard deviation vector}}$

STOCHASTIC MECHANICAL SYSTEMS & AUTOMATION (SMSA) LABORATORY UNIVERSITY OF PATRAS

PAGE 19

I. Prediction Error (PE) & Maximum Likelihood (ML)

Prediction Error (PE) estimation

$\hat{\vartheta} = \arg \min_{\vartheta} \sum_{t=1}^N \lambda[t] \cdot e^2[t, \vartheta]$ **WLS criterion**

$\lambda[t]$: weighting function $(\lambda[t] \equiv 1 \rightsquigarrow \text{OLS criterion})$

~ **Remark:** The estimation criterion is *parametrized* in terms of $\hat{\vartheta}$ alone.

Parameter Estimation for FS-TAR models

The FS-TAR model is expressed as:

$x[t] + \underbrace{\sum_{i=1}^{n_a} \sum_{j=1}^{p_a} a_{i,j} \cdot G_{ba(j)}[t] \cdot x[t-i]}_{\text{AR part}} = e[t, \vartheta] \implies x[t] = \phi_{\text{AR}}^T[t] \cdot \vartheta + e[t, \vartheta]$ ~ linear in ϑ

$\phi_{\text{AR}}[t] \triangleq [-G_{ba(1)}[t] \cdot x[t-1] \dots -G_{ba(p_a)}[t] \cdot x[t-n_a]]^T$

STOCHASTIC MECHANICAL SYSTEMS & AUTOMATION (SMSA) LABORATORY UNIVERSITY OF PATRAS

PAGE 20

✓ The *Weighted Least Squares (WLS)* estimator:

$\hat{\vartheta} = \left(\sum_{t=1}^N \lambda[t] \cdot \phi_{\text{AR}}[t] \cdot \phi_{\text{AR}}^T[t] \right)^{-1} \cdot \left(\sum_{t=1}^N \lambda[t] \cdot \phi_{\text{AR}}[t] \cdot x[t] \right)$

~ **Remark:** According to the *Gauss-Markov theorem* we expect that the WLS estimator will be *optimal* (minimal covariance of $\hat{\vartheta}$) for

$\lambda[t] = \frac{1}{\sigma_e^2[t]}$

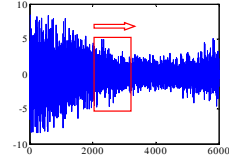
Once $\hat{\vartheta}$ has been obtained, the *innovations standard deviation* coefficient of projection vector s is estimated as follows:

STOCHASTIC MECHANICAL SYSTEMS & AUTOMATION (SMSA) LABORATORY UNIVERSITY OF PATRAS

Step 1. Non-parametric estimation

→ The innovations variance $\hat{\sigma}_e^2[t]$ is non-parametrically estimated via a **moving average filter** (sliding window):

$$\hat{\sigma}_e^2[t] = \frac{1}{2M+1} \sum_{\tau=t-M}^{t+M} e^2[\tau, \hat{\vartheta}]$$

**Step 2. Parametric estimation**

→ \mathbf{s} is estimated by **projecting** the square root of the **estimated innovations variance** on the selected **functional subspace**:

$$\hat{\sigma}_e[t] = \sum_{j=1}^{p_s} s_j \cdot G_{b_s(j)}[t]$$

This is solved for the **coefficients of projection s_j** in a **least squares** sense.

Alternative scheme. Residual Standard Deviation Vector Estimation (Grenier 1983)

→ \mathbf{s} is estimated by **projecting** the sequence of the **estimated innovations absolute values** on the selected **functional subspace (least squares problem)**:

$$E\{|e[t]|\} = \sqrt{2/\pi} \cdot \hat{\sigma}_e[t] = \sqrt{2/\pi} \cdot \sum_{j=1}^{p_s} s_j \cdot G_{b_s(j)}[t] \implies \hat{\mathbf{s}} = \arg \min_{\mathbf{s}} \frac{1}{N} \sum_{t=1}^N \left(|e[t]| - \sqrt{\frac{2}{\pi}} \cdot \sum_{j=1}^{p_s} s_j \cdot G_{b_s(j)}[t] \right)^2$$

Maximum Likelihood (ML) estimation

→ Estimate ϑ and $\hat{\sigma}_e^2$ by **maximizing the Gaussian conditional likelihood** $\mathcal{L}(\vartheta, (\hat{\sigma}_e^2)_1^N | x^N)$ of ϑ and $(\hat{\sigma}_e^2)_1^N$, given the observations $x^N \triangleq \{x[1], \dots, x[N]\}$:

$$\{\hat{\vartheta}, \hat{\sigma}_e^2[1], \dots, \hat{\sigma}_e^2[N]\} = \arg \max_{\vartheta, (\hat{\sigma}_e^2)_1^N} \ln \mathcal{L}(\vartheta, (\hat{\sigma}_e^2)_1^N | x^N)$$

$$\mathcal{L}(\vartheta, (\hat{\sigma}_e^2)_1^N | x^N) = f(x^N) = f(e^N) = \prod_{t=1}^N \frac{1}{\sqrt{2\pi\hat{\sigma}_e^2[t]}} \cdot \exp \left[-\frac{e^2[t, \vartheta]}{2\hat{\sigma}_e^2[t]} \right] \implies$$

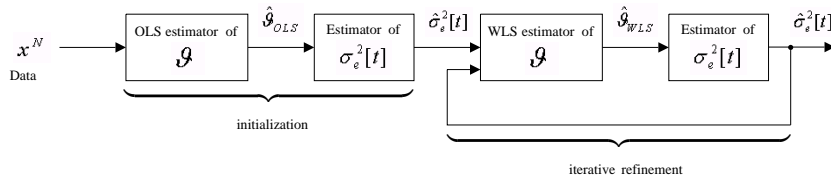
$$\ln \mathcal{L}(\vartheta, (\hat{\sigma}_e^2)_1^N | x^N) = -\frac{1}{2} \left\{ N \cdot \ln 2\pi + \sum_{t=1}^N \ln \hat{\sigma}_e^2[t] + \sum_{t=1}^N \frac{e^2[t, \vartheta]}{\hat{\sigma}_e^2[t]} \right\}$$

$f(\cdot)$: probability density function

Non-parametrized innovations variance case

$$\frac{\partial \ln \mathcal{L}}{\partial \hat{\sigma}_e^2[\tau]} = 0 \Leftrightarrow -\frac{1}{2} \cdot \left[\frac{1}{\hat{\sigma}_e^2[\tau]} - \frac{e^2[\tau, \vartheta]}{\hat{\sigma}_e^4[\tau]} \right] = 0 \Leftrightarrow \hat{\sigma}_e^2[\tau] = e^2[\tau, \vartheta], \quad (\tau \in (1, N))$$

$$\frac{\partial^2 \ln \mathcal{L}}{\partial (\hat{\sigma}_e^2[\tau])^2} \Big|_{\hat{\sigma}_e^2[\tau]=e^2[\tau, \vartheta]} = -\frac{1}{2} \cdot \left[\frac{-1}{\hat{\sigma}_e^4[\tau]} + \frac{2e^2[\tau, \vartheta]}{\hat{\sigma}_e^6[\tau]} \right] \Big|_{\hat{\sigma}_e^2[\tau]=e^2[\tau, \vartheta]} = -\frac{1}{2} \cdot \left[\frac{2}{\hat{\sigma}_e^4[\tau]} - \frac{1}{\hat{\sigma}_e^4[\tau]} \right] = -\frac{1}{2\hat{\sigma}_e^4[\tau]} < 0$$

Bootstrap implementation of the optimal WLS estimator:**Parameter Estimation for FS-TARMA models**

The **FS-TARMA** model **cannot** be written as a **linear function** of ϑ . Indeed:

$$x[t] + \underbrace{\sum_{i=1}^{n_a} \sum_{j=1}^{p_a} a_{i,j} \cdot G_{b_a(j)}[t] \cdot x[t-i]}_{\text{AR part}} = e[t, \vartheta] + \underbrace{\sum_{i=1}^{n_c} \sum_{j=1}^{p_c} c_{i,j} \cdot G_{b_c(j)}[t] \cdot e[t-i, \vartheta]}_{\text{MA part}} \implies$$

$$\implies x[t] = \phi_{\text{ARMA}}^T[t, \vartheta] \cdot \vartheta + e[t, \vartheta]$$

$\phi_{\text{ARMA}}[t, \vartheta] \triangleq \begin{bmatrix} -G_{b_a(1)}[t] \cdot x[t-1] & \dots & -G_{b_a(p_a)}[t] \cdot x[t-n_a] & G_{b_c(1)}[t] \cdot e[t-1, \vartheta] & \dots & G_{b_c(p_c)}[t] \cdot e[t-n_c, \vartheta] \end{bmatrix}^T$
Hence the **OLS** and **WLS** criteria lead to **nonlinear** estimators characterized by several **local minima**.

From the above equations it follows that:

$$\{\hat{\vartheta}, (\hat{\sigma}_e^2)_1^N\} = \arg \max_{\vartheta, (\hat{\sigma}_e^2)_1^N} \left\{ \ln \mathcal{L}(\vartheta, (\hat{\sigma}_e^2)_1^N | x^N) \Big|_{\hat{\sigma}_e^2[\tau]=e^2[\tau, \vartheta]} \right\} \iff$$

$$\iff \hat{\vartheta} = \arg \max_{\vartheta} \left\{ -\frac{1}{2} \sum_{t=1}^N \ln e^2[t, \vartheta] \right\} = \left\{ -\frac{1}{2} \ln \left(\prod_{t=1}^N e^2[t, \vartheta] \right) \right\}, \quad \hat{\sigma}_e^2[t] = e^2[t, \vartheta]$$

Parametrized innovations variance case

$$\hat{\vartheta} = \arg \max_{\vartheta} \left\{ -\frac{1}{2} \sum_{t=1}^N \left[\ln \left(\sum_{j=1}^{p_s} \mathbf{s}_j \cdot G_{b_s(j)}[t] \right)^2 + \frac{e^2[t, \vartheta]}{\left(\sum_{j=1}^{p_s} \mathbf{s}_j \cdot G_{b_s(j)}[t] \right)^2} \right] \right\} \quad \begin{aligned} \vartheta &\triangleq [\vartheta^T : \mathbf{s}^T]^T \\ \mathbf{s} &\triangleq [\mathbf{a}^T : \mathbf{c}^T]^T \\ \mathbf{s} &\triangleq [s_1 \dots s_{p_s}]^T \end{aligned}$$

$$\frac{\partial \ln \mathcal{L}}{\partial s_r} = 0 \Leftrightarrow \sum_{t=1}^N \left\{ \frac{2 \cdot G_{b_s(r)}[t]}{\sum_{j=1}^{p_s} \mathbf{s}_j \cdot G_{b_s(j)}[t]} - \frac{2 \cdot e^2[t, \vartheta] \cdot G_{b_s(r)}[t]}{\left(\sum_{j=1}^{p_s} \mathbf{s}_j \cdot G_{b_s(j)}[t] \right)^3} \right\} = 0 \Leftrightarrow ???$$

→ **Non-linear** optimization problem due to the **non-quadratic** dependence on:

▷ The innovations variance vector \mathbf{s} (FS-TAR and FS-TARMA case).

▷ The **MA** projection coefficients (FS-TARMA case)

PARAMETRIC TIME-DOMAIN METHODS FOR NON-STATIONARY RANDOM VIBRATION IDENTIFICATION 25

II. Multi-Stage Estimation Methods

⇒ **Multi-stage** methods tackle the problem by “*breaking*” it up into **simpler subproblems**. These are *either* **quadratic** (⇒ linear techniques applicable) *or* **non-quadratic** but of **lower dimension**.

The Two-Stage Least Squares (2SLS) method (Grenier 1989; Poulimenos and Fassois 2003)

STAGE 1. Inverse Function Estimation:
A truncated n_i -order inverse function model:

$$I[\mathcal{B}, t, \mathbf{i}] \cdot x[t] = e[t, \mathbf{i}]$$

$$\mathbf{i}$$
: inverse function coefficient of projection vector.

is estimated via an **OLS** or **WLS** estimator.

STAGE 2. AR/MA Projection Coefficient Estimation:
Estimates of the residuals $e[t]$ are obtained as $e[t, \hat{\mathbf{i}}]$ and the AR/MA coefficients of projection in the model:

$$x[t] + \sum_{i=1}^{n_a} \sum_{j=1}^{p_a} a_{i,j} \cdot G_{b_a(j)} \cdot x[t-i] = \sum_{i=1}^{n_c} \sum_{j=1}^{p_c} c_{i,j} \cdot G_{b_c(j)} \cdot e[t-i, \hat{\mathbf{i}}] + e[t, \vartheta]$$

are obtained via an **OLS** or **WLS** estimator.

STAGE 3. Innovations Standard Deviation Estimation:
The residual standard deviation $\sigma_e[t]$ is **non-parametrically/parametrically** estimated.

STOCHASTIC MECHANICAL SYSTEMS & AUTOMATION (SMSA) LABORATORY UNIVERSITY OF PATRAS

PARAMETRIC TIME-DOMAIN METHODS FOR NON-STATIONARY RANDOM VIBRATION IDENTIFICATION 26

The Three-Stage LS/ML method

Motivation:

Given an **estimate of \mathbf{s}** , the ln-likelihood simplifies to a **Weighted Least Squares** criterion:

$$\ln \mathcal{L}(\vartheta | x^N) = -\frac{1}{2} \sum_{t=1}^N \left(\ln(\mathbf{g}_s^T[t] \cdot \hat{\mathbf{s}})^2 + \frac{e^2[t, \vartheta]}{(\mathbf{g}_s^T[t] \cdot \hat{\mathbf{s}})^2} \right) = -\left(\frac{1}{2} \sum_{t=1}^N \frac{e^2[t, \vartheta]}{(\mathbf{g}_s^T[t] \cdot \hat{\mathbf{s}})^2} \right) + \text{const.}$$

$$\mathbf{g}_s[t] \triangleq [G_{b_s(1)}[t] \dots G_{b_s(p_s)}[t]]^T$$

▷ **Weighted Linear Least Squares (WLLS)** estimation may be applied in the **FS-TAR** case ($e[t, \vartheta]$ depends linearly on ϑ)

▷ **Weighted Non-linear Least Squares (WNLS)** estimation may be applied in the **FS-TARMA** case ($e[t, \vartheta]$ depends non-linearly on ϑ)
⇒ *This problem may be relaxed and treated suboptimally via linear techniques as in the P-A and 2SLS methods (Poulimenos and Fassois 2004)*

⇒ **This multistage estimator is asymptotically equivalent to the ML estimator**

STOCHASTIC MECHANICAL SYSTEMS & AUTOMATION (SMSA) LABORATORY UNIVERSITY OF PATRAS

PARAMETRIC TIME-DOMAIN METHODS FOR NON-STATIONARY RANDOM VIBRATION IDENTIFICATION 27

STAGE 1. Initial AR/MA Projection Coefficient Estimation (OLS)

$$\hat{\vartheta}_{OLS} = \arg \min_{\vartheta} \sum_{t=1}^N e^2[t, \vartheta]$$

FS-TAR case [Ordinary **Linear** Least Squares (OLLS) estimation]:

$$\hat{\vartheta}_{OLS} = \left(\sum_{t=1}^N \phi_{AR}[t] \cdot \phi_{AR}^T[t] \right)^{-1} \cdot \left(\sum_{t=1}^N \phi_{AR}[t] \cdot x[t] \right)$$

FS-TARMA case [Ordinary **Non-linear** Least Squares (ONLS) estimation]:
Initial P-A or 2SLS estimation (suboptimum)
+
refinement by the **ONLS** estimator using iterative optimization techniques.

STOCHASTIC MECHANICAL SYSTEMS & AUTOMATION (SMSA) LABORATORY UNIVERSITY OF PATRAS

PARAMETRIC TIME-DOMAIN METHODS FOR NON-STATIONARY RANDOM VIBRATION IDENTIFICATION 28

STAGE 2. Residual Standard Deviation Estimation (ML)

FS-TAR / TARMA case [Maximum Likelihood (ML) estimation]:

$$\hat{\mathbf{s}}_{ML} = \arg \max_{\mathbf{s}} \left\{ -\frac{1}{2} \sum_{t=1}^N \left(\ln(\mathbf{g}_s^T[t] \cdot \mathbf{s})^2 + \frac{e^2[t, \hat{\vartheta}_{OLS}]}{(\mathbf{g}_s^T[t] \cdot \mathbf{s})^2} \right) \right\}$$

⇒ **Non-linear** optimization problem of **lower dimension**

Implementation:

Initial estimation via a **Least Squares** estimator (Grenier, 1983):

$$\hat{\mathbf{s}} = \arg \min_{\mathbf{s}} \frac{1}{N} \sum_{t=1}^N \left(|e[t, \hat{\vartheta}_{OLS}]| - \sqrt{\frac{2}{\pi}} \cdot \mathbf{g}_s^T[t] \cdot \mathbf{s} \right)^2 = \sqrt{\frac{\pi}{2}} \cdot \left(\sum_{t=1}^N \mathbf{g}_s^T[t] \cdot \mathbf{g}_s^T[t] \right)^{-1} \cdot \left(\sum_{t=1}^N \mathbf{g}_s^T[t] \cdot |e[t, \hat{\vartheta}_{OLS}]| \right)$$

+
Refinement by the **ML** estimator using iterative optimization techniques.

STOCHASTIC MECHANICAL SYSTEMS & AUTOMATION (SMSA) LABORATORY UNIVERSITY OF PATRAS

PARAMETRIC TIME-DOMAIN METHODS FOR NON-STATIONARY RANDOM VIBRATION IDENTIFICATION 29

STAGE 3. Final AR/MA Projection Coefficient Estimation

$$\hat{\boldsymbol{\vartheta}} = \arg \min_{\boldsymbol{\vartheta}} \sum_{t=1}^N \frac{e^2[t, \boldsymbol{\vartheta}]}{(\mathbf{g}_s^T[t] \cdot \hat{\mathbf{s}})^2}$$

FS-TAR case [Weighted **Linear** Least Squares (WLLS) estimation problem]:

$$\hat{\boldsymbol{\vartheta}} = \left(\sum_{t=1}^N \frac{\boldsymbol{\phi}_{\text{AR}}[t] \cdot \boldsymbol{\phi}_{\text{AR}}^T[t]}{(\mathbf{g}_s^T[t] \cdot \hat{\mathbf{s}})^2} \right)^{-1} \cdot \left(\sum_{t=1}^N \frac{\boldsymbol{\phi}_{\text{AR}}[t] \cdot \mathbf{x}[t]}{(\mathbf{g}_s^T[t] \cdot \hat{\mathbf{s}})^2} \right)$$

FS-TARMA case [Weighted **Non-linear** Least Squares (WNLS) estimation problem]:

Initial (suboptimum) P-A or 2SLS estimation (WLS versions)
+
refinement by the WNLS estimator using iterative optimization techniques.

STOCHASTIC MECHANICAL SYSTEMS & AUTOMATION (SMSA) LABORATORY UNIVERSITY OF PATRAS

PARAMETRIC TIME-DOMAIN METHODS FOR NON-STATIONARY RANDOM VIBRATION IDENTIFICATION 30

4. ASYMPTOTIC ANALYSIS FOR FS-TARMA ESTIMATORS

~ Refers to the **estimator properties** as the number of **observations** tends to infinity

▷ **Consistency:** Probabilistic convergence of the estimator to its “true” ($\boldsymbol{\theta}^o$) value:

$$\hat{\boldsymbol{\theta}}_N \xrightarrow{p} \boldsymbol{\theta}^o$$

▷ **Asymptotic Normality:** Approximation of the estimator distribution by a **normal law**:

$$\hat{\boldsymbol{\theta}}_N \xrightarrow{A} \mathcal{N} \left(\boldsymbol{\theta}^o, \frac{1}{N} \mathbf{P} \right), \quad \left(\frac{1}{N} \mathbf{P} \right) \text{ : estimator covariance matrix } \right)$$

↔ **A physical interpretation:**
“As the number of observations increases more information of the same kind is added”.

Question: How more and more observations concerning a **general (non-periodic) non-stationary** phenomenon can be collected?

~ A **general non-stationary** phenomenon takes place in a **specific time interval**, thus:

more observations ($N \rightarrow \infty$) \iff **more dense observations** ($T_s \rightarrow 0$)
(Dahlhaus, 1997)

STOCHASTIC MECHANICAL SYSTEMS & AUTOMATION (SMSA) LABORATORY UNIVERSITY OF PATRAS

PARAMETRIC TIME-DOMAIN METHODS FOR NON-STATIONARY RANDOM VIBRATION IDENTIFICATION 31

Problem Formulation

~ **Difficulty:** The “true” discrete-time system changes as $N \rightarrow \infty$ via $T_s \rightarrow 0$

~ The “true” parameter is considered as a sequence of “true” parameters $\{\boldsymbol{\theta}_N^o\}$:

$$\left\{ \boldsymbol{\theta}_N^o = \left[\boldsymbol{\theta}_N^{o,T} : \mathbf{s}_N^{o,T} \right]^T \right\} : \quad x_N[t] + \sum_{i=1}^{n_a} a_i[t, \boldsymbol{\theta}_N^o] \cdot x_N[t-i] = e_N[t] + \sum_{i=1}^{n_c} c_i[t, \boldsymbol{\theta}_N^o] \cdot e_N[t-i]$$

$$e_N[t] \sim \mathcal{N}(0, \sigma_e^2[t, \mathbf{s}_N^o]), \quad t = 1, \dots, N, \quad N = 1, 2, 3, \dots$$

~ **Asymptotic considerations:**

▷ **Consistency:** Probabilistic convergence of the **distance** between the estimator and its “true” value $\rho(\hat{\boldsymbol{\theta}}_N, \boldsymbol{\theta}_N^o)$ to zero:

$$\rho(\hat{\boldsymbol{\theta}}_N, \boldsymbol{\theta}_N^o) \xrightarrow{p} 0 \quad \rightsquigarrow \quad \hat{\boldsymbol{\theta}}_N \xrightarrow{p} \boldsymbol{\theta}_N^o \text{ (large } N\text{)} \quad \xrightarrow{p} \text{ indicating convergence in probability}$$

▷ **Asymptotic Normality:** Convergence of the normalized estimator distribution to the standard normal law:

$$\lambda^T \mathbf{P}^{-\frac{1}{2}}(\boldsymbol{\theta}_N^o) \sqrt{N} (\hat{\boldsymbol{\theta}}_N - \boldsymbol{\theta}_N^o) \xrightarrow{d} \mathcal{N}(0, 1), \quad \forall \lambda : \lambda^T \cdot \lambda = 1 \quad \rightsquigarrow \quad \hat{\boldsymbol{\theta}}_N \xrightarrow{A} \mathcal{N} \left(\boldsymbol{\theta}_N^o, \frac{1}{N} \mathbf{P}(\boldsymbol{\theta}_N^o) \right) \text{ (large } N\text{)}$$

$\frac{1}{N} \mathbf{P}(\boldsymbol{\theta}_N^o)$: asymptotic covariance matrix \xrightarrow{d} : convergence in distribution

STOCHASTIC MECHANICAL SYSTEMS & AUTOMATION (SMSA) LABORATORY UNIVERSITY OF PATRAS

PARAMETRIC TIME-DOMAIN METHODS FOR NON-STATIONARY RANDOM VIBRATION IDENTIFICATION 32

Consistency Analysis

~ It may be shown under **general conditions** concerning the FS-TARMA model **stability**, **invertibility** and **identifiability** that:

$$\begin{aligned} \rho(\hat{\boldsymbol{\theta}}_N^{OLS}, \boldsymbol{\theta}_N^o) &\xrightarrow{p} 0, & \rho(\hat{\boldsymbol{\theta}}_N^{WLS}, \boldsymbol{\theta}_N^o) &\xrightarrow{p} 0 \\ \rho(\hat{\boldsymbol{\theta}}_N^{ML}, \boldsymbol{\theta}_N^o) &\xrightarrow{p} 0, & \rho(\hat{\boldsymbol{\theta}}_N^{MS}, \boldsymbol{\theta}_N^o) &\xrightarrow{p} 0 \end{aligned}$$

Asymptotic Normality

~ It may be shown under the same general conditions that:

$$\begin{aligned} \mathbf{P}_{OLS}^{-\frac{1}{2}}(\boldsymbol{\theta}_N^o) \cdot \sqrt{N} \cdot (\hat{\boldsymbol{\theta}}_N^{OLS} - \boldsymbol{\theta}_N^o) &\xrightarrow{d} \mathcal{N}(\mathbf{0}, \mathbf{I}) \\ \mathbf{P}_{WLS}^{-\frac{1}{2}}(\boldsymbol{\theta}_N^o) \cdot \sqrt{N} \cdot (\hat{\boldsymbol{\theta}}_N^{WLS} - \boldsymbol{\theta}_N^o) &\xrightarrow{d} \mathcal{N}(\mathbf{0}, \mathbf{I}) \\ \mathbf{P}_{ML}^{-\frac{1}{2}}(\boldsymbol{\theta}_N^o) \cdot \sqrt{N} \cdot (\hat{\boldsymbol{\theta}}_N^{ML} - \boldsymbol{\theta}_N^o) &\xrightarrow{d} \mathcal{N}(\mathbf{0}, \mathbf{I}) \\ \mathbf{P}_{MS}^{-\frac{1}{2}}(\boldsymbol{\theta}_N^o) \cdot \sqrt{N} \cdot (\hat{\boldsymbol{\theta}}_N^{MS} - \boldsymbol{\theta}_N^o) &\xrightarrow{d} \mathcal{N}(\mathbf{0}, \mathbf{I}) \end{aligned}$$

STOCHASTIC MECHANICAL SYSTEMS & AUTOMATION (SMSA) LABORATORY UNIVERSITY OF PATRAS

PARAMETRIC TIME-DOMAIN METHODS FOR NON-STATIONARY RANDOM VIBRATION IDENTIFICATION 33

Cramèr-Rao Bound

→ Imposes a *lower bound* on the *asymptotic covariance* matrix.

$$\frac{1}{N} \mathbf{P}(\boldsymbol{\theta}_N^o) \geq [\mathbf{J}(\boldsymbol{\theta}_N^o)]^{-1} = \left[\mathbb{E} \left\{ \left[\frac{\partial}{\partial \boldsymbol{\theta}} \mathcal{L}(\boldsymbol{\theta} | x^N) \right] \cdot \left[\frac{\partial}{\partial \boldsymbol{\theta}} \mathcal{L}(\boldsymbol{\theta} | x^N) \right]^T \right\}_{\boldsymbol{\theta}_N^o} \right]^{-1} = \left[\mathbb{E} \left\{ \frac{\partial^2}{\partial \boldsymbol{\theta} \partial \boldsymbol{\theta}^T} \mathcal{L}(\boldsymbol{\theta} | x^N) \right\}_{\boldsymbol{\theta}_N^o} \right]^{-1}$$

Fisher's Information Matrix ($\mathbf{J}(\boldsymbol{\theta}_N^o)$):

$$\mathbf{J}(\boldsymbol{\theta}_N^o) = \sum_{t=1}^N \begin{bmatrix} \mathbb{E} \left\{ \left[\frac{\partial}{\partial \boldsymbol{\theta}} e[t, \boldsymbol{\theta}] \right] \cdot \left[\frac{\partial}{\partial \boldsymbol{\theta}} e[t, \boldsymbol{\theta}] \right]^T \right\}_{\boldsymbol{\theta}_N^o} & \mathbf{0} \\ \hline \mathbb{E} \left\{ \frac{\partial \mathcal{L}}{\partial \boldsymbol{\theta}} \cdot \frac{\partial \mathcal{L}}{\partial \boldsymbol{\theta}^T} \right\} & \mathbb{E} \left\{ \frac{\partial \mathcal{L}}{\partial \boldsymbol{\theta}} \cdot \frac{\partial \mathcal{L}}{\partial \boldsymbol{\theta}^T} \right\} \\ \mathbf{0} & 2 \cdot \frac{\mathbf{g}_s[t] \cdot \mathbf{g}_s^T[t]}{(\mathbf{g}_s^T[t] \cdot \mathbf{s}_N^o)^2} \\ \hline \mathbb{E} \left\{ \frac{\partial \mathcal{L}}{\partial \boldsymbol{s}} \cdot \frac{\partial \mathcal{L}}{\partial \boldsymbol{\theta}^T} \right\} & \mathbb{E} \left\{ \frac{\partial \mathcal{L}}{\partial \boldsymbol{s}} \cdot \frac{\partial \mathcal{L}}{\partial \boldsymbol{\theta}^T} \right\} \end{bmatrix}$$

$$\mathbf{P}_{ML}(\boldsymbol{\theta}_N^o) = \mathbf{P}_{MS}(\boldsymbol{\theta}_N^o) = [\mathbf{J}(\boldsymbol{\theta}_N^o)]^{-1}$$

STOCHASTIC MECHANICAL SYSTEMS & AUTOMATION (SMSA) LABORATORY UNIVERSITY OF PATRAS

PARAMETRIC TIME-DOMAIN METHODS FOR NON-STATIONARY RANDOM VIBRATION IDENTIFICATION 34

Monte Carlo study

Chebyshev II basis functions: $G_0[t] = 1$, $G_1[t] = 4 \frac{t-1}{N-1} - 2$, $G_k[t] = G_1[t] \cdot G_{k-1}[t] - G_{k-2}[t]$, $t = 1, \dots, N$, $n = 2, 3, \dots$

FS-TARMA(2,2)^[3,3,3]

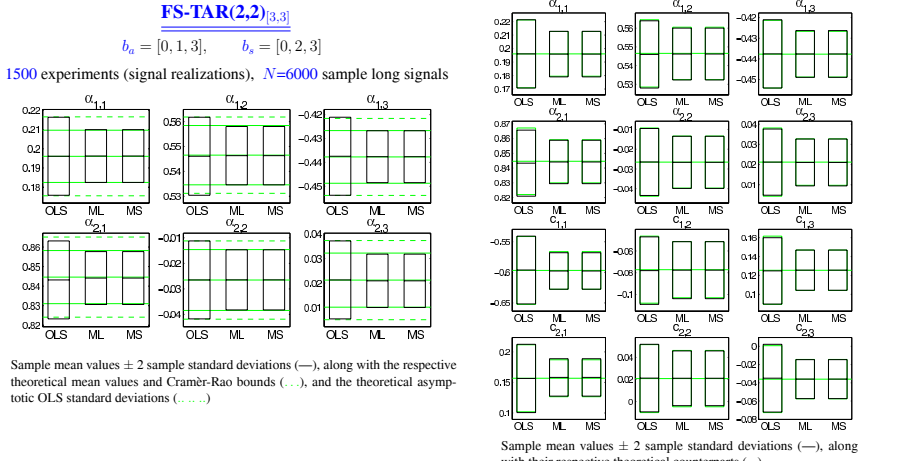
$b_a = [0, 1, 3]$, $b_s = [0, 2, 3]$

1500 experiments (signal realizations), $N=6000$ sample long signals

FS-TAR(2,2)^[3,3]

$b_a = [0, 1, 3]$, $b_s = [0, 2, 3]$

1500 experiments (signal realizations), $N=6000$ sample long signals



Sample mean values ± 2 sample standard deviations (—), along with the respective theoretical mean values and Cramèr-Rao bounds (…), and the theoretical asymptotic OLS standard deviations (....)

STOCHASTIC MECHANICAL SYSTEMS & AUTOMATION (SMSA) LABORATORY UNIVERSITY OF PATRAS

PARAMETRIC TIME-DOMAIN METHODS FOR NON-STATIONARY RANDOM VIBRATION IDENTIFICATION 35

5. MODEL STRUCTURE ESTIMATION & VALIDATION

MODEL STRUCTURE ESTIMATION

“Estimation of the model orders and additional structural parameters for a selected model class”

$$\begin{aligned} \mathcal{M} &\stackrel{\Delta}{=} \{n_a, n_c\} & n_a, n_c : \text{AR/MA orders} \\ \mathcal{M}_{SP} &\stackrel{\Delta}{=} \{n_a, n_c, \kappa\} & \kappa : \text{smoothness constraint order} \\ \mathcal{M}_{FS} &\stackrel{\Delta}{=} \{n_a, n_c, \mathcal{F}_{\text{AR}}, \mathcal{F}_{\text{MA}}, \mathcal{F}_{\sigma_e^2}\} & \mathcal{F} : \text{functional subspace} \end{aligned}$$

General approach: minimization of the Bayesian Information Criterion (BIC) or the negative log-likelihood function.

$$BIC = \left[\frac{N}{2} \cdot \ln 2\pi + \frac{1}{2} \sum_{t=1}^N \left(\ln(\sigma_e^2[t]) + \frac{e^2[t]}{\sigma_e^2[t]} \right) \right] + \frac{\ln N}{2} \cdot d$$

d: number of independently estimated model parameters

STOCHASTIC MECHANICAL SYSTEMS & AUTOMATION (SMSA) LABORATORY UNIVERSITY OF PATRAS

PARAMETRIC TIME-DOMAIN METHODS FOR NON-STATIONARY RANDOM VIBRATION IDENTIFICATION 36

A heuristic method
(Pouliomenos and Fassois 2004)

PHASE I. Model Order Selection
Based upon *initial* “extended” and “complete” functional subspaces (ensuring *subspace adequacy*) via *minimization* of the *BIC*:

$$\{n_a, n_c\} = \arg \min_{n_a, n_c} BIC(\mathcal{M})$$

using *trial and error* techniques.

PHASE II. Functional Subspace Selection
Optimization of the *initial*, “extended”, subspaces by detecting “excess” basis functions through either the *BIC* or the *APD* criterion:

$$APD \stackrel{\Delta}{=} \sum_{i=1}^{n_a} \Delta a_i + \sum_{i=1}^{n_c} \Delta c_i + \Delta s$$

$\Delta a_i, \Delta c_i, \Delta s$: normalized *deviations* of the *current model parameters* from their *initial model* counterparts (Phase I result)

using *backward* procedures.

STOCHASTIC MECHANICAL SYSTEMS & AUTOMATION (SMSA) LABORATORY UNIVERSITY OF PATRAS

246

Integer Optimization Scheme

(Poulimenos and Fassois 2003)

Minimization of the BIC is achieved via a “*direct*”, “*hybrid*”, two-phase optimization scheme:

PHASE I. *Coarse (“global”) optimization.*

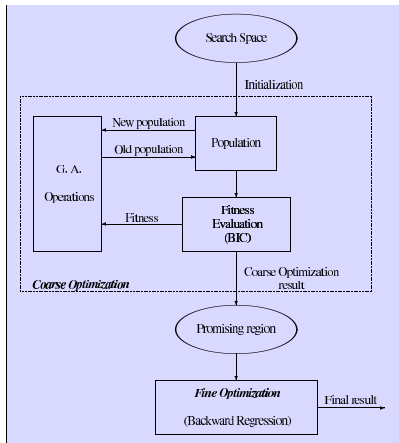
→ applied to the complete search space aiming at locating promising regions.

→ Approach: *Genetic Algorithms*

PHASE II. *Fine (“local”) optimization.*

→ operates in the neighborhood of each Phase I result aiming at locating the exact optimum point.

→ Approach: *Backward Regression*



MODEL VALIDATION

The residual series is **non-stationary**. A test based upon the number of **sign changes** in the residual series is applied.

(++)(−−−)(+)(−−)(+++)(−)(++)(−−)

Let: z be the number of “runs” (groups with common sign)

z_1 be the total number of positive residuals

z_2 be the total number of negative residuals

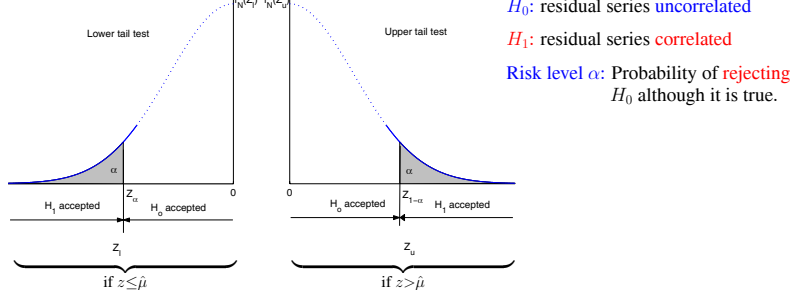
The **sign test** examines whether a pattern is “unusual” for a **zero-mean uncorrelated series** or not.

The **mean** and **variance** of the random variable z may be estimated as:

$$\hat{\mu} = \frac{2z_1 z_2}{z_1 + z_2} + 1, \quad \hat{\sigma}^2 = \frac{2z_1 z_2 \cdot (2z_1 z_2 - z_1 - z_2)}{(z_1 + z_2)^2 \cdot (z_1 + z_2 - 1)}$$

For large samples, the tails of the distribution of z may be approximated by **Gaussian curves**.

→ Lower tail statistic $Z_\ell = \frac{z - \hat{\mu} + 1/2}{\hat{\sigma}} \sim \text{lower tail of } \mathcal{N}(0, 1)$
 → Upper tail statistic $Z_u = \frac{z - \hat{\mu} - 1/2}{\hat{\sigma}} \sim \text{upper tail of } \mathcal{N}(0, 1)$ } under H_0



6. MODEL BASED ANALYSIS

The Impulse Response Function

It may readily obtained as:

$$h[t, \tau] = \begin{cases} 0, & t < \tau \\ c_{t-\tau}[t] - \sum_{j=1}^{t-\tau} a_j[t] \cdot h[t-j, \tau], & t \geq \tau \end{cases}$$

The Autocovariance Function

$$\gamma[t_1, t_2] = \sum_{i=-\infty}^{\min(t_1, t_2)} \bar{h}[t_1, i] \cdot \bar{h}[t_2, i] \implies \gamma[t_1, t_2] = \sum_{i=-\infty}^{\min(t_1, t_2)} h[t_1, i] \cdot h[t_2, i] \cdot \sigma_e^2[i]$$

$$(\bar{h}[t, \tau]) \triangleq h[t, \tau] \cdot \sigma_e[\tau]$$

Time-frequency Distributions

“Frequency Response”

$$H(e^{j\omega T_s}, t) \triangleq \frac{\text{response of the system to } e^{j\omega T_s t}}{e^{j\omega T_s t}}$$

ω : frequency
 $j = \sqrt{-1}$
 T_s : sampling period

$$H(e^{j\omega T_s}, t) = \sum_{i=0}^{\infty} h[t, t-i] \cdot e^{-j\omega T_s i}$$

PARAMETRIC TIME-DOMAIN METHODS FOR NON-STATIONARY RANDOM VIBRATION IDENTIFICATION 41

The Wigner-Ville distribution:

$$S_{WV}(\omega, t) = \sum_{\tau=-\infty}^{\infty} \gamma \left[t - \frac{\tau}{2}, t + \frac{\tau}{2} \right] \cdot e^{-j\omega T_s \tau}$$

The Melard-Tjøstheim distribution:

$$S_{MT}(\omega, t) = |\bar{H}(e^{j\omega T_s}, t)|^2 = \left| \sum_{\tau=-\infty}^t \bar{h}[t, \tau] \cdot e^{j\omega T_s \tau} \right|^2$$

The “Frozen” distribution:

$$S_F(\omega, t) = \left| \frac{A[e^{-j\omega T_s}, t]}{C[e^{-j\omega T_s}, t]} \right|^2 \cdot \sigma_e^2[t] \quad A[e^{-j\omega T_s}, t] = A[\mathcal{B}, t] \text{ for } \mathcal{B} = e^{-j\omega T_s}$$

✓ The “frozen” characteristics correspond to the characteristics that the system would have if it were actually “frozen” at a specific time instant.

A **frozen frequency response function (frf)** may be defined as:

$$H_F(e^{j\omega T_s}, t) = \frac{A[e^{-j\omega T_s}, t]}{C[e^{-j\omega T_s}, t]}$$

Similarly **frozen natural frequencies** and **damping ratios** may be obtained as:

$$\omega_m[t] = \frac{|\ln \lambda_i[t]|}{T_s} \quad (\text{rad/time unit}), \quad \zeta_i[t] = -\cos(\arg(\ln \lambda_i[t]))$$

λ_i : designating the i -th discrete-time “frozen” pole

STOCHASTIC MECHANICAL SYSTEMS & AUTOMATION (SMSA) LABORATORY UNIVERSITY OF PATRAS

PARAMETRIC TIME-DOMAIN METHODS FOR NON-STATIONARY RANDOM VIBRATION IDENTIFICATION 42

7. A COMPARATIVE STUDY BASED ON MONTE CARLO EXPERIMENTS
(Pouliimenos and Fassois 2006)

THE PROBLEM: Modeling, analysis and prediction of non-stationary vibration.

The Underlying System

Time-varying stiffnesses $k_2(t)$ and $k_3(t)$:

$$k_1(t) = k_{1,0} + k_{1,1} \cdot \sin(2\pi t/P_{1,1}) + k_{1,2} \cdot \sin(2\pi t/P_{1,2})$$

Symbol	Value
m_1	0.5 kg
m_2	1.5 kg
m_3	1.0 kg
c_2	0.5 N/(m/s)
c_3	0.3 N/(m/s)
k_1	300 N/m
$k_2(t)$	$k_{2,0} = 100 \text{ (N/m)}, k_{2,1} = 60, k_{2,2} = 20 \text{ (N/m)}$ $P_{2,1} = 170, P_{2,2} = 85 \text{ (s)}$
$k_3(t)$	$k_{3,0} = 120 \text{ (N/m)}, k_{3,1} = 72, k_{3,2} = 24 \text{ (N/m)}$ $P_{3,1} = 141.67, P_{3,2} = 94.44 \text{ (s)}$

STOCHASTIC MECHANICAL SYSTEMS & AUTOMATION (SMSA) LABORATORY UNIVERSITY OF PATRAS

PARAMETRIC TIME-DOMAIN METHODS FOR NON-STATIONARY RANDOM VIBRATION IDENTIFICATION 43

System Properties

The Non-stationary Vibration Signal

STFT

STOCHASTIC MECHANICAL SYSTEMS & AUTOMATION (SMSA) LABORATORY UNIVERSITY OF PATRAS

PARAMETRIC TIME-DOMAIN METHODS FOR NON-STATIONARY RANDOM VIBRATION IDENTIFICATION 44

Identified Models

Model Class	Identification Method	Method Characteristics	Identified Model
Unstructured	ST-ARMA	$M = 301; m = 10$; PE estimation	ST-ARMA(6,3)
Parameter Evolution	RML-TARMA	(Levenberg-Marquardt); termination rule $ \hat{\vartheta}_i - \hat{\vartheta}_{i-1} < 10^{-6}$	RML-TARMA(6,3)
Stochastic Parameter Evolution	SP-TARMA*	ELS-like estimation; $\alpha = 10^4$ $\hat{\nu} = 4.988 \times 10^{-8}$	SP-TARMA(6,3) $\kappa = 2$
Deterministic Parameter Evolution	SP-TARMA (smoothed)*	"	"
Deterministic Parameter Evolution	FS-TARMA (2SLS) [†]	$n_i = 20$; QR implementation of OLS	FS-TARMA(6,3) ^[41,2,19]
Deterministic Parameter Evolution	FS-TARMA (2SLS-PE) [†]	"	"
Deterministic Parameter Evolution	FS-TARMA (RELS) [†]	(Levenberg-Marquardt); init. covariance $\alpha = 10^4$	"

* SP-TARMA(6,3) models: $\alpha_i[t] = 2 \cdot \alpha_i[t-1] - \alpha_i[t-2] + w_{\alpha_i}[t], \quad c_i[t] = 2 \cdot c_i[t-1] - c_i[t-2] + w_{c_i}[t]$

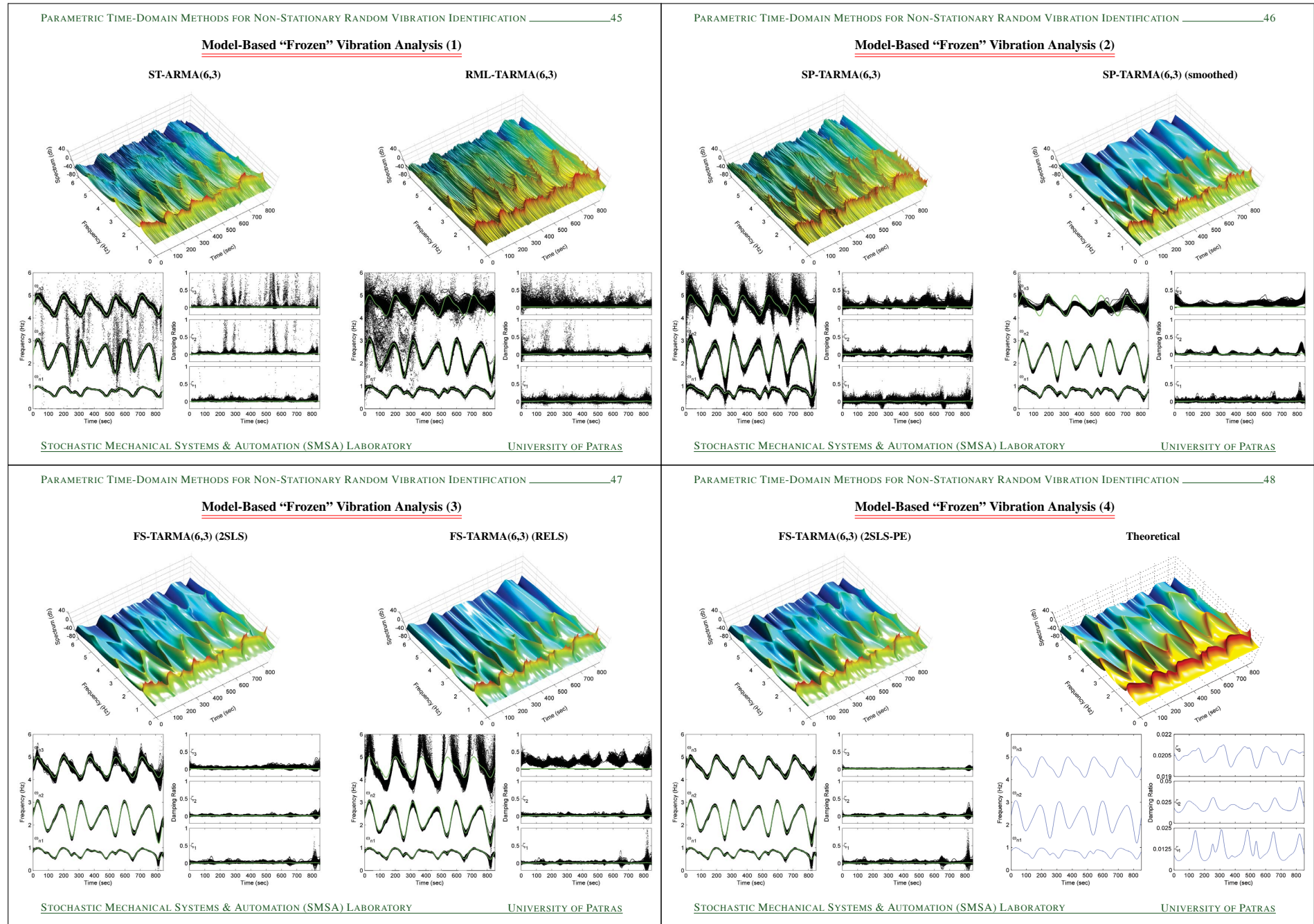
† FS-TARMA(6,3) models: trigonometric functional subspaces

$G_0[t] = 1, \quad G_{2k-1}[t] = \sin\left[\frac{k\pi t}{N-1}\right], \quad G_{2k}[t] = \cos\left[\frac{k\pi t}{N-1}\right], \quad k = 1, 2, \dots$

$b_a = [0, \dots, 34, 36, 38, 42, 44, 46, 48]$
 $b_c = [0, 2]$
 $b_s = [0, 1, 2, 4, 6, 7, 8, 10, 12, 13, 14, 16, 17, 18, 22, \dots, 26]$

STOCHASTIC MECHANICAL SYSTEMS & AUTOMATION (SMSA) LABORATORY UNIVERSITY OF PATRAS

248



PARAMETRIC TIME-DOMAIN METHODS FOR NON-STATIONARY RANDOM VIBRATION IDENTIFICATION _____ 49

8. APPLICATION EXAMPLES

8.a Earthquake Ground Motion Modelling, Analysis and Synthesis

(Fouskitakis and Fassois 2002)

Acceleration (cm/sec²)

Time series index

(a)

Power Spectral Density (STFT)

Frequency (Hz)

Time series index

(b)

AIMS:

- ~ Modelling and synthesis of the 1979 El Centro (California) accelerogram via FS-TAR/TARMA (DPE-TARMA) modelling.
- ~ Critical comparisons with RML-TARMA (UPE-TARMA) modelling.

STOCHASTIC MECHANICAL SYSTEMS & AUTOMATION (SMSA) LABORATORY UNIVERSITY OF PATRAS

PARAMETRIC TIME-DOMAIN METHODS FOR NON-STATIONARY RANDOM VIBRATION IDENTIFICATION _____ 50

Earthquake Ground Motion Signal Modelling

- FS-TARMA modelling: P-A estimation method + non-linear PE (refinement).
- FS-TAR modelling: OLS estimation.
- Recursive TARMA modelling: Recursive Maximum Likelihood estimation.

FS-TARMA structure selection

(a)

(b)

FS-TARMA/RML-TARMA one-step ahead predictions

(c)

(d)

Model

Model	RSS	RSS/SSS(%)	AIC	BIC	SPP [†]
FS-TAR(6) ₈ ^{Haar}	7,958	1.505	2.243	2.319	23
FS-TARMA(2, 4) _[8,8] ^{Haar}	7,698	1.455	2.207	2.286	23
RML-TARMA(4, 1) _{0.966}	11,287	2.134	(2.531)	(2.389)	(224)

FS-TAR

$b_0 = [0, 2, 4, 17, 70, 71, 142, 146]$

FS-TARMA

$b_0 = [0, 2, 4, 17, 70, 71, 142, 146]$

$b_c = [0, 2, 4, 17, 70, 71, 142, 146]$

[†] Samples Per (estimated model) Parameter

STOCHASTIC MECHANICAL SYSTEMS & AUTOMATION (SMSA) LABORATORY UNIVERSITY OF PATRAS

PARAMETRIC TIME-DOMAIN METHODS FOR NON-STATIONARY RANDOM VIBRATION IDENTIFICATION _____ 51

Earthquake Ground Motion Signal Synthesis

- Based upon the estimated FS-TARMA (2,4)_[8,8] / RML-TARMA(4,1) models.

Acceleration (cm/sec²)

Time series index

El Centro

Frequency (Hz)

Time series index

(a)

Acceleration (cm/sec²)

Time series index

TARMA(2,4)₈

Frequency (Hz)

Time series index

(b)

Acceleration (cm/sec²)

Time series index

RARMA(4,1)_{0.966}

Frequency (Hz)

Time series index

(c)

STOCHASTIC MECHANICAL SYSTEMS & AUTOMATION (SMSA) LABORATORY UNIVERSITY OF PATRAS

PARAMETRIC TIME-DOMAIN METHODS FOR NON-STATIONARY RANDOM VIBRATION IDENTIFICATION _____ 52

Model-based Synthesis Assessment

- In terms of critical signal characteristics like the Peak Ground Acceleration (PGA) and the Root Mean Square Acceleration (RMSA):

PGA $\triangleq \max_t |x[t]|$,

•: actual, □: simulated mean

(a)

RMSA $\triangleq \sqrt{\frac{1}{N} \sum_{t=1}^N x^2[t]}$

•: actual, □: simulated mean

(b)

RESULTS:

- ✓ Accurate FS-TAR/TARMA model based *modelling* and *synthesis*.
- ✓ FS-TAR/TARMA models *outperform* their RML-TARMA counterparts in terms of signal *modelling*, *synthesis* and representation *parsimony*.
- ✓ FS-TARMA modelling *outperforms* pure FS-TAR modelling in terms of *accuracy*, *synthesis* and representation *parsimony*.

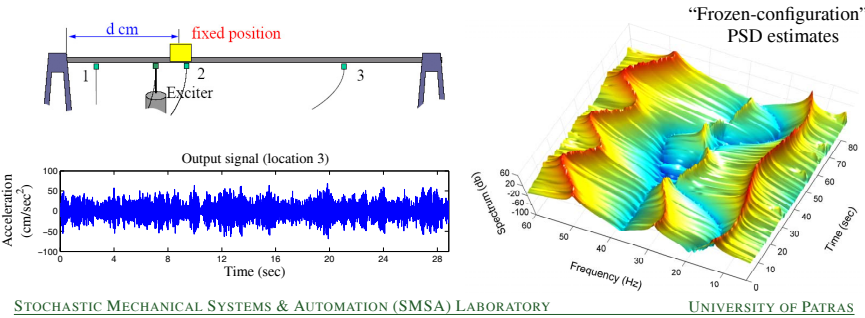
STOCHASTIC MECHANICAL SYSTEMS & AUTOMATION (SMSA) LABORATORY UNIVERSITY OF PATRAS

PARAMETRIC TIME-DOMAIN METHODS FOR NON-STATIONARY RANDOM VIBRATION IDENTIFICATION 57

Baseline modelling: “Frozen-configuration” representation

The underlying **structural dynamics** corresponding to **various mass positions** are identified via exhaustive **stationary experiments** and subsequent analysis.

▷ **Exhaustive ARMA modelling:**

$$\left\{ x_m[t] + \sum_{i=1}^{n_a} a_i[m] \cdot x_m[t-i] = e_m[t] + \sum_{i=1}^{n_c} c_i[m] \cdot e_m[t-i]; \quad e_m[t] \sim \text{NID}(0, \sigma_{e_m}^2); \quad m = 1, \dots, 120 \right\}$$


STOCHASTIC MECHANICAL SYSTEMS & AUTOMATION (SMSA) LABORATORY UNIVERSITY OF PATRAS

PARAMETRIC TIME-DOMAIN METHODS FOR NON-STATIONARY RANDOM VIBRATION IDENTIFICATION 58

Structural Identification & Analysis Results

→ AR/MA orders: TARMA(n, n) models, $n = 2, \dots, 12$

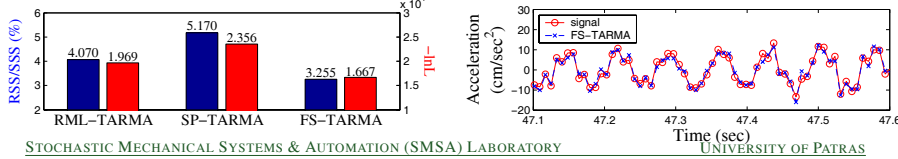
- BIC in the FS-TARMA case and (RSS) in the RML-TARMA and SP-TARMA cases.

Model Class	Identification Method	Method Characteristics	Identified Model
Unstructured	RML-TARMA	$\lambda = 0.9905$	RML-TARMA(8, 8)
Parameter Evolution		$\alpha = 10^4$	
Stochastic	SP-TARMA	$\nu = 2.757 \times 10^{-11}$	SP-TARMA(8, 8) $\kappa = 2$
Parameter Evolution		$\alpha = 10^4$	
Deterministic	FS-TARMA	Gauss-Newton	FS-TARMA(8, 8)[11, 15, 15]
Parameter Evolution			

• **FS-TARMA** model: trigonometric functional subspaces

$$G_0[t] = 1, \quad G_{2k-1}[t] = \sin \left[\frac{k \pi t}{N-1} \right], \quad G_{2k}[t] = \cos \left[\frac{k \pi t}{N-1} \right], \quad k = 1, 2, \dots$$

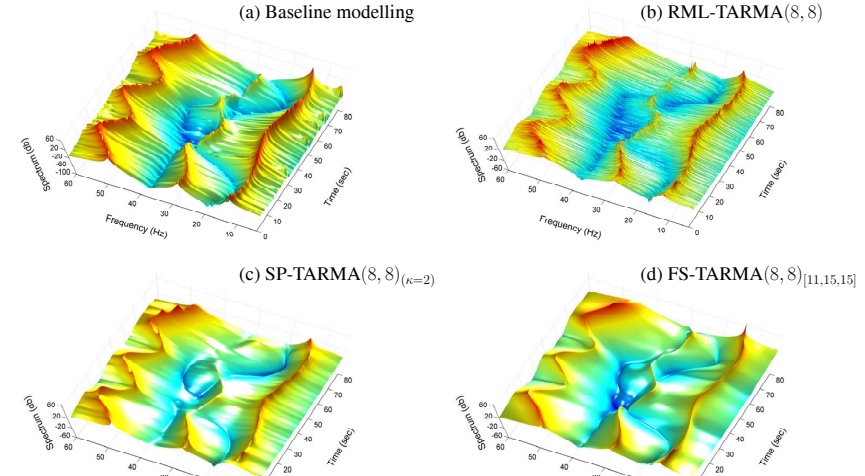
$b_a = [0, \dots, 10]$
 $b_c = [0, \dots, 14]$
 $b_s = [0, \dots, 6, 8, 9, 10, 12, 13, 14, 17, 19]$



STOCHASTIC MECHANICAL SYSTEMS & AUTOMATION (SMSA) LABORATORY UNIVERSITY OF PATRAS

PARAMETRIC TIME-DOMAIN METHODS FOR NON-STATIONARY RANDOM VIBRATION IDENTIFICATION 59

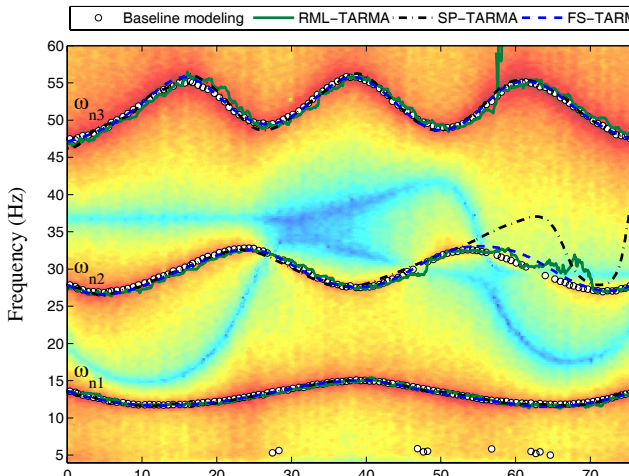
Model-Based Time-Varying Power Spectral Density Estimates



STOCHASTIC MECHANICAL SYSTEMS & AUTOMATION (SMSA) LABORATORY UNIVERSITY OF PATRAS

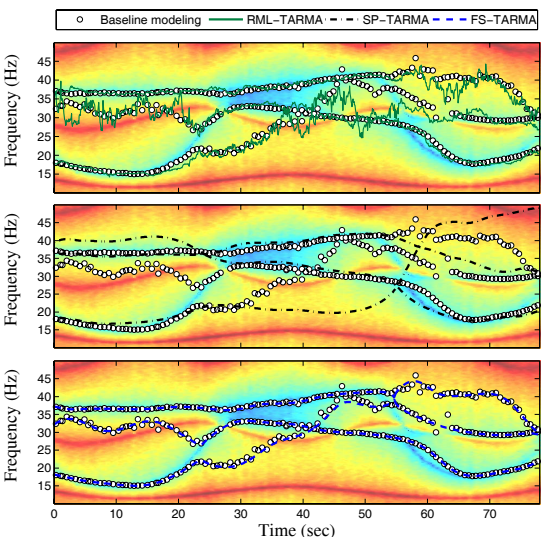
PARAMETRIC TIME-DOMAIN METHODS FOR NON-STATIONARY RANDOM VIBRATION IDENTIFICATION 60

Model-Based Natural Frequency Estimates



STOCHASTIC MECHANICAL SYSTEMS & AUTOMATION (SMSA) LABORATORY UNIVERSITY OF PATRAS

Model-Based Antiresonant Frequency Estimates



9. CONCLUDING REMARKS & OUTLOOK

1. A summary of parametric models and methods for non-stationary random vibration identification were reviewed and classified as:
 - a. Unstructured Parameter Evolution (UPE) (RARMA models)
 - b. Stochastic Parameter Evolution (SPE) (SP-TARMA models)
 - c. Deterministic Parameter Evolution (DPE) (FS-TARMA models)
2. A framework for complete identification (parameter estimation, structure selection, model validation) of TARMA models was presented – AIC/BIC criteria not always effective.
3. A framework for asymptotic analysis of FS-TARMA estimators was presented.
4. The methods' performance characteristics were assessed via Monte Carlo experiments – Representative practical applications were also presented.
5. Issues for future investigation on FS-TARMA model identification include:
 - i. algorithmic instability problem alleviation
 - ii. more flexible & fully automated basis function selection
 - iii. identification with short data records
 - iv. extensions to vector models and alternative estimation criteria

Nonlinear Dynamic Optimization in Control Engineering – Algorithms and Applications

Moritz Diehl,
Optimization in Engineering Center (OPTEC)
K.U. Leuven, Belgium

Benelux Meeting on Systems and Control,
March 15, 2007

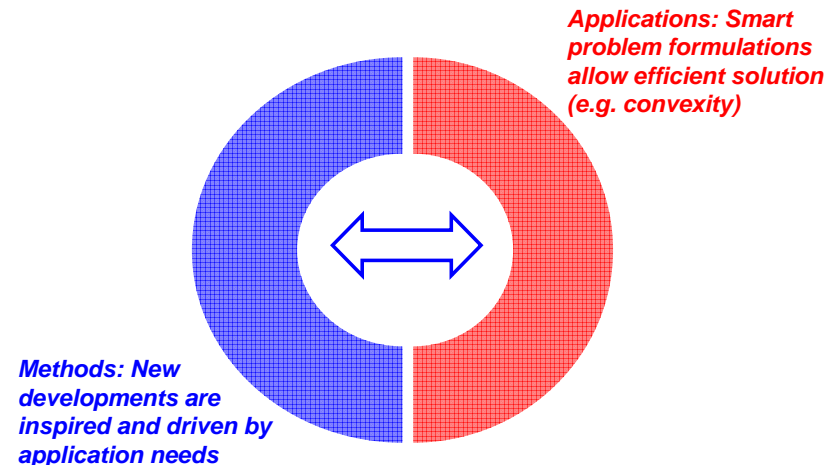
Overview

- What is the Optimization in Engineering Center OPTEC?
- Dynamic Optimization Example: Control of Batch Reactors
- How to Solve Dynamic Optimization Problems?
- Three Challenging Applications:
 - Robust Open-Loop Control of Batch Reactor
 - Periodic and Robust Optimization for „Flying Windmills“
 - Model Predictive Control (MPC) of Kites and Engines

Moritz Diehl



OPTEC Aim: Connect Optimization Methods & Applications



Moritz Diehl



History of Optimization in Engineering Center

Founded as “K.U. Leuven Center of Excellence: Optimization in Engineering”

Five year project with 500.000 Euro per year, from 2005 to 2010

Promoted by four engineering departments:

- Chemical Engineering
- Computer Science
- Electrical Engineering
- Mechanical Engineering

New positions:

- 4-6 PhD
- 2-4 Postdoc
- 1 new professorship (located at ESAT) for „Principal Investigator“

Moritz Diehl



Quarterly and Weekly OPTEC Lecture Series

● **Quarterly „Simon Stevin Lecture on Optimization in Engineering“:**

- Dec. 6: **Larry Biegler**, CMU Pittsburgh (past)
- Mar. XX: **David Mayne**, Imperial, London (tent.)
- July XX: **Steven Wright**, Wisconsin
- Oct 26: **Manfred Morari**, ETH Zurich



Simon Stevin,
1548-1620



● „K.U. Leuven Seminar on Optimization in Engineering“:

- Jan. 31: Mario Milanese (Torino): MPC of semi-active damping
- Feb. 8: Philippe Toint (Namur): large scale optimization methods
- Feb. 22: Peter Kuehl (Heidelberg): Robust optimal feedback control
- March 1: Yurii Nesterov (UCL)/ Florian Jarre (Duesseldorf): new optimization algorithms

Moritz Diehl



Some OPTEC Workshops

- 1st International Workshop on Modelling and Optimization of **Power Generating Kites**, January 30, 2007, Leuven

- one week **Athens-course** „Dynamic Process and System Optimization“ March 19-23, 2007, Leuven

- 13th CFG07 **Optimization Conference**, September 17-21, 2007, Heidelberg

- 2-day **parameter estimation and experimental design** workshop on October 3 & 4, 2007, Leuven

Moritz Diehl



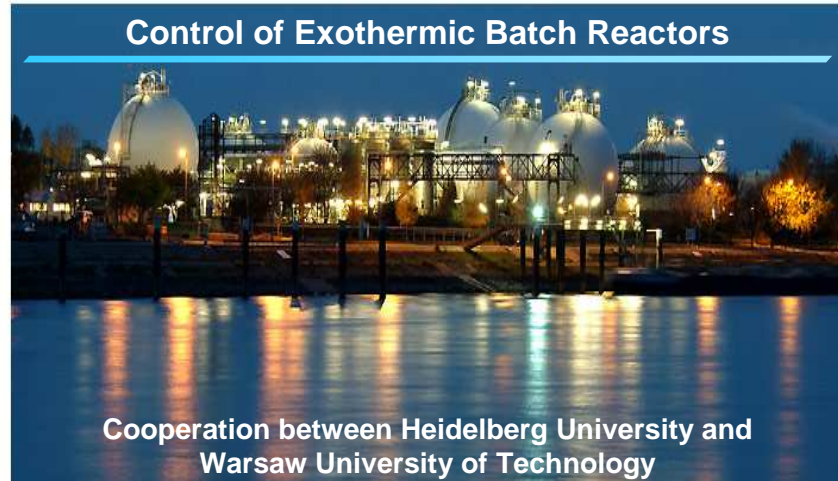
Overview

- What is the Optimization in Engineering Center OPTEC?
- **Dynamic Optimization Example: Control of Batch Reactors**
- How to Solve Dynamic Optimization Problems?
- Three Challenging Applications:
 - Robust Open-Loop Control of Batch Reactor
 - Periodic and Robust Optimization for „Flying Windmills“
 - Model Predictive Control (MPC) of Kites and Engines

Moritz Diehl



Control of Exothermic Batch Reactors



Cooperation between Heidelberg University and Warsaw University of Technology



Work of **Peter Kühl** (Heidelberg)
with A. Milewska, E. Molga (Warsaw)

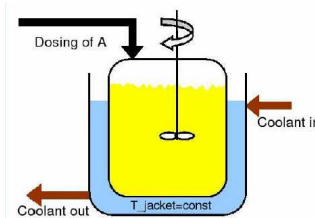


Batch Reactor in Warsaw [Peter Kuehl, Aleksandra Milewska]

Esterification of 2-Butanol (B) by propionic anhydride (A): exothermic reaction, fed-batch reactor with cooling jacket

Aim: complete conversion of B, **avoid explosion!**

Control: dosing rate of A



Moritz Diehl



Differential (Algebraic) Equation Model

$$\begin{aligned} \dot{n}_A &= u - r V \\ \dot{n}_B &= -r V \\ \dot{n}_C &= r V \end{aligned} \quad \begin{aligned} (C_{p,I} + C_p) \dot{T}_R &= r H V - q_{\text{dil}} - U \Omega (T_R - T_J) \\ &\quad -\alpha (T_R - T_a) - u c p_A (T_R - T_d), \end{aligned} \quad (1)$$

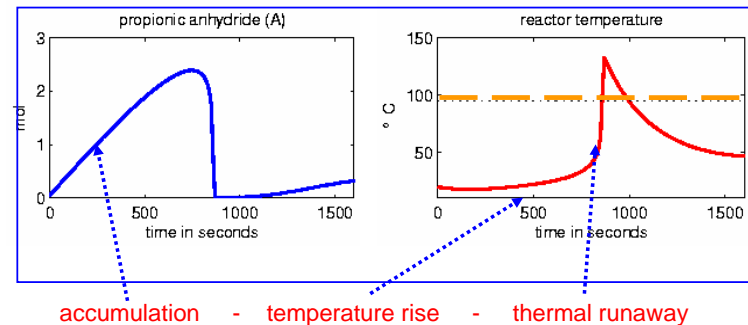


$$\begin{aligned} \rho_i &= 1000 M_i \left(P_i Q_i^{\left(1 - \left(\frac{T_R}{T_{c,i}}\right)^{\alpha}\right)} \right)^{-1}, \quad i = A, B, C, D \\ c_{p,i} &= a_i + b_i T_R + c_i T_R^2 + d_i T_R^3, \quad i = A, B, C, D \\ C_p &= \sum_{i=A,B,C,D} c_{p,i} n_i \\ C_{p,I} &= C_{p,I1} + \frac{C_{p,I2} - C_{p,I1}}{V_2 - V_1} (V - V_1) \\ V &= 1000 \left(\frac{n_A M_A}{\rho_A} + \frac{n_B M_B}{\rho_B} + \frac{n_C M_C}{\rho_C} + \frac{n_D M_D}{\rho_D} \right) \\ \Omega &= \Omega_{\min} + 4 \frac{V - V_{\min}}{1000 d} \end{aligned} \quad (2)$$

Moritz Diehl



Safety Risk: Thermal Runaways



Try to avoid by requiring upper bounds on

- reactor temperature T_R , and hypothetical
- *adiabatic temperature* S that would result if all A reacts with B

Moritz Diehl



Dynamic Optimization Problem for Batch Reactor

Constrained optimal control problem:

$$\begin{aligned} \min_u & \int_0^{t_f} n_B(\tau)^2 d\tau \\ \text{subject to} & \quad (1), (2) \\ & 0 \text{ mol/s} \leq u(t) \leq 0.005 \text{ mol/s} \\ & \int_{t_0=0}^{t_f} u(\tau) d\tau = 6.89396 \text{ mol} \\ & T_R(t) \leq 343.15 \text{ K} \\ & S(t) \leq 363.15 \text{ K}, \\ & S(t) = T_R(t) + \min(n_A, n_B) \frac{H_A}{\rho c_p V} \end{aligned}$$

minimize remaining B
subject to dosing rate and temperature constraints

$$\begin{aligned} \text{Generic optimal control problem:} \\ \min_{x(\cdot), u(\cdot)} & \int_0^T L(x(t), u(t)) dt + E(x(T)) \\ \text{subject to} & \quad x(0) - x_0 = 0, \\ & \dot{x}(t) - f(x(t), u(t)) = 0, \quad t \in [0, T], \\ & h(x(t), u(t)) \geq 0, \quad t \in [0, T], \\ & r(x(T)) \geq 0 \end{aligned}$$

Moritz Diehl



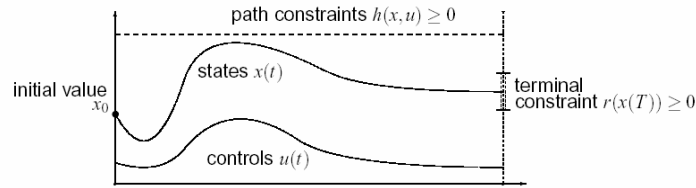
Overview

- What is the Optimization in Engineering Center OPTEC?
- Dynamic Optimization Example: Control of Batch Reactors
- How to Solve Dynamic Optimization Problems?
- Three Challenging Applications:
 - Robust Open-Loop Control of Batch Reactor
 - Periodic and Robust Optimization for „Flying Windmills“
 - Model Predictive Control (MPC) of Kites and Engines

Moritz Diehl



Optimal Control Problem in Simplest Form



$$\underset{x(\cdot), u(\cdot)}{\text{minimize}} \quad \int_0^T L(x(t), u(t)) dt + E(x(T))$$

subject to

$$\begin{aligned} x(0) - x_0 &= 0, & (\text{fixed initial value}) \\ \dot{x}(t) - f(x(t), u(t)) &= 0, & t \in [0, T], & (\text{ODE model}) \\ h(x(t), u(t)) &\geq 0, & t \in [0, T], & (\text{path constraints}) \\ r(x(T)) &\geq 0 & & (\text{terminal constraints}). \end{aligned}$$

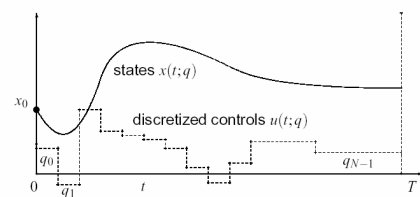
Moritz Diehl



First Approach: Single Shooting

Discretize controls $u(t)$ on fixed grid

$$0 = t_0 < t_1 < \dots < t_N = T,$$

regard states $x(t)$ on $[0, T]$ as dependent variables.Use numerical integration routine to obtain state as function $x(t; q)$ of finitely many control parameters

$$q = (q_0, q_1, \dots, q_{N-1})$$

Moritz Diehl



Nonlinear Program (NLP) in Single Shooting

- After control discretization, obtain NLP:

$$\underset{q}{\text{minimize}} \quad \int_0^T L(x(t; q), u(t; q)) dt + E(x(T; q))$$

subject to

$$\begin{aligned} h(x(t_i; q), u(t_i; q)) &\geq 0, & i = 0, \dots, N, & (\text{discretized path constraints}) \\ r(x(T; q)) &\geq 0. & & (\text{terminal constraints}) \end{aligned}$$

- Solve with NLP solver, e.g. Sequential Quadratic Programming (SQP)

Moritz Diehl



Sequential Quadratic Programming (SQP)

Summarize problem as

$$\min_q F(q) \text{ s.t. } H(q) \geq 0.$$

Solve iteratively, start with guess q^0 for controls. Set $k = 0$.

1. Evaluate $F(q^k), H(q^k)$ and derivatives (ODE solution).
Obtain "Hessian matrix" A^k e.g. by updates.
2. Compute Δq^k that solves **Quadratic Program (QP)**:

$$\min_{\Delta q} \nabla F(q_k)^T \Delta q + \frac{1}{2} \Delta q^T A^k \Delta q \text{ s.t. } H(q^k) + \nabla H(q^k)^T \Delta q \geq 0.$$

3. Perform step

$$q^{k+1} = q^k + \alpha_k \Delta q^k$$

with step length $\alpha_k \in [0, 1]$ determined e.g. by line search. $k = k + 1$.

Moritz Diehl



Toy Problem with One ODE for Illustration

$$\underset{x(\cdot), u(\cdot)}{\text{minimize}} \quad \int_0^3 x(t)^2 + u(t)^2 dt$$

subject to

$$\begin{aligned} x(0) &= x_0, && \text{(initial value)} \\ \dot{x} &= (1+x)x + u, \quad t \in [0, 3], && \text{(ODE model)} \\ \begin{pmatrix} 1-x(t) \\ 1+x(t) \\ 1-u(t) \\ 1+u(t) \end{pmatrix} &\succeq \begin{pmatrix} 0 \\ 0 \\ 0 \\ 0 \end{pmatrix}, && t \in [0, 3], \text{ (bounds)} \\ x(3) &= 0. && \text{(zero terminal constraint).} \end{aligned}$$

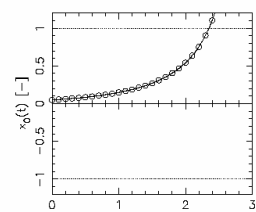
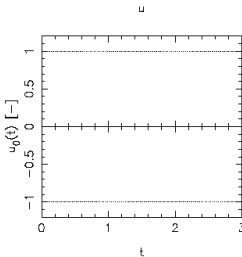
Mildly nonlinear and unstable system.

Moritz Diehl



Single Shooting

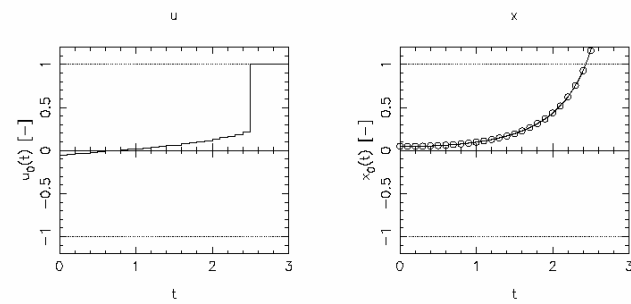
- Choose $N = 30$ equal control intervals.
- Initialize with steady state controls $u(t) \equiv 0$.



Moritz Diehl



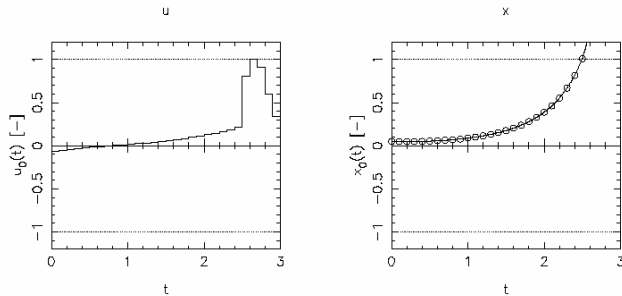
Single Shooting: First Iteration



Moritz Diehl



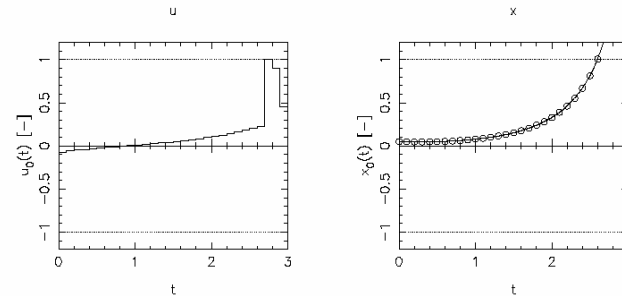
Single Shooting: Second Iteration



Moritz Diehl



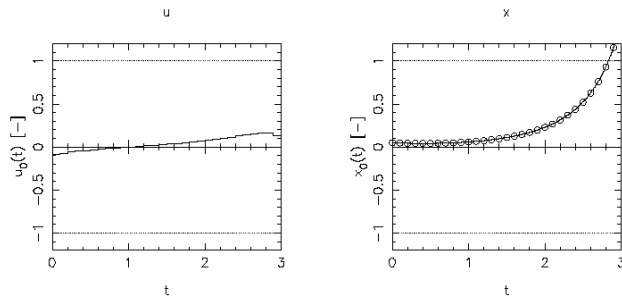
Single Shooting: Third Iteration



Moritz Diehl



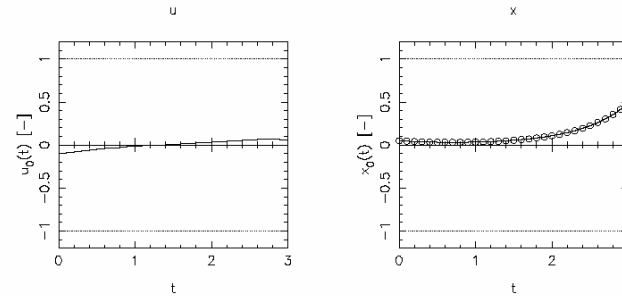
Single Shooting: 4th Iteration



Moritz Diehl



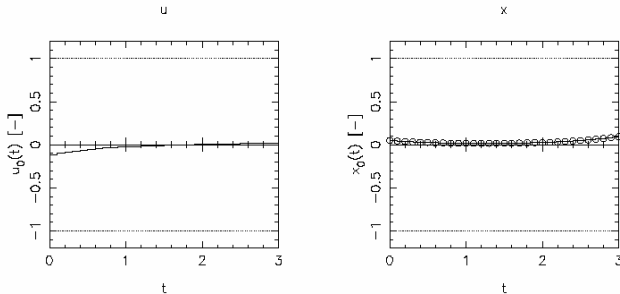
Single Shooting: 5th Iteration



Moritz Diehl



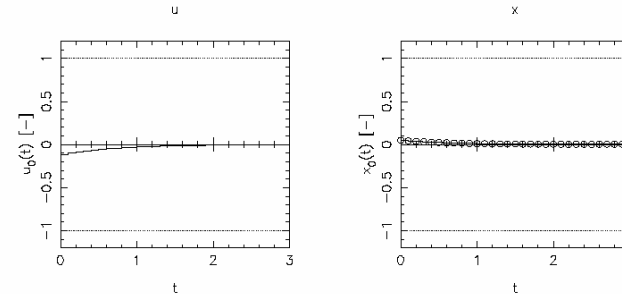
Single Shooting: 6th Iteration



Moritz Diehl



Single Shooting: 7th Iteration (Solution)



Moritz Diehl



260

Single Shooting: Pros and Cons

- + Can use state-of-the-art ODE/DAE solvers.
- + Few degrees of freedom even for large ODE/DAE systems.
- + Active set changes easily treated.
- + Need only initial guess for controls q .
- Cannot use knowledge of x in initialization (e.g. in tracking problems).
- ODE solution $x(t; q)$ can depend very nonlinearly on q .
- Unstable systems difficult to treat.

Moritz Diehl



2nd Approach: Direct Multiple Shooting [Bock, Plitt 1981]

- Discretize controls piecewise on a coarse grid

$$u(t) = q_i \quad \text{for } t \in [t_i, t_{i+1}]$$

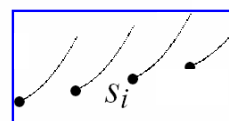
- Solve ODE on each interval $[t_i, t_{i+1}]$ numerically, starting with artificial initial value s_i :

$$\begin{aligned} \dot{x}_i(t; s_i, q_i) &= f(x_i(t; s_i, q_i), q_i), \quad t \in [t_i, t_{i+1}], \\ x_i(t_i; s_i, q_i) &= s_i. \end{aligned}$$

Obtain trajectory pieces $x_i(t; s_i, q_i)$.

- Also compute integrals

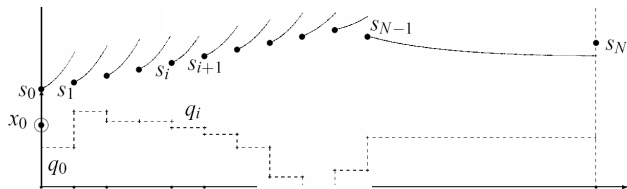
$$l_i(s_i, q_i) := \int_{t_i}^{t_{i+1}} L(x_i(t; s_i, q_i), q_i) dt$$



Moritz Diehl



Nonlinear Program in Multiple Shooting



$$\begin{aligned}
 & \underset{s, q}{\text{minimize}} && \sum_{i=0}^{N-1} l_i(s_i, q_i) + E(s_N) \\
 & \text{subject to} && \\
 & s_0 - x_0 = 0, && \text{(initial value)} \\
 & s_{i+1} - x_i(t_{i+1}; s_i, q_i) = 0, && \text{(continuity)} \\
 & h(s_i, q_i) \geq 0, && \text{(discretized path constraints)} \\
 & r(s_N) \geq 0. && \text{(terminal constraints)}
 \end{aligned}$$

SQP for Multiple Shooting

Summarize NLP:

$$\min_w F(w) \text{ s.t. } \begin{cases} G(w) = 0, \\ H(w) \geq 0. \end{cases}$$

- Summarize all variables as $w := (s_0, q_0, s_1, q_1, \dots, s_N)$.
- In each iteration, solve Quadratic Program:

$$\min_{\Delta w} \nabla F(w^k)^T \Delta w + \frac{1}{2} \Delta w^T A^k \Delta w \text{ s.t. } \begin{cases} G(w^k) + \nabla G(w^k)^T \Delta w = 0 \\ H(w^k) + \nabla H(w^k)^T \Delta w \geq 0. \end{cases}$$

- Jacobians $\nabla G(w^k)^T$, $\nabla H(w^k)^T$ and Hessian A^k are block sparse.

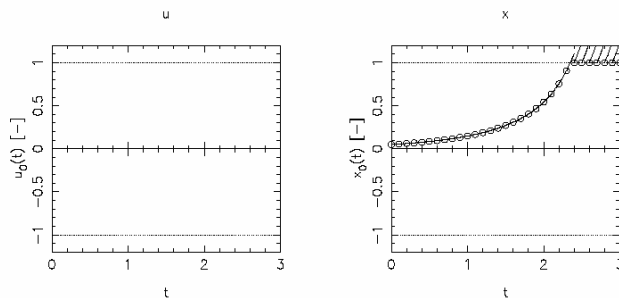
Moritz Diehl



Moritz Diehl



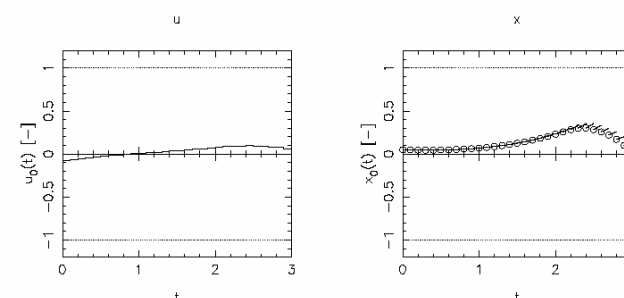
Toy Example: Multiple Shooting Initialization



Moritz Diehl



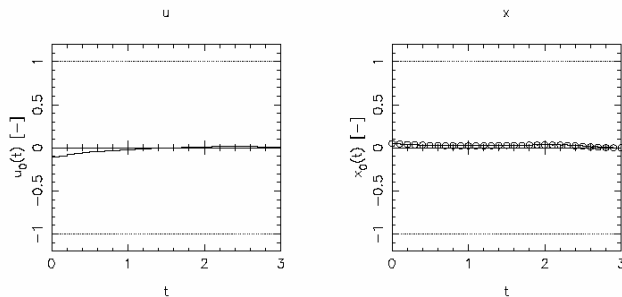
Multiple Shooting: First Iteration



Moritz Diehl



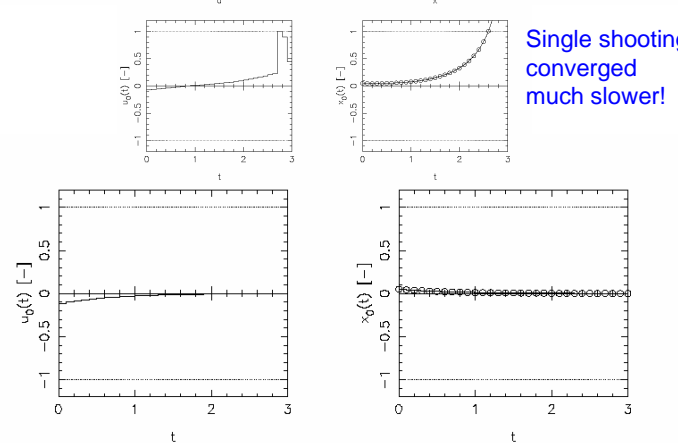
Multiple Shooting: Second Iteration



Moritz Diehl



Multiple Shooting: 3rd Iteration (already solution!)



Moritz Diehl



Multiple Shooting: Pros and Cons

- + can use knowledge of x in initialization
- + can treat unstable systems well.
- + robust handling of path and terminal constraints.
- + easy to parallelize.

*Optimal control package **MUSCOD-II** (C/C++/Fortran) for large ODE/DAE models continuously developed in Heidelberg and Leuven
 (Leineweber, Schäfer, Diehl, Sager, Albersmeyer, Potschka, ..., 1999 -)*

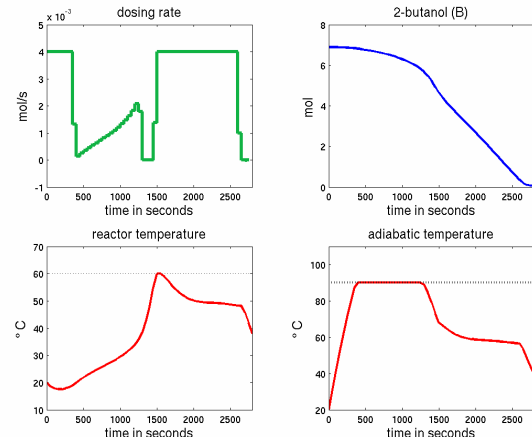
Moritz Diehl



The MUSCOD Developer Team in Heidelberg



Solution of Peter's Batch Reactor Problem



Moritz Diehl



Experimental Results for Batch Reactor

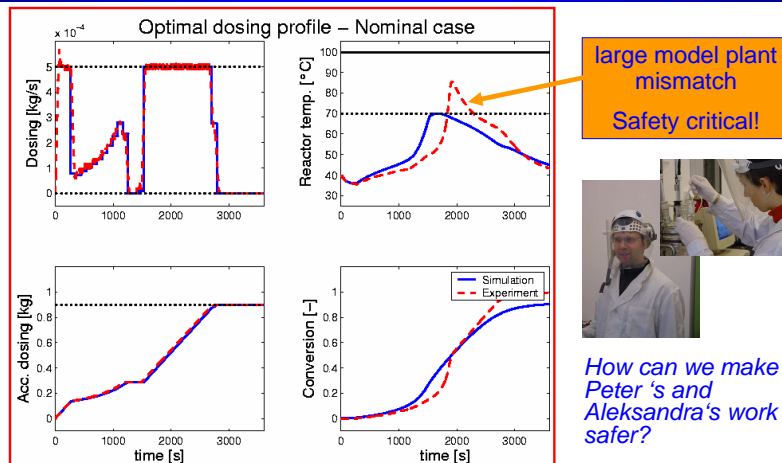


- Mettler-Toledo test reactor R1
- batch time: 1 h
- end volume: ca. 2 l

Moritz Diehl



Experimental Results for Batch Reactor (Red)



Moritz Diehl



Overview

- What is the Optimization in Engineering Center OPTEC?
- Dynamic Optimization Example: Control of Batch Reactors
- How to Solve Dynamic Optimization Problems?
- Three Challenging Applications:
 - Robust Open-Loop Control of Batch Reactor
 - Periodic and Robust Optimization for „Flying Windmills“
 - Model Predictive Control (MPC) of Kites and Engines

Moritz Diehl



Robust Worst Case Formulation

$$\begin{array}{ll} \min_{u \in \mathcal{U}} & J[x(u, p), u] \\ \text{s.t.} & h_i(x, u, p) \leq 0, \quad i = 1 \dots n, \\ & \tilde{h}(x, u, p) \leq 0, \end{array}$$

Make sure safety critical constraints are satisfied for **all possible** parameters p !



$$\begin{array}{ll} \min_{u \in \mathcal{U}} & J[x(u, \bar{p}), u] \\ \text{s.t.} & \max_{\|p - \bar{p}\|_{2, \Sigma^{-1}} \leq \gamma_i} h_i(x, u, p) \leq 0, \quad i = 1 \dots n, \\ & \tilde{h}(x, u, \bar{p}) \leq 0. \end{array}$$



Semi-infinite optimization problem, difficult to tackle...

Moritz Diehl



Approximate Robust Formulation [Körkel, D., Bock, Kostina 04, 05]

Fortunately, it is easy to show that up to first order:

$$\max_{\|p - \bar{p}\|_{2, \Sigma^{-1}} \leq \gamma_i} h_i(x, u, p) \approx h_i(x, u, \bar{p}) + \gamma_i \left\| \frac{d}{dp} h_i(x, u, \bar{p}) \right\|_{2, \Sigma}$$

So we can approximate robust problem by:

$$\begin{array}{ll} \min_{u \in \mathcal{U}} & J[x(u, \bar{p}), u] \\ \text{s.t.} & h_i(x, u, \bar{p}) + \gamma_i \left\| \frac{d}{dp} h_i(x, u, \bar{p}) \right\|_{2, \Sigma} \leq 0, \quad i = 1, \dots, n_r, \\ & \tilde{h}(x, u, \bar{p}) \leq 0. \end{array}$$

Intelligent safety margins (influenced by controls)

Moritz Diehl



Numerical Issues for Robust Approach

- for optimization, need further derivatives of $\frac{d}{dp} h_i(x, u, \bar{p})$
- treat second order derivatives by internal numerical differentiation in ODE/DAE solver
- implemented in MUSCOD-II Robust -Framework [C. Kirches]
- use homotopy: start with nominal solution, increase γ_i slowly, employ warm starts

Moritz Diehl



Estimated Parameter Uncertainties for Test Reactor

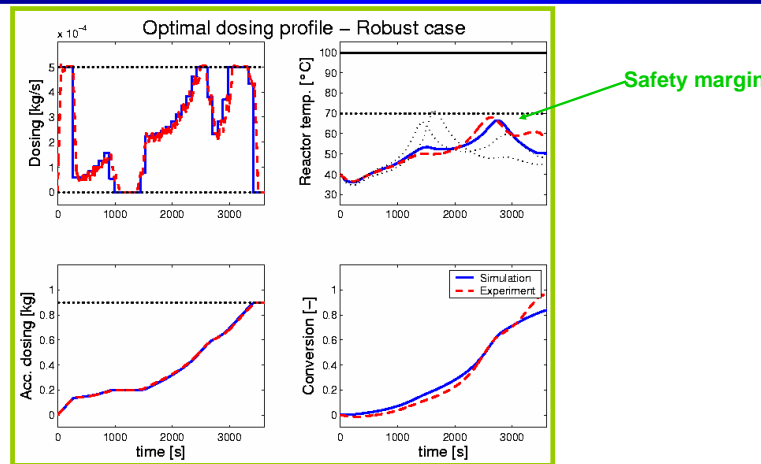
	Standard deviation	gamma
T_{jacket}	0.3 K	3.0
m_{catalyst}	0.5 g (~10 %)	3.0
U_A	10.0 W/(m ² K) (~10 %)	2.0
u_{offset}	$5.0 \cdot 10^{-5}$ kg/s (~10 % of upper bound)	3.0



Moritz Diehl



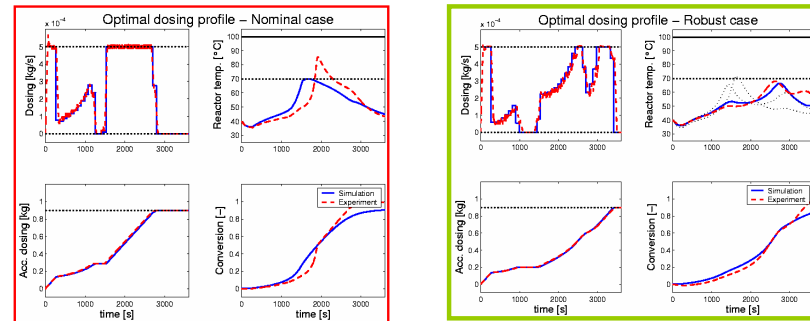
Robust Optimization Result and Experimental Test



Moritz Diehl



Comparison Nominal and Robust Optimization



Different solution structure. Model plant mismatch and runaway risk considerably reduced. Complete conversion.

Moritz Diehl



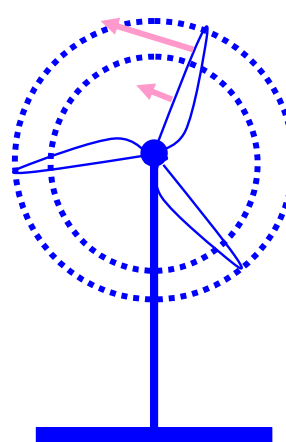
Overview

- What is the Optimization in Engineering Center OPTEC?
- Dynamic Optimization Example: Control of Batch Reactors
- How to Solve Dynamic Optimization Problems?
- Three Challenging Applications:
 - Robust Open-Loop Control of Batch Reactor
 - Periodic and Robust Optimization for „Flying Windmills“
 - Model Predictive Control (MPC) of Kites and Engines

Moritz Diehl



Conventional Wind Turbines

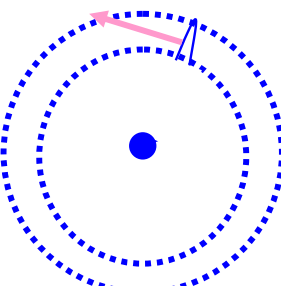


- Due to high speed, wing tips are **most efficient** part of wing
- High torques at wings and mast limit size and height of wind turbines
- But best winds are in high altitudes!

Moritz Diehl



Conventional Wind Turbines



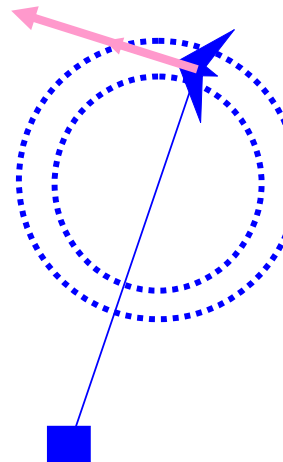
- Due to high speed, wing tips are **most efficient** part of wing
- High torques at wings and mast limit size and height of wind turbines
- But best winds are in high altitudes!

Could we construct a wind turbine with only **wing tips and generator**?

Moritz Diehl



Crosswind Kite Power (Loyd 1980)



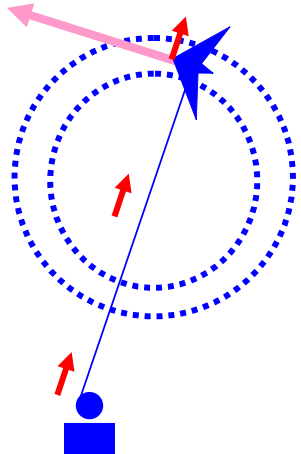
- use **kite with high lift-to-drag-ratio**
- use **strong line**, but no mast and basement
- **automatic control** keeps kites looping

But where could a **generator** be driven?

Moritz Diehl



New Power Generating Cycle



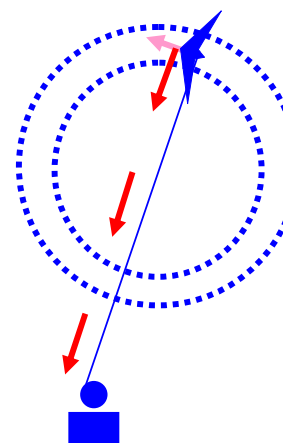
New cycle consists of two phases:

- **Power generation phase:**
 - add **slow downwind motion** by prolonging line (1/3 of wind speed)
 - **generator at ground** produces power due to large pulling force

Moritz Diehl



New Power Generating Cycle



New cycle consists of two phases:

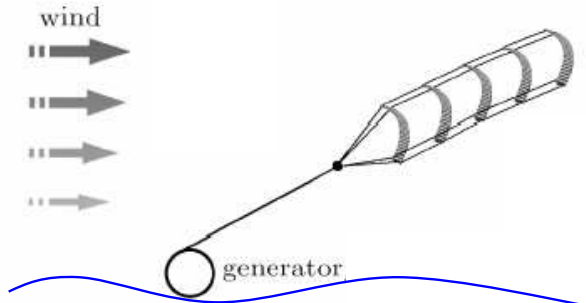
- **Power generation phase:**
 - add **slow downwind motion** by prolonging line (1/3 of wind speed)
 - **generator at ground** produces power due to large pulling force
- **Retraction phase:**
 - change kite's angle of attack to **reduce pulling force**
 - pull back line

Cycle produces same average power as wind turbine of same wing size, but much larger units possible
(independently patented by Ockels, Ippolito/Milanese, D.)

Moritz Diehl



Can stack kites, can use on sea

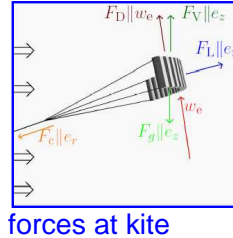


Moritz Diehl



Periodic Optimal Control (with Boris Houska)

Have to regard also cable elasticity



forces at kite

ODE Model with 12 states and 3 controls

- Differential states: $x := (r_0, r, \phi, \theta, \dot{r}_0, \dot{r}, \dot{\phi}, \dot{\theta}, n, \Psi, C_L, W)^T$
- Controls: $u := (\ddot{r}_0, \dot{\Psi}, \dot{C}_L)^T$

Control inputs:

- line length
- roll angle (as for toy kites)
- lift coefficient (pitch angle)

Moritz Diehl



Some Kite Parameters

Name	Symbol	Value
mass of the kite	m_k	850 kg
area	A	500 m ² (circled)
volume	V	720 m ³
pure drag	$c_{D,0}$	0.04
reference wind	w_0	10 m/s (circled)
gravit. const.	g	9.81 m/s ²
air density	ρ	1.23 kg/m ³
cable density	ρ_c	1450 kg/m ³
cable friction	$c_{D,C}$	1.0
internal friction	b_0	10 ⁵ kg/sm ²
elastic modulus	E	1.5 * 10 ¹¹ Pa

e.g. 10 m x 50 m,
like Boeing wing,
but much lighter
material

standard wind velocity
for nominal power of
wind turbines

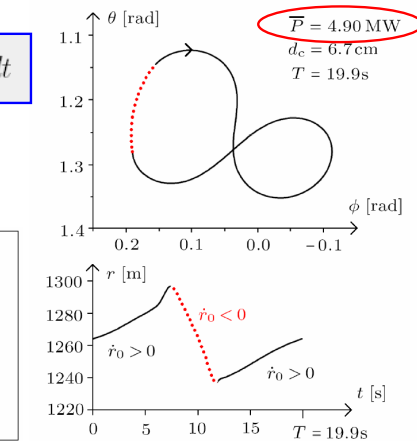
Solution of Periodic Optimization Problem

Maximize mean power production:

$$\bar{P} := \frac{1}{T} W(T) := \frac{1}{T} \int_0^T F_c \dot{r}_0 dt$$

by varying line thickness, period duration, controls, subject to periodicity and other constraints:

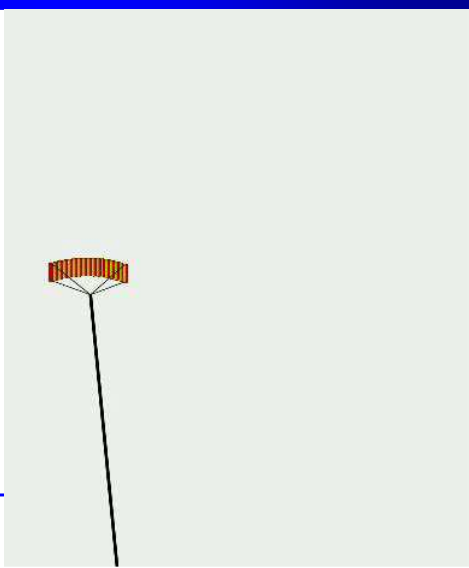
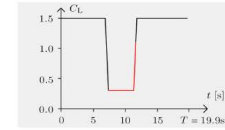
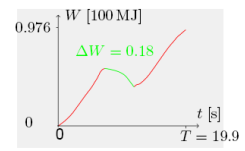
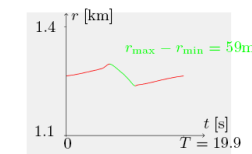
$$\begin{aligned} & \text{maximize}_{x(\cdot), u(\cdot), d_c, T} \bar{P}(x(T), T) \\ & \text{subject to:} \\ & \forall t \in [0, T]: \dot{x}(t) = f(x(t), u(t), d_c) \\ & \forall t \in [0, T]: 0 \geq \eta(x(t), u(t), d_c) \\ & 0 = \chi(x(0), x(T)) \end{aligned}$$



Moritz Diehl



Visualization of Periodic Solution

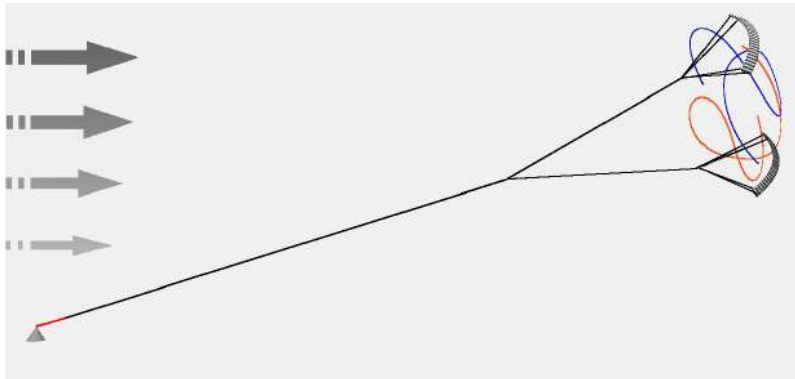


Prototype built by Partners in Torino and Delft



268

What about 'dancing' kites ?

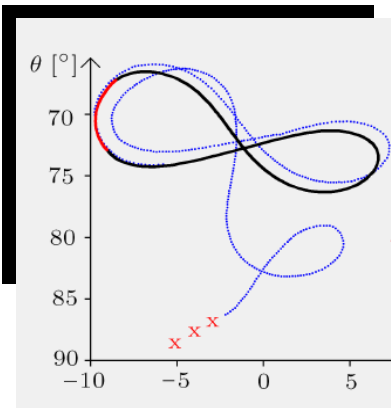


Moritz Diehl

Optimization with 'dancing' kites: 14 MW possible



Question: could kite also fly without feedback?



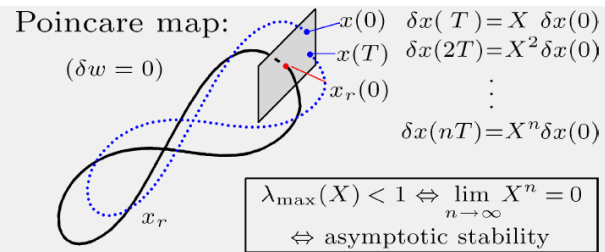
Stability just by smart choice of open-loop controls?

Moritz Diehl



Linearization of Poincare Map determines stability

„Monodromy matrix“ = linearization of Poincare Map.



Stability \Leftrightarrow Spectral radius smaller than one.

Cons of Spectral radius:

- Nonsmooth criterion difficult for optimization
- uncertainty of parameters not taken into account

Moritz Diehl



Periodic Lyapunov Equations

THEOREM [Houska and D., 2007]:
Nonlinear system

$$\dot{x}(t) = f(x(t), u(t), \delta w(t))$$

stable against perturbations if and only if

\Leftrightarrow periodic Lyapunov Equation

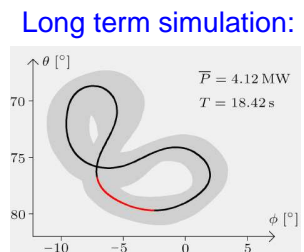
$$\begin{aligned} \dot{P}(t) &= A(t)P(t) + P(t)A(t)^T + B(t)B(t)^T \\ P(0) &= P(T) \end{aligned}$$

with $A = \frac{\partial f}{\partial x}$ has finite solution.
 $B = \frac{\partial f}{\partial w}$

Moritz Diehl



Orbit optimized for stability (using periodic Lyapunov eq.)



Open-loop stability only possibly due to nonlinearity!

Moritz Diehl



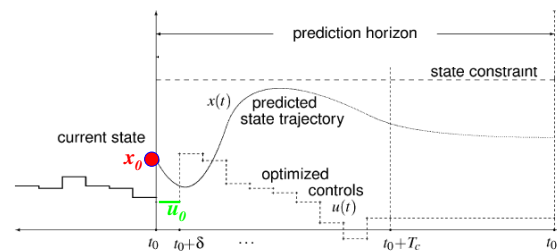
Overview

- What is the Optimization in Engineering Center OPTEC?
- Dynamic Optimization Example: Control of Batch Reactors
- How to Solve Dynamic Optimization Problems?
- Three Challenging Applications:
 - Robust Open-Loop Control of Batch Reactor
 - Periodic and Robust Optimization for „Flying Windmills“
 - Model Predictive Control (MPC) of Kites and Engines

Moritz Diehl



Principle of Model Predictive Control (MPC)



- Estimate current system state x_0 (and parameters) from measurements.
- Solve *in real-time* an optimal control problem:

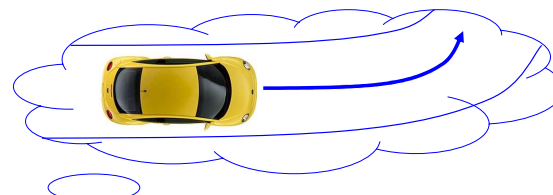
$$\min_{x,z,u} \int_{t_0}^{t_0+T_p} \bar{L}(x,z,u) dt + E(x(t_0+T_p)) \text{ s.t. } \begin{cases} x(t_0) - x_0 = 0, \\ \dot{x} - f(x,z,u) = 0, t \in [t_0, t_0+T_p] \\ g(x,z,u) = 0, t \in [t_0, t_0+T_p] \\ h(x,z,u) \geq 0, t \in [t_0, t_0+T_p] \\ r(x(t_0+T_p)) \geq 0. \end{cases}$$

- Implement first control u_0 for time δ at real plant. Set $t_0 = t_0 + \delta$ and go to 1.

270

Model Predictive Control When We Drive a Car

Always look a bit into the future!

Brain predicts and optimizes:
e.g. slow down **before** curve**Main challenge for MPC:** fast and reliable real-time optimization!

Moritz Diehl



Nonlinear MPC Computation from 1998 to 2006

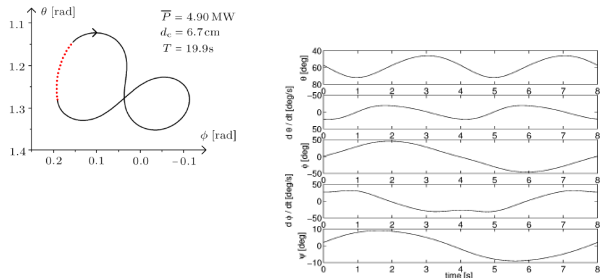


- 1998: 5th order distillation model allows sampling times of only 5 minutes [Allgower, Findeisen, 1998]
- 2001: 206th order distillation model, sampling times of 20 seconds [D. et al., '01]
- 2006: 5th order engine model, sampling times of 10-20 milliseconds [Ferreau et al. '06]
- 5*60*1000 / 20 = 15 000 times faster, due to Moore's law + Algorithm Development**

Moritz Diehl

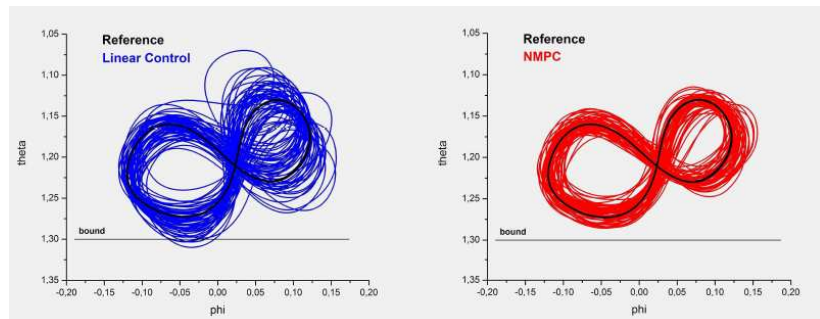


Kite MPC Setup [Diploma A. Ilzhofer]



- optimize quadratic deviation from “lying eight”
- choose one second sampling time
- use new real-time algorithms

Kite MPC: Comparison with LTV Control



Moritz Diehl



271

Kite: Control after turn of wind direction



EU Project PREDIMOT - Predictive Motor Control



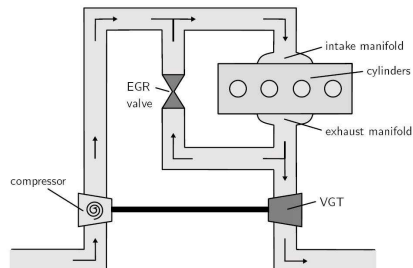
North East South West
INTERREG IIIC

PROJECT PART-FINANCED
BY THE EUROPEAN UNION

Moritz Diehl



Diesel Engine Airpath Control in Linz, Austria

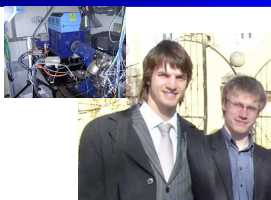


- **Control objective:** Track Mass Air Flow (**MAF**) and intake Manifold Pressure (**MAP**)
- **Controls:** Exhaust Gas Recirculation (**EGR**) and Variable Geometry of Turbocharger (**VGT**)
- Challenge for MPC: solve every **50 ms** a complex quadratic program on slow dSPACE processor

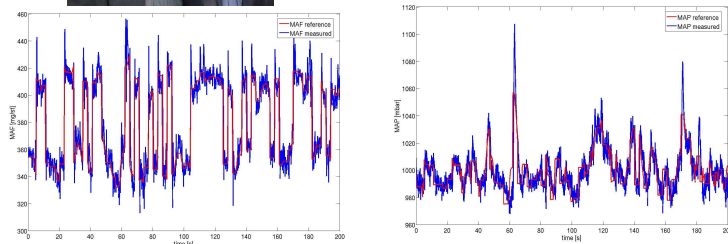
Moritz Diehl



Real-World Experiments [P. Ortner, J. Ferreau, 2007]



- Model Identification based on Data Series
- State Estimation with Kalman Filter
- MPC Setup: predict 5 intervals of 50 ms
- Use novel **Online Active Set Strategy**
- Implement control system on dSPACE

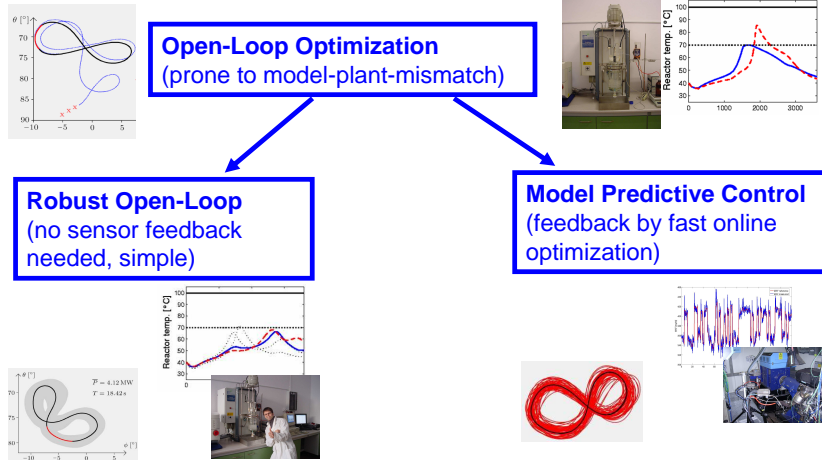


MPC aggressive but effective. Computation fast enough!

Moritz Diehl



Summary: Nonlinear Dynamic Optimization



Moritz Diehl



Two events of interest this year

- Workshop on NMPC Software and Applications (NMPC-SOFAP), Loughborough, United Kingdom, April 19-20, 2007.
(inv. speakers: Biegler, Findeisen, Kerrigan, Richalet, Schei)
- 13th Czech-French-German Conference on Optimization (CFG07), Heidelberg, Germany, September 17-21, 2007.
(inv. speakers: Fletcher, Scherer, Trelat, Waechter,...) Traditionally strong in optimal control.

Moritz Diehl



For weekly information,
join the OPTEC Mailing List:
1) google „Listserv OPTEC“
2) subscribe as indicated

(New OPTEC Website at www.esat.kuleuven.be/~optec under construction)

Moritz Diehl



Thank you very much for your attention!

Moritz Diehl



Part 4

List of Participants

Part 5

Organizational Comments

Welcome

The Organizing Committee has the pleasure of welcoming you to the *26th Benelux Meeting on Systems and Control*, at “CenterParcs De Vossemere” in Lommel, Belgium.

Aim

The aim of the Benelux Meeting is to promote research activities and to enhance cooperation between researchers in Systems and Control. This is the twenty-sixth in a series of annual conferences that are held alternately in Belgium and The Netherlands.

Overview of the Scientific Program

1. Plenary lectures by invited speakers

- *Graham C. Goodwin* (University of Newcastle, Australia)
 - **Sampling in Signal Processing**
 - **Quantization in Signal Processing and Control**
 - **Sampling and Quantization in Modelling and System Identification**
- *Spiliotis D. Fassois* (University of Patras, Greece)
 - **Parametric Time Domain Methods for Non-Stationary Random Vibration Identification: An Overview of Methods and Applications**
- *Moritz Diehl* (Katholieke Universiteit Leuven, Belgium)
 - **Nonlinear Dynamic Optimization in Control Engineering – Algorithms and Applications**

2. Contributed short lectures, see the list of sessions for the titles and authors of these lectures.

Directions for speakers

For a contributed lecture the available time is 25 minutes. Please leave a few minutes of this period for discussion and room changes and adhere to the indicated schedule. In each room overhead projectors and beamers will be available. Be careful with this equipment, because the beamers are supplied by some of the participating groups. When using a beamer, you have to provide a notebook yourself and you have to start your lecture with the notebook up and running and the external video port switched on.

Organization

The Organizing Committee of the Benelux Meeting consists of

D. Aeyels (Univ. of Ghent), G. Bastin (Univ. catholique de Louvain), O.H. Bosgra (Delft Univ. of Technology), R.F. Curtain (Univ. of Groningen), B. de Jager (Eindhoven Univ. of Technology), B. Demeulenaere (K.U.Leuven), B.L.R. De Moor (K.U.Leuven), M. Gevers (Univ. catholique de Louvain), P. Guillaume (VUB), H. Nijmeijer (Eindhoven Univ. of Technology), R. Pintelon (VUB), J. Schoukens (VUB), J.M. Schumacher (Tilburg Univ.), I. Smets (K.U.Leuven), M. Steinbuch (Eindhoven Univ. of Technology), J. Swevers (K.U.Leuven), P.M.J. Van den Hof (Delft Univ. of Technology), A.J. van der Schaft (Univ. of Twente), J. Van Impe (K.U.Leuven), G. van Straten (Wageningen Univ.), S. Weiland (Eindhoven Univ. of Technology), H. Zwart (Univ. of Twente).

This meeting has been organized by:

Jan De Caigny (K.U.Leuven, Div. PMA), Bram Demeulenaere (K.U.Leuven, Div. PMA), Béatrice De Geest (K.U.Leuven, Dept of Chemical Engineering) Bart De Moor (K.U.Leuven, ESAT-SISTA), Patrick Guillaume (VUB, Dept. MECH), Bart Motmans (K.U.Leuven, ESAT-SISTA), Lieve Notre (K.U.Leuven, Div. PMA), Ilse Pardon (K.U.Leuven, ESAT-SISTA), Ann Pintelon (VUB, Dept. ELEC), Rik Pintelon (VUB, Dept. ELEC), Goele Pipeleers (K.U.Leuven, Div. PMA), Johan Schoukens (VUB, Dept. ELEC), Ilse Smets (K.U.Leuven, Dept of Chemical Engineering), Jan Swevers (K.U.Leuven, Div. PMA), Bert Stallaert (K.U.Leuven, Div. PMA), Ida Tassens (K.U.Leuven, ESAT-SISTA), Jan Van Impe (K.U.Leuven, Dept of Chemical Engineering)

The meeting is sponsored by ICCoS (Identification and Control of Complex Systems), a Scientific Research Network of the Research Foundation - Flanders (FWO-Vlaanderen) and supported by the Belgian Programme on Interuniversity Poles of Attraction DYSCO (Dynamic Systems, Control and Optimization), initiated by the Belgian State, Prime Minister's Office for Science.

Facilities

The facilities at the center include restaurants, bars, and recreation and sports facilities. We refer to the reception desk of the

center for detailed information about the use of these facilities. Breakfast will be served in the "Market Grill Restaurant", from 7:00 until 9:30 (only for the people that registered with accommodation). Lunches take place in the "Market Grill Restaurant", from 12:30 until 14:00. The dinner on Tuesday takes place in the "Hammonds Restaurant", from 19:00 until 21:00. The dinner on Wednesday takes place in the "Savanna Restaurant", from 19:00 until 21:00.

Best junior presentation award

Continuing a tradition begun in 1996, junior speakers at the Benelux Meeting will contend for the Best Junior Presentation Award. As the name indicates, the prize honors the best presentation at the Benelux Meeting by a junior speaker, *i.e.*, a researcher working towards a PhD degree. The award is given specifically for presentation technique rather than for content, so in principle it would be possible that the winner gave a beautiful presentation of irrelevant, trivial or even incorrect results. This is of course not to say that content is not important; however, the BJP Award is intended to help remedy a lack of attention for presentation technique that has been sometimes perceived.

The awarding of the prize proceeds as follows. The chairs of sessions in which a junior speaker gives a presentation will be asked to find three volunteers in the audience who are willing to fill out an evaluation form. After the session, the completed forms will be collected by the Prize Commissioners who will then compute a ranking. The winner will be announced immediately after the final lectures of the meeting. The prize consists of a trophy that is made available by DISC and that is to be kept by the winner for one year (until the next Benelux Meeting). The winner will also get an award certificate. This year's Prize Commissioners are: Ilse Smets and Jan Van Impe (Katholieke Universiteit Leuven) and Ton van den Boom (Delft University of Technology).

Some detailed information concerning the prize competition is provided below or the session chairs, for the volunteers in the audience who will complete the evaluation forms, and for the prize candidates.

For the session chairs

You will receive a set of envelopes corresponding to each of the junior researchers who are giving a presentation during your session, as well as a spare envelope. Each envelope contains a set of evaluation forms. Please find three volunteers in the audience (preferably not belonging to the research group that the speaker comes from) who are willing to complete a form. After the talk please collect the forms, check that they are indeed completed, and put them back into the envelope. Please hand all envelopes to one of the Prize Commissioners.

For the jurors

The effect of the BJP Award depends on the efforts of those who volunteer as jurors; so your assistance is most appreciated. Please tick one box in each line; take the leftmost box if you agree with the statement on the left, the rightmost box if the statement on the right seems adequate, or choose a box in between to indicate an intermediate position. An attempt has been made to order the questions in such a way that you may already begin putting marks during the talk. The twelve categories appearing in the form are to be interpreted as follows.

Question 1 asks whether the speaker clearly sets out what the talk is about and why the subject is of interest. Question 2 is about the speaker's use of English. Although full grammatical correctness is not an absolute requisite for effective communication, errors such as misuse of words and wrong pronunciation can be distracting and, therefore, should be counted negatively. Questions 3 and 4 deal with the speaker's ability to make effective use of facilities; question 3 is about the 'human' facilities (voice, facial expression, gestures), question 4 about the technical equipment (transparencies, overhead projector, beamer). Question 5 asks whether the speaker is able to make contact with the audience. Handling a question properly doesn't necessarily imply a long answer, but rather refers to an appropriate action by the speaker.

Questions 6 to 8 deal with several aspects of *clarity*. The main points of the talks should not only be announced as such, but the audience should also be given sufficient time to take these points in (question 6). Talks usually have a hierarchical structure in which main goals lead to subgoals; question 7 asks whether this structure was clear. If several transparencies made you wonder about the purpose of what was written there, then you'll have to tick one of the boxes at the left end on line 7. The speaker should take into account that the attention span of the audience is limited and that some listeners may have lost the thread of the reasoning; at least every ten minutes there should be a moment where everyone is enabled to catch up, even when not all details of what was said before were understood. This is the subject of question 8.

Question 9 asks whether the speaker made a confident impression and appeared to give the talk as planned. A speaker who puts on a slide and then pulls it away after two seconds saying "oh well, this is not too important anyway" will get bad marks here. In question 10 there should be low marks both when the audience was overestimated and when it was underestimated by the speaker. Since the forms will be returned to the speaker, it will be useful if you underline 'too high' or 'too low' if and when appropriate.

Finally, questions 11 and 12 deal with the way that the talk is concluded. The speaker should clearly summarize what was achieved in the work described in the talk, and relate this to the goals stated at the beginning of the presentation (question 11). The talk should be timed in such a way that it can be completed without an increase of pace at the end, and with a few minutes left for discussion. Running out of time, but also finishing very early, are signs of inadequate time planning and should result in low marks for question 12.

If you have any specific hints or suggestions for the speaker,

please write these on the back side of the evaluation form. As already noted, the forms will be returned to the speakers, and they will be grateful for any help you can provide in improving their presentations.

For the contestants

So, here's your chance to boost your career and to amaze your family, friends and colleagues with the shiny BJP Award that makes Oscar and Emmy look pale in comparison. All you have to do is to give a brilliant talk at the Benelux Meeting, ... But seriously, a few comments are in order. First of all, what counts in the first place is the scientific quality of the work that you are doing, and this is *not* what the BJP Award is for; the prize is for quality of presentation rather than for quality of content. Secondly, the ranking system associated with the prize is based on marks given by volunteers who probably do not all use the same standards, and so there is an unavoidable element of chance in the system. Therefore, the prize shouldn't be taken too seriously, and certainly should not give rise to an atmosphere of fierce competition. For the proud winner: congratulations, and please take good care of the trophy since it will be awarded again next year. For all the others: the envelope with your results will be available immediately after the winner has been announced, in the same room. Looking over your marks and reading the suggestions that some jurors may have placed on the back side of the form may give you some ideas of how to improve your presentation technique; and then take another chance next year.

For all further information regarding the BJP Award, please contact the Prize Commissioners: Ilse Smets, Jan Van Impe or Ton van den Boom.

Meetings

The following meetings are scheduled:

- DISC bestuursvergadering; Tuesday, March 13, 21:00–22:00, Seaside zaal.
- Lunch meeting Unit DISC; Wednesday, March 14, 12:30–14:00, Market Grill Restaurant.
- Dinner meeting of the Programme Committee of the Graduate School in Systems and Control: Wednesday, March 14, 19:00–21:00, Savanna Restaurant.
- DISC management team vergadering: Wednesday, March 14, 21:00–22:00, Seaside zaal.

Tuesday March 13

		Conference Centre			
		<i>Registration</i>			
		Les Arcades			
		<i>Welcome and Opening</i>			
		Les Arcades			
09:00 – 10:40					
10:40 – 10:55					
11:30 – 12:30		Plenary lecture: "Sampling in Signal Processing" G. Goodwin			
12:30 – 14:00		Lunch (Market Grill Restaurant)			
room	Les Arcades	Bloemenzaal	Impresario zaal	Western zaal	Emanuel zaal
TuP	TuP01 <i>Control applications 1</i>	TuP02 <i>Control</i>	TuP03 <i>Reservoir monitoring & control</i>	TuP04 <i>System theory 1</i>	TuP05 <i>Chemical reactors</i>
14:00 – 14:25	van Oort	Oomen	Douma	Toth	Gins
14:25 – 14:50	De Laet	van Helvoort	Leskens	Collins	Vande Wouwer
14:50 – 15:15	Smitis	Aangenent	van Doren	Peeters	Sauvage
15:15 – 15:40	Donné	Habets	Zandvliet	Vanhuylen	Mesbah
15:40 – 16:05	Schitter	Wei	van Essen	Nencova	Simeonova
16:05 – 16:35				Break	D'hane
TuE	TuE01 <i>Control applications 2</i>	TuE02 <i>Traffic, motion control</i>	TuE03 <i>Bio / Human</i>	TuE04 <i>System theory 2</i>	TuE05 <i>Bio reactors</i>
16:35 – 17:00	van Hulzen	van Ast	Daye	Favache	Dewasme
17:00 – 17:25	Bruynen	Michiels	Bonjean	Tuna	De Sitter
17:25 – 17:50	Stolte	Baskar	Urbain	Callier	David
17:50 – 18:15	Gajdusek	Scardovi	Shi	Jetsma	Winkin
18:15 – 18:40	van den Berg	Cloosterman	Van Herpe	Jungers	Sharciog
19:00 – 21:00				Dinner (Hammonds Restaurant)	Boerlage
21:00 – 22:00				Bestuursvergadering DISC (Seaside zaal)	Reynders

Wednesday March 14

Les Arcades		Plenary lecture: "Parametric Time Domain Methods for Non-Stationary Random Vibration Identification: An Overview of Methods and Applications"	
08:30 – 09:30		S.Fassois	
09:30 – 10:00		Break	
10:00 – 11:00		Plenary lecture: "Quantization in Signal Processing and Control"	
11:00 – 11:15		Les Arcades	
room	Les Arcades	Bloemenzaal	Impresario zaal
WeM	WeM01 Control applications 3	WeM02 Special session: "target round-robin"	WeM03 Tubular reactors
11:15 – 11:40	Gerard	Rotain	Van Erdghem
11:40 – 12:05	van der Meulen	Logist	Trottemant
12:05 – 12:30	Stallaert	Vandereycken	Collins
12:30 – 14:00			Lunch (Market Grill Restaurant)
WeP	WeP01 Control applications 4	WeP02 Distributed systems	WeP03 Optimization
14:00 – 14:25	van Eekelen	Grosfils	Pipeleers
14:25 – 14:50	van Helvoirt	Wattanwar	Haverbeke
14:50 – 15:15	Delwiche	van Mourik	De Caigny
15:15 – 15:40	Iokic	Napp	Vanbiervliet
15:40 – 16:05	Balini	Ellenbroek	Camino
16:05 – 16:35			Debrouwe
WeE	WeE01 Control applications 5	WeE02 Miscellaneous	WeE03 Numerical techniques
16:35 – 17:00	Vanderborght	Petit	Ho
17:00 – 17:25	Deckers	van der Laan	de Kerchove
17:25 – 17:50	Van Damme	Naus	Journée
17:50 – 18:15	van Lierop		Warnez
19:00 – 21:00			Dinner (Savanna Restaurant) Graduate School Dinner Meeting
21:00 – 22:00			DISC management team vergadering (Seaside zaal)

Thursday March 15

Les Arcades											
08:30 – 09:30		Plenary lecture: "Nonlinear Dynamic Optimization in Control Engineering – Algorithms and Applications"									
09:30 – 10:00		M. Diehl									
10:00 – 11:00		Break									
11:00 – 11:15		Les Arcades									
room	Les Arcades	Bloemenzaal	Impresario zaal	Western zaal	Emanuel zaal	Seaside zaal					
ThM	ThM01	ThM02	ThM03	ThM04	ThM05	ThM06					
Control applications 6											
11:15 – 11:40	van Mourik	Saha	MPC 1	Non linear control systems	Learning 2	State estimation					
11:40 – 12:05	van Ooteghem	Ionescu	Barjas Blanco	van Oort	Smolders	Witters					
12:05 – 12:30	Lepore	van Belzen	Galvez-Carillo	Sonneveldt	Defourny	Goffaux					
12:30 – 14:00	Break										
ThP	ThP01	ThP02	ThP03	ThP04	ThP05	ThP06					
Control applications 7											
14:00 – 14:25	Merry	Bos	Aguadelo	Tien Hung	van Dijk	Vries					
14:25 – 14:50	Pajmans	Voss	Bonilla	Wei	Rogge	Goffaux					
14:50 – 15:15	van de Loo	Meyroneinc	ter Meer	Pajmans	de Weerdt	Lendek					
15:45 – 16:15		Les Arcades									
Best Junior Presentation Award											
Closing											

